

**Modulation of transglutaminase
2 by the A₁ adenosine receptor
and β₂-adrenoceptor in
cardiomyoblasts: a role in cell
survival**

Falguni Satish Vyas

A thesis submitted in partial fulfilment of the
requirements of Nottingham Trent University
for the degree of Doctor of Philosophy.

July 2017

This work is the intellectual property of the author. You may copy up to 5% of this work for private study, or personal, non-commercial research. Any re-use of the information contained within this document should be fully referenced, quoting the author, title, university, degree level and pagination. Queries or requests for any other use, or if a more substantial copy is required, should be directed in the owner(s) of the Intellectual Property Rights.

Publications:

Vyas FS, Hargreaves AJ, Bonner PL, Boocock DJ, Coveney C, Dickenson JM. (2016) A₁ adenosine receptor-induced phosphorylation and modulation of transglutaminase 2 activity in H9c2 cells: A role in cell survival. *Biochem Pharmacol* **107**:41-58.

Vyas FS, Nelson CP, Freeman F, Boocock DJ, Hargreaves AJ, Dickenson JM. (2017) β_2 -adrenoceptor-induced modulation of transglutaminase 2 transamidase activity in cardiomyoblasts. *Eur J Pharmacol* **813**:105-121.

Vyas FS, Nelson CP, Dickenson JM. (2018) Role of transglutaminase 2 in A₁ adenosine receptor- and β_2 -adrenoceptor-mediated pharmacological pre- and post-conditioning against hypoxia-reoxygenation-induced cell death in H9c2 cells. *Eur J Pharmacol* **819**:144-160.

Conference presentations:

School of Science and Technology 11th Annual Research Conference (STAR conference), Nottingham Trent University (May 2017). Poster presentation entitled "Role of Transglutaminase 2 in β_2 -AR-induced cardioprotection". P42.

15th Annual East Midlands Proteomics Workshop, Nottingham Trent University (November 2016). Poster presentation entitled: "Identification of β_2 -adrenoceptor-stimulated transglutaminase 2 substrates by SWATH-MS". P05.

Gordon Research Conference on Transglutaminases in Human Disease Processes, PGA Catalunya Business and Convention Centre, Girona, Spain (July 2016). Poster presentation entitled: "Modulation of transglutaminase-2 activity by the A₁ adenosine receptor". P58.

British Pharmacological Society 6th Focused Meeting on Cell Signalling, University of Leicester (April 2016). Poster presentation entitled: "A₁ adenosine receptor-induced modulation of transglutaminase 2 activity in H9c2 cardiomyoblasts" *Proceedings of the British Pharmacological Society* Vol**12** Issue3 024P.

School of Science and Technology 9th Annual Research Conference (STAR conference), Nottingham Trent University (May 2015). Poster presentation entitled "Regulation of Transglutaminase-2 by Adenosine A₁ Receptor". P31

Abstract

Transglutaminase 2 (TG2) is a multifunctional enzyme possessing transamidating, GTPase and protein disulphide isomerase activity. Due to its diverse nature and ubiquitous distribution TG2 is implicated in the regulation of many physiological processes, including cell adhesion, migration, growth, differentiation, survival and apoptosis. Recently, TG2 has been shown to be modulated by PKC and PKA and to play a role in cardioprotection. However, the precise mechanism(s) of its modulation by G-protein coupled receptors coupled to PKC and PKA activation are not fully understood. The present study investigated the molecular mechanisms underlying TG2 modulation by GPCRs (A_1 adenosine receptor (A_1R) and β_2 -adrenoceptor (β_2 -AR)) and its role in cardioprotection. Transglutaminase transamidation activity was determined using amine-incorporating (*in vitro* and *in situ*) and protein cross-linking assays. TG2 phosphorylation was assessed via immunoprecipitation and Western blotting. The role of TG2 in A_1R - or β_2 -AR-induced cytoprotection was investigated by monitoring hypoxia- and hypoxia/reoxygenation-induced cell death. Novel TG2 substrates/interacting proteins were identified using SWATH MS.

Stimulation of the A_1R (with the selective agonist CPA and endogenous agonist adenosine) and β_2 -AR (with the selective agonist formoterol and non-selective agonist isoprenaline) resulted in activation of TG2 in a time- and concentration-dependent manner, which was attenuated by the TG2 inhibitors Z-DON and R283. Responses to CPA and adenosine were blocked by pharmacological inhibition of PKC (Ro 31-8220), MEK1/2 (PD 98059), p38 MAPK (SB 203580) and JNK1/2 (SP 600125) and by removal of extracellular Ca^{2+} . CPA triggered robust increases in the levels of TG2-associated phosphoserine and phosphothreonine, which were attenuated by PKC, MEK1/2 and JNK1/2 inhibitors. Responses to formoterol, whilst insensitive to pertussis toxin (PTX; G_i -protein inactivator), were abolished by PKA (*Rp*-cAMPs), MEK1/2, and PI-3K γ (AS 605240) inhibitors. Responses to isoprenaline were blocked by PTX and inhibitors of MEK1/2 and PI-3K γ . Formoterol triggered robust increases in the levels of TG2-associated phosphoserine and phosphothreonine, which were attenuated by PKA, MEK1/2 PI-3K γ inhibitors and by removal of extracellular Ca^{2+} .

Furthermore, the A_1R - or β_2 -AR-mediated TG2 activation (with the exception of formoterol-induced TG2 activation) was protective against hypoxia- and hypoxia/reoxygenation-induced cell death. Finally, identification of novel TG2 substrates/interacting proteins using SWATH MS illustrated differential modulation of substrates by TG2 upon stimulation of the A_1R - or β_2 -AR which may contribute to differences in their cellular/physiological responses. The present study provides the first detailed characterisation of the molecular mechanisms underlying the modulation of TG2 by the A_1R - or β_2 -AR and describes a role for TG2 in cardioprotection, along with identifying novel substrates/interacting proteins which may be involved in mediating this protection.

Acknowledgements

I'd like to express my gratitude to my supervisory team, Dr John Dickenson, Dr Phillip Bonner and Dr Alan Hargreaves for their help and support. A special thanks goes to Dr Carl Nelson for being my unofficial supervisor throughout my PhD, whose knowledge and expertise have been an invaluable asset to me. An added thank you goes to both John and Carl for believing in me and being understanding, supportive, calm and positive during difficult days and you know there have been many! Your constant reminders that "it's my PhD" kept me motivated and your incredible sense of humour made my time here both enjoyable and productive - better supervisors I could not have asked for.

I would like to thank David in JvG for his help with mass spectrometry, Fiona for her help with PCR and Gordon for his help in microscopy.

My thanks also go to members of labs 107 and 106 (both past and present) for putting up with me and listening to rants about unsuspecting students! Thanks for making life so much fun and eventful in IBRC. In particular, James and Shatha, for accepting me into your group when I wasn't a part of it and teaching me the basic techniques like cell culture and maintenance of the lab; Tom, for being extremely patient, understanding and assisting me with crazy ideas for people's birthdays (thanks my fluorescent man!); Jess, for always being there and teaching me document formatting without which my thesis would not look the way it does; Nina, for teaching me western blotting and Lyndsey for teaching me how to develop blots flawlessly (none of my blots would look how they look if it wasn't for you two). A special thanks goes to Giulia for her company and constant encouragement and support in the lab throughout. Thank you for making me laugh no matter what mood I'm in, and countless coffees, you have a friend for life in me.

More importantly, my sincere thanks goes to my mum and dad, who have always supported me in every way possible, even when they had no clue of what I was going on about! Thank you for funding all my studies right from nursery till my PhD. Without your support I couldn't have achieved what I have so far and hope to achieve much more to make you even more proud.

Abbreviations

A ₁ R	A ₁ adenosine receptor
AC	Adenylyl cyclase
AIDA	Advanced Image Data Analysis software
ANT1	Adenine nucleotide translocator 1
β ₂ -AR	β ₂ -adrenoceptor
BAD	Bcl-2-associated death promoter
Bax	Bcl-2-associated X protein
Bcl	B-cell lymphoma
BSA	Bovine serum albumin
BXC	Biotin X cadaverine
cAMP	Adenosine 3', 5'-cyclic monophosphate
CICR	Calcium-Induced Calcium Release
CREB	cAMP response element-binding protein
CYP	Cytochrome P450
DAG	Diacylglycerol
DMEM	Dulbecco's Modified Eagle's Medium
DMSO	Dimethyl sulphoxide
DNA-PK	DNA-dependent protein kinase
DTT	Dithiothreitol
ECL	Enhanced chemiluminescence
ECM	Extracellular matrix
EDTA	Ethylenediaminetetraacetic acid
ERK1/2	Extracellular signal-regulated kinase ½
FBS	Foetal bovine serum
GDP	Guanosine 5'-diphosphate
GEF	Guanine nucleotide exchange factor
GPCR	G-protein-coupled receptors
GTP	Guanosine 5'-triphosphate
HIF1β	Hypoxia inducible factor 1β
HK1	Hexokinase 1
IL	Interleukin
IP ₃	Inositol 1,4,5-trisphosphate
JNK	c-Jun N-terminal kinase
LDH	Lactate dehydrogenase
LTCC	L-type calcium channels
MAPK	Mitogen-activated protein kinase
mPTP	Mitochondrial permeability transition pore
mTORC	Mammalian target of rapamycin Complex
NF-κB	Nuclear factor kappa B
NHE	Sodium/hydrogen exchanger
PBS	Phosphate-buffered saline
PDI	Protein disulphide isomerase
PDK	Phosphoinositide dependent protein kinase
PI-3K	Phosphoinositol-3 kinase
PIP ₂	Phosphatidylinositol 4,5-bisphosphate
PIP ₃	Phosphatidylinositol (3,4,5)-trisphosphate
PKA	Protein kinase A

PKB/Akt	Protein kinase B/Akt
PKC	Protein kinase C
PLC	Phospholipase C
PTEN	Phosphatase and tensin homolog
PTX	Pertussis toxin
Rb	Retinoblastoma protein
RISK	Reperfusion Injury Salvage Kinase
ROS	Reactive oxygen species
RyR	Ryanodine receptors
SDS	Sodium dodecyl sulphate
SERCA	Sarcoplasmic/Endoplasmic Reticulum Calcium ATPase
SWATH MS	Sequential Windowed Acquisition of all Theoretical fragment ion Mass Spectra
TG	Transglutaminase
TG2	Transglutaminase 2
TGF- β	Tumour growth factor- β
TNF- α	Tumour necrosis factors- α
VDAC-1	Voltage dependent anion channel 1

Contents:

CHAPTER I:

Introduction.....	1
1.1 Cardiovascular diseases.....	1
1.2 Ischaemia/reperfusion injury.....	1
1.3 Ischaemic pre- and post-conditioning.....	5
(i) Signalling pathways involved in ischaemic pre- and post-conditioning.....	6
1.4 Transglutaminases.....	9
1.5 Tissue transglutaminase.....	12
(i) <i>Functions of TG2.</i>	13
(ii) <i>Role of TG2 in disease.</i>	19
(iii) <i>Role of TG2 in cell death and cell survival.</i>	21
(iv) <i>TG2 and cardioprotection.</i>	23
1.6 The G-protein Coupled Receptor (GPCR) family.....	24
(i) <i>Structure of GPCRs.</i>	24
1.7 Adenosine receptors.....	27
(i) <i>Role of the A₁ adenosine receptor in cardioprotection.</i>	31
1.8 Adrenoceptors.....	32
1.9 Beta-adrenoceptors.....	36
(i) <i>Biased agonism of the β₂ adrenoceptors.</i>	38
(ii) <i>β₂ adrenoceptor signalling in cardiomyocytes.</i>	39
(iii) <i>Cardioprotective effects of β₂ adrenoceptors.</i>	39
1.10 H9c2 cells as a model system for cardioprotection.....	41
1.11 Aims of this project.....	43
Chapter II: Methods.....	44
2.1 Materials.....	44
2.2 Cell culture.....	46
2.3 Tissue transglutaminase activity assays.....	46
2.4 Expression of GPCRs and TGs in H9c2 cells.....	49
2.5 Functional Expression of GPCRs in H9c2 cells.....	51
(i) <i>cAMP accumulation assay</i>	51
(ii) <i>Measurement of intracellular calcium.</i>	52
2.6 SDS-PAGE and Western blot analysis.....	52
(i) <i>Preparation of cell lysates for western blotting.</i>	52
(ii) <i>BCA protein assay.</i>	52
(iii) <i>SDS-PAGE (Sodium Dodecyl Sulphate-Polyacrylamide Gel Electrophoresis)</i>	53
(iv) <i>Coomassie staining of gels.</i>	53
(v) <i>Western blotting.</i>	54
2.7 Immunoprecipitation analysis of TG2 phosphorylation.....	55

2.8 GPCR-mediated protection against hypoxia- and hypoxia/reoxygenation-induced cell death.....	55
(i) Simulation of ischaemia and/or ischaemia/reperfusion injury.....	55
(ii) MTT reduction assay.....	59
(iii) LDH release assay.....	59
(iv) Caspase-3 activation.....	60
2.9 Proteomic analysis of TG2 biotin-X-cadaverine labelled substrates.....	60
(i) CaptAvidin™-agarose sedimentation based affinity purification.....	60
(ii) Mass spectrometry.....	61
(iii) Bio-informatics analysis of mass spectrometry identified substrates.....	61
(iv) Validation of mass spectrometry derived substrates of TG2.....	62
2.10 Statistical analysis.....	62
CHAPTER III Functional GPCR and Transglutaminase expression in H9c2 cells.....	64
3.1. Functional expression of adenosine receptors on H9c2 cells.....	64
3.2. Functional expression of β-adrenoceptors on H9c2 cells.....	67
3.3. Characterisation of TG expression pattern in H9c2 cells.....	74
3.4 Discussion.....	75
Chapter IV: Modulation of TG2 activity by the A₁ adenosine receptor in H9c2 cells.....	83
4.1 Effect of A ₁ R activation on TG2-mediated biotin cadaverine amine incorporation and protein cross-linking activity.....	83
4.2 The effect of selective A ₁ R antagonist and TG2 inhibitors on A ₁ R induced TG2 activity.....	86
4.3 The role of Ca ²⁺ in A ₁ R induced TG2 activity.....	86
4.4 The effect of pertussis toxin and protein kinase inhibitors on A ₁ adenosine receptor-induced TG2 activity.....	89
4.5 Visualisation of <i>in situ</i> TG2 activity following A ₁ R activation.....	97
4.6 A ₁ R induced TG2 phosphorylation.....	103
4.7 Discussion.....	107
Chapter V: Modulation of TG2 activity by the β₂ adrenoceptor in H9c2 cells.....	114
5.1 Effect of β ₂ -AR activation on TG2-mediated biotin cadaverine amine incorporation and protein cross-linking activity.....	114
5.2 The effect of β-AR antagonists and TG2 inhibitors on β ₂ -AR induced TG2 activity.....	117
5.3 The role of Ca ²⁺ in β ₂ -AR induced TG2 activity.....	117
5.4 The effect of protein and lipid kinase inhibitors on β ₂ -AR induced TG2 activity.....	120
5.5 Visualisation of <i>in situ</i> TG2 activity following β ₂ -AR activation.....	137
5.6 β ₂ -AR induced TG2 phosphorylation.....	143

5.7 Discussion.....	149
Chapter VI: Cardioprotective role of A₁ adenosine receptor and β₂ adrenoceptor-induced TG2 activation.....	157
6.1 Determination of time period for hypoxia and hypoxia/re-oxygenation-induced cell death.....	157
6.2 Role of TG2 in A ₁ R-induced cell survival against hypoxia-induced cell death.....	159
6.3 Role of TG2 in β ₂ -AR-induced cell survival against hypoxia-induced cell death....	163
6.4 Role of TG2 in A ₁ R-induced cell survival against hypoxia/re-oxygenation-induced cell death.....	167
6.5 Role of TG2 in β ₂ -AR-induced cell survival against hypoxia/ re-oxygenation-induced cell death.....	175
6.6 Discussion.....	181
Chapter VII: Proteomic identification of agonist-mediated TG2 substrates and associated proteins.....	184
7.1 CaptAvidin™-agarose affinity chromatography.....	184
7.2 SWATH MS identification of proteins.....	186
7.3 Pathway analysis.....	197
7.4 Western blot confirmation of VDAC1 and HK1.....	201
7.5 Discussion.....	204
Chapter VIII: Conclusions and further work.....	211
8.1 General conclusions.....	211
8.2 Further work.....	211
8.3 Concluding remarks.....	213
Bibliography.....	215
Appendix I.....	278

CHAPTER I: Introduction

1.1 Cardiovascular diseases.

Currently, cardiovascular disease is the leading cause of death in the world with 17.5 million deaths in 2012 worldwide (WHO statistics database; <http://www.who.int/mediacentre/factsheets/fs317/en/>). Of those deaths, 7.4 million were due to ischaemic heart disease (WHO statistics database). In 2015, over 70,000 deaths in the UK were due to ischaemic heart disease (BHF statistics database; <https://www.bhf.org.uk/research/heart-statistics>) and it is predicted if not controlled, it will rise by 25% in 2025 (Gaziano et al, 2010). Ischaemic heart disease occurs when the coronary artery is blocked, usually by an atherosclerotic plaque. This blockage reduces the blood flow to myocardial tissue resulting in angina pectoris (chest pain and discomfort) and myocardial infarction (heart attack). There are several risk factors that play a role in development of this atherosclerotic plaque such as age, diet, obesity, high blood pressure, high levels of cholesterol, smoking and other lifestyle choices (Nichols et al, 2014). Even though there is plenty of research regarding ischaemic heart diseases and their underlying mechanisms, there are not many pharmacological agents that have made it successfully into clinical trials. Therefore, it is of utmost necessity to comprehend the pathophysiology of ischaemic heart disease in order to develop novel therapeutic strategies and identify potential targets which could be manipulated by the use of pharmacological agents to be used in clinical studies and scenarios.

1.2 Ischaemia/reperfusion injury.

Ischaemia is a pathological condition suffered by tissues and organs which are deprived of nutrients and oxygen due to inadequate blood supply. This imbalance in oxygen demand and supply results in changes in metabolic and cellular responses of the cells. Myocardial cells when exposed to ischaemia can show either myocardial stunning and/or myocardial hibernation. Myocardial stunning is described as delayed return of the contractile function of the heart following ischaemia although complete restoration of the blood flow is achieved (Depre and Taegtmeyer, 2000). Myocardial hibernation is described as recurring stunning as a result of a chronic ischaemic insult (Kim et al, 2003).

Under normal physiological conditions, cardiac cells generate ATP from metabolites and oxidative phosphorylation (aerobic respiration) in order to meet the oxygen supply and demand. The heart changes this chemical energy into mechanical energy (Carvajal and Moreno-Sanchez, 2003; Solaini and Harris, 2005). During ischaemia, mitochondrial respiration is switched from aerobic to anaerobic in order to match the oxygen demand and supply. This leads to inhibition of phosphofructokinase, accumulation of hydrogen ions and lactate as well as accumulation of sodium ions via inhibition of the sodium/potassium pump (Na^+/K^+ -ATPase) and activation of sodium/hydrogen exchanger (NHE). Inhibition of phosphofructokinase leads to

reduction in sensitivity of Troponin C to calcium resulting in asystole (Di Lisa et al, 1998). Inhibition of the Na^+/K^+ -ATPase increases efflux of potassium ions and influx of sodium and chloride ions as well as water into the cardiac cells, which leads to cell swelling. High intracellular sodium ion concentration activates the sodium/calcium exchanger ($\text{Na}^+/\text{Ca}^{2+}$ exchanger), thereby increasing intracellular levels of calcium. Normal calcium concentration cannot be restored by the Sarcoplasmic/Endoplasmic Reticulum Calcium ATPase (SERCA) due to reduction in ATP levels. This high calcium concentration activates calcium dependent proteases such as calpain which results in cytoskeletal damage and membrane rupture leading to ischaemic cell death (Schaper and Kostin, 2005; for an overview refer to figure 1.1). Ischaemic cell death (apoptosis during ischaemia) is characterised by swelling of the cells, increase in membrane permeability, non-specific DNA degradation, nuclear chromatin condensation and blebbing (Majno and Joris, 1995; Buja, 2005). Apoptosis or programmed cell death is characterised by cell shrinkage, nuclear condensation, fragmentation of DNA and formation of apoptotic bodies, which are phagocytosed without evoking an inflammatory response (Majno and Joris, 1995; Edinger and Thompson, 2004). Cells can be rescued from ischaemic cell death, however if not rescued, necrosis sets in. Necrosis is characterised by further degradation of cytoplasmic membrane and constituents as well as changes in the nucleus and as such represents irreversible cell death (for review see Trump and Berezsky, 1996; Adameova et al, 2016).

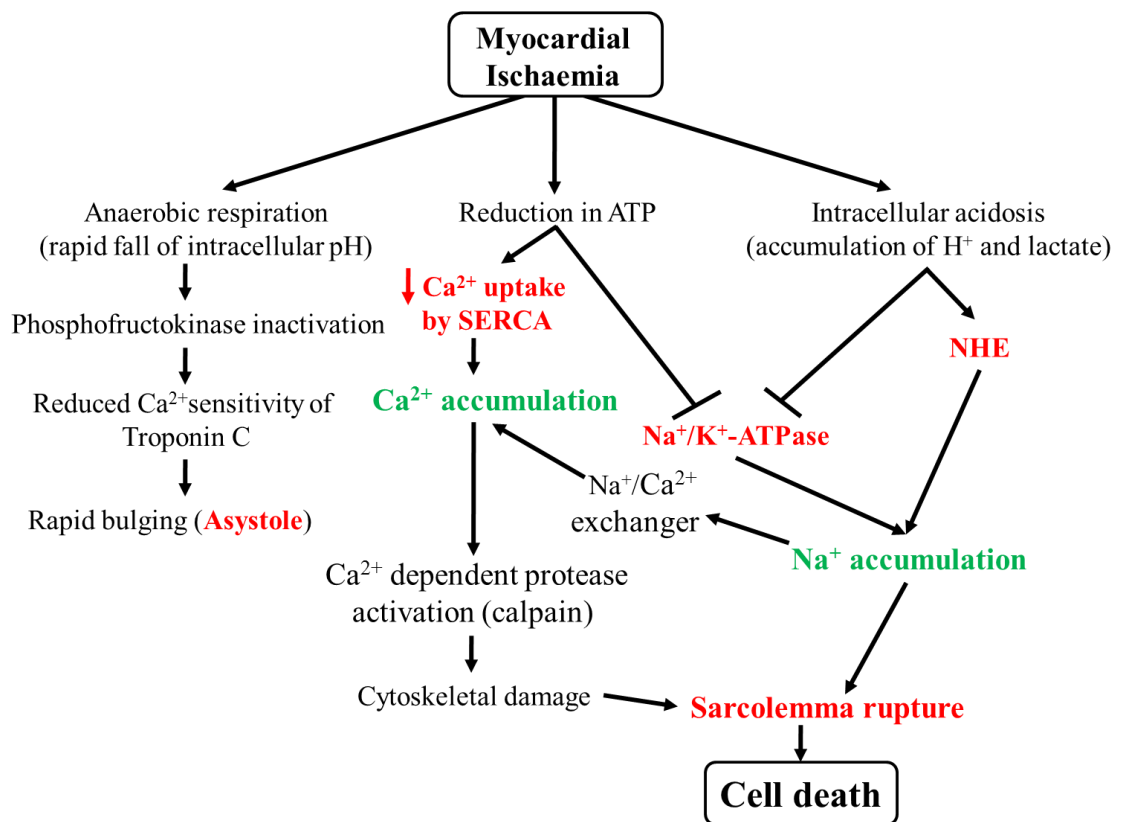


Fig 1.1: Proposed series of events leading from myocardial ischaemia to cell death. Anaerobic respiration along with reduced formation of ATP and intracellular acidosis causes sarcolemma to rupture and lead to cell death.

Reperfusion is the restoration of blood flow following an ischemic insult for more than 10 min. It was initially thought that reperfusion can rescue the damage caused by ischaemia to cells and tissues; however, it is now known that it leads to further complications such as arrhythmia, stunning, decrease in contractility and more pronounced necrosis (Moens et al, 2005). Neutrophils accumulate surrounding the damaged cells and tissues during ischaemia (Hansen, 1995). Upon reoxygenation, neutrophils generate more reactive oxygen species (ROS), proteases and cause activation of inflammatory cascades (Jordan et al, 1999). Apart from neutrophil activation, restoration of oxygen causes mitochondrial respiration to switch back to aerobic from anaerobic resulting in additional production of ROS (Korge et al, 2008). ROS generation can cause further damage by attacking lipids, proteins and nucleic acid components of the cell as well as dysregulating ion transport, fluidity, protein synthesis and enzyme activity within the cell (Becker, 2004). ROS generation causes activation (opening) of mitochondrial permeability transition pore (mPTP) thereby setting off either apoptosis via release of cytochrome c and activation of caspase cascade or necrosis via ATP hydrolysis and dysregulation of intracellular calcium concentration (Lopez-Neblina and Toledo-Pereyra, 2006). This Ca^{2+} overload leads to activation of calcium-dependent proteases such as calpains. These proteases degrade intracellular proteins and cause cytoskeletal damage leading to cell death (Piper et al, 2006). Also during reperfusion, Nuclear factor kappa B (NF- κ B) activates various cell adhesion molecules and adheres leukocytes to the endothelium of the myocardium (Baldwin, 2001). This leads to vasoconstriction and microvascular dysfunction reducing perfusion resulting in "no-flow" phenomenon which ultimately leads to myocardial infarction (Moens et al, 2005; for an overview refer to figure 1.2).

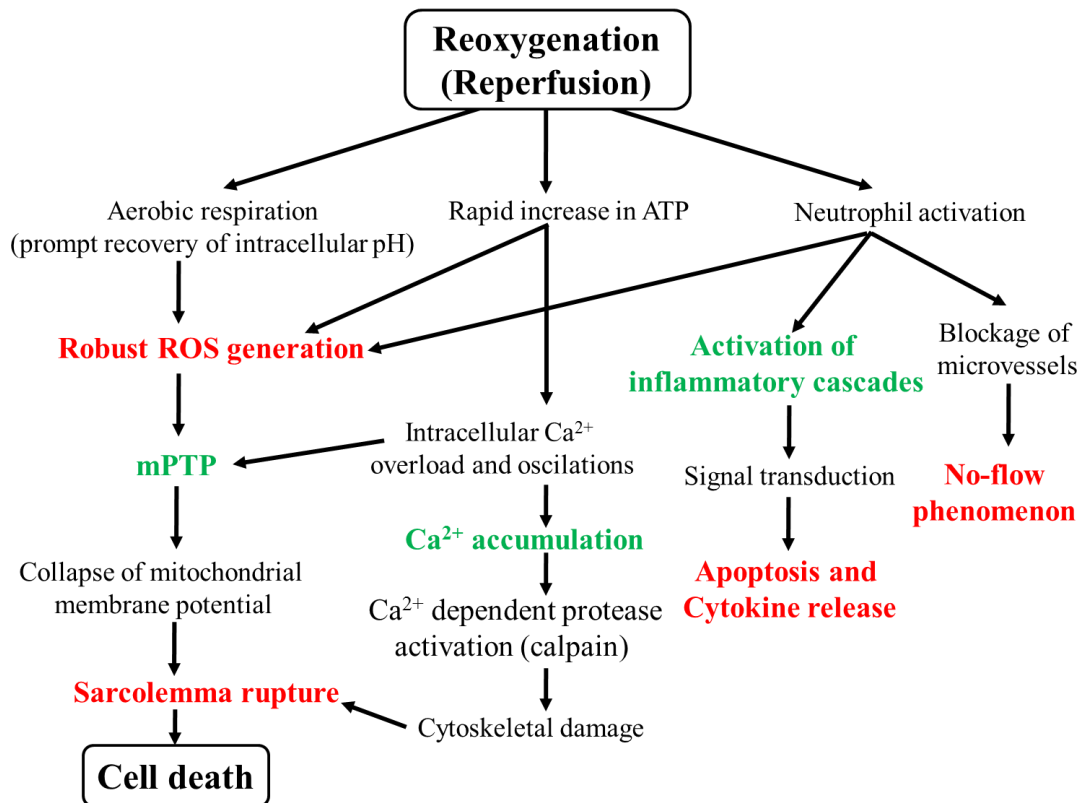


Fig 1.2: Proposed series of events leading from myocardial ischaemia/reperfusion injury to cell death. Switch from anaerobic respiration to aerobic respiration along with rapid formation of ATP and neutrophil activation causes a series of events that lead to cell death.

Both ischaemia and ischaemia/reperfusion are known to induce a combination apoptosis and necrosis. Apoptosis is the preferred pathway until ATP levels are too low to sustain this energy-dependent pathway and then necrosis sets in (Tatsumi et al, 2003; Otani et al, 2006). This greatly depends on the conditions used to simulate ischaemia or ischaemia/reperfusion and model type used in the study. For instance, in neonatal and adult rat cardiomyocytes, ischaemia is known to induce apoptosis (Tanaka et al, 1994; de Moissac et al, 2000). However, in Langendorff-perfused mouse heart, apoptosis was only observed when ischaemia was accompanied with reperfusion, hence necrosis dominates (Webster et al, 1999). Also the apoptotic pathway stimulated depends on the conditions used to simulate ischaemia or ischaemia/reperfusion. For example, in Jurkat cells, a caspase-3 dependent apoptotic cascade was activated when ischaemia was simulated in glucose-free medium (Malhotra et al, 2001). Similar observations have also been reported in H9c2 cardiomyoblasts (Ekhterae et al, 1999). However, in Jurkat cells, simulating ischaemia in glucose-containing medium (3 mM glucose) activated a caspase-3 independent apoptotic cascade (Malhotra et al, 2001). Having said this, overall, there is strong evidence that apoptosis is induced in cardiomyocytes during ischaemia (Itoh et al, 1995; Long et al, 1997; Saraste et al, 1997) or ischaemia/reperfusion injury (Gottlieb et al, 1994; Fliss and Gattinger, 1996; Aikawa et al, 1997; Xia et al, 2016).

1.3 Ischaemic pre- and post-conditioning.

The pilot study carried out by Murry and colleagues reported that brief periods of discontinuous ischaemia and reperfusion prior to subsequent prolonged lethal ischaemia was able to protect against ischaemia/reperfusion damage in a canine model (Murry et al, 1986). This is called ischaemic preconditioning or classical/early phase preconditioning. There are many clinical limitations to ischaemic preconditioning as it is quite difficult to predict the timing of a myocardial infarction. However, this phenomenon is very useful in cases of cardiac bypass surgery as well as coronary artery bypass graft surgery, where ischaemic events are predicted (Wu et al, 2002; Yellon et al, 2005). This preconditioning offers transient benefits for 1-2 hours against ischaemic insult. Various survival kinases such as PKA, PKB, PKC and ERK1/2 are involved in mediating protection via this mechanism (for reviews see Sanada and Kitakaze, 2004; Bolli, 2007).

Zhao and colleagues were the first to describe the term ischaemic postconditioning (Zhao et al, 2003). It is described as brief periods of ischaemia and reperfusion following an ischaemic insult but prior to reperfusion (Zhao et al, 2003). It is shown to have similar protective effects as pre-conditioning (Hausenloy et al, 2006), however, post-conditioning is more clinically relevant as reperfusion following myocardial infarction can be predicted. Figure 1.3 represents a basic outline of ischaemic pre- and post-conditioning.

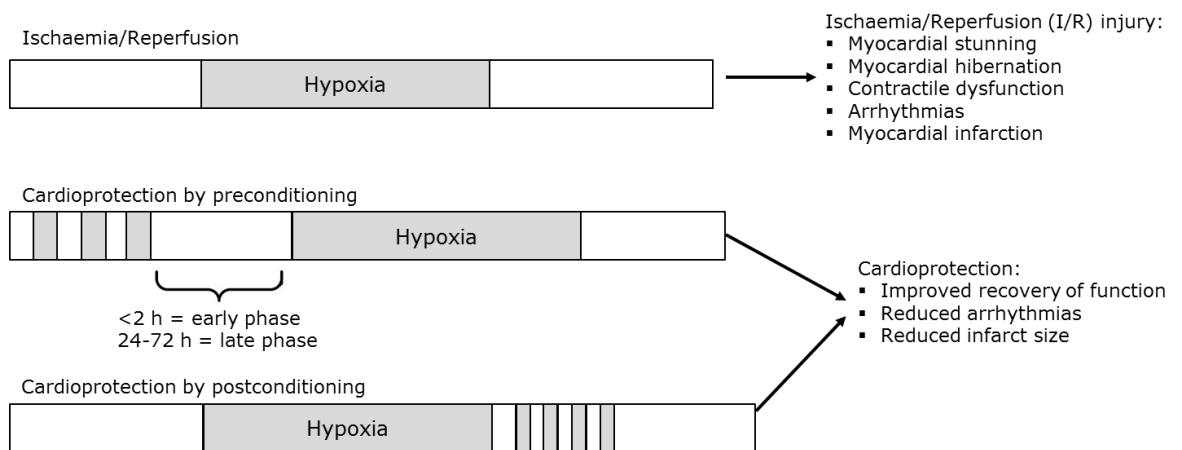


Fig 1.3: Graphical representation of ischaemia/reperfusion injury and pre- /post-conditioning. Areas in grey indicate ischaemia and white represent normal perfusion. Figure adapted from Ferdinandy et al, 2007.

(i) Signalling pathways involved in ischaemic pre- and post-conditioning.

Both ischaemic pre- and post-conditioning are known to activate several survival kinases such as ERK1/2, PKC, PKA, PKB and p38 MAPK, which have well documented roles (Hausenloy and Yellon, 2006). During an ischaemic insult, autacoid triggers such

as adenosine (Headrick, 1996; Pac-soo et al, 2015), catecholamines (Schomig, 1990; Pac-soo et al, 2015) and many others are released from the myocardial tissue. These triggers stimulate specific GPCRs which activate signal transduction cascades (for reviews see Halestrap and Richardson, 2015; Altamirano et al, 2015; Pac-soo et al, 2015; Bice et al, 2016).

The Reperfusion Injury Salvage Kinase (RISK) pathway plays a key role in mediating protection. The important targets of the RISK pathway are ERK1/2 and PKB (Hausenloy and Yellon, 2006). ERK1/2 phosphorylation is significantly increased following pre- and post-conditioning in Langendorff-perfused rat heart (Hausenloy et al, 2005) as well as rat (Fryer et al, 2001) and pig hearts *in vivo* (Schwartz and Lagranha, 2006). In order to activate the ERK1/2 pathway, GTP-bound Ras recruits and phosphorylates Raf at the cell membrane. Phosphorylated Raf then phosphorylates MAPK/ERK Kinase 1 and 2 (MEK1 and MEK2). Phosphorylated MEK1/2 then phosphorylates ERK1/2. Once ERK1/2 is phosphorylated, it can then activate downstream effectors such as p90 ribosomal S6 kinase (p90RSK; Herrera and Sebolt-leopold, 2002). Figure 1.4 summarises the ERK1/2 pathway. P90RSK inactivates BAD and inhibits BAD-mediated cytochrome-c release and caspase activation (Downward, 1999). The A₁ adenosine receptor activation causes phosphorylation of ERK1/2 and its role in protecting neonatal rat cardiomyocytes via pre-conditioning is well documented (Germack and Dickenson, 2005).

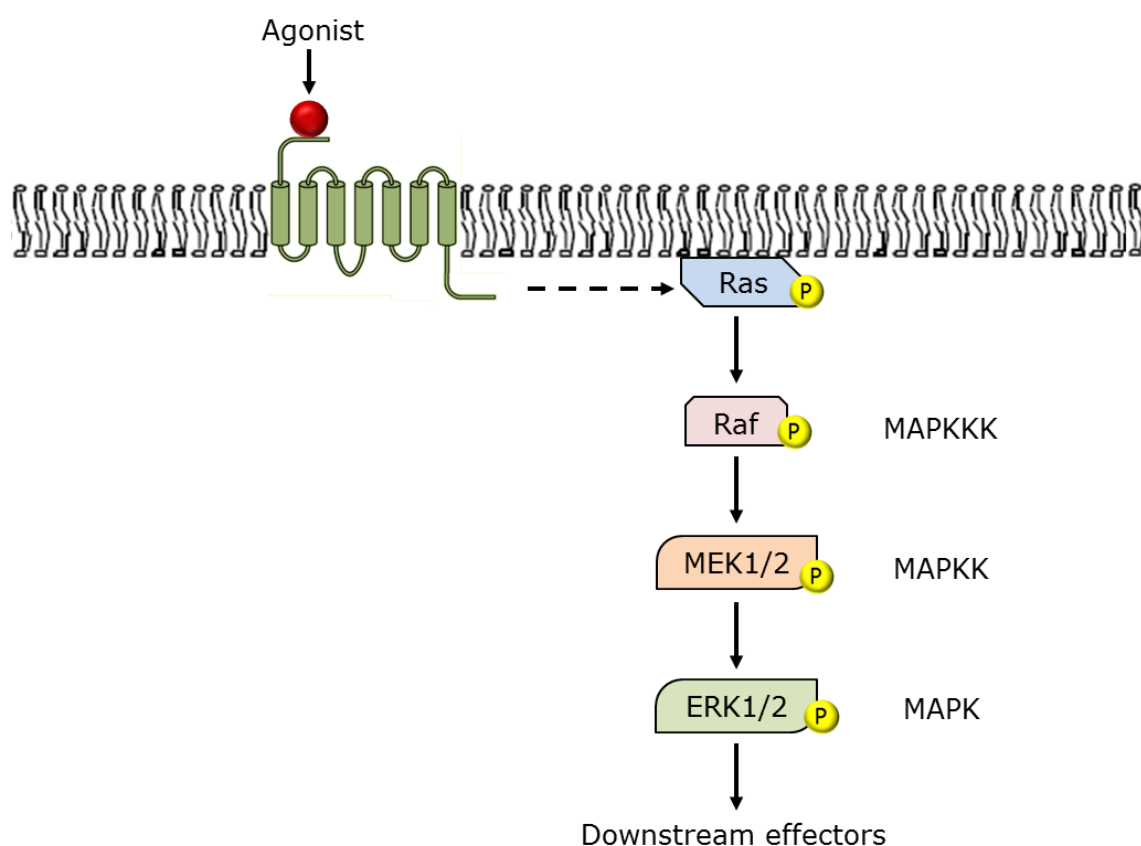


Fig 1.4: The steps leading to activation of ERK1/2. For detailed description, see main body of text.

Phosphorylation of PKB is significantly increased following pre- and post-conditioning in Langendorff-perfused rat and rabbit hearts (Hausenloy et al, 2005; Solenkova et al, 2006) as well as pig hearts *in vivo* (Schwartz and Lagranha, 2006). The PKB pathway is activated via phosphorylation of PIP₂ to PIP₃ by PI-3K. PIP₃ recruits phosphoinositide dependent protein kinase (PDK) to the cell membrane where PKB is phosphorylated at Thr³⁰⁸ by PDK1 while Ser⁴⁷³ can be phosphorylated by a number of kinases such as PDK2 (Vanhaesebroeck and Alessi, 2000), integrin-linked kinase (ILK; Osaki et al, 2004), mechanistic target of rapamycin complex (mTORC; Sarbassov et al, 2005) and DNA-dependent protein kinase (DNA-PK; Hemmings and Restuccia, 2012). For an extensive review on AKT/PKB signalling and regulation, see Bayascas and Alessi, 2005 and Risso et al, 2015. Phosphatase and tensin homolog (PTEN) counter regulates PI-3K activity by dephosphorylating PIP₃ to PIP₂, thereby inhibiting the PKB pathway (Carracedo and Pandolfi, 2008). Along with PTEN, the pathway is also modulated by protein phosphatase 2A (PP2A) and PH domain and Leucine rich repeat protein phosphatases (PHLPP) that dephosphorylate PKB at Thr³⁰⁸ and Ser⁴⁷³ respectively (for an extensive review see Carracedo and Pandolfi, 2008). Figure 1.5 summarises the PKB pathway.

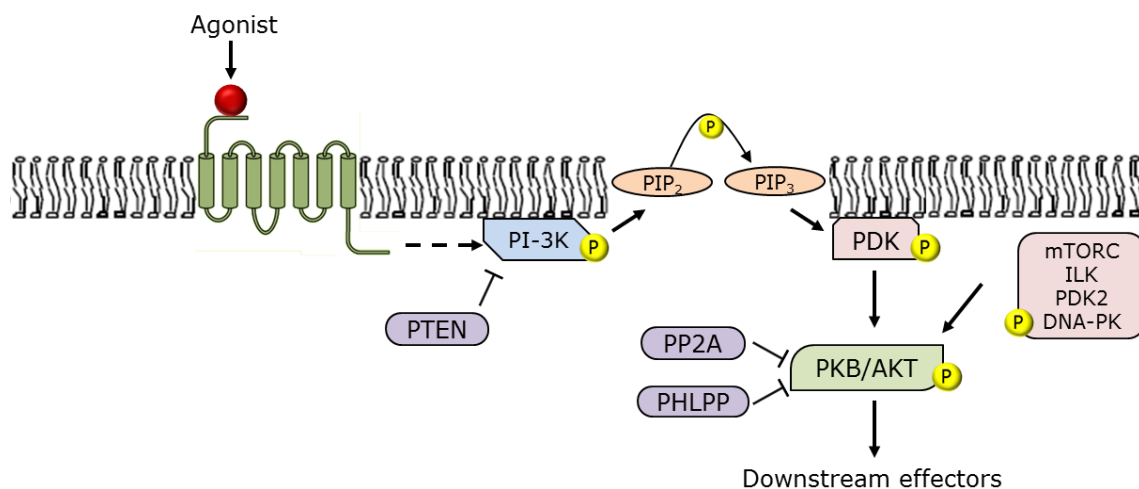


Fig 1.5: The steps leading to activation of PKB. For detailed description, see main body of text

Phosphorylated PKB is redistributed to the mitochondria (Miyamoto et al, 2008) and/or nucleus (Toker and Marmiroli, 2014) where it inhibits BAD-mediated cytochrome-c release (Datta et al, 1997). Furthermore, Gottlob and colleagues have reported that PKB enhances the interaction between hexokinase and voltage dependent anion channel 1 (VDAC-1) thereby preserving the mitochondrial membrane integrity (Gottlob et al, 2001; Abu-Hamad et al, 2008).

There is some evidence that PKA activation prior to an ischaemic insult significantly reduces the infarct size in canine heart and that increases in cAMP levels during

ischaemia might be necessary to offer protection (Sanada et al, 2004). However, the same could not be demonstrated for rat hearts as inhibition of PKA reduced the infarct size and improved recovery (Makaula et al, 2005). Another protein kinase involved in cardioprotection is PKC. There are 10 isoforms of PKC, however, PKC δ and PKC ϵ are dominant in murine heart (Schreiber et al, 2001). While PKC α , PKC β I and PKC β II are dominant in human ventricles, PKC γ and PKC δ in atria and PKC ϵ and PKC λ are distributed equally in both (Simonis et al, 2007). Hence, there is inconsistency in the PKC isoform essential to trigger cardioprotection as these depend on the model system used. PKC ϵ appears to be somewhat consistently expressed and is essential for cardioprotection (Zatta et al, 2006) across various models, for instance, in rabbit and human myocardium (Liu et al, 1999; Sivaraman et al, 2009). While inhibition of PKC δ has been reported to reduce the infarct size and improve recovery in murine hearts (Inagaki et al, 2003).

Overall, evidence points that cardioprotection via pre- and post-conditioning is dependent on protein kinases even though the exact mechanisms are not well understood (Hausenloy et al, 2005). Interpretation of the signal transduction cascades and their downstream effectors involved in cardioprotection via pre- and post-conditioning would provide clear understanding and pharmacological tools to exert beneficial effects during ischaemia and ischaemia/reperfusion injury.

1.4 Transglutaminases.

Transglutaminases (TG) are a family of multifunctional enzymes that catalyse calcium dependent post-translational modifications of proteins. Clarke and colleagues provided the first data documenting a TG that was obtained from guinea pig liver (Clarke et al, 1957). The official name 'transglutaminase' was coined by Mycek and colleagues in 1959 (Mycek et al, 1959). Nine proteins have been identified in the TG family. Eight of them are enzymatically active (TG1-7 and Factor XIII A), however the ninth one (Band 4.2) is structurally related to the family but is not enzymatically active due to the fact that it lacks a catalytically active site (Grenard et al, 2001; Lorand and Graham, 2003). Transglutaminases mainly catalyse an acyl transfer reaction between γ -carboxamides of glutamines and ϵ -amino group of lysine residues. This reaction can form various products by incorporation of polyamines into proteins, deamidation of proteins as well as protein crosslinks (Lorand and Conrad, 1984; Nurminskaya and Belkin, 2012; Eckert et al, 2014). Hence TGs can affect protein structure, signal transduction, membrane stabilisation, etc. and these may slightly vary up on kinetics of the reaction and differences in substrates (Facchiano and Facchiano, 2009). The family of TGs and their physiological impact is summarised in Table 1.

Table 1. The family of transglutaminases and their physiological impact.

Name	Alternative names	Mol wt	Gene name	Location	Function	Pathology	References
Factor XIIIa	Plasma transglutaminase, fibrin stabilising factor, fibrinolygase, Laki-Lorand factor	83 kDa	<i>F13A1</i>	Platelets, placenta, synovial fluid, chondrocytes, astrocytes, macrophages, osteoclasts and osteoblasts, heart, eye, dendritic cells in the dermis	Blood clotting, wound healing, bone growth and synthesis	Impaired wound healing, severe bleeding tendency, spontaneous abortion during pregnancy, subcutaneous and intramuscular haematomas	Odi and Coussons, 2014; Eckert <i>et al</i> , 2014
TG1	Keratinocyte transglutaminase, particulate TG, type 1 TG, TGK	90 kDa	<i>TGM1</i>	Cytosol, membrane, squamous epithelia, keratinocytes	Cell envelope formation in the differentiation of keratinocytes, cornified envelope assembly in surface epithelia, barrier function in stratified squamous epithelia	Lamellar ichthyosis	Candi <i>et al</i> , 1998; Odi and Coussons, 2014; Eckert <i>et al</i> , 2005; Eckert <i>et al</i> , 2014
TG2	Tissue transglutaminase, type 2 TG, G_{oh} , cytosolic transglutaminase, transglutaminase type II, liver TG, erythrocyte TG, endothelial TG, TGC	78kDa	<i>TGM2</i>	Ubiquitous distribution in different tissues, membrane, cytosol, nucleus, extracellular	Cell differentiation, matrix stabilisation, adhesion protein, apoptosis, transmembrane signalling, GTPase activity, cell survival, endocytosis	Autoimmune diseases, neurodegenerative disorders, metabolic diseases, malignancies	Facchianoet <i>al</i> , 2006; Eckert <i>et al</i> , 2014; Nurminskaya and Belkin, 2012; Odi and Coussons, 2014
TG3	Epidermal transglutaminase, callus TG, hair follicle TG, bovine snout TG, type 3 TG, TGE	77 kDa	<i>TGM3</i>	Cytosol, hair follicle, brain, epidermis	Cell envelope formation during keratinocyte differentiation, terminal differentiation of keratinocytes and hair follicle, GTPase activity	Human epidermis diseases	Odi and Coussons, 2014, Eckert <i>et al</i> , 2014
TG4	Prostatic transglutaminase, androgen-regulated major secretory protein, vesiculase, dorsal prostate protein 1 (DP1), type 4 TG, TGP	77 kDa	<i>TGM4</i>	Prostate gland, prostatic fluids and seminal plasma	Reproductive function involving semen coagulation esp. in rodents, cell-matrix adhesion of prostate cancer cells	Prostate cancer progression	Odi and Coussons, 2014; Jiang <i>et al</i> , 2013; Eckert <i>et al</i> , 2014

TG5	Type 5 TG, TGX	81 kDa	<i>TGM5</i>	Ubiquitously expressed but predominant in female reproductive tissues, foetal tissues, cytosol, foreskin keratinocytes, skeletal muscular striatum, epithelial barrier lining	Keratinocyte differentiation and cornified cell envelope assembly, adhesion of stratum corneum to stratum granulosum, epidermal differentiation	Over-expressed or absent in different areas of the Darier's disease lesions, secondarily involved in hyperkeratotic phenotype in ichthyosis and in psoriasis	Odi and Coussons, 2014; Candiet <i>et al</i> , 2002; Toone, 2011; Eckert <i>et al</i> , 2014
TG6	Type 6 TG, TGY	78 kDa	<i>TGM6</i>	Cytosol, membrane, testis, lung, brain	Development of central nervous system, GTPase activity, motor function, late stage cell envelope formation in epidermis and hair follicle	Spinocerebellar ataxias, polyglutamine (polyQ) diseases	Odi and Coussons, 2014; Wang <i>et al</i> , 2010; Sailer and Houlden, 2012; Guan <i>et al</i> , 2013; Eckert <i>et al</i> , 2014
TG7	Type 7 TG, TGZ	81 kDa	<i>TGM7</i>	Ubiquitously expressed but predominant in testis and lungs	Not characterised	Not characterised	Odi and Coussons, 2014; Eckert <i>et al</i> , 2014
Band 4.2	Erythrocyte membrane protein band 4.2, B4.2, ATP-binding erythrocyte membrane protein band 4.2	72 kDa	<i>EPB42</i>	Erythrocyte membranes, spleen, bone marrow, foetal liver	Maintains erythrocyte shape and mechanical properties, membrane integrity, cell attachment, signal transduction	Spherocyticelliptocytosis	Odi and Coussons, 2014; Eckert <i>et al</i> , 2014; Kalfaet <i>et al</i> , 2014

1.5 Tissue transglutaminase.

Tissue transglutaminase or TG2 is an ubiquitously expressed member of the TG family (Lorand and Graham, 2003). It is a multifunctional enzyme possessing a transamidating activity, GTPase activity, protein disulphide isomerase activity and can also function as a scaffolding protein. It is due to its diverse nature and ubiquitous distribution that TG2 is implicated in regulation of many physiological processes such as cell adhesion and migration, growth and differentiation, survival and apoptosis as well as organisation of the extracellular matrix. Given that TG2 has a myriad of functions, it is involved in many pathologies such as neurodegenerative disorders, coeliac disease, few cancers, inflammation, ischaemia/reperfusion injury, etc. TG2 is composed of four domains: N terminal β -sandwich (aa 1-139), catalytic domain (aa 140-460), β -barrel-1 (aa 461-586) and β -barrel-2 (aa 587-687; see figure 1.6). The N-terminus contains a fibronectin binding site that mediates high affinity interaction between TG2 and fibronectin, which is involved in cell adhesion (Akimov et al, 2000). The catalytic domain contains the catalytic triad (cys277, His335, Asp358) which is essential for its transamidating activity (Griffin et al, 2002). The β -barrel-1 contains the GTP/GDP-binding domain. However, the catalytic domain also contains 15 residues spanning between amino acids 159-173 involved in the GTP/GDP-binding activity. Apart from these residues Trp332 and Arg579 have been recently identified as being important for GTP binding activity of TG2 (Murthy et al, 2002; Ruan et al 2008; Lai and Greenberg, 2013). The β -barrel-2 domain contains 20 residues spanning between amino acids 657-677 which are essential to recognise and activate phospholipase C δ 1 (PLC δ 1) and promotes α_{1B} adrenoceptor-mediated signal transduction (Das et al, 1993; Hwang et al, 1995; Baek et al, 2001; Kang et al, 2002).

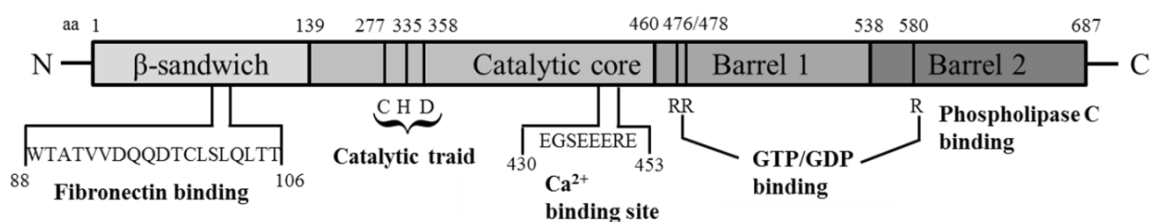


Fig 1.6: Schematic illustration of the structure of tissue transglutaminase (TG2). TG2 is composed of four domains: N terminal β -sandwich, catalytic core, β -barrel-1 and 2. Figure adapted from Lai and Greenberg, 2012.

(i) Functions of TG2.

(a) GTPase activity:

In 1990, a novel G-protein was identified, termed $G_{\alpha h}$ (Im and Graham, 1990). Further investigation revealed that $G_{\alpha h}$ had a 74 kDa α -subunit and a 50 kDa $\beta\gamma$ -subunit (Das et al, 1993; Baek et al, 1993) which made it atypical to heterotrimeric G-proteins that have a 45 kDa α -subunit and a 35-40 kDa $\beta\gamma$ -heterodimer (Milligan and Kostenis, 2006). In 1994, $G_{\alpha h}$ was found to be TG2 (Nakoka et al., 1994). It transmits signals from α_{1B} and α_{1D} adrenoceptors, thromboxane A₂, oxytocin and follicle-stimulating hormone receptors. All these receptors activate phospholipase C $\delta 1$ (PLC- $\delta 1$) which leads to increased inositol 1,4,5-trisphosphate (IP₃) levels and downstream signalling (Baek et al, 1993; Das et al, 1993; Baek et al, 1996; Feng et al, 1996; Im and Graham, 1990; Im et al, 1990; Lorand and Graham, 2003; Mhaouty-Kodja, 2004; Park et al, 1998; Vezza, 1999). $G_{\alpha h}$ or TG2 binds and hydrolyses GTP with similar affinity and catalytic rate as observed in the classical G-proteins (Begg et al, 2006; Begg et al, 2006a). Also, the G-protein cycle is similar to that of the heterotrimeric G-proteins (Lorand and Graham, 2003; Mhaouty-Kodja, 2004). Extensive characterisation of $G_{\alpha h}$ /TG2 revealed Val⁶⁶⁵-Lys⁶⁷² region in the β -barrel-2 domain as the effector contact region required to bind and activate PLC- $\delta 1$ (Hwang et al, 1995). This is similar to that of heterotrimeric G-protein as C-terminal of the α -subunit contains an effector contact region. For instance, Trp²⁶³, Leu²⁶⁸ and Arg²⁶⁹ of $G_{\alpha s}$ are the effector contact region required to bind and activate adenylyl cyclase (Itoh and Gilman, 1991; Berlot and Bourne, 1992).

Apart from these TG2 is also known to regulate other signalling pathways. It activates ERK1/2 in cardiomyocytes (Lee et al, 2003), increases adenylyl cyclase activity in neuroblastoma cells (Tucholski and Johnson, 2003) while inhibits adenylyl cyclase activity in fibroblasts and endothelial cells (Gentile et al, 1997). TG2 also promotes fibroblast migration (Stephens et al, 2004), however inhibits vascular smooth muscle migration by binding to the cytoplasmic tail of $\alpha 5$ integrin (Kang et al, 2004). In vascular smooth muscle, TG2 also activates large-conductance Ca²⁺-activated K⁺ channels (Lee et al, 1997). This implies that regulation of signalling pathways depends on the cell background and type (Eckert et al, 2014).

Regardless of the recent progress in understanding this function of TG2, its role in pathophysiology is still poorly understood. In NIH3T3 and HeLa cells, this activity of TG2 is pro-survival and cytoprotective independent of its transamidating function (Datta et al, 2007). In an ischaemic heart, TG2 GTPase activity is strikingly reduced suggesting it is an important factor in cardiac failure (Hwang et al, 1995). However, cardiac-specific overexpression of TG2 does not alter PLC- $\delta 1$ activity proposing that it functions as a TG rather than GTPase (Small et al, 1999) or through a non-PLC- $\delta 1$ pathway such as many outlined above.

(b) Kinase activity:

In 2004, it was reported that TG2 has intrinsic kinase activity (Mishra and Murphy, 2004). It was found that TG2 phosphorylates insulin-like growth factor binding protein-3 (IGFBP-3) and insulin-like growth factor binding protein-5 (IGFBP-5) in breast cancer cells. Furthermore, inhibition of TG2 using chemical inhibitors abolished phosphorylation of both these proteins (Mishra and Murphy, 2004). This phosphorylation was at multiple serine residues in the central domain of these proteins. Also, increasing intracellular calcium concentration inhibited TG2 kinase activity and enhanced its crosslinking activity in a concentration dependent manner (Mishra and Murphy, 2004).

Furthermore, it was found that the kinase activity of TG2 is responsible for phosphorylation of histones H1, H2A, H2B, H3 and H4 (Mishra et al, 2006). This phosphorylation occurred at functionally important serine residues such as Ser¹⁰, Ser²⁸ and amino-terminal region of histones, further illustrating the kinase activity of TG2 (Mishra et al, 2006). TG2 is also responsible for phosphorylating p53 oncoprotein (Mishra and Murphy, 2006). TG2 phosphorylates p53 at Ser¹⁵ and Ser²⁰ residues which reduces the ability of p53 to interact with mouse double minute 2 (Mdm2), thereby facilitating apoptosis (Dumaz et al, 2001; Ito et al, 2004; Mishra and Murphy, 2006).

TG2 phosphorylates retinoblastoma protein (Rb) at Ser⁷⁸⁰ residue which is important for binding of Rb to E2F family of transcription factors (Mishra et al, 2007). Moreover, Medina and colleagues reported that in FRTL-5 thyroid cells, cAMP-induced proliferation involved both phosphorylation of Rb and PKA activation (Medina et al, 2000). It is possible that phosphorylation of Rb by TG2 is important however was not investigated in these studies.

TG2 can be phosphorylated by PKA which attenuates its transamidating activity and enhances its kinase activity (Mishra et al, 2007). PKA activation by dibutyryl-cAMP enhanced TG2 and Rb phosphorylation in mouse embryonic fibroblasts which was reversed by PKA inhibitor H-89 (Mishra et al, 2007). Nurminskaya and colleagues reported that in differentiation of pre-osteoblasts in the periosteal bone, there is an inter-relationship between TG2 and PKA dependent signalling pathways. According to this study, TG2 can inhibit PKA-mediated signalling however the underlying mechanisms remain unexplored (Nurminskaya et al, 2003). It was recognised that TG2 has a Ser²¹⁶ residue which is phosphorylated by PKA and creates a binding pocket for 14-3-3 protein (Mishra and Murphy, 2006). 14-3-3 forms a complex with retinoblastoma associated protein RbAp48 (Imhof and Wolffe, 1999). Also, 14-3-3 protein interacts with various other proteins involved in apoptosis and signalling pathways (Mackintosh, 2004; Porter et al, 2006). Hence interaction of 14-3-3 with TG2 might be important in regulation of TG2 function as well as for crosstalk amongst signalling pathways.

Furthermore, phosphorylation of TG2 at Ser²¹⁶ residue by PKA causes TG2-mediated activation of NF- κ B, which induces down regulation of PTEN, resulting in activation of AKT in mouse embryonic fibroblasts, MCF-7 and T-47D breast cancer cells (Wang et al, 2012). Use of mutant TG2 lacking the Ser²¹⁶ residue and H-89 (PKA inhibitor) completely blocked activation of NF- κ B and down regulation of PTEN (Wang et al, 2012). Rodolfo and colleagues identified BH3 motif in TG2 which facilitates its interaction with Bax but not with Bcl-2 and Bcl-X_L (Rodolfo et al, 2004). Phosphorylation of Ser¹¹² in BH3 motif of BAD facilitates its interaction with Bcl-X_L as well as increases accessibility to Ser¹⁵⁵ which is phosphorylated by PKA in the BH3 motif (Macdonald et al, 2006). Phosphoproteomic studies have revealed that TG2 apart from Ser²¹⁶ has an additional serine residue Ser²¹² which is present in PKA consensus phosphorylation site (Wang et al, 2012). These potential sites can be phosphorylated by many kinases such as calmodulin-dependent protein kinase II, casein kinase II, MAPK, PKC, RSK and CDK5 (Rikova et al, 2007; Guo et al, 2008; Wang et al, 2012) and once phosphorylated may play a role in interaction of TG2 with Bcl-2 which attenuates its pro-apoptotic function and enhances its anti-apoptotic function (Wang et al, 2012).

TG2 has also been shown to play a role in activation of Rho A and MAPK (ERK1/2, JNK1/2 and p38 MAPK) pathways (Singh et al, 2003), CREB activation (Tucholski and Johnson, 2003) and PLC activation (Nakaoka et al, 1994). It remains unclear if TG2 kinase activity is necessary for activating these kinases.

(c) Protein disulphide isomerase activity:

In 2003, protein disulphide isomerase activity (PDI) of TG2 was reported (Hasegawa et al, 2003). PDI's are enzymes that catalyse formation of disulphide bonds within proteins to ensure correct protein folding. Once certain proteins are folded in the correct conformation, they can be activated, e.g. inactive RNase A was reported to be folded properly into an active form by TG2 (Hasegawa et al, 2003). It is observed that TG2 might modulate the respiratory chain by facilitating formation of di-sulphide bridges in the mitochondrial complex I (NADH-ubiquinone oxidoreductase), II (succinate-ubiquinone oxidoreductase), IV (cytochrome c oxidase) and V (ATP synthase) (Mastroberardino et al, 2006). It was also found that there is a reduction in ATP production in TG2 knockout mouse cardiomyocytes and skeletal muscles. This reduction could be due to lack of di-sulphide bridges formed by TG2 (Krasnikov et al, 2005). Adenine nucleotide translocator 1 (ANT1) is another target for TG2 PDI activity (Malorni et al, 2009). Oligomerisation of ANT1 is necessary for its activity, however TG2 knockout mice have increased thiol-dependent ANT1 oligomerisation which results in high ANT1 mediated ADP/ATP exchange activity in the cardiac myocyte mitochondria (Malorni et al, 2009). It was also found that interaction of Bax and ANT1, as well as their co-localisation is dependent on TG2. Overall, this suggests that TG2

PDI activity in conjunction with ANT1 might play a role during impairment of mitochondrial activity (Malorni et al, 2009; Sarang et al, 2009).

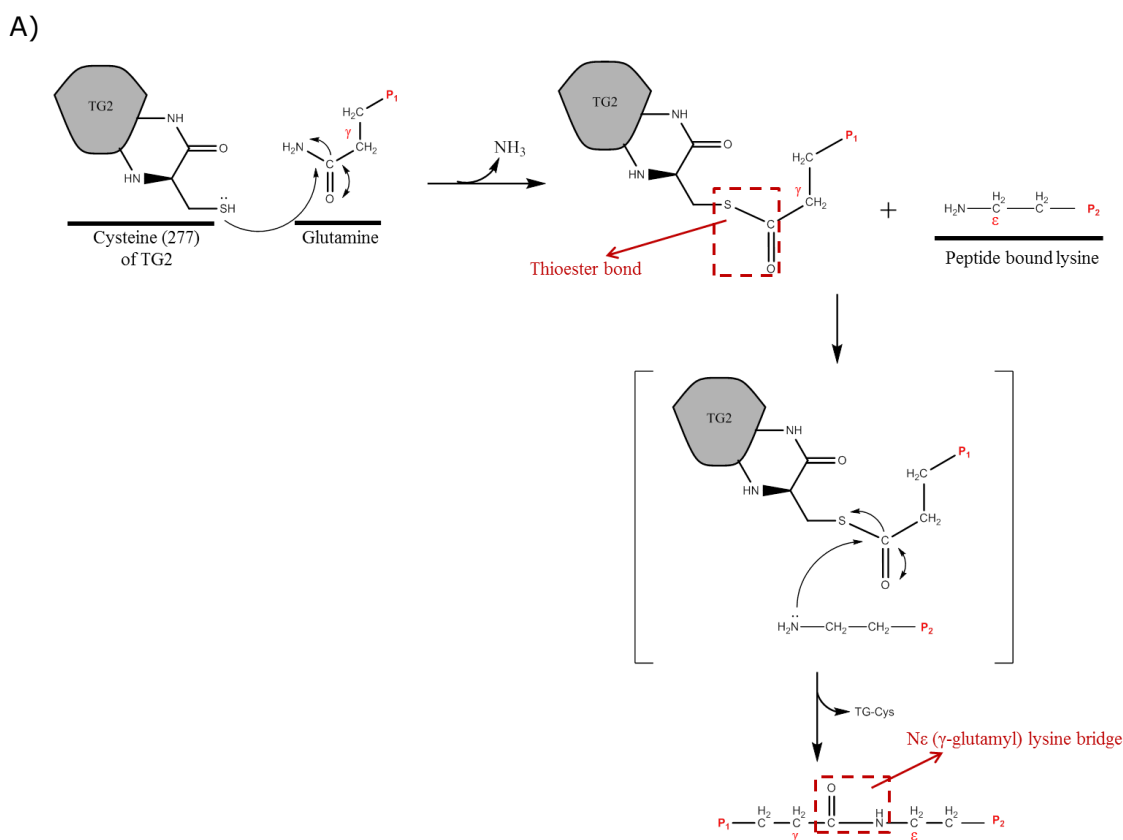
Overexpression of TG2 in other mitochondrial models resulted in increased cell death (Piacentini et al, 2002; Ruan et al, 2007). Piacentini and colleagues have shown that there was hyperpolarisation of the mitochondria and increased levels of reactive oxygen species (ROS) in TG2 overexpressing cells in response to staurosporine treatment (Piacentini et al, 2002). Cyclosporin A (mitochondrial transition pore inhibitor) was successful in protecting the cells from apoptosis, however, the mitochondria remained hyperpolarised due to overexpression of TG2 (Piacentini et al, 2002). In a related study using TG2 overexpressing striatal cells reported that thapsigargin treatment increased mitochondrial hyperpolarisation and ROS production. They also found that this treatment elevated cytochrome c release and caspase-3 activation which led to increased cell death (Ruan et al, 2007). These studies suggest that regulation of TG2 PDI activity is necessary for normal mitochondrial function. It should be noted that this activity of TG2 is independent of its transamidating activity (Krasnikov et al, 2005).

(d) Transamidating activity:

TGs require Ca^{2+} to catalyse transamidation reactions, however the Ca^{2+} binding sites have not been conclusively identified yet. Kiraly and colleagues have identified six putative Ca^{2+} binding sites on TG2, all of which are located in the catalytic domain (aa 149, 228, 236, 305, 395 and 432). Mutagenesis studies have shown that mutation of any one of the Ca^{2+} binding site results in complete loss of the transamidating function. This suggests that there is some level of co-operation between the Ca^{2+} binding domains to TG2 (Bergamini, 1998; Kiraly et al, 2011). Apart from this, a membrane lipid sphingosylphosphocholine (Lyso-Sm) has been shown to modulate TG2 transamidase activity by enhancing it at 10 μM Ca^{2+} concentrations. Lyso-Sm induces a conformational change in TG2 influencing its Ca^{2+} binding affinity while not affecting its substrate binding affinity (Lai et al, 1997). Another study has shown that the transient rise in Ca^{2+} levels because of tissue injury or other stimuli can reduce TG2's affinity for GTP thereby resulting in activation of its transamidating function (Begg et al, 2006a). This rise in intracellular levels of Ca^{2+} can be induced by a number of factors such as rapid ATP production (aerobic metabolism), reactive oxygen species (ROS), growth factors (e.g. Insulin-like growth factor binding protein-3, nerve growth factor) and chemokines (e.g. CXCL 10, CXCL 12) which can release Ca^{2+} from intracellular stores (De Bernardi et al, 1996; Seurin et al, 2013; Nelson and Gruol, 2004; Agle et al, 2010). To further support this argument, most of the potential substrates of TG2 are primarily cytoplasmic proteins (Facchiano and Facchiano, 2009). Stamnaes and colleagues have reported that two intra-molecular disulphide bonds (C370-C371 and C370-C270) appear to influence the transamidating activity of TG2 (Stamnaes et al, 2010). Post-translational modifications such as S-nitrosylation have

also been shown to attenuate TG2 transamidating function (Santhanam et al, 2010). These findings indicate that Ca^{2+} levels are not the only factor regulating the transamidating activity of TG2 but it seems that this activity is highly regulated by multiple factors (e.g. Ca^{2+}).

Transglutaminases are capable of catalysing various transamidation reactions. When an acyl transfer reaction takes place between γ -carboxamides of glutamines and primary amines, it leads to post-translational modification of proteins by amine incorporation. When an acyl transfer reaction takes place between γ -carboxamides of glutamines and ϵ -amino group of lysine residues, it leads to formation of an isopeptide bond and crosslinks the two proteins (see figure 1.7A). When the same reaction occurs between γ -carboxamides of glutamines and primary amines, it leads to formation of an amide bond (see figure 1.7B). When an acyl transfer reaction takes place between γ -carboxamides of glutamines and a water molecule, deamidation occurs (Lorand, 2003; see figure 1.7C). The mechanism of transamidation comprises of two steps. Firstly, the acyl acceptor (glutamine residues) binds to the active site cysteine 277 of TG2 forming a thioester bond (intermediary step) and releases an ammonia molecule. Secondly, the amine donors such as primary amines (free amines) or a peptide bound lysine, nucleophilically attacks the thioester bond releasing TG2 to its original active form (Folk, 1983). However, if the attacking group is water, then it leads to deamidation.



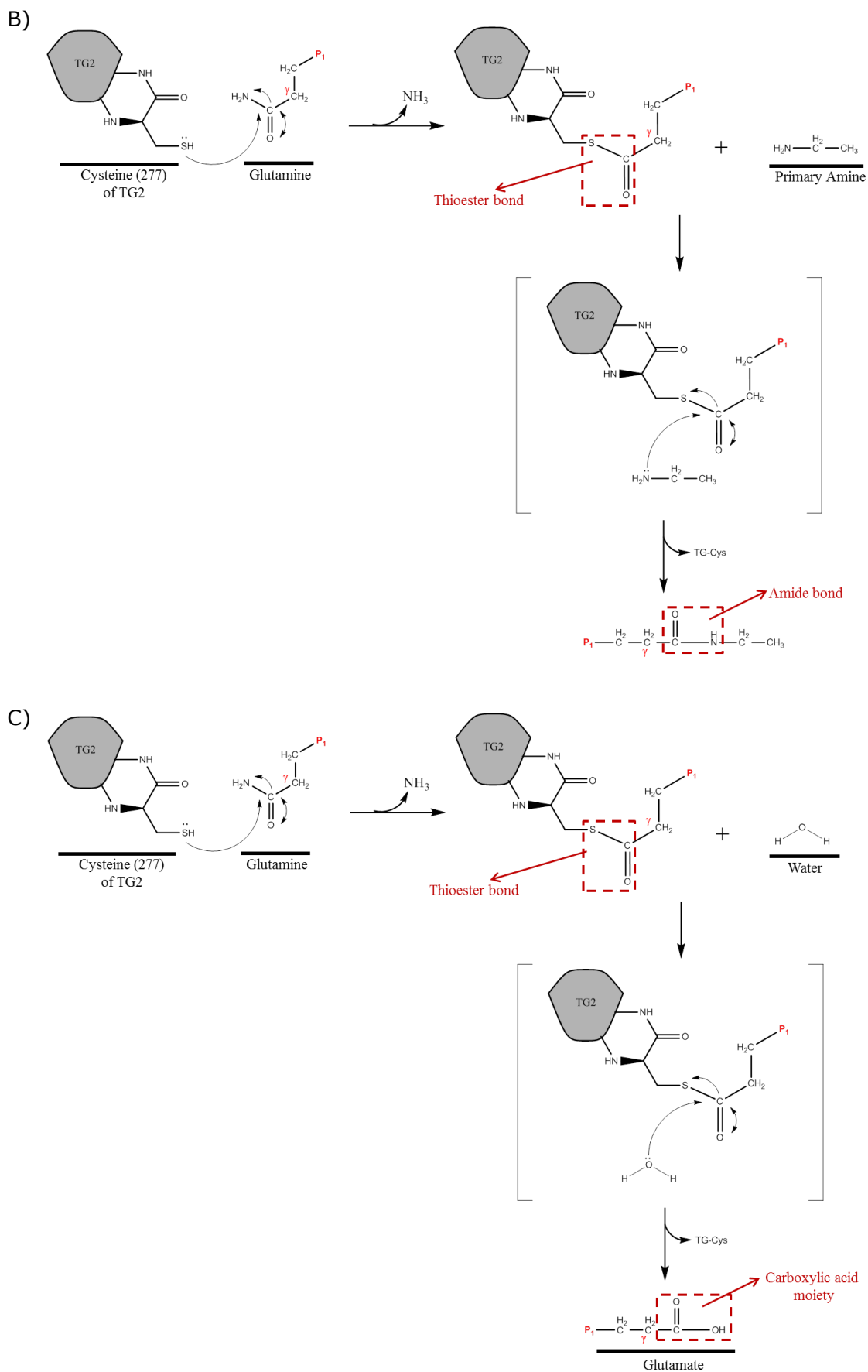


Fig 1.7: Transamidation reactions catalysed by TG2. TG2 is capable of catalysing various transamidation reactions, which can lead to (A) an isopeptide bond formation, (B) an amide bond formation and (C) deamidation.

(e) Protein Scaffolding function:

Apart from the enzymatic functions, protein scaffolding functions of TG2 have also been recognised (Park et al., 2010). Interaction of TG2 with fibronectin and β -integrins (β 1, β 3 and β 5) leads to stronger cell adhesion and stabilisation of the extracellular matrix (Akimov et al 2000, Akimov and Belkin, 2001). TG2 also affects adhesion-dependent signalling pathways such as constitutive activation of focal adhesion kinase (FAK) (Verma and Mehta, 2007) and its ablation causes a decrease in renal fibrosis as a result of lower collagen I synthesis and reduced activity of TGF β (Shweke et al, 2008). Another example of TG2 acting as a scaffolding function is in cell migration. In EGF-stimulated cancer cells, TG2 binds to actin and recruits proteins that aid in actin polymerisation (Antonyak et al, 2009). TG2 functions as a scaffold for a variety of non-enzymatic interacting partners and its role has been well documented. Few examples include interaction of TG2 with calmodulin and huntingtin (Zainelli et al, 2004), with calreticulin and integrin (Coppolino et al, 1997), with small ubiquitin-like modifiers (SUMO-1) and E3 SUMO protein ligase (PIASy; Luciani et al, 2009), with RhoA, PKA, AKAP13 (Lewis et al, 2005), and with syndecan, fibronectin and integrin (Telci et al, 2008). For an extensive review on scaffolding function of TG2, see Nurminskaya and Belkin, 2012; Eckert et al, 2014; Kanchan et al, 2015.

(ii) Role of TG2 in disease.

(a) Neurodegenerative diseases:

TG2 has been suggested to contribute to neurodegeneration by generating cytotoxic soluble and insoluble protein aggregates (Jeitner et al, 2009; Grosso and Mouradian, 2012). The activity and expression of TG2 is elevated during Alzheimer's disease (Kim et al, 1999), Parkinson's disease (Andringa et al, 2004) and Huntington's disease (Karpuj et al, 1999). Alzheimer's disease is characterised by the presence of extracellular senile plaques formed of aggregated amyloid β protein along with intracellular neurofibrillary tangles formed of phosphorylated tau protein (Przedborski et al, 2003; Siegel and Khosla, 2007). Amyloid β is a substrate for TG2, crosslinking of which resembles the polymers seen in Alzheimer's disease (Hartley et al, 2008; Martin et al, 2011). α -synuclein is a substrate for TG2 in the context of Parkinson's disease. Parkinson's disease is characterised by degradation of dopaminergic neurons within the substantia nigra along with formation of Lewy bodies (α -synuclein protein aggregates; Hoffner and Djian, 2005). Crosslinking of α -synuclein monomer leads to the aggregation of α -synuclein in Lewy bodies (Andringa et al, 2004).

Huntington's disease is characterised by the presence of insoluble huntingtin protein aggregates. It is an autosomal dominant disorder caused by expansion of CAG repeats which encodes for glutamine and this expansion leads to production of huntingtin protein with a poly glutamine N-terminus. Since glutamine is a substrate for TG2, it has been highly implicated in formation of insoluble huntingtin protein aggregates

(MacDonald et al, 1993; Hoffner and Djian, 2005). During Huntington's disease, it has been recorded that deletion of TG2 extends the life span in mouse models (Bailey and Johnson, 2005; Mastroberardino and Piacentini, 2010; Altuntas et al, 2014). These studies provide evidence of involvement of TG2 in neurodegenerative disorders and that it plays an important role in their progression.

(b) Coeliac disease:

It is well established that TG2 acts as a master regulator of coeliac disease. Coeliac disease is a systemic autoimmune disorder characterised by villous atrophy and crypt hyperplasia of the small intestine due to indigestion of dietary wheat, rye and barley derived gluten (Learner et al, 2015; Rauhavirta et al, 2016). The glutamine residues in gluten need to be deamidated to provoke an immune response. This is performed by TG2 (Schuppan and Hahn, 2002). Previous studies have demonstrated that patients suffering from coeliac disease have high levels of anti-TG2 antibody in their serum (Sollid and Scott, 1998), higher expression and activity of TG2 in the intestinal mucosa (Caputo et al, 2004) and localisation of TG2 in the extracellular matrix and small intestinal mucosa as compared to all layers of the small intestinal wall (Hansson et al, 2002; Caputo et al, 2004). Despite, having ample evidence of involvement of TG2, its role is still being unravelled and new therapeutic strategies are being developed for coeliac disease.

(c) Cancer:

Elevated levels of TG2 have been reported in malignant melanoma (Fok et al, 2006), glioblastoma (Yuan et al, 2007), breast carcinoma (Mehta et al, 2004), ovarian carcinoma (Hwang et al, 2008), pancreatic carcinoma (Verma et al, 2006) and lung carcinoma (Park et al, 2010). Cancer cells expressing high levels of TG2 show higher resistance to chemotherapeutic drugs (Mehta et al, 2006). TG2 has conflicting roles in cancer with respect to cell survival or apoptosis. For instance, enhancement in adhesion to fibronectin and promotion of cell migration in ovarian carcinoma which leads to survival of cancer cells has been observed (Satpathy et al, 2007). However, down regulation of TG2 in primary tumours causes metastasis (Verma and Mehta, 2007). On the other hand, transamidation activity causes apoptosis in some cancer cells (Milakovic et al, 2004). These studies illustrate that TG2 can either prevent or promote cancer metastasis which greatly depends on cancer cell type and stage.

(d) Inflammation and wound healing:

TG2 expression is up-regulated by tumour necrosis factor- α (TNF- α) (Kuncio et al, 1998), interleukin-1 (IL1) (Johnson et al, 2001), interleukin-6 (IL6) (Suto et al, 1993) and tumour growth factor- β 1 (TGF- β 1) (Quan et al, 2005). Recently, it has also been reported that TG2 expression is up-regulated via β ₂ adrenoceptors in macrophages and promotes differentiation of T-helper type 17 cells, thereby promoting inflammation (Yanagawa et al, 2014). Reduced kidney injury, renal fibrosis and

scarring was observed in TG2^{-/-} mice as compared to wild type mice (Verderio et al, 2004; Shweke et al, 2008). This effect was due to reduced activation of TGF- β and collagen I along with reduced inflammatory response. It was also recently observed that deletion of TG2 causes autoimmunity due to impairment of macrophage-mediated phagocytosis of apoptotic cells (Toth et al, 2009). TG2 can protect cells by enhancing attachment and motility in an inflammatory background as TG2-overexpressing fibroblasts show increased cell attachment and migration (Gross et al, 2003). As suggested by these studies, TG2 is an important player in cell death mechanisms and inflammatory responses.

(e) Ischaemia/reperfusion injury:

Elevated expression of TG2 in response to ischaemia has been reported in several studies (Tolentino et al, 2004; Filiano et al, 2010). Filiano and colleagues have reported neuroprotective effects of TG2 in both primary rat cortical neurons and SH-SY5Y human neuroblastoma cell line (Filiano et al, 2008; Filiano et al, 2010). This protection was observed due to interaction of TG2 with hypoxia inducible factor-1 β (HIF1 β) which results in negative regulation of HIF1 transcriptional activity and attenuation of the pro-apoptotic gene, Bnip3. Another study from the same group reported that astrocytes from TG2^{-/-} mice showed resistance to ischaemia/reperfusion injury and were able to increase survival of neurons (Colak et al, 2012). This conflict shows that TG2 differentially modulates ischaemic cell death in neurons and astrocytes. Szondy and colleagues in another study have shown that TG2 is cardioprotective against ischaemia/reperfusion injury (Szondy et al, 2006). This study suggests that TG2 acts at a mitochondrial level and maintains mitochondrial respiratory function by ATP synthesis. These studies collectively show that TG2 is involved in cellular mechanisms underlying ischaemia/reperfusion injury and that it might have a protective role depending on the cell background.

Overall, looking at these studies we can conclude that TG2 is able to contribute to both cell survival and cell death depending on cell background and disease pathology. Therefore, it is of great interest and importance to get a better understanding of function and role of TG2 in numerous pathological conditions as it represents a potential target.

(iii) Role of TG2 in cell death and cell survival.

TG2 is a complex enzyme, which is regulated by various factors. Hence, conflicting roles in the same pathological and/or physiological system have been reported. These opposing roles could be due to differences in the enzymatic as opposed to non-enzymatic functions (Fesus and Szondy, 2005; Iismaa et al, 2009; Kiraly et al, 2011), conformational structure (open verses closed) (Fesus and Szondy, 2005; Iismaa et al, 2009), genetic variations such as short or truncated form (TG2-S) in comparison with long form (TG2-L) (Tee et al, 2010) or single-nucleotide polymorphism (Kiraly et al,

2011) as well as the genetic background of cell systems or animal models used during the study (Iismaa et al, 2009; Tatsukawa and Kojima, 2010).

Currently, the role of TG2 in cell survival and cell death is widely acknowledged and numerous studies are being focused to identify what triggers TG2 to act in a pro- or anti-apoptotic manner (Nurminskaya and Belkin, 2012; Tatsukawa et al, 2016). In TG2 overexpressing mice neurons and N2a neuronal cell line, TG2 exerts a protective effect against hypoxia-induced cell death (Filiano et al, 2010). This protective effect is observed due to overexpression of TG2 and its localisation in the nucleus (Filiano et al, 2010). On the other hand, TG2 knockout or inhibition of TG2 in transgenic mice attenuated the progression of neurodegenerative disorders (Bailey and Johnson, 2005; Mastroberardino et al, 2002; Karpuj et al, 2002; Andringa et al, 2004; Dudek and Johnson, 1994). TG2 enhances cancer development by increasing EGFR expression in glioblastomas (Zhang et al, 2013), attenuation of apoptosis in thapsigargin-treated HEK293 cells (Milakovic et al, 2004) and retinoic acid treated NIH3T3 and embryonic lung fibroblast cells (Boehm et al, 2002), increasing resistance to chemotherapeutic drug in breast cancer metastasis (Mehta et al, 2010; Mangala et al, 2007) and stabilising adhesive interactions in melanoma cells for metastasis (Kong and Korthuis, 1997). However, TG2 can also suppress cancer by excessive stabilisation and accumulation of ECM crosslinks (Johnson et al, 1994; Shrestha et al, 2015) and can also facilitate apoptosis in retinoic acid treated U937 cells and phosphorylation of retinoblastoma (Rb) protein in MCF-7 cells (Tatsukawa et al, 2011; Mishra et al, 2007; Oliverio et al, 1997).

TG2^{-/-} mice show impaired glucose-stimulated insulin secretion and glucose intolerance compared to control mice (Bungay et al, 1986; Gomis et al, 1983; Sener et al, 1985; Bernassola et al, 2002; Porzio et al, 2007). However, it should be noted that inhibition of TG2 did not prevent insulin secretion induced by cAMP or phorbol ester and could only prevent insulin-secretion induced by calcium (Lindsay et al, 1990; Iismaa et al, 2013). TG2 can enhance angiogenesis through VEGF signalling in the endothelium (Dardik and Inbal, 2006; Haroon et al, 1999). It can also facilitate migration and tubule formation of the human umbilical vein endothelial cells (HUVEC) (Wang et al, 2011). It is observed that inhibition of TG2 causes a reduction in fibronectin deposition and matrix-bound VEGFA and therefore promotes angiogenesis in a VEGF-dependent manner (Wang et al, 2011). TG2 is also known to enhance angiogenesis by co-localisation and binding with endostatin- a C-terminal domain of collagen XVIII (Faye et al, 2009; Faye et al, 2010), organisation of the cytoskeleton, as well as endothelial sprouting and migration of both endothelial and vascular mesenchymal cells (Myrsky et al, 2008).

TG2 is also reported to promote spreading and adhesion of human endothelial cells ECV304 via its adhesion/scaffolding activity with fibronectin and/or integrin (Gaudry et al, 1999; Jones, et al, 1997). However, TG2 is also known to inhibit angiogenesis by

excessive stabilisation and accumulation of ECM crosslinks resulting in a reduction of organised vasculature (Jones et al, 2006) and can also cause retinoic acid-mediated apoptosis in vascular smooth muscle cells (Ou et al, 2000). TG2 can protect hepatocytes against carbon tetrachloride and FAS-induced liver injury through dimerization leading to activation of Sp1 (Han and Park, 2000; Nardacci et al, 2003; Sarang et al, 2005). However, it can also promote liver injury and fibrosis in alcoholic steatohepatitis and non-alcoholic steatohepatitis free fatty acid-treated human 293T cells and NZB/W F1 mice (Kuo et al, 2012; D'Argenio et al, 2010; Kojima et al, 2010; Hsu et al, 2008). Thus, it is clear that the complex balance between pro- and anti-apoptotic functions of TG2 need further investigation and that they are dependent on numerous factors (Tatsukawa et al, 2016).

In NIH3T3 fibroblast cells, exposure to LY 294002 (PI-3K inhibitor) causes a substantial decrease in the ability of TG2 to bind to GTP. This indicates that PI-3K regulates the switch between GTPase and transamidase activity of TG2, along with changes in Ca^{2+} concentration. Also the Ras-ERK1/2 pathway influences the switch between pro-apoptotic transamidating function and pro-survival GTPase function (Antonyak et al, 2003). There is evidence that is contradictory as to whether TG2 is pro or anti-apoptotic. The mechanism by which TG2 modulates apoptosis greatly depends on the cell type and stimulus involved (Gundemir et al, 2012). It has been shown that there is a role for TG2 transamidase activity in tissue injury/repair following ischaemic/reperfusion injury (Gundemir et al, 2013) and during ischaemia or hypoxia TG2 binds to hypoxia inducible factor 1 β (HIF1 β) and suppresses HIF activity (Gundemir et al, 2013).

(iv) TG2 and cardioprotection.

TG2 has been shown to be cardioprotective against ischaemia/reperfusion injury in mice (Szondy et al, 2006). Wild type and TG2 knockout mouse hearts were subjected to ischaemia/reperfusion injury. It was observed that TG2^{-/-} hearts had significantly increased infarct size and ventricular fibrillation when compared to TG2^{+/+} hearts under ischaemia/reperfusion injury. It should be noted that infarct size and ventricular fibrillation of both TG2^{+/+} and TG2^{-/-} ischaemia/reperfused hearts were significantly increased as compared to control TG2^{+/+} and TG2^{-/-} normoxic hearts (Szondy et al, 2006). It was found that TG2 is necessary for maintenance of intact mitochondrial respiration and knockout of TG2 leads to severe failure in ATP production. This failure in ATP production was hypothesised to be a result of reduced post-translational modifications of mitochondrial regulatory proteins along with abolished action of TG2 on mitochondrial substrate proteins (Szondy et al, 2006). However, further investigation is warranted to identify these mitochondrial substrate proteins and elucidate which activity of TG2 (kinase, transamidase, etc.) is vital for ATP production.

Recently, it has been shown that TG2 can be activated by PKA and PKC (Almami *et al*, 2014). Activation of these pathways by forskolin and phorbol ester, respectively, contributed to cytoprotection of H9c2 cardiomyoblasts against hydrogen peroxide-induced cell death. Inhibition of TG2 using chemical inhibitors attenuated the protection offered by forskolin and phorbol ester, suggesting TG2 to have an important role in facilitating cytoprotection (Almami *et al*, 2014).

These studies suggest a role for TG2 in mediating cellular response to ischaemia/reperfusion injury and it could potentially be a pharmacological target for treatment for ischaemia-induced pathologies. Since GPCRs are capable of initiating pathways which lead to activation of protein kinases such as PKA and PKC, it is possible that GPCRs can modulate TG2 activity. However, at present very little is known about regulation of TG2 by GPCRs and its role in cardioprotection.

1.6 The G-protein Coupled Receptor (GPCR) family.

G-protein coupled receptors (GPCRs) are the largest (>1200 GPCRs identified in the human genome) and most studied family of membrane proteins (Insel *et al*, 2012). They are widely distributed across various cell and tissue types and are responsible for mediating physiological responses by interacting with a wide variety of stimuli such as peptides, non-peptides, hormones, light, catecholamines, etc. (Katritch *et al*, 2013; Kingwell, 2016). The prime reason for studying these receptors is due to the fact that currently about 40% of therapeutic drugs on the market target one or more GPCRs (Cooke *et al*, 2015; Heifetz *et al*, 2016).

(i) Structure of GPCRs:

GPCRs are characterised by seven α -helical transmembrane spanning domains separated by alternating intra- and extra-cellular loops, an intracellular carboxyl terminal and an extracellular amino terminal (Rosenbaum *et al*, 2009). GPCRs also undergo post-translational modifications such as glycosylation of the amino terminus or extracellular loops, which is often necessary for their localisation; palmitoylation of cysteine residues within the intracellular loops and/or carboxyl terminal tail is required to strengthen membrane association; reversible phosphorylation of the intracellular loops and/or carboxyl terminal tail is important for G-protein anchorage as well as desensitisation and internalisation of the receptor (see figure 1.8; Goddard and Watts 2012). Rhodopsin, the light sensitive receptor was the first to have its crystal structure reported which has been extensively used to determine the structure and function of other GPCRs (Palczewski, 2006).

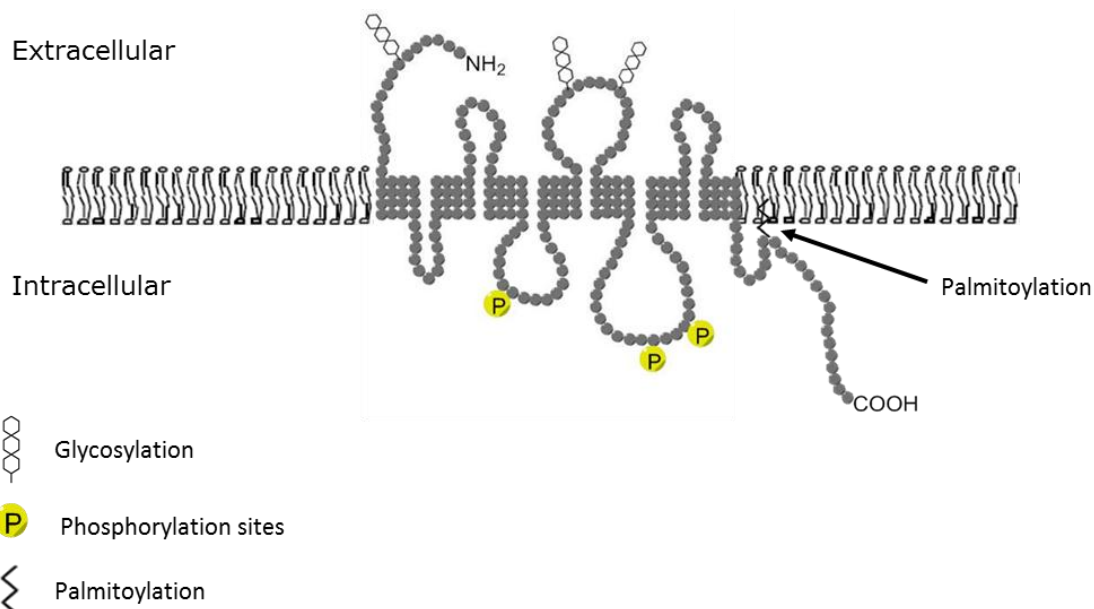


Fig 1.8: Schematic representation of the basic structure of class A GPCR. Class A GPCRs interact with ligands and initiate a cascade of events ultimately leading to an intracellular response.

Rhodopsin-like/Class A are the largest sub-group of GPCRs that includes receptors for a vast variety of neurotransmitters, peptides, hormones and other small molecules such as pheromones, taste, vision and olfactory senses (Alexander et al, 2015). Ligands bind to the receptor and cause a conformational change which leads to receptor activation and activation of heterotrimeric G-proteins (Hillenbrand et al, 2015; for an overview refer to figure 1.9). In the inactive state, there is strong association between GDP- bound $G\alpha$ -subunit and the $\beta\gamma$ -dimer. When a ligand binds to the receptor, it acts as a guanine nucleotide exchange factor (GEF) catalysing the exchange of GDP for GTP. This exchange reduces the affinity of $G\alpha$ -subunit for the $\beta\gamma$ -dimer, which results in their dissociation. Once dissociated the $G\alpha$ -bound GTP and $\beta\gamma$ -subunits can act on their downstream effectors and generate a response. Termination of this signal occurs via the intrinsic GTPase activity of the $G\alpha$ -subunit that cleaves GTP to GDP. This completes the cycle by re-associating the $G\alpha$ -subunit and the $\beta\gamma$ -dimer hence impeding interaction with their downstream effectors (Cabrera-Vera et al, 2003; Sunahara and Insel, 2016). Two of the GPCRs discussed in this thesis (adenosine A₁ receptors and β_2 adrenoceptors) belong to the class A sub-group of GPCRs.

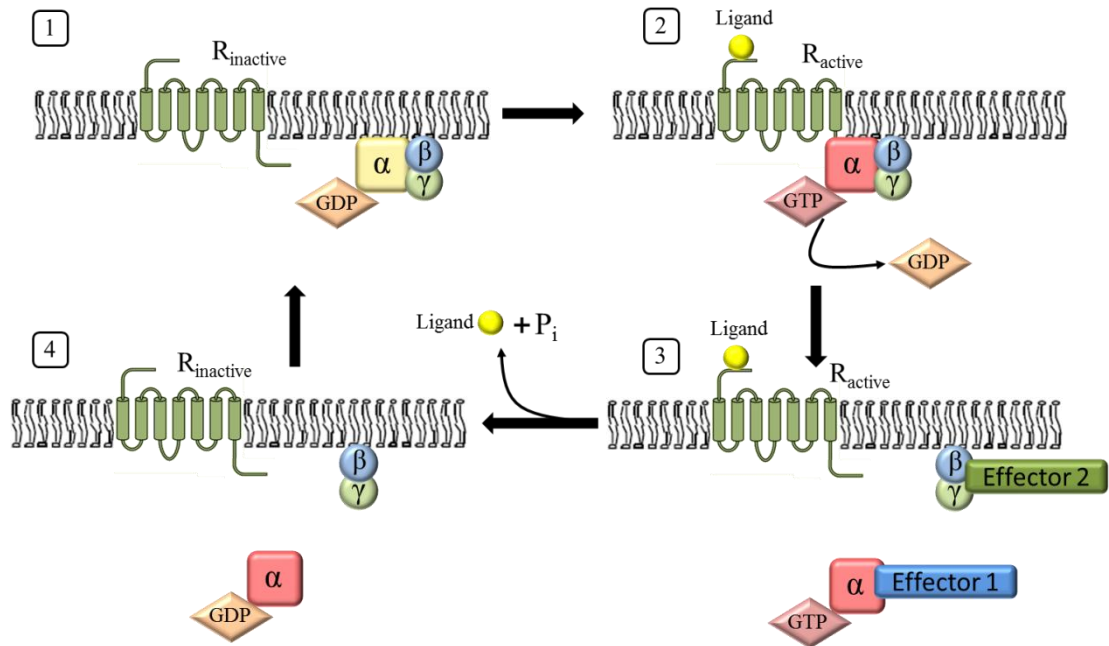


Fig 1.9: Conformational changes during GPCR activation. (1) In the resting state, the heterotrimeric G-protein is bound to GDP. (2) Upon ligand binding, a conformational change causes receptor to become active which exposes a catalytic component which causes exchange of GDP to GTP. (3) The active G_α-GTP subunit dissociates from membrane bound G_{βγ} subunit and both these subunits exert a downstream effect. (4) Termination of the signal by hydrolysis of GTP to GDP by the intrinsic GTPase activity of G_α subunit, which causes the receptor and G-protein to return to its inactive/resting state.

G-proteins are further classified depending upon their G_α-subunit (see figure 1.10). They are broadly categorised into four subtypes: G_{α_s}, G_{α_{i/o}}, G_{α_{q/11}}, G_{α_{12/13}}. G_{α_s} proteins have a stimulatory effect on the enzyme adenylyl cyclase while the G_{α_{i/o}} proteins have an inhibitory effect on it. Adenylyl cyclase produces the second messenger cAMP and activates PKA-mediated signalling. G_{α_s} proteins are selectively activated by cholera toxin while G_{α_{i/o}} proteins are inhibited by pertussis toxin. G_{α_{12/13}} act on the guanine exchange factors (GEF) of the Rho family of GTPases. The G_{α_{q/11}} proteins activate phospholipase C-β (PLCβ) which cleaves phosphatidylinositol bisphosphate (PIP₂) into diacylglycerol (DAG) and inositol triphosphate (IP₃). DAG further activates protein kinase C (PKC) and IP₃ modulates intracellular calcium concentration. The G_{α_{q/11}} proteins are insensitive to cholera and pertussis toxin therefore distinguishing them from the other G-proteins (Neves et al, 2002; Wettschureck and Offermanns, 2005; Syrovatkina et al, 2016).

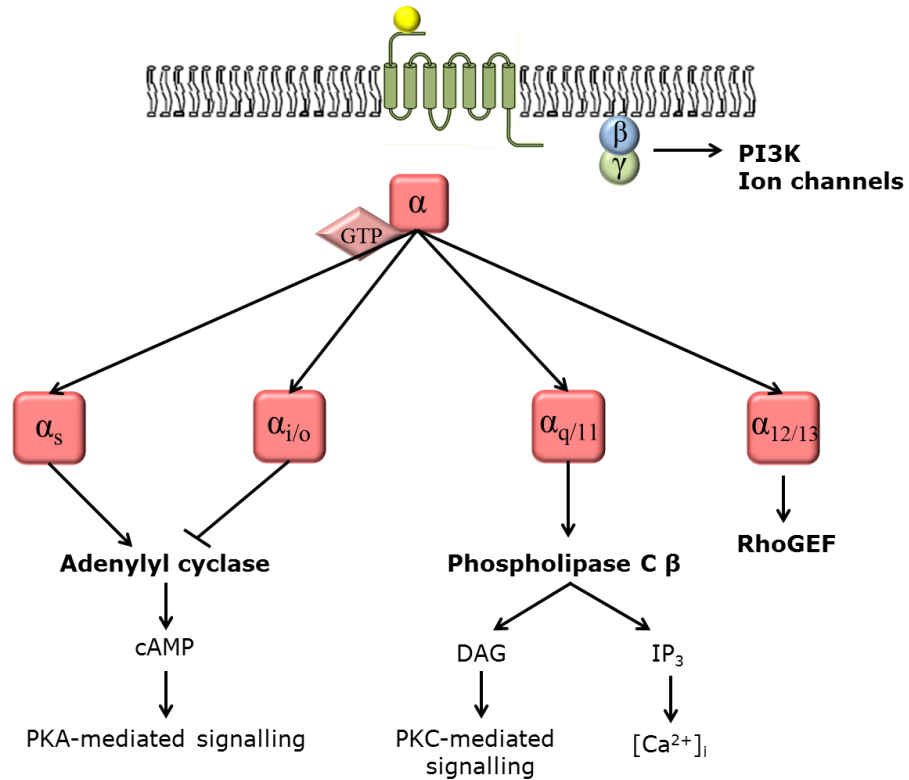


Fig 1.10: Signalling pathways mediated by main classes of G_α proteins. G_{α_s}, G_{α_{i/o}} proteins have stimulatory and inhibitory effects on adenylyl cyclase and its downstream effectors respectively. G_{α_{q/11}} protein activates phospholipase C thereby activating protein kinase C and calcium signalling while G_{α_{12/13}} proteins activate guanine nucleotide exchange factors of the Rho family.

Many of these GPCRs are expressed in the heart where they contribute to cardioprotection, including the adenosine receptors and the beta-adrenoceptors. Hence, studying their signalling mechanisms is of utmost importance in order to identify potential pharmacological targets, which could protect against myocardial injury.

1.7 Adenosine receptors.

Adenosine is a naturally occurring purine molecule which is formed by degradation of adenine nucleotides (ATP, ADP and AMP) both intra- and extracellularly. Adenosine formation is increased in response to various stimuli such as ischaemic/reperfusion injury, necrotic cell death, inflammation (Schulte and Fredholm, 2003; Fredholm, 2014) and exerts several effects such as vasodilation, negative inotropic, chronotropic and dromotropic effects (Sheth et al, 2014). Adenosine exerts these effects via the four cloned and characterised adenosine receptors (A₁, A_{2A}, A_{2B} and A₃) belonging to the GPCR superfamily. Among these the A₁ and A₃ couple to G_{i/o} proteins which are sensitive to pertussis toxin and inhibit cAMP signalling while A_{2A} and A_{2B} couple to G_s proteins and activate cAMP signalling (Fredholm et al, 2011; Headrick et al, 2013). Furthermore, A₁ and A₃ adenosine receptors also activate phospholipase C (PLC) signalling via βγ subunits released from G_i-proteins (Smrcka and Sternweis,

1993; Rebecchi and Pantyala, 2000; Schulte and Fredholm, 2003). Adenosine is known to balance cellular energy supply and demand and has several roles in maintaining normal physiological regulation including cardiac impulse generation and conduction, contractility and adrenergic responsiveness (Headrick et al, 2011; Headrick et al, 2013; Fredholm, 2014). Its physiological range is about 30-200 nM, however, during ischaemia or ischaemia/reperfusion injury, extracellular levels of adenosine can increase up to 10 μ M, a concentration which then exerts its cardioprotective effects against ischaemia or ischaemia/reperfusion injury (Ballarin et al, 1991; Fryer et al, 2002; Schulte and Fredholm, 2003; Fredholm, 2014).

All the four adenosine receptor subtypes are expressed in the heart. The majority of the A₁ adenosine receptor population is distributed in the atrial myocytes, ventricular myocytes, AV and SA nodes (Burns, 1990; Germack and Dickenson, 2004; Fredholm et al, 2011) while the A₃ adenosine receptor population is found in coronary vascular smooth muscle cells and ventricular myocytes (Burns, 1990; Auchamp and Bolli, 1999; Germack and Dickenson, 2004; Fredholm et al, 2011). The A_{2A} adenosine receptor population can be found in the coronary endothelium and coronary vascular smooth muscle cells of guinea pigs and mice (Burns, 1990; Auchamp and Bolli, 1999; Hein et al, 2001; Fredholm et al, 2011) as well as ventricular myocytes while the A_{2B} adenosine receptor population is distributed in the coronary endothelium and coronary vascular smooth muscle cells of rats (Burns, 1990; Feoktistov and Biaggioni, 1990; Germack and Dickenson, 2004; Fredholm et al, 2011). All four adenosine receptors exert cardiovascular effects. which are summarised in table 2 and play a role in cardioprotection (Ralevic and Burnstock, 1998; Salvatore et al, 2000; Fredholm et al, 2011; Headrick et al, 2013). However, the major focus of this thesis will be on the A₁ adenosine receptor and its role in cardioprotection.

Table 2. Adenosine receptor subtype and their effects on cardiovascular tissue.

Adenosine receptor subtype	Tissue distribution	G-protein subunits	Signalling pathways modulated	Physiological effects on cardiovascular tissue	References
A ₁	Atrial and ventricular myocytes, AV and SA nodes, cortex, cerebellum, hippocampus, spinal cord, eye, adrenal gland, skeletal muscle, adipose tissue, bronchi, oesophagus, kidney, liver, colon, testis, pancreas.	G _{o/i1/2/3}	<p>↓cAMP</p> <p>↑IP₃/DAG (PLC)</p> <p>↓ Q, P, N-type Ca²⁺ channels</p> <p>↑K⁺ channels</p> <p>↑choline /DAG (PLD)</p> <p>↑ Arachidonic acid (PLA₂)</p>	Bradycardia (negative chronotropy), A-V nodal conduction slowing (negative dromotropy), reduction of atrial contractility (negative inotropy), inhibition of cardiac pacemaker cells, anti-β-adrenergic effect, ischaemic pre-conditioning and post-conditioning (tolerance to hypoxia), glycolysis (depending on metabolism of ATP can increase or decrease).	Belardinelli and Isenberg, 1983; Munshi et al, 1991; Scholz and Miller, 1991; Freund et al, 1994; Jockers et al, 1994; Gerwins and Fredholm, 1995; Shryock and Belardinelli, 1997; Dickenson and Hill, 1998; Ralevic and Burnstock, 1998; Freissmuth et al, 1999; Salvatore et al, 2000; Fredholm et al, 2001; Straiker et al, 2002; Ciruela et al, 2010; Headrick et al, 2011; Fredholm et al, 2011; Headrick et al, 2013.
A _{2A}	Coronary endothelium, coronary vascular smooth muscle cells, ventricular myocytes, thymus, leukocytes, platelets, blood vessels, olfactory bulb, GABAergic neurons, peripheral nerves, eye, lung.	<p>G_s</p> <p>G_{olf}</p> <p>G_{15/16}</p>	<p>↑cAMP</p> <p>↑cAMP</p> <p>↑IP₃,</p> <p>↓ Ca²⁺ channels</p>	Vasodilation (hypotension), inhibition of platelet aggregation to vascular endothelium, inhibition of adherence of activated neutrophils to vascular endothelium, inhibition of superoxide release.	Offermanns and Simon, 1995; Olah, 1997; Shryock and Belardinelli, 1997; Ralevic and Burnstock, 1998; Kull et al, 2000; Salvatore et al, 2000; Corvol et al, 2001; Fredholm et al, 2001; Li et al, 2009; Ciruela et al, 2010; Headrick et al, 2011; Fredholm et al, 2011; Hasko and Pacher, 2012; Headrick et al, 2013.

A _{2B}	Coronary endothelium, coronary vascular smooth muscle cells, blood vessels, eye, adrenal gland, brain, pituitary gland, lung, mast cells, adipose tissue, cecum, colon, bladder, ovaries, kidney, liver.	G _s G _{q/11}	↑cAMP ↑Ca ²⁺ channels ↑IP ₃ /DAG (PLC)	Vasodilation (hypotension), inhibition of platelet aggregation to vascular endothelium, inhibition of adherence of activated neutrophils to vascular endothelium, inhibition of superoxide release.	Pierce et al, 1992; Shryock and Belardinelli, 1997; Ralevic and Burnstock, 1998; Linden et al, 1999; Gao et al, 1999; Salvatore et al, 2000; Fredholm et al, 2001; Ciruela et al, 2010; Headrick et al, 2011; Fredholm et al, 2011; Headrick et al, 2013.
A ₃	Coronary vascular smooth muscle cells, ventricular myocytes, cerebellum, hippocampus, microglia cells, lung, mast cells, spleen, testis, pineal gland, thyroid, adrenal gland, liver, kidney, intestine.	G _{q/11} G _{i2/3/o}	↑IP ₃ /DAG (PLC) ↓cAMP ↑IP ₃ /DAG (PLC) ↑K ⁺ -ATP channels ↑choline /DAG (PLD) ↑Cl ⁻ channels	Ischaemic pre-conditioning (tolerance to hypoxia), increase in mast cell activation, inhibition of inflammatory pain.	Abbracchio et al, 1995; Palmer et al, 1995; Shryock and Belardinelli, 1997; Parsons et al, 2000; Ralevic and Burnstock, 1998; Tracey et al, 1998; Carre et al, 2000; Mitchell et al, 1999; Salvatore et al, 2000; Fredholm et al, 2001; Ciruela et al, 2010; Headrick et al, 2011; Fredholm et al, 2011; Headrick et al, 2013.

(i) Role of the A₁ adenosine receptor in cardioprotection:

The pilot study undertaken by Liu et al, 1991 reported that ischaemic pre-conditioning reduced, infarct size in rabbits and that this protection was lost following infusion of non-selective adenosine receptor antagonists (Liu et al, 1991). A subsequent study showed that selective antagonism of the A₁ adenosine receptor completely abolished the protection, indicating that the A₁ adenosine receptor appears to have a central role in offering protection against ischaemia/reperfusion injury (Thornton et al, 1992). Thornton and colleagues also showed that infusion of a selective A₁ adenosine receptor agonist significantly reduced the infarct size, providing further evidence for the role of A₁ adenosine receptor in protection (Thornton et al, 1992). Pharmacological post-conditioning using adenosine was effective in reducing infarct size in canines which was abolished in the presence of a selective A₁ adenosine receptor antagonist indicating a role for the A₁ adenosine receptor (Velasco et al, 1991). However, similar post-conditioning had no effect in isolated rabbit hearts (Xu et al, 2001). Hochhauser and colleagues have shown that in isolated hearts from rats (both normotensive and hypertensive), activation of the A₁ adenosine receptor triggers early- and late-phases of pre-conditioning which results in protection (Hochhauser et al, 2007). Another study undertaken in canines found that pre-conditioning with adenosine not only reduces the infarct size but also preserves myocardial function. However, this treatment also had side effects such as increase in energy requirement and oxygen wasting (Phillips and Ko, 2007). There have been many subsequent studies evaluating the role of adenosine in cardioprotection (Kersten et al, 1997; Mangoni and Barrere-lemire, 2004; Peart and Headrick, 2007; Bonney et al, 2014; Yeung and Kolathuru, 2015; Contractor et al, 2016; Randhawa and Jaggi, 2016).

Given that all the four adenosine receptors play a role in cardioprotection, there is a lot of synergistic effects amongst them. For instance, Cohen and Downey have shown that protection delivered by adenosine during ischaemia or ischaemia/reperfusion injury triggers activation of the A₁ and A₃ adenosine receptors which signal via G_i and activate PKC. PKC further activates the A_{2B} adenosine receptor, which then offers protection by targeting effector proteins such as mitochondrial permeability transition pore (mPTP) (Cohen and Downey, 2008). Another study reported that in H9c2 cells adenosine-mediated protection was due to co-operation between A₁, A_{2A} and A_{2B} receptors (Urmaliya *et al*, 2009). Boucher and colleagues reported that pre-conditioning of the A_{2A} adenosine receptor resulted in reduction of the infarct size (Boucher et al, 2004). The A_{2B} adenosine receptor exhibits protection via pharmacological pre- and/or post-conditioning in rabbit hearts (Kuno et al, 2007; Philipp et al, 2006). However, no protection was observed in the A₁ adenosine receptor knock-out mice (Xi et al, 2008) suggesting that the mechanism of protection exhibited by the adenosine receptors greatly depends on the model system used.

There appears to be a role for PKB in adenosine-mediated cardioprotection. Qin and colleagues demonstrated that protection in isolated rabbit hearts via pre-conditioning with adenosine is independent of PI-3K (Qin et al, 2003). However, another similar study reported that protection of isolated rabbit hearts by adenosine is through phosphorylation of PKB during reperfusion (Solenkova et al, 2006). Furthermore, Germack and colleagues have shown that in neonatal rat hearts, PKB phosphorylation is involved in adenosine mediated signalling but not in adenosine-mediated cardioprotection (Germack et al, 2004).

From these examples, it is clear that there is a role for adenosine receptors in cardioprotection and that understanding the underlying signal transduction mechanism is of the utmost importance as it could potentially modulate proteins which exert these cardioprotective effects. A₁ adenosine receptor-mediated signalling is very well documented. Although the A₁ adenosine receptor stimulation is traditionally associated with inhibition of adenylyl cyclase, it also can trigger the activation of additional signalling cascades involving PKB, PKC, ERK1/2 and p38 MAPK (Dickenson et al, 1998; Germack and Dickenson, 2000; Robinson and Dickenson, 2001; Germack and Dickenson, 2004, Germack et al, 2005; Yang et al, 2009). Since PKC and ERK1/2 are also associated with modulation of transglutaminase activity (Mishra et al, 2007; Bollag et al, 2005), it is conceivable that the A₁ adenosine receptor can modulate transglutaminase activity as well. This will form one of the major areas of investigation undertaken by this thesis.

1.8 Adrenoceptors.

The catecholamines, adrenaline and noradrenaline play dual roles as neurotransmitters as well as hormones. They are synthesised from tyrosine by tyrosine hydroxylase to produce dihydroxyphenylalanine (L-DOPA) in the postganglionic sympathetic nerve ending and chromaffin cells of the adrenal gland (Guimaraes and Moura, 2001). The signal provided by these hormones is transduced to a cellular response by a family of GPCRs called the adrenoceptors. There are nine adrenoceptor subtypes identified, based upon both genetic and functional studies. The family is further split into two divisions, α and β , comprising of six alpha (α_{1A} , α_{1B} , α_{1D} , α_{2A} , α_{2B} and α_{2C}) and three beta (β_1 , β_2 and β_3) adrenoceptors (Brodde et al, 2006; Guimaraes and Moura, 2001; McGrath, 2015). The existence of a fourth atypical beta adrenoceptor (β_4 adrenoceptor) was proposed by various studies and it was suggested to mediate glucose uptake in muscle cells and chronotropic and ionotropic functions in rat and human cardiac cells (Roberts et al, 1993; Roberts et al, 1995; Kaumann and Molenaar, 1997 Sarsero et al, 1999). Few studies demonstrated that in rat aorta the β_4 adrenoceptor mediated lusitropic effects (Shafiei and Mahmoudian, 1999; Brawley et al, 2000a; Brawley et al, 2000b) and that the β_4 adrenoceptor is present in rat mesenteric arteries (Kozłowska et al, 2003). However, other studies failed to confirm these findings (Brahmadevara et al, 2003; Brahmadevara et al, 2004; Briones et al,

2005). Follow up studies have shown that β_4 adrenoceptor is rather an altered conformational state of the β_1 or β_3 adrenoceptor and this conformational change causes it to lose its affinity for specific ligands and gain affinity towards other agonists (Konkar et al, 2000; Granneman, 2001; Jost et al, 2002; Lewis et al, 2004; Baker, 2005). Thus, the existence of β_4 adrenoceptor remains unclear.

The α_1 adrenoceptor subtypes couple to $G_{q/11}$ protein and activate phospholipase C- β (PLC β) which further activates protein kinase C (PKC) and releases intracellular calcium stores (Minneman, 1988; Terzic et al, 1993) while the α_2 adrenoceptor subtypes couple to G_i and inhibit cAMP signalling (Civantos and Aleixandre, 2001). There is evidence that the α_1 adrenoceptors are present in the heart, however, no α_2 adrenoceptors are found in the heart (Simpson, 1983; Bylund et al, 1998). There appears to be a substantial role for alpha adrenoceptors in the vasculature, where stimulation causes constriction of peripheral vessels, thereby controlling blood pressure (Guimaraes and Moura, 2001).

Table 3. Adrenoceptor subtype and their effects on cardiovascular tissue.

Adrenoceptor subtype	Tissue distribution	G-protein subunits	Signalling pathways modulated	Physiological effects on cardiovascular tissue	References
α_{1A}	Coronary vascular smooth muscle cells, Atrial and ventricular myocytes, cortex, glutamatergic neurons, eye, Liver, kidney, lung, uterus smooth muscle, salivary gland, platelets, stomach and intestinal smooth muscle.	$G_{q/11}$	$\uparrow IP_3/DAG$ (PLC)	Positive chronotropy, positive inotropy, vasoconstriction	Bristow et al, 1986; Wu et al, 1995; Reiter, 2004; Zaugg et al, 2004; Zaugg and Schaub, 2005; Rozec and Gauthier, 2006; Zaugg et al, 2008 ; Cotecchia, 2010; Jensen et al, 2011.
α_{1B}	Coronary vascular smooth muscle cells, Atrial and ventricular myocytes, cortex, glutamatergic neurons, eye, Liver, kidney, lung, uterus smooth muscle, salivary gland, platelets, stomach and intestinal smooth muscle.	$G_{q/11}$	$\uparrow IP_3/DAG$ (PLC)	Positive chronotropy, positive inotropy, vasoconstriction	Bristow et al, 1986; Wu et al, 1995; Reiter, 2004; Zaugg et al, 2004; Zaugg and Schaub, 2005; Rozec and Gauthier, 2006; Zaugg et al, 2008 ; Cotecchia, 2010; Jensen et al, 2011.
α_{1D}	Coronary vascular smooth muscle cells, Atrial and ventricular myocytes, cortex, glutamatergic neurons, eye, Liver, kidney, lung, uterus smooth muscle, salivary gland, platelets, stomach and intestinal smooth muscle.	$G_{q/11}$	$\uparrow IP_3/DAG$ (PLC)	Positive inotropy, vasoconstriction	Bristow et al, 1986; Wu et al, 1995; Reiter, 2004; Zaugg et al, 2004; Zaugg and Schaub, 2005; Rozec and Gauthier, 2006; Zaugg et al, 2008.; Cotecchia, 2010; Jensen et al, 2011.
α_{2A}	cortex, cerebellum, hippocampus, spinal cord, pre- and post-synaptic nerve terminals, hypothalamus, coronary vascular smooth muscle cells, atrial and ventricular myocytes, adipocytes, platelets, kidney, intestinal smooth muscle, pancreas.	$G_{\alpha/i1/2/3}$	$\downarrow cAMP$ $\uparrow IP_3/DAG$ (PLC)	Lowers BP	Bristow et al, 1986; Gesek, 1996; Schwartz, 1997; Reiter, 2004; Zaugg et al, 2004; Zaugg and Schaub, 2005; Rozec and Gauthier, 2006; Zaugg et al, 2008; Bondar and Lazar, 2017.

α_{2B}	Coronary vascular smooth muscle cells, atrial and ventricular myocytes, hippocampus, thalamus, olfactory bulb, blood vessels, intestinal smooth muscle, pancreas.	$G_{o/i1/2/3}$	↓cAMP ↑IP ₃ /DAG (PLC)	vasoconstriction	Bristow et al, 1986; Gesek, 1996; Schwartz, 1997; Reiter, 2004; Zaugg et al, 2004; Zaugg and Schaub, 2005; Rozec and Gauthier, 2006; Zaugg et al, 2008.
α_{2C}	Coronary vascular smooth muscle cells, atrial and ventricular myocytes, cortex, hippocampus, thalamus, olfactory bulb, eye, blood vessels, intestinal smooth muscle, pancreas.	$G_{o/i1/2/3}$	↓cAMP ↑IP ₃ /DAG (PLC)	Lowers BP, vasoconstriction	Bristow et al, 1986; Gesek, 1996; Schwartz, 1997; Reiter, 2004; Zaugg et al, 2004; Zaugg and Schaub, 2005; Rozec and Gauthier, 2006; Zaugg et al, 2008.
β_1	Atrial and ventricular myocytes, AV and SA nodes, cortex, salivary gland, kidney, adipocytes, vasculature, urinary bladder, stomach and intestinal smooth muscle.	G_s $G_{o/i1/2/3}$	↑cAMP ↑L-type Ca ²⁺ opening ↑IP ₃ /DAG (PLC)	Positive inotropy, positive lusitropy, positive chronotropy, positive dromotropy	Bristow et al, 1986; Martin et al, 2004; Reiter, 2004; Zaugg et al, 2004; Zaugg and Schaub, 2005; Rozec and Gauthier, 2006; Zaugg et al, 2008 ; Bernstein et al, 2011.
β_2	Atrial and ventricular myocytes, AV and SA nodes, coronary vascular smooth muscle cells, blood vessels, cerebellum, motor nerve terminals, olfactory bulb, eye, kidney, lung, vasculature, liver, mast cells, salivary glands, pancreas, gastrointestinal and uterus smooth muscle, striated and skeletal muscle.	G_s $G_{o/i1/2/3}$	↑cAMP ↑IP ₃ /DAG (PLC) ↑PI-3K (PKB)	Positive inotropy, positive lusitropy, positive chronotropy, vasodilation	Bristow et al, 1986; Xiao, 2001; Heubach et al, 2004; Reiter, 2004; Zaugg et al, 2004; Zaugg and Schaub, 2005; Rozec and Gauthier, 2006; Zaugg et al, 2008; Galaz-Montoya et al, 2017
β_3	Adipocytes, lung, gall bladder, urinary bladder.	G_s $G_{o/i1/2/3}$	↑cAMP ↑IP ₃ /DAG (PLC) ↑eNOS/nNOS	Negative chronotropy, negative inotropy, positive lusitropy, vasodilation	Bristow et al, 1986; Reiter, 2004; Zaugg et al, 2004; Zaugg and Schaub, 2005 ; Rozec and Gauthier, 2006; Zaugg et al, 2008 ; Tchivileva et al, 2009 ; Cannavo and Koch, 2017.

1.9 Beta-adrenoceptors.

Evidence shows that the human heart consists of both β_1 and β_2 adrenoceptors. In the atria the ratio between β_1 : β_2 adrenoceptors is 70%:30% while in ventricles its 80%:20% (Brodde et al, 2006). Both β_1 and β_2 adrenoceptors can stimulate cardiac contractility (positive inotropy) and are involved in vasodilation, while the β_2 adrenoceptors can also stimulate lusitropy (cardiac relaxation). The β_3 adrenoceptors are usually associated with decreasing cardiac contractility (negative inotropy; Motomura et al, 1990; Kaumann and Sanders, 1993; MacDougall et al, 2012). The β_1 and β_2 adrenoceptors couple to G_s although under certain circumstances, there is evidence that β_2 adrenoceptors can couple to G_i proteins (Xiang and Kobilka, 2003). Whereas the β_3 adrenoceptors consistently couple to G_i proteins (Wallukat, 2002).

Both β_1 and β_2 adrenoceptors play a very important role in cardiac contractility. Usually, noradrenaline selectively activates β_1 adrenoceptors and controls the heart rate and contractibility (Brodde et al, 2006). However, during cardiac insult or stress, adrenaline is released which stimulates the β_2 adrenoceptors, increasing heart rate and contractibility thereby increasing the cardiac output, ensuring adequate tissue perfusion (Brodde, 1988). Once activated, both β_1 and β_2 adrenoceptors couple to G_s , activating cAMP signalling thereby activating protein kinase A (PKA), which further phosphorylates protein targets involved in chronotropy and inotropy (Brodde et al, 2006). Increases in intracellular calcium concentration leads to contraction (inotropy) while decreases in intracellular calcium concentration leads to relaxation (lusitropy). The L-type calcium channels (LTCC) are responsible for regulating the calcium concentration in cardiomyocytes (Kamp and Hell, 2000). Hulme and colleagues demonstrated that stimulation of isolated ventricular myocytes with isoprenaline caused a significant increase in intracellular calcium concentration (Hulme et al, 2006). This increase was observed as a result of phosphorylation of serine-1928, a residue present at the C-terminal end of the L-type calcium channels, via activation of PKA (Hulme et al, 2006). They also suggested that activation of β_1 adrenoceptors activates the L-type calcium channels by increasing cAMP concentrations throughout the cells, while β_2 adrenoceptors only produce a smaller population of cAMP near the cell surface, which regulates cardiac T-tubules and ryanodine receptors (Hulme et al, 2006). This assumption was verified by various studies using frog cardiomyocytes, which only express β_2 adrenoceptors, as well as FRET-based techniques using cAMP-FRET sensor called hyperpolarisation activated cyclic nucleotide-gated potassium channel 2 (HCN2-cAMP; for reviews see Chen-lzu et al, 2000; Skeberdis et al, 1997; Nikolaev et al, 2006; Nikolaev et al, 2010).

Ryanodine receptors are involved in a process called Calcium-Induced Calcium Release (CICR) and are located on the membrane of the sarcoplasmic reticulum of cardiomyocytes. Zhou and colleagues reported that stimulation of isolated ventricular myocytes with isoprenaline caused an increase in activation of ryanodine receptors

following activation of L-type Ca^{2+} channels. PKA was shown to be the key player in this study as inhibiting PKA with Rp-8-CPT-cAMP resulted in elimination of ryanodine receptors being activated (Zhou et al, 2009). The cardiac relaxation (lusitropy) is regulated by SERCA, which is responsible for removal of Ca^{2+} from the cytoplasm and back into the sarcoplasmic reticulum. At rest, phospholamban (sarcoplasmic reticulum membrane protein) is dephosphorylated and inhibits SERCA. Activation of PKA by β adrenoceptors leads to phosphorylation of phospholamban and activation of SERCA (Kaumann et al, 1999). Ca^{2+} is quickly quenched from the cytoplasm to the sarcoplasmic reticulum and results in relaxation (positive lusitropy) (Frank et al, 2002; see figure 1.11). Furthermore, phosphorylation of troponin I and myosin-binding protein C via PKA reduce myofilament sensitivity to Ca^{2+} causing ventricular relaxation (Frank et al, 2002). Apart from cardiac excitation-contraction coupling, β adrenoceptors can also activate glycogen phosphorylase kinase, thereby increasing glucose available for metabolism necessary due to increased cardiac output (Xiao and Lakatta, 1993).

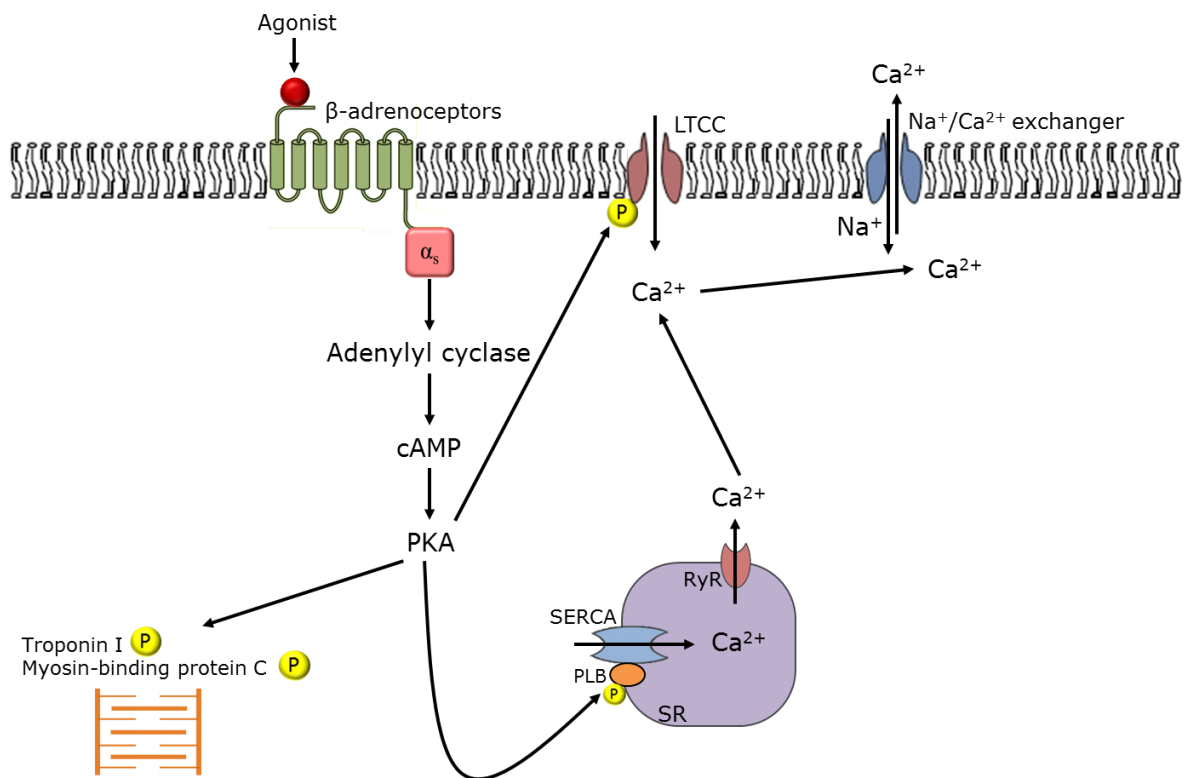


Fig 1.11: β -adrenoceptor mediated cardiac excitation-contraction coupling. β -adrenoceptor couples to G_{α_s} activating adenylyl cyclase and cAMP mediated PKA activation. PKA phosphorylates phospholamban (PLB) and enhances sarcoplasmic reticulum (SR) calcium uptake. Activation of L-type calcium channels (LTCC) are responsible for entry of calcium ions, which causes activation of ryanodine receptors (RyR) thereby inducing Calcium-Induced Calcium Release (CICR). Figure adapted from Champion and Kass, 2004.

(i) Biased agonism of the β_2 adrenoceptors:

Recently, the 'linear efficacy' of GPCRs has been proven incorrect for many GPCRs (Reiter et al, 2012). Many GPCRs via their agonist signalling are 'biased' towards multiple G-proteins or β arrestin-dependent signalling pathways. This 'pluridimensional efficacy' occurs when an agonist preferentially activates one or multiple signalling pathways from the same receptor (Reiter et al, 2012). β_2 adrenoceptors have been shown to demonstrate this property in response to multiple agonists. Noradrenaline (the endogenous full agonist) can fully activate β_2 adrenoceptor-mediated G_s signalling/cAMP signalling pathway (Heubach et al, 2003; Wang et al, 2008). Whereas Clenbuterol (full agonist) solely activates β_2 adrenoceptor mediated G_i signalling/IP₃ signalling pathway (Siedlecka et al, 2008). Similar biased agonist properties have been exhibited by isoprenaline and adrenaline (both full agonists; Heubach et al, 2003; Wang et al, 2008; Liu et al, 2009). The biased agonism phenomenon for the β_2 adrenoceptor may involve phosphorylation of the receptor by PKA (Daaka et al, 1997) or GRK2 (Liu et al, 2009). Once the agonist is bound, the conformational shift in the receptor is sufficient to reveal further allosteric sites (Staus et al, 2014). These sites are revealed only during adrenaline biased agonism while for noradrenaline these sites are not present (Wang et al, 2008). β_2 adrenoceptors can be rapidly desensitised and re-sensitised and it appears that dual phosphorylation of the receptor by PKA and GRK2 is necessary for this (Xin et al, 2008).

There are several mechanisms produced to explain the phenomenon of biased agonism. For instance, the differences in relative efficacy and potency were implied to determine ligand bias (Holloway et al, 2002; Sneddon et al, 2004; Gay et al, 2004; Urban et al, 2007). For extensive discussion on biased agonism see Kenakin, 2007; Kekani, 2009; Kenakin et al, 2012; Kenakin and Christopoulos, 2013; Rajagopal, 2013; Brust et al, 2015; Stahl et al, 2015; Rankovic et al, 2016. The currently accepted model for biased agonism is the 'competitive model' developed by Kenakin et al, 2013 and modified to accommodate weak partial agonists by Sthal et al, 2015. Liu and colleagues identified conformational change in helix VI for G-protein dependent signalling while conformational change in helix VII for arrestin-biased ligands at the β_2 adrenoceptor using one-dimensional ¹⁹F NMR spectroscopic studies (Liu et al, 2012). Recently, β -adrenoceptor subtypes were quantified in airway smooth muscles of β -arrestin knockout mice using this competitive model (Hegde et al, 2015). However, Onaran and colleagues screened 11 β_2 adrenoceptor agonists coupling to G_s , G_i or β -arrestin with varying efficacy to confirm this competitive model. They found a high level of false positive results along with a lack of correlation between the other models used in this study (Onaran et al, 2017). Clearly further studies are necessary to successfully identify biased agonists at the β_2 adrenoceptor.

(ii) β_2 adrenoceptor signalling in cardiomyocytes:

Liu and colleagues have shown that biased agonism phenomenon occurs at β_2 adrenoceptors in cardiomyocytes only at supra-physiological levels of adrenaline and isoprenaline (Liu et al, 2009). They reported that adrenaline induces rapid desensitisation and re-sensitisation while noradrenaline just induces desensitisation (Liu et al, 2009). This could be seen as a further regulation of β_2 adrenoceptor-mediated G_i binding and it is well known that G_i is localised separately to β_2 adrenoceptors (Head et al, 2005). This biased agonism of the β_2 adrenoceptor can allow the receptor function to switch from being positive inotropy to negative inotropy. The $\beta\gamma$ subunit of G_i activates downstream effectors such as MAPKs via the Src/Ras pathway (Daaka et al, 1997). MAPKs can inhibit PKA induced phosphorylation of phospholamban and hence reduce cardiac contractility (Crespo et al, 1995). Communal and colleagues have shown that MAPK activation can protect the cardiomyocyte from noradrenaline-induced apoptosis (Communal et al, 2000). The β_2 adrenoceptor-mediated G_i binding exerts an anti-apoptotic effect via ERK and AKT signalling (Chesley et al, 2000; Shizukuda and Buttrick, 2002). The activation of p38 MAPK exerts negative inotropic effects in adult cardiomyocytes and its inhibition causes strong reversible cardiac inotropy (Liao et al, 2002). Heubach and colleagues have shown that β_2 adrenoceptor-overexpressing muscle strips from mice represent a bell-shaped concentration response curve when stimulated with adrenaline. However, this was not observed with noradrenaline. β_2 adrenoceptor-mediated G_s signalling causes positive inotropy when stimulated with adrenaline; however, at higher concentrations, β_2 adrenoceptor-mediated G_i signalling kicks in and inhibits this positive inotropy, bringing contraction to baseline levels (Heubach et al, 2003). This suggests that β_2 adrenoceptor-mediated G_i signalling occurs only at higher agonist concentrations, while at physiological levels of adrenaline the β_2 adrenoceptor couples to G_s .

(iii) Cardioprotective effects of β_2 adrenoceptors:

Cardiovascular effects of the β adrenoceptors lies in their ability to couple to different G-proteins. Communal and colleagues (1999) demonstrated that β_1 adrenoceptors induce apoptosis while β_2 adrenoceptors prevent it. This was established by inhibiting G_i -proteins by treating the cardiomyocytes with pertussis toxin, which led to a significant increase in the number of apoptotic cells (Communal et al, 1999). Based on this study it was suggested that β_1 adrenoceptors have cardiotoxic effects while β_2 adrenoceptors have cardioprotective effects and that this is based on the ability of receptors coupling to different G-proteins. This could explain why prolonged stimulation of the β adrenoceptors causes apoptosis (Shizakuda and Buttrick, 2002). Activation of phosphoinositide 3 kinase (PI-3K), PKB and ERK1/2 by G_i -proteins promotes cell survival (Xiao, 2001; Chesley et al, 2000, Zhu et al, 2003). The β_1 adrenoceptor is also known to promote cardiac hypertrophy and abnormal calcium

signalling by activating CAMKII and exchange protein directly activated by cAMP (Epac1 and Epac2; Schafer et al, 2000; Morisco et al, 2001; Zhu et al, 2003). Epac activation is also known to be associated with pro-hypertrophy by activation of NFAT/calcineurin signalling (Metrich et al, 2008; Pereira et al, 2013). Epac2 signalling can cause leakage of Ca^{2+} from intracellular stores resulting in Ca^{2+} sparks, arrhythmia and hypertrophy (Wu et al, 2002; Hothi et al, 2008; Pereira et al, 2013).

β_1 adrenoceptor antagonists are prescribed to prevent cardiotoxic effects of β_1 adrenoceptors, which leads to various cardiovascular diseases such as chronic stable angina and hypertrophy (Messerli et al, 2009). The mechanism by which these antagonists prevent cardiovascular diseases is by inhibiting the sympathetic activation of heart and also limiting the myocardial oxygen demand so that it matches the supply. This measure was used in pre-operative and perioperative patients with cardiovascular risk factors to decrease myocardial oxygen demand, which conferred cardiac protection (Mangano and Goldman, 1995; Poldermans et al, 1999; Messerli et al, 2009). However, some clinical studies have shown adverse effects, such as increased incidence of stroke and mortality (Devereaux et al, 2008; Beattie et al, 2010; Brady et al, 2005; Wallace et al, 2011; Yang et al, 2006). Some studies have shown that the β_2 adrenoceptors are cardioprotective (Bernstein et al, 2005; Fajardo et al, 2006; Shizukuda and Buttrick, 2002; Chelsey et al, 2000; Devic et al, 2001). For instance, β_2 adrenoceptors protects the heart against doxorubicin-mediated toxicity by activating survival pathways (Fajardo et al, 2011). Overall, these studies support the hypothesis that β_1 adrenoceptors have cardiotoxic effects while β_2 adrenoceptors have cardioprotective effects.

Yano and colleagues have reported that in H9c2 cardiomyocytes, the β_2 adrenoceptors couples to G_i and activates pro-survival kinases such as PI-3K (Yano et al, 2007). PI-3K is a central compound in the RISK pathway and it has also been demonstrated that β_2 adrenoceptors can activate the ERK1/2 pathway, which is another key player in the RISK pathway (Hausenloy et al, 2005; Galandrin and Bouvier, 2006; Tutor et al, 2007). A pilot study by Strasser and colleagues reported that in Langendorff-perfused rat heart, exposure to ischaemia for short periods resulted in increased levels of β adrenoceptors, which led to increased activity of adenylyl cyclase. However, longer periods of ischaemia resulted in decreased levels of β adrenoceptors and in turn decreased activity of adenylyl cyclase (Strasser et al, 1990). A subsequent study using neonatal rat ventricular myocytes reported a similar observation (Rocha-Singh et al, 1991). These initial studies demonstrated a role for β adrenoceptors during ischaemia. Many studies have looked at β adrenoceptors agonists as a potential preventive measure against ischaemia. In mouse heart, cardioprotection is mediated via β_2 adrenoceptors and its switching from G_s to G_i -mediated signalling (Tong et al, 2005). The β adrenoceptor(s) responsible for cardioprotection in rat heart remain unclear (Lange et al, 2006; Lochner et al, 1999; Marais et al, 2001; Moolman et al, 2006a;

Moolman et al, 2006c; Nasa et al, 1997; Robinet et al, 2005; Tong et al, 2005; Yabe et al, 1998; Yates et al, 2003). In the Langendorff-perfused rat heart, pre-conditioning with β adrenoceptors results in decrease in cytokine release, apoptosis and infarct size. The key pathways identified as mediating these protective effects are PI-3K, PKA, PKC and p38 MAPK (Nasa et al, 1997; Robinet et al, 2005 ; Moolman et al, 2006a; Moolman et al, 2006c). However, the β adrenoceptor activating these kinases is yet to be identified.

There is a potential role for β_2 adrenoceptors in post-conditioning. β_2 adrenoceptors can activate PI-3K and ERK1/2, which are both key players of the RISK pathway (Galandrin and Bouvier, 2006; Tutor et al, 2007). RISK pathways are activated during reperfusion and so it is entirely possible that activation of β_2 adrenoceptors could mimic post-conditioning. Preliminary evidence exists that activation of β_2 adrenoceptors via post-conditioning in langendoff perfused rat hearts can offer cardioprotection (Tota et al, 2012; Tota et al, 2014).

1.10 H9c2 cells as a model system for cardioprotection.

H9c2 cells are derived from embryonic rat heart tissue and exhibit similar biochemical, morphological and electrophysiological properties to primary cardiac cells (Kimes and Brandt, 1976; Hescheler et al, 1991). These cells are increasingly being used as an *in vitro* model for studies relating to cardioprotection (see Han et al, 2005; Chen et al, 2010; Crawford et al, 2003; Sun et al, 2016) and H9c2 cells have been shown to be a good model for ischaemia/reperfusion injury (Fretwell and Dickenson, 2009; Urmaliya et al, 2009; Zhu et al, 2011; Sun et al, 2015; Hu et al, 2016; Khaliulin et al, 2017; Li et al, 2017; Liu et al, 2017; Wang et al, 2017; Xu et al, 2017). Furthermore, recent studies have demonstrated that H9c2 cells are energetically more similar to primary cardiac myocytes than mouse atrial HL-1 cells and thus represent a viable *in vitro* model to investigate simulated cardiac ischaemia/reperfusion injury (Kuznetsov et al. 2015). It should also be noted that HL-1 cell medium contains adenosine (a cardioprotective agent) and hence cannot be used to assess cardioprotective potential especially with the adenosine receptors (Peter et al, 2016). In addition to their increasing use in studies exploring cardioprotection, H9c2 cells show hypertrophic responses comparable to primary neonatal cardiac myocytes and therefore also represent a useful cell model system to study heart disease (Watkins et al. 2011). H9c2 cells also contain multiple cytochrome P450 (CYP) genes which are comparable to those expressed in primary cardiomyocytes thus offering a unique *in vitro* model to investigate cardiac metabolic activity (Zordoky and El-Kadi, 2007). Zhou and colleagues have reported that even though H9c2 cells do not have a beating function, they have the ability to contract and expand. Therefore, they represent a suitable model for investigating contraction and relaxation characteristics of cardiomyocytes as well as for pre-assessment for toxicological studies of cardiovascular drugs where high

throughput and repetitions are required (Zhou et al, 2016). Comparative analysis of H9c2 cells with other cardiac cells is summarised in table 4.

Table 4. Comparative analysis of H9c2 cells with other cardiac cells (adapted from Peter et al, 2016).

	Neonatal cardiomyocytes (NRVMs/NMVMs)	Adult cardiomyocytes (ARVMs/AMVMs)	H9c2 cardiomyoblasts	HL-1 cardiomyocytes	Human embryonic and pluripotent stem cells (ESCs)
Origin	Neonatal ventricular origin	Adult ventricular origin	Ventricular origin	Derived from AT-1 atrial tumour cell lineage	Ventricular origin
Isolation	Easy isolation	Technically challenging isolation	Immortalised	Immortalised	Immortalised
Maintenance	Can be maintained in a serum-free culture medium up to 28 days after isolation	Can be maintained in a serum-free culture medium for a short time after isolation	Media must be supplemented with an atrial differentiation factor in order to differentiate in cardiomyocytes and express cardiomyocyte lineage markers	Have to be maintained in medium containing a cardioprotective agent, a hypertrophic stimulus, and an atrial differentiation factor	Technically challenging to maintain in a serum-free culture medium. Numerous protocols for differentiation.
Phenotype	Immature	Mature sarcomeric structure is ideal for patch-clamp/ contractility studies. Presence of mature ion channels are ideal for Ca ²⁺ imaging studies	Immature	Immature	Immature unless maintained in culture for 12–15 week
Homogeneity/heterogeneity	Can produce both homogeneous and/or heterogeneous cultures	Can produce both homogeneous and/or heterogeneous cultures	Homogeneous	Homogeneous	Heterogeneous
Transfection/manipulation	Easily transfectable with lipid or electroporation methodologies	Can only be transfected with viral vectors	Easily manipulated	Easily manipulated	Easily manipulated
Contraction in culture (beating)	Spontaneously beat in culture	Do not spontaneously beat in culture	Do not spontaneously beat in culture	Contract spontaneously in ideal culture conditions	Contract spontaneously in ideal culture conditions
Respond to hypertrophic stimuli	Yes	Yes	Yes	No	Yes
Cost	Cost-effective	Cost-effective	Cost-effective	Cost-effective	Expensive

It has been previously shown that pre- and post-conditioning with adenosine via A₁ adenosine receptor protects H9c2 cells against simulated ischaemia (Nagarkitti and Shaafi, 1998; Fretwell and Dickenson, 2011; Fretwell and Dickenson, 2009). A recent study showed that TG2 can be modulated by PKC and PKA and that it plays a role in cardioprotection in H9c2 cells (Almami *et al*, 2014). However, this study did not investigate the GPCR(s) involved in TG2-induced protection as general activators of PKA (forskolin) and PKC (PMA) were used. Since PKC and ERK1/2 pathways are also associated with modulation of TG activity (Mishra *et al*, 2007; Bollag *et al*, 2005), it is conceivable that the A₁ adenosine receptor could modulate TG2 activity and thereby play a role in cardioprotection in these cells. The role of β -adrenoceptors in mediating cardioprotection in H9c2 cells has not been uncovered yet. However, since PKA is known to be activated by β -adrenoceptors, it is also conceivable that β -adrenoceptors could modulate TG2 activity and hence have a role in cardioprotection in H9c2 cells.

1.11 Aims of this project.

The main aims of this project are:

- 1) To establish functional expression of GPCRs (adenosine receptors and β -adrenoceptors) and TG2 in H9c2 cells.
- 2) To investigate modulation of TG2 activity by the A₁ adenosine receptor.
- 3) To investigate modulation of TG2 activity by the β ₂-adrenoceptor.
- 4) To identify and validate substrates of TG2 that are modulated by the aforementioned GPCRs.
- 5) To assess the cardioprotective potential of GPCR-induced TG2 activity.

Chapter II: Methods

2.1 Materials.

Akt inhibitor XI, AS 605240, BAPTA/AM, forskolin, PD 98059, CGP 20712, Ro-31-8220, Rp-8-Cl-cAMPs, N6-cyclopentyladenosine, SB 203580, SP 600125, CL 316243, cimaterol, dobutamine, formoterol, ICI 118,551, KT 5720, LY 294002, propranolol, thapsigargin and wortmannin were obtained from Tocris Bioscience (Bristol, UK).

Adenosine, casein, DPCPX (1,3-dipropylcyclopentylxanthine), IBMX, IGEPAL, Isoprenaline, MTT (3-(4-5-dimethylthiazol-2-yl)-2,5-diphenyltetrazolium bromide), N',N'-dimethylcasein, paraformaldehyde, pertussis toxin, protease inhibitor cocktail, phosphatase inhibitor cocktail 2 and 3, ExtrAvidin[®]-HRP and ExtrAvidin[®]-FITC and Triton[™] X-100 were obtained from Sigma-Aldrich Co. Ltd. (Gillingham, UK). Fluo-8/AM was purchased from Stratech Scientific Ltd (Newmarket, UK). 5X MMLV buffer, 10 mM dNTPs, random primers, RNAsin, MMLV enzyme and 100 bp DNA ladder were purchased from Promega[®] (Southampton, UK). Biomix red taq polymerase was obtained from Bioline (London, UK). The TG2 inhibitors Z-DON (Z-ZON-Val-Pro-Leu-OMe) and R283 along with purified standard guinea-pig liver TG2 were obtained from Zedira GmbH (Darmstadt, Germany). Biotin-TVQQEL was purchased from Pepceuticals (Enderby, UK). DAPI was from Vector Laboratories Inc (Peterborough, UK). Coomassie blue (Instant Blue[™] stain) was purchased from Expedeon (Swavesey, UK). Biotin cadaverine (N-(5-Aminopentyl) biotinamide) and biotin-X-cadaverine (5-([(N-(Biotinoyl)amino)hexanoyl]amino)pentylamine) were purchased from Invitrogen UK (Loughborough, UK). DMEM (Dulbecco's modified Eagle's medium), foetal bovine serum, trypsin (10X), L-glutamine (200mM), penicillin (10,000 U/ml)/streptomycin (10,000 µg/ml) were purchased from Lonza, (Castleford, UK). All other reagents were purchased from Sigma-Aldrich Co. Ltd. (Gillingham, UK) and were of analytical grade.

Table 2.1. Primary antibodies employed in this study.

Antigen	Antibody	Catalogue number	Company	Working dilution (Western Blot)	Working dilution (Immunofluorescence)
phospho-specific JNK (Thr ¹⁸³ /Tyr ¹⁸⁵)	Rabbit monoclonal	9251	New England Biolabs, UK	1:500	N/A
Total unphosphorylated JNK	Rabbit polyclonal	9252	New England Biolabs, UK	1:500	N/A
phospho-specific PKB (Ser ⁴⁷³)	Rabbit polyclonal	9271	New England Biolabs, UK	1:500	N/A
Total unphosphorylated PKB	Rabbit polyclonal	9272	New England Biolabs, UK	1:500	N/A
phospho-specific ERK1/2 (Thr ²⁰² /Tyr ²⁰⁴)	Mouse monoclonal	M8159	Sigma-Aldrich, UK	1:1000	N/A
Total unphosphorylated ERK1/2	Mouse monoclonal	9107	New England Biolabs, UK	1:1000	N/A
phospho-specific p38 MAPK (Thr ¹⁸⁰ /Tyr ¹⁸²)	Rabbit monoclonal	9216	New England Biolabs, UK	1:500	N/A
Total unphosphorylated p38 MAPK	Rabbit polyclonal	9212	New England Biolabs, UK	1:500	N/A
Cleaved caspase-3 (Asp ¹⁷⁵)	Rabbit monoclonal	9661	New England Biolabs, UK	1:200	N/A
anti-TG2 (CUB 7402)	Mouse monoclonal	MA5-12739	Thermo Scientific, UK	1:1000	1:1000
anti-phosphoserine	Rabbit polyclonal	ab9332	Abcam, UK	1:1000	N/A
anti-phosphothreonine	Rabbit polyclonal	ab9337	Abcam, UK	1:1000	N/A
anti-TG1	Rabbit polyclonal	A018	Zedira GmbH, Germany	1:1000	1:1000
anti-TG3	Rabbit polyclonal	A015	Zedira GmbH, Germany	1:1000	1:1000
GAPDH	Rabbit monoclonal	2118	New England Biolabs, UK	1:1000	N/A
Hexokinase-1	Rabbit monoclonal	2024	New England Biolabs, UK	1:1000	N/A
VDAC-1	Rabbit monoclonal	4661	New England Biolabs, UK	1:1000	N/A

It should be noted that the anti-phosphoserine and anti-phosphothreonine are sold as they're directed towards all phosphoproteins. However, there's a possibility they might not do so due to the protein conformation resulting in epitope not being exposed and also there could be a loss in epitope due to harsh reducing conditions of SDS and Laemmli.

Table 2.2. Secondary antibodies employed in this study.

Secondary antibody	Catalogue number	Company	Working dilution (Western Blot)	Working dilution (Ex/Em-Immunofluorescence)
Horse anti-mouse IgG, HRP-linked	7076	New England Biolabs, UK	1:1000	N/A
Goat anti-rabbit IgG, HRP-linked	7074	New England Biolabs, UK	1:1000	N/A
FITC conjugated goat anti-rabbit IgG, H&L	ab6717	Abcam, UK	N/A	1:1000 (493/528nm)
FITC conjugated goat anti-mouse IgG, H&L	ab6785	Abcam, UK	N/A	1:1000 (493/528nm)

2.2 Cell culture.

Rat embryonic cardiomyoblast-derived H9c2 cells (European Collection of Animal Cell Cultures, Salisbury, UK) were cultured in 75 cm² flasks in Dulbecco's Modified Eagles Medium (DMEM) supplemented with 10% (v/v) foetal bovine serum, 2 mM L-glutamine and 100 U/ml penicillin/streptomycin for the duration of this project. Cells were maintained in a humidified incubator (95% air / 5% CO₂, 37°C) and grown up to 70-80% confluency as observed by light microscopy. Beyond 80% confluency, cells start to differentiate and hence change their morphology. Typically, H9c2 cells were sub-cultured with a 1:10 split using trypsin (0.05% w/v)/EDTA (0.02% w/v). Cells for MTT, LDH and functional receptor expression assays were grown in 24 well plates and/or 96 well plates (Sarstedt; NÜmbrecht, Germany).

(i) Differentiation of H9c2 cells:

H9c2 cells were differentiated by culturing the cells for 7 days in the continued presence of 10 nM *all-trans* retinoic acid in Dulbecco's Modified Eagles Medium (DMEM) supplemented with 1 % (v/v) foetal bovine serum. The differentiation medium was replaced every 48 h and to confirm differentiation. The cells were observed under the microscope to form cardiomyocyte-like phenotype by the formation of multinucleated elongated myotubes as described by Daubney et al, 2015.

2.3 Tissue transglutaminase activity assays.

(i) Preparation of cell lysates for tissue transglutaminase activity assays:

H9c2 cells were grown in T75 cm² tissue culture flasks. Following the treatments, cells were washed twice with ice cold PBS and then subjected to 500 µl of lysis buffer (50 mM Tris-HCl pH 8.0, 0.5% (w/v) sodium deoxycholate, 0.1% (v/v) protease inhibitor cocktail and 1% (v/v) phosphatase inhibitor cocktail 2 and 3). The cells were incubated in the lysis buffer on ice for 30 min, scraped and clarified by centrifugation

at 4°C for 10 min at 14000xg. The supernatant was collected and stored at -80°C until use.

(ii) Amine incorporating assay:

The amine incorporating activity of TG2 was measured via biotin-cadaverine incorporation into N, N'-dimethylcasein as described by Slaughter et al., (1992) with modifications of Lilley et al., (1998). 96-well microtitre plates were coated overnight at 4°C with 250 µl of N, N'-dimethylcasein (10 mg/ml in 100mM Tris-HCl, pH 8.0). After incubation, plates were washed twice with distilled water and blocked with 250 µl of 3% (w/v) BSA in 100 mM Tris-HCl, pH 8.0 and incubated at room temperature for 1 h with gentle agitation. The plate was then washed twice with distilled water and 150 µl of either 6.67 mM calcium chloride (required for enzyme activity) or 13.3 mM EDTA (added to identify background activity) containing 225 µM biotin-cadaverine and 2mM 2-mercaptoethanol was added in the respective wells. The reaction was started by the addition of either 50 µl samples or negative or positive controls. 50 ng/well of guinea pig liver TG2 was used as a positive control and 100 mM Tris-HCl, pH 8.0 was used as a negative control. The plates were incubated at 37°C for 1 h. After incubation, the plates were washed twice with distilled water and 200 µl of 100 mM Tris-HCl, pH 8.0 containing 1% BSA and 1:5000 dilution of ExtrAvidin®-peroxidase conjugate was added to each well. The plates were then incubated at 37°C for 45 min and washed as before. The reaction was developed by the addition of 200 µl of freshly prepared developing buffer (7.5 µg ml⁻¹ 3, 3', 5, 5'-tetramethylbenzidine (TMB) and 0.0005% (v/v) hydrogen peroxide in 100 mM sodium acetate, pH 6.0) and incubated at room temperature for 15 min. The development of colour was terminated using 50 µl of 5.0 M sulphuric acid and the absorbance read at 450 nm using a standard 96-well plate reader. Each experiment was performed in triplicate and the results are expressed as specific activity of TG2 in units. One unit of TG2 was defined as a change in absorbance at 450nm/1 h. The order of drug treatments on the layout of the plate was randomised to avoid experimental design bias.

(iii) Peptide crosslinking assay:

The crosslinking activity of TG2 was measured via biotin-TVQQEL peptide incorporation into casein as described by Trigwell et al., 2004 with minor modifications. 96-well microtitre plates were coated overnight at 4°C with 250 µl of casein (1 mg/ml in 100mM Tris-HCl, pH 8.0). After incubation, plates were washed twice with distilled water and blocked with 250 µl of 3% (w/v) BSA in 100 mM Tris-HCl, pH 8.0 and incubated at room temperature for 1 h with gentle agitation. The plate was then washed twice with distilled water and 150 µl of either 6.67 mM calcium chloride (required for enzyme activity) or 13.3 mM EDTA (added to detect background activity) containing 5 µM biotin-TVQQEL peptide and 2 mM 2-mercaptoethanol was added in

the respective wells. The reaction was started by the addition of 50 μ l samples or negative and positive controls. 50 ng/well of guinea pig liver TG2 was used as a positive control and 100 mM Tris-HCl, pH 8.0 was used as a negative control. The plates were incubated at 37°C for 1 h. After incubation, the plates were washed twice with distilled water and 200 μ l of 100 mM Tris-HCl, pH 8.0 containing 1% BSA and 1:5000 dilution of ExtrAvidin®-peroxidase conjugate was added to each well. The plates were then incubated at 37°C for 45 min and washed as before. The reaction was developed by the addition of 200 μ l of freshly prepared developing buffer (7.5 μ g/ml 3, 3', 5, 5'-tetramethylbenzidine (TMB) and 0.0005% (v/v) hydrogen peroxide in 100 mM sodium acetate, pH 6.0) and incubating at room temperature for 15 min. The development of colour was terminated using 50 μ l of 5.0 M sulphuric acid and the absorbance read at 450 nm using a standard 96-well plate reader. Each experiment was performed in triplicate and the results are expressed as specific activity of TG2 in units. One unit of TG2 was defined as a change in absorbance at 450nm/1 h. The order of drug treatments on the layout of the plate was randomised to avoid experimental design bias.

(iv) Visualisation of in-situ TG2 transamidating activity via ExtrAvidin® FITC and confocal microscopy:

H9c2 cells were seeded into 8-well chamber slides (15000 cells/well) and cultured for 24 h in fully supplemented DMEM. The next day, cells were exposed to fresh fully supplemented DMEM containing 1 mM biotin-x-cadaverine and incubated for 6 h (Perry et al., 1995). Following incubation, cells were treated as described in Figure legends. After treatment(s), cells were washed three times (five min per wash) with PBS. 200 μ l of 3.7% (w/v) paraformaldehyde in PBS was added into each well and incubated at room temperature for 15 min in order to fix cells. The cells were washed twice (five min per wash) with PBS. 200 μ l of 0.1% (v/v) Triton-X100 in PBS was added into each well and incubated at room temperature for 15 min in order to permeabilise the cells. The cells were washed again as described previously and blocked with 3% (w/v) BSA in PBS for 1 h at room temperature. Transglutaminase mediated transamidating activity was detected by FITC-conjugated ExtrAvidin® (1:200 v/v) in blocking buffer. The slides were incubated overnight at 4°C. The next day, cells were washed as before and nuclei counter-stained using DAPI in Vectorshield mounting medium. The slides were sealed with coverslips and secured with nail varnish and stored at 4°C until required. Images were acquired using Leica TCS SP5 II confocal microscope (Leica Microsystems, GmbH, Mannheim, Germany) equipped with a 20x air objective. Optical sections were typically 1–2 μ m and the highest fluorescence intensity was acquired using either forskolin (10 μ M) or CPA (100 nM) as a positive control. Using the look-up table overlay option, saturation was observed and avoided by setting the gain accordingly. The output laser power, acquisition mode, pinhole

diameter, detector gain and amplifier offset were standardised for all samples analysed. Images were acquired using a sequential scan to avoid cross-excitation of fluorochromes and to distinguish between extracellular, cell surface and intracellular TG2. The images were analysed and quantified using Leica LAS AF software from minimum of five fields of view per treatment. Each experiment had a negative control (no application of FITC) and the FITC fluorescence intensity values of the negative control (i.e. background) were subtracted from the FITC fluorescence intensity values of each treatment in that experiment. Following this, the value obtained for each treatment was divided by the fluorescence intensity of DAPI for that treatment in that experiment to get fluorescence per nuclei. This normalised FITC fluorescence intensity per nuclei values were plotted and further analysed using GraphPad Prism[®] software (GraphPad Software, Inc., USA).

2.4 Expression of GPCRs and TGs in H9c2 cells.

(i) RT-PCR for GPCR expression:

(a) cDNA synthesis:

Total RNA was isolated from mitotic and differentiated H9c2 cells, rat heart, rat lung, rat brain and rat eye using a GenElute[®] total RNA isolation kit (Sigma-Aldrich Co. Ltd, Gillingham, UK) according to the manufacturer's instructions. First strand complementary DNA (cDNA) was synthesized using 10 µl of 5X MMLV buffer, 10 µl of 10 mM dNTPs, 1 µl of random primers, 1 µl of RNAsin, 1 µl of MMLV enzyme and 27 µl of 2 µg mRNA (Promega[®], Southampton, UK).

After gentle mixing of the reagents, each sample was subjected to 42°C for 90 min. Following this incubation, residual RNA was preserved in 0.1 vol of 3M sodium acetate and 2.5 vol of 100% ethanol. Samples were then gently mixed and stored at -20°C.

(b) PCR:

PCR was performed using gene-specific primer sequences (Eurofins Genomics, Wolverhampton, UK) for adenosine receptors and beta adrenoceptors as well as the housekeeping gene GAPDH. The primers used are shown in Table 2.3.

Table 2.3. Primer sequences designed along with melting temperature and product sizes.

Receptor	Primer	Sequence	T _m	Product size
Adenosine A ₁ Receptor	Forward	GCTCCATTCTGGCTCTGCT	60°C	207
	Reverse	CACTGCCGTTGGCTCTCC	60°C	
Adenosine A _{2A} Receptor	Forward	TTCGCTATCACCATCAGCAC	60°C	249
	Reverse	GTTCCAGCCCAGCATGGG	60°C	
Adenosine A _{2B} Receptor	Forward	TTCGCCATCCCCTTTGCCA	60°C	250
	Reverse	GGAAAGGAGTCAGTCCAATG	60°C	
Adenosine A ₃ Receptor	Forward	CCACGCTTCCATCATGTCC	60°C	237
	Reverse	CCGACCACGGAACGGAAG	60°C	
β ₁ adrenoceptor	Forward	TACTCCTGGCGCTCATCGT	60°C	599
	Reverse	CTCGCAGCTGTCGATCTTC	60°C	
β ₂ adrenoceptor	Forward	AGCCACACGGGAATGACAG	60°C	323
	Reverse	CCAGAACTCGCACCAGAA	60°C	
β ₃ adrenoceptor	Forward	AGTCCTGGTGTGGATCGTG	60°C	724
	Reverse	ACGCTCACCTTCATAGCCAT	60°C	
GAPDH	Forward	CAAGTTCAACGGCACAGTCA	60°C	392
	Reverse	GAGTGGCAGTGATGGCATG	60°C	

Eight thin-walled PCR tubes were prepared consisting of 1 µl forward primer, 1 µl reverse primer, 1 µl cDNA, 12.5 µl Biomix red taq polymerase (Bioline, London, UK) and 9.5 µl DEPC water. The PCR conditions for the adenosine receptors, beta adrenoceptor and GAPDH were 40 cycles of 94°C for 1 min, 59°C for 1.5 min, and 72°C for 1 min. Samples were held at 4°C. Negative controls were performed using an identical protocol but lacking the cDNA template.

(c) Agarose gel electrophoresis:

1.5% (w/v) agarose gels were cast in Tris-acetate-EDTA (TAE) buffer (40mM Tris, 20mM acetic acid, 1mM EDTA) supplemented with 0.5 µg/ml of ethidium bromide. 5 µl of 100 bp DNA ladder (Promega®, Southampton, UK) and 25 µl of PCR product were loaded on the gel. Gels were run at 100 V for 30 min. DNA was visualised under UV illumination and images were captured by U:Genius3 (Syngene, Cambridge, UK).

(ii) Immunofluorescence for TG expression:

H9c2 cells were seeded into 8-well chamber slides (15,000 cells/well) and cultured for 24 h in fully supplemented DMEM. The next day, medium was removed and cells were washed twice (five min per wash) with PBS. 200 µl of 3.7% (w/v) paraformaldehyde in PBS was added into each well and incubated at room temperature for 15 min in order to fix cells. The cells were washed three times (five min per wash) with PBS. 200 µl of 0.1% (v/v) Triton-X100 in PBS was added into each well and incubated at room temperature for 15 min in order to permeabilise the cells. The cells were then again washed as described above and blocked with 3% (w/v) BSA in PBS for 1 h at room temperature. The slides were incubated overnight at 4°C in blocking buffer with one of the following primary antibodies (1:1000 unless otherwise stated): TG1 (A018), TG2 (CUB 7402) and TG3 (A015). After incubation, the primary antibody was removed and the slides washed three times (five min per wash) with PBS. Slides were then incubated with appropriate secondary antibody (FITC conjugated goat anti-rabbit/anti-mouse antibody; 1:1000) in blocking buffer for 2 h at room temperature. After incubation with secondary antibody, the slides were washed three times (five min per wash) with PBS and the nuclei counter stained using DAPI in Vectorshield® mounting medium. The slides were sealed with coverslips, secured with nail varnish and stored at 4°C until required. Images were acquired using Leica TCS SP5 II confocal microscope (Leica Microsystems, GmbH, Mannheim, Germany) and the images were analysed and quantified, as described above.

2.5 Functional Expression of GPCRs in H9c2 cells.

(i) cAMP accumulation assay:

H9c2 cells (5000 cells/well) were seeded in a white 96 well microtitre plate, with clear-bottomed wells (Fisher Scientific, Loughborough, UK) and cultured for 24 h in fully supplemented DMEM. The medium was removed and the monolayer treated with agonists for 20 min in serum-free DMEM (40 µl/well) in the presence of 1 M MgCl₂ and 500 µM 3-isobutyl-1-methylxanthine (IBMX; phosphodiesterase inhibitor). Where appropriate, cells were pre-treated with antagonists for 30 min in similar media. Following stimulation, cAMP levels within cells were determined using the cAMP-Glo™ Max Assay kit (Promega®, Southampton, UK). Briefly, following antagonist/agonist

incubation, 10 μ l of cAMP detection solution was added to all wells and incubated for 20 min at room temperature while gently shaking. After incubation, Kinase-Glo[®] reagent (50 μ l/well) was added and incubated for 10 min at room temperature under shaking conditions, following which luminescence levels across the plate were read using a plate-reading FLUOstar Optima luminometer (BMG Labtech Ltd, Aylesbury, UK). Forskolin 10 μ M was used as a positive control and the luminescence values were converted to cAMP levels using a cAMP standard curve (0-100 nM), according to manufacturer's instructions.

(ii) Measurement of intracellular calcium:

H9c2 cells were seeded in 24-well flat-bottomed plates (15,000 cells/well) and cultured for 24 h in fully supplemented DMEM. Cells were loaded with Fluo-8 AM (5 μ M, 30–40 min) before mounting on the stage of a Leica TCS SP5 II confocal microscope (Leica Microsystems, GmbH, Mannheim, Germany) equipped with a 20x air objective. Cells were incubated at 37°C using a temperature controller and micro incubator (The Cube, Life Imaging Services, Basel, Switzerland) in the presence of imaging buffer (134 mM NaCl, 6 mM KCl, 1.3 mM CaCl₂, 1 mM MgCl₂, 10 mM HEPES, and 10 mM glucose; pH 7.4). Using an excitation wavelength of 490 nm, emissions over 514 nm were collected. Images were collected every 1.7 s for 10 min. Increases in intracellular Ca²⁺ were defined as F/F_0 where F was the fluorescence at any given time, and F₀ was the initial basal level of fluorescence.

2.6 SDS-PAGE and Western blot analysis.

(i) Preparation of cell lysates for western blotting:

H9c2 cells were grown in T25 tissue culture flasks. Following treatments, cells were washed twice with PBS (room temperature) and subjected to 300 μ l of boiling lysis buffer (0.1% SDS in Tris buffered saline). The cells were immediately scraped and collected in 1.5 ml Eppendorf™ tubes and boiled for 10 min. The lysates were stored at -20°C until use.

(ii) BCA protein assay:

The protein content of samples was assessed using the commercially available kit from Sigma-Aldrich based on the bicinchoninic acid (BCA) protocol (Smith et al, 1985) using dilutions of bovine serum albumin (BSA) as standard. Protein standards were prepared using dilutions of 1 mg/ml BSA to produce a linear standard curve as shown in table 2.4. 20 μ l of standards and samples were added to a 96 well flat-bottomed plate in triplicate. 200 μ l of working BCA reagent (50 parts of reagent A to 1 part of reagent B) was added to each of the wells and the plate incubated at 37°C for 30 min. Absorbance was read at 570 nm using a standard 96-well plate reader. Protein content

of samples was obtained by measuring them against the standard curve. The order of drug treatments on the layout of the plate was randomised to avoid experimental design bias.

Table 2.4. BSA standard curve.

Protein concentration (mg/ml)	1 mg/ml BSA (μ l)	Distilled water (μ l)
0	0	20
0.2	4	16
0.4	8	12
0.6	12	8
0.8	16	4
1	20	0

(iii) SDS-PAGE (Sodium Dodecyl Sulphate-Polyacrylamide Gel Electrophoresis):

Once the protein concentration of the samples was estimated, the desired amount of protein was dissolved in a 3:1 ratio with 4x reducing Laemmli buffer (125mM Tris-HCl, pH 6.8, 20% (v/v) glycerol, 4% (v/v) SDS, 10% (v/v) 2- β -mercaptoethanol and 0.004% bromophenol blue) (Laemmli et al., 1970) and boiled for 10 min at 95°C to denature. The gels were prepared according to manufacturer's instructions. Briefly, 1.5 mm thickness 10% acrylamide gel (8.0 ml deionised water, 6.6 ml ProtoGel[®] acrylamide mix (30 % acrylamide solution 37.5:1 ratio, Geneflow Ltd, Staffordshire, UK), 5.0 ml 1.5 M Tris-HCl pH 8.8, 200 μ l 10% SDS solution (10% (w/v) sodium dodecyl sulphate in deionised water), 200 μ l APS solution (10% (w/v) ammonium persulphate in deionised water), 20 μ l TEMED) were cast using the Bio-Rad Mini-Protean III system. Once the resolving gel was poured to about 75% of the glass plates, water was added to ensure level polymerisation of the gel. Once the resolving gel had polymerised, water was removed and the stacking gel was poured (12.3 ml deionised water, 2.5 ml ProtoGel[®] acrylamide mix, 5.0 ml 1.0 M Tris-HCl pH 6.8, 200 μ l 10% SDS solution (10% (w/v) sodium dodecyl sulphate in deionised water), 200 μ l APS solution (10% (w/v) ammonium persulphate in deionised water), 20 μ l TEMED). Immediately once the stacking gel was poured, a plastic comb was placed to form wells. Following polymerisation, the gels were placed in the electrophoretic tank and filled with electrophoresis buffer (25mM Tris, 192mM Glycine and 0.1% (w/v) SDS, pH 8.5). The protein samples (20-50 μ g/well; depending on target protein) were loaded along with 5 μ l of protein ladder. Electrophoresis was conducted at 120 V through the stacking gel and then at 160 V through the resolving gel.

(iv) Coomassie staining of gels:

Following electrophoresis, the gel was washed twice with distilled water and 20 ml of Instant Blue stain (Expedeon, Cambridge, UK) was added. The gel was incubated for 1

h at room temperature with gentle agitation. After incubation, the gel was washed three times (ten min per wash) with distilled water. Subsequently, the gel was visualised and images were captured by LAS 4000 system (GE healthcare life sciences, Buckinghamshire, UK).

(v) Western blotting:

After electrophoresis, the proteins were transferred to nitrocellulose membranes using Bio-Rad Trans-blot system according to previously established protocols (Towbin et al., 1979). Briefly sponges, filter paper, nitrocellulose membrane and electrophoresed gels were soaked in ice-cold transfer buffer (25mM Tris, 192mM glycine, pH 8.3 and 20% (v/v) methanol). The western blot sandwich was prepared in the following manner: sponge, filter paper, nitrocellulose membrane, gel, filter paper, sponge. A roller was used to remove any air bubbles trapped in the sandwich. The layers were clamped together and placed in a western blotting cassette and then into the tank along with a cooling block. The tank was filled with ice-cold transfer buffer and the transfer was performed at 180 mA for 75 min. Following transfer, membranes were stained with Ponceau S stain to visualise the protein bands. Once stained the protein bands were cut above the predicted molecular weight. Initially, full length blots were used to check if there was any non-specific binding of the antibody. However, since no non-specific binding was observed, the blots were cut to reduce antibody consumption. The membrane strips were destained using Tris-buffered saline Tween-20 (TBST; 0.1% (v/v) Tween-20 in 25mM Tris, 150mM NaCl). After destaining, the membrane was blocked with 5% (w/v) skimmed milk powder in TBST for 1 h at room temperature with gentle agitation. The blots were then incubated overnight with gentle agitation at 4°C in blocking buffer with one of the following primary antibodies (1:1000 unless otherwise stated): Phospho-specific ERK1/2, phospho-specific JNK (1:500), phospho-specific p38 MAPK (1:500), phospho-specific PKB (1:500), cleaved active caspase-3 (1:200), GAPDH, TG1, TG2, TG3, anti-phosphoserine, anti-phosphothreonine, hexokinase-1, VDAC-1. After incubation, the primary antibody was removed and the membrane washed three times for 5 min each with TBST. Blots were then incubated with appropriate secondary antibody (1:1000) conjugated to horseradish peroxidase (New England Biolabs (UK) Ltd) in blocking buffer for 2 h at room temperature with gentle agitation. After incubation with secondary antibody, the blots were washed three times for 5 min each with TBST and developed using the Enhanced Chemiluminescence (ECL) detection system. Digital images of the blots were captured by the LAS 4000 system and the bands were quantified by densitometry using Advanced Image Data Analysis software (AIDA). Samples were also analysed using primary antibodies that recognise total ERK1/2, PKB, p38 MAPK and JNK (1:1000) in order to confirm the uniformity of protein loading.

2.7 Immunoprecipitation analysis of TG2 phosphorylation.

H9c2 cells were grown in T175 tissue culture flasks. Following treatments, cells were washed twice with ice cold PBS. The cells were then scraped, collected in 5 ml of PBS and subjected to centrifugation at 300xg (1000 rpm) at room temperature for 5 min. The supernatant was discarded and cell pellet resuspended in 500 µl of ice cold lysis buffer (2 mM EDTA, 1.5 mM MgCl₂, 10% (v/v) glycerol, 0.5% (v/v) IGEPAL, 0.1% (v/v) protease inhibitor cocktail (AEBSF – [4-(2-Aminoethyl)benzenesulfonyl fluoride hydrochloride], Aprotinin, Bestatin hydrochloride, E-64 – [N-(trans-Epoxy succinyl)-L-leucine 4-guanidinobutylamide], Leupeptin hemisulfate salt, Pepstatin A), and 1% (v/v) phosphatase inhibitor cocktail 2 (sodium orthovanadate, sodium molybdate, sodium tartrate and imidazole) and 3 (Cantharidin, (-)-p-Bromolevamisole oxalate, Calyculin A) in PBS). The cells were incubated with lysis buffer for 30 min and then clarified by centrifugation at 4°C for 10 min at 14000xg. The supernatant was collected and following protein estimation, 500 µg of protein was incubated overnight at 4°C with 2 µg of anti-TG2 monoclonal antibody (CUB 7402) or IgG. Immune complexes were precipitated using Pierce™ Classic Magnetic IP/Co-IP kit (Thermo Scientific, Loughborough, UK). The eluted proteins were resolved by 10% SDS-PAGE and western blotting, and then probed using anti-phosphoserine or anti-phosphothreonine antibodies (1:1000). The blots were developed using the Enhanced Chemiluminescence (ECL) detection system and quantified by densitometry, as described above.

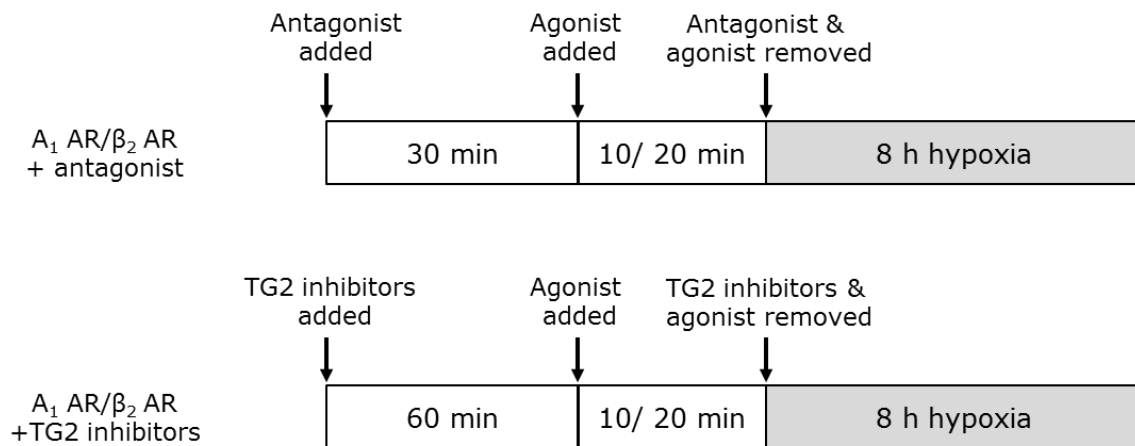
2.8 GPCR-mediated protection against hypoxia- and hypoxia/reoxygenation-induced cell death.

(i) Simulation of ischaemia and/or ischaemia/reperfusion injury:

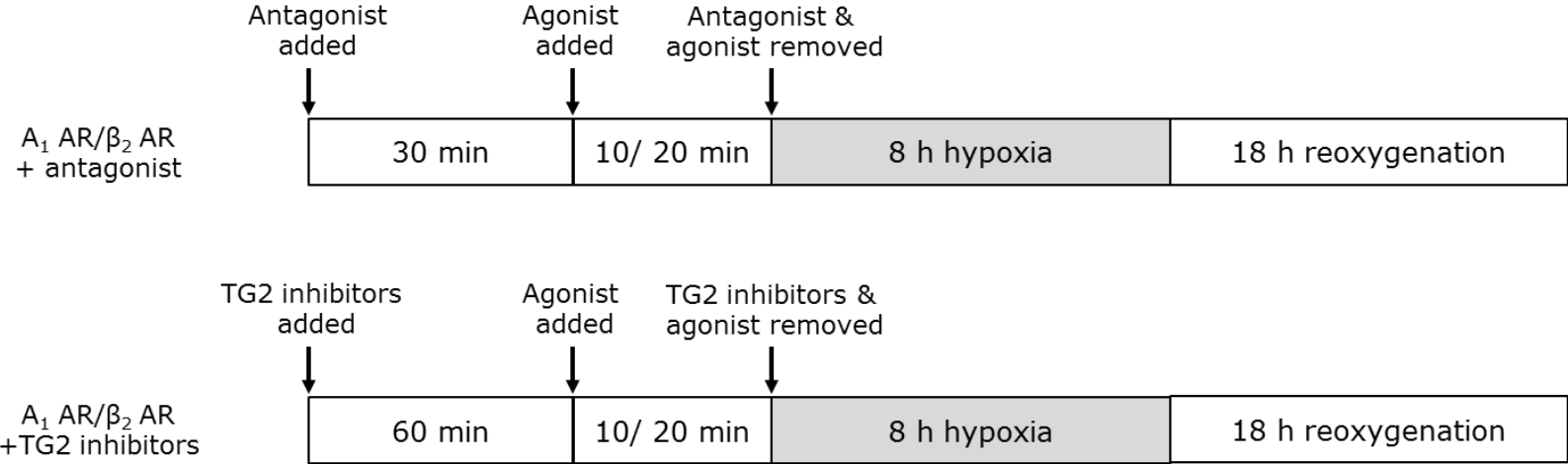
Ischaemia was simulated by means of hypoxia while ischaemia/reperfusion injury was simulated by hypoxia/reoxygenation. Hypoxia was induced by means of Panasonic® O₂/CO₂ incubator. 80% confluent H9c2 cells were placed in glucose- and serum-free DMEM and exposed to 8 h (except for time course experiments) hypoxia using a hypoxic incubator (5% CO₂/1% O₂; 37°C) in which O₂ was replaced with N₂. Normoxic incubation of similar passage numbers were used as controls. Where pharmacological pre- or post-conditioning was needed, cells were incubated with GPCR agonists in 200 µl (96-well microtitre plates), 500 µl (24-well microtitre plates) or 5 ml (T25 tissue culture flasks) serum-free DMEM for 10 min (for A₁ adenosine receptor) or 20 min (for β₂ adrenoceptor); this medium was then discarded and replaced with glucose- and serum-free DMEM for the hypoxic/normoxic incubation. Where appropriate, cells were also treated with GPCR antagonists for 30 min or TG2 inhibitors for 60 min prior to the addition of agonist.

For hypoxia/reoxygenation experiments, cells were exposed to hypoxia for 8 h as described above, and then reoxygenated for 18 h in DMEM containing glucose and 1% serum. Preconditioning was performed prior to hypoxia, Postconditioning occurred at the start of reoxygenation, treatment protocol as before (see Figure 2.1 for summary).

(A) Hypoxia



(B) Hypoxia/reoxygenation preconditioning



(C) Hypoxia/reoxygenation postconditioning

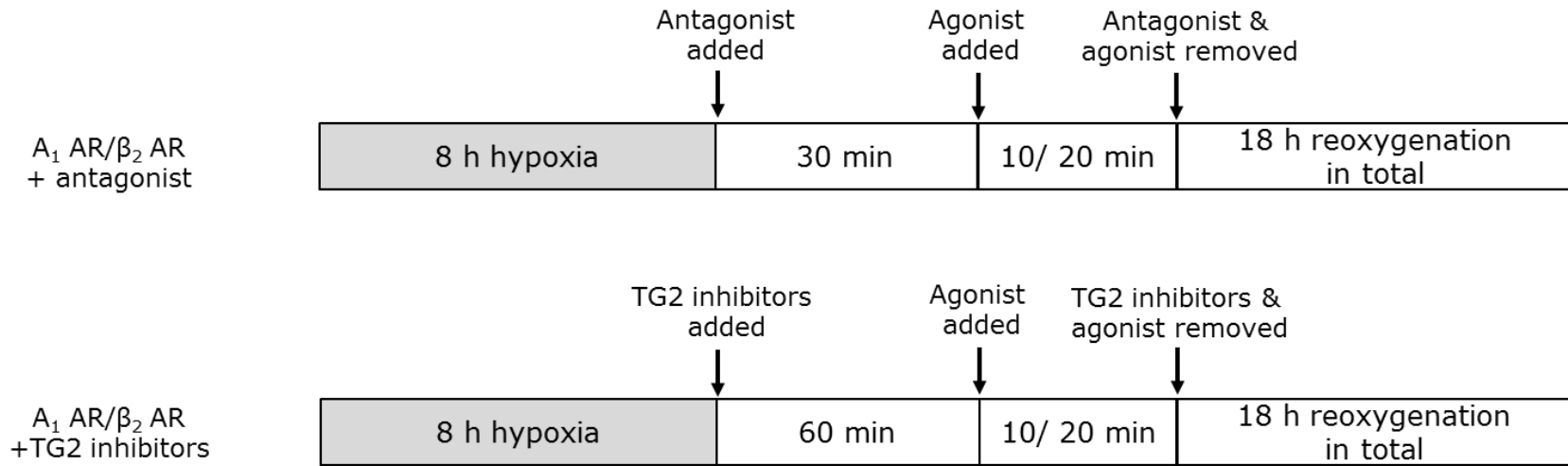


Fig 2.1 Protocol for hypoxia and hypoxia/reoxygenation experiments. Time-matched normoxic and hypoxic controls were performed for each experimental condition.

(ii) MTT reduction assay:

H9c2 cells were seeded in 24-well flat-bottomed plates (15,000 cells/well) and cultured for 24 h in fully supplemented DMEM. Incubations were performed in 500 μ l of the relevant media and an hour prior to completion of periods of hypoxia or hypoxia/reoxygenation, 0.5 mg/ml of MTT (3-(4,5-dimethylthiazol-2-yl)-2,5-diphenyltetrazolium bromide) in the relevant media was added to each well. After completion of this final hour, the medium was aspirated carefully not disturbing the blue insoluble formazan crystals at the bottom of the well. 500 μ l of DMSO was added to each well and gently agitated to solubilise the formazan product. 200 μ l of the resulting solution was transferred to 96-well flat-bottomed plates and the absorbance read at 570 nm using a standard plate reader. Results are expressed as percentage of basal MTT reduction and represent the mean \pm S.E.M. from four independent experiments, each performed in quadruplicate. The order of drug treatments on the layout of the plate was randomised to avoid experimental design bias.

(iii) LDH release assay:

H9c2 cells were seeded in 96-well flat-bottomed plates (5000 cells/well) and cultured for 24 h in fully supplemented DMEM. Incubations were performed in 200 μ l of the relevant media and the cell death measured using the colorimetric CytoTox 96[®] non-radioactive cytotoxicity assay kit (Promega[®], Southampton, UK). This kit measures lactate dehydrogenase (LDH) leakage from the cell membrane, thereby providing an indirect method of measuring cell toxicity. There are two reactions involved. Firstly, the LDH released from the cells catalyses lactate and NAD^+ to form pyruvate and NADH. The second reaction is catalysed by the dehydrogenase enzyme diaphorase (present in substrate mix provided in the kit) which involves formation of NAD^+ and red formazan product which is then measured colorimetrically.

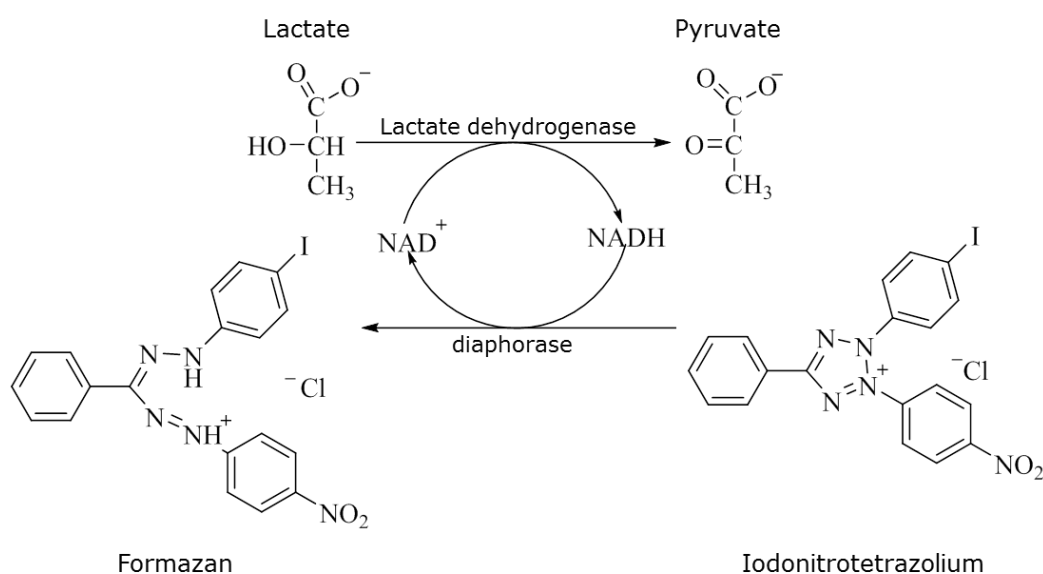


Fig 2.2 Reactions involved in detection of cell viability using LDH release assay.

Once incubations were finished, the plates were centrifuged at 300xg for 5 min to sediment any cell debris. 50 μ l of the supernatant was transferred to a new non-sterile 96-well flat-bottomed plates and 50 μ l of reconstituted assay buffer substrate solution (10 ml of assay buffer in one bottle of substrate provided in the kit) was added to each well. The assay plate was wrapped in foil and incubated for 30 min at room temperature with gentle agitation. The reaction was terminated by addition of 50 μ l stop solution (1 M acetic acid, provided in the kit) to each well and the absorbance read at 490 nm using a standard plate reader. Results are expressed as percentage of basal LDH release and represent the mean \pm S.E.M. from four independent experiments, each performed in sextuplicate. The order of drug treatments on the layout of the plate was randomised to avoid experimental design bias.

(iv) Caspase-3 activation:

H9c2 cells were cultured in T25 tissue culture flasks, until 80% confluent, in fully supplemented DMEM. Where appropriate, treatments were performed in 5 ml of respective media. This was replaced with 5 ml glucose- and serum-free DMEM for the 8 h incubation under hypoxic conditions and/or DMEM containing glucose and 1% serum during reoxygenation. Following incubations, cells were lysed and subjected to western blotting as described above to detect cleaved caspase-3.

2.9 Proteomic analysis of TG2 biotin-X-cadaverine labelled substrates.

(i) CaptAvidinTM-agarose sedimentation based affinity purification:

Cellular proteins acting as substrates for endogenous TG2-catalysed polyamine incorporation reactions were investigated as described by Singh et al., (1995). Briefly, H9c2 cells were grown in T175 tissue culture flasks and cultured until 80% confluent in fully supplemented DMEM. Cells were then exposed to fresh fully supplemented DMEM containing 1 mM biotin-x-cadaverine and incubated for 6 h (Perry et al., 1995). Following incubation, cells were treated as described in Figure legends. Following treatments, cells were washed twice with ice cold PBS and subjected to 500 μ l of lysis buffer (50 mM Tris-HCl pH 8.0, 0.5% (w/v) sodium deoxycholate, 0.1% (v/v) protease inhibitor cocktail and 1% (v/v) phosphatase inhibitor cocktail 2 and 3). The cells were incubated in the lysis buffer on ice for 30 min, scraped and clarified by centrifugation at 4°C for 10 min at 14000xg. The supernatant was collected and following protein estimation, 500 μ g of protein was incubated overnight at 4°C along with 500 μ l of biotin binding buffer (50 mM citrate phosphate buffer pH 4.0) and 200 μ l of CaptAvidinTM-agarose sedimentation beads (Life Technologies, UK). The next day, protein substrates were eluted according to the manufacturer's protocol and the elution's subjected to 4-15% gradient SDS-PAGE. The separated proteins were stained with Coomassie blue and visualised using LAS 4000 system. The bands were

quantified by densitometry using Advanced Image Data Analysis software (AIDA) as described previously.

(ii) Mass spectrometry:

Following pre-treatment with 1 mM biotin-X-cadaverine, H9c2 cells were treated with A₁ adenosine receptor or β_2 adrenoceptor agonists and lysed as described above. The proteins labelled with biotin-X-cadaverine were enriched using CaptAvidinTM-agarose and these biotin-X-cadaverine labelled proteins were processed for trypsin digestion (Trypsin, proteomics grade; Sigma-Aldrich, UK). For trypsin digestion: samples (~50 μ g protein) were reduced and alkylated (1 μ l 0.5 M DTT, 56°C for 20 min; 2.7 μ l 0.55 M iodoacetamide, room temperature 15 min in the dark), dried in a vacuum concentrator (Eppendorf, UK) and re-suspended in 100 μ l 50 mM tri-ethyl ammonium bicarbonate (TEAB). Sigma Trypsin (2 μ g) was added in 2 μ l of 1 mM HCl, and incubated overnight at 37°C in a thermo mixer. Samples were then evaporated to dryness in a vacuum concentrator and resuspended in 5% (v/v) acetonitrile/0.1% (v/v) formic acid (20 μ l) and transferred to a HPLC vial for SWATH MS (Sequential Windowed Acquisition of all Theoretical fragment ion Mass Spectra) analysis. For the A₁ adenosine receptor, samples (3 μ l) were directly injected by an autosampler (Eksigent nano LC 425 LC system) at 5 μ l/min onto a YMC Triart-C18 column (25 cm, 3 μ m, 300 μ m inner diameter). For the β_2 adrenoceptor, samples (3 μ l) were injected onto an automated trapelute column prior to injecting onto the column. The column was eluted using a gradient elution (2–40% mobile phase B over mobile phase A, followed by wash at 80% mobile phase B and re-equilibration at 5% mobile phase B) over 120 min run time (for spectral library construction using data/information dependent acquisition DDA/IDA) or 60 min run time for SWATH/DIA (Data Independent Acquisition) analysis (Huang et al., 2015). Mobile phases consisted of A: 2% (v/v) acetonitrile, 5% (v/v) DMSO in 0.1% (v/v) formic acid and B: acetonitrile containing 5% (v/v) DMSO in 0.1% (v/v) formic acid. A spectral library was constructed using the output from ProteinPilot 5 (SCIEX) combining 4 IDA runs per group (control and treated) and filtered and aligned to spiked in iRT peptides (Biognosys, Switzerland) using PeakView 2.1 SWATH micro app (SCIEX). SWATH data extraction, quantitation and fold change analysis were carried out using SCIEX OneOmics cloud processing software (<https://basespace.illumina.com/home/index>; Lambert et al., 2013). Further details on this method are given in chapter VII.

(iii) Bio-informatics analysis of mass spectrometry identified substrates:

Following identification by SWATH MS, TG2 substrates representing increased/decreased levels of proteins in eluates from CaptAvidinTM-agarose beads following stimulation of either the A₁ adenosine receptor and β_2 adrenoceptor were further analysed using the Database for Annotation, Visualisation and Integrated

Discovery (DAVID) v6.8 (<https://david.ncifcrf.gov/home.jsp>; Dennis et al, 2003). Once input of the protein substrates was completed, DEFINE KEGG pathway annotation results were chosen. The parameters were set to be stringent by ensuring the p value used was <0.05 and that a minimum of two proteins existed in that pathway. Fold enrichment values were calculated by the software and used to create a graphical representation of the pathway.

(iv) Validation of mass spectrometry derived substrates of TG2:

Following pre-treatment with 1 mM biotin-X-cadaverine, H9c2 cells were treated with A1 adenosine receptor or β_2 adrenoceptor agonists and lysed as described above. The proteins labelled with biotin-X-cadaverine were enriched using CaptAvidinTM-agarose and subjected to immunoprecipitation as described previously, using specific primary antibodies against mass spectrometry-identified proteins. Following immunoprecipitation, western blotting was carried out using with ExtrAvidin[®]-HRP (1:5000 dilution) as neither primary antibody nor secondary antibody was used. After incubation, the blots were washed three times for 5 min each with TBST and developed using the Enhanced Chemiluminescence (ECL) detection system. Digital images of the blots were captured by LAS 4000 system and the bands were quantified by densitometry using Advanced Image Data Analysis software (AIDA) as described previously.

2.10 Statistical analysis

All graphs and statistics (one-way ANOVA followed by Dunnett's multiple comparison test and two-way ANOVA followed by Dunnett's (to compare one mean to other means) or Sidak's (to compare sets of means e.g. normoxia vs hypoxia or hypoxia/reoxygenation) multiple comparison test for group comparison) were performed using GraphPad Prism[®] software (GraphPad Software, Inc., USA). Results represent mean \pm S.E.M. and p values <0.05 were considered statistically significant.

For all concentration responses, a four-parameter logistic equation was used to fit the curve which accounts for top, bottom, slope of the curve and EC₅₀ values. Curve fits were performed using GraphPad Prism[®] software (GraphPad Software, Inc., USA). The drug concentrations, particularly antagonist concentrations, were chosen after calculating the receptor occupancy for each antagonist using the Hill-Langmuir equation. As the affinity (K_A) of the ligand for that receptor is known from the literature, the proportional occupancy (p_A) at a given concentration (x_A) of the drug was calculated using the Hill-Langmuir equation:

$$P_A = (x_A/K_A) / ((x_A/K_A) + (x_B/K_B) + 1).$$

For example, the affinity of Isoprenaline at the β_1 -adrenoceptor is 0.871 μ M and at the β_2 -adrenoceptor is 0.229 μ M and that of the selective β_2 -adrenoceptor antagonist ICI

118551 at the β_1 -adrenoceptor is 302 nM and at the β_2 -adrenoceptor is 0.55 nM (affinity values obtained from Baker, 2005; Baker, 2010). The receptor occupancies in the presence of both ligands were calculated as follows:

Proportion occupied (p_A) by 100 nM (x_A) ICI 118551 (K_A) in the presence of 1 μ M (x_B) isoprenaline (K_B) for β_2 -adrenoceptors:

$$P_A = (x_A/K_A) / ((x_A/K_A) + (x_B/K_B) + 1).$$

$$P_A = (100/0.55) / ((100/0.55) + (1/0.229) + 1).$$

$$P_A = 181.8 / (181.8 + 4.37 + 1).$$

$$P_A = 181.8 / 187.17.$$

$$P_A = 0.971.$$

The proportion occupied (p_A) can be converted to percentage occupied by multiplying it by 100.

$$P_A = 97\%$$

Proportion occupied (p_A) by 100 nM (x_A) ICI 118551 (K_A) in the presence of 1 μ M (x_B) isoprenaline (K_B) for β_1 -adrenoceptors:

$$P_A = (x_A/K_A) / ((x_A/K_A) + (x_B/K_B) + 1).$$

$$P_A = (100/302) / ((100/302) + (1/0.871) + 1).$$

$$P_A = 0.33 / (0.33 + 1.15 + 1).$$

$$P_A = 0.33 / 2.48.$$

$$P_A = 0.133.$$

The proportion occupied (p_A) can be converted to percentage occupied by multiplying it by 100.

$$P_A = 13\%$$

All other receptor occupancies were calculated in the same way.

CHAPTER III: Functional GPCR and Transglutaminase expression in H9c2 cells

Prior to investigating the modulation of TG2 activity by GPCRs and its cardioprotective effects, it is necessary to determine whether TG2 and other TG isoforms along with the GPCRs intended to target (adenosine receptors and β -adrenoceptors) are functionally expressed in H9c2 cells. Hence, this chapter aims to determine the mRNA expression and functional expression of adenosine receptors and β -adrenoceptors via RT-PCR analysis, cAMP accumulation and calcium imaging. Subsequently, to determine which TG isoforms (TG1, TG2 and TG3) are expressed in these cells via western blotting and confocal microscopy.

3.1. Functional expression of adenosine receptors on H9c2 cells.

RT-PCR analysis

A_{1R} , A_{2AR} , A_{2BR} and A_{3R} adenosine receptor mRNA expression in both mitotic and differentiated H9c2 cells was determined by RT-PCR analysis. As shown in figure 3.1, mRNA encoding for A_{1R} and A_{3R} adenosine receptors was observed in mitotic H9c2 cells, whereas only mRNA for the A_{2AR} adenosine receptor was present in differentiated H9c2 cells. Faint expression of the A_{1R} adenosine receptor was observed in differentiated H9c2 cells. There was no observable expression of the A_{2BR} adenosine receptor in either mitotic or differentiated H9c2 cells.

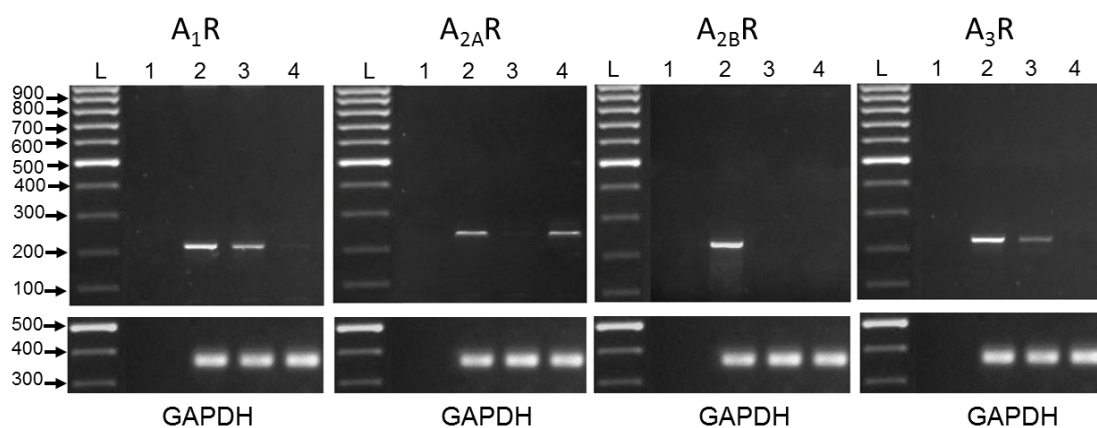


Fig. 3.1: Adenosine receptor mRNA expression in H9c2 cells. mRNA isolated from H9c2 cells was subjected to RT-PCR using intron spanning A_{1R} , A_{2AR} , A_{2BR} and A_{3R} adenosine receptor gene-specific primers. mRNA sample isolated from rat brain (A_{1R}), rat eye (A_{2AR} and A_{2BR}) and rat lung (A_{3R}) were used as positive controls. L: 100 bp DNA standard; lane 1: no DNA control (DEPC water); lane 2: positive control; lane 3: mitotic H9c2 cell-derived mRNA; lane 4: differentiated H9c2 cell-derived mRNA. mRNA control using GAPDH primers is shown in the lower panel. The predicted transcript sizes for A_{1R} , A_{2AR} , A_{2BR} , A_{3R} adenosine receptor and GAPDH are 207, 2049, 250, 237 and 392 bp. The results presented are representative of three independent experiments.

cAMP accumulation

Following mRNA assessment, functional expression of adenosine receptors on H9c2 cells was investigated using a cAMP accumulation assay and calcium imaging. The selective A_1 adenosine receptor agonist, CPA, revealed substantial inhibition of forskolin-induced cAMP accumulation ($pEC_{50} = 9.19 \pm 0.16$; $n=4$; figure 3.2) in mitotic H9c2 cells. However, 10 μ M CPA resulted in beginning of reversal of the inhibition of cAMP accumulation observed at lower concentrations suggesting G_s -coupling. CGS 21680, the selective A_{2A} adenosine receptor agonist, did not generate any cAMP accumulation (figure 3.3) suggesting that even though mRNA was detected, this receptor is not functionally expressed in differentiated H9c2 cells.

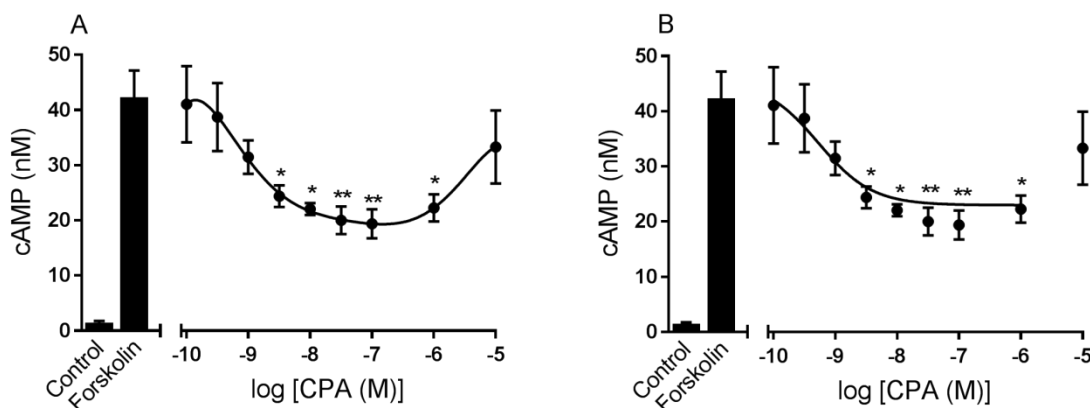


Fig 3.2 Effect of the selective A_1 adenosine receptor agonist CPA on cAMP accumulation in H9c2 cells. Cells were pre-treated with the indicated concentrations of CPA for 5 min prior to addition of 10 μ M forskolin for 10 min. Levels of cAMP were determined as described in section 2.5 (i) of chapter II. Data are presented as levels of cAMP in nM. The results represent the mean \pm S.E.M. of four experiments each performed in triplicate. * $P < 0.05$, ** $P < 0.01$, (A) a polynomial curve fit to illustrate G_s -coupling and (B) sigmoidal four-parameter logistic curve fit to determine the EC_{50} values.

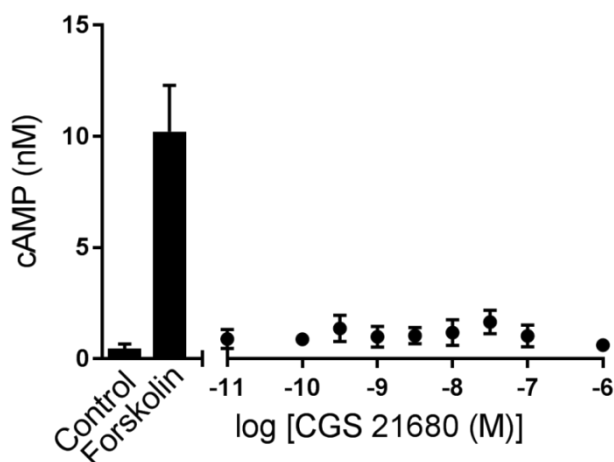


Fig 3.3: Effect of the selective A_{2A} adenosine receptor agonist CGS 21680 on cAMP accumulation in differentiated H9c2 cells. Cells were pre-treated with the indicated concentrations of CGS 21680 for 15 min. Levels of cAMP were determined as described in section 2.5 (i) of chapter II. Data are presented as levels of cAMP in nM. The results represent the mean \pm S.E.M. of four experiments each performed in triplicate.

A₁ adenosine receptor-mediated Ca²⁺ signalling

Experiments were performed to assess whether the A₁ adenosine receptor triggers intracellular Ca²⁺ responses in H9c2 cells. CPA (100 nM) triggered intracellular Ca²⁺ oscillations (figure 3.4A, B) which were dependent on extracellular Ca²⁺ (figure 3.4C). Furthermore, pertussis toxin (PTX, 100 ng/ml for 16 h; figure 3.4D) and the A₁ adenosine receptor antagonist DPCPX (1 μM; figure 3.4E) blocked CPA-induced Ca²⁺ signalling.

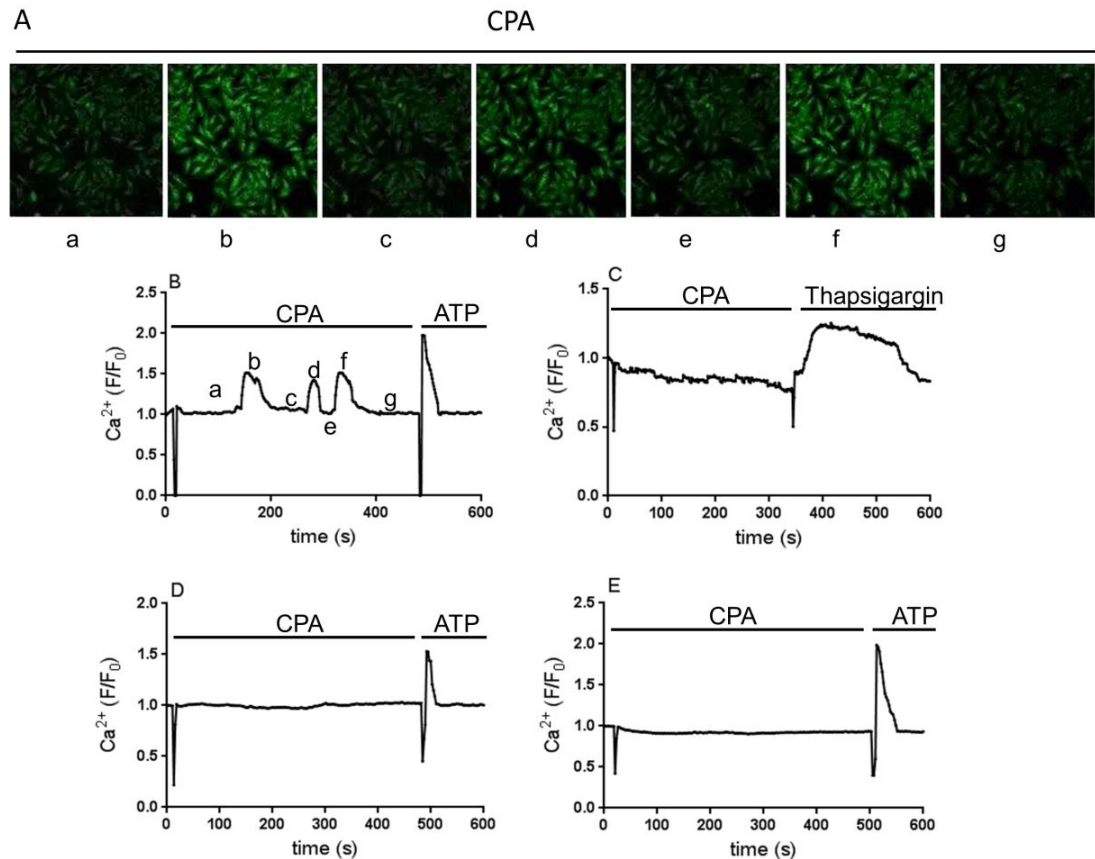


Fig 3.4: Effect of the A₁ adenosine receptor agonist CPA on [Ca²⁺]_i in H9c2 cells. (A) Confocal images of CPA (100 nM)-induced Ca²⁺ oscillations in the presence of extracellular Ca²⁺ (1.3 mM). The panel letters (a–g) correspond to the time points shown in trace B. (B) The A₁ adenosine receptor agonist CPA triggered pronounced Ca²⁺ oscillations in the presence of extracellular Ca²⁺ (1.3 mM). (C) Oscillations induced by CPA were absent during experiments performed in nominally Ca²⁺-free buffer and 0.1 mM EGTA. In these experiments, depletion of intracellular Ca²⁺ stores with thapsigargin (5 μM) was still evident which suggested that the intracellular Ca²⁺ stores were still intact. (D) Responses to CPA in the presence of extracellular Ca²⁺ were abolished by the A₁ adenosine receptor antagonist DPCPX (1 μM) and (E) following treatment with PTX (100 ng/ml for 16 h). ATP (10 μM) was added where indicated as a positive control. Similar results were obtained in three other experiments, each of several replicates.

Adenosine (100 μM) also triggered intracellular Ca²⁺ responses (figure 3.5A, B) which were also dependent on extracellular Ca²⁺ (figure 3.5C). Furthermore, DPCPX (1 μM) and PTX (100 ng/ml for 16 h; figure 3.5D, E respectively) blocked adenosine-induced Ca²⁺ signalling confirming the role of G_{i/o}-proteins and the A₁ adenosine receptor in adenosine-mediated responses.

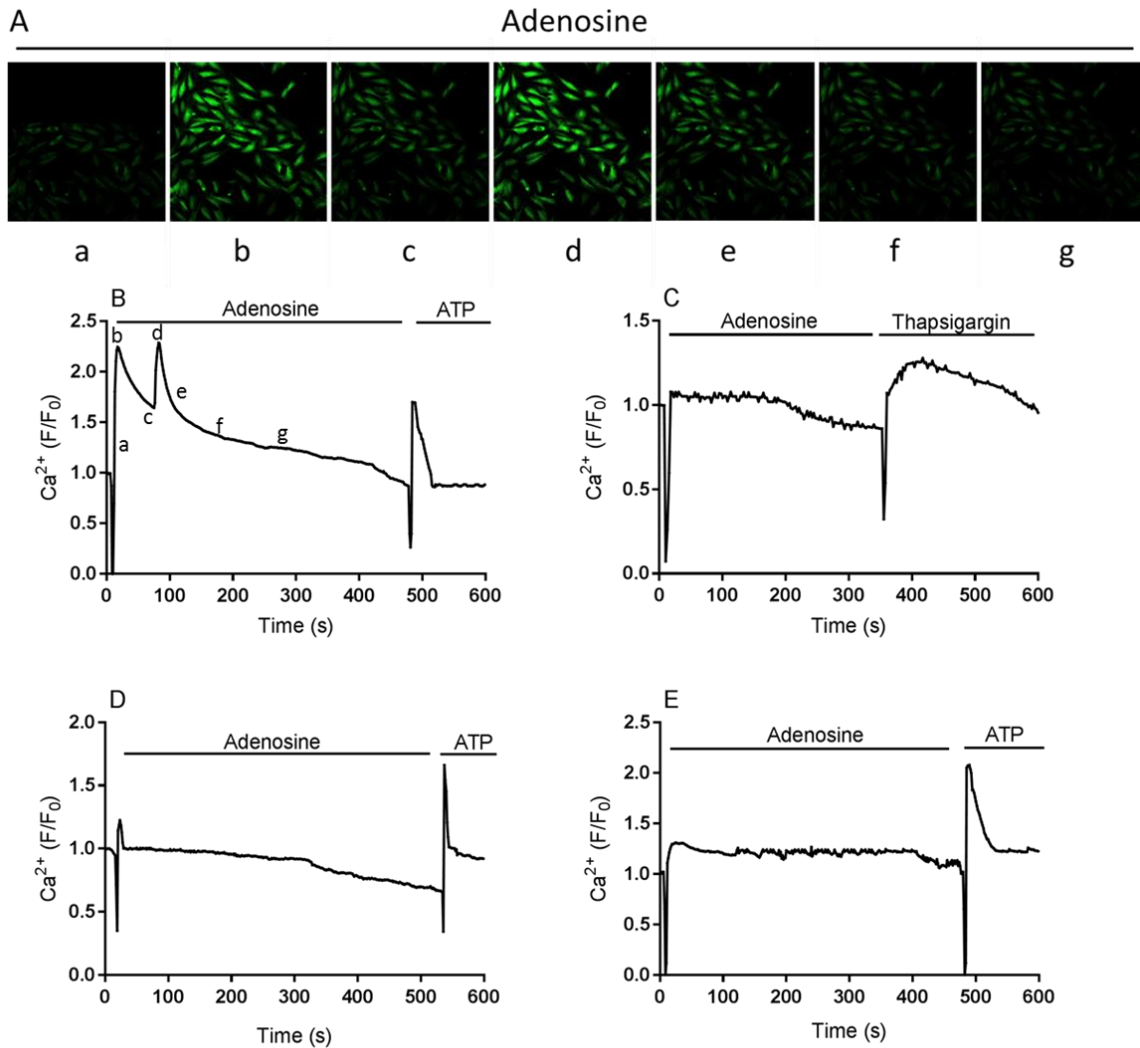


Fig 3.5: Effect of adenosine on $[Ca^{2+}]_i$ in H9c2 cells. (A) Confocal images of adenosine (100 μ M)-induced Ca^{2+} responses in the presence of extracellular Ca^{2+} (1.3 mM). The panel letters (a–g) correspond to the time points shown in trace B. (B) Adenosine triggered pronounced Ca^{2+} responses in the presence of extracellular Ca^{2+} (1.3 mM). (C) Responses induced by adenosine were absent during experiments performed in nominally Ca^{2+} -free buffer and 0.1 mM EGTA. In these experiments, depletion of intracellular Ca^{2+} stores with thapsigargin (5 μ M) was still evident which suggested that the intracellular Ca^{2+} stores were still intact. (D) Responses to adenosine in the presence of extracellular Ca^{2+} were abolished by the A_1 adenosine receptor antagonist DPCPX (1 μ M) and (E) following treatment with PTX (100 ng/ml for 16 h). ATP (10 μ M) was added where indicated as a positive control. Similar results were obtained in three other experiments, each of several replicates.

These data suggest that mitotic H9c2 cells functionally express the A_1 adenosine receptors. However, the A_{2A} adenosine receptor mRNA is encoded but is not functionally expressed in differentiated H9c2 cells.

3.2. Functional expression of β -adrenoceptors on H9c2 cells.

RT-PCR analysis

β_1 , β_2 and β_3 adrenoceptors mRNA expression was determined in mitotic and differentiated H9c2 cells by RT-PCR analysis. As shown in figure 3.6, mRNA was

detected in mitotic and differentiated H9c2 cells for all three β -adrenoceptor subtypes with a rank order of $\beta_2 > \beta_1 = \beta_3$.

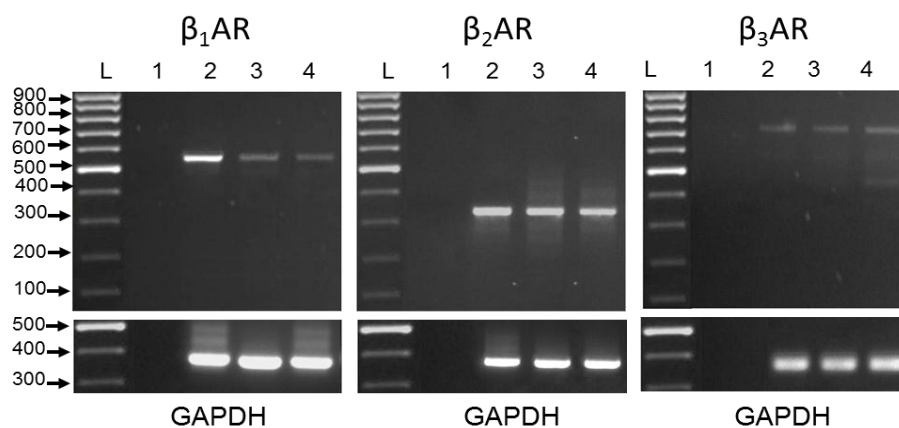


Fig 3.6: β -adrenoceptor mRNA expression in H9c2 cells. mRNA isolated from mitotic and differentiated H9c2 cells was subjected to RT-PCR using intron spanning β_1 , β_2 and β_3 -adrenoceptor gene specific primers. mRNA samples isolated from rat heart (β_1 -adrenoceptor) and rat lung (β_2 and β_3 -adrenoceptor) were used as positive controls. L: 100 bp DNA standard; lane 1: no DNA control; lane 2: positive control; lane 3: mitotic H9c2 cell-derived mRNA; lane 4: differentiated H9c2 cell-derived mRNA. mRNA control using GAPDH primers is shown in the lower panel. The predicted transcript sizes for β_1 , β_2 and β_3 -adrenoceptor and GAPDH are 599, 323, 724 and 392 bp. The results presented are representative of three independent experiments.

cAMP accumulation

Following mRNA assessment, functional expression of β -adrenoceptor subtypes on mitotic H9c2 cells was investigated using a cAMP accumulation assay. The selective β_2 -AR agonist formoterol ($pEC_{50} = 8.9 \pm 0.1$; $n=3$) stimulated a robust increase in cAMP (90% of forskolin max response), confirming the functional expression of the β_2 -AR in H9c2 cells (figure 3.7B). Initial experiments using the non-selective β -AR agonist isoprenaline revealed only a modest increase in cAMP (figure 3.7A; $pEC_{50} = 7.63 \pm 0.07$; $n=4$; 22% of forskolin max response). However, following treatment of cells with PTX ($G_{i/o}$ -protein in-activator; 100 ng/ml) for 16 h, isoprenaline triggered a near maximal cAMP response (figure 3.7A; $pEC_{50} = 8.68 \pm 0.09$; $n=4$; 96% of forskolin max response). In marked contrast, cAMP accumulation in response to formoterol was insensitive to PTX (figure 3.7B; $pEC_{50} = 8.70 \pm 0.24$; $n=4$; 89% of forskolin max response). These data suggest that in the absence of PTX, isoprenaline-induced cAMP accumulation is suppressed due to $G_{i/o}$ -protein coupling. From here on all isoprenaline-induced cAMP accumulation was performed in the presence of PTX. The selective β_3 -AR agonist CL 316243 did not generate any cAMP accumulation (figure 3.7C) suggesting that even though the mRNA is detected, this subtype is not functional in H9c2 cells.

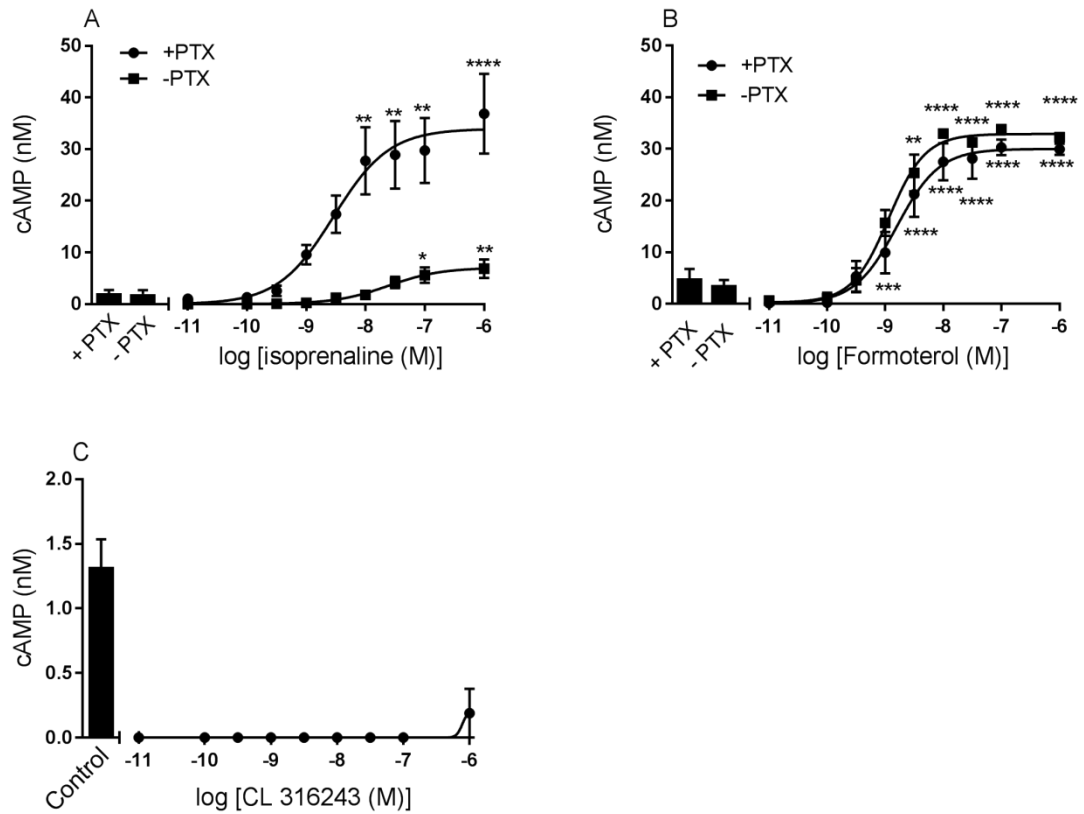


Fig. 3.7: β -adrenoceptor agonist-induced cAMP accumulation in H9c2 cells. Where indicated cells were pre-treated for 16 h with 100 ng/ml PTX. Cells were stimulated for 20 min with the indicated concentrations of (A) isoprenaline, (B) formoterol and (C) CL 316243. Levels of cAMP were determined as described in section 2.5 (i) of chapter II. Data are presented as mean levels of cAMP (in nM) \pm S.E.M. of four experiments each performed in triplicate. ** $P < 0.01$ and **** $P < 0.0001$.

Isoprenaline-induced cAMP responses were abolished by the non-selective β -adrenoceptor antagonist propranolol (100 nM) and the selective β_2 -AR antagonist ICI 118,551 (100 nM), while the selective β_1 -AR antagonist CGP 20712 (100 nM) part-inhibited the response (figure 3.8A). This indicates that there is some activity of the β_1 -AR in H9c2 cells. Formoterol-induced cAMP responses were blocked by the non-selective β -adrenoceptor antagonist propranolol (100 nM) and the selective β_2 -AR antagonist ICI 118,551 (100 nM), whereas the selective β_1 -AR antagonist CGP 20712 (100 nM) had no effect (figure 3.8B).

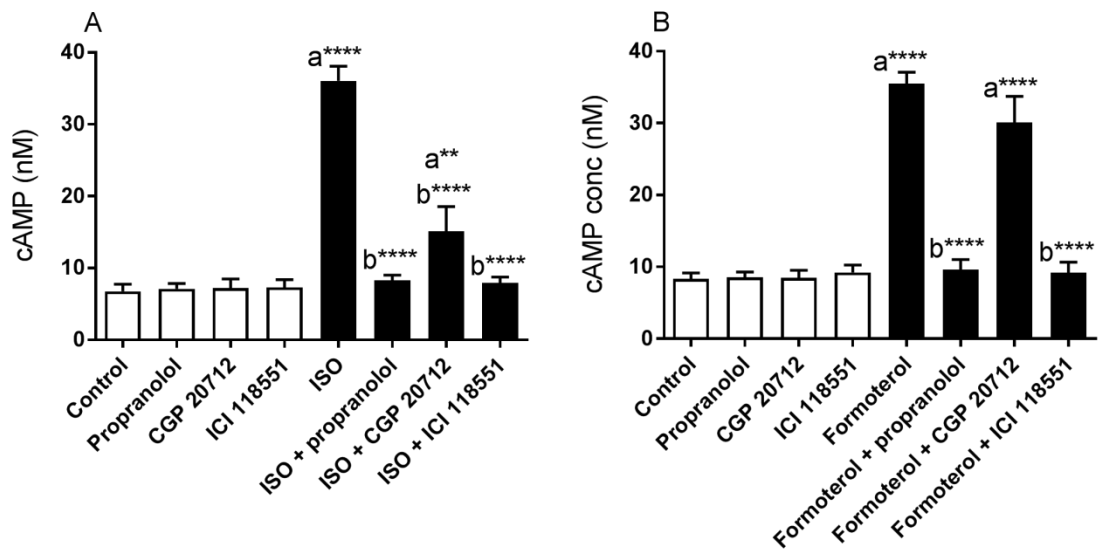


Fig. 3.8: Effect of β -adrenoceptor antagonists on isoprenaline and formoterol-induced cAMP accumulation in H9c2 cells. Cells were pre-treated for 30 min with propranolol (100 nM), CGP 20712 (100 nM), or ICI 118551 (100 nM) prior to 20 min stimulation with (A) isoprenaline (10 nM) or (B) formoterol (10 nM). Levels of cAMP were determined as described in section 2.5 (i) of chapter II. Data are presented as mean levels of cAMP (in nM) \pm S.E.M. of four experiments each performed in triplicate. **** P <0.0001, (a) versus control and (b) versus 10 nM isoprenaline or 10 nM formoterol alone.

To confirm the functional expression of β_2 -AR, cimaterol (β_2 -AR selective agonist) was investigated. Cimaterol ($pEC_{50} = 7.50 \pm 0.06$; $n=4$) stimulated a modest increase in cAMP, confirming the functional expression of the β_2 -AR in H9c2 cells (figure 3.9A). Cimaterol-induced cAMP responses were blocked by the non-selective β -adrenoceptor antagonist propranolol (100 nM) and the selective β_2 -AR antagonist ICI 118,551 (100 nM), whereas the selective β_1 -AR antagonist CGP 20712 (100 nM) had no effect (figure 3.9C). These data support the previous finding suggesting that the β_2 -AR is functionally active in H9c2 cells. Dobutamine as a partial agonist of the β_2 -AR stimulated only a small cAMP response ($pEC_{50} = 7.40 \pm 0.09$; $n=3$; figure 3.9B). Due to the lack of a selective β_1 -AR agonist, the functional expression of this subtype was assessed by determining dobutamine-induced cAMP accumulation (non-selective β_1 and β_2 agonist). Dobutamine-induced cAMP responses were blocked by the non-selective β -adrenoceptor antagonist propranolol and the selective β_2 -AR antagonist ICI 118,551, whereas the selective β_1 -AR antagonist CGP 20712 had no effect (figure 3.9D). Overall these data suggest functional expression of only the β_2 -AR in mitotic H9c2 cells.

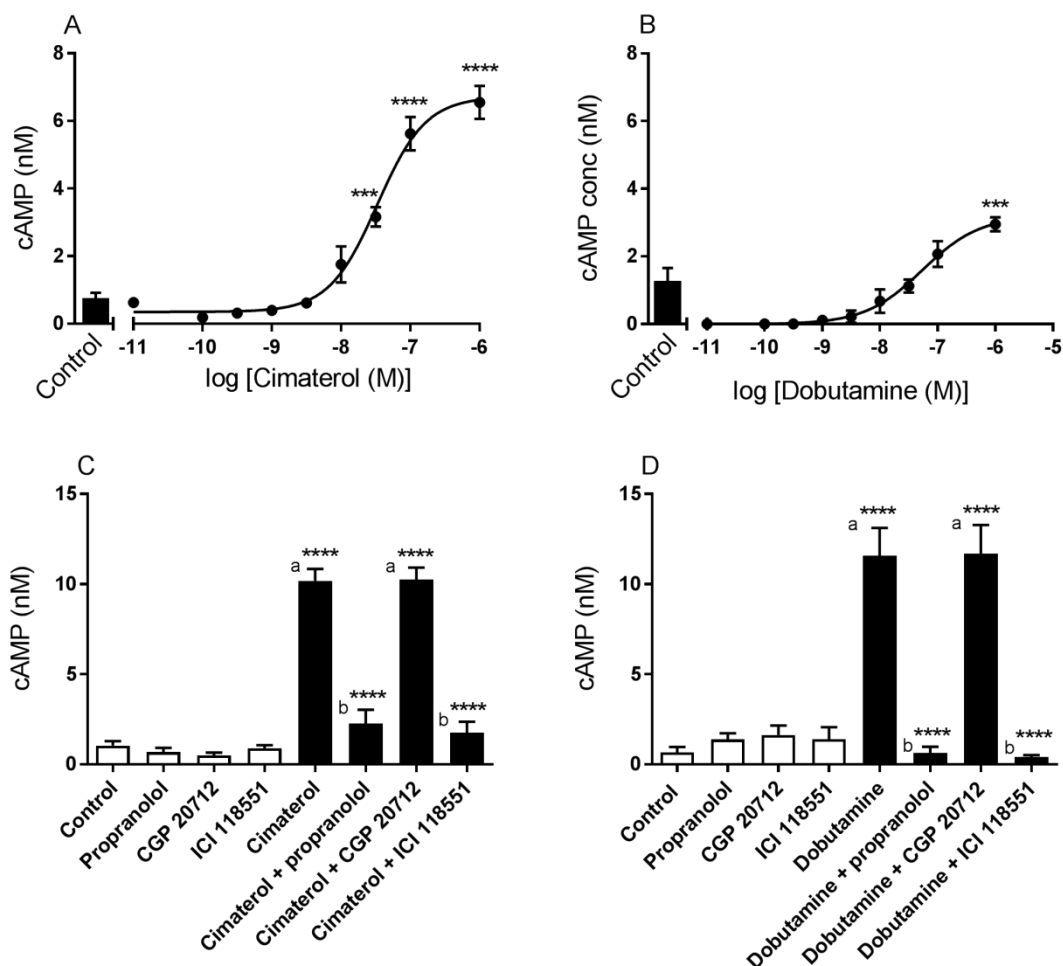


Fig. 3.9: β -adrenoceptor agonist-induced cAMP accumulation in H9c2 cells. Cells were stimulated for 20 min with the indicated concentrations of (A) cimaterol and (B) dobutamine. Cells were pre-treated for 30 min with propranolol (100 nM), CGP 20712 (100 nM), or ICI 118551 (100 nM) prior to 20 min stimulation with (C) cimaterol (1 μ M) and (D) dobutamine (1 μ M). Levels of cAMP were determined as described in section 2.5 (i) of chapter II. Data are presented as mean levels of cAMP (in nM) \pm S.E.M. of four experiments each performed in triplicate. *** P <0.001, and **** P <0.0001, (a) versus control and (b) versus 1 μ M cimaterol or 1 μ M dobutamine alone.

Since the response generated by cimaterol and dobutamine was modest, it was of interest to determine whether these agonists also coupled to $G_{i/o}$ -protein. To determine this, cimaterol and dobutamine along with isoprenaline, formoterol, CL 316243 and forskolin were used at their maximal concentrations in presence and absence of PTX. Also, to verify if the $G_{i/o}$ -protein coupling observed with isoprenaline (and perhaps with the above mentioned agonists) was an event occurring only in H9c2 cells, BEAS-2B R1 cells (human bronchial epithelial cells) which endogenously express the β_2 -AR (Kelsen et al, 1997) were used as a positive control. Culturing and seeding of BEAS-2B R1 cells was similar to H9c2 cells as described in section 2.2 of chapter II. Isoprenaline (10 μ M) and cimaterol (10 μ M) only generated a modest cAMP-response in the absence of PTX in H9c2 cells (figure 3.10A), whereas they generated robust cAMP-accumulation in the presence of PTX (figure 3.10B). In contrast, responses to formoterol (1 μ M), CL 316243 (10 μ M), dobutamine (10 μ M) and forskolin (10 μ M) in

H9c2 cells were unaffected by PTX pre-treatment. The above mentioned agonists (except for CL 316243) generated robust cAMP-accumulation in BEAS-2B R1 cells (figure 3.10C) suggesting the β_3 -AR subtype is not functionally expressed on these cells. No significant changes were observed in the cAMP response profiles of these agonists following PTX pre-treatment, except for dobutamine which generated slightly more cAMP following PTX pre-treatment (figure 3.10D; 68% of forskolin max response in presence of PTX as compared to 40% of forskolin max response in absence of PTX) suggesting that the $G_{i/o}$ -protein coupling event is exclusive to H9c2 cells (at least for isoprenaline and cimaterol).

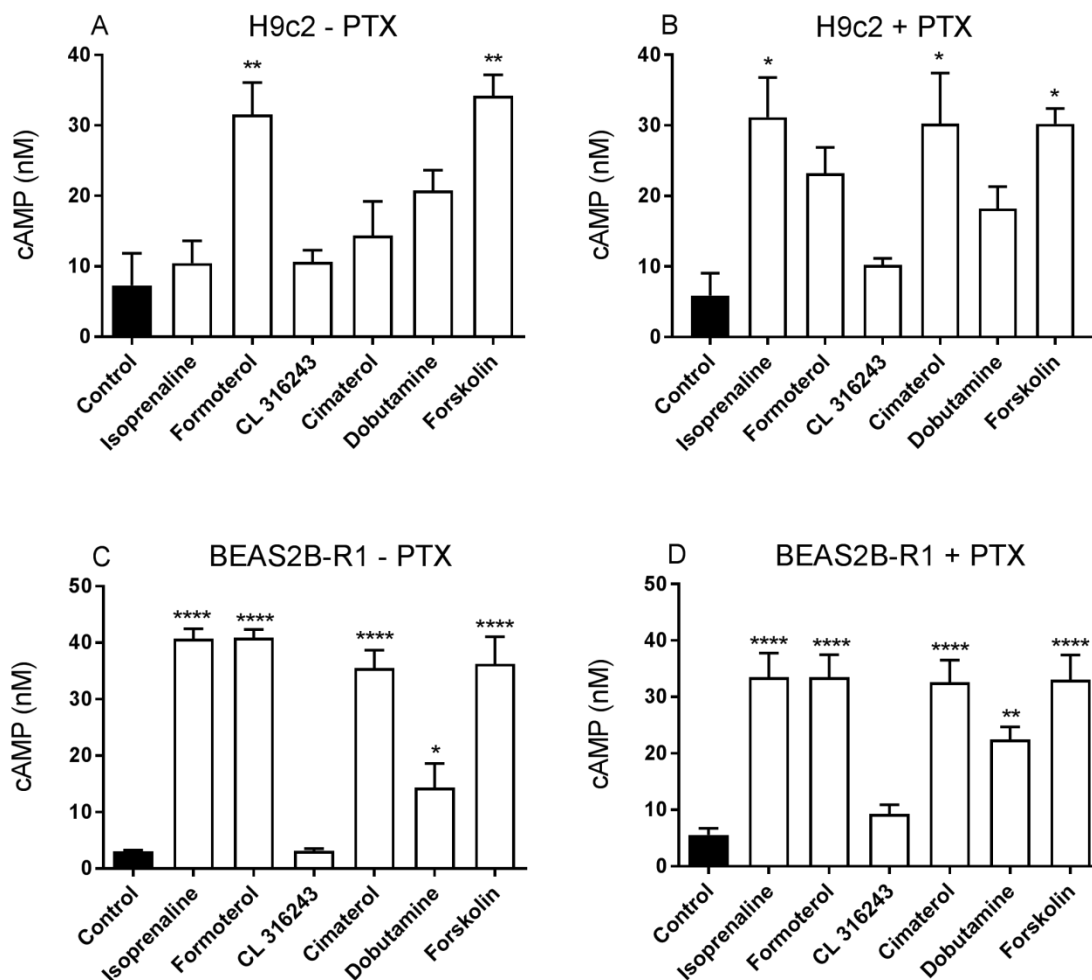


Fig. 3.10: β -adrenoceptor agonist-induced cAMP accumulation in H9c2 and BEAS-2B R1 cells. H9c2 cells were treated with isoprenaline (10 μ M), formoterol (1 μ M), CL 316243 (10 μ M), cimaterol (10 μ M), dobutamine (10 μ M) and forskolin (10 μ M) for 20 min in absence of PTX pre-treatment (A) and following 16 h pre-treatment with PTX ($G_{i/o}$ -protein in-activator; 100 ng/ml; B). BEAS-2B R1 cells were treated with isoprenaline (10 μ M), formoterol (1 μ M), CL 316243 (10 μ M), cimaterol (10 μ M), dobutamine (10 μ M) and forskolin (10 μ M) for 20 min in absence of PTX pre-treatment (C) and following 16 h pre-treatment with PTX ($G_{i/o}$ -protein in-activator; 100 ng/ml; D). Levels of cAMP were determined as described in section 2.5 (i) of chapter II. Data are presented as mean levels of cAMP (in nM) \pm S.E.M. of four experiments each performed in triplicate. * P <0.05, ** P <0.01, and **** P <0.0001 relative to control.

Beta-adrenoceptor-mediated Ca^{2+} signalling

To determine if formoterol and isoprenaline were able to generate Ca^{2+} responses in H9c2 cells, Ca^{2+} imaging was performed. Formoterol (1 μ M) did not trigger any intracellular Ca^{2+} responses (figure 3.11A; over three independent experiments 18 wells were observed and no response was observed). Isoprenaline (10 μ M) on occasion did trigger intracellular Ca^{2+} responses. Figure 3.11B represents a trace in which isoprenaline did not generate any Ca^{2+} response while figure 3.11C, D represent a trace in which isoprenaline did generate a Ca^{2+} response (over three independent experiments 18 wells were observed and in 7 wells isoprenaline generated a response i.e. 39%). It is important to note that in all experiments, ATP was used as a positive control to check if the Ca^{2+} stores were still intact.

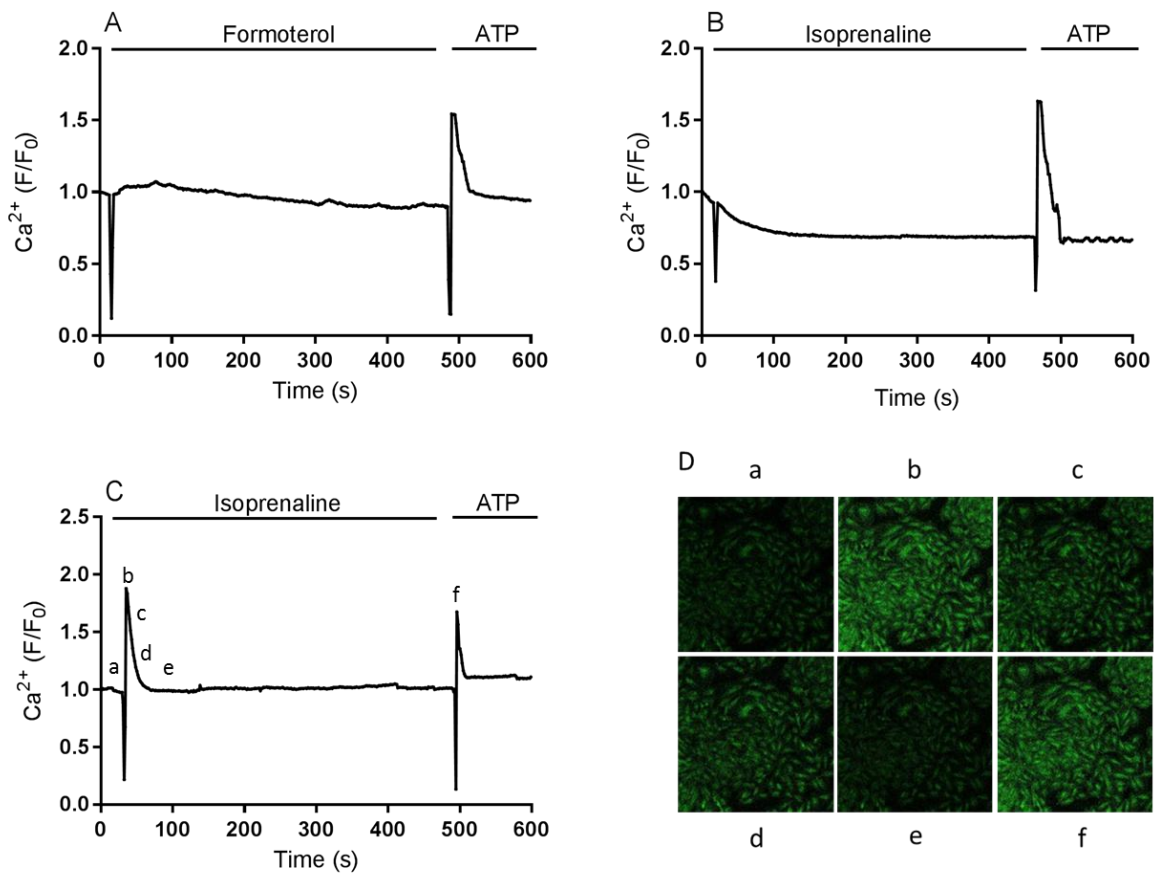


Fig 3.11: Effect of β -adrenoceptor agonists on $[Ca^{2+}]_i$ responses in H9c2 cells. (A) No Ca^{2+} responses were observed when treated with formoterol (1 μ M). (B) Isoprenaline triggered no Ca^{2+} responses on occasion. (C) Isoprenaline on occasion (38.88%) triggered pronounced Ca^{2+} responses in the presence of extracellular Ca^{2+} (1.3 mM). (D) Confocal images of isoprenaline (1 μ M)-induced Ca^{2+} responses in the presence of extracellular Ca^{2+} (1.3 mM). The panel letters (a–f) correspond to the time points shown in trace C. ATP (10 μ M) was added as a positive control. Similar results were obtained in three other experiments.

3.3. Characterisation of TG expression pattern in H9c2 cells.

Western blot analysis was performed to compare the expression of TG isoforms in mitotic and differentiated H9c2 cells. TG1, TG2 and TG3 expression were detected in both mitotic and differentiated H9c2 cells (figure 3.12). This indicates that not only TG2 but other TG isoforms are present in H9c2 cells.

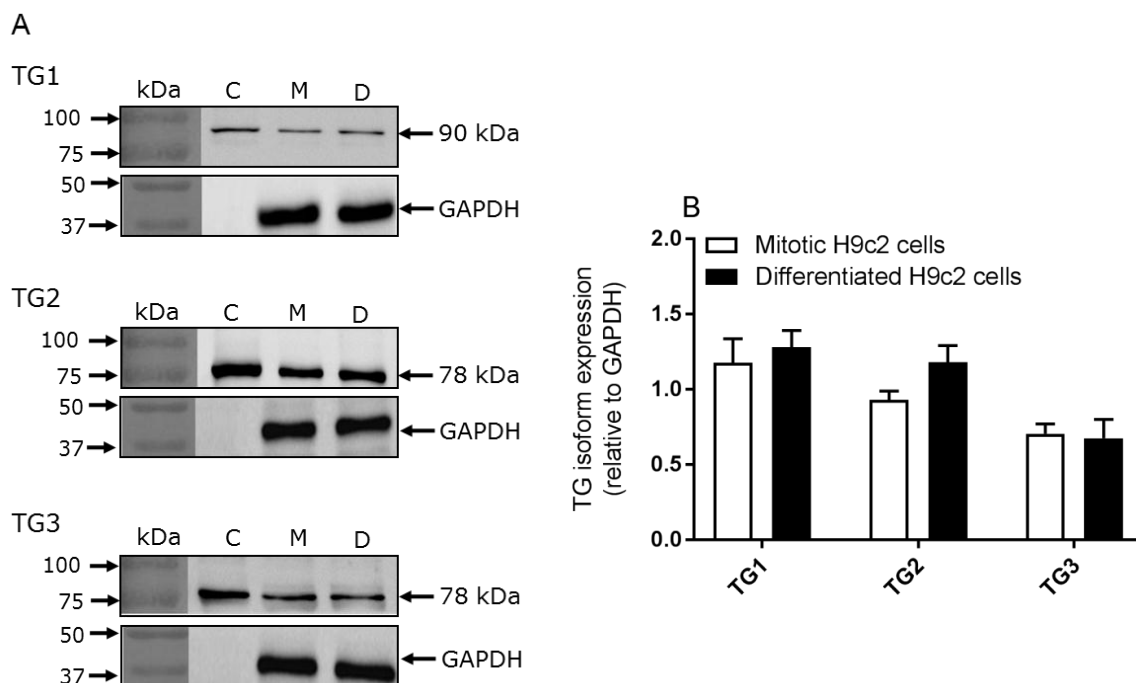


Fig 3.12: Protein expression of TG isoforms in mitotic and differentiated H9c2 cells. (A) cell lysates (20 μ g) from mitotic (M) and differentiated (D) H9c2 cells were analysed for TG1, TG2 and TG3 expression by western blotting using TG isoform-specific antibodies. Loading control using GAPDH is shown in the lower panel. 0.1 ng from purified enzymes (C) were used as positive control. (B) Quantified data are expressed as the ratio of TG isoform to GAPDH and represent the mean \pm S.E.M. from three independent experiments.

Furthermore, to determine if the levels expressed are localised to a particular area of the cell, immunofluorescence by confocal microscopy was performed using TG isoform-specific antibodies and counterstained by the nuclear stain DAPI (figure 3.13). Immunofluorescence staining indicated that TG1 and TG3 are mainly localised in the perinuclear region. TG1 is also sparsely localised in the cytoplasm. TG2 is distributed ubiquitously but is predominantly localised in the cytoplasm.

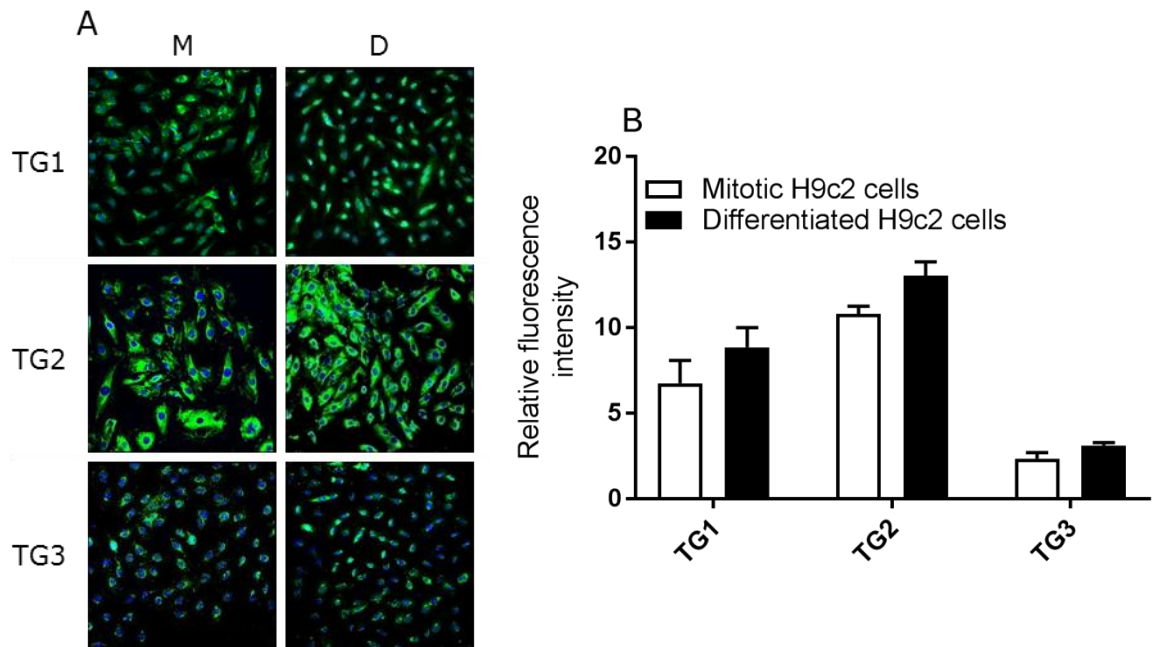


Fig 3.13: Protein expression of TG isoforms in mitotic and differentiated H9c2 cells. (A) Images acquired from immunofluorescence by confocal microscopy are presented from one experiment and are representative of three independent experiments. (B) Quantified immunofluorescence data represent the mean \pm S.E.M. of fluorescence intensity relative to DAPI stain for five fields of view from each of three independent experiments.

3.4 Discussion.

The initial aim of this study was to identify functional expression of adenosine receptor and β -adrenoceptor subtypes on H9c2 cells along with characterisation of TG isoforms.

Functional expression of adenosine receptors on H9c2 cells:

H9c2 cardiomyoblasts derived from embryonic rat heart myoblasts are widely used as an in-vitro model for cardiac cells since they are electrophysiologically and biochemically similar to cardiomyocytes (Heschelet et al, 1991). It has been previously reported that rat ventricular myocytes express A_1 , A_{2A} and A_3 adenosine receptors (Martens et al, 1987; Linden, 1994; Dixon et al, 1996; Dobson and Fenton, 1997; Germack and Dickenson, 2004). Fretwell and Dickenson, reported the functional expression of the A_1 adenosine receptor on H9c2 cells using cAMP accumulation assay (Fretwell and Dickenson, 2009). However, to further investigate, mRNA and functional expression of adenosine receptors via RT-PCR analysis, cAMP accumulation and calcium imaging was performed. As reported by Fretwell and Dickenson, CPA mediated a biphasic modulation of forskolin-stimulated cAMP accumulation in mitotic H9c2 cells (figure 3.2). Although CPA-induced inhibition of forskolin-stimulated cAMP accumulation was seen at nM concentrations (≤ 100 nM), at higher concentrations (> 100 nM) this inhibition was partially reversed. In agreement with previous findings, this observation suggests that at higher agonist concentrations, the A_1 adenosine receptor can also couple to G_s -protein in mitotic H9c2 cells (Fretwell and Dickenson,

2009). Due to the extremely low level detection of A_1 adenosine receptor mRNA in differentiated H9c2 cells, work was performed using mitotic H9c2 cells.

The selective A_{2A} adenosine receptor agonist, CGS 21680 caused no measurable cAMP accumulation (figure 3.3) suggesting that even though the mRNA for A_{2A} adenosine receptor is detectable (figure 3.1), this receptor is not functional in differentiated H9c2 cells. It should be noted that IBMX was implemented in this cAMP accumulation assay to inhibit phosphodiesterase activity. However, IBMX also functions as a non-selective antagonist of adenosine receptors (Beavo et al, 1970; Morgan et al, 1993). Therefore, it is possible that the lack of cAMP response was due to antagonism of CGS 21680 by IBMX and hence the use of an alternative phosphodiesterase inhibitor e.g. rolipram should be implemented in further studies. The mRNA profile of the adenosine receptors shows no expression of A_{2B} adenosine receptor and hence no functional studies were undertaken for this receptor. Although the mRNA profile is positive for the A_3 adenosine receptor, previous studies have found it not to be functionally expressed in these cells (Fretwell and Dickenson, 2009). Hence it was not studied any further.

Convincing evidence exists that the A_1 adenosine receptor directly stimulates inositol phospholipid hydrolysis through $G_{i/o}$ -protein $\beta\gamma$ subunit-mediated activation of phospholipase C in many cell types (White et al, 1992; Dickenson et al, 1995; Murthy and Makhlof, 1995; Tomura et al, 1997; Linden, 2001; Sheth et al, 2014). In this study, CPA triggered increases in intracellular Ca^{2+} levels which were characterised by pronounced Ca^{2+} oscillations (figure 3.4). These responses were eliminated following removal of extracellular Ca^{2+} , suggesting that these responses are dependent upon extracellular Ca^{2+} influx as the intracellular stores were still intact. Similar observations were made with the endogenous agonist adenosine (figure 3.5). In order to clarify the involvement of the A_1 adenosine receptor in mediating these Ca^{2+} responses, the selective A_1 adenosine receptor antagonist DPCPX and the $G_{i/o}$ -protein blocker pertussis toxin were used. As expected, intracellular Ca^{2+} responses observed with both CPA and adenosine were blocked when cells were pre-treated with either DPCPX and PTX, thus confirming the involvement of the A_1 adenosine receptor.

This influx of extracellular Ca^{2+} upon stimulation of the A_1 adenosine receptor is in contrast to previous findings in basal forebrain cholinergic neurons, human bronchial smooth muscle cells and the smooth muscle cell line DDT₁MF-2 which suggest that the A_1 adenosine receptor stimulates the release of intracellular Ca^{2+} stores (Dickenson and Hill, 1993; Basheer et al, 2002; Ethier and Madison, 2006). In relation to the current data, it is unlikely that voltage-gated Ca^{2+} channels are involved as activation of the $G_{i/o}$ -protein coupled A_1 adenosine receptor is associated with the inhibition of P/Q- and N-type voltage-dependent Ca^{2+} channels (Gundlfinger et al, 2007). Sabourine and colleagues have recently provided an alternative mechanism for the A_1

adenosine receptor-induced Ca^{2+} influx in cardiomyocytes which occurs via store-operated Ca^{2+} channels (Sabourine et al, 2012). Furthermore, there is some evidence that the A_1 adenosine receptor can modulate L-type Ca^{2+} channels in rat atria (Fassina et al, 1991; Braganca et al, 2016). At present the mechanisms associated with the A_1 adenosine receptor-induced Ca^{2+} influx in H9c2 cells are not established, however it would be of interest to investigate the mechanisms underlying this phenomena. Collectively, these data sufficiently demonstrate the functional expression of the A_1 adenosine receptor on H9c2 cells.

Functional expression of β -adrenoceptors on H9c2 cells:

In contrast to the heart where the β_1 -AR is the dominant adrenoceptor subtype (Woo and Xiao, 2012), previous studies have shown that H9c2 cells have a β -AR subtype ratio of 71% β_2 -AR to 29% β_1 -AR (Dangel et al, 1996). In this study, RT-PCR analysis revealed expression of β_1 , β_2 , and β_3 -AR mRNA in mitotic and differentiated H9c2 cells (figure 3.6), with a rank order of β_2 -AR > β_1 -AR = β_3 -AR. Since all of the three β -AR subtypes couple to G_s -proteins and activate adenylyl cyclase, their functional expression was assessed by measuring cAMP accumulation in mitotic cells. Mitotic H9c2 cells were chosen for further investigation even though the mRNA of receptor is detected in differentiated cells because it would be more suitable to determine TG2 activation by GPCRs (adenosine receptors and adrenoceptors) in the same cell background. The selective β_3 -AR agonist CL 316243 did not generate any cAMP accumulation (figure 3.7), suggesting that even though the mRNA is detected, this subtype is not functionally expressed on H9c2 cells. However, recently it has been reported that the β_3 -AR is functionally active in mouse heart and is involved in cardioprotection (Dessy and Balligand, 2010; Niu et al, 2012; Cannavo and Koch, 2017).

In this study, the selective β_2 -AR agonist formoterol revealed a robust increase in cAMP accumulation whilst the non-selective β -AR agonist isoprenaline revealed only a modest increase in cAMP accumulation (figure 3.7). There is some evidence that in rat cardiomyocytes many β_2 -AR agonists have been shown to activate both G_s and $G_{i/o}$ proteins, with the exception of fenoterol which exclusively activates only G_s protein (Xiao et al, 2003). Hence it was of interest to check if isoprenaline were coupling to $G_{i/o}$ -protein in H9c2 cells. Following treatment of cells with PTX for 16 h, isoprenaline triggered a robust cAMP response, thus suggesting that in H9c2 cells isoprenaline couples to $G_{i/o}$ -proteins. In contrast, treatment with PTX had no effect on formoterol-induced robust increase in cAMP accumulation. These data suggest that the cAMP responses to isoprenaline were augmented by PTX indicating dual coupling to G_s and G_i , whereas responses to formoterol were insensitive to PTX indicating coupling only to G_s proteins. There is some evidence that formoterol promotes the receptor to exclusively couple to G_s proteins. For instance, in HEK293 cells and isolated rat heart,

formoterol-induced cAMP accumulation was insensitive to PTX (Somvanshi et al, 2011; Salie et al, 2011). However there are several studies that claim isoprenaline couples to $G_{i/o}$ proteins in mouse cardiomyocytes (for details see Daaka et al, 1997; Davel et al, 2014; Fu et al, 2014).

To confirm these results, subtype-selective antagonists were employed. From the data shown in figure 3.8, it is clear that the cAMP response to β -AR agonists is via the β_2 -AR. Formoterol-induced cAMP responses were blocked by the non-selective β -AR antagonist propranolol and the selective β_2 -AR antagonist ICI 118,551, whereas the selective β_1 -AR antagonist CGP 20712 had no effect. Isoprenaline-induced cAMP responses in the presence of PTX were attenuated by the non-selective β -AR antagonist propranolol and the selective β_2 -AR antagonist ICI 118,551, while the selective β_1 -AR antagonist CGP 20712 could only modestly block the response. This indicates that there is some activity of the β_1 -AR in H9c2 cells. The majority of evidence is consistent with β_2 -AR being functionally active, with the exception of isoprenaline in presence of the selective β_1 -AR antagonist CGP 20712. However, it is not clear how the response could be dependent up on either β_1 - or β_2 -AR. Previous studies by Somvanshi and colleagues have implied functional expression of β_1 -AR in H9c2 cells via isoprenaline-induced apoptosis and signalling responses such as CREB and ERK1/2 (Somvanshi et al, 2013). However it should be noted that isoprenaline is a non-selective β -AR agonist and was reported to induce PI-3K activity which was inhibited by the β_2 -AR antagonist ICI 118,551 but not the β_1 -AR antagonist CGP 20712 in H9c2 cells (Yano et al, 2007). Overall, these data suggest functional expression of the β_2 -AR but not β_1 -AR or β_3 -AR subtypes in H9c2 cells.

Due to the slight discrepancy observed in antagonising the isoprenaline- and formoterol-induced cAMP accumulation, two additional β -AR agonists were implemented. The selective β_2 -AR agonist cimaterol and the β_1/β_2 agonist dobutamine (figure 3.9) both generated modest cAMP accumulation which was in each case blocked by the non-selective β -AR antagonist propranolol and the selective β_2 -AR antagonist ICI 118,551, whereas the selective β_1 -AR antagonist CGP 20712 had no effect. These data confirm the functional expression of the β_2 -AR but not β_1 -AR or β_3 -AR subtypes in H9c2 cells. Since both of these agonists could only generate a modest cAMP response, it became of interest to identify if the cAMP response to these agonists is limited by $G_{i/o}$ -protein-coupling in H9c2 cells, as seen with isoprenaline. Also, to identify if the phenomenon of isoprenaline-induced coupling to $G_{i/o}$ -protein is an effect observed only in H9c2 cells, BEAS-2B R1 cells (human bronchial epithelial cells which endogenously express β_2 -AR; Kelsen et al, 1997) were employed as a positive control (figure 3.10). Data obtained with H9c2 cells in the presence and absence of PTX, suggest that not only isoprenaline but also cimaterol promotes β_2 -AR coupling to $G_{i/o}$ -protein in H9c2 cells. This may explain why cimaterol could only generate a modest

cAMP response compared to formoterol. All the other agonists used in this study at their maximal concentrations did not have any effect upon treatment with PTX, suggesting they do not promote β_2 -AR coupling to $G_{i/o}$ -protein in H9c2 cells.

The data obtained from BEAS-2B R1 cells suggest that the phenomenon of isoprenaline and cimaterol coupling to $G_{i/o}$ -protein is exclusive to H9c2 cells. However, it should be noted that there was a slight increase in dobutamine-mediated cAMP accumulation in BEAS-2B R1 cells treated with PTX. One reason for these agonists coupling to $G_{i/o}$ -proteins in H9c2 cardiomyocytes could be due to compartmentalisation of the β_2 -AR. Myocytes contain abundant lipid rafts and caveolae with high expression of the β_2 -AR (Patel et al, 2008; Xiang, 2011). This distribution facilitates signalling molecules such as cAMP to signal in a location-dependent manner. Using real time imaging of live myocytes, it was reported that stimulation of the β_2 -AR at one end of elongated adult myocytes generates a spatially confined cAMP response, whereas, similar stimulation of the β_1 -AR generates a diffused cAMP response reaching inside the cells (Nikolaev et al, 2006; Nikolaev et al, 2010). Furthermore, only certain isoforms of adenylyl cyclase are enriched in the caveolae (e.g. AC6) and are known to couple to the β_1 -AR more effectively than to the β_2 -AR (Ostrom et al, 2001). Also, disruption of caveolae and lipid rafts causes enhancement of isoprenaline-induced cAMP response (Head et al, 2006). Hence, it is plausible that because of the low availability of G_s -protein/adenylyl cyclase these agonists couple to $G_{i/o}$ -protein.

Apart from this, it is also known that in mouse heart, genetic disruption of β_1 -AR does not alter the function of β_2 -AR and vice versa (Rohrer et al, 1996; Chruscinski et al, 1999; Devic et al, 2001; Soto et al, 2009). This suggests that these two receptors reside in different compartments in mouse heart. Kuschel and colleagues have reported that inhibition of $G_{i/o}$ -protein using PTX allowed switching of the localised cAMP response to a global phenomenon, confirming that β_2 -AR coupling to $G_{i/o}$ -protein restricts the cAMP response to the sarcolemma of rat ventricular myocytes (Kuschel et al, 1999b). Interestingly, some studies have shown that in neonatal cardiac myocytes β_2 -AR coupling to $G_{i/o}$ -proteins is PKA and GRK phosphorylation dependent and it is associated with receptor internalisation and recycling (Xiang et al, 2002; Xiang and Kobilka, 2003; Wang et al, 2007; Wang et al, 2008; Liu et al, 2009; Xiang, 2011). However, further studies are needed to confirm if this coupling to $G_{i/o}$ -proteins in H9c2 cardiomyocytes is due to compartmentalisation. At present, the levels of $G_{i/o}$ -protein and G_s -protein as well as expression of different $G_{i/o}$ -protein subtypes (G_{i1} -, G_{i2} -, G_{i3} -, G_{o1} - and G_{o2} -protein) in H9c2 cells are not known. Furthermore, the different cell backgrounds used in various studies could also be a potential reason for these agonists to couple to $G_{i/o}$ -protein.

To determine if β_2 -AR activation initiated Ca^{2+} responses in H9c2 cells, Ca^{2+} imaging was performed. Formoterol consistently produced no measurable Ca^{2+} responses,

whilst isoprenaline in a proportion of experiments triggered intracellular Ca^{2+} responses (figure 3.11). It can be conceivable that the reason for formoterol not triggering any Ca^{2+} responses could be because it does not promote the β_2 -AR to couple to $G_{i/o}$ -protein. It is important to note that the concentrations of the agonists used to determine intracellular Ca^{2+} responses are not the same as those used for cAMP accumulation studies. This is simply because as shown in Chapter V, modulation of TG2 activity occurs at higher concentrations and since TG2 is a calcium dependent enzyme, it was necessary to use the same concentration for comparison purposes. As for the cAMP accumulation, it was important to use the agonists and antagonists at their selective concentrations to be able to determine the subtype functionally expressed on H9c2 cells.

On quantification, it was observed that over three independent experiments 18 wells were assessed and in 7 wells isoprenaline generated a response i.e. 39%. The intracellular Ca^{2+} responses observed could be a result of activation of L-type Ca^{2+} channels (LTCCs). LTCCs, along with ryanodine receptors (RyRs) and Sarcoplasmic/Endoplasmic Reticulum Calcium ATPase type 2 (SERCA2), are known substrates of PKA which are involved in Ca^{2+} responses and recycling (Kamp and Hell, 2000; Manni et al, 2008; Kranias and Hajjar, 2012). Convincing evidence exists that there is localisation of a subpopulation of LTCCs in caveolae and that activation of β_2 -AR coupling causes a localised cAMP response which might be sufficient to spatially activate PKA, which leads to activation of caveolar LTCCs (Xiao et al, 1994; Chen-Izu et al, 2000; Fu et al, 2013).

Finally, a number of studies have also shown that activation of β -AR induces activation of Ca^{2+} /calmodulin-dependent kinase II (CaMKII), which causes phosphorylation of phospholamban and ryanodine receptors which play a role in myocardial hypertrophy (Zhang et al, 2005; Anderson et al, 2011; Swaminathan et al, 2012). This activation of CaMKII via β -AR can occur due to PKA-dependent increases in local Ca^{2+} concentrations via LTCCs and RyRs as well as through G_s -protein mediated up-regulation of LTCCs and cAMP/EPAC-dependent signalling pathways (Lader et al, 1998; Oestreich et al, 1998; Ferrero et al, 2007; Soltis and Saucerman, 2010; Fu et al, 2013). Several studies have shown that activation of the β_2 -AR following inhibition of $G_{i/o}$ -protein with PTX caused switching of the localised cAMP response to a global phenomenon and complete phosphorylation of phospholamban by PKA was observed (Xiao et al, 1995; Kuschel et al, 1999b). Furthermore, in rat ventricular myocytes, several studies have shown dual coupling of β_2 -AR to G_s - and $G_{i/o}$ -proteins and this dual coupling leads to reduced cAMP response resulting in highly localised Ca^{2+} responses (Xiao et al, 1995; Daaka et al, 1997; Xiao et al, 1999; Chen-Izu et al, 2000). These responses appear to be dependent on cAMP/PKA-signalling as inhibition of PKA with RpCamps and peptide inhibitors abolished these Ca^{2+} responses. A similar

phenomenon was observed in frog ventricular myocytes which are known to be rich in β_2 -AR (Zhou et al, 1997; Kuschel et al, 1999a; Kuznetsov et al, 1995; Hartzell et al, 1991; Hartzell and Fischmeister, 1992; Skeberdis et al, 1997b). Together these studies show that inhibition of $G_{i/o}$ -protein caused the β_2 -AR to signal in a similar fashion to the β_1 -AR. At present it is still not clear if the isoprenaline-induced intracellular Ca^{2+} responses are dependent on $G_{i/o}$ -protein coupling in H9c2 cardiomyoblasts and hence further investigation is warranted. Overall, the data presented clearly show functional expression of the β_2 -AR on H9c2 cells.

Characterisation of TG expression pattern in H9c2 cells:

At present few studies have shown differential expression of transglutaminase isoforms in heart. For instance, Factor XIIIIA mRNA and protein levels have been identified in mouse heart (Sane et al, 2007; Myneni et al, 2014) and its up-regulation in cardiac myxoma (Berrutti and Silverman, 1996). There is also evidence of strong mRNA expression for TG3 in mouse heart (Zhang et al, 2005). However, to the authors knowledge no studies relating to TG1, TG4, TG5, TG6, TG7 and Band 4.2 have been carried out in the cardiovascular field. There are a significant number of studies which have reported TG2 mRNA and protein levels in mouse heart (Small et al, 1999; Sane et al, 2007; Iismaa et al, 2009; Deasey and Numinskaya, 2013) and neonatal rat cardiomyocytes (Li et al, 2009). TG2 is implied in cardiac disorders such as atherosclerosis, cardiac hypertrophy and stiffness. The role of TG2 is debatable in these disorders as there are contrasting studies suggesting that TG2 does not play a role in plaque stability during atherosclerosis (Williams et al, 2010), while another study claims that its activity is important in regulating the atherosclerotic plaque (Matlung et al, 2012). In an ischaemic heart, TG2 GTPase activity is strikingly reduced suggesting that it is an important factor in cardiac failure (Hwang et al, 1995). However, cardiac-specific overexpression of TG2 does not alter PLC- δ 1 activity, suggesting that it functions as a TG rather than a GTPase (Small et al, 1999). TG2 is also involved in cardiac hypertrophy (Iismaa and Graham, 2003) and cardiovascular stiffness (Jung et al, 2013; Steppan et al, 2014; Steppan et al, 2017), but its role in their progression is debatable. All of the above studies were carried out in mouse/rat models and hence it was important to determine which TG isoform is expressed in H9c2 cardiomyocytes. It is apparent from the data shown in figures 3.12 and 3.13 that TG1, TG2 and TG3 are expressed in both mitotic and differentiated H9c2 cells. In mitotic and differentiated H9c2 cells, TG1 and TG3 are mainly localised in the perinuclear region with TG1 being sparsely localised in the cytoplasm. TG2 is distributed ubiquitously, however, it is predominantly localised in the cytoplasm. It is clear from these data that differentiation of H9c2 cells does not affect the localisation of TG1, TG2 and TG3. Although it would have been ideal to check the expression of all TG isoforms, this was not technically possible due to lack of specific antibodies and

time constraints. However, it should be noted that some of the TG isoforms which were not assessed in this study, might not be expressed in H9c2 cardiomyocytes as TGs have been named according to their specific localisation. For instance TG4 or prostate TG is only expressed in the prostate gland, prostatic fluids and seminal plasma. From this study it can be concluded that mitotic and differentiated H9c2 cells express TG1, TG2 and TG3.

In conclusion, these data provide sufficient evidence of functional expression of the A₁ adenosine receptor, β_2 -adrenoceptor and TG2 in mitotic H9c2 cardiomyocytes.

Chapter IV: Modulation of TG2 activity by the A₁ adenosine receptor in H9c2 cells

This chapter aims to investigate modulation of TG2 by the A₁ adenosine receptor in mitotic H9c2 cells via TG2 amine incorporating and peptide crosslinking assays along with *in-situ* TG2 activity.

4.1 Effect of A₁R activation on TG2-mediated biotin cadaverine amine incorporation and protein cross-linking activity.

Initially the effect of the selective A₁R agonist CPA on TG2 activity in H9c2 cardiomyoblasts was investigated. H9c2 cells were treated with CPA (1 μM) for varying periods of time and the cell lysates subjected to both biotin cadaverine amine-incorporation assay (Slaughter et al, 1992) and biotin-labelled peptide (biotin-TVQQEL) cross-linking assay (Trigwell et al, 2004). CPA (figure 4.1A) produced time-dependent increases in TG2-catalysed biotin-cadaverine incorporation activity, peaking at 10 min. In addition, CPA (pEC₅₀ = 8.87 ± 0.17; n=6; figure 4.1C) stimulated concentration-dependent increases in biotin-cadaverine incorporation activity. CPA also triggered time-dependent increases in TG2-mediated protein cross-linking activity peaking at 10 min (figure 4.1B) along with concentration-dependent increases in protein cross-linking activity (pEC₅₀ = 8.61 ± 0.20; n=6; figure 4.1D). Similar to CPA, the endogenous adenosine receptor agonist adenosine (100 μM) also triggered transient increases in TG2 catalysed biotin-cadaverine incorporation and protein cross-linking activity, peaking at 10 min (figure 4.2A and B). Furthermore, adenosine stimulated concentration-dependent increases in both biotin-amine incorporation activity (figure 4.2C; pEC₅₀ = 6.90 ± 0.11; n=7) and protein cross-linking activity (figure 4.2D; pEC₅₀ = 7.08 ± 0.16; n=7). It should be noted that activation of A₁R using CPA and adenosine reveals a trend towards a decrease in both amine incorporation and protein cross-linking activities of TG2 at 1 min.

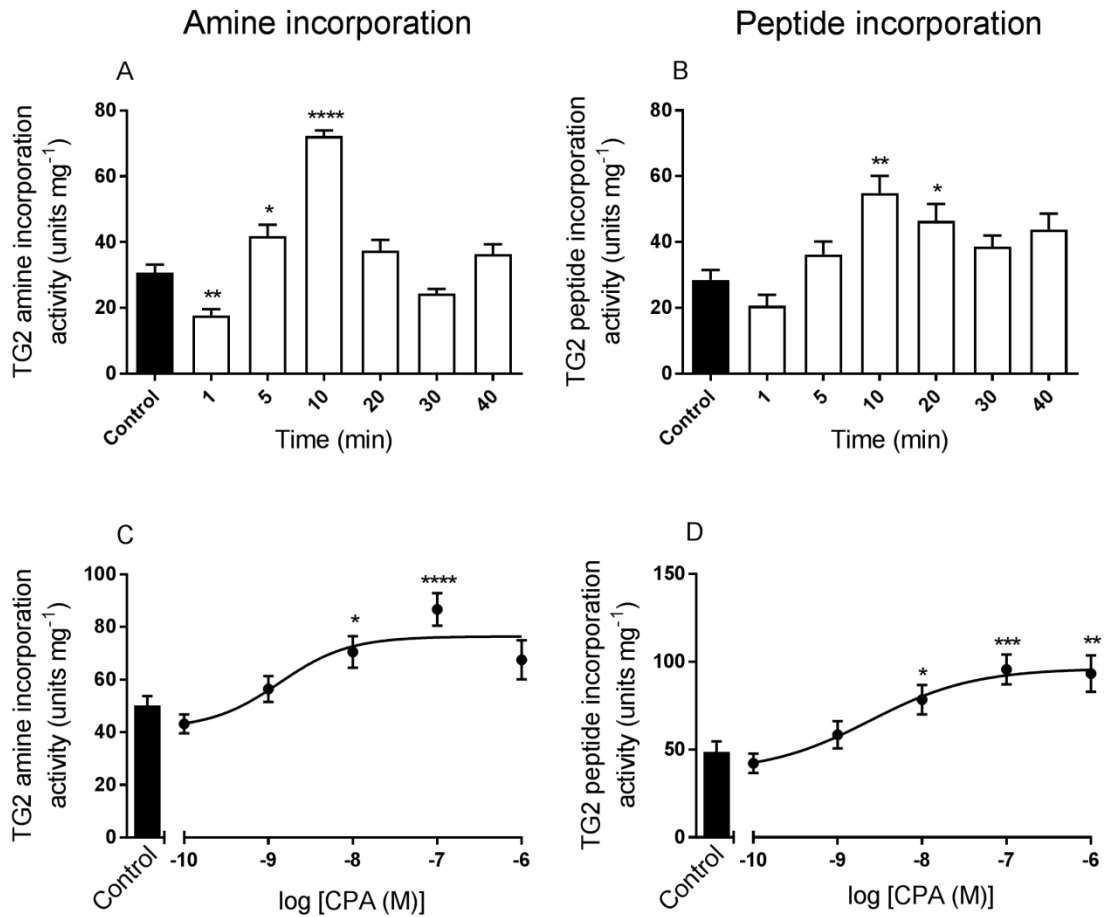


Fig 4.1: Effect of the selective A₁ adenosine receptor agonist CPA on TG2 activity in H9c2 cells. Cells were stimulated with CPA (1 μM) for the indicated time intervals (panels A and B). Concentration-response curves for CPA in cells treated with agonist for 10 min (panels C and D). Cell lysates were subjected to biotin-cadaverine incorporation (panels A and C) or the peptide cross-linking assay (panels B and D). Data points represent the mean ± S.E.M. for TG2 specific activity from four independent experiments. **P*<0.05, ***P*<0.01, ****P*<0.001 and *****P*<0.0001 versus control response.

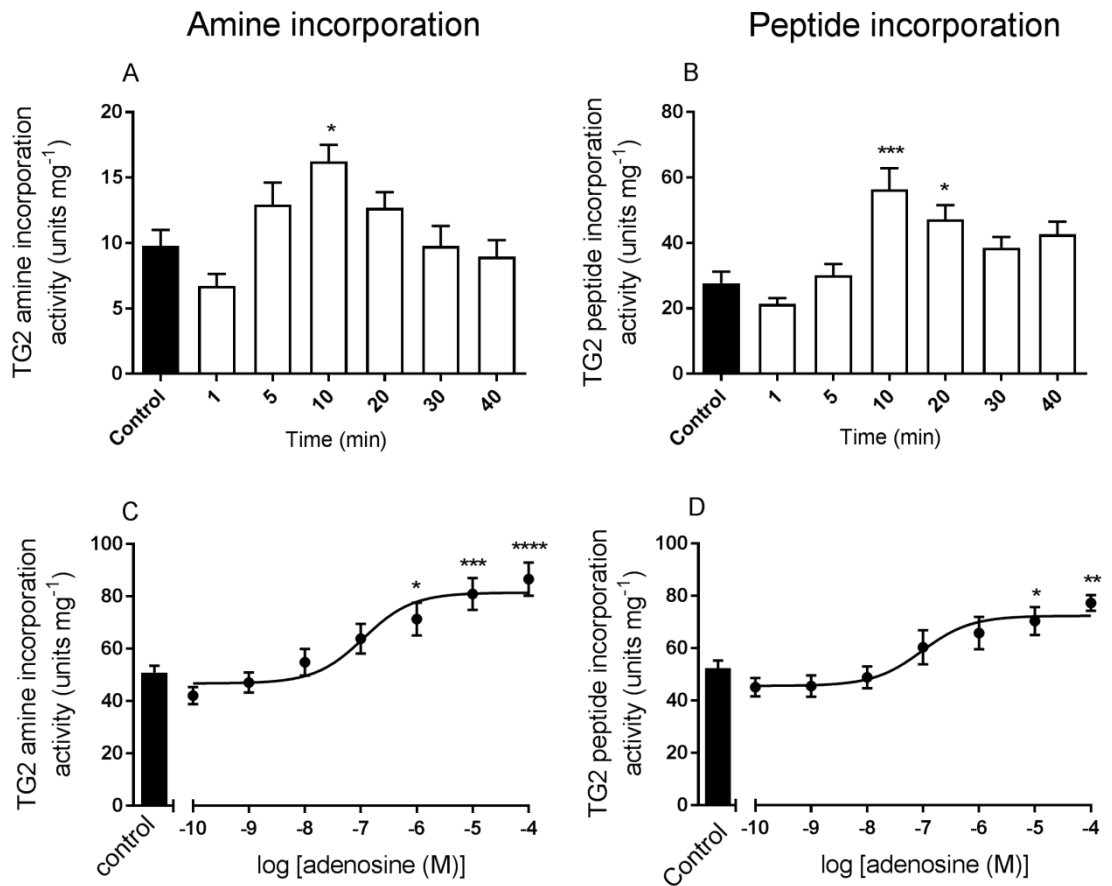


Fig 4.2: Effect of the endogenous adenosine receptor agonist adenosine on TG2 activity in H9c2 cells. Cells were stimulated with adenosine (100 μ M) for the indicated time intervals (panels A and B). Concentration-response curves for adenosine in cells treated with agonist for 10 min (panels C and D). Cell lysates were subjected to biotin-cadaverine incorporation (panels A and C) or the peptide cross-linking assay (panels B and D). Data points represent the mean \pm S.E.M. for TG2 specific activity from four independent experiments. * P <0.05, ** P <0.01, *** P <0.001 and **** P <0.0001 versus control response.

4.2 The effect of selective A₁R antagonist and TG2 inhibitors on A₁R induced TG2 activity.

To determine if the evoked TG2 activity was via the A₁R, H9c2 cells were pre-treated for 30 min with the selective A₁R antagonist DPCPX (1 μM) prior to stimulation with CPA (100 nM) and/or adenosine (100 μM) for 10 min. DPCPX blocked CPA-elicited (figure 4.3A and B) and adenosine-induced (figure 4.3C and D) TG2 activity, thus confirming that the activity was mediated by the A₁R. To confirm that TG2 is responsible for the A₁R induced transglutaminase activity in H9c2 cells, two structurally different cell permeable TG2 specific inhibitors were tested: R283 (a small molecule; Freund et al, 1994) and Z-DON (peptide-based; Schaertl et al, 2010). H9c2 cells were pre-treated for 1 h with Z-DON (150 μM) or R283 (200 μM) prior to stimulation with CPA (100 nM) and/or adenosine (100 μM) for 10 min. Both inhibitors blocked CPA-induced and adenosine-induced TG-mediated amine incorporation (figure 4.3A and C) and peptide cross-linking activity (figure 4.3B and D), confirming the involvement of TG2. As these are TG2 inhibitors, they are also lowering the basal enzyme activity.

4.3 The role of Ca²⁺ in A₁R induced TG2 activity.

The role of Ca²⁺ in A₁R-induced TG2 activation was determined because TG2 is a Ca²⁺-dependent enzyme. The role of extracellular Ca²⁺ was assessed by measuring TG2 responses in the absence of extracellular Ca²⁺ using nominally Ca²⁺-free Hanks/HEPES buffer containing 0.1 mM EGTA (pH was confirmed). Removal of extracellular Ca²⁺ abolished CPA- and adenosine-induced TG2 activity (figure 4.4A and B). To assess the role of intracellular Ca²⁺, measurements of TG2 activation were also performed using cells pre-incubated with the Ca²⁺ chelator BAPTA-AM (50 μM for 30 min) in the absence of extracellular Ca²⁺. Loading cells with BAPTA in the absence of extracellular Ca²⁺ did not lead to further inhibition of CPA- and adenosine-induced TG2 activation (figure 4.4A and B). These observations indicate that the A₁R-induced TG2 activation is dependent upon the influx of extracellular Ca²⁺.

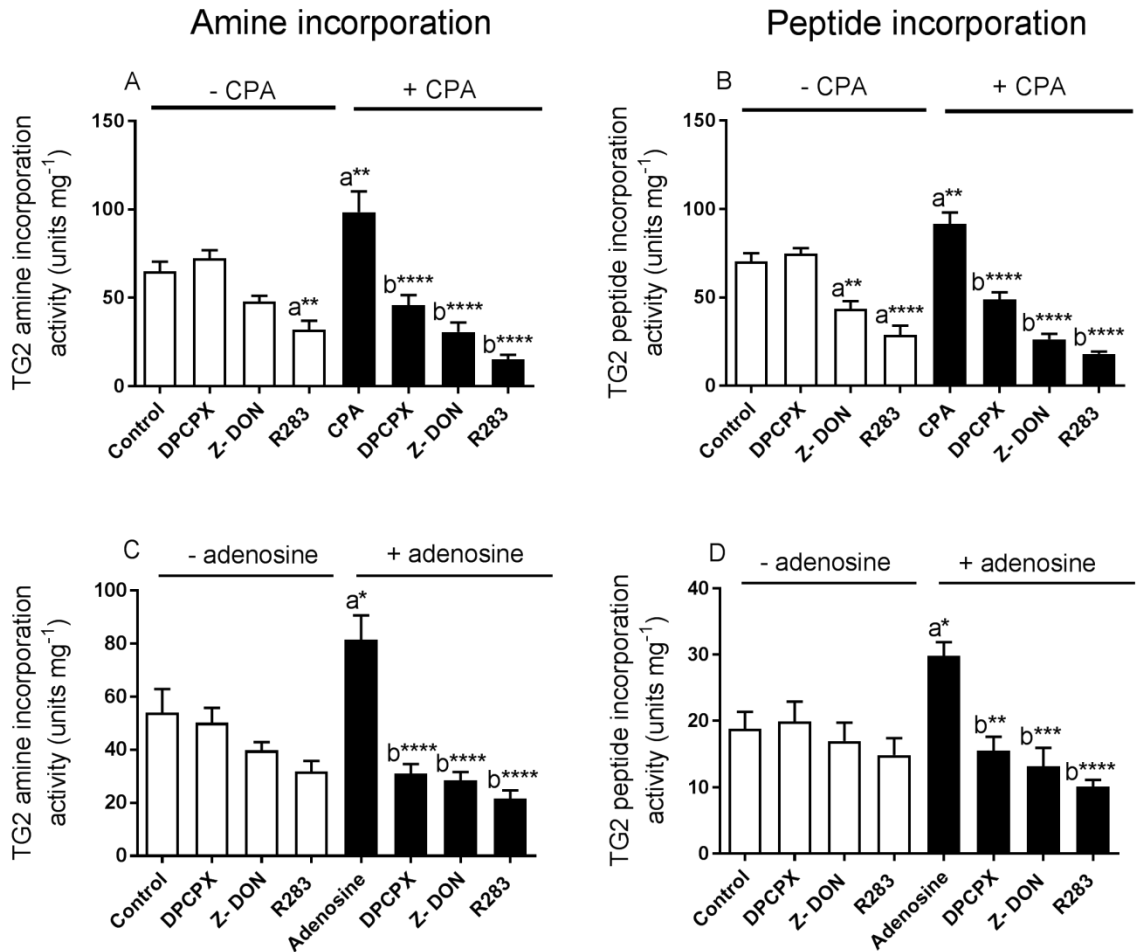


Fig 4.3: Effect of the A₁ adenosine receptor antagonist DPCPX and TG2 inhibitors on CPA and adenosine-induced TG2 activity. H9c2 cells were pre-treated for 30 min with the selective A₁ adenosine receptor antagonist DPCPX (1 μM) or for 1 h with the TG2 inhibitors Z-DON (150 μM) and R283 (200 μM) prior to 10 min stimulation with CPA (100 nM) or adenosine (100 μM). Cell lysates were subjected to biotin cadaverine amine incorporation assay (panels A and C) or peptide cross-linking assay (panels B and D). Data points represent the mean ± S.E.M for TG2 specific activity from four independent experiments. **P*<0.05, ***P*<0.01, ****P*<0.001, and *****P*<0.0001, (a) versus control and (b) versus 100 nM CPA or 100 μM adenosine alone.

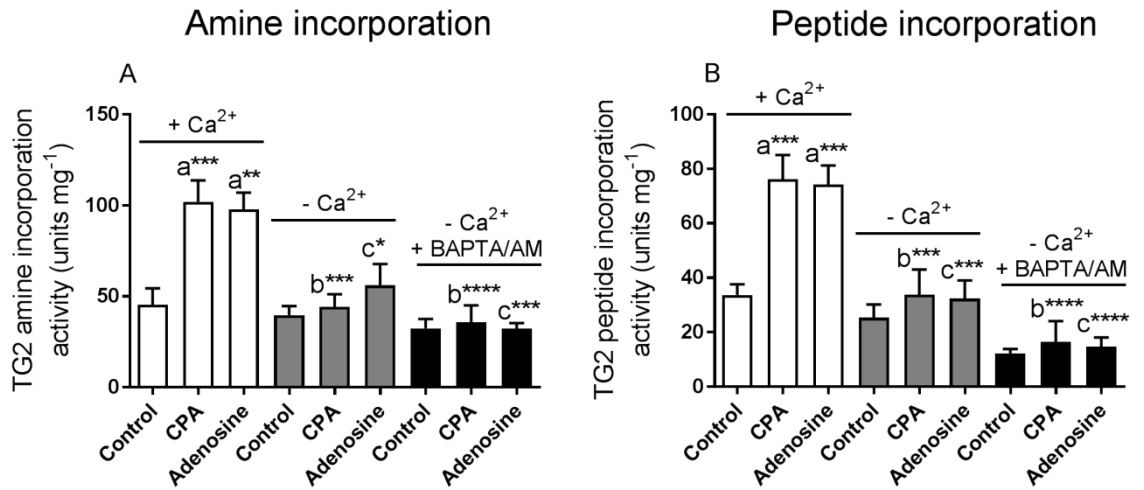


Fig 4.4: The role of extracellular Ca²⁺ in CPA- and adenosine-induced TG2 activation. H9c2 cells were stimulated for 10 min with CPA (100 nM) or adenosine (100 μM) either in the presence of extracellular Ca²⁺ (1.8 mM) or in its absence using nominally Ca²⁺-free Hanks/HEPES buffer containing 0.1 mM EGTA. Experiments were also performed using cells pre-incubated for 30 min with 50 μM BAPTA/AM and in the absence of extracellular Ca²⁺ (nominally Ca²⁺-free Hanks/HEPES buffer containing 0.1 mM EGTA) to chelate intracellular Ca²⁺. Cell lysates were subjected to biotin-cadaverine incorporation assay (panel A) or peptide cross-linking assays (panel B). Data points represent the mean ± S.E.M for TG specific activity from four independent experiments. **P*<0.05, ***P*<0.01, ****P*<0.001 and *****P*<0.0001, (a) versus control in presence of extracellular Ca²⁺, (b) versus 100 nM CPA in the presence of extracellular Ca²⁺, (c) versus 100 μM adenosine in the presence of extracellular Ca²⁺.

4.4 The effect of pertussis toxin and protein kinase inhibitors on A₁ adenosine receptor-induced TG2 activity.

Pre-treatment with the G_{i/o}-protein inactivating pertussis toxin (100 ng/ml for 16 h) completely abolished CPA- and adenosine-induced transglutaminase amine incorporation activity and peptide cross-linking activity, confirming the involvement of G_{i/o}-proteins (figure 4.5).

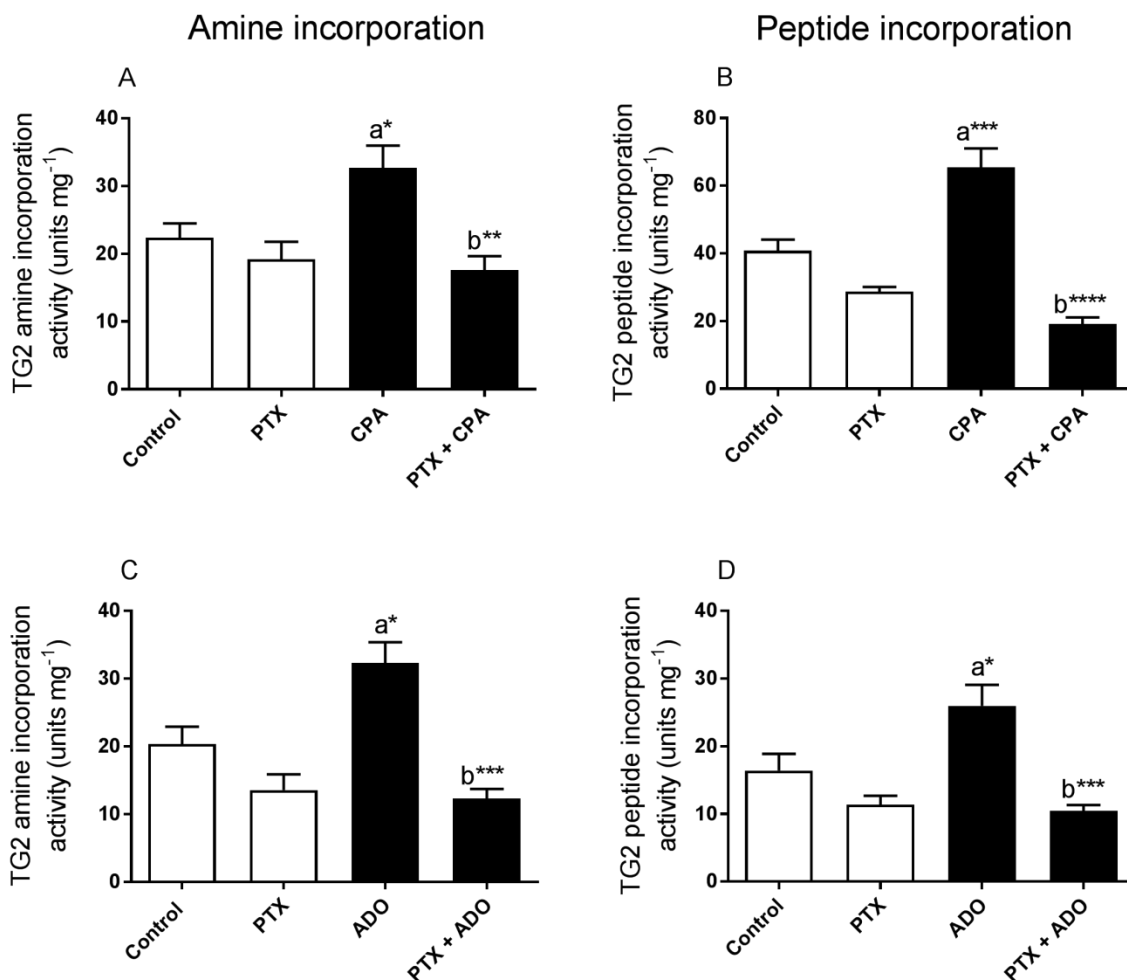


Fig 4.5: Effect of pertussis toxin on A₁ adenosine receptor-induced TG2 activity. H9c2 cells were pre-treated for 16 h with pertussis toxin (100 ng/ml) prior to 10 min stimulation with CPA (100 nM) or adenosine (ADO; 100 μ M). Cell lysates were subjected to biotin-cadaverine incorporation assay (panels A and C) or peptide cross-linking assay (panels B and D). Data points represent the mean \pm S.E.M for TG2 specific activity from four independent experiments. * P <0.05, ** P <0.01, *** P <0.001 and **** P <0.0001, (a) versus control and (b) versus 100 nM CPA or 100 μ M adenosine alone.

It is evident from previous literature that the A₁R activates other protein kinases including PKB (Germack and Dickenson, 2000; Germack et al, 2005), p38 MAPK (Robinson and Dickenson, 2001) and JNK1/2 (Brust et al, 2007). Modulation of ERK1/2, p38 MAPK, JNK1/2 and PKB activity following A₁R activation was assessed in H9c2 cells

by Western blotting using phospho-specific antibodies that recognise phosphorylated motifs within activated ERK1/2 (pTEpY), p38 MAPK (pTGpY), JNK1/2 (pTPpY) and PKB (pS⁴⁷³). CPA (100 nM for 10 min) and adenosine (100 μ M for 10 min) stimulated significant increases in ERK1/2 phosphorylation in H9c2 cells (figure 4.6). As expected, pre-treatment with the MEK1/2 inhibitor PD 98059 (50 μ M) blocked CPA- and adenosine-induced activation of ERK1/2 (figure 4.6). Moreover, PD 98059 (50 μ M) also blocked CPA- and adenosine-induced induced TG-mediated amine incorporation activity and peptide cross-linking activity (figure 4.7). As shown in figure 4.7, the PKC inhibitor Ro 318220 (10 μ M) also blocked CPA- and adenosine-induced TG2 activity suggesting the involvement of ERK1/2 and PKC.

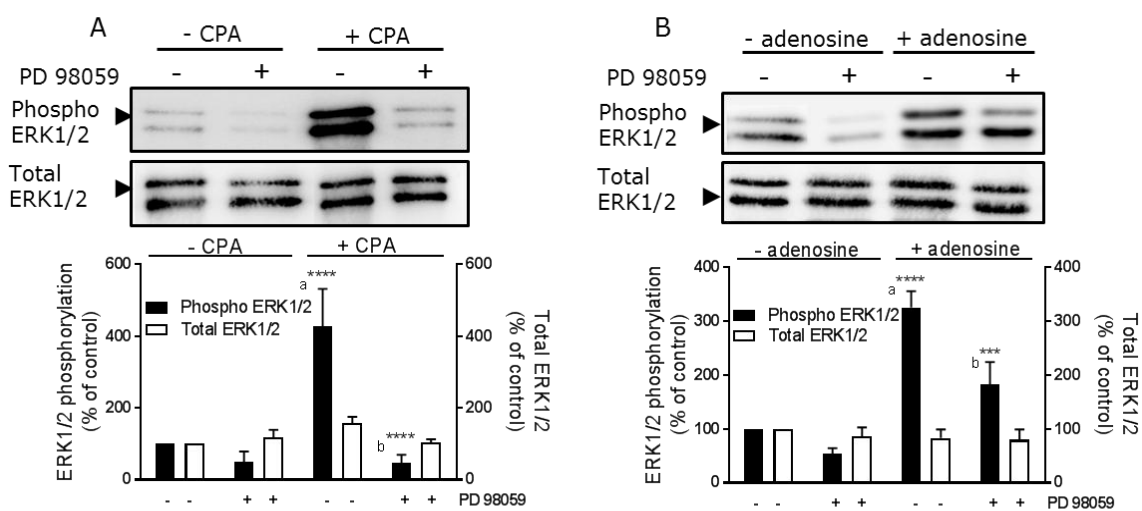


Fig 4.6: Effect of CPA and adenosine on ERK1/2 phosphorylation in H9c2 cells. H9c2 cells were pre-treated for 30 min with PD 98059 (50 μ M) prior to stimulation with CPA (100 nM) or adenosine (100 μ M) for 10 min. Cell lysates were analysed by Western blotting for activation of ERK1/2 using phospho-specific antibodies. Samples were subsequently analysed on separate blots using antibodies that recognize total ERK1/2. Data are expressed as the percentage of values for control cells (=100%) in the absence of protein kinase inhibitor and represent the mean \pm S.E.M. of four independent experiments. *** P <0.001 and **** P <0.0001, (a) versus control and (b) versus 100 nM CPA or 100 μ M adenosine alone.

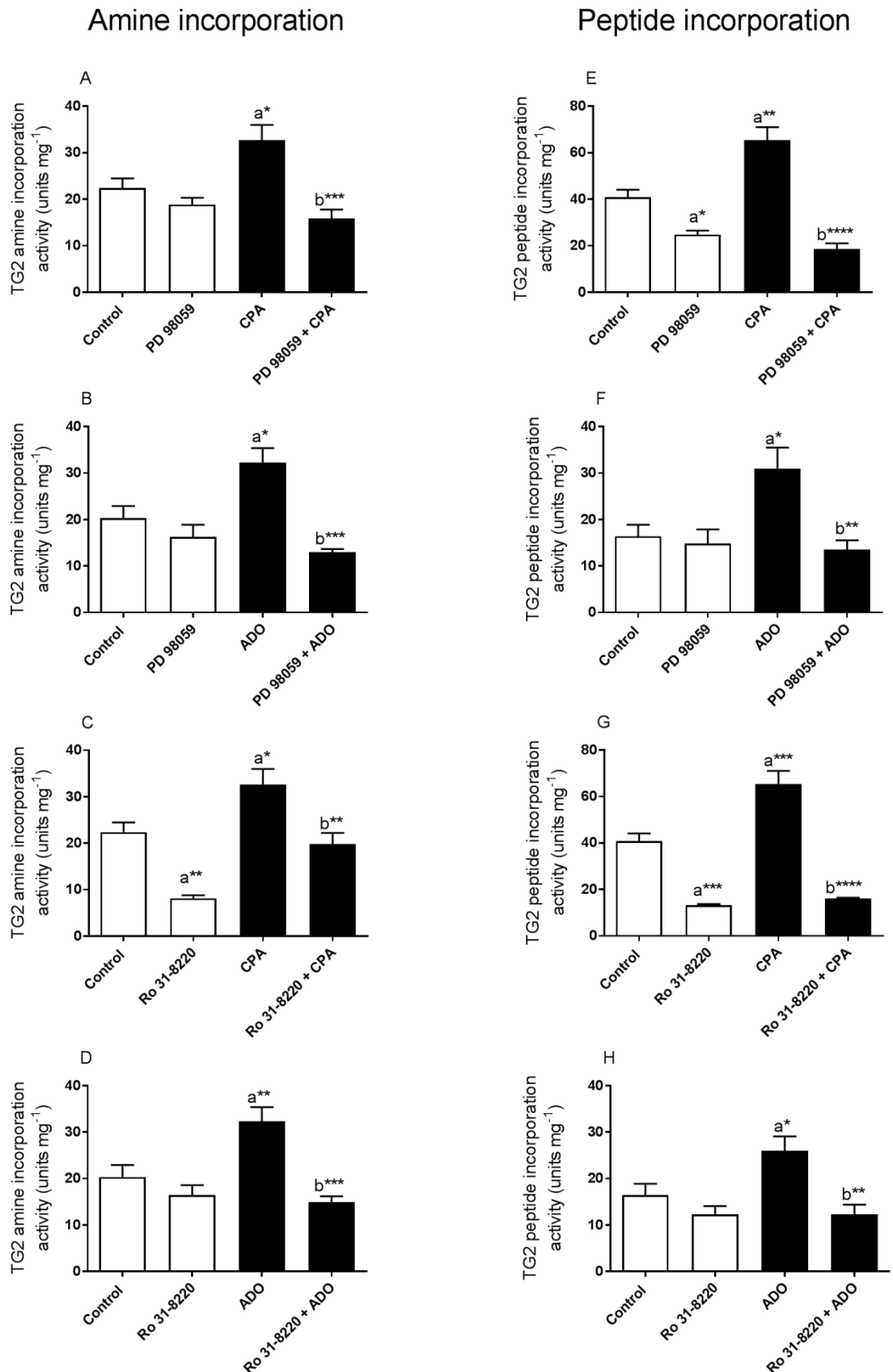


Fig 4.7: Effect of ERK1/2 and PKC inhibitors on the A₁ adenosine receptor-induced TG2 activity. H9c2 cells were pre-treated for 30 min with PD 98059 (50 μ M) or Ro 31-8220 (10 μ M) prior to 10 min stimulation with CPA (100 nM) or adenosine (ADO; 100 μ M). Cell lysates were subjected to protein biotin-cadaverine amine incorporation assay (panels A to D) or peptide cross-linking assay (panels E and H). Data points represent the mean \pm S.E.M for TG2 specific activity from four independent experiments. * P <0.05, ** P <0.01, *** P <0.001 and **** P <0.0001, (a) versus control and (b) versus 100 nM CPA or 100 μ M adenosine alone.

CPA (100 nM for 10 min) and adenosine (100 μ M for 10 min) also stimulated significant increases in p38 MAPK and JNK1/2 phosphorylation in H9c2 cells (figure 4.8). As expected, pre-treatment with SB 203580 (20 μ M; p38 MAPK inhibitor) and SP 600125 (20 μ M; JNK1/2 inhibitor) blocked CPA- and adenosine-induced activation of p38 MAPK and JNK1/2, respectively (figure 4.8). Furthermore, SB 203580 and SP 600125 blocked CPA- and adenosine-induced TG-mediated amine incorporation activity and peptide cross-linking activity (figure 4.9). On the other hand, no activation of PKB by CPA and adenosine was observed in H9c2 cells (figure 4.10). This was confirmed by the pan PI-3K inhibitors wortmannin (100 nM) and LY 294002 (30 μ M) did not block CPA and adenosine-induced TG2 activity (figure 4.11).

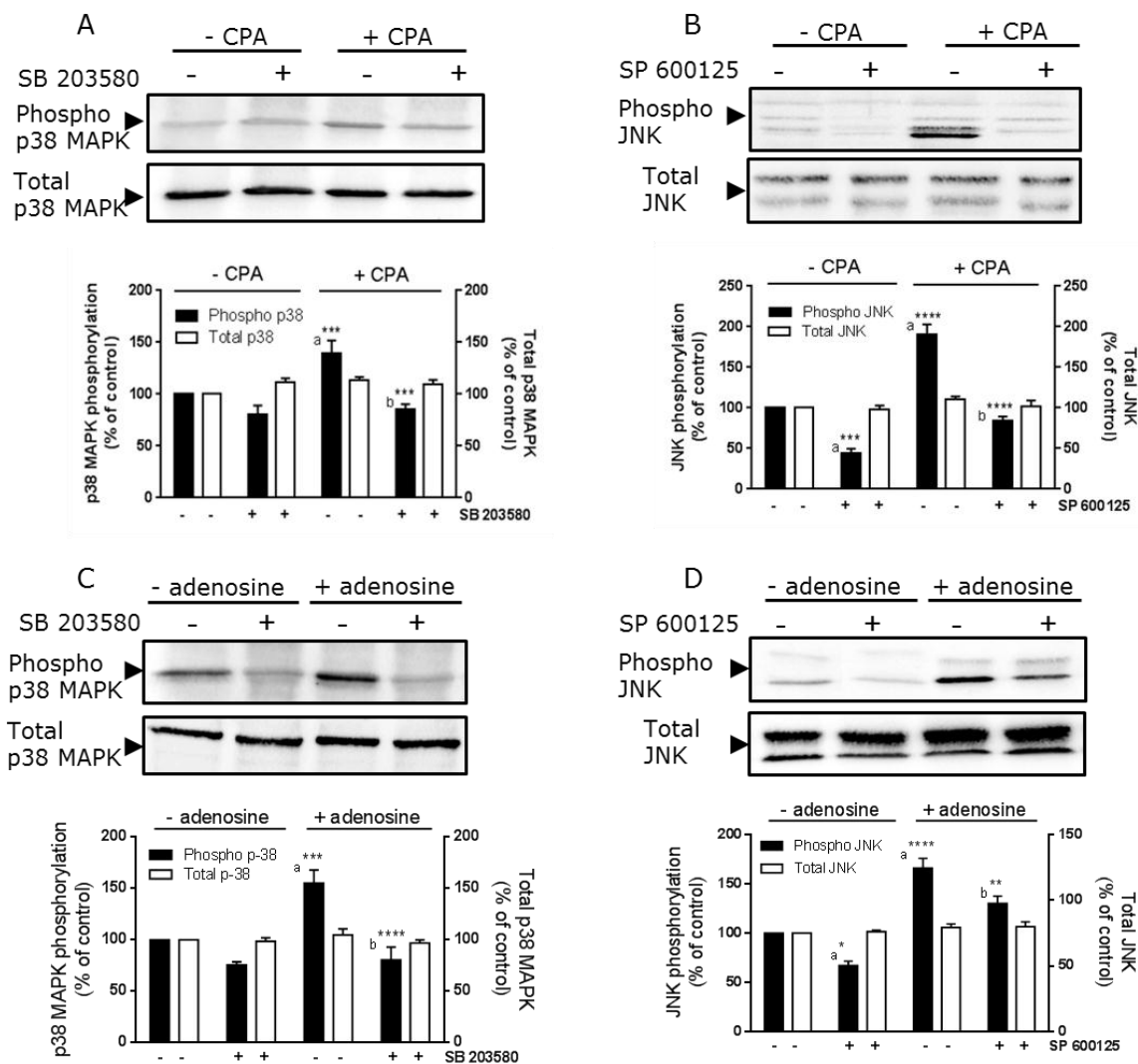


Fig 4.8: Effect of CPA and adenosine on p38 MAPK and JNK1/2 phosphorylation in H9c2 cells. Where indicated, H9c2 cells were pre-treated for 30 min with SB 203580 (20 μ M; panels A and C) or SP 600125 (20 μ M; panels B and D) prior to stimulation with either CPA (100 nM) or adenosine (100 μ M) for 10 min. Cell lysates were analysed by Western blotting for activation of p38 MAPK and JNK1/2 using phospho-specific antibodies. Samples were subsequently analysed on separate blots using antibodies that recognise total p38 MAPK and JNK1/2. Data are expressed as the percentage of values for control cells (=100%) in the absence of protein kinase inhibitor and represent the mean \pm S.E.M. of four independent experiments. * P <0.05, ** P <0.01, *** P <0.001 and **** P <0.0001, (a) versus control and (b) versus 100 nM CPA or 100 μ M adenosine alone.

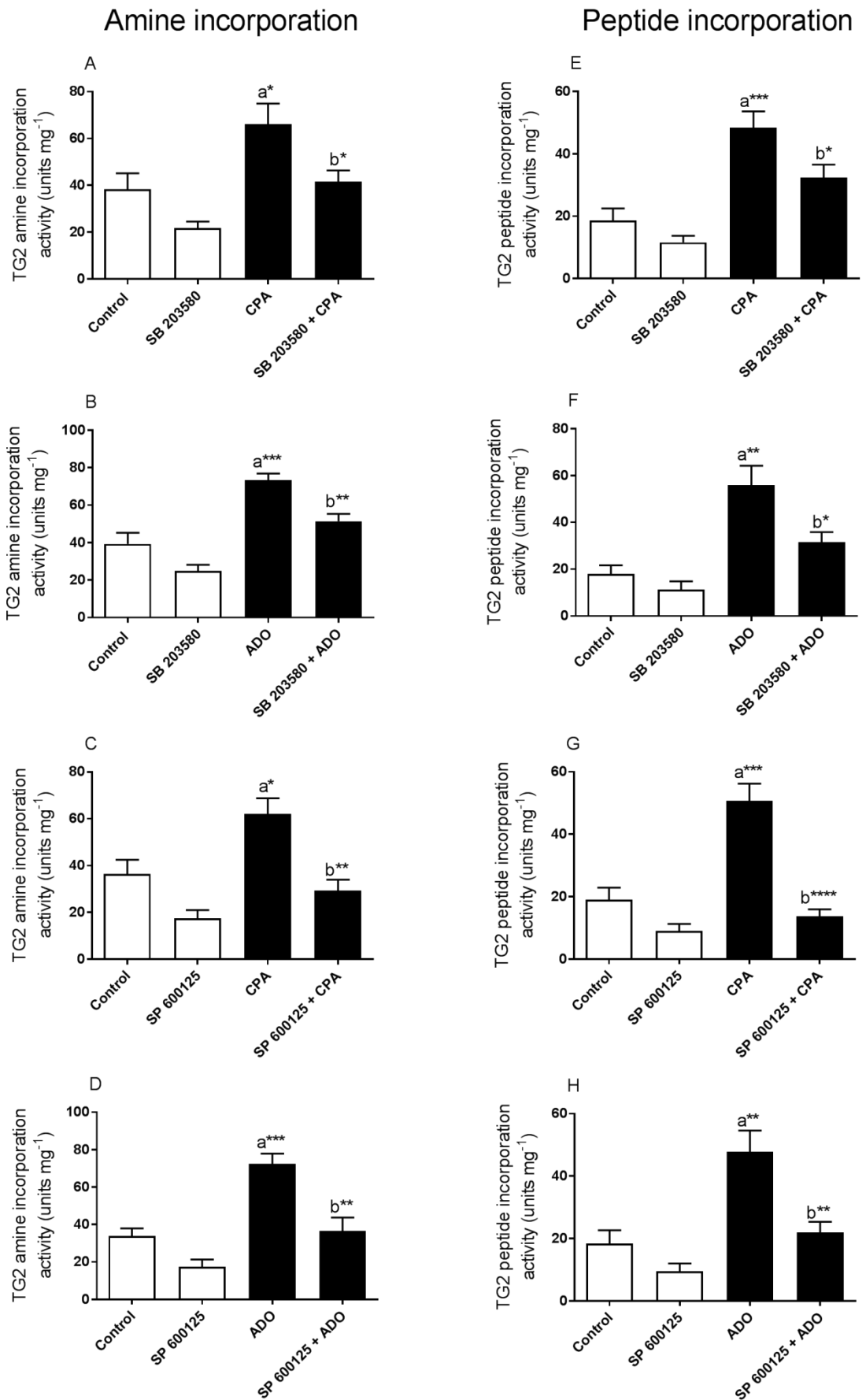


Fig 4.9: Effect of p38 MAPK and JNK1/2 inhibitors on the A₁ adenosine receptor-induced TG2 activity. H9c2 cells were pre-treated for 30 min with SB 203580 (20 μM) or SP 600125 (20 μM) prior to 10 min stimulation with CPA (100 nM) or adenosine (ADO; 100 μM). Cell lysates were subjected to protein biotin-cadaverine amine

incorporation assay (panels A to D) or peptide cross-linking assay (panels E and H). Data points represent the mean \pm S.E.M for TG2 specific activity from four independent experiments. * P <0.05, ** P <0.01, *** P <0.001 and **** P <0.0001, (a) versus control and (b) versus 100 nM CPA or 100 μ M adenosine alone.

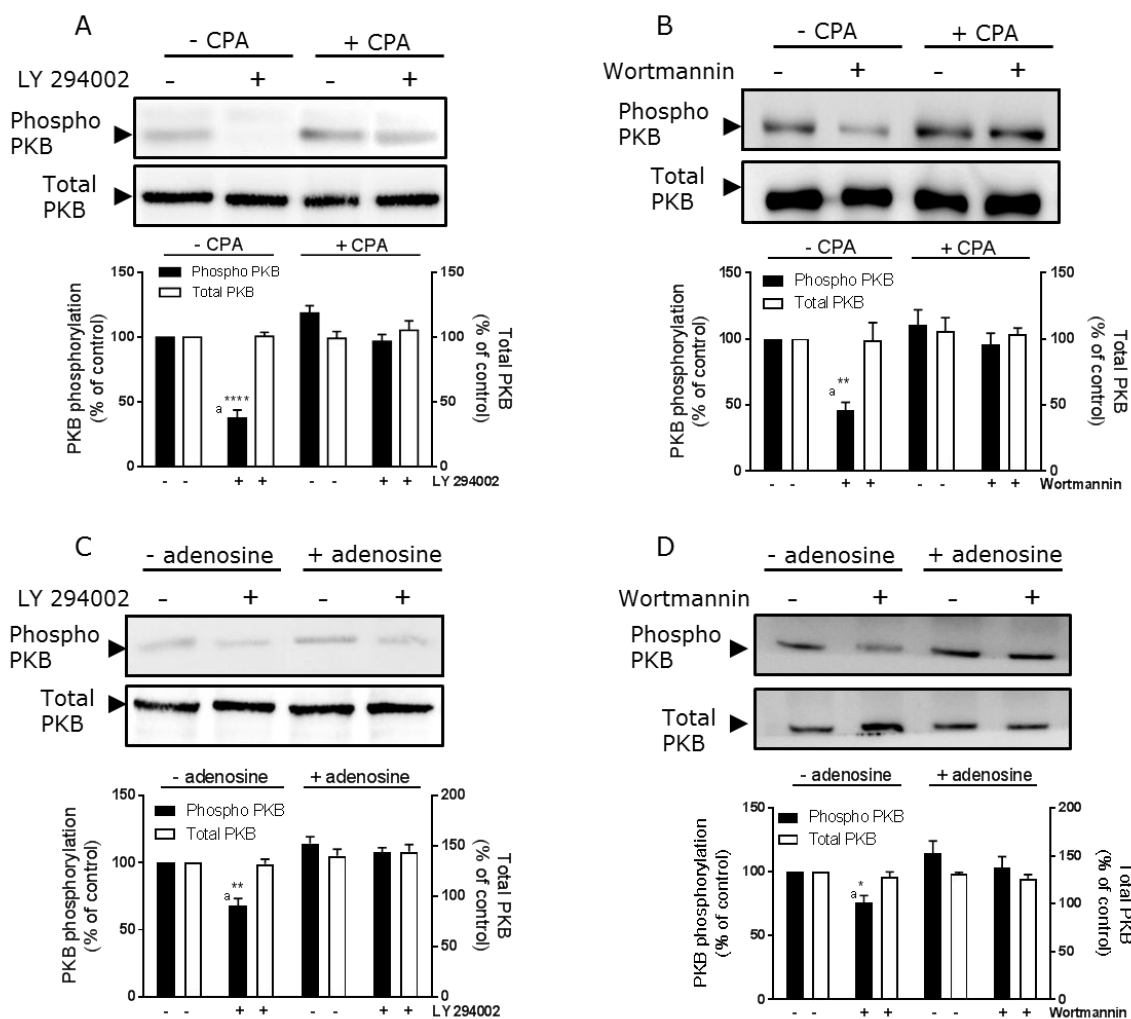


Fig 4.10: Effect of CPA and adenosine on PKB phosphorylation in H9c2 cells. Where indicated, H9c2 cells were pre-treated for 30 min with LY 294002 (30 μ M; panels A and C) and wortmannin (100 nM; panels B and D) prior to stimulation with CPA (100 nM) or adenosine (100 μ M) for 10 min. Cell lysates were analysed by Western blotting for activation of PKB using phospho-specific antibodies. Samples were subsequently analysed on separate blots using antibodies that recognize total PKB. Data are expressed as the percentage of values for control cells (=100%) in the absence of protein kinase inhibitor and represent the mean \pm S.E.M. of four independent experiments. * P <0.05, ** P <0.01, *** P <0.001 and **** P <0.0001, (a) versus control and (b) versus 100 nM CPA or 100 μ M adenosine alone.

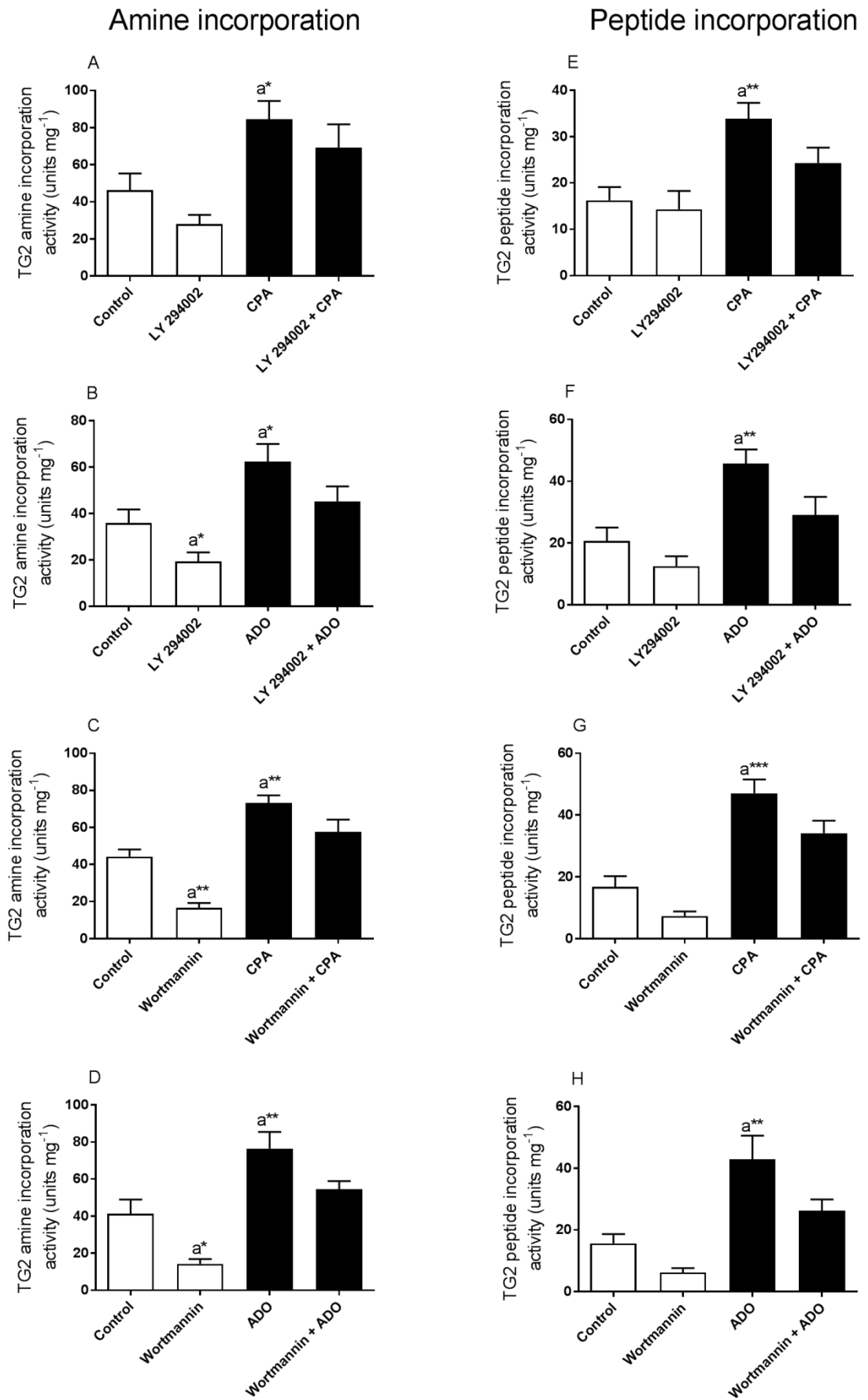


Fig 4.11: Effect of pan PI-3K inhibitors on the A₁ adenosine receptor-induced TG2 activity. H9c2 cells were pre-treated for 30 min with wortmannin (100 nM) or LY 294002 (30 μM) prior to 10 min stimulation with CPA (100 nM) or adenosine (ADO; 100 μM). Cell lysates were subjected to protein biotin-cadaverine amine incorporation

assay (panels A to D) or peptide cross-linking assay (panels E and H). Data points represent the mean \pm S.E.M for TG2 specific activity from four independent experiments. * P <0.05, ** P <0.01 and *** P <0.001, (a) versus control.

It is important to note that Ro 31-8220, PD 98059, SB 203580, SP 600125, LY 294002, wortmannin and other compounds used in this study had no significant effect on purified guinea pig liver TG2 activity (table 4.1). Overall, these data suggest that TG2 activity is modulated in H9c2 cells by the A₁ adenosine receptor via a multi protein kinase-dependent signalling pathway.

Table 4.1: Effect of compounds used in this study on purified guinea pig liver TG2 activity.

Compound	Concentration	Effect on in-vitro TG2 activity (% of control)	
		Amine Incorporation	Cross linking
Adenosine	100 μ M	102 \pm 6	95 \pm 2
CPA	100 nM	94 \pm 3	97 \pm 4
DMSO	10 mM	103 \pm 2	94 \pm 3
DPCPX	1 μ M	89 \pm 9	100 \pm 1
Forskolin	10 μ M	96 \pm 1	99 \pm 1
LY 294002	30 μ M	108 \pm 8	93 \pm 6
PD 98059	50 μ M	100 \pm 2	103 \pm 2
PTX	100 ng/ml	109 \pm 4	101 \pm 5
Ro 31-8220	10 μ M	103 \pm 5	97 \pm 1
SB 203580	30 μ M	98 \pm 3	97 \pm 1
SP 600125	20 μ M	90 \pm 5	110 \pm 1
Wortmannin	100 nM	103 \pm 3	96 \pm 6

TG2 amine incorporating and peptide crosslinking assays were carried out using purified guinea pig liver TG2 (50 ng/ well). Briefly, 50 ng of purified guinea pig liver TG2 was incubated with concentrations of the compounds listed in table 5.1 for 30 min prior to 1 h incubation in presence of either 6.67 mM calcium chloride or 13.3 mM EDTA containing 225 μ M biotin-cadaverine and 2 mM 2-mercaptoethanol. Following incubation, the plates were processed as described in section 2.3 (ii) and (iii) of chapter II.

4.5 Visualisation of *in situ* TG2 activity following A₁R activation.

Biotin-X-cadaverine, a cell penetrating biotin-labelled primary amine, acts as the acyl-acceptor during intracellular TG2-mediated transamidating reactions and is incorporated into endogenous protein substrates of TG2, which can subsequently be visualised by reporters such as FITC- and HRP-ExtrAvidin[®] (Lee et al, 1993). H9c2 cells were pre-incubated with 1 mM biotin-X-cadaverine for 6 h at 37°C prior to treatment with either CPA or adenosine for 1, 5, 10, 20, 30 and 40 min. After fixation and permeabilisation, intracellular proteins with covalently attached biotin-X-cadaverine were visualised using FITC-ExtrAvidin[®]. As shown in figure 4.12 and figure 4.13, CPA (100 nM) and adenosine (100 μM) induced time-dependent increases in the incorporation of biotin-X-cadaverine into endogenous protein substrates of TG2. These data are comparable to the transient time-dependent increases in TG2 activity observed *in vitro* (see figure 4.1 and 4.2). Surprisingly, given the covalent nature of biotin-X-cadaverine incorporation, fluorescence staining returned to control levels following 30 min incubation with CPA or 40 min incubation with adenosine. CPA-mediated biotin-X-cadaverine incorporation was also concentration-dependent ($pEC_{50} = 8.07 \pm 0.12$; $n=4$; figure 4.12). Similarly, adenosine-mediated biotin-X-cadaverine incorporation was also concentration-dependent ($pEC_{50} = 5.94 \pm 0.72$; $n=3$; figure 4.13).

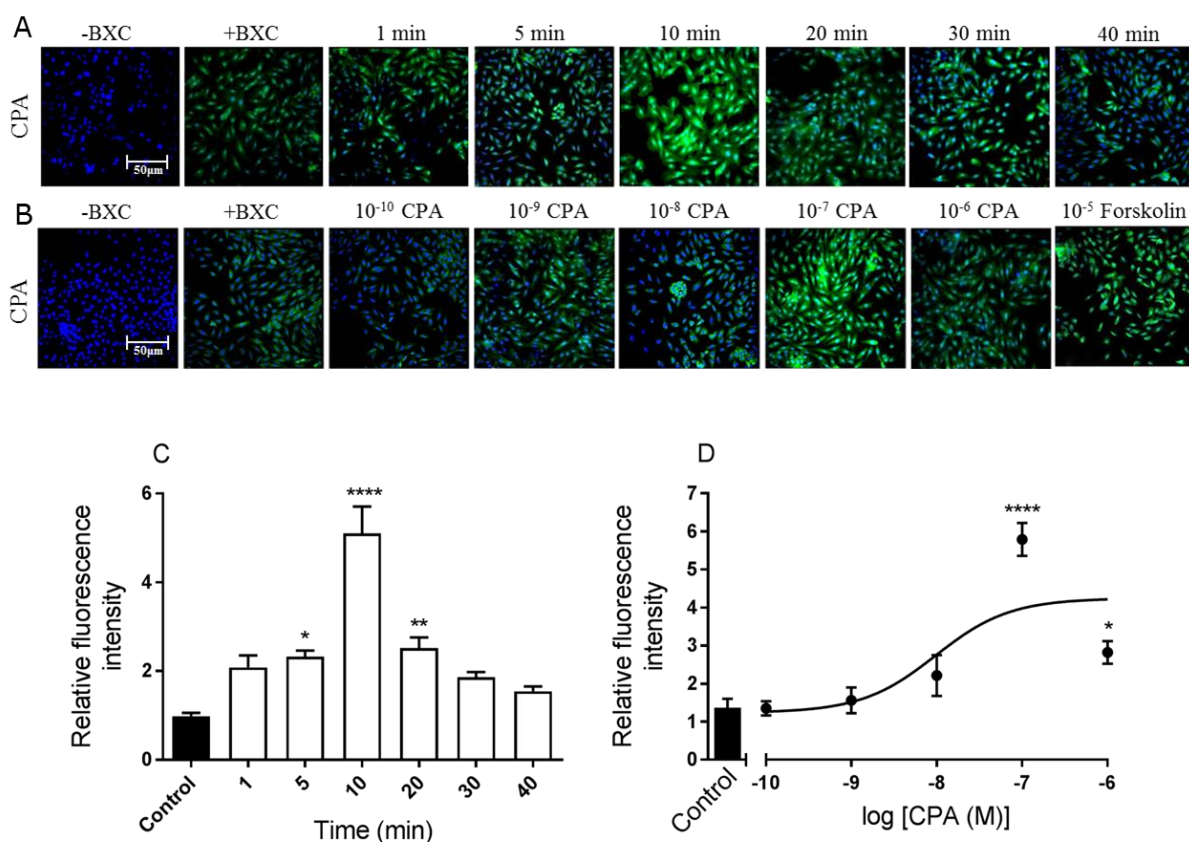


Fig 4.12: CPA-induced *in situ* TG2 activity in H9c2 cells. Cells were incubated with 1 mM biotin-X-cadaverine (BXC) for 6 h, after which they were treated with (A) 1 μM CPA for 1, 5, 10, 20, 30 or 40 min or (B) the indicated concentrations (in M) of CPA for 10 min. TG2-mediated biotin-X-cadaverine incorporation into intracellular proteins was

visualized using FITC-ExtrAvidin[®] (green). Nuclei were stained with DAPI (blue) and viewed using a Leica TCS SP5 II confocal microscope (20x objective lens). Images presented are from one experiment and representative of three independent experiments. Quantified data points for (C) time course and (D) concentration-response curve experiments represent the mean \pm S.E.M. of fluorescence intensity relative to DAPI stain for five fields of view each from three independent experiments. * $P < 0.05$, ** $P < 0.01$ and **** $P < 0.0001$ versus control response.

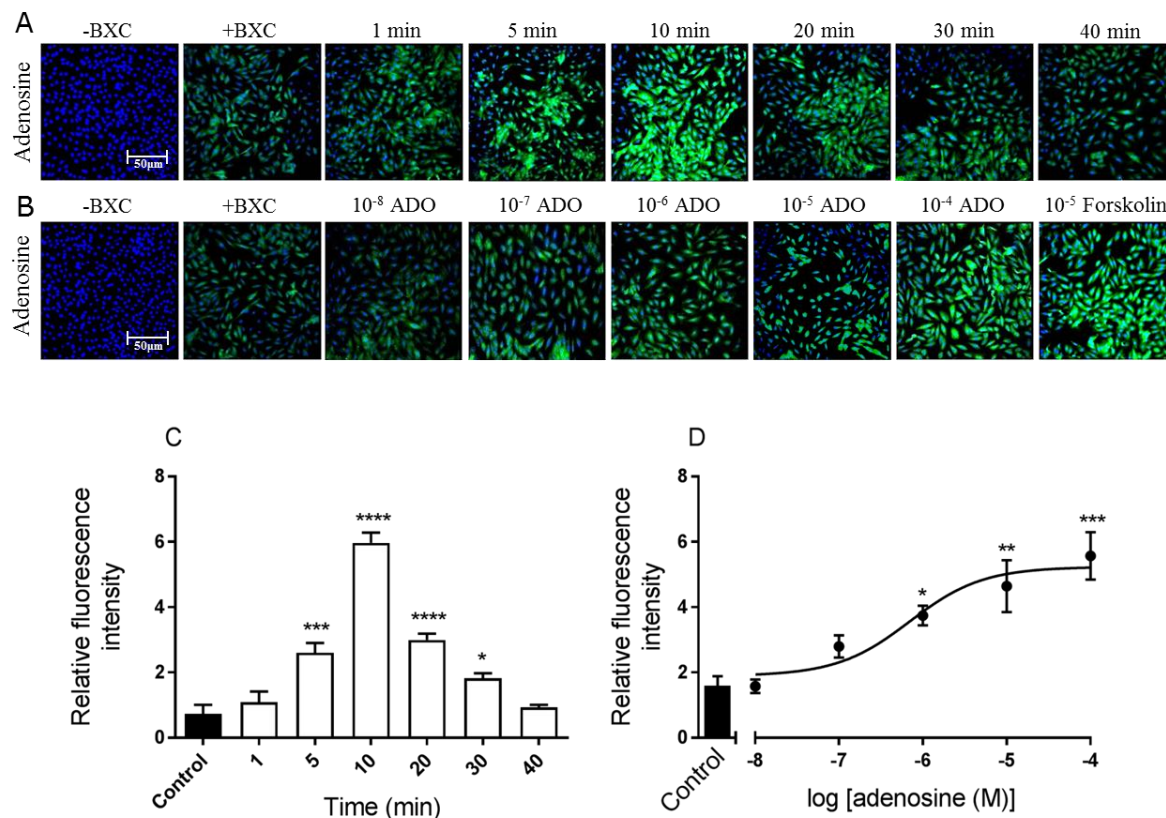


Fig 4.13: Adenosine-induced *in situ* TG2 activity in H9c2 cells. Cells were incubated with 1 mM biotin-X-cadaverine (BXC) for 6 h, after which they were treated with (A) 100 μ M adenosine (ADO) for 1, 5, 10, 20, 30 or 40 min or (B) the indicated concentrations (in M) of adenosine for 10 min. TG2-mediated biotin-X-cadaverine incorporation into intracellular proteins was visualized using FITC-ExtrAvidin[®] (green). Nuclei were stained with DAPI (blue) and viewed using a Leica TCS SP5 II confocal microscope (20x objective lens). Images presented are from one experiment and representative of three independent experiments. Quantified data points for (C) time course and (D) concentration-response curve experiments represent the mean \pm S.E.M. of fluorescence intensity relative to DAPI stain for five fields of view each from three independent experiments. * $P < 0.05$, ** $P < 0.01$, *** $P < 0.001$ and **** $P < 0.0001$ versus control response.

To confirm the involvement of the A₁R and G_{i/o}-proteins, cells were treated with the A₁R selective antagonist DPCPX (1 μ M) for 30 min and G_{i/o}-protein inactivating pertussis toxin (100 ng/ml) for 16 h prior to incubation with either CPA (100 nM) or adenosine (100 μ M) for 10 min. Pre-treatment of cells with DPCPX and PTX resulted in the complete inhibition of CPA- and adenosine-mediated biotin-X-cadaverine

incorporation into protein substrates (figure 4.14), confirming that the induced TG2 activity was mediated by the A₁R.

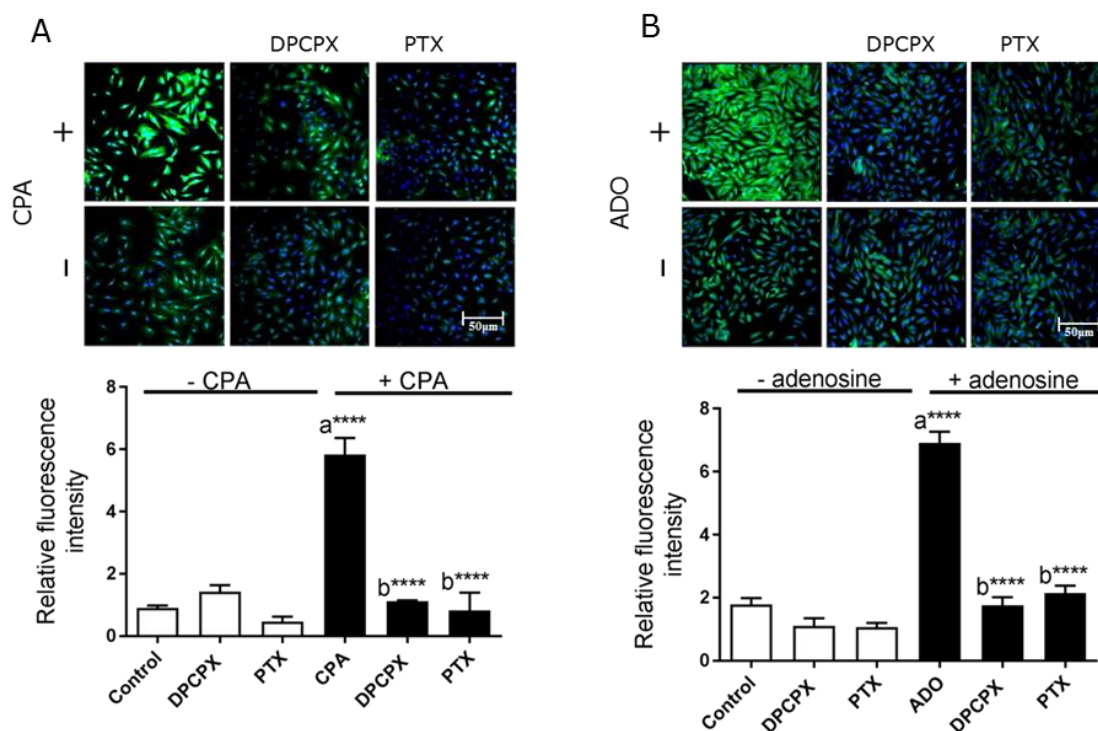


Fig 4.14: Effect of the A₁ adenosine receptor selective antagonist DPCPX and G_{i/o}-protein inactivating pertussis toxin on *in situ* TG2 activity. H9c2 cells were pre-treated for 30 min with the selective A₁ adenosine receptor antagonist DPCPX (1 μM) or 16 h with G_{i/o}-protein inactivating pertussis toxin (100 ng/ml) prior to 10 min stimulation with CPA (100 nM) or adenosine (100 μM). Cells were subsequently lysed with 0.1 M Tris buffer pH 8.0 containing protease and phosphatase inhibitors and cell lysates subjected to biotin cadaverine amine incorporation assay (panels A and C) or peptide cross-linking assay (panels Band D). Data points represent the mean ± S.E.M for TG2 specific activity from four independent experiments. *****P*<0.0001, (a) versus control and (b) versus 100 nM CPA or 100 μM adenosine alone.

To confirm the involvement of TG2 activation, cells were treated with the TG2 inhibitors Z-DON (150 μM) and R283 (200 μM) for 1 h prior to incubation with either CPA (100 nM) or adenosine (100 μM) for 10 min. Pre-treatment of cells with Z-DON and R283 resulted in the complete inhibition of CPA-mediated biotin-X-cadaverine incorporation into protein substrates (figure 4.15A). The *in situ* responses to CPA were also attenuated by inhibitors of PKC (Ro 31-8220; 10 μM), MEK1 (PD 98059, 50 μM), p38 MAPK inhibitor (SB 203580; 20 μM), JNK1/2 inhibitor (SP 600125; 20 μM) and following removal of Ca²⁺ (figure 4.15).

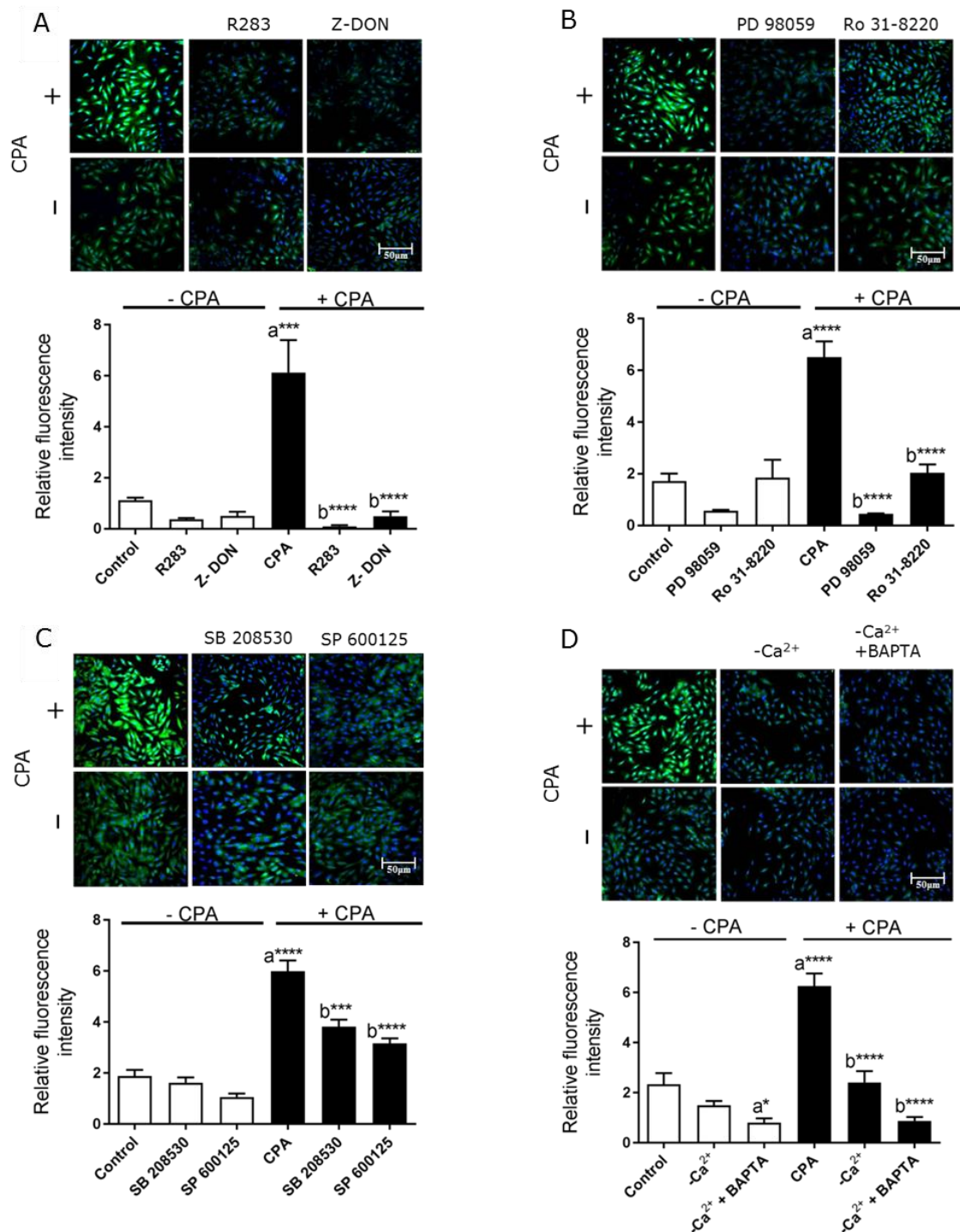


Fig 4.15: Effects of TG2, PKA, ERK1/2, p38 MAPK, JNK1/2 inhibitors and removal of Ca²⁺ on *in situ* TG2 activity in H9c2 cells following stimulation with CPA. Cells were incubated with 1 mM biotin-X-cadaverine (BXC) for 6 h after which they were treated as follows: (A) 1 h with the TG2 inhibitors Z-DON (150 μ M) or R283 (200 μ M), (B) 30 min with PD 98059 (50 μ M) or Ro 31-8220 (10 μ M), (C) 30 min with SB 203580 (20 μ M) or SP 600125 (20 μ M), and (D) in the absence of extracellular Ca²⁺ for 30 min (nominally Ca²⁺-free Hanks/HEPES buffer containing 0.1 mM EGTA) or pre-incubated for 30 min with 50 μ M BAPTA/AM and in the absence of extracellular Ca²⁺ (nominally Ca²⁺-free Hanks/HEPES buffer containing 0.1 mM EGTA) to chelate intracellular Ca²⁺, prior to 10 min stimulation with CPA (100 nM). TG2-mediated biotin-X-cadaverine incorporation into intracellular proteins was visualized using FITC-ExtrAvidin[®] (green).

Nuclei were stained with DAPI (blue) and viewed using a Leica TCS SP5 II confocal microscope (20x objective lens). Images presented are from one experiment and are representative of three independent experiments. Quantified data points represent the mean \pm S.E.M. of fluorescence intensity relative to DAPI stain for five fields of view from each of three independent experiments. *** $P < 0.001$ and **** $P < 0.0001$, (a) versus control and (b) versus 100 nM CPA alone.

Similarly, adenosine-mediated biotin-X-cadaverine incorporation into protein substrates was sensitive to TG2 (Z-DON; 150 μ M and R283; 200 μ M), PKC (Ro 31-8220; 10 μ M), MEK1/2 (PD 98059; 50 μ M), p38 MAPK (SB 203580; 20 μ M), and JNK1/2 (SP 600125; 20 μ M) inhibitors and following the removal of Ca^{2+} (figure 4.16).

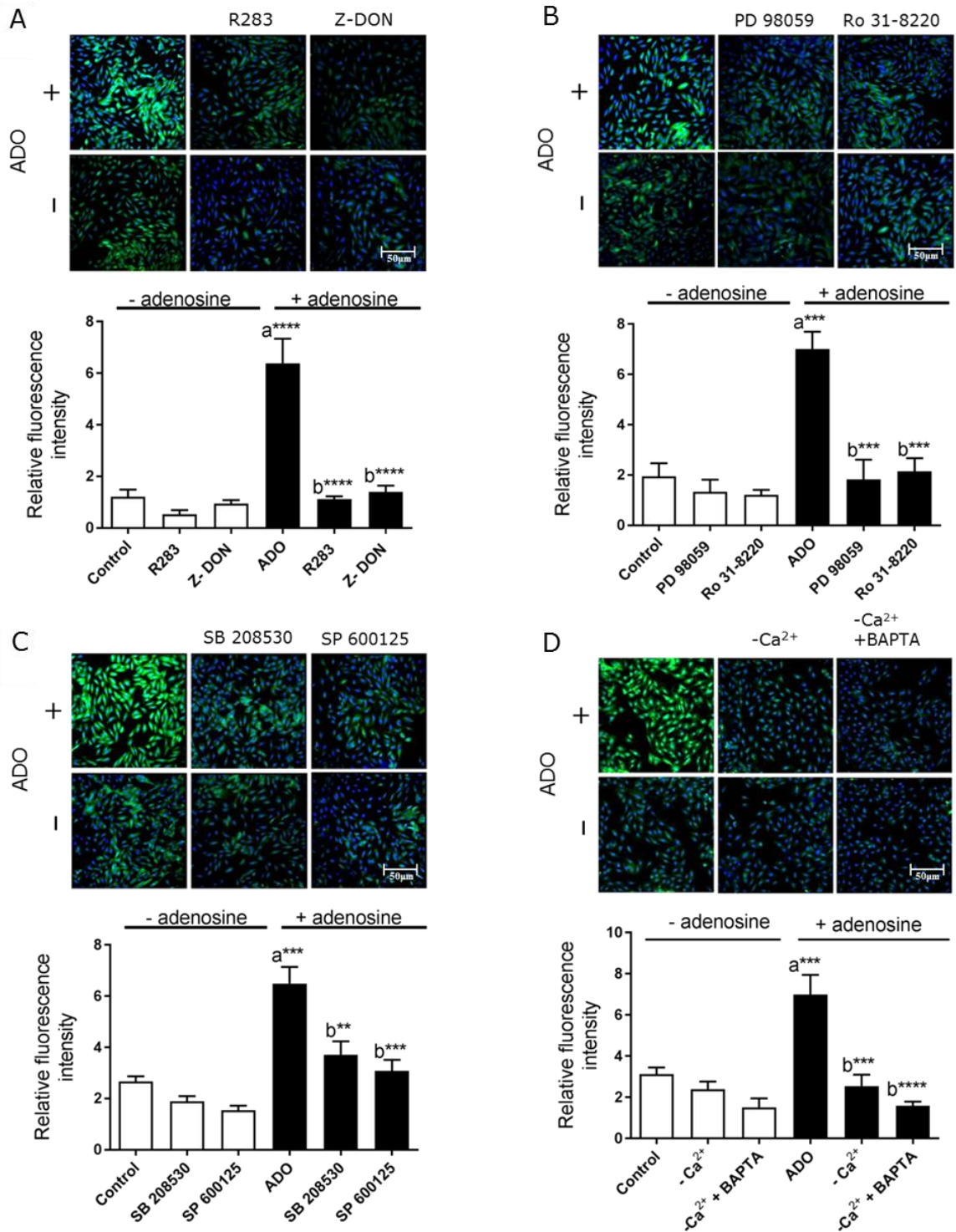


Fig 4.16: Effects of TG2, PKA, ERK1/2, p38 MAPK, JNK1/2 inhibitors and removal of Ca^{2+} on *in situ* TG2 activity in H9c2 cells following stimulation with adenosine. Cells were incubated with 1 mM biotin-X-cadaverine (BXC) for 6 h after which they were treated as follows: (A) 1 h with the TG2 inhibitors Z-DON (150 μM) or R283 (200 μM), (B) 30 min with PD 98059 (50 μM) or Ro 31-8220 (10 μM), (C) 30 min with SB 203580 (20 μM) or SP 600125 (20 μM), and (D) in the absence of extracellular Ca^{2+} for 30 min (nominally Ca^{2+} -free Hanks/HEPES buffer containing 0.1 mM EGTA) or pre-incubated for 30 min with 50 μM BAPTA/AM and in the absence of extracellular Ca^{2+} (nominally Ca^{2+} -free Hanks/HEPES buffer containing 0.1 mM EGTA) to chelate

intracellular Ca^{2+} , prior to 10 min stimulation with adenosine (ADO; 100 μM). TG2-mediated biotin-X-cadaverine incorporation into intracellular proteins was visualized using FITC-ExtrAvidin[®] (green). Nuclei were stained with DAPI (blue) and viewed using a Leica TCS SP5 II confocal microscope (20x objective lens). Images presented are from one experiment and are representative of three independent experiments. Quantified data points represent the mean \pm S.E.M. of fluorescence intensity relative to DAPI stain for five fields of view from each of three independent experiments. *** $P < 0.001$ and **** $P < 0.0001$, (a) versus control and (b) versus 100 μM adenosine alone.

4.6 A₁R induced TG2 phosphorylation.

The effect of CPA on TG2 phosphorylation was examined via immunoprecipitation of TG2, followed by SDS-PAGE and Western blot analysis using anti-phosphoserine and anti-phosphothreonine antibodies. As shown in figure 4.17 and 4.18, CPA (100 nM) enhanced the phosphoserine and phosphothreonine residues within TG2. Pre-treatment with Ro 318220 (10 μM), PD 98059 (50 μM) and SP 600125 (20 μM) attenuated CPA-induced TG2 phosphorylation (figure 4.17 and 4.18). However, SB 203580 (20 μM) had no significant effect on CPA-induced TG2 phosphorylation (figure 4.18).

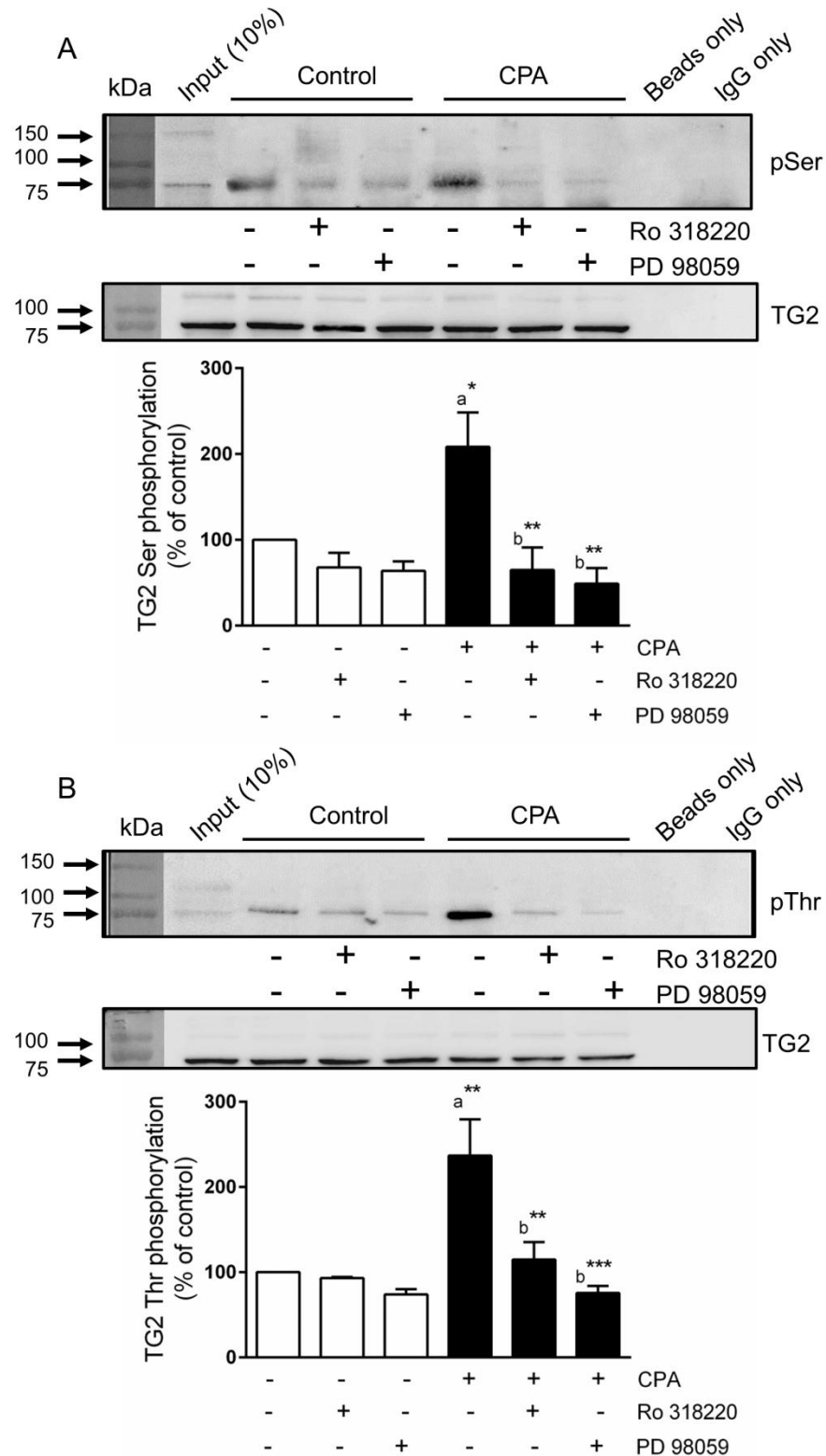


Fig 4.17: Effect of PKC and ERK1/2 inhibition on CPA-induced phosphorylation of TG2. Where indicated, H9c2 cells were incubated for 30 min with Ro 318220 (10 μ M) or PD 98059 (50 μ M) prior to stimulation with CPA (100 nM) for 10 min. Following stimulation, cell lysates were subjected to immunoprecipitation using an anti-TG2 monoclonal antibody as described in section 2.7 of chapter II. The resultant immunoprecipitated protein(s) were subjected to SDS-PAGE and analysed via Western blotting using (A) anti-phosphoserine and (B) anti-phosphothreonine antibodies.

10% of the input was added to the first lane to show the presence of phosphorylated proteins prior to immunoprecipitation and negative controls with the immunoprecipitation performed with beads or IgG only were included to demonstrate the specificity of the bands shown. Quantified data for formoterol-induced increases in TG2-associated serine and threonine phosphorylation are expressed as a percentage of that observed in control cells (100%). Data points represent the mean \pm S.E.M. from three independent experiments. * P <0.05, ** P <0.01 and *** P <0.001 (a) versus control and (b) versus CPA alone.

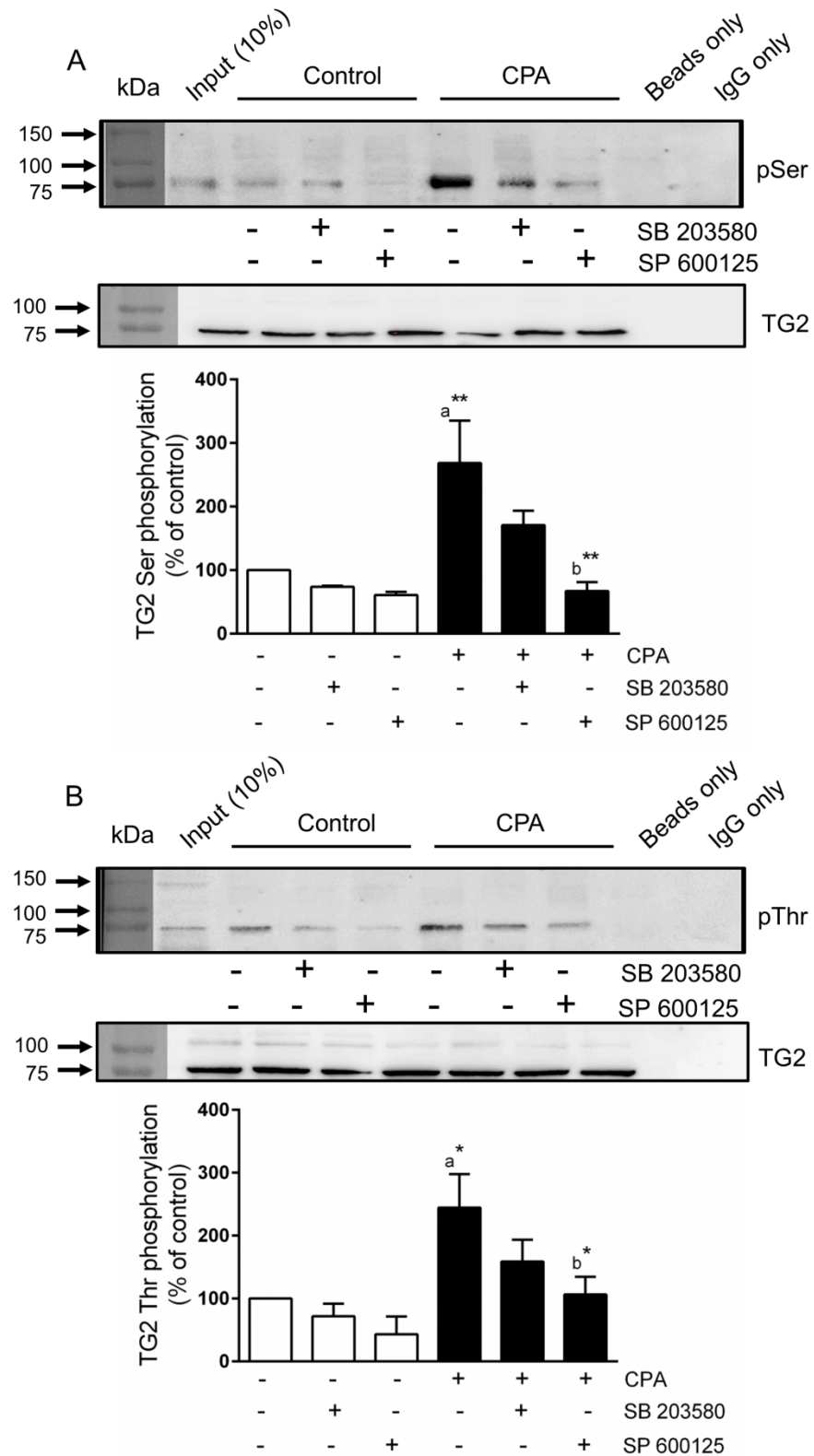


Fig 4.18: Effect of p38 MAPK and JNK1/2 inhibition on CPA-induced phosphorylation of TG2. Where indicated, H9c2 cells were incubated for 30 min with SB 203580 (20 μ M) or SP 600125 (20 μ M) prior to stimulation with CPA (100 nM) for 10 min. Following stimulation, cell lysates were subjected to immunoprecipitation using an anti-TG2 monoclonal antibody as described in section 2.7 of chapter II.. The resultant immunoprecipitated protein(s) were subjected to SDS-PAGE and analysed via Western blotting using (A) anti-phosphoserine and (B) anti-phosphothreonine antibodies.

10% of the input was added to the first lane to show the presence of phosphorylated proteins prior to immunoprecipitation and negative controls with the immunoprecipitation performed with beads or IgG only were included to demonstrate the specificity of the bands shown. Quantified data for formoterol-induced increases in TG2-associated serine and threonine phosphorylation are expressed as a percentage of that observed in control cells (100%). Data points represent the mean \pm S.E.M. from three independent experiments. * P <0.05 and ** P <0.01 (a) versus control and (b) versus CPA alone.

In conclusion, the data shown in this chapter provide sufficient evidence that supports the notion that TG2 activity is modulated by the A₁ adenosine receptor in mitotic H9c2 cells via a multi kinase dependent pathway.

4.7 Discussion.

The aims of this chapter were to identify if TG2 is modulated by the A₁ adenosine receptor in H9c2 cells and to determine the molecular mechanisms underlying this modulation.

In vitro modulation of TG2 by the A₁R:

Recently Almami and colleagues reported that PMA (a PKC activator) triggers increases in TG2-mediated transamidase activity in H9c2 cells (Almami et al, 2014). Hence, it was of interest to investigate if the A₁R, which couples to PKC, could modulate TG2-mediated transamidase activity in rat H9c2 cardiomyoblasts. Activation of the A₁R with the selective agonist CPA or the endogenous agonist adenosine triggered time- and concentration-dependent increases in the amine-incorporating and protein cross-linking activity of TG2 (figures 4.1 and 4.2). It was observed that there was a trend towards a decrease in both amine incorporation and protein cross-linking activities of TG2 at 1 min following activation of A₁R using CPA and adenosine. At present, it is not known how A₁R activation promotes an apparent inhibition of TG2 amine incorporation activity. Moreover, experiments performed with the selective A₁R antagonist DPCPX and the G_{i/o}-protein inactivating pertussis toxin further clarify that the responses obtained occur through the A₁R and G_{i/o}-protein-mediated signalling (figure 4.3 and 4.5). Finally, involvement of TG2 was confirmed as responses to agonists were blocked by R283 and Z-DON, two structurally different TG2 inhibitors (Freund et al, 1994; Schaertl et al, 2010; figure 4.3). It should be noted that these TG2 inhibitors are poorly cell-permeable and inhibition of cellular TG2 is only achievable at concentrations significantly above their IC₅₀ value versus purified enzyme (Schaertl et al, 2010; Freund et al, 1994). Hence, from these results, it is clear that the A₁R is able to modulate TG2 mediated amine- and peptide-incorporating activities.

At present there is insufficient knowledge regarding the regulation of TG2 enzymatic activity by GPCRs. Some examples in the literature include muscarinic receptor-

mediated increases in TG2 activity in SH-SY5Y cells (Zhang et al, 1998) and 5-HT_{2A} receptor mediated transamidation (TG-catalysed) of the small G-protein Rac1 in the rat A1A1v cells (Dai et al, 2008). Zhang and colleagues (1998) measured *in situ* TG2 activity (polyamine incorporation) triggered by the muscarinic agonist carbachol, whereas Dai and colleagues (2008) reported TG2-catalysed incorporation of 5-hydroxytryptamine into Rac1. 5-HT_{2A} receptor-mediated incorporation of 5-HT into the small GTPases RhoA and Rab4 was also observed in platelets (Walther et al, 2003). It has been suggested that 5-HT_{2A} and muscarinic receptor-mediated release of Ca²⁺ from intracellular Ca²⁺ stores might be responsible for triggering TG transamidating activity (Zhang et al, 1998; Walther et al, 2003).

Role of extracellular Ca²⁺ in A₁R-induced TG2 activation:

The amine- and peptide-incorporating activities of TG2 are dependent upon Ca²⁺ (Slaughter et al, 1992; Trigwell et al, 2004), therefore the role of extracellular and intracellular Ca²⁺ in A₁R-induced TG2 activation was investigated. Although coupled to G_{i/o}-proteins, the A₁R directly stimulates inositol phospholipid hydrolysis and Ca²⁺ signalling through G-protein βγ subunit-mediated activation of phospholipase C in DDT₁MF-2 cells, rat ventricular myocytes, rat atria and mouse heart (White et al, 1992; Dickenson & Hill, 1993, Dickenson et al, 1995; Sterin-Borda et al, 2002; Fenton et al, 2010). Removal of extracellular Ca²⁺ inhibited CPA- and adenosine-induced TG2-mediated amine- and peptide-incorporating activities (figure 4.4). As shown in chapter III (see figures 3.4 and 3.5), CPA and adenosine triggered increases in intracellular Ca²⁺ levels in H9c2 cells loaded with Fluo-8 AM which were characterised by pronounced Ca²⁺ oscillations and abolished following removal of extracellular Ca²⁺. As the A₁R-induced TG2 activation was also abolished following removal of extracellular Ca²⁺, it suggests that extracellular Ca²⁺ has an important role in modulation of TG2. Further studies are warranted to determine precisely how A₁R-induced Ca²⁺ influx and TG2 activation occur in H9c2 cells. However, it is known that the A₁R promotes receptor-operated Ca²⁺ influx in cardiomyocytes via a phospholipase C and PKC-dependent pathway (Sabourin et al, 2012) and hence the kinase-dependent pathways outlined in the present study could be central to these novel aspects of TG2 modulation by the A₁R.

Role of protein kinases in A₁R-induced TG2 activity:

The role of PKC and other protein/lipid kinases in CPA- and adenosine-induced TG2 activation were investigated using appropriate pharmacological inhibitors. Even though TG2 activity can be modulated by intracellular [Ca²⁺] changes, there is growing evidence that TG activity can also be regulated by phosphorylation (Bollag et al, 2005; Mishra et al, 2007). PKB was not activated following stimulation of A₁R (figure 4.10) suggesting that this pathway is not involved. Similarly, the pan PI-3K inhibitors LY 294002 and wortmannin did not have any effect on A₁R induced TG2 activation (figure

4.11), further confirming that these protein kinases are not involved. As illustrated in figure 4.6, CPA and adenosine induced robust increases in ERK1/2. The broad spectrum PKC inhibitor Ro 31-8220 and the MEK1/2 (up-stream activator of ERK1/2) inhibitor PD 98059 completely abolished CPA and adenosine-induced TG2 activity (figure 4.7), suggesting prominent roles for PKC and ERK1/2. Although ERK1/2 has been implicated in regulating the cross-linking activity of TG1 (Bollag et al, 2005) there is no prior evidence suggesting a role for this protein kinase in TG2 regulation. It is interesting to note that ERK1/2 activation by the A₁R is sensitive to PKC inhibition in both neonatal rat cardiomyocytes (Germack and Dickenson, 2004) and H9c2 cells (Fretwell and Dickenson, 2009) and, therefore, the role of PKC in TG2 activation may be up-stream of ERK1/2.

As indicated in figure 4.8, CPA and adenosine also induced robust activation of p38 MAPK and JNK1/2. The p38 MAPK and JNK1/2 inhibitors SB 203580 and SP 600125 blocked CPA and adenosine-induced TG2 activation (figure 4.9), further confirming the role of these protein kinases. Previous studies have shown activation of p38 MAPK occurs upon stimulation of A₁R in adult rat ventricular myocytes, Langendorff-perfused rat hearts, isolated rabbit ventricular myocytes and a human cardiomyocyte-derived cell line (Carroll and Yellon, 2000; Dana et al, 2000; Mocanu et al, 2000; Liu and Hofmann, 2003; Ballard-Croft et al, 2005). In all of these cases, activation of p38 by the A₁R was crucial for A₁R-mediated preconditioning against ischaemia-reperfusion injury. Furthermore, activation of JNK1/2 following stimulation of A₁R is not known to occur in cardiac cells. However, there are several studies reporting activation of JNK1/2 following stimulation of A₁R in rat hippocampus (Burst et al, 2007; Chen et al, 2014; Stockwell et al, 2017).

There appears to be general constitutive activity of the enzyme TG2 in H9c2 cells. This activity could be a result of constitutive activity of the A₁R or that TG2 is regulated by other constitutively active GPCRs. However, this is unlikely as there have been no studies investigating constitutive activation of GPCRs in H9c2 cells. There also seems to be a trend that the protein kinases assessed in this study can lower TG2 basal activity. As mentioned previously, there are some examples of TG2 being modulated by GPCRs and therefore, these kinases could be activated by a different GPCR (apart from A₁R) and modulate the basal activity of TG2. Furthermore, it is possible that TG2 activity is not only modulated by GPCRs but also by other receptors that activate protein kinases e.g. Receptor Tyrosine Kinases (RTKs; Sivaramakrishnan et al, 2013), post-translational modifications (phosphorylation; Mishra and Murphy, 2006) and direct activation of kinases by intracellular peptides (such as polyubiquitin chains; Xia et al, 2009). Therefore it is not surprising that the basal TG2 activity is lowered when treated with inhibitors of protein kinases on their own. Overall, these data suggest that the A₁R regulates TG2 activity in H9c2 cells via a multi-protein kinase dependent

pathway. Although protein kinase inhibition and removal of extracellular Ca^{2+} both inhibit A_1R -induced TG2 activation, the relationship between the two is yet to be explored.

A_1R -induced phosphorylation of TG2:

Given the apparent role of multiple serine/threonine kinases in modulation of TG2, it was of interest to investigate the phosphorylation status of TG2 following A_1R stimulation. The data obtained demonstrate that TG2 is phosphorylated in response to A_1R activation (figure 4.17 and 4.18). Hence, the modulation of TG2 phosphorylation may represent a prominent downstream target of A_1R signalling. Previous studies have revealed that TG2 is phosphorylated by PKA at Ser²¹⁵ and Ser²¹⁶ (Mishra and Murphy, 2006) and at an unknown site(s) by PTEN-induced putative kinase 1 (PINK1; Min et al, 2015). It is also known that phosphorylation of TG2 by PKA at Ser²¹⁶ inhibits its transamidase activity and enhances its kinase activity (Mishra et al, 2007; Wang et al, 2012). Phosphoproteomic studies have also identified numerous phosphorylation sites in human (Ser⁵⁶, Ser⁶⁰, Tyr²¹⁹, Thr³⁶⁸, Tyr³⁶⁹, Ser⁴¹⁹, Ser⁴²⁷, Ser⁵³⁸, Ser⁵⁴¹ and Ser⁶⁰⁸; Rikova et al, 2007; Imami et al, 2008; Kettenbach et al, 2011; Bian et al, 2014; Palacios-Moreno et al, 2015) and rat (Tyr⁴⁴, Thr⁵⁸, Ser⁶⁸ and Ser⁴⁴⁹; Hoffert et al, 2006; Lundby et al, 2012) TG2. Therefore, it is of great interest to identify the specific serine and threonine residue(s) within TG2 that are phosphorylated following A_1R activation as well as the functional consequence(s) of A_1R -induced TG2 phosphorylation.

Given the multiple protein kinases implicated in A_1R -induced TG2 activation, the influence of protein kinase inhibitors on TG2 phosphorylation were also investigated. CPA-induced increases in TG2 serine and threonine phosphorylation were significantly reduced following pharmacological inhibition of PKC (Ro 31-8220), MEK1/2 (PD 98059) or JNK1/2 (SP 600125). However, further studies are required to confirm whether these protein kinases directly catalyse the phosphorylation of TG2. It is notable that the p38 MAPK inhibitor SB203580 did not attenuate TG2 phosphorylation despite being able to block A_1R -induced TG2 activation, suggesting that p38 MAPK modulates other targets involved in TG2 activation. Finally, as TG2 possesses kinase activity, it is conceivable that CPA-induced increases in TG2-bound serine and threonine phosphorylation may involve auto-phosphorylation. However, further work to identify the phosphorylation site(s) involved in auto-phosphorylation and phosphorylation following A_1R activation would be of value and necessary.

In situ A_1R -induced polyamine incorporation into protein substrates:

In situ TG2 activity following A_1R stimulation increased in a time- and concentration-dependent manner, which was comparable to CPA- and adenosine-induced amine incorporation activity observed *in vitro* (figure 4.12 and 4.13). The role of the A_1R and $\text{G}_{i/o}$ -proteins in inducing *in situ* TG2 activity was confirmed using the selective A_1R

antagonist DPCPX and the $G_{i/o}$ -protein inactivating pertussis toxin, which were able to reverse *in situ* TG2 activity (figure 4.14). However, given the covalent nature of biotin-X-cadaverine incorporation into protein substrates, it was surprising to observe that *in situ* TG2 activity returned to basal levels after 40 min. Possible explanations for this include reversal of amine incorporation catalysed by TG (Stamnaes et al, 2008), targeting of biotin-cadaverine-labelled proteins for degradation or their rapid expulsion from the cell. The rapid export of biotin-cadaverine-labelled proteins from PMA- or forskolin-stimulated H9c2 cells has been previously observed (Almami *et al.*, 2014), so a similar mechanism may be occurring following A_1R activation. The role of TG2 in *in situ* A_1R -induced polyamine incorporation into protein substrates was confirmed using TG2 inhibitors Z-DON and R283, which were able to significantly reverse *in situ* TG2 activity (figures 4.15A and 4.16A). A_1R -induced *in situ* TG2 responses were also sensitive to pharmacological inhibition of PKC (Ro 31-8220), MEK1/2 (PD 98059), p38 MAPK (SB203580), JNK1/2 (SP 600125) and removal of Ca^{2+} (figures 4.15 and 4.16), confirming the role of these signalling pathways. In summary, these data demonstrate that A_1R mediated incorporation of polyamines via TG2 is dependent up on range of protein kinases.

In conclusion, this present study has revealed that A_1R -mediated activation of TG2 occurs via a multi-protein kinase pathway in H9c2 cells. Figure 4.19 and table 4.2 summarises the findings of this chapter.

Table 4.2: Summary of the effect of treatments on A₁R-induced TG2 activities.

A ₁ R-induced TG2 activation						
TG2 activity	Amine incorporation		peptide crosslinking		<i>in-situ</i>	
Treatments	CPA	ADO	CPA	ADO	CPA	ADO
1 μM DPCPX	Y	Y	Y	Y	Y	Y
150 μM Z-DON	Y	Y	Y	Y	Y	Y
200 μM R283	Y	Y	Y	Y	Y	Y
Nominally Ca ²⁺ -free Hanks/HEPES buffer containing 0.1 mM EGTA	Y	Y	Y	Y	Y	Y
50 μM BAPTA-AM in nominally Ca ²⁺ -free Hanks/HEPES buffer containing 0.1 mM EGTA	Y	Y	Y	Y	Y	Y
100 ng/ml PTX	Y	Y	Y	Y	Y	Y
50 μM PD 98059	Y	Y	Y	Y	Y	Y
10 μM Ro 31-8220	Y	Y	Y	Y	Y	Y
20 μM SB 208530	Y	Y	Y	Y	Y	Y
20 μM SP 600125	Y	Y	Y	Y	Y	Y
30 μM LY 294002	N	N	N	N		
100 nM Wortmannin	N	N	N	N		

Effects of a range of treatments used in this study were investigated for TG2 amine incorporating, peptide crosslinking and *in-situ* activities in H9c2 cells, following stimulation with either CPA or adenosine. H9c2 cells were treated with above mentioned treatments in presence of CPA (100 nM) or adenosine (ADO; 100 μM) and cell lysates subjected to determine TG2 amine incorporating, peptide crosslinking and *in-situ* activities according to the protocols described in chapter II section 2.3.

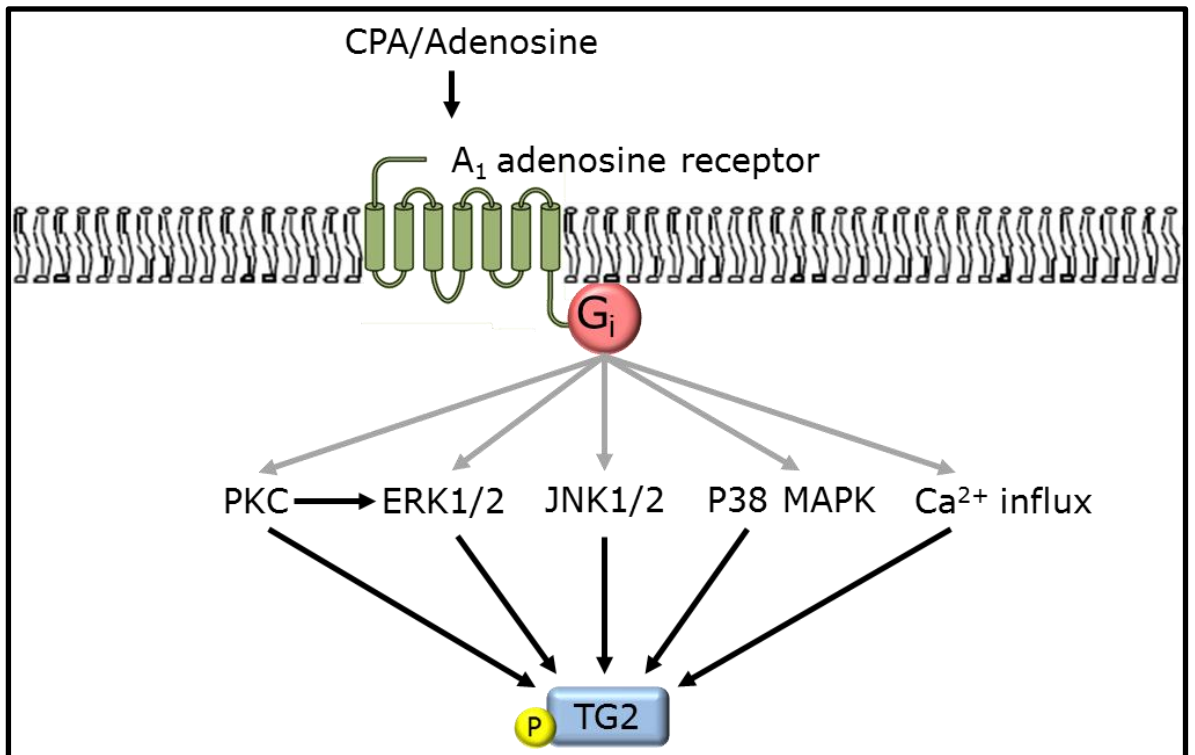


Fig 4.19: Summary of the findings presented in this study. Stimulation of the A₁ adenosine receptor (A₁R) by selective and endogenous agonists (CPA and adenosine, respectively) triggers activation of protein kinases (PKC, ERK1/2, JNK1/2 and p38 MAPK) along with influx of extracellular Ca²⁺ leading to increases in TG2 activity and TG2 phosphorylation. Solid black arrows represent findings of this study and grey arrows represent published findings (not from the present study).

Chapter V: Modulation of TG2 activity by the β_2 adrenoceptor in H9c2 cells

This chapter aims to investigate modulation of TG2 by the β_2 adrenoceptor in mitotic H9c2 cells via TG2 amine incorporating and peptide crosslinking assays along with *in-situ* TG2 activity. It also investigates the signalling mechanisms underlying its modulation.

5.1 Effect of β_2 -AR activation on TG2-mediated biotin cadaverine amine incorporation and protein cross-linking activity.

Initially the effect of the selective β_2 -AR agonist formoterol on TG2 activity in H9c2 cardiomyoblasts was investigated. H9c2 cells were treated with formoterol (100 nM) for varying intervals of time and the cell lysates subjected to both biotin cadaverine amine-incorporation assay (Slaughter et al, 1992) and biotin-labelled peptide (biotin-TVQQEL) cross-linking assay (Trigwell et al, 2004). Formoterol (figure 5.1A) produced increases in TG2-catalysed biotin-cadaverine incorporation activity, peaking at 20 min. In addition, formoterol ($pEC_{50} = 7.85 \pm 0.09$; $n=4$; figure 5.1C) stimulated concentration-dependent increases in biotin-cadaverine incorporation activity. Formoterol also triggered time-dependent increases in TG2-mediated protein cross-linking activity peaking at 20 min (figure 5.1B), which was concentration-dependent ($pEC_{50} = 7.69 \pm 0.15$; $n=4$; figure 5.1D). Even though the β_2 -AR couples to G_s and G_i proteins (Daaka et al, 1997; Zamah et al, 2002), pre-treatment with pertussis toxin ($G_{i/o}$ -protein blocker; 100 ng/ml) for 16 h had no significant effect on formoterol-induced TG2 activity (figure 5.1E and F). Similar to formoterol, the non-selective β -AR agonist isoprenaline (10 μ M) also triggered transient increases in TG2 catalysed biotin-cadaverine incorporation and protein cross-linking activity, peaking at 20 min (figure 5.2A and B). Furthermore, isoprenaline stimulated concentration-dependent increases in both biotin-amine incorporation activity (figure 5.2C; $pEC_{50} = 6.13 \pm 0.15$; $n=4$) and protein cross-linking activity (figure 5.2D; $pEC_{50} = 7.11 \pm 0.17$; $n=4$). It is notable that TG2 responses to isoprenaline were blocked by pertussis toxin indicating a role for $G_{i/o}$ -proteins (figure 5.2E and F).

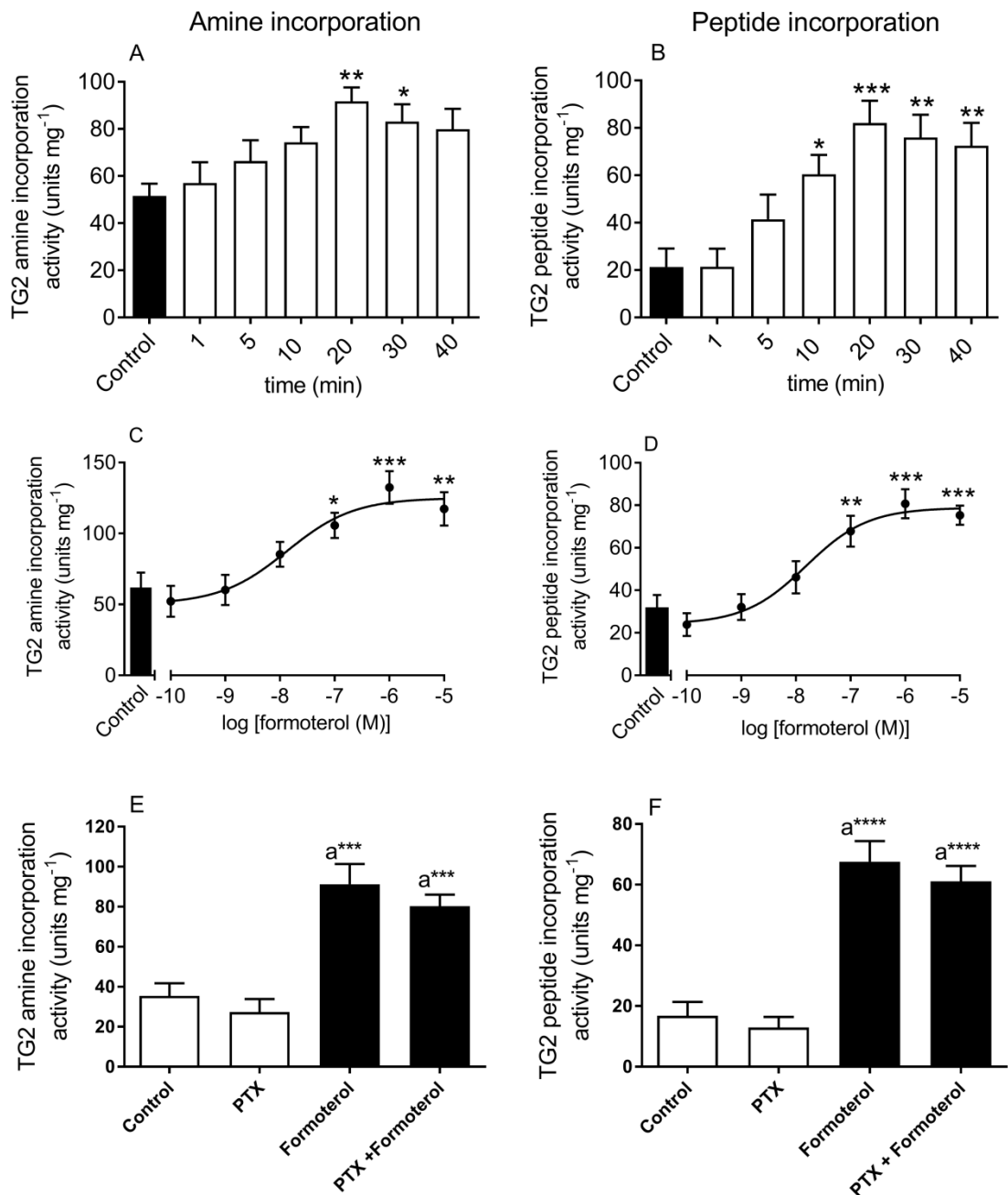


Fig 5.1: Effect of the β_2 -AR agonist formoterol on TG2 activity in H9c2 cells. Cells were stimulated with formoterol (100 nM) for the indicated time intervals (panels A and B). Concentration-response curves for formoterol in cells treated with agonist for 20 min (panels C and D). Where indicated H9c2 cells were pre-treated for 16 h with 100 ng/ml pertussis toxin (PTX) prior to 20 min stimulation with 100 nM formoterol (panels E and F). Cell lysates were subjected to the biotin-cadaverine incorporation (panels A, C and E) or the peptide cross-linking assay (panels B, D and F). Data points represent the mean \pm S.E.M. for TG2 specific activity from four independent experiments. * $P < 0.05$, ** $P < 0.01$, *** $P < 0.001$ and **** $P < 0.0001$, (a) versus control response.

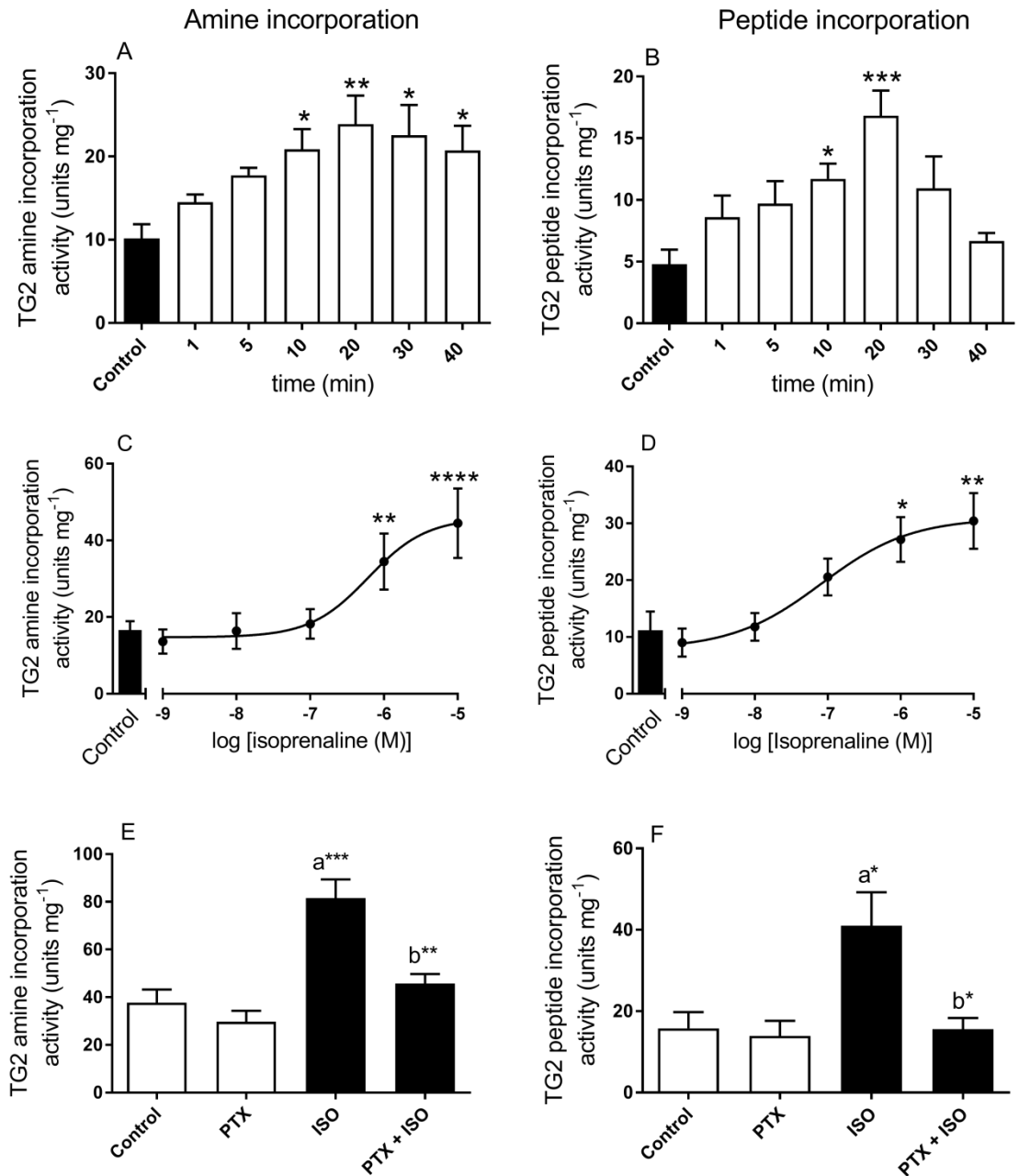


Fig 5.2: Effect of the non-selective β -AR agonist isoprenaline on TG2 activity in H9c2 cells. Cells were stimulated with isoprenaline (10 μ M) for the indicated time periods (panels A and B). Concentration-response curves for isoprenaline in cells treated with agonist for 20 min are also shown (panels C and D). Where indicated, H9c2 cells were pre-treated for 16 h with 100 ng/ml pertussis toxin (PTX) prior to 20 min stimulation with 10 μ M isoprenaline (ISO; panels E and F). Cell lysates were subjected to the biotin-cadaverine incorporation (panels A, C and E) or the peptide cross-linking assay (panels B, D and F). Data points represent the mean \pm S.E.M. for TG2 specific activity from four independent experiments. * P <0.05, ** P <0.01, *** P <0.001 and **** P <0.0001, (a) versus control response and (b) versus 10 μ M isoprenaline alone.

5.2 The effect of β -AR antagonists and TG2 inhibitors on β ₂-AR induced TG2 activity.

To determine whether the formoterol- and isoprenaline-induced TG2 activity occurred via activation of the β ₂-AR, the selective β ₂-AR antagonist ICI 118,551 and the non-selective β -adrenoceptor receptor antagonist propranolol were implemented. H9c2 cells were pre-treated for 30 min with ICI 118,551 (1 μ M) or propranolol (1 μ M) prior to stimulation with formoterol (1 μ M) and/or isoprenaline (10 μ M) for 20 min. ICI 118,551 and propranolol blocked formoterol-induced (figure 5.3A and D) and isoprenaline-induced (figure 5.4A and D) TG2 activity, thus confirming that the induced activity was mediated by the β ₂-AR. To confirm that TG2 is responsible for the β ₂-AR induced transglutaminase activity in H9c2 cells, two structurally different cell permeable TG2 specific inhibitors were tested; R283 (a small molecule; Freund et al, 1994) and Z-DON (peptide-based; Schaertl et al, 2010). H9c2 cells were pre-treated for 1 h with Z-DON (150 μ M) or R283 (200 μ M) prior to stimulation with formoterol (1 μ M) and/or isoprenaline (10 μ M) for 20 min. Both inhibitors blocked formoterol-induced and isoprenaline-induced TG-mediated amine incorporation (figure 5.3B and 5.4B) and peptide cross-linking activity (figure 5.3D and 5.4D), confirming the involvement of TG2.

5.3 The role of Ca^{2+} in β ₂-AR induced TG2 activity.

The role of Ca^{2+} in β ₂-AR-induced TG2 activation was determined because TG2 is a Ca^{2+} -dependent enzyme (Kiraly et al, 2011; Nurminskaya and Belkin, 2012; Eckert et al, 2014). The role of extracellular Ca^{2+} was assessed by measuring TG2 responses in the absence of extracellular Ca^{2+} using nominally Ca^{2+} -free Hanks/HEPES buffer containing 0.1 mM EGTA. Removal of extracellular Ca^{2+} partially attenuated formoterol- (figure 5.3C and F) and isoprenaline-induced TG2 activity (figure 5.4C and F). To assess the role of intracellular Ca^{2+} , measurements of TG2 activation were also performed using cells pre-incubated with the Ca^{2+} chelator BAPTA-AM (50 μ M for 30 min) in the absence of extracellular Ca^{2+} . Loading cells with BAPTA in the absence of extracellular Ca^{2+} did not lead to further inhibition of formoterol-induced (figure 5.3C and F) and isoprenaline-induced TG2 activation (figure 5.4C and F). These observations indicate that the β ₂-AR induced TG2 activation is partially dependent upon the influx of extracellular Ca^{2+} .

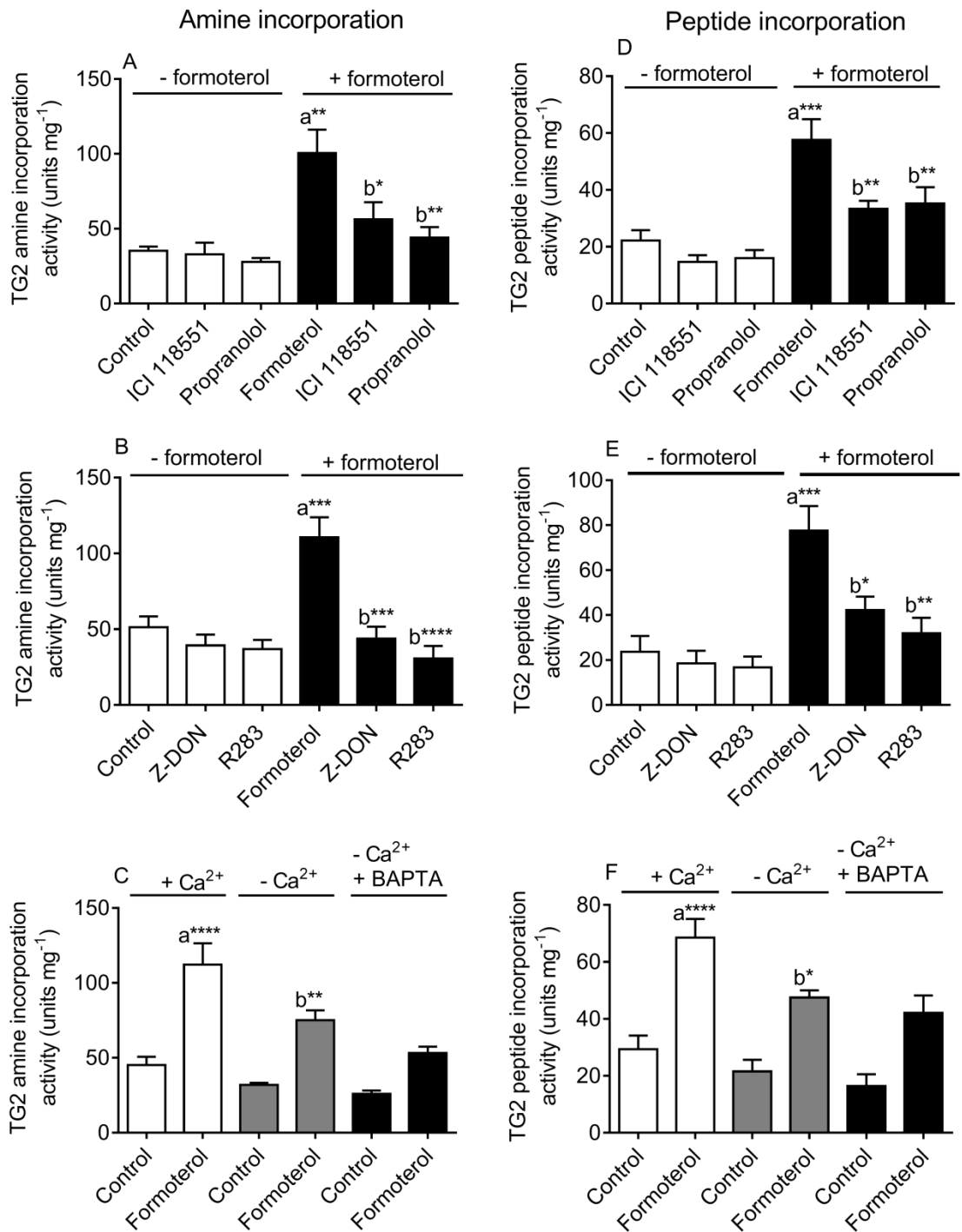


Fig 5.3: Effect of β -adrenoceptor antagonists, inhibitors of TG2 and removal of extracellular Ca^{2+} on formoterol-induced TG2 activity in H9c2 cells. H9c2 cells were pre-treated for 30 min with the antagonists ICI 118,551 (1 μM ; β_2 -AR selective) and propranolol (1 μM ; non-selective β .adrenoceptor) or for 1 h with the TG2 inhibitors Z-DON (150 μM) and R283 (200 μM) prior to stimulation with formoterol (1 μM ; 20 min). H9c2 cells were also stimulated for 20 min with formoterol (1 μM) either in the presence of extracellular Ca^{2+} (1.8 mM) or in its absence using nominally Ca^{2+} -free Hanks/HEPES buffer containing 0.1 mM EGTA. Experiments were also performed using cells pre-incubated for 30 min with 50 μM BAPTA/AM and in the absence of extracellular Ca^{2+} (nominally Ca^{2+} -free Hanks/HEPES buffer containing 0.1 mM EGTA) to chelate intracellular Ca^{2+} . Cell lysates were subjected to the biotin-cadaverine incorporation assay (panels A, B and C) or peptide cross-linking assay (panels D, E and F). Data points represent the mean \pm S.E.M. for TG2 specific activity from four independent experiments. * $P < 0.05$, ** $P < 0.01$, *** $P < 0.001$ and **** $P < 0.0001$, (a) versus control and (b) versus 1 μM formoterol in the presence of extracellular Ca^{2+} .

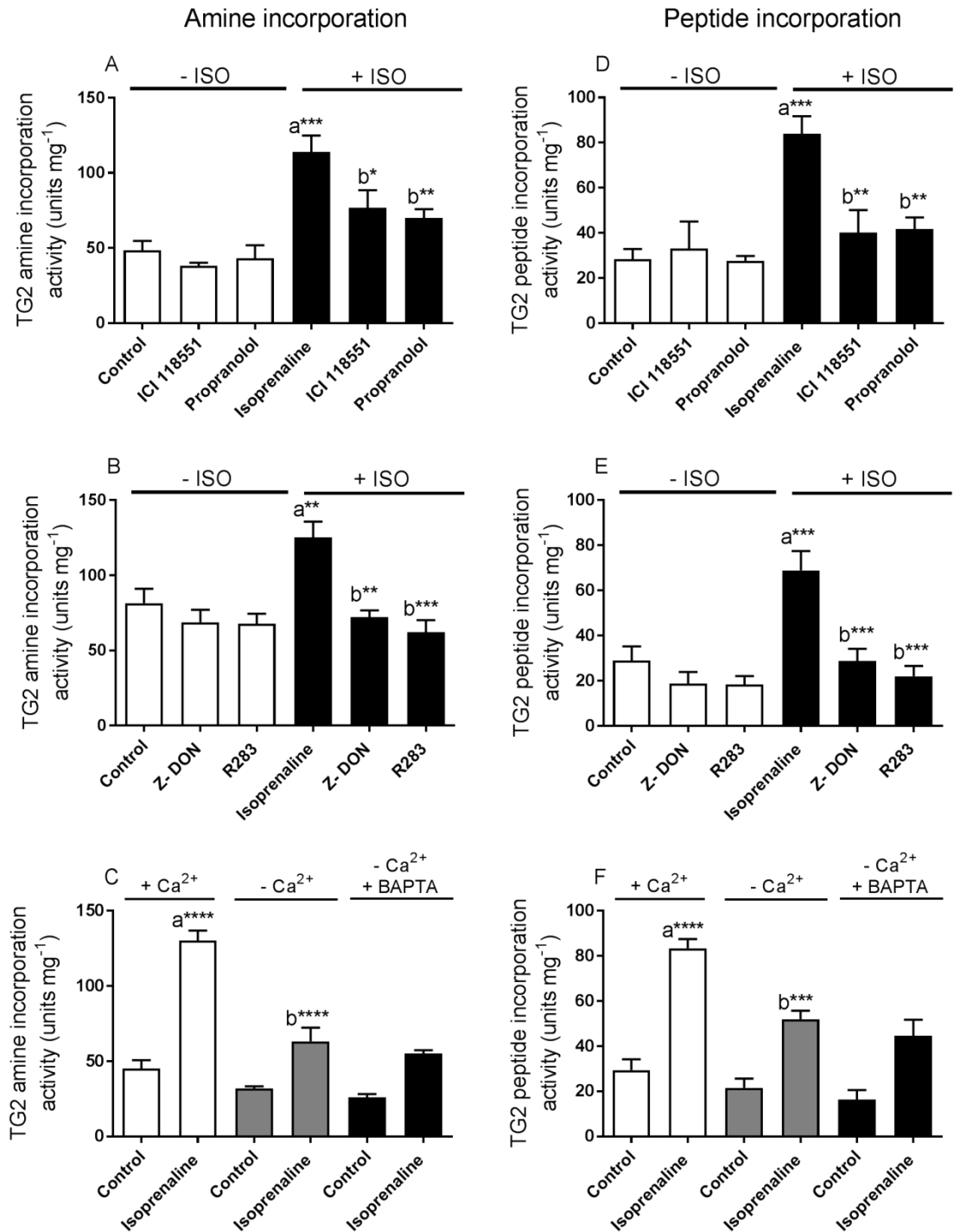


Fig 5.4: Effect of β -adrenoceptor antagonists, inhibitors of TG2 and removal of extracellular Ca^{2+} on isoprenaline-induced TG2 activity in H9c2 cells. H9c2 cells were pre-treated for 30 min with the antagonists ICI 118,551 (1 μM ; β_2 -AR selective) and propranolol (1 μM ; non-selective β -adrenoceptor) or for 1 h with the TG2 inhibitors Z-DON (150 μM) and R283 (200 μM) prior to stimulation with isoprenaline (10 μM ; 20 min). H9c2 cells were also stimulated for 20 min with isoprenaline (10 μM) either in the presence of extracellular Ca^{2+} (1.8 mM) or in its absence using nominally Ca^{2+} -free Hanks/HEPES buffer containing 0.1 mM EGTA. Experiments were also performed using cells pre-incubated for 30 min with 50 μM BAPTA/AM and in the absence of extracellular Ca^{2+} (nominally Ca^{2+} -free Hanks/HEPES buffer containing 0.1 mM EGTA) to chelate intracellular Ca^{2+} . Cell lysates were subjected to the biotin-cadaverine incorporation assay (panels A, B and C) or peptide cross-linking assay (panels D, E and F). Data points represent the mean \pm S.E.M. for TG2 specific activity from four

independent experiments. * $P < 0.05$, ** $P < 0.01$, *** $P < 0.001$ and **** $P < 0.0001$, (a) versus control and (b) versus 10 μM isoprenaline in the presence of extracellular Ca^{2+} .

5.4 The effect of protein and lipid kinase inhibitors on β_2 -AR induced TG2 activity.

The β_2 -AR activates the cAMP/PKA pathway and therefore the effect of two structurally different PKA inhibitors, *Rp*-cAMPs (de Wit et al, 1984) and KT-5720 (Kase et al, 1987), on formoterol-induced and isoprenaline-induced TG2 activity was assessed. As shown in figure 5.5, pre-treatment with *Rp*-cAMPs (50 μM) or KT 5720 (5 μM) partially attenuated formoterol-induced TG-mediated amine incorporation and protein cross-linking activity, suggesting the involvement of PKA. Pre-treatment with *Rp*-cAMPs (50 μM) or KT 5720 (5 μM) partially attenuated isoprenaline-induced TG-mediated amine incorporation, suggesting the involvement of PKA. It should be noted that the effect of *Rp*-cAMPs on isoprenaline-induced protein cross-linking activity was not statistically significant. Moreover, the effect of KT 5720 on formoterol- and isoprenaline-induced protein cross-linking activity was also not statistically significant. Overall, these data indicate that PKA plays a role in β_2 -AR induced TG2 activity.

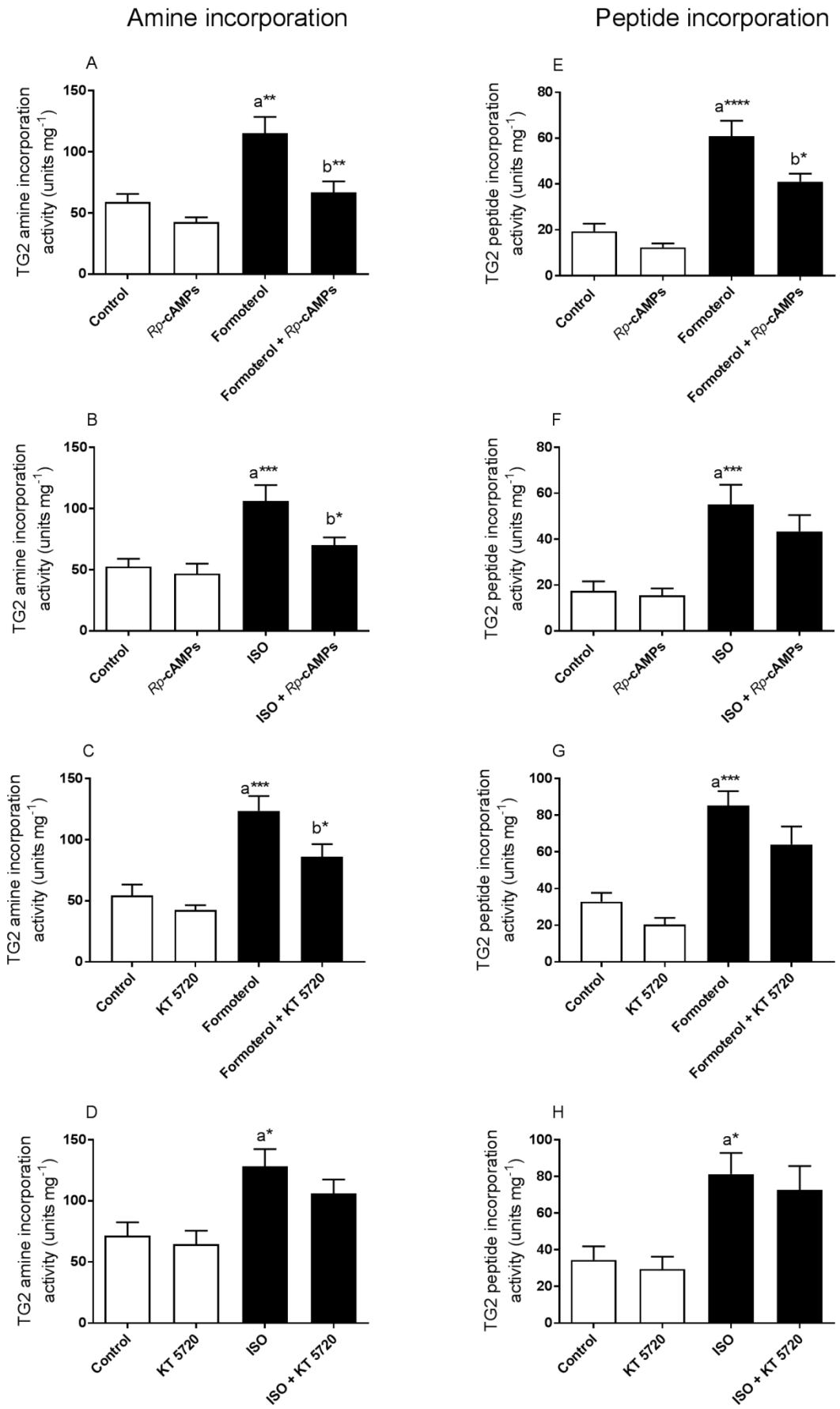


Fig 5.5: Effect of PKA inhibitors KT-5720 and *Rp*-cAMPs on formoterol- and isoprenaline-induced TG2 activity. H9c2 cells were pre-treated for 30 min with *Rp*-cAMPs (50 μ M) or KT-5720 (5 μ M) prior to 20 min stimulation with either formoterol (1 μ M) or isoprenaline (ISO; 10 μ M). Cell lysates were subjected to biotin-cadaverine

incorporation (panels A to D) or peptide cross-linking assays (panels E to H). Data points represent the mean \pm S.E.M. for TG2 specific activity from four independent experiments. * P <0.05, ** P <0.01, *** P <0.001 and **** P <0.0001, (a) versus control and (b) versus 1 μ M formoterol or 10 μ M isoprenaline alone.

It is clear from previous studies that the β_2 -AR triggers the activation of signalling cascades involving ERK1/2, p38 MAPK, JNK1/2 and PKB in a variety of cell backgrounds (Daaka et al, 1997; Okamoto et al, 1991; Steinberg, 1999; Yano et al, 2007). Modulation of ERK1/2, p38 MAPK, JNK1/2 and PKB activity following β_2 -AR activation was assessed in H9c2 cells by Western blotting using phospho-specific antibodies that recognise phosphorylated motifs within activated ERK1/2 (pTEpY), p38 MAPK (pTGpY), JNK1/2 (pTPpY) and PKB (pS⁴⁷³). Formoterol (1 μ M for 20 min) and isoprenaline (10 μ M for 20 min) did not stimulate p38 MAPK or JNK1/2 activation (figure 5.6). This is consistent with the data showing no significant effect on formoterol- and isoprenaline-induced TG2 activity upon treatment with SB 203580 (20 μ M; p38 MAPK inhibitor) and SP 600125 (20 μ M; JNK1/2 inhibitor; figure 5.7).

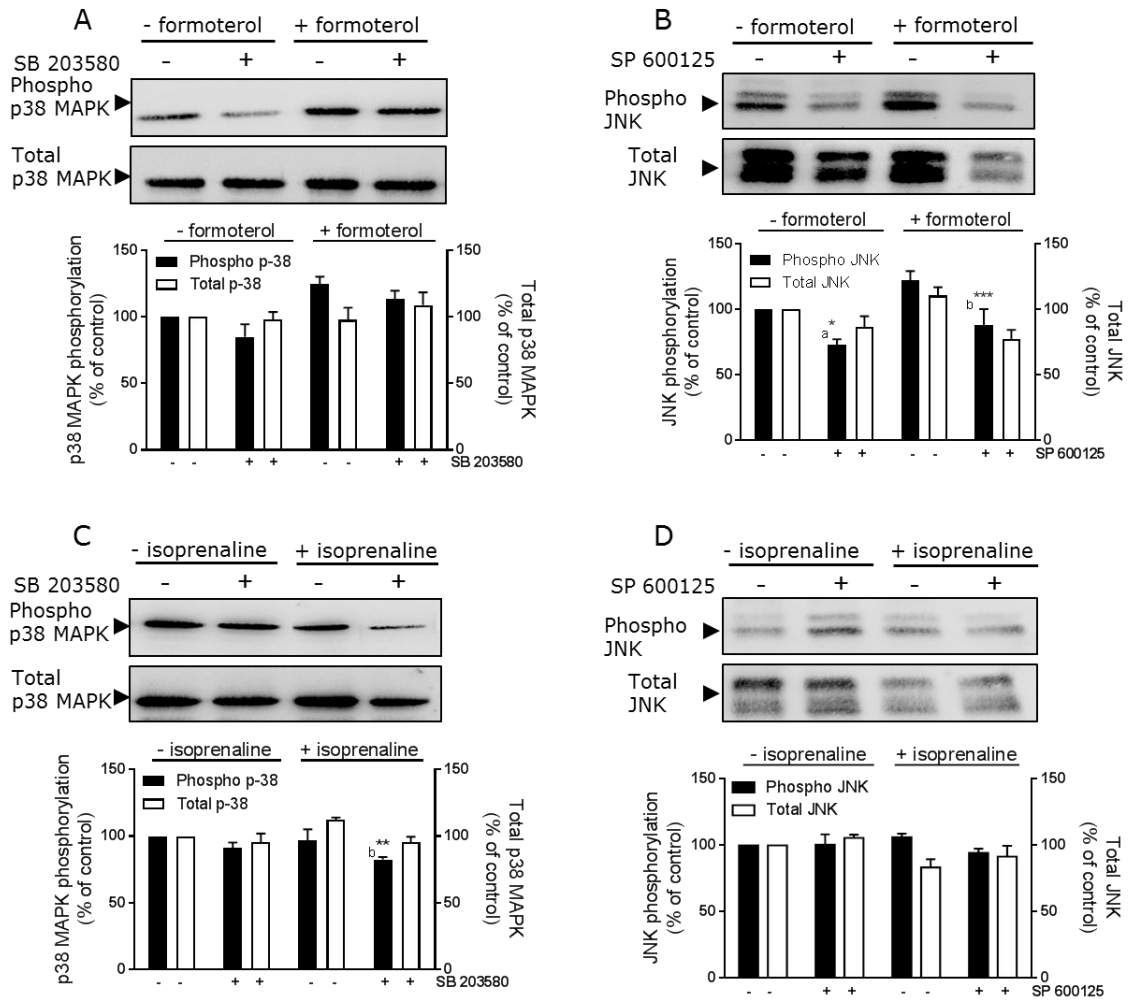


Fig 5.6: Effect of formoterol and isoprenaline on p38 MAPK and JNK1/2 phosphorylation in H9c2 cells. Where indicated, H9c2 cells were pre-treated for 30 min with SB 203580 (20 μ M; panels A and C) or SP 600125 (20 μ M; panels B and D) prior to stimulation with either formoterol (1 μ M) or isoprenaline (10 μ M) for 20 min. Cell lysates were analysed by Western blotting for activation of p38 MAPK and JNK1/2 using phospho-specific antibodies. Samples were subsequently analysed on separate blots using antibodies that recognize total p38 MAPK and JNK1/2. Data are expressed as the percentage of values for control cells (=100%) in the absence of protein kinase inhibitor and represent the mean \pm S.E.M. of four independent experiments. *** P <0.001, (b) versus 1 μ M formoterol alone.

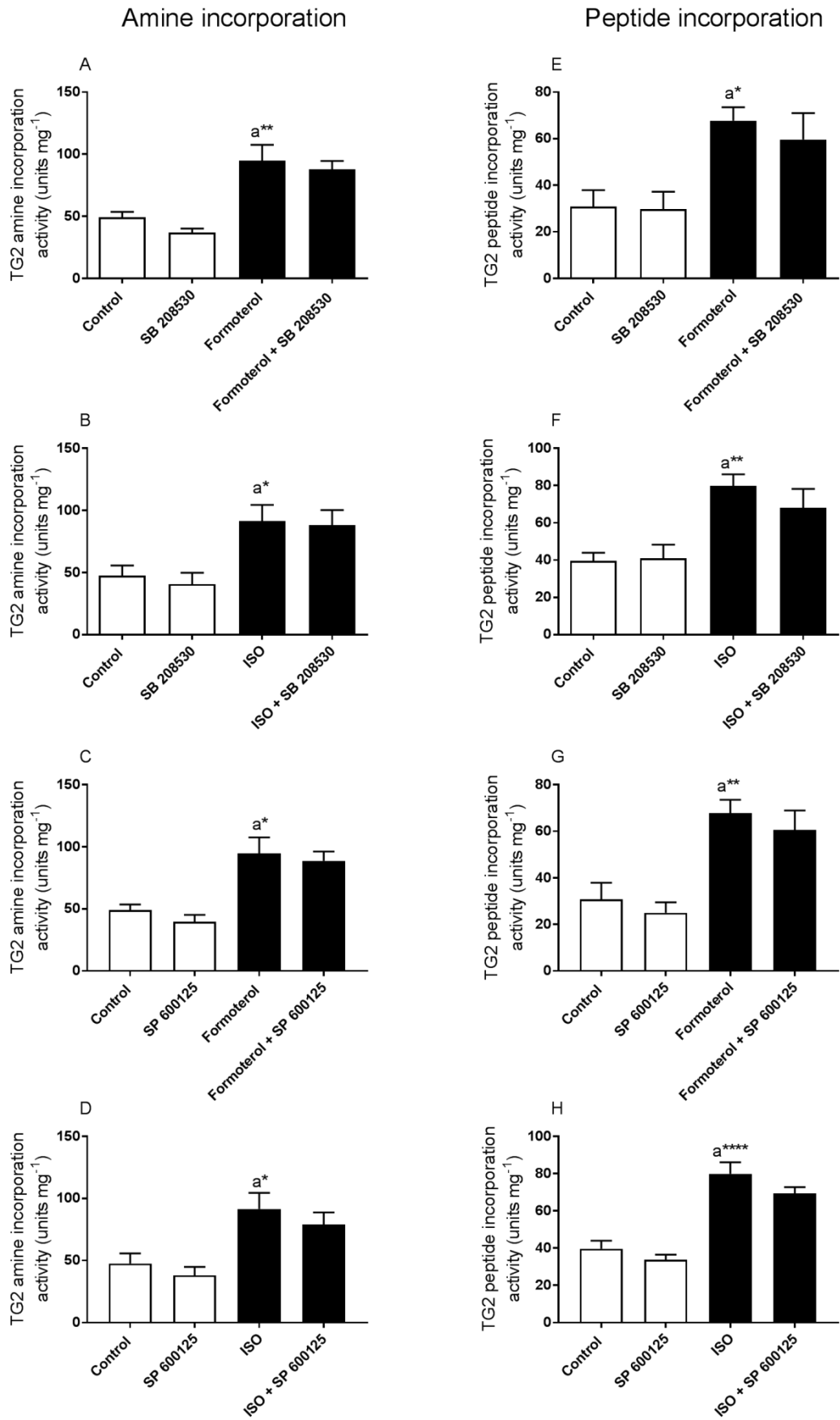


Fig 5.7: Effect of p38 MAPK and JNK1/2 inhibitors on formoterol and isoprenaline-induced TG2 activity. H9c2 cells were pre-treated for 30 min with SB 203580 (20 μ M) or SP 600125 (20 μ M) prior to 20 min stimulation with formoterol (1 μ M) or isoprenaline (ISO; 10 μ M). Cell lysates were subjected to the protein biotin-cadaverine

amine incorporation assay (panels A to D) or peptide cross-linking assay (panels E to H). Data points represent the mean \pm S.E.M. TG2 specific activity from four independent experiments. * P <0.05, ** P <0.01 and **** P <0.0001, (a) versus control.

Formoterol (1 μ M for 20 min) and isoprenaline (10 μ M for 20 min) stimulated significant increases in ERK1/2 (figure 5.8) and PKB phosphorylation (figure 5.10) in H9c2 cells. As expected, pre-treatment with PD 98059 (50 μ M; MEK1 inhibitor) blocked formoterol- (figure 5.8A) and isoprenaline-induced activation of ERK1/2 (figure 5.8B). Furthermore, treatment with PD 98059 (50 μ M) also blocked formoterol- and isoprenaline-induced TG-mediated amine incorporation and protein cross-linking activity, suggesting a role for ERK1/2 in regulating these activities (figure 5.9). Pre-treatment with wortmannin (100 nM) and LY 294002 (30 μ M) blocked formoterol- (figure 5.10A and B) and isoprenaline-induced activation of PKB (figure 5.10C and D).

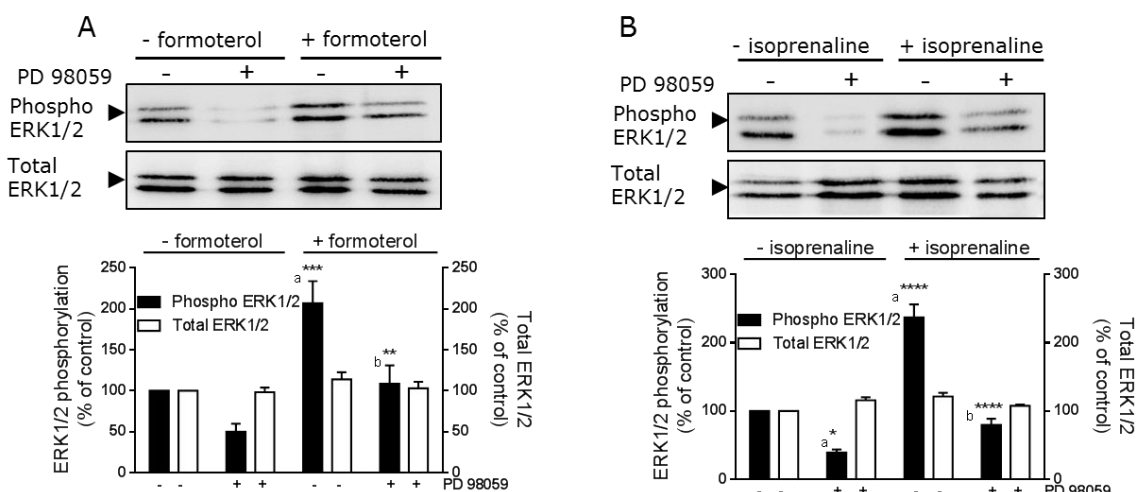


Fig 5.8: Effect of formoterol and isoprenaline on ERK1/2 phosphorylation in H9c2 cells. H9c2 cells were pre-treated for 30 min with PD 98059 (50 μ M) prior to stimulation with formoterol (1 μ M) or isoprenaline (10 μ M) for 20 min. Cell lysates were analysed by Western blotting for activation of ERK1/2 using phospho-specific antibodies. Samples were subsequently analysed on separate blots using antibodies that recognize total ERK1/2. Data are expressed as the percentage of values for control cells (=100%) in the absence of protein kinase inhibitor and represent the mean \pm S.E.M. of four independent experiments. * P <0.05, ** P <0.01, *** P <0.001 and **** P <0.0001, (a) versus control and (b) versus 1 μ M formoterol or 10 μ M isoprenaline alone.

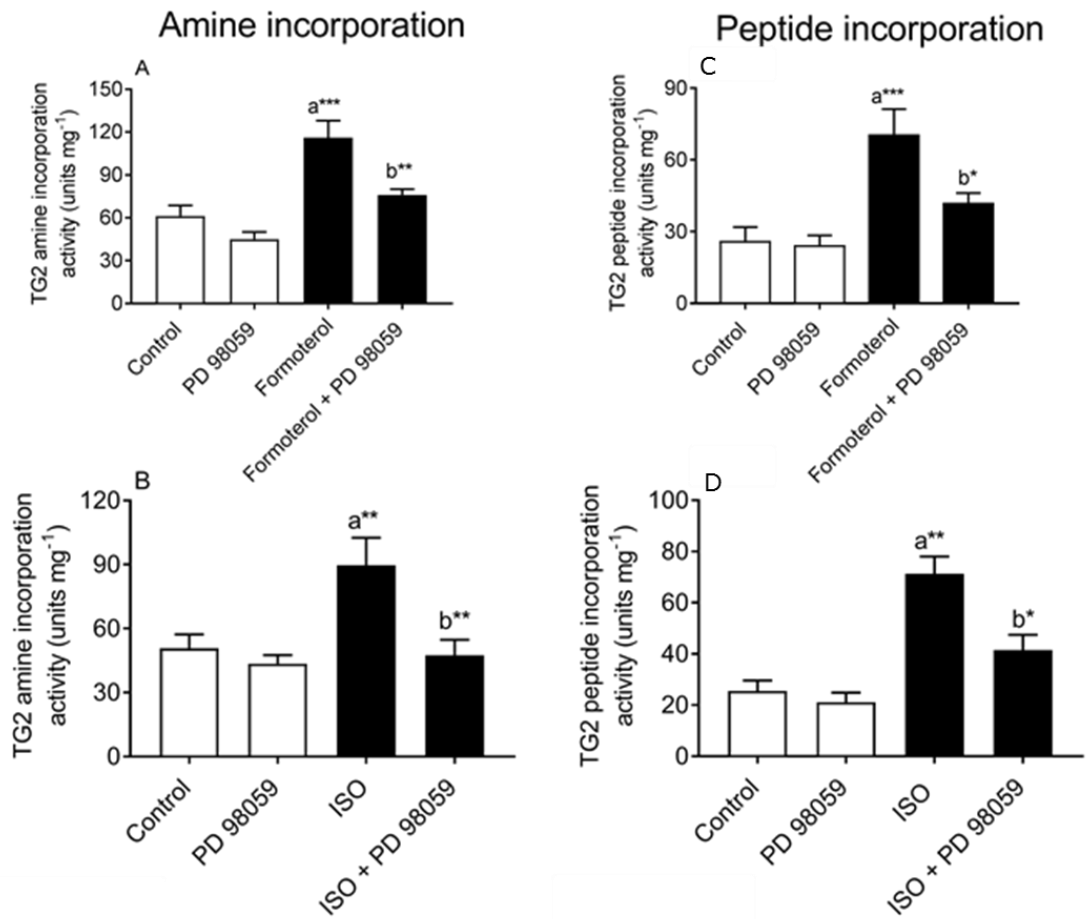


Fig 5.9: Effect of ERK1/2 inhibitor on formoterol- and isoprenaline-induced TG2 activity. H9c2 cells were pre-treated for 30 min with PD 98059 (50 μ M) prior to 20 min stimulation with formoterol (1 μ M) or isoprenaline (ISO; 10 μ M). Cell lysates were subjected to the protein biotin-cadaverine amine incorporation assay (panels A and B) or peptide cross-linking assay (panels C and D). Data points represent the mean \pm S.E.M. TG2 specific activity from four independent experiments. * P <0.05, ** P <0.01 and *** P <0.001, (a) versus control and (b) versus 1 μ M formoterol or 10 μ M isoprenaline alone.

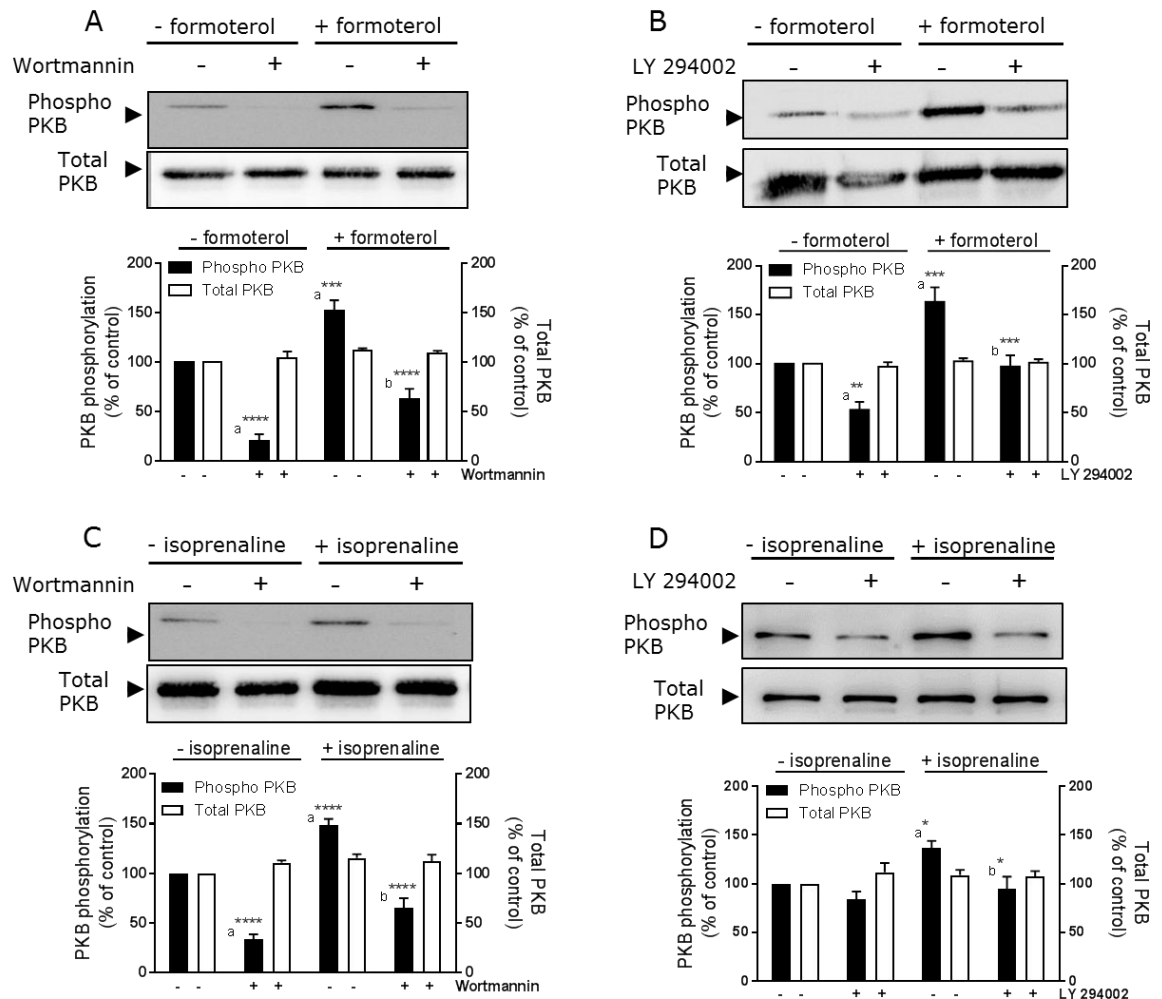


Fig 5.10: Effect of formoterol and isoprenaline on PKB phosphorylation in H9c2 cells. Where indicated, H9c2 cells were pre-treated for 30 min with wortmannin (100 nM; panels A and C) and LY 294002 (30 μ M; panels B and D) prior to stimulation with formoterol (1 μ M) or isoprenaline (10 μ M) for 20 min. Cell lysates were analysed by Western blotting for activation of PKB using phospho-specific antibodies. Samples were subsequently analysed on separate blots using antibodies that recognize total PKB. Data are expressed as the percentage of values for control cells (=100%) in the absence of protein kinase inhibitor and represent the mean \pm S.E.M. of four independent experiments. * P <0.05, ** P <0.01, *** P <0.001 and **** P <0.0001, (a) versus control and (b) versus 1 μ M formoterol or 10 μ M isoprenaline alone.

In this study the pan PI-3K inhibitors wortmannin (100 nM) and LY 294002 (30 μ M) blocked formoterol and isoprenaline-induced TG2 activity (figure 5.11). Furthermore, to determine if PI-3K γ were involved, the effect of the selective PI-3K γ inhibitor AS 605240 was assessed. AS 605240 inhibited PKB phosphorylation (IC_{50} = 31.84 nM; $p[IC_{50}]$ = 7.50 ± 0.03 ; $n=3$; figure 5.12A) and ERK1/2 phosphorylation (IC_{50} = 61.17 nM; $p[IC_{50}]$ = 7.25 ± 0.10 ; $n=3$; figure 5.12B) in a concentration-dependent manner. AS 605240 (1 μ M) significantly inhibited formoterol and isoprenaline-induced PKB phosphorylation (figure 5.12C and D). The selective PI-3K γ inhibitor AS 605240 (1 μ M) also blocked formoterol- and isoprenaline-induced TG2 activity (figure 5.13).

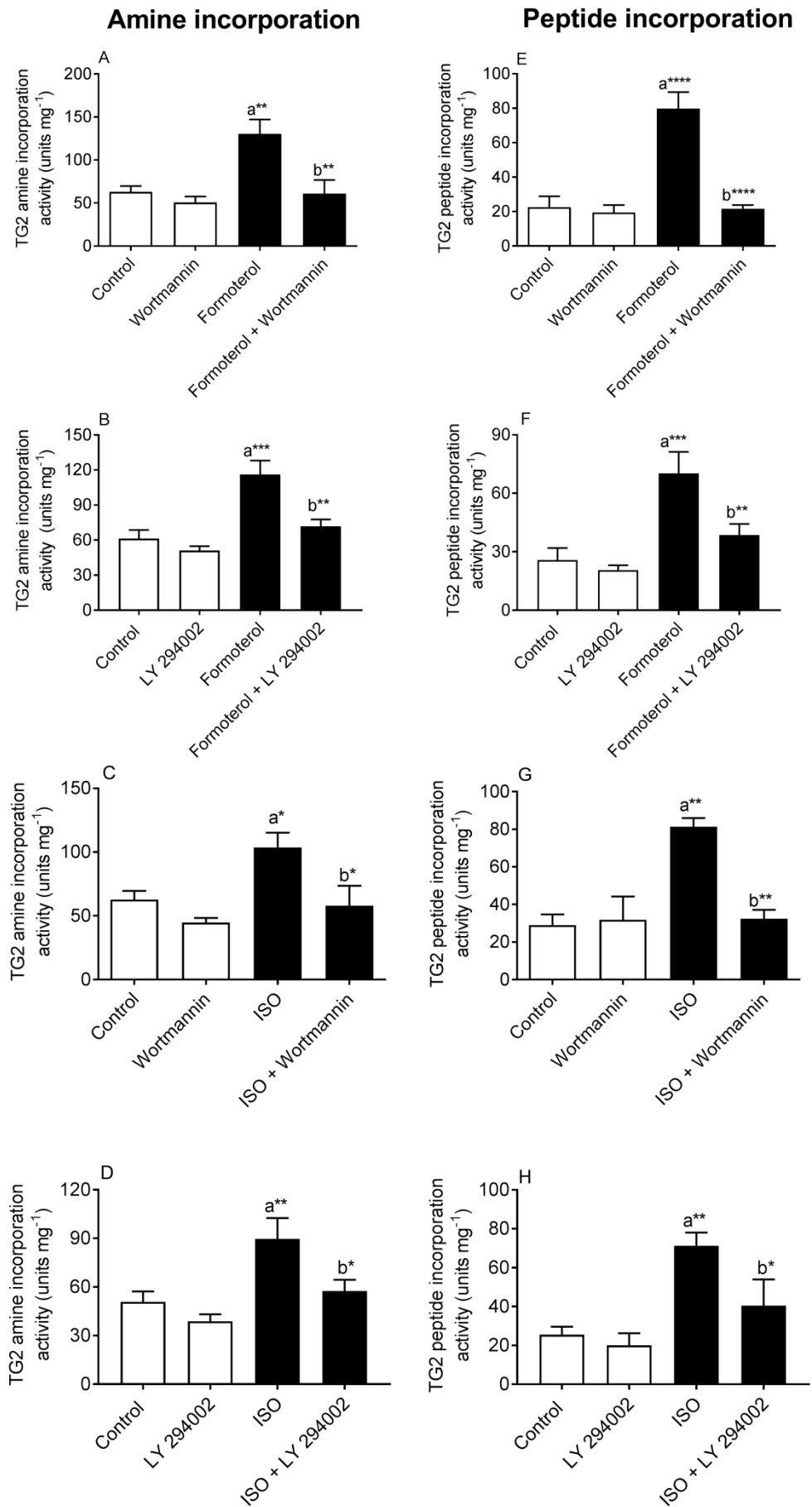


Fig 5.11: Effect of pan PI-3K inhibitors on formoterol- and isoprenaline-induced TG2 activity. H9c2 cells were pre-treated for 30 min with wortmannin (100 nM) or LY 294002 (30 μ M) prior to 20 min stimulation with formoterol (1 μ M) or isoprenaline

(ISO; 10 μ M). Cell lysates were subjected to the protein biotin-cadaverine amine incorporation assay (panels A to D) or peptide cross-linking assay (panels E to H). Data points represent the mean \pm S.E.M. TG2 specific activity from four independent experiments. * P <0.05, ** P <0.01, *** P <0.001 and **** P <0.0001, (a) versus control and (b) versus 1 μ M formoterol or 10 μ M isoprenaline alone.

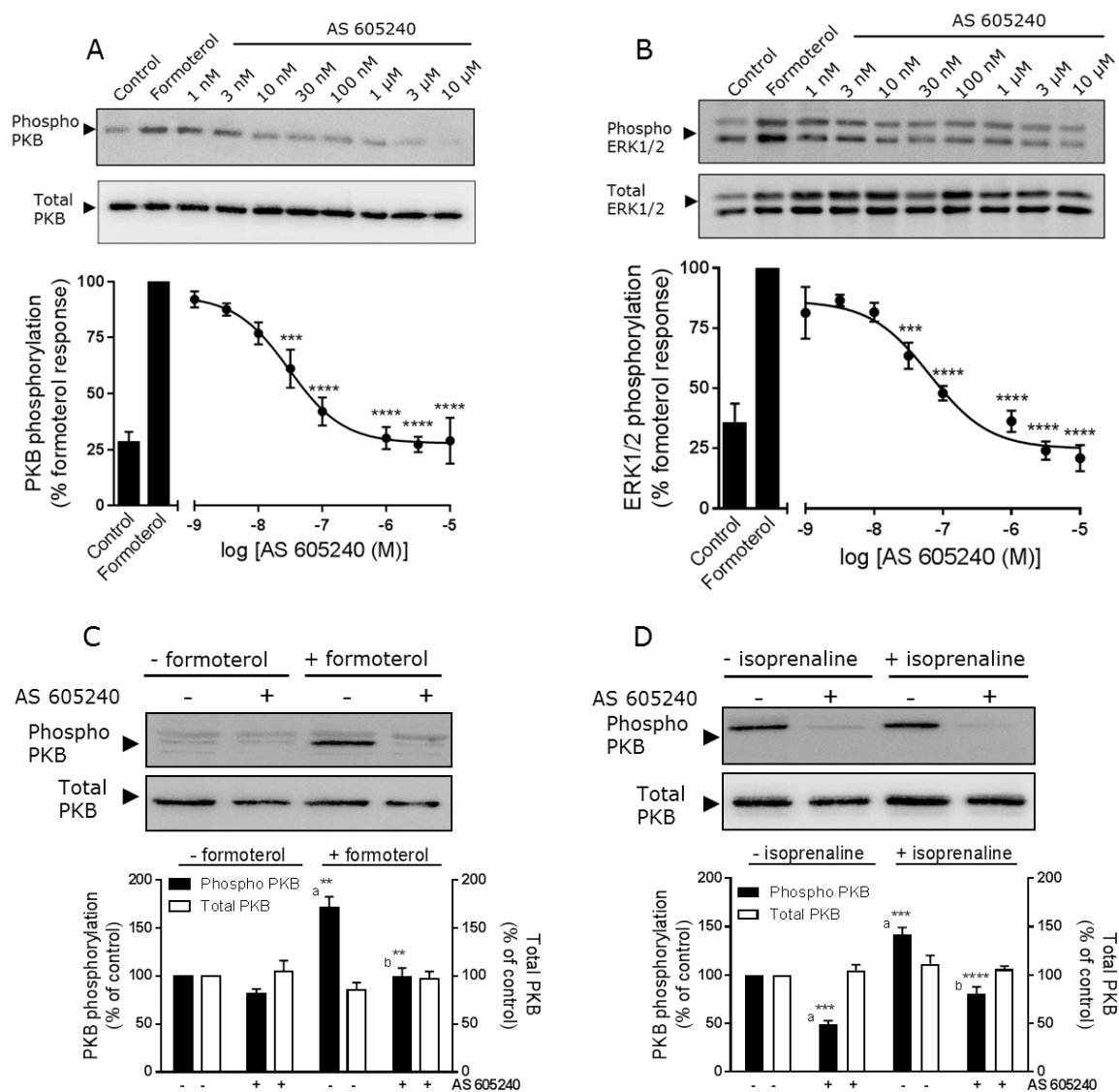


Fig 5.12: Effect of PI-3K γ inhibitor AS 605240 on formoterol and isoprenaline on PKB and ERK1/2 phosphorylation. H9c2 cells were pre-treated for 30 min with indicated concentrations of AS 605240 prior to 20 min stimulation with formoterol (1 μ M; panels A and B). H9c2 cells were pre-treated for 30 min with AS 605240 (1 μ M) prior to 20 min stimulation with formoterol (1 μ M) or isoprenaline (ISO; 10 μ M; panels C and D). Cell lysates were analysed by Western blotting for activation of PKB and ERK1/2 using phospho-specific antibodies. Samples were subsequently analysed on separate blots using antibodies that recognize total PKB and ERK1/2. Data are expressed as the percentage of values for control cells (=100%) in the absence of protein kinase inhibitor and represent the mean \pm S.E.M. of four independent experiments. ** P <0.01, *** P <0.001 and **** P <0.0001, (a) versus control and (b) versus 1 μ M formoterol or 10 μ M isoprenaline alone.

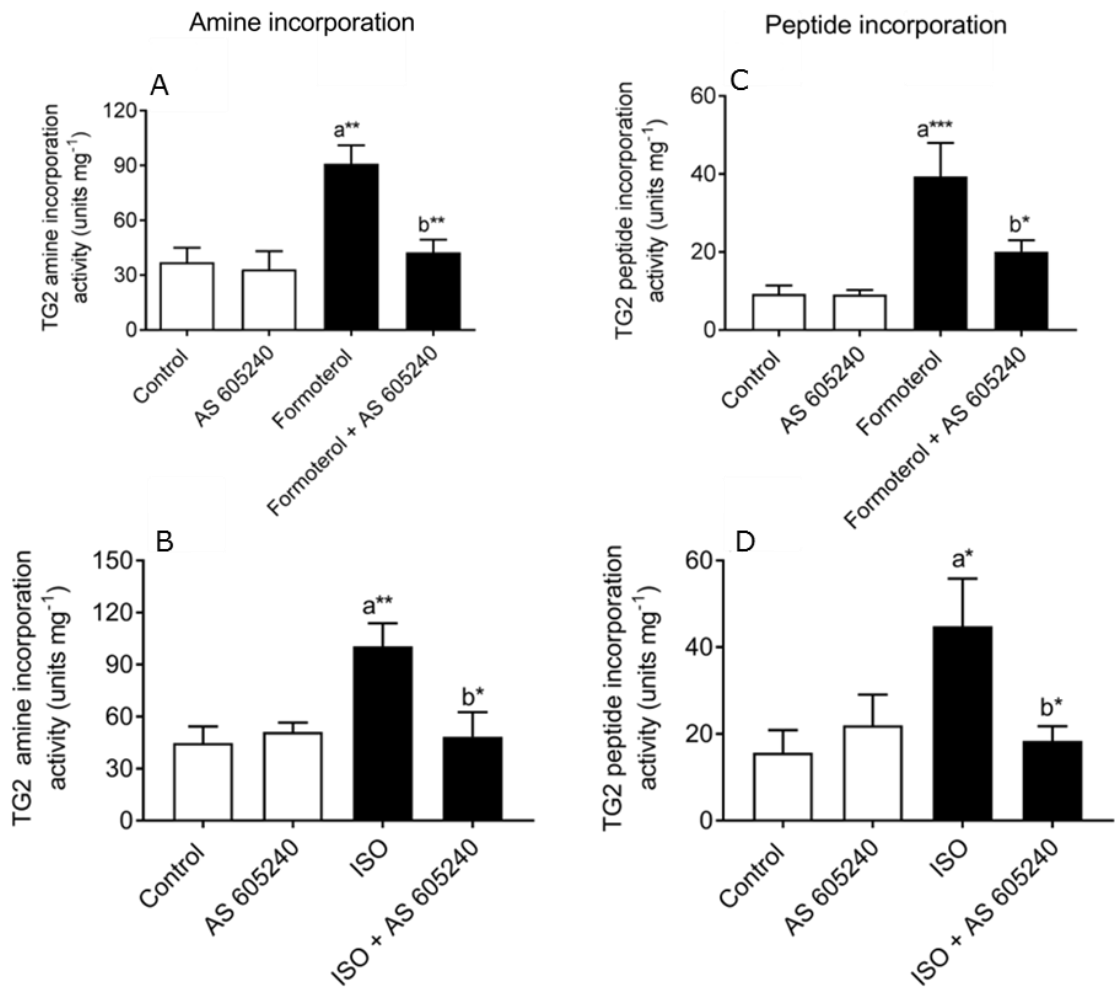


Fig 5.13: Effect of PI-3K γ inhibitor (AS 605240) on formoterol- and isoprenaline-induced TG2 activity. H9c2 cells were pre-treated for 30 min with AS 605240 (1 μ M) prior to 20 min stimulation with formoterol (1 μ M) or isoprenaline (ISO; 10 μ M). Cell lysates were subjected to the protein biotin-cadaverine amine incorporation assay (panels A and B) or peptide cross-linking assay (panels C and D). Data points represent the mean \pm S.E.M. TG2 specific activity from four independent experiments. * P <0.05, ** P <0.01 and *** P <0.001, (a) versus control and (b) versus 1 μ M formoterol or 10 μ M isoprenaline alone.

To assess the role of PKB, Akt inhibitor XI, the selective inhibitor of PKB (Barve et al, 2006) was employed. Akt inhibitor XI (IC₅₀ = 6.86 nM; p[IC₅₀] = 6.20 \pm 0.10; n=3; figure 5.14A) inhibited PKB phosphorylation in a concentration-dependent manner. Akt inhibitor XI (1 μ M) significantly inhibited formoterol- and isoprenaline-induced PKB phosphorylation (figure 5.14B and C). However, treatment with Akt inhibitor XI (1 μ M) had no significant effect on formoterol- and isoprenaline-induced TG2 activity (figure 5.15).

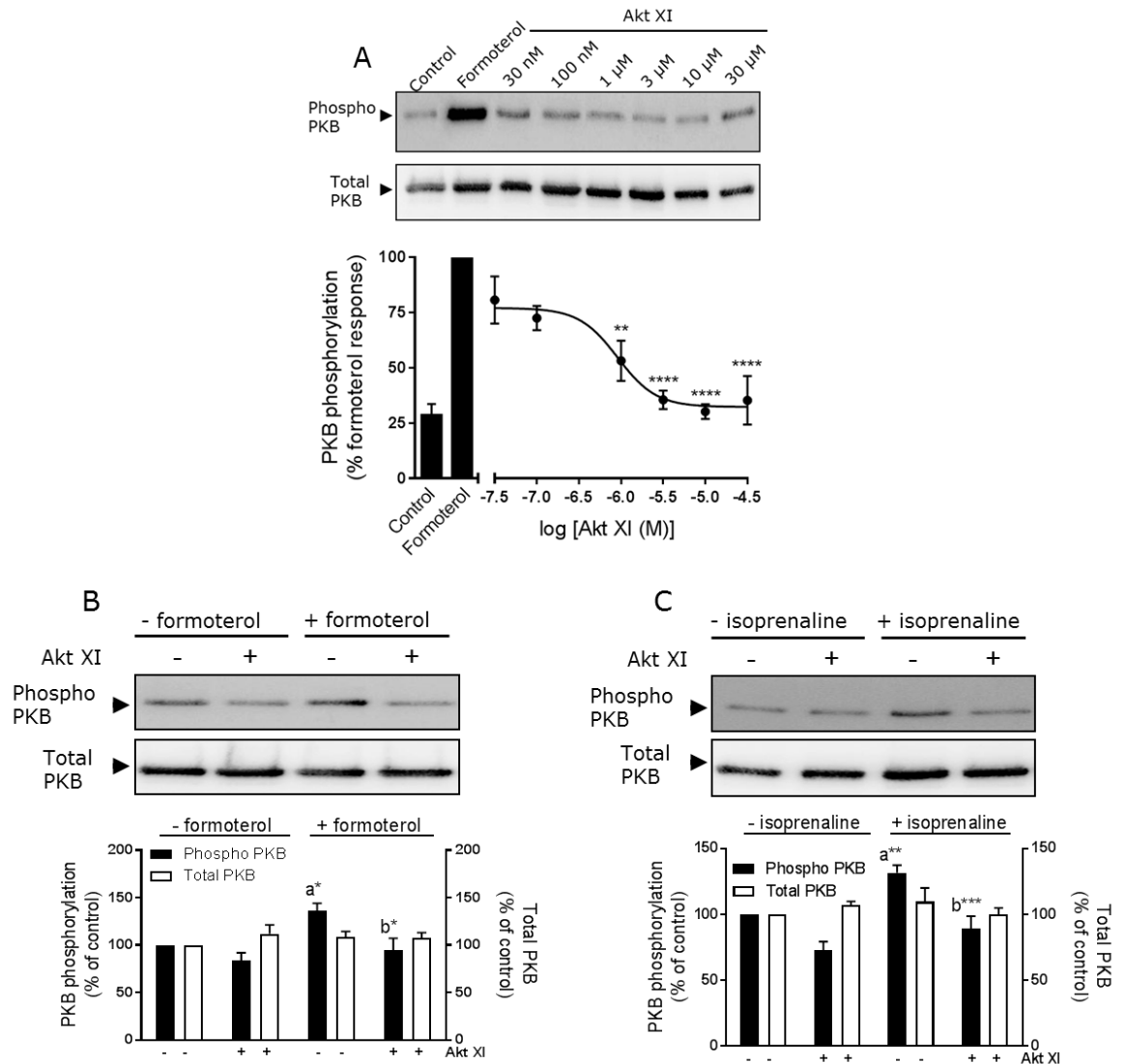


Fig 5.14: Effect of PKB inhibitor on formoterol- and isoprenaline-mediated PKB phosphorylation. H9c2 cells were pre-treated for 30 min with indicated concentrations of Akt inhibitor XI prior to 20 min stimulation with formoterol (1 μ M; panel A). H9c2 cells were pre-treated for 30 min with Akt inhibitor XI (1 μ M) prior to 20 min stimulation with formoterol (1 μ M) or isoprenaline (ISO; 10 μ M; panels B and C). Cell lysates were analysed by Western blotting for activation of PKB using phospho-specific antibodies. Samples were subsequently analysed on separate blots using antibodies that recognize total PKB. Data are expressed as the percentage of values for control cells (=100%) in the absence of protein kinase inhibitor and represent the mean \pm S.E.M. of four independent experiments. * P <0.05, ** P <0.01, *** P <0.001 and **** P <0.0001, (a) versus control and (b) versus 1 μ M formoterol or 10 μ M isoprenaline alone.

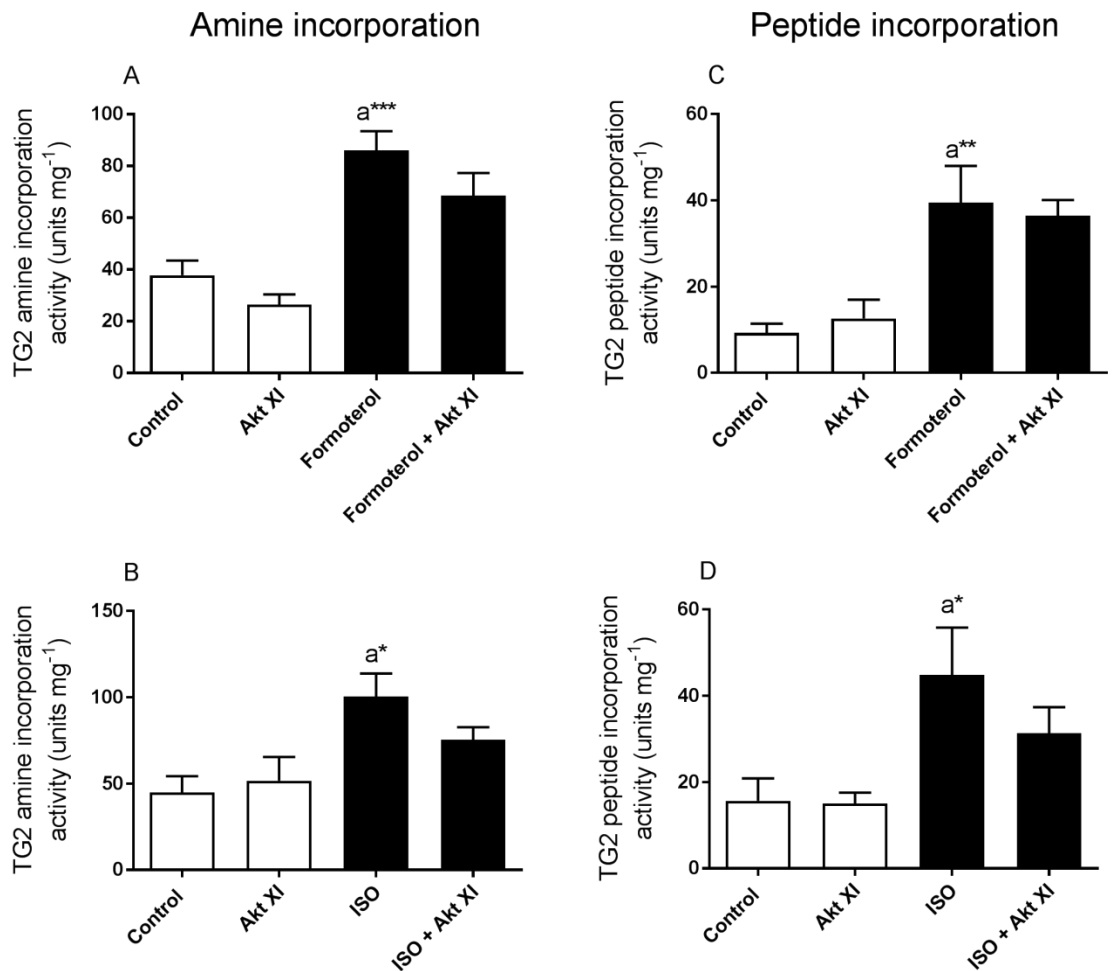


Fig 5.15: Effect of PKB inhibitor on formoterol- and isoprenaline-induced TG2 activity. H9c2 cells were pre-treated for 30 min with Akt inhibitor XI (1 μ M) prior to 20 min stimulation with formoterol (1 μ M) or isoprenaline (ISO; 10 μ M). Cell lysates were subjected to the protein biotin-cadaverine amine incorporation assay (panels A and B) or peptide cross-linking assay (panels C and D). Data points represent the mean \pm S.E.M. TG2 specific activity from four independent experiments. * P <0.05, ** P <0.01 and *** P <0.001, (a) versus control and (b) versus 1 μ M formoterol or 10 μ M isoprenaline alone.

Since formoterol- and isoprenaline-induced TG2 activation is dependent on ERK1/2, PI-3K and extracellular Ca²⁺, it was of interest to determine whether PI-3K and extracellular Ca²⁺ play an up-stream role in ERK1/2 activation. The pan PI-3K inhibitors wortmannin and LY 294002, the selective PI-3K γ inhibitor AS 605240 and removal of extracellular Ca²⁺ attenuated formoterol- and isoprenaline-induced ERK1/2 activation (figure 5.16 and 5.17) suggesting that they are upstream of ERK1/2.

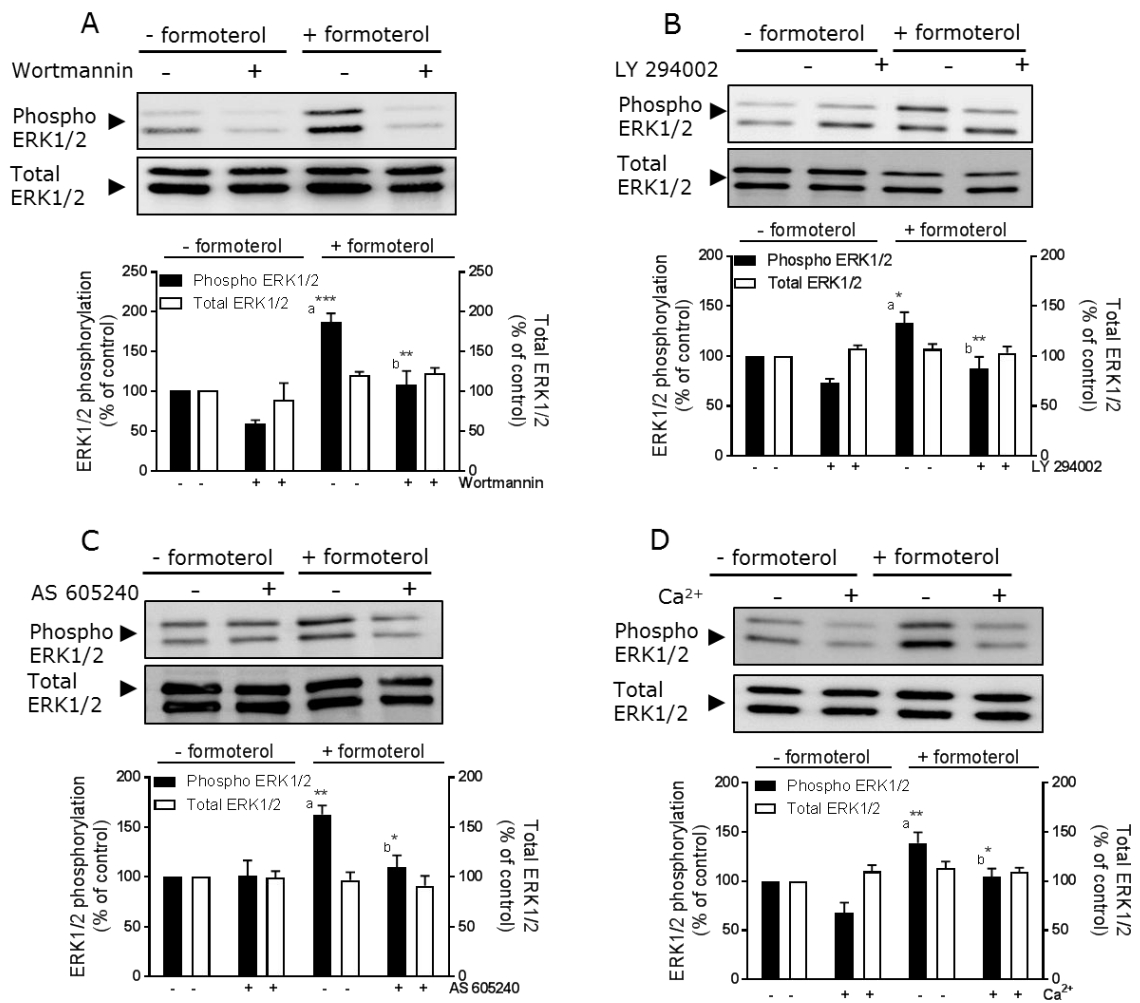


Fig 5.16: Effect of formoterol on ERK1/2 phosphorylation in H9c2 cells. Where indicated, H9c2 cells were pre-treated for 30 min with (A) wortmannin (100 nM), (B) LY 294002 (30 μ M), or (C) AS 605240 (1 μ M) prior to stimulation with formoterol (1 μ M) for 20 min. In Panel (D) cells were stimulated for 20 min with formoterol (1 μ M) either in the presence of extracellular Ca²⁺ (1.3 mM) or in its absence using nominally Ca²⁺-free Hanks/HEPES buffer containing 0.1 mM EGTA. Cell lysates were analysed by Western blotting for activation of ERK1/2 using phospho-specific antibodies. Samples were subsequently analysed on separate blots using antibodies that recognize total ERK1/2. Data are expressed as the percentage of values for control cells (=100%) in the absence of protein kinase inhibitor and represent the mean \pm S.E.M. of four independent experiments. * P <0.05, ** P <0.01 and *** P <0.001, (a) versus control and (b) versus 1 μ M formoterol alone.

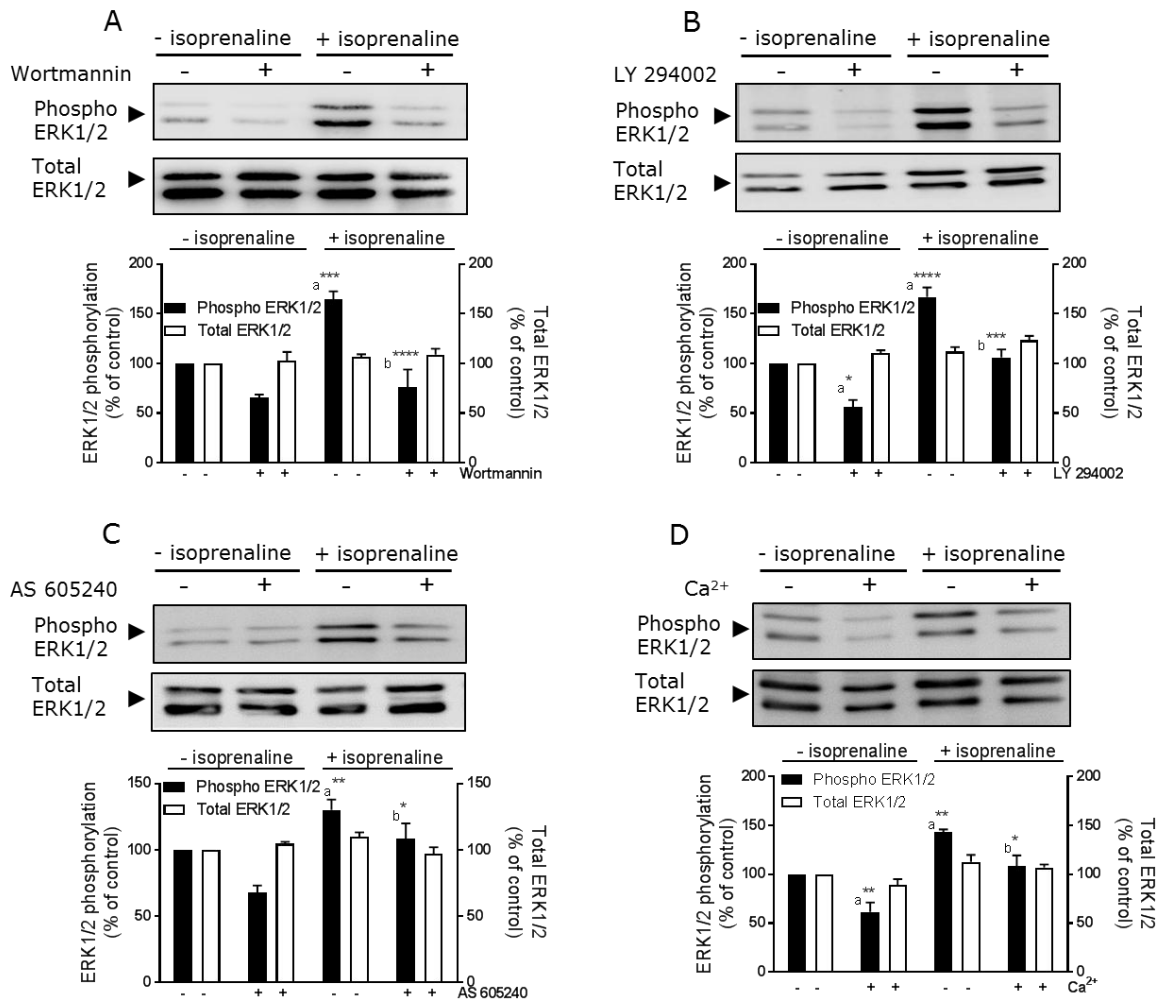


Fig 5.17: Effect of isoprenaline on ERK1/2 phosphorylation in H9c2 cells. Where indicated, H9c2 cells were pre-treated for 30 min with (A) wortmannin (100 nM), (B) LY 294002 (30 μ M), or (C) AS 605240 (1 μ M) prior to stimulation with isoprenaline (10 μ M) for 20 min. In Panel (D) cells were stimulated for 20 min with isoprenaline (10 μ M) either in the presence of extracellular Ca²⁺ (1.3 mM) or in its absence using nominally Ca²⁺-free Hanks/HEPES buffer containing 0.1 mM EGTA. Cell lysates were analysed by Western blotting for activation of ERK1/2 using phospho-specific antibodies. Samples were subsequently analysed on separate blots using antibodies that recognize total ERK1/2. Data are expressed as the percentage of values for control cells (=100%) in the absence of protein kinase inhibitor and represent the mean \pm S.E.M. of four independent experiments. * P <0.05, ** P <0.01, *** P <0.001 and **** P <0.0001, (a) versus control and (b) versus 10 μ M isoprenaline alone.

Moreover, *Rp*-cAMPs and pertussis toxin (figure 5.18A and B) had no significant effect on formoterol-induced ERK1/2 activation. However, isoprenaline-induced ERK1/2 activation was inhibited by pertussis toxin and *Rp*-cAMPs (figure 5.18C and D). These data suggest formoterol activates ERK1/2 via a PKA-independent but PI-3K γ and Ca²⁺-dependent pathway while isoprenaline-induced ERK1/2 activation is dependent upon G_i-protein, PI-3K γ , extracellular Ca²⁺ and PKA.

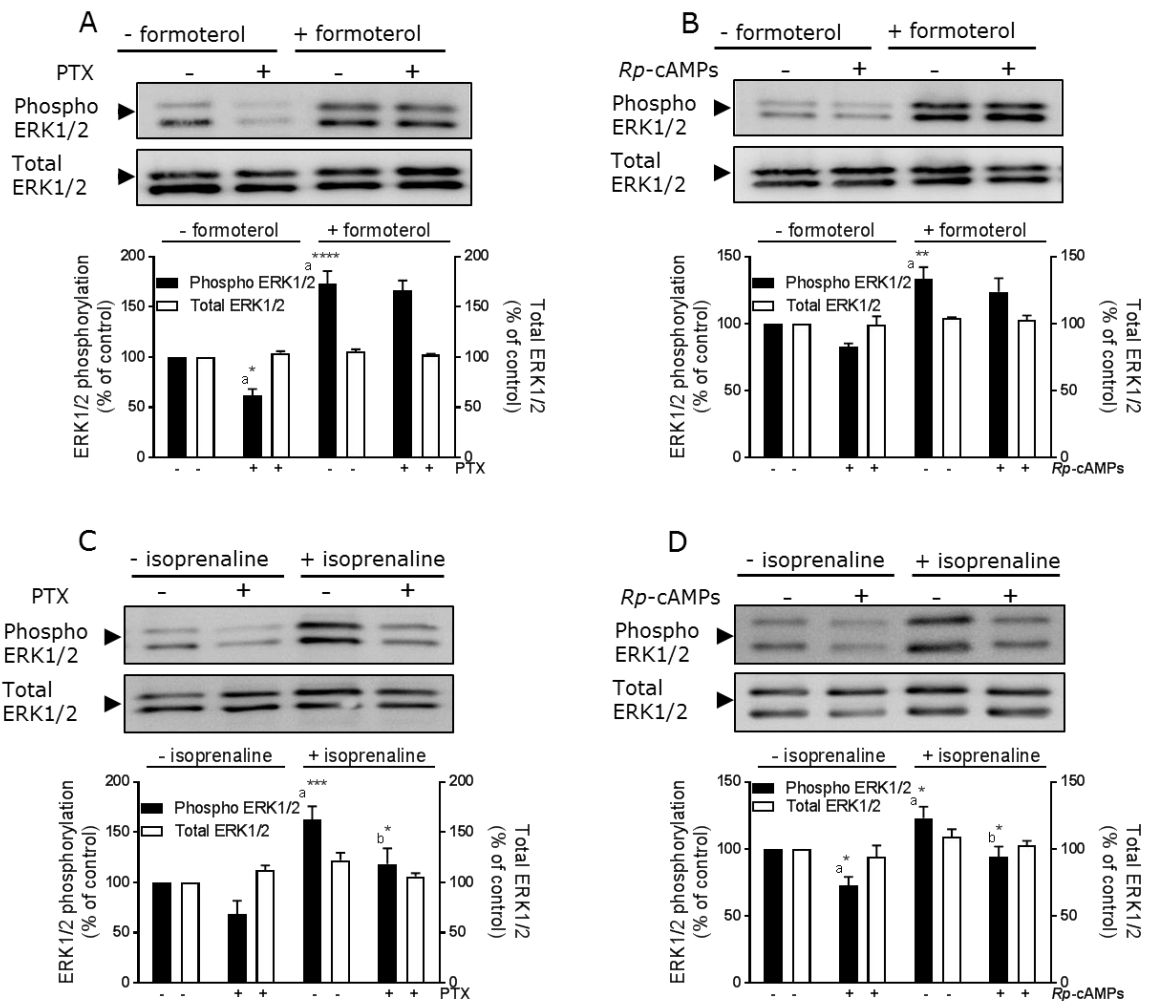


Fig 5.18: Effect of formoterol and isoprenaline on ERK1/2 phosphorylation in H9c2 cells. Where indicated, H9c2 cells were pre-treated for 16 h with 100 ng/ml pertussis toxin (panels A and C) or 30 min with *Rp*-cAMPS (50 μ M; panels B and D) prior to 20 min stimulation with formoterol (1 μ M) or isoprenaline (10 μ M). Cell lysates were analysed by Western blotting for activation of ERK1/2 using phospho-specific antibodies. Samples were subsequently analysed on separate blots using antibodies that recognize total ERK1/2. Data are expressed as the percentage of values for control cells (=100%) in the absence of protein kinase inhibitor and represent the mean \pm S.E.M. of four independent experiments. * P <0.05, ** P <0.01, *** P <0.001 and **** P <0.0001, (a) versus control and (b) versus 1 μ M formoterol or 10 μ M isoprenaline alone.

It is important to note that KT-5720, *Rp*-cAMPS, PD 98059, Akt inhibitor XI, SB 203580, SP 600125, LY 294002, AS 605240 and other compounds used in this study had no significant effect on purified guinea pig liver TG2 activity (table 5.1). H-89 had an inhibitory effect on the purified guinea pig liver TG2 activity (table 5.1) and hence was not used in this study. Overall, these data suggest that TG2 activity is modulated in H9c2 cells by the β_2 -AR via a pathway involving PKA, ERK1/2 and PI-3K γ .

Table 5.1: Effect of compounds used in this study on purified guinea pig liver TG2 activity.

Compound	Concentration	Effect on in-vitro TG2 activity (% of control)	
		Amine Incorporation	Cross linking
Akt inhibitor XI	1 μ M	87 \pm 3	85 \pm 3
AS 605240	1 μ M	103 \pm 2	88 \pm 4
CGP 20712	1 μ M	93 \pm 2	96 \pm 8
Cimaterol	10 μ M	91 \pm 3	86 \pm 1
DMSO	10 mM	103 \pm 1	94 \pm 3
Dobutamine	10 μ M	90 \pm 3	107 \pm 4
Formoterol	1 μ M	99 \pm 2	108 \pm 4
Forskolin	10 μ M	95 \pm 1	99 \pm 1
H-89	1 μM	51 \pm 5	56 \pm 3
ICI 118,551	1 μ M	97 \pm 4	81 \pm 5
Isoprenaline	10 μ M	98 \pm 4	86 \pm 4
KT-5720	2 μ M	93 \pm 6	93 \pm 3
LY 294002	30 μ M	108 \pm 8	93 \pm 7
PD 98059	50 μ M	100 \pm 2	102 \pm 2
Procaterol	10 μ M	98 \pm 5	108 \pm 1
Propranolol	1 μ M	109 \pm 2	106 \pm 2
PTX	100 ng/ml	110 \pm 4	101 \pm 5
<i>Rp</i> -cAMPs	50 μ M	107 \pm 3	108 \pm 1
SB 203580	30 μ M	98 \pm 3	97 \pm 1
SP 600125	20 μ M	90 \pm 5	110 \pm 2
Wortmannin	100 nM	103 \pm 3	96 \pm 6

TG2 amine incorporating and peptide crosslinking assays were carried out using purified guinea pig liver TG2 (50 ng/ well). Briefly, 50 ng of purified guinea pig liver TG2 was incubated with concentrations of the compounds listed in table 5.1 for 30 min prior to 1 h incubation in presence of either 6.67 mM calcium chloride or 13.3 mM EDTA containing 225 μ M biotin-cadaverine and 2mM 2-mercaptoethanol. Following incubation, the plates were processed as described in section 2.3 (ii) and (iii) of chapter II. H-89 had a significant effect on purified guinea pig liver TG2 activity (indicated in red) with $**P < 0.01$ for amine incorporating and $*P < 0.05$ for peptide crosslinking activity of TG2 versus control.

5.5 Visualisation of *in situ* TG2 activity following β_2 -AR activation.

Biotin-X-cadaverine, a cell penetrating biotin-labelled primary amine, acts as the acyl-acceptor during intracellular TG2-mediated transamidating reactions and is incorporated into endogenous protein substrates of TG2, which can subsequently be visualised by reporters such as FITC- and HRP-ExtrAvidin[®] (Lee et al, 1993). H9c2 cells were pre-incubated with 1 mM biotin-X-cadaverine for 6 h at 37°C prior to treatment with either formoterol or isoprenaline for 1, 5, 10, 20, 30 and 40 min. After fixation and permeabilisation, intracellular proteins with covalently attached biotin-X-cadaverine were visualised using FITC-ExtrAvidin[®]. As shown in figure 5.19 and figure 5.20, formoterol (100 nM) and isoprenaline (10 μ M) induced a time-dependent increase in the incorporation of biotin-X-cadaverine into endogenous protein substrates of TG2. These data are comparable to the time-dependent increases in TG2 activity observed *in vitro* (see figure 5.1 and 5.2). Formoterol-mediated biotin-X-cadaverine incorporation was also concentration-dependent ($pEC_{50} = 7.65 \pm 0.27$; $n=4$; figure 5.19). Similarly, isoprenaline-mediated biotin-X-cadaverine incorporation was also concentration-dependent ($pEC_{50} = 6.94 \pm 0.14$; $n=3$; figure 5.20).

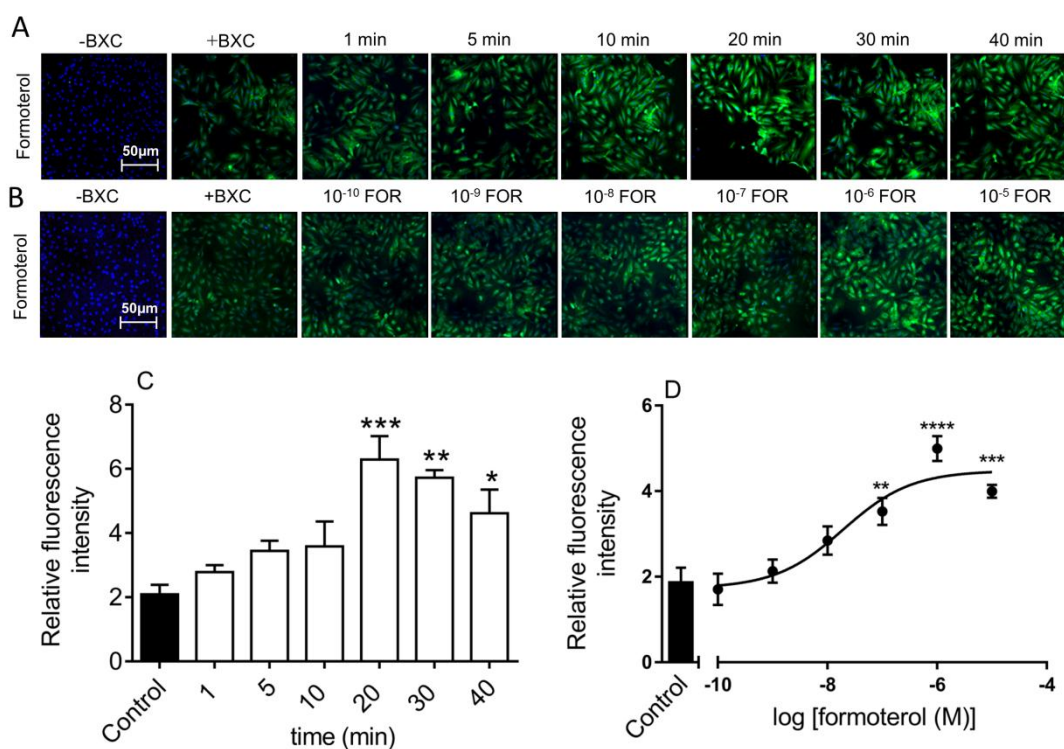


Fig 5.19: Formoterol-induced *in situ* TG2 activity in H9c2 cells. Cells were incubated with 1 mM biotin-X-cadaverine (BXC) for 6 h, after which they were treated with (A) 100 nM formoterol for 1, 5, 10, 20, 30 or 40 min or (B) the indicated concentrations (in M) of formoterol for 20 min. TG2-mediated biotin-X-cadaverine incorporation into intracellular proteins was visualized using FITC-ExtrAvidin[®] (green). Nuclei were stained with DAPI (blue) and viewed using a Leica TCS SP5 II confocal microscope (20x objective lens). Images presented are from one experiment and representative of three independent experiments. Quantified data points for (C) time course and (D) concentration-response curve experiments represent the mean \pm S.E.M. of fluorescence intensity relative to DAPI stain for five fields of view from each of three independent experiments. * $P < 0.05$, ** $P < 0.01$, *** $P < 0.001$ and **** $P < 0.0001$ versus control response.

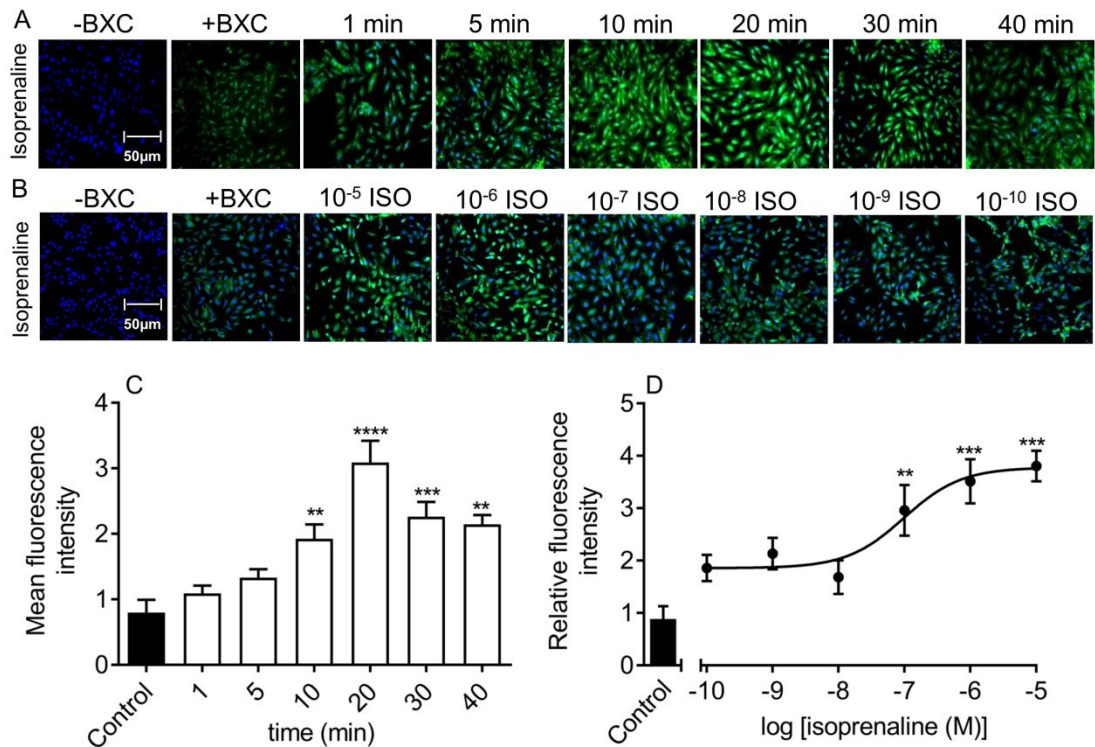


Fig 5.20: Isoprenaline-induced *in situ* TG2 activity in H9c2 cells. Cells were incubated with 1 mM biotin-X-cadaverine (BXC) for 6 h, after which they were treated with (A) 10 μ M isoprenaline for 1, 5, 10, 20, 30 or 40 min or (B) the indicated concentrations (in M) of isoprenaline for 20 min. TG2-mediated biotin-X-cadaverine incorporation into intracellular proteins was visualized using FITC-ExtrAvidin[®] (green). Nuclei were stained with DAPI (blue) and viewed using a Leica TCS SP5 II confocal microscope (20x objective lens). Images presented are from one experiment and representative of three independent experiments. Quantified data points for (C) time course and (D) concentration-response curve experiments represent the mean \pm S.E.M. of fluorescence intensity relative to DAPI stain for five fields of view from each of three independent experiments. * P <0.05, ** P <0.01, *** P <0.001 and **** P <0.0001 versus control response.

To confirm the involvement of TG2 activation, cells were treated with the TG2 inhibitors Z-DON (150 μ M) and R283 (200 μ M) for 1 h prior to incubation with either formoterol (1 μ M) or isoprenaline (10 μ M) for 20 min. Pre-treatment of cells with Z-DON and R283 resulted in the complete inhibition of formoterol-mediated biotin-X-cadaverine incorporation into protein substrates (figure 5.21A). The *in situ* responses to formoterol were also attenuated by inhibitors of PKA (KT 5720 and Rp-cAMPs), PI-3K (LY 294002 and AS 605240) and MEK1 (PD 98059) and following removal of extracellular Ca²⁺ (figure 5.21).

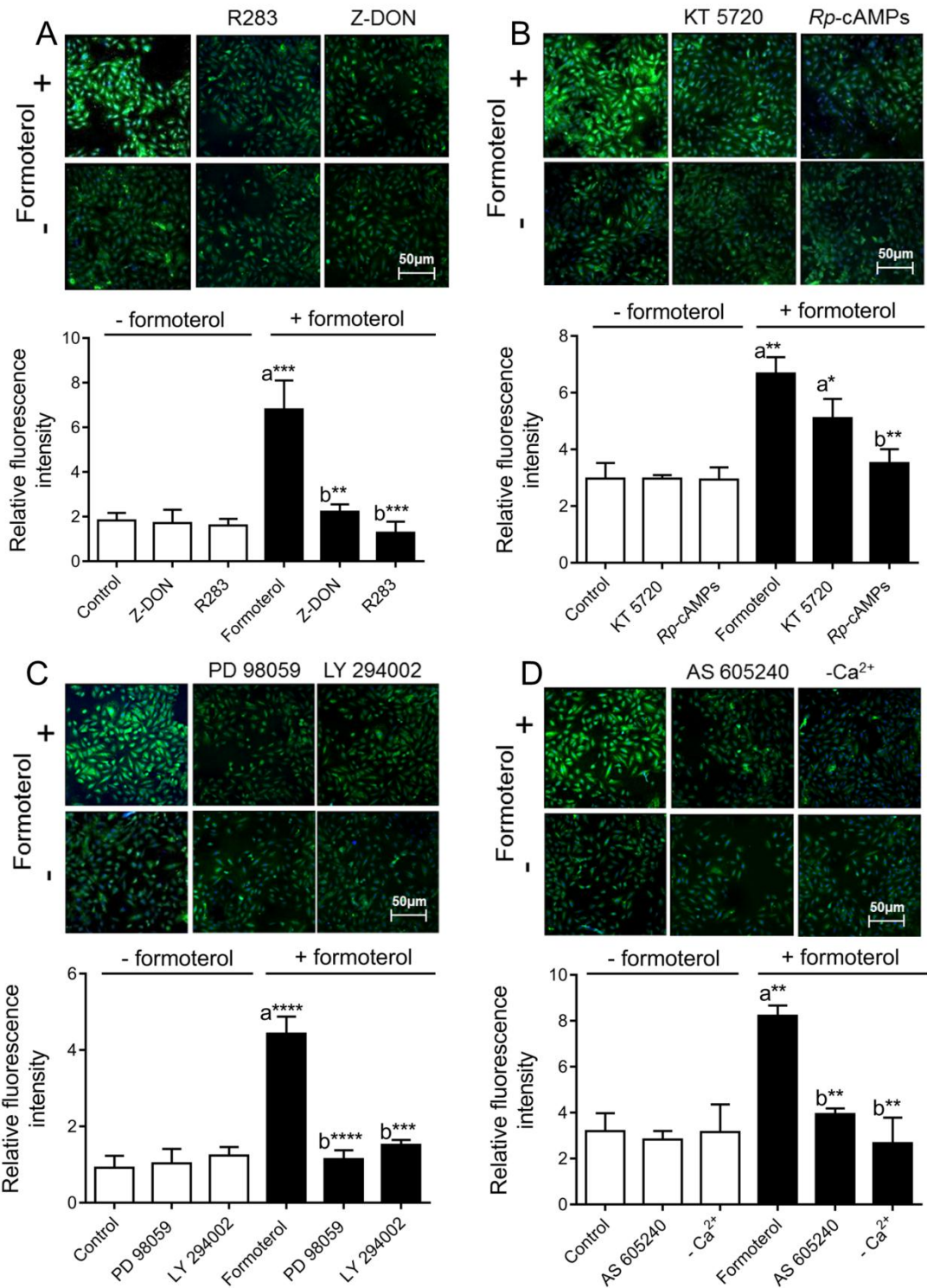


Fig 5.21: Effects of TG2, PKA, ERK1/2, PI-3K inhibitors and removal of extracellular Ca²⁺ on *in situ* TG2 activity in H9c2 cells following stimulation with formoterol. Cells were incubated with 1 mM biotin-X-cadaverine (BXC) for 6 h after which they were treated as follows: (A) 1 h with the TG2 inhibitors Z-DON (150 μ M) or R283 (200 μ M), (B) 30 min with KT 5720 (5 μ M) or Rp-cAMPS (50 μ M), (C) 30 min with PD 98059 (50 μ M) or LY 294002 (30 μ M) or (D) 30 min with AS 605240 (1 μ M) or in the absence of extracellular Ca²⁺ for 30 min (nominally Ca²⁺-free Hanks/HEPES buffer containing 0.1 mM EGTA), prior to 20 min stimulation with formoterol (1 μ M). TG2-mediated biotin-X-cadaverine incorporation into intracellular proteins was visualized using FITC-ExtrAvidin[®] (green). Nuclei were stained with DAPI (blue) and viewed using a Leica TCS SP5 II confocal microscope (20x objective lens). Images presented are from one experiment and are representative of three independent experiments. Quantified data

points represent the mean \pm S.E.M. of fluorescence intensity relative to DAPI stain for five fields of view from each of three independent experiments. * P <0.05, ** P <0.01, *** P <0.001 and **** P <0.0001, (a) versus control and (b) versus 1 μ M formoterol alone.

Similarly, isoprenaline-mediated biotin-X-cadaverine incorporation into protein substrates was sensitive to TG2 (Z-DON and R283), PKA (KT 5720 and *Rp*-cAMPs), PI-3K (LY 294002, AS 605240, wortmannin) and MEK1 (PD 98059) inhibitors and following removal of extracellular Ca^{2+} (figure 5.22 and 5.23).

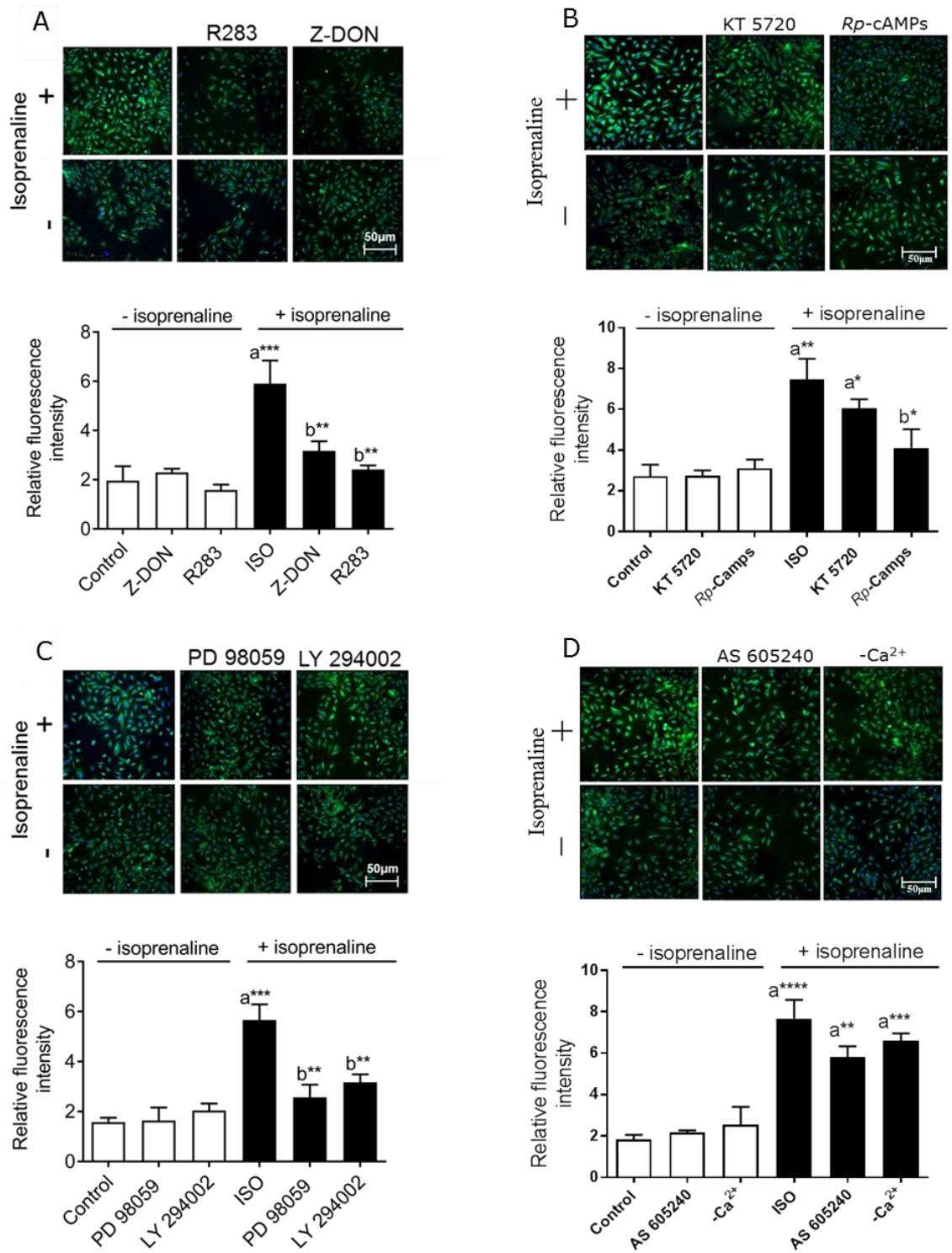


Fig 5.22: Effects of TG2, PKA, ERK1/2, PI-3K inhibitors and removal of extracellular Ca²⁺ on *in situ* TG2 activity in H9c2 cells following stimulation with isoprenaline. Cells were incubated with 1 mM biotin-X-cadaverine (BXC) for 6 h after which they were treated as follows: (A) 1 h with the TG2 inhibitors Z-DON (150 μ M) or R283 (200 μ M), (B) 30 min with KT 5720 (5 μ M) or Rp-cAMPS (50 μ M), (C) 30 min with PD 98059 (50 μ M) or LY 294002 (30 μ M) or (D) 30 min with AS 605240 (1 μ M) or in the absence of extracellular Ca²⁺ for 30 min (nominally Ca²⁺-free Hanks/HEPES buffer containing 0.1 mM EGTA), prior to 20 min stimulation with isoprenaline (ISO; 10 μ M). TG2-mediated biotin-X-cadaverine incorporation into intracellular proteins was visualized using FITC-ExtrAvidin[®] (green). Nuclei were stained with DAPI (blue) and viewed using a Leica TCS SP5 II confocal microscope (20x objective lens). Images presented are from one experiment and are representative of three independent experiments. Quantified data

points represent the mean \pm S.E.M. of fluorescence intensity relative to DAPI stain for five fields of view from each of three independent experiments. * P <0.05, ** P <0.01, *** P <0.001 and **** P <0.0001, (a) versus control and (b) versus 10 μ M isoprenaline alone.

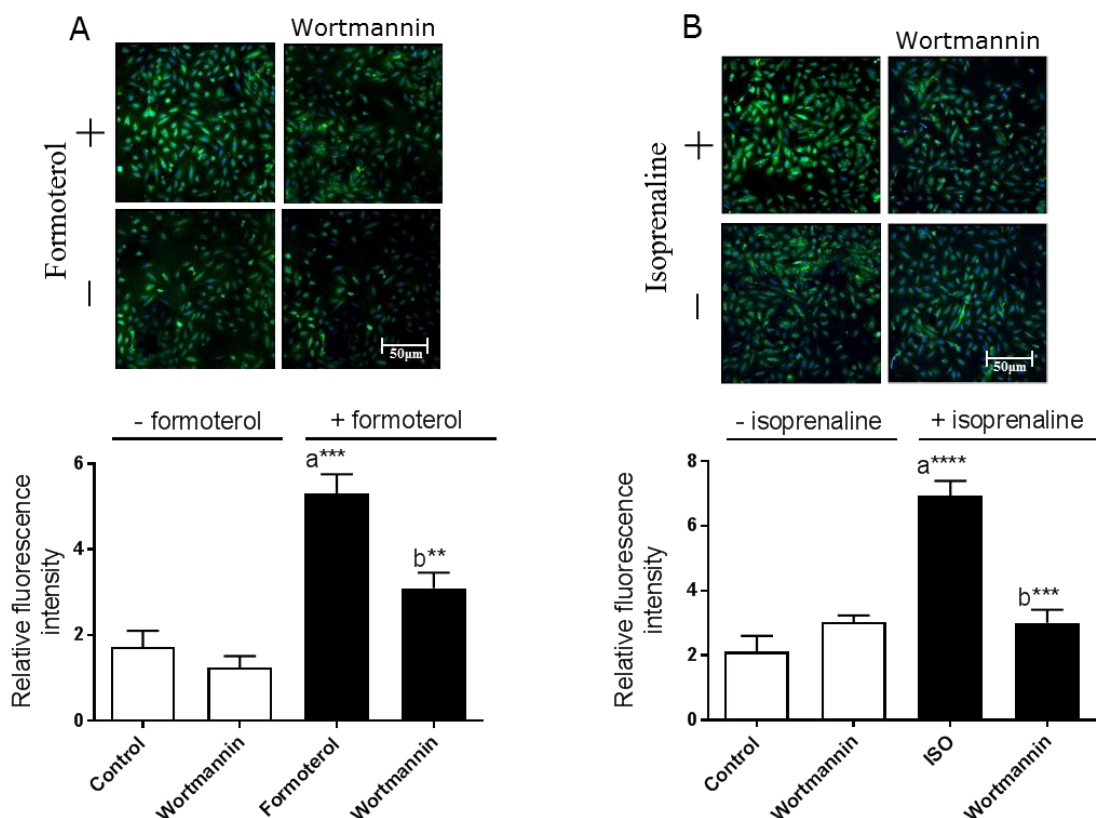


Fig 5.23: Effects of pan PI-3K inhibitor wortmannin on *in situ* TG2 activity in H9c2 cells following stimulation with formoterol and isoprenaline. Cells were incubated with 1 mM biotin-X-cadaverine (BXC) for 6 h after which they were treated with wortmannin (100 nM) prior to 20 min stimulation with formoterol (1 μ M) or isoprenaline (ISO; 10 μ M). TG2-mediated biotin-X-cadaverine incorporation into intracellular proteins was visualized using FITC-ExtrAvidin[®] (green). Nuclei were stained with DAPI (blue) and viewed using a Leica TCS SP5 II confocal microscope (20x objective lens). Images presented are from one experiment and are representative of three independent experiments. Quantified data points represent the mean \pm S.E.M. of fluorescence intensity relative to DAPI stain for five fields of view from each of three independent experiments. ** P <0.01, *** P <0.001 and **** P <0.0001, (a) versus control and (b) versus 1 μ M formoterol or 10 μ M isoprenaline alone.

To confirm the involvement of the β_2 -AR, cells were treated with the β_2 -AR selective antagonist ICI 118,551 (1 μ M) and non-selective β -AR antagonist propranolol (1 μ M) for 30 min prior to incubation with either formoterol (1 μ M) or isoprenaline (10 μ M) for 20 min. Pre-treatment of cells with ICI 118,551 and propranolol resulted in the complete inhibition of formoterol- and isoprenaline-mediated biotin-X-cadaverine incorporation into protein substrates (figure 5.24). This confirms that the induced TG2 activity was mediated by the β_2 -AR.

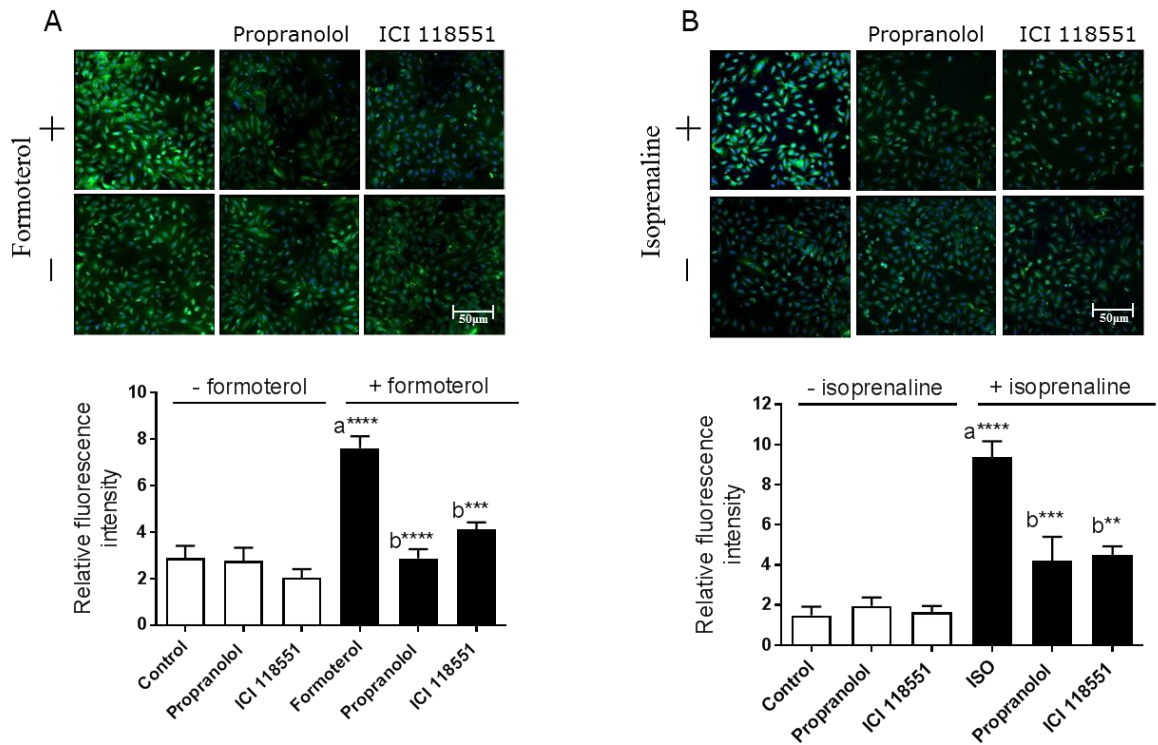


Fig 5.24: Effect of β -adrenoceptor antagonists on *in situ* TG2 activity in H9c2 cells following stimulation with formoterol and isoprenaline. Cells were incubated with 1 mM biotin-X-cadaverine (BXC) for 6 h after which they pre-treated for 30 min with the antagonists ICI 118,551 (1 μ M; β_2 -AR selective) and propranolol (1 μ M; non-selective β -adrenoceptor) prior to 20 min stimulation with formoterol (1 μ M) or isoprenaline (ISO; 10 μ M). TG2-mediated biotin-X-cadaverine incorporation into intracellular proteins was visualized using FITC-ExtrAvidin[®] (green). Nuclei were stained with DAPI (blue) and viewed using a Leica TCS SP5 II confocal microscope (20x objective lens). Images presented are from one experiment and are representative of three independent experiments. Quantified data points represent the mean \pm S.E.M. of fluorescence intensity relative to DAPI stain for five fields of view from each of three independent experiments. ** P <0.01, *** P <0.001 and **** P <0.0001, (a) versus control and (b) versus 1 μ M formoterol or 10 μ M isoprenaline alone.

5.6 β_2 -AR induced TG2 phosphorylation.

The effect of formoterol on TG2 phosphorylation was examined via immunoprecipitation of TG2, followed by SDS-PAGE and Western blot analysis using anti-phosphoserine and anti-phosphothreonine antibodies. As shown in figure 5.25 and 5.26, formoterol (1 μ M) enhanced the phosphoserine and phosphothreonine residues within TG2. Pre-treatment with *Rp*-cAMPs (50 μ M), PD 98059 (50 μ M) and AS 605240 (1 μ M) attenuated formoterol-induced TG2 phosphorylation (figure 5.25 and 5.26). Furthermore, removal of extracellular Ca^{2+} also resulted in attenuation of formoterol-induced TG2 activity (figure 5.26). Additionally, formoterol-induced increases in TG2 phosphorylation were also blocked by the pan PI-3K inhibitors wortmannin and LY 294002 (figure 5.27).

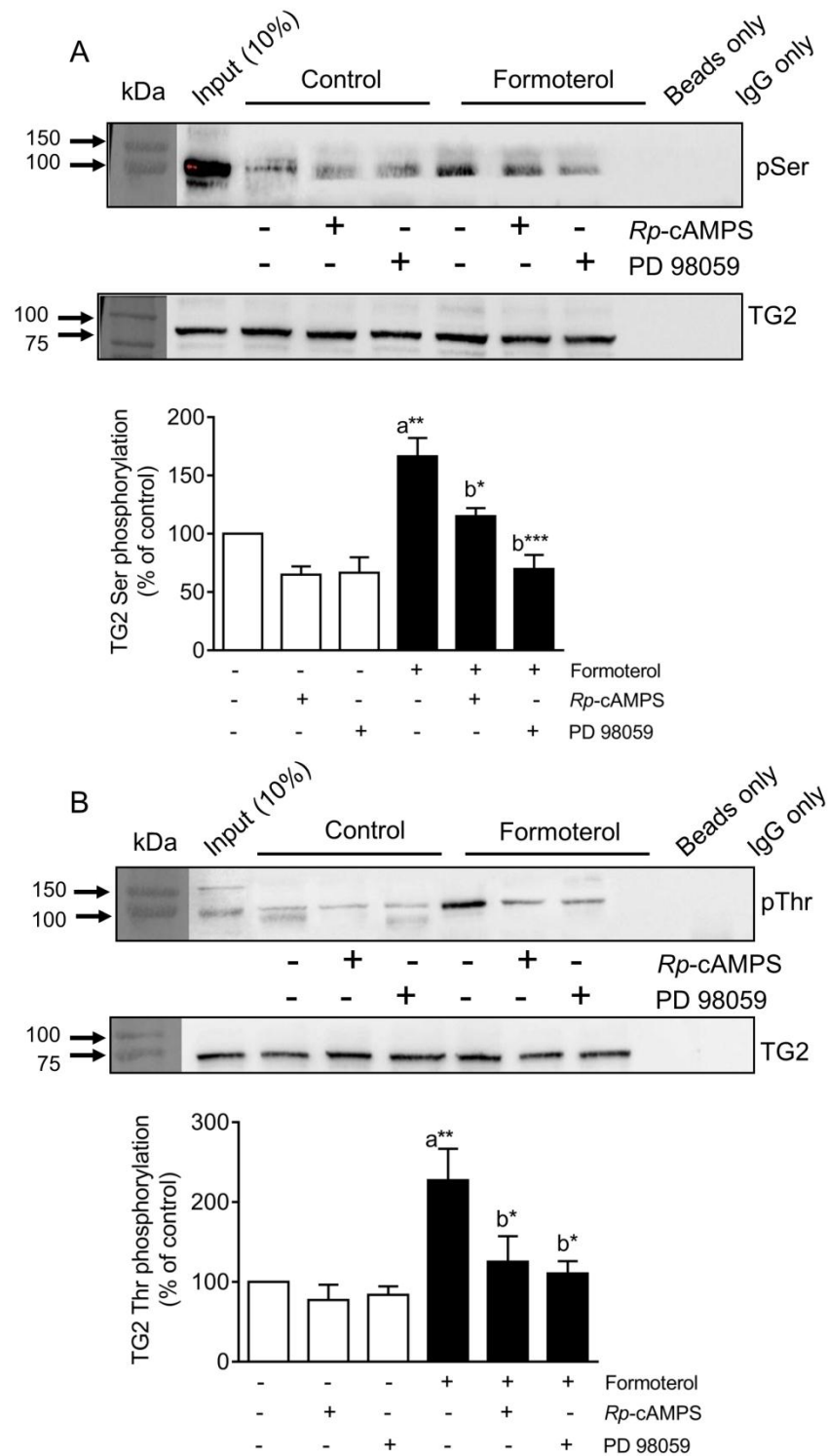


Fig 5.25: Effect of PKA and ERK1/2 inhibition on formoterol-induced phosphorylation of TG2. Where indicated, H9c2 cells were incubated for 30 min with *Rp*-cAMPS (50 μ M) or PD 98059 (50 μ M) prior to stimulation with formoterol (1 μ M) for 20 min. Following stimulation, cell lysates were subjected to immunoprecipitation using an anti-TG2 monoclonal antibody as described in section 2.7 of chapter II. The resultant immunoprecipitated protein(s) were subjected to SDS-PAGE and analysed via Western blotting using (A) anti-phosphoserine and (B) anti-phosphothreonine antibodies. 10% of the input was added to the first lane to show the presence of phosphorylated proteins prior to immunoprecipitation and negative controls with the immunoprecipitation performed with beads or IgG only were included to demonstrate the specificity of the bands shown. Quantified data for formoterol-induced increases in

TG2-associated serine and threonine phosphorylation are expressed as a percentage of that observed in control cells (100%). Data points represent the mean \pm S.E.M. from three independent experiments. * P <0.05, ** P <0.01 and *** P <0.001 (a) versus control and (b) versus formoterol alone.

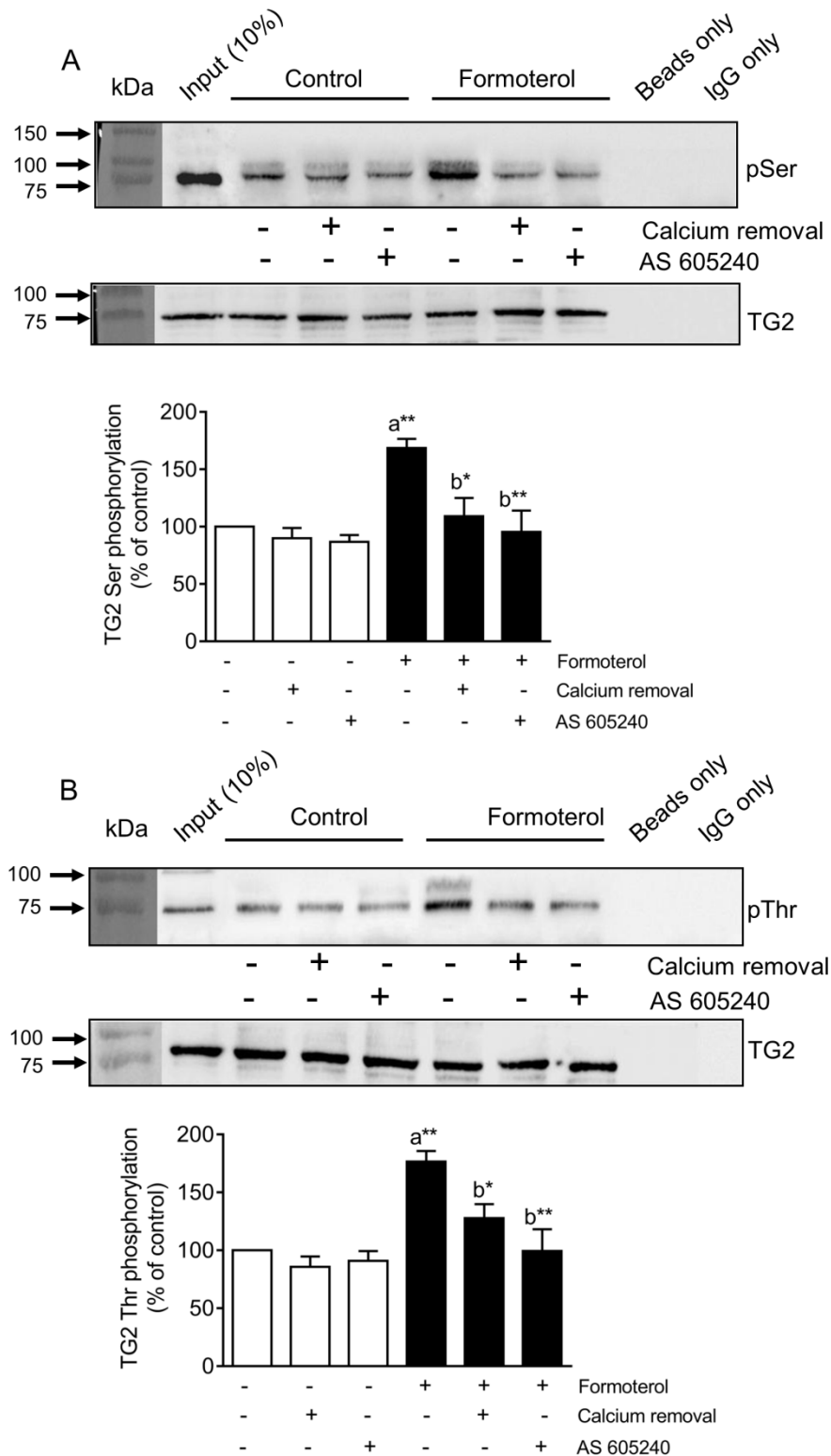


Fig 5.26: Roles of extracellular Ca^{2+} and PI-3K γ in formoterol-induced phosphorylation of TG2. Measurements of formoterol-induced TG2 phosphorylation were performed either in the absence of extracellular Ca^{2+} using nominally Ca^{2+} -free Hanks/HEPES buffer containing 0.1 mM EGTA, as indicated, or in cells incubated for 30 min with AS 60540 (1 μM) prior to stimulation with formoterol (1 μM) for 20 min. Following stimulation, cell lysates were subjected to immunoprecipitation using an anti-TG2 monoclonal antibody as described in section 2.7 of chapter II. The resultant immunoprecipitated protein(s) were subjected to SDS-PAGE and Western blot analysis using (A) anti-phosphoserine and (B) anti-phosphothreonine antibodies. 10% of the input was added to the first lane to show the presence of phosphorylated proteins prior to immunoprecipitation and negative controls with the

immunoprecipitation performed with beads or IgG only were included to demonstrate the specificity of the bands shown. Quantified data for formoterol-induced increases in TG2-associated serine and threonine phosphorylation are expressed as a percentage of that observed in control cells (100%). Data points represent the mean \pm S.E.M. from three independent experiments. * P <0.05 and ** P <0.01 (a) versus control and (b) versus formoterol alone.

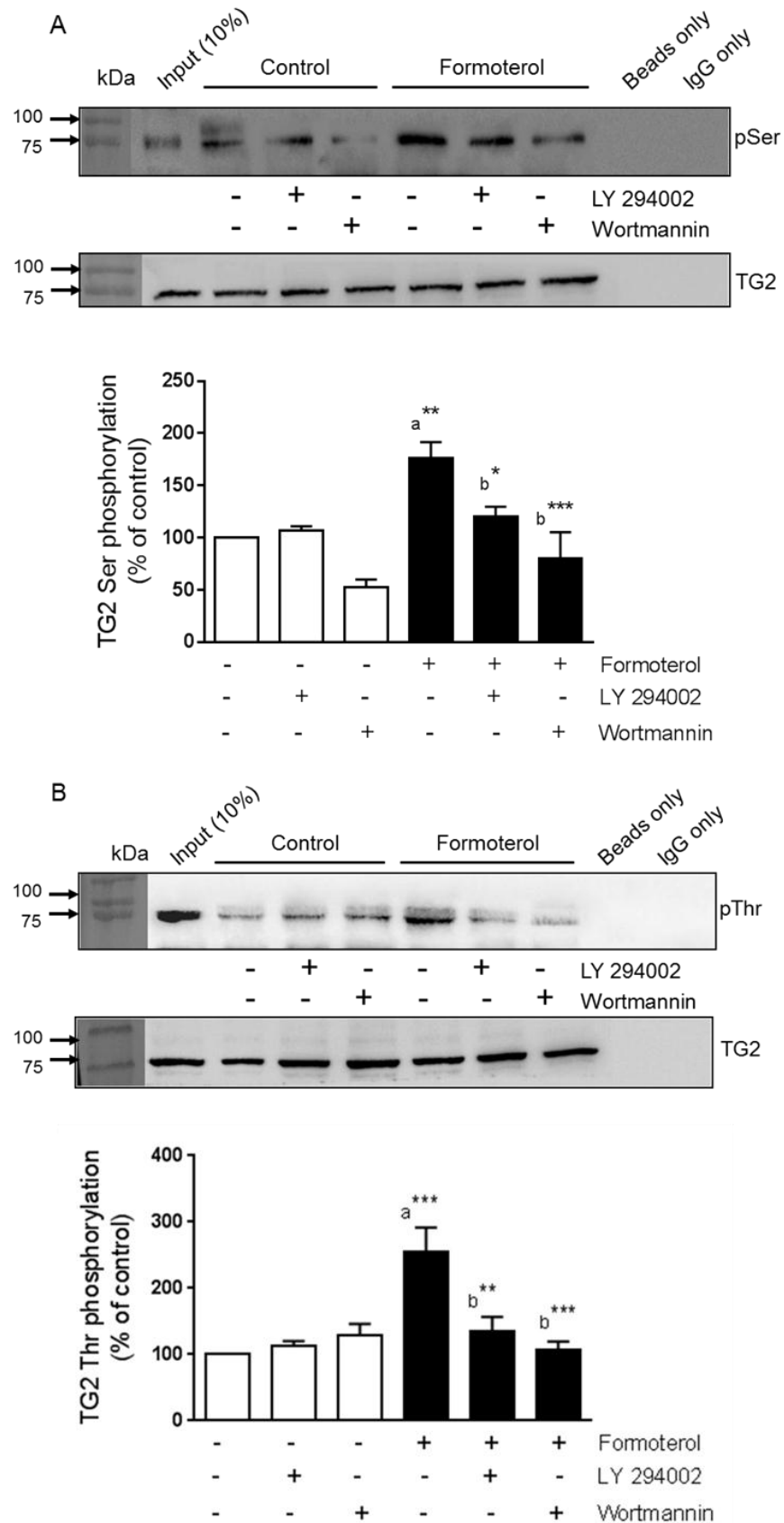


Fig 5.27: Effect of pan PI-3K inhibitors on formoterol-induced phosphorylation of TG2. Where indicated, H9c2 cells were incubated for 30 min with wortmannin (100 nM) or LY 294002 (30 μ M) prior to stimulation with formoterol (1 μ M) for 20 min. Following stimulation, cell lysates were subjected to immunoprecipitation using an anti-TG2

monoclonal antibody as described in section 2.7 of chapter II. The resultant immunoprecipitated protein(s) were subjected to SDS-PAGE and analysed via Western blotting using (A) anti-phosphoserine and (B) anti-phosphothreonine antibodies. 10% of the input was added to the first lane to show the presence of phosphorylated proteins prior to immunoprecipitation and negative controls with the immunoprecipitation performed with beads or IgG only were included to demonstrate the specificity of the bands shown. Quantified data for formoterol-induced increases in TG2-associated serine and threonine phosphorylation are expressed as a percentage of that observed in control cells (100%). Data points represent the mean \pm S.E.M. from three independent experiments. * P <0.05, ** P <0.01 and *** P <0.001 (a) versus control and (b) versus formoterol alone.

In conclusion, the data shown in this chapter provide sufficient evidence which supports the notion that TG2 activity is modulated by the β_2 adrenoceptor in mitotic H9c2 cells via a PKA, PI-3K γ and ERK1/2 dependent pathway.

5.7 Discussion.

The aim of this chapter was to identify if TG2 is modulated by the β_2 adrenoceptor in H9c2 cells along with determining the molecular mechanisms underlying it.

In vitro modulation of TG2 by the β_2 -AR

Recently Almami and colleagues have reported that forskolin (AC activator) triggers increases in TG2-mediated transamidase activity in H9c2 cells (Almami et al, 2014). Hence it was of interest to investigate if the β_2 -AR which couples to cAMP/PKA could modulate TG2-mediated transamidase activity in rat H9c2 cardiomyoblasts. Activation of the β_2 -AR with either the selective long-acting β_2 -AR agonist formoterol or the non-selective β -AR agonist isoprenaline triggered time- and concentration-dependent increases in the amine incorporating and protein cross-linking activity of TG2 (figures 5.1 and 5.2). It is important to note that the potency for both of these agonists in mediating biotin-cadaverine incorporation and protein cross-linking is lower than that for agonist-stimulated cAMP accumulation. One possible explanation for these differences in potency might be due to the top of the curve being different. This could be because of less data points on the curve and therefore would need higher concentrations of agonist to achieve the top of the curve. These differences may be a consequence of biased agonism between agonist-induced cAMP accumulation versus TG2 activation (Rajagopal et al, 2011). Alternatively, it could also be a consequence of the multiple signalling pathways e.g. PI-3K, ERK1/2 and Ca²⁺ shown to be required for TG2 modulation by the β_2 -AR. Moreover, administration of the non-selective β -AR antagonist propranolol and the selective β_2 -AR antagonist ICI 118,551 further clarifies that the responses obtained are from the β_2 -AR as the induced TG2 activity was completely reversed (figure 5.3 and 5.4). Finally, involvement of TG2 was confirmed as responses to agonists were blocked by R283 and Z-DON, two structurally different TG2 inhibitors (Freund et al, 1994; Schaertl et al, 2010; figure 5.3 and 5.4). Hence

from these results, it is clear that the β_2 -AR is able to modulate TG2 mediated amine- and peptide-incorporating activities.

Role of extracellular Ca^{2+} in β_2 -AR induced TG2 activation

It is well known that the amine- and peptide-incorporating activities of TG2 are dependent upon Ca^{2+} (Slaughter et al, 1992; Trigwell et al, 2004), therefore the role of extracellular and intracellular Ca^{2+} in β_2 -AR-induced TG2 activation was investigated. Removal of extracellular Ca^{2+} partially inhibited formoterol-induced TG2-mediated amine- and peptide-incorporating activities (figure 5.3). As shown in chapter III figure 3.11, formoterol did not trigger observable increases in intracellular $[Ca^{2+}]$ in H9c2 cells loaded with Fluo-8 AM. At present the reason(s) for this discrepancy are unclear but it may reflect very localized formoterol-induced increases in intracellular $[Ca^{2+}]$ (as a consequence of Ca^{2+} influx) that, whilst sufficient to trigger TG2 activation, were not detectable using the methodology employed for imaging. It is important to note that, although changes in intracellular $[Ca^{2+}]$ required for TG2 activation are typically in the order 3-100 μ M (Király et al., 2011), there is growing evidence that intracellular $[Ca^{2+}]$ can reach levels sufficient to activate TG2. For instance, interaction of TG2 with protein binding partners and/or membrane lipids have been proposed to induce a conformational change that promotes activation at lower levels of intracellular $[Ca^{2+}]$ (Király et al, 2011). Hence it is possible that formoterol-induced TG2 activation may require the sensitization of TG2 to low levels of intracellular $[Ca^{2+}]$. Interestingly, removal of extracellular Ca^{2+} also partially inhibited isoprenaline-induced TG2-mediated amine- and peptide-incorporating activities (figure 5.4). As shown in chapter III figure 3.11, isoprenaline occasionally did trigger increases in intracellular $[Ca^{2+}]$ in H9c2 cells loaded with Fluo-8 AM. This could be a result of isoprenaline coupling to $G_{i/o}$ -proteins as treatment with PTX resulted in reversal of isoprenaline-induced TG2-mediated amine- and peptide-incorporating activities (figure 5.2) but PTX pre-treatment had no effect in formoterol-induced TG2-mediated amine- and peptide-incorporating activities (figure 5.1). Clearly, further studies are warranted to determine precisely how β_2 -AR-induced TG2 activation occurs in the absence of detectable increases in intracellular Ca^{2+} (in case of formoterol) and in case of isoprenaline, it is necessary to confirm the isoprenaline-induced intracellular Ca^{2+} responses and their relation with TG2. However, the kinase-dependent pathways outlined in the present study could be central to these novel aspects of TG2 modulation by the β_2 -AR. Furthermore, many protein kinases (e.g. ERK1/2 and PKC; Chuderland and Seger, 2008; Steinberg, 2012) display Ca^{2+} sensitivity. This Ca^{2+} sensitivity of protein kinases can lead to potential crosstalk and might be crucial in modulation of TG2.

Role of protein and lipid kinase inhibitors on β_2 -AR induced TG2 activity

The role of PKA and other protein/lipid kinases in formoterol- and isoprenaline-induced TG2 activation were investigated using the appropriate pharmacological inhibitors. There was no activation of p38 MAPK or JNK1/2 following stimulation of β_2 -AR (figure 5.6) suggesting that these pathways are not involved. Similarly, the p38 MAPK and JNK1/2 inhibitors SB 203580 and SP 600125 did not have any effect on β_2 -AR-induced TG2 activation (figure 5.7) further confirming no involvement of these protein kinases. The PKA inhibitors *Rp*-cAMPs and KT 5720 attenuated formoterol-induced TG2 amine incorporating and peptide crosslinking activities, suggesting a role for PKA in β_2 -AR induced TG2 activation (figure 5.5). Interestingly, the PKA inhibitors *Rp*-cAMPs and KT 5720 did not inhibit isoprenaline-induced TG2 amine incorporating and peptide crosslinking activities, suggesting there might be a different pathway by which isoprenaline induces TG2 activation. It has been shown in this study that isoprenaline can couple to $G_{i/o}$ -proteins and hence TG2 activation might occur via a pathway that is dependent on $G_{i/o}$ -proteins.

As indicated in figure 5.8, formoterol and isoprenaline also induced robust increases in ERK1/2. The MEK1/2 (up-stream activator of ERK1/2) inhibitor PD 98059 abolished formoterol- and isoprenaline-induced TG2 activation (figure 5.9). Previous studies have reported that ERK1/2 activation by the β_2 -AR involves PKA-dependent activation of the small G-protein Rap1 and subsequent activation of B-Raf (Schmitt and Stork, 2000). However, in H9c2 cells formoterol-induced ERK1/2 activation was insensitive to PKA inhibition while isoprenaline-induced ERK1/2 activation was sensitive to PKA inhibition. Therefore the role of PKA in TG2 activation remains unclear (figure 5.18).

In addition to the pathway outlined above, the β_2 -AR can also trigger ERK1/2 activation via two other pathways; one G_s/G_i -protein dependent and the other β -arrestin-dependent but G-protein independent (Shenoy et al, 2006). In H9c2 cells, formoterol-induced ERK1/2 and TG2 activation were pertussis toxin insensitive and therefore are independent of $G_{i/o}$ -proteins and suggests involvement of G_s -proteins and/or β -arrestin. In contrast, isoprenaline-induced ERK1/2 and TG2 activation were sensitive to pertussis toxin suggesting the involvement of $G_{i/o}$ -proteins (figure 5.1, 5.2 and 5.18). The fact that removal of extracellular Ca^{2+} abolished formoterol- and isoprenaline-induced ERK1/2 activation, suggests a prominent role for Ca^{2+} influx (figure 5.16 and 5.17). Previous studies have shown that G_s coupled receptors can also stimulate ERK1/2 via cAMP-mediated (PKA independent) activation of EPAC (exchange protein directly activated by cAMP), which is a guanine nucleotide exchange factor for Rap1 (Goldsmith and Dhanasekaran, 2007). Overall, these observations suggest that signalling pathways leading to ERK1/2 and TG2 activation by the β_2 -AR appear to be ligand dependent. It would be of interest to investigate further the mechanism(s) underlying β_2 -AR-induced ERK1/2 activation in H9c2 cells.

Chesley and colleagues have shown that the β_2 -AR triggers the activation of PI-3K γ via a G $_i$ -protein dependent pathway (Chesley et al, 2000). Furthermore, PI-3K γ plays a prominent role in the regulation of cardiac contractility by attenuating cAMP levels via phosphodiesterase 4 activation (Gregg et al, 2010). It has also been previously reported that isoprenaline activates PI-3K α via the sequential activation of G $_i$ /G $\beta\gamma$, Src and PDGFR in H9c2 cells (Yano et al, 2007) and the β_2 -AR has been shown to activate PI-3K α via the transactivation of the platelet-derived growth factor receptor (PDGFR; Yano et al, 2007). In the present study we have shown that formoterol- and isoprenaline-induced TG2 (figure 5.11 and 5.13) and ERK1/2 (figure 5.16 and 5.17) activation are sensitive to the pan PI-3K inhibitors wortmannin and LY 294002 and the selective PI-3K γ inhibitor AS 605240. From these data a substantial role for PI-3K α in β_2 -AR-induced TG2 activation would seem unlikely. Furthermore, since formoterol-induced ERK1/2 activation is pertussis toxin insensitive, it is likely that the β_2 -AR-induced PI-3K γ activation proceeds via a G $_i$ -protein independent pathway in H9c2 cells. Interestingly, in adult rat cardiomyocytes the β_1 -AR stimulates PI-3K via a signalling pathway involving G $_s$ /PKA and G $_{s\beta\gamma}$ /GRK2 (Leblais et al, 2004). Overall, these observations suggest that PI-3K γ plays a prominent up-stream role in ERK1/2 stimulation and TG2 activation by the β_2 -AR in H9c2 cells. Clearly, further studies are required to elucidate the mechanism(s) governing β_2 -AR-induced PI-3K γ activation in H9c2 cells.

Apart from PI-3K γ and ERK1/2 activation in H9c2 cells, PKB activation upon stimulation of β_2 -AR was investigated as PI-3k is closely associated with PKB. It was found that the pan PI-3K inhibitors wortmannin and LY 294002 and the selective PI-3K γ inhibitor AS 605240 could inhibit PKB phosphorylation (figures 5.10 and 5.12) and TG2 activation (figures 5.11 and 5.13) further confirming the role of PI-3K γ . Implementation of the selective PKB inhibitor, Akt inhibitor XI significantly attenuated β_2 -AR-induced PKB activation in H9c2 cells (figure 5.14). In pulmonary vascular smooth muscle cells, TG2 promotes Akt signalling by Akt serotonylation i.e. covalent attachment of 5-HT via transamidase activity of TG2 (Penumatsa et al, 2014). Similarly, in several cancers such as pancreatic cancer cells, HeLa cells, meningioma and breast cancer cells, TG2 expression is associated with activation of the PAK/Akt survival pathway, inhibition of ROS formation and modulation of tumour suppressor phosphatase PTEN which results in cell survival (Bae et al, 2006; Verma et al, 2008; Verma et al, 2008; Agnihotri et al, 2013; Huang et al, 2014; Huang et al, 2015). However, Akt inhibitor XI had no effect on β_2 -AR-induced TG2 activation (figure 5.15), thus suggesting that even though PKB is being activated, it does not play a role in modulation of TG2 activity upon stimulation of the β_2 -AR.

β₂-AR-induced phosphorylation of TG2

Given the apparent role of PKA and ERK1/2 in modulation of TG2, it was of interest to investigate the phosphorylation status of TG2 following β₂-AR stimulation. The data obtained demonstrate that TG2 is phosphorylated in response to β₂-AR activation (figure 5.25, 5.26 and 5.27). Hence it is conceivable that the modulation of TG2 phosphorylation represents a downstream target of β₂-AR signalling. Previous studies have shown that TG2 is phosphorylated by PKA at Ser²¹⁵ and Ser²¹⁶ (Mishra and Murphy, 2006) and at an unknown site(s) by PTEN-induced putative kinase 1 (PINK1; Min et al., 2015). It is also known that phosphorylation of TG2 by PKA at Ser²¹⁶ inhibits its transamidase activity and enhances its kinase activity (Mishra et al, 2007; Wang et al, 2012). Phosphoproteomic studies have also identified numerous phosphorylation sites in human (Ser⁵⁶, Ser⁶⁰, Tyr²¹⁹, Thr³⁶⁸, Tyr³⁶⁹, Ser⁴¹⁹, Ser⁴²⁷, Ser⁵³⁸, Ser⁵⁴¹ and Ser⁶⁰⁸; Rikova et al, 2007; Imami et al, 2008; Kettenbach et al, 2011; Bian et al, 2014; Palacios-Moreno et al, 2015) and rat (Tyr⁴⁴, Thr⁵⁸, Ser⁶⁸ and Ser⁴⁴⁹; Hoffert et al, 2006; Lundby et al, 2012) TG2.

It is interesting to note that PKA-mediated phosphorylation of TG2 has several potential consequences, including promotion of protein-protein interactions, enhancement of TG2 kinase activity and inhibition of transamidating activity (Mishra and Murphy, 2006; Mishra et al, 2007), whereas PINK1-mediated phosphorylation of TG2 blocks its proteasomal degradation (Min et al, 2015). In this study β₂-AR-induced PKA activation promoted TG2 transamidating activity. Mishra and colleagues showed using histidine-tagged TG2 immobilized on nickel-agarose and incubated with purified PKA that PKA inhibited *in vitro* TG2 crosslinking activity (Mishra et al, 2007). Hence, *in vivo* regulation of TG2 activity by PKA may be influenced by interaction of TG2 with other proteins and/or lipids. Thus, further studies are required to determine the consequence(s) of β₂-AR induced TG2 phosphorylation. In view of the multiple protein/lipid kinases (PKA, ERK1/2, PI-3Kγ) implicated in β₂-AR-induced TG2 activation, investigation of the influence of kinase inhibitors on TG2 phosphorylation was carried out. Formoterol-induced increases in TG2 serine and threonine phosphorylation were significantly reduced following pharmacological inhibition of PKA (*Rp*-cAMPs), MEK1/2 (PD 98059), PI-3K (AS 605240, wortmannin, LY 294002) and removal of extracellular Ca²⁺. Although the inhibition of TG2 phosphorylation following PI-3Kγ inhibition is most likely due to the upstream role of PI-3Kγ in ERK1/2 activation, it is possible that the protein kinase activity of PI-3Kγ could directly phosphorylate TG2 (Hunter 1995; Naga Prasad et al, 2005). Further studies are necessary to establish whether PKA, ERK1/2 and/or indeed PI-3Kγ directly catalyse the phosphorylation of TG2.

It is also important to note that removal of extracellular Ca²⁺ inhibited formoterol-induced TG2 phosphorylation. The role of extracellular Ca²⁺ in formoterol-induced ERK1/2 activation is apparent from these data. Alternatively, it is also possible that

conformational changes in TG2 triggered by Ca^{2+} facilitate its subsequent phosphorylation by PKA and/or ERK1/2. Conversely, it could be that TG2 phosphorylation sensitizes TG2 to activation in the presence of low intracellular Ca^{2+} levels. Finally, as TG2 possesses kinase activity, it is conceivable that formoterol-induced increases in TG2-bound serine and threonine phosphorylation may involve auto-phosphorylation. However, further work to identify the phosphorylation sites involved would be necessary.

In situ β_2 -AR-induced polyamine incorporation into protein substrates

Intracellular polyamines (e.g. spermine, spermidine, and putrescine) play an important role the regulation of gene expression, cell proliferation, and the response of cells to stress (Miller-Fleming et al, 2015). Polyamines can also be covalently attached onto proteins via TG2-mediated transamidation activity, resulting in the incorporation of a positively charged group into the target protein. Hence, TG2-mediated polyamination may promote changes in protein conformation, which could lead to alterations in protein function (Yu et al, 2015). For instance, constitutive G-protein activity is a consequence of TG2-mediated incorporation of polyamines into RhoA (Makitie et al, 2009; Shin et al, 2008; Singh et al, 2001), while the incorporation of polyamines into phospholipase A_2 results in a 2-3 fold increase in its activity which causes release of arachidonic acid from membrane phospholipids (Cordella-Miele et al, 1993). In the present study, *in situ* TG2 activity increased following stimulation of the β_2 -AR in a time- and concentration-dependent manner which is comparable to amine incorporation activity observed *in vitro* (figures 5.19 and 5.20). The role of TG2 was confirmed using TG2 inhibitors Z-DON and R283 which were able to significantly reverse *in situ* TG2 activity (figures 5.21A and 5.22A). These β_2 -AR induced-TG2 responses were also sensitive to pharmacological inhibition of PKA (*Rp*-cAMPs, KT 5720), MEK1/2 (PD 98059), PI-3K (AS 605240, LY 294002, Wortmannin) and removal of extracellular Ca^{2+} (figures 5.21, 5.22 and 5.23), confirming the role of these signalling pathways. The role of β_2 -AR in inducing TG2 activity was confirmed using the selective β_2 -AR antagonist ICI 118,551 and the non-selective β -AR antagonist propranolol which were able to reverse *in situ* TG2 activity (figure 5.24). From the data presented in this study, it could be speculated that β_2 -AR mediated incorporation of polyamines might regulate the function of a range of cellular targets and may represent a new paradigm in β_2 -AR signalling and regulation of cellular function.

In conclusion, this present study has revealed that the activation of TG2 occurs by the β_2 -AR via a PKA, PI-3K and ERK1/2 dependent pathway in H9c2 cells. Figure 5.28 and table 5.2 summarise the findings of this chapter.

Table 5.2: Summary of the effect of treatments on β_2 -AR-induced TG2 activities.

β_2 -AR-induced TG2 activation						
TG2 activity	Amine incorporation		peptide crosslinking		<i>in-situ</i>	
Treatments	FORM	ISO	FORM	ISO	FORM	ISO
100 ng/ml PTX	N	Y	N	Y		
1 μ M ICI 118551	Y	Y	Y	Y	Y	Y
1 μ M Propranolol	Y	Y	Y	Y	Y	Y
150 μ M Z-DON	Y	Y	Y	Y	Y	Y
200 μ M R283	Y	Y	Y	Y	Y	Y
Nominally Ca^{2+} -free Hanks/HEPES buffer containing 0.1 mM EGTA	Y	Y	Y	Y	Y	N
50 μ M BAPTA-AM in nominally Ca^{2+} -free Hanks/HEPES buffer containing 0.1 mM EGTA	N	N	N	N		
50 μ M <i>Rp</i> -cAMPs	Y	Y	Y	N	Y	Y
5 μ M KT 5720	Y	N	N	N	N	N
20 μ M SB 208530	N	N	N	N		
20 μ M SP 600125	N	N	N	N		
50 μ M PD 98059	Y	Y	Y	Y	Y	Y
30 μ M LY 294002	Y	Y	Y	Y	Y	Y
100 nM Wortmannin	Y	Y	Y	Y	Y	Y
1 μ M AS 605240	Y	Y	Y	Y	Y	N
1 μ M AKT XI inhibitor	N	N	N	N		

Effects of a range of treatments used in this study were investigated for TG2 amine incorporating, peptide crosslinking and *in-situ* activities in H9c2 cells, following stimulation with either formoterol or isoprenaline. H9c2 cells were treated with above mentioned treatments in presence of formoterol (FORM; 1 μ M) or isoprenaline (ISO; 10 μ M) and cell lysates subjected to determine TG2 amine incorporating, peptide crosslinking and *in-situ* activities according to the protocols described in chapter II section 2.3.

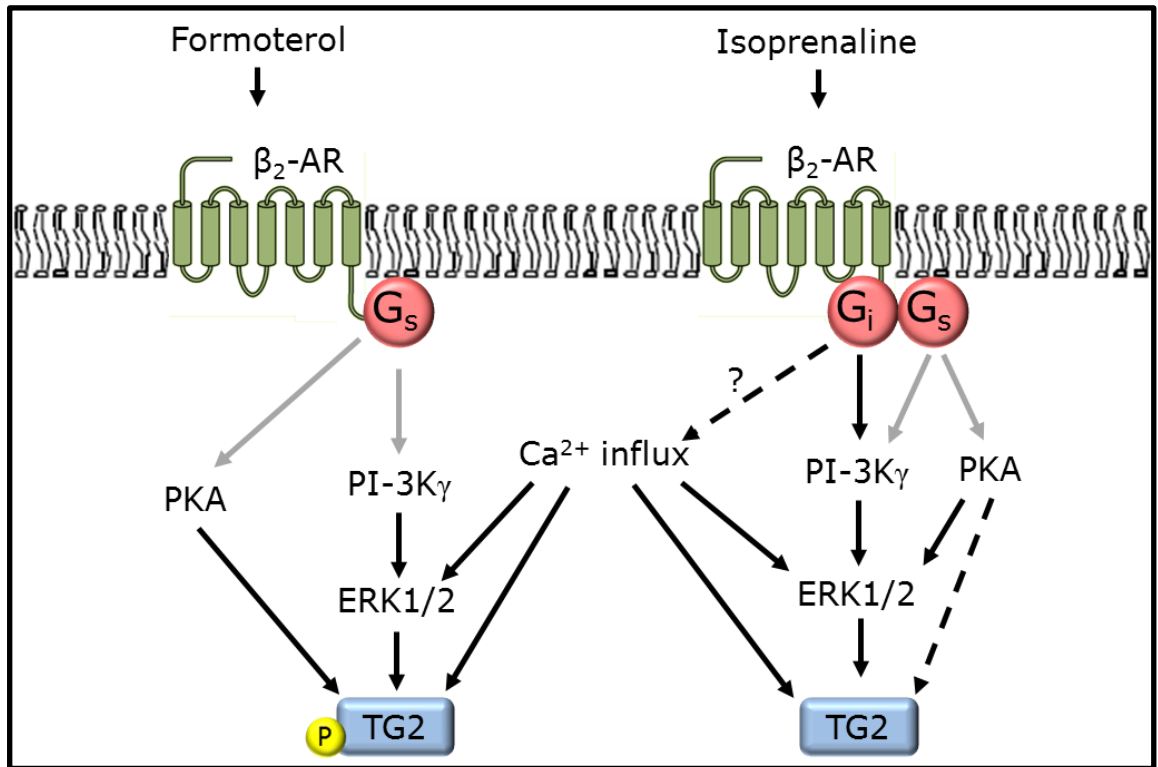


Fig 5.28: Summary of the findings presented in this study. Stimulation of the β_2 -adrenoceptor (β_2 -AR) by selective and non-selective agonists (formoterol and isoprenaline, respectively) triggers activation of protein kinases (PKA, PI-3K γ and ERK1/2) along with influx of extracellular Ca²⁺ leading to increases in TG2 activity and TG2 phosphorylation. Solid black arrows represent findings of this study, dashed arrows represent findings of this study which need further work or were inconclusive and grey arrows represent published findings (not from the present study).

Chapter VI: Cardioprotective role of A₁ adenosine receptor and β₂ adrenoceptor-induced TG2 activation

This chapter aims to assess the cardioprotective potential of the A₁ adenosine receptor and β₂ adrenoceptor-induced TG2 activity during simulated hypoxia and hypoxia/re-oxygenation injury. Cell viability assays and activation of caspase-3 were used to investigate if activation of TG2 via the aforementioned receptors is cytoprotective.

6.1 Determination of time period for hypoxia and hypoxia/re-oxygenation-induced cell death.

Initially the effect of hypoxia on cell viability in H9c2 cardiomyoblasts was investigated. H9c2 cells were exposed to hypoxia for varying intervals of time and assessed for cell viability using reduction in MTT, release of LDH and activation of caspase-3. As shown in figure 6.1, ~60% cell death was successfully achieved at 8 h of incubation with hypoxia (reduction in MTT was 37 ± 3% of control; n=4; figure 6.1A; release of LDH was 543 ± 34% of control; n=4; figure 6.1B; increase in caspase-3 activity was 342 ± 62% of control; n=4; figure 6.1D) and hence was chosen for further experiments.

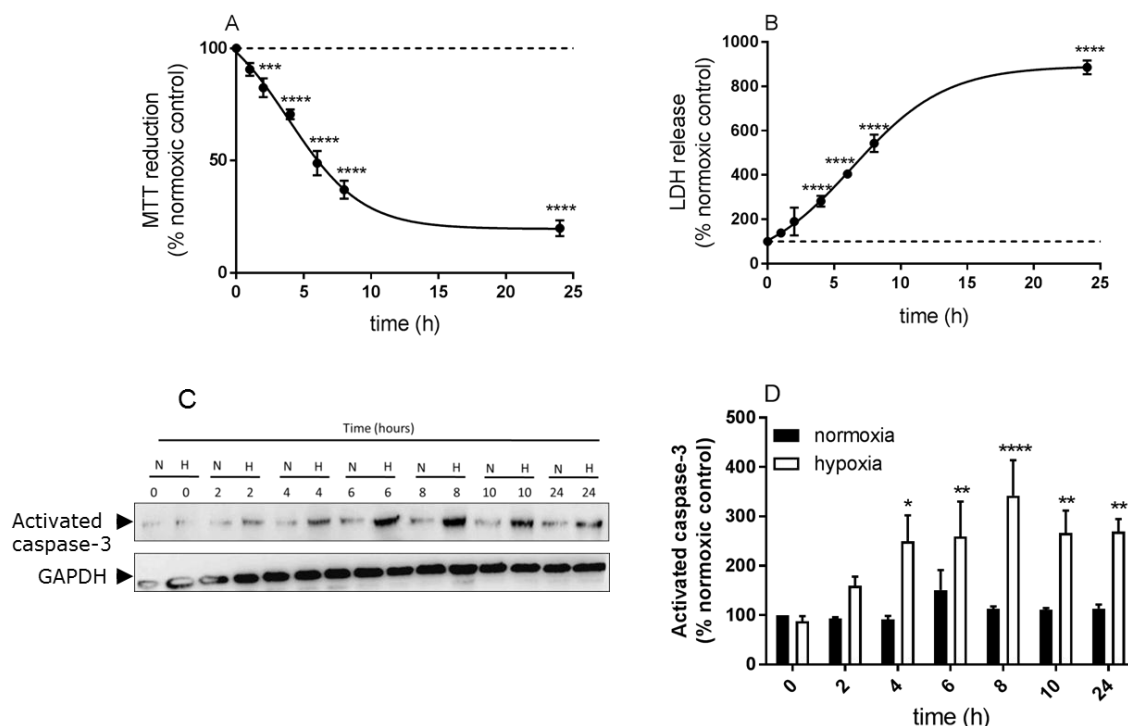


Fig 6.1: Effect of hypoxia on cell viability in H9c2 cells. Cells were exposed to hypoxia for varying intervals of time (1, 2, 4, 6, 8 and 24 h for MTT and LDH assays; 1, 2, 4, 6, 8, 10 and 24 h for caspase-3 activation). Cell viability was assessed by measuring the metabolic reduction of MTT by cellular dehydrogenases (A) and release of LDH into the culture medium (B). Caspase-3 activation was assessed via Western blotting using anti-activated caspase-3 antibody (C) and quantified caspase-3 data (D) are expressed as a percentage of normoxia control cell values (=100%). Data are expressed as a percentage of normoxia control cell values (=100%) and represent the mean ± S.E.M. from four independent experiments. * $P < 0.05$, ** $P < 0.01$, *** $P < 0.001$ and **** $P < 0.0001$ versus control.

Subsequently the effect of hypoxia/re-oxygenation-induced cell death in H9c2 cardiomyoblasts was investigated. H9c2 cells were exposed to 8 h of hypoxia followed by varying intervals of time of re-oxygenation and assessed for cell viability using reduction in MTT, release of LDH and activation of caspase-3. As shown in figure 6.2, further reduction in cell viability was successfully achieved at 18 h of re-oxygenation (reduction in MTT was $22 \pm 2\%$ of control; $n=4$; figure 6.2A; release of LDH was $637 \pm 22\%$ of control; $n=4$; figure 6.2B; increase in caspase-3 activity was $418 \pm 26\%$ of control; $n=4$; figure 6.2D) and was chosen for further experiments so that all experiments could be completed in a working day.

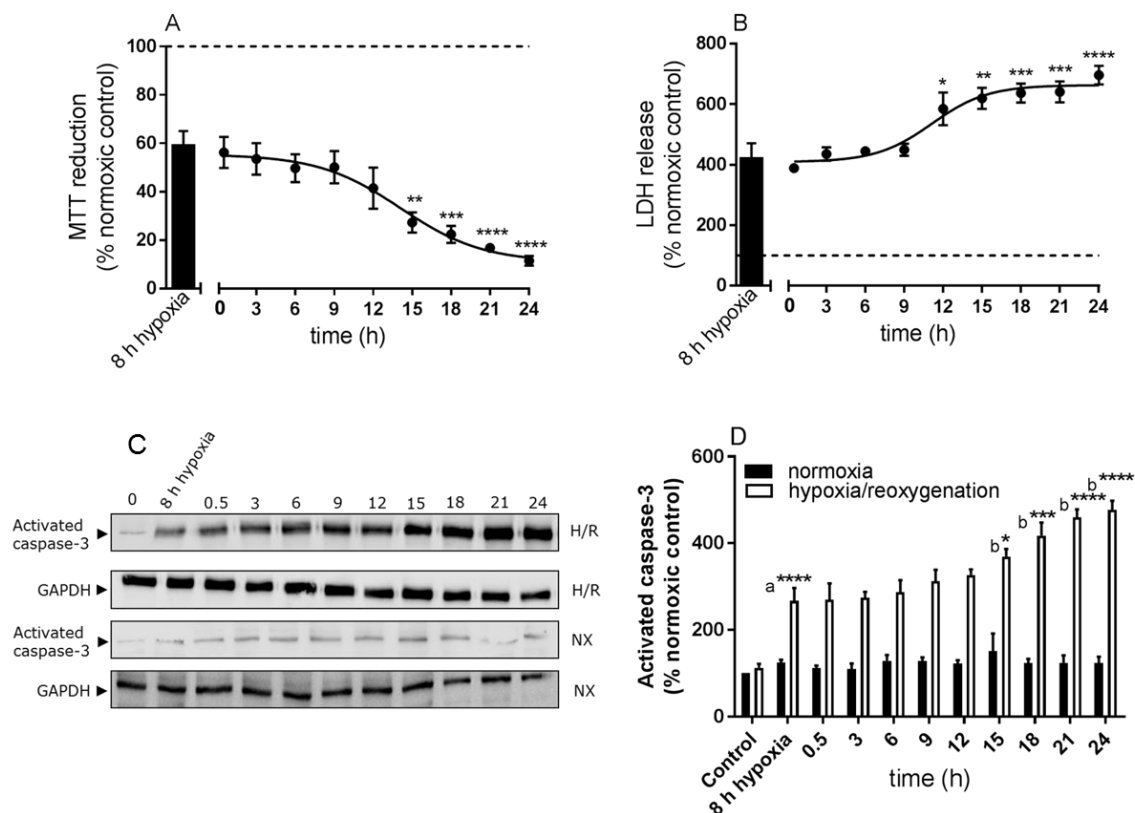


Fig 6.2: Effect of hypoxia/re-oxygenation on cell viability in H9c2 cells. Cells were exposed to 8 h of hypoxia followed by re-oxygenation for varying intervals of time (0.5, 3, 6, 9, 12, 15, 18, 21 and 24 h; H/R). Cell viability was assessed by measuring the metabolic reduction of MTT by cellular dehydrogenases (A) and release of LDH into the culture medium (B). Caspase-3 activation was assessed via Western blotting using anti-activated caspase-3 antibody (C) and quantified caspase-3 data (D) are expressed as a percentage of normoxia control (NX) cell values (=100%). Data are expressed as a percentage of normoxia control cell values (=100%) and represent the mean \pm S.E.M. from four independent experiments. * $P<0.05$, ** $P<0.01$, *** $P<0.001$ and **** $P<0.0001$, (a) versus normoxia control, (b) versus hypoxic control.

6.2 Role of TG2 in A₁R-induced cell survival against hypoxia-induced cell death.

The A₁R agonists CPA and adenosine were both cytoprotective against hypoxic injury. Briefly, H9c2 cells were treated with CPA (100 nM) or adenosine (100 μM) for 10 min prior to exposure to 8 h of hypoxia. Following hypoxic incubation, cell viability was assessed. Both CPA and adenosine were successful in increasing reduction in MTT, reducing both release of LDH and activation of caspase-3, thus offering protection (figure 6.3, 6.4, 6.5 and 6.6). This protection was abolished when H9c2 cells were pre-treated for 30 min with the selective A₁R antagonist DPCPX (1 μM) prior to stimulation (figure 6.3). Furthermore, pre-treatment with the G_{i/o}-protein inactivating pertussis toxin (100 ng/ml for 16 h) abolished CPA- and adenosine-induced cell survival (figure 6.4), confirming the involvement of G_{i/o}-proteins.

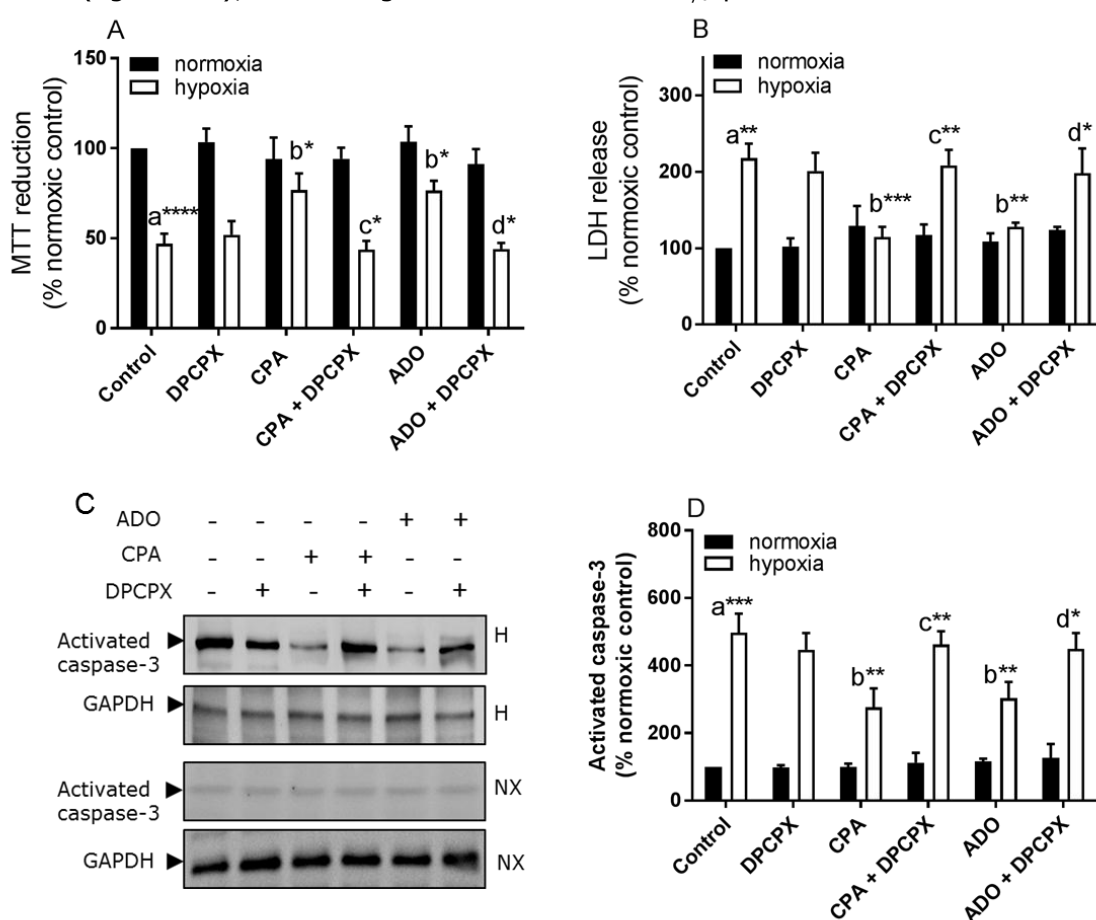


Fig 6.3: The effect of A₁R activation on hypoxia-induced cell death. Where indicated, H9c2 cells were pre-treated for 30 min with DPCPX (1 μM) before the addition of CPA (100 nM) or adenosine (ADO; 100 μM) for 10 min prior to 8 h hypoxia (H; 1% O₂) or normoxia (NX). Cell viability was assessed by measuring the metabolic reduction of MTT by cellular dehydrogenases (A) and release of LDH into the culture medium (B). Caspase-3 activation was assessed via Western blotting using anti-activated caspase-3 antibody (C) and quantified caspase-3 data (D) are expressed as a percentage of normoxia control cell values (=100%). Data are expressed as a percentage of normoxia control cell values (=100%) and represent the mean ± S.E.M. from four independent experiments. **P*<0.05, ***P*<0.01, ****P*<0.001 and *****P*<0.0001, (a) versus normoxia control, (b) versus hypoxic control, (c) versus 100 nM CPA in the presence of hypoxia, (d) versus 100 μM ADO in the presence of hypoxia.

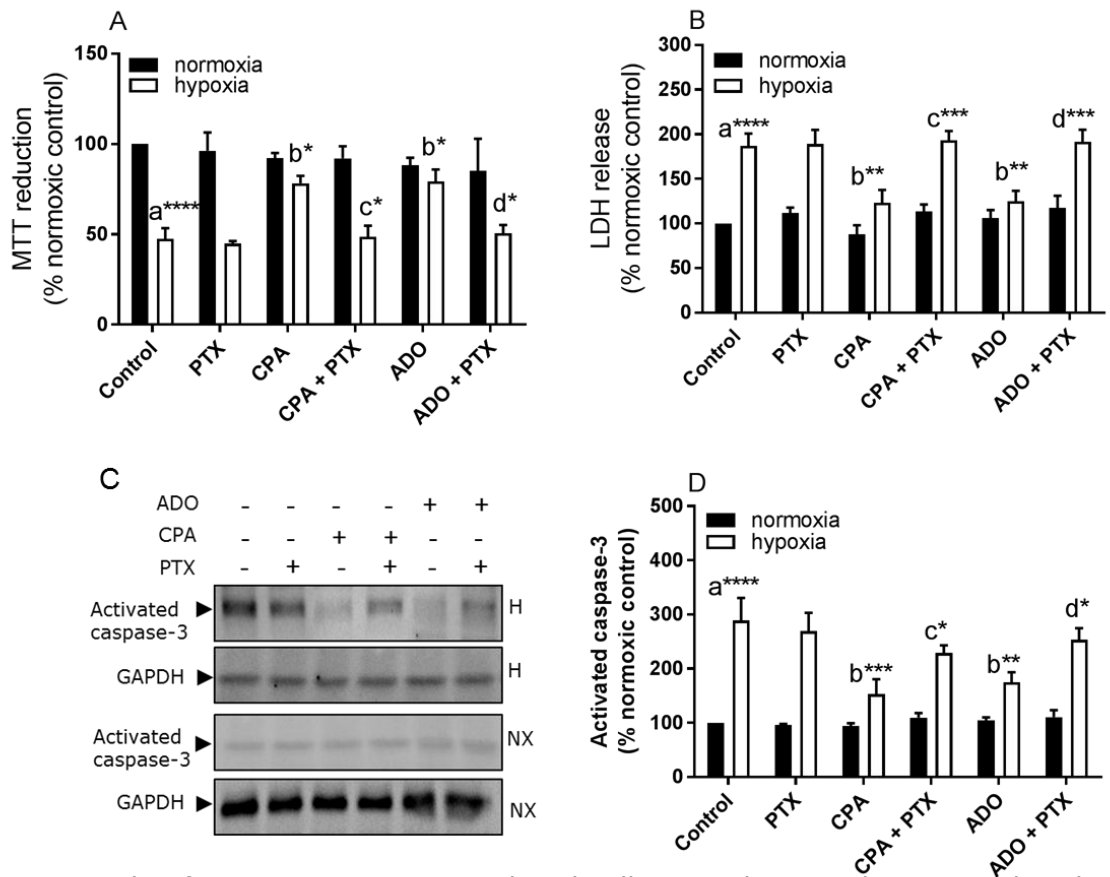


Fig 6.4: Role of $G_{i/o}$ -proteins in A_1R -induced cell survival versus hypoxia-induced cell death. Where indicated, H9c2 cells were pre-treated for 16 h with pertussis toxin (100 ng/ml) before the addition of CPA (100 nM) or adenosine (ADO; 100 μ M) for 10 min prior to 8 h hypoxia (H; 1% O_2) or normoxia (NX). Cell viability was assessed by measuring the metabolic reduction of MTT by cellular dehydrogenases (A) and release of LDH into the culture medium (B). Caspase-3 activation was assessed via Western blotting using anti-activated caspase-3 antibody (C) and quantified caspase-3 data (D) are expressed as a percentage of normoxia control cell values (=100%). Data are expressed as a percentage of normoxia control cell values (=100%) and represent the mean \pm S.E.M. from four independent experiments. * P <0.05, ** P <0.01, *** P <0.001 and **** P <0.0001, (a) versus normoxia control, (b) versus hypoxic control, (c) versus 100 nM CPA in the presence of hypoxia, (d) versus 100 μ M ADO in the presence of hypoxia.

To confirm that TG2 is responsible for the A_1R -induced cell survival in H9c2 cells, two structurally different cell permeable TG2 specific inhibitors were tested; R283 (a small molecule; Freund et al, 1994) and Z-DON (peptide-based; Schaertl et al, 2010). H9c2 cells were pre-treated for 1 h with Z-DON (150 μ M) or R283 (200 μ M) prior to stimulation with CPA (100 nM) and/or adenosine (100 μ M) for 10 min. Both inhibitors blocked CPA- and adenosine-induced cell survival (figure 6.5 and 6.6), confirming the involvement of TG2.

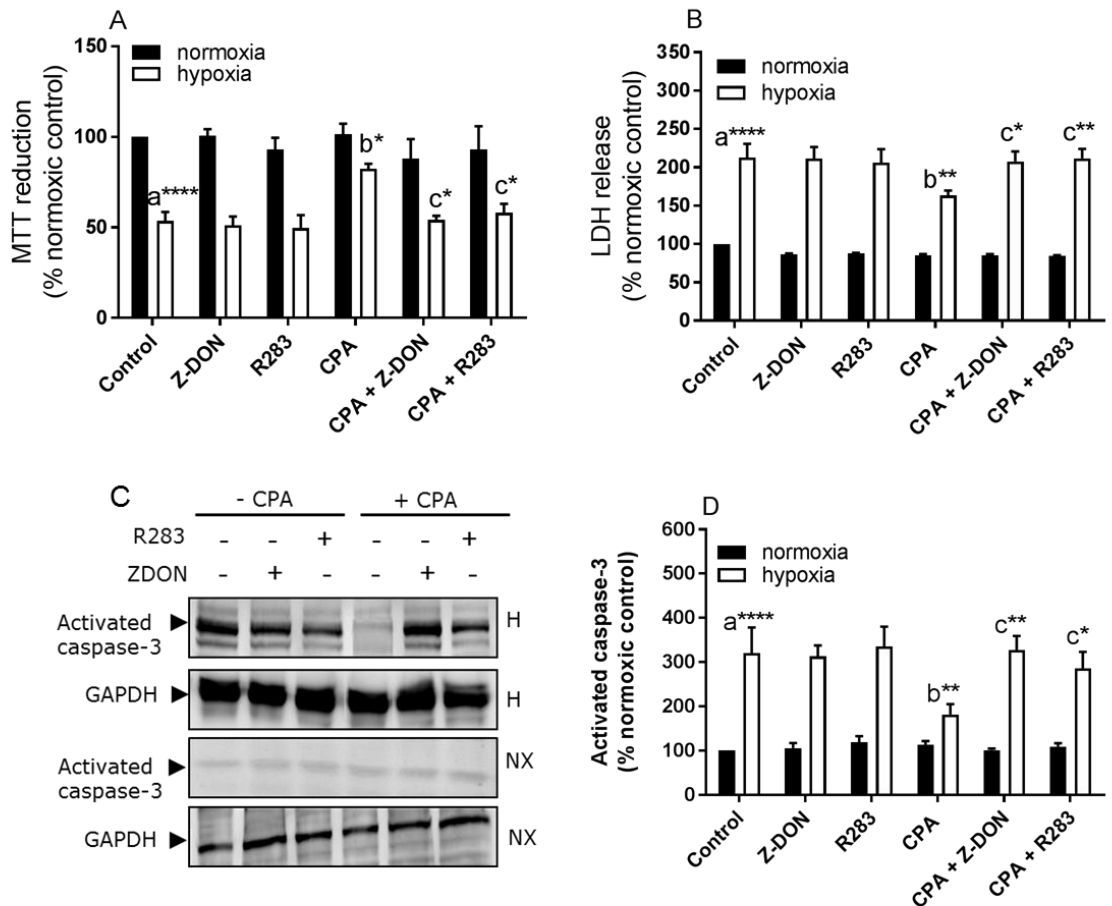


Fig 6.5: Role of TG2 in CPA-induced cell survival versus hypoxia-induced cell death. Where indicated, H9c2 cells were pre-treated for 1 h with Z-DON (150 μ M) or R283 (200 μ M) before the addition of CPA (100 nM) for 10 min prior to 8 h hypoxia (H; 1% O₂) or normoxia (NX). Cell viability was assessed by measuring the metabolic reduction of MTT by cellular dehydrogenases (A) and release of LDH into the culture medium (B). Caspase-3 activation was assessed via Western blotting using anti-activated caspase-3 antibody (C) and quantified caspase-3 data (D) are expressed as a percentage of normoxia control cell values (=100%). Data are expressed as a percentage of normoxia control cell values (=100%) and represent the mean \pm S.E.M. from four independent experiments. * P <0.05, ** P <0.01, *** P <0.001 and **** P <0.0001, (a) versus normoxia control, (b) versus hypoxic control, (c) versus 100 nM CPA in the presence of hypoxia.

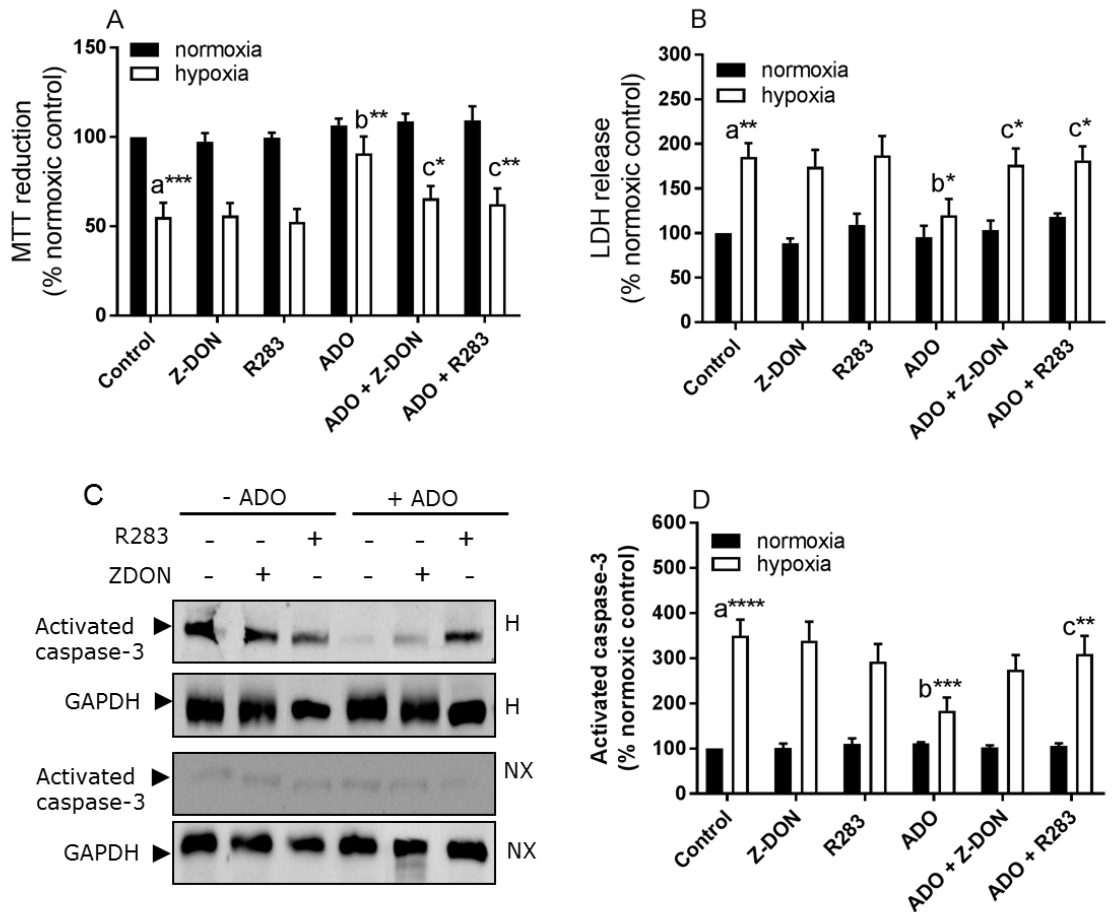


Fig 6.6: Role of TG2 in adenosine-induced cell survival versus hypoxia-induced cell death. Where indicated, H9c2 cells were pre-treated for 1 h with Z-DON (150 μ M) or R283 (200 μ M) before the addition of adenosine (ADO; 100 μ M) for 10 min prior to 8 h hypoxia (H; 1% O₂) or normoxia (NX). Cell viability was assessed by measuring the metabolic reduction of MTT by cellular dehydrogenases (A) and release of LDH into the culture medium (B). Caspase-3 activation was assessed via Western blotting using anti-activated caspase-3 antibody (C) and quantified caspase-3 data (D) are expressed as a percentage of normoxia control cell values (=100%). Data are expressed as a percentage of normoxia control cell values (=100%) and represent the mean \pm S.E.M. from four independent experiments. * P <0.05, ** P <0.01, *** P <0.001 and **** P <0.0001, (a) versus normoxia control, (b) versus hypoxic control, (c) versus 100 μ M ADO in the presence of hypoxia.

6.3 Role of TG2 in β_2 -AR-induced cell survival against hypoxia-induced cell death.

To determine the role of TG2 in β_2 -AR-induced cell survival, H9c2 cells were treated with formoterol (1 μ M) or isoprenaline (10 μ M) for 20 min prior to exposure to 8 h of hypoxia. Following hypoxic incubation, cell viability was assessed. Pre-treatment with formoterol had no significant effect on hypoxia-induced decrease in MTT reduction or release of LDH (figure 6.7). In contrast, isoprenaline significantly attenuated hypoxia-induced reduction in MTT, release of LDH and activation of caspase-3, thus offering protection (figure 6.8, 6.9 and 6.10). This protection was abolished when H9c2 cells were pre-treated for 30 min with the β_2 -AR selective and non-selective β -AR antagonists ICI 118551 (1 μ M) and propranolol (1 μ M), respectively prior to stimulation (figure 6.8). Furthermore, pre-treatment with the $G_{i/o}$ -protein inactivating pertussis toxin (100 ng/ml for 16 h) abolished isoprenaline-induced cell survival (figure 6.9), suggesting a prominent role for $G_{i/o}$ -proteins. However, formoterol had no significant effect even when cells were pre-treated with pertussis toxin. These observations indicate that the β_2 -AR-induced cell survival is dependent upon $G_{i/o}$ -protein and the differences in signalling mapped out in chapter V between isoprenaline and formoterol could be a potential cause of formoterol not offering protection. Therefore, all further experiments will be performed with isoprenaline.

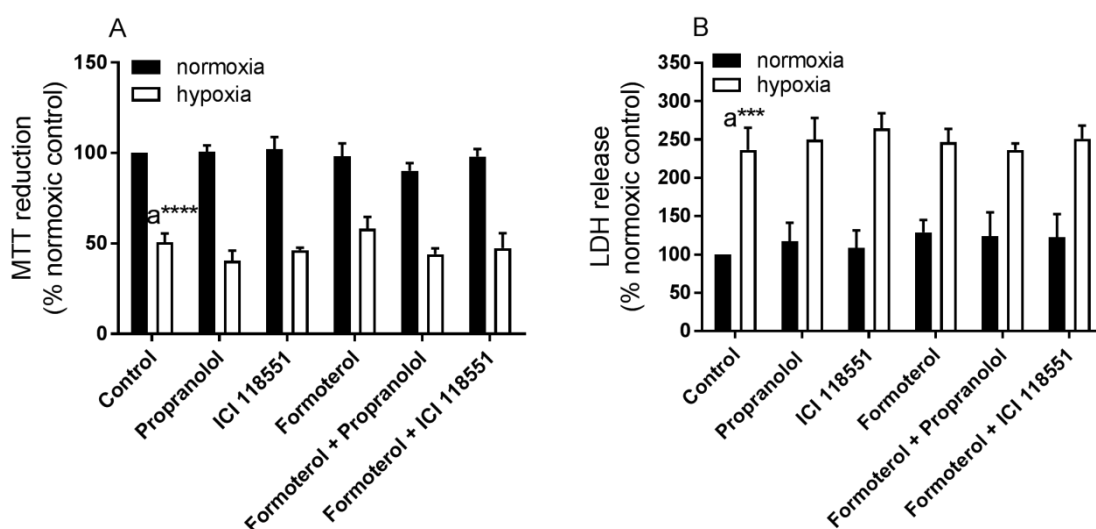


Fig 6.7: The effect of formoterol on hypoxia-induced cell death. Where indicated, H9c2 cells were pre-treated for 30 min with ICI 118551 (1 μ M) or propranolol (1 μ M) before the addition of formoterol (1 μ M) for 20 min prior to 8 h hypoxia (1% O_2) or normoxia (NX). Cell viability was assessed by measuring the metabolic reduction of MTT by cellular dehydrogenases (A) and release of LDH into the culture medium (B). Data are expressed as a percentage of normoxia control cell values (=100%) and represent the mean \pm S.E.M. from four independent experiments. *** P <0.001 and **** P <0.0001, (a) versus normoxia control.

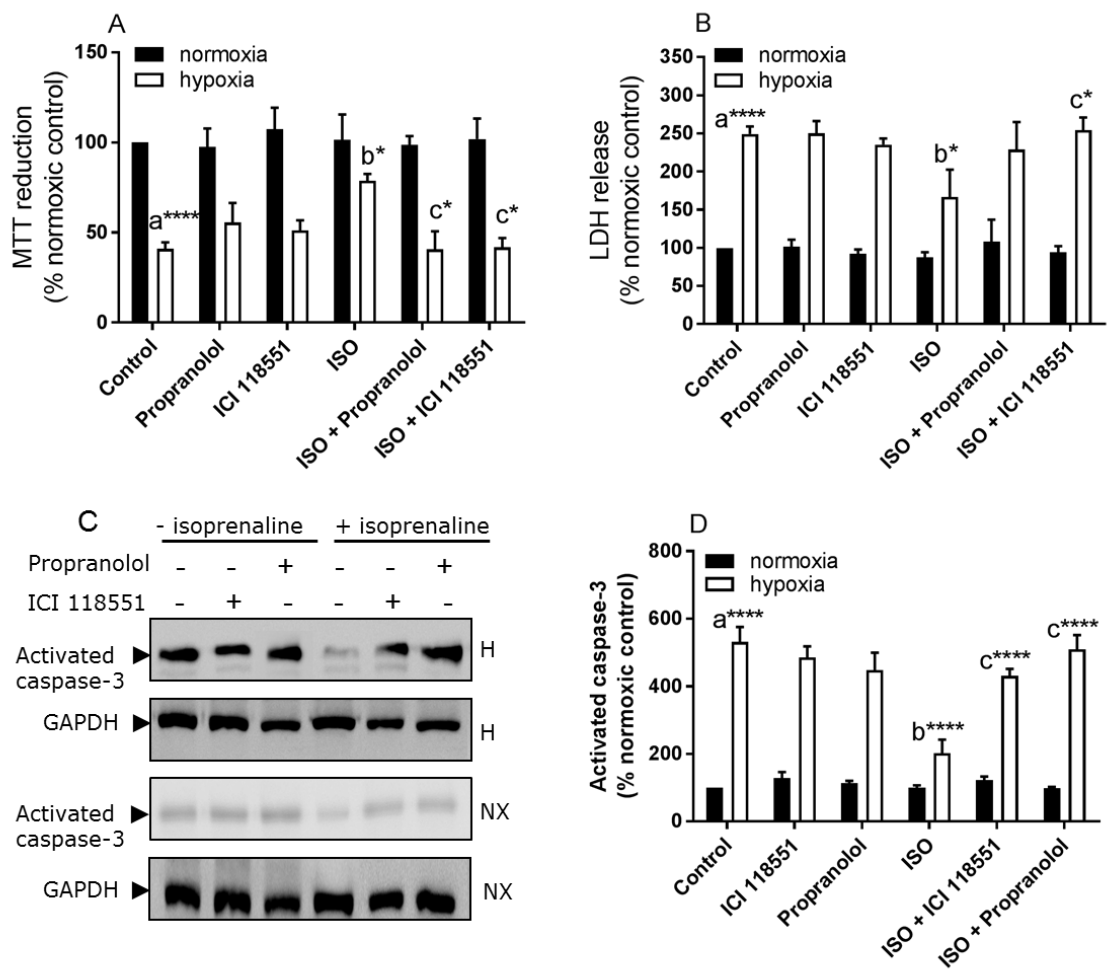


Fig 6.8: The effect of isoprenaline on hypoxia-induced cell death. Where indicated, H9c2 cells were pre-treated for 30 min with ICI 118551 (1 μ M) or propranolol (1 μ M) before the addition of isoprenaline (10 μ M) for 20 min prior to 8 h hypoxia (H; 1% O₂) or normoxia (NX). Cell viability was assessed by measuring the metabolic reduction of MTT by cellular dehydrogenases (A) and release of LDH into the culture medium (B). Caspase-3 activation was assessed via Western blotting using anti-activated caspase-3 antibody (C) and quantified caspase-3 data (D) are expressed as a percentage of normoxia control cell values (=100%). Data are expressed as a percentage of normoxia control cell values (=100%) and represent the mean \pm S.E.M. from four independent experiments. * P <0.05 and **** P <0.0001, (a) versus normoxia control, (b) versus hypoxic control, (c) versus 10 μ M isoprenaline in the presence of hypoxia.

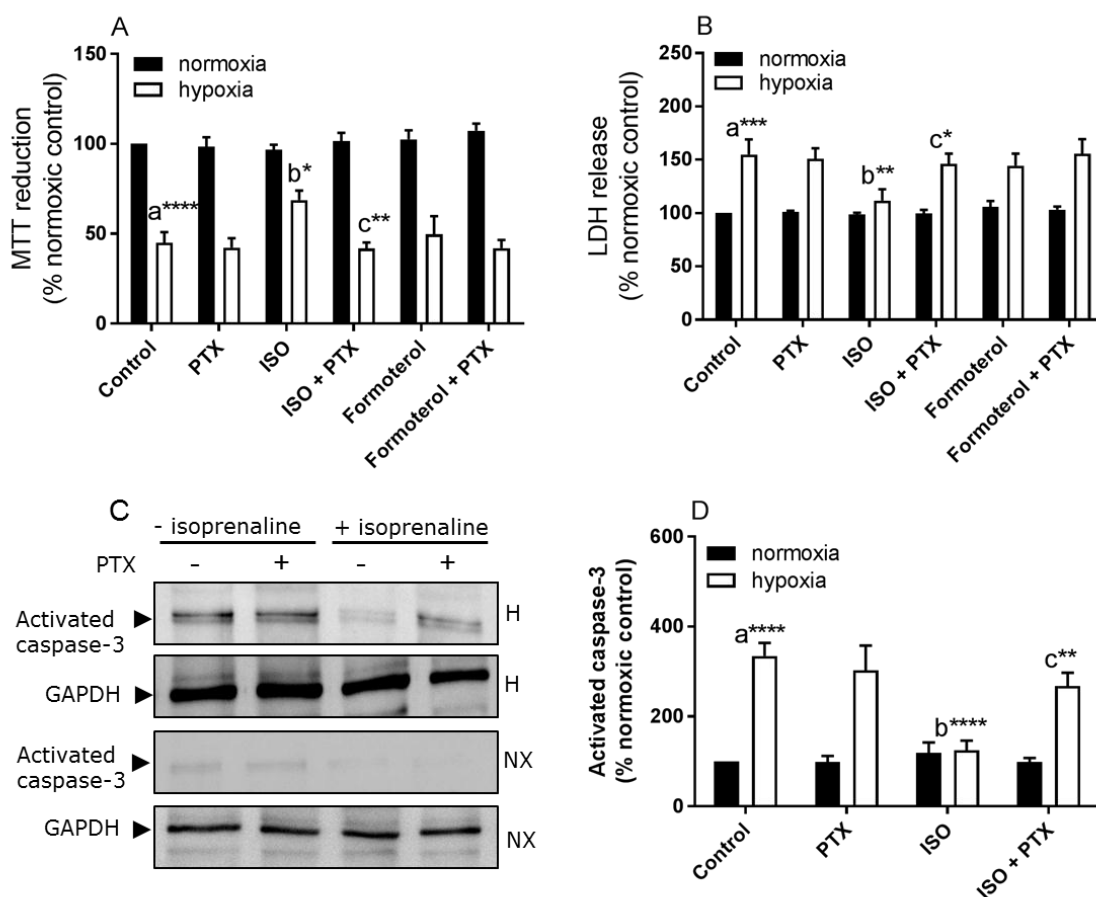


Fig 6.9: Role of $G_{i/o}$ -proteins in β_2 -AR-induced cell survival versus hypoxia-induced cell death. Where indicated, H9c2 cells were pre-treated for 16 h with pertussis toxin (100 ng/ml) before the addition of isoprenaline (10 μ M) for 20 min prior to 8 h hypoxia (H; 1% O_2) or normoxia (NX). Cell viability was assessed by measuring the metabolic reduction of MTT by cellular dehydrogenases (A) and release of LDH into the culture medium (B). Caspase-3 activation was assessed via Western blotting using anti-activated caspase-3 antibody (C) and quantified caspase-3 data (D) are expressed as a percentage of normoxia control cell values (=100%). Data are expressed as a percentage of normoxia control cell values (=100%) and represent the mean \pm S.E.M. from four independent experiments. * P <0.05, ** P <0.01, *** P <0.001 and **** P <0.0001, (a) versus normoxia control, (b) versus hypoxic control, (c) versus 10 μ M isoprenaline in the presence of hypoxia.

To confirm that TG2 is responsible for the β_2 -AR-induced cell survival in H9c2 cells, TG2 specific inhibitors R283 and Z-DON were implemented. H9c2 cells were pre-treated for 1 h with Z-DON (150 μ M) or R283 (200 μ M) prior to stimulation with isoprenaline (10 μ M) for 20 min. Both inhibitors blocked isoprenaline-induced cell survival (figure 6.10), confirming the involvement of TG2.

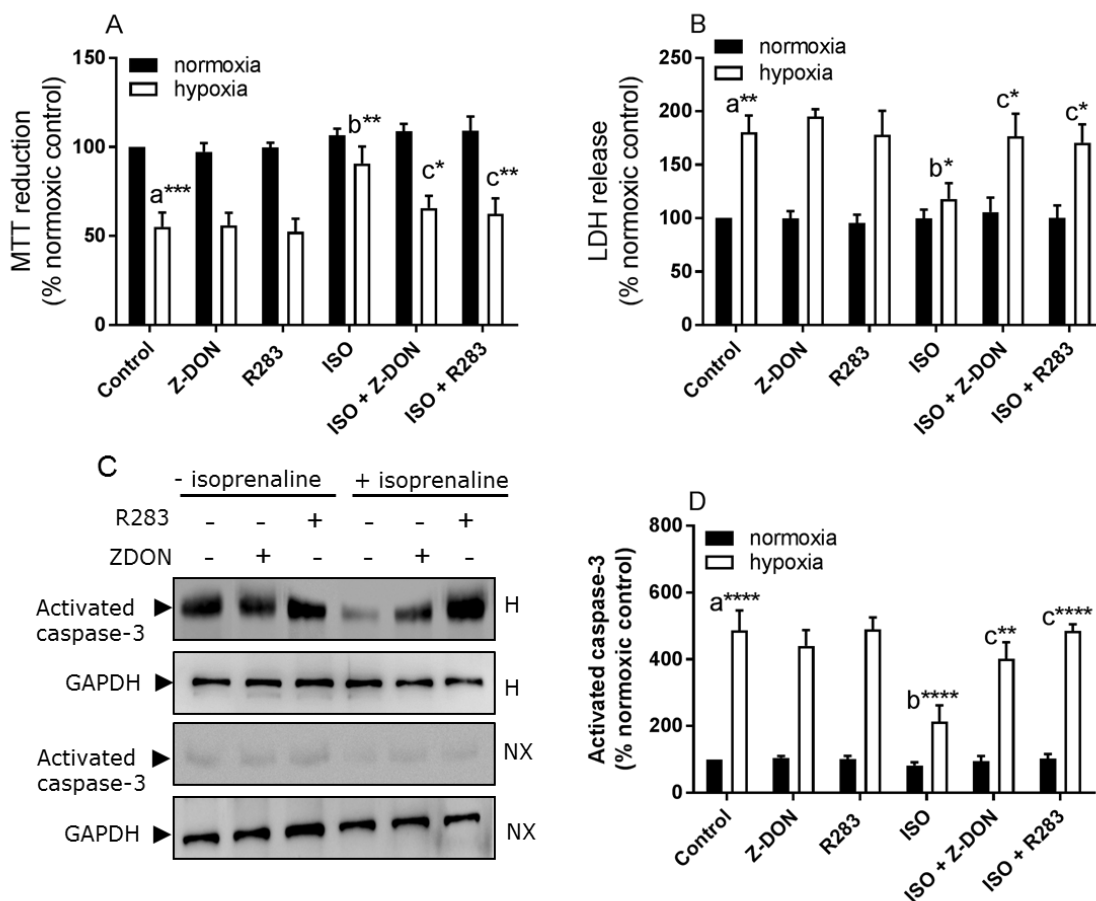


Fig 6.10: Role of TG2 in β_2 -AR-induced cell survival versus hypoxia-induced cell death. Where indicated, H9c2 cells were pre-treated for 1 h with Z-DON (150 μ M) or R283 (200 μ M) before the addition of isoprenaline (10 μ M) for 20 min prior to 8 h hypoxia (H; 1% O₂) or normoxia (NX). Cell viability was assessed by measuring the metabolic reduction of MTT by cellular dehydrogenases (A) and release of LDH into the culture medium (B). Caspase-3 activation was assessed via Western blotting using anti-activated caspase-3 antibody (C) and quantified caspase-3 data (D) are expressed as a percentage of normoxia control cell values (=100%). Data are expressed as a percentage of normoxia control cell values (=100%) and represent the mean \pm S.E.M. from four independent experiments. * P <0.05, ** P <0.01, *** P <0.001 and **** P <0.0001, (a) versus normoxia control, (b) versus hypoxic control, (c) versus 10 μ M isoprenaline in the presence of hypoxia.

6.4 Role of TG2 in A₁R-induced cell survival against hypoxia/re-oxygenation-induced cell death.

A₁R-induced pre-conditioning

For pre-conditioning, H9c2 cells were treated with the pharmacological agents prior to the onset of hypoxic incubation. Activation of the A₁R provided protection against hypoxia/re-oxygenation-induced cell death. H9c2 cells were treated with CPA (100 nM) or adenosine (100 μM) for 10 min prior to exposure to 8 h of hypoxia followed by 18 h re-oxygenation. Both CPA and adenosine significantly attenuated hypoxia/re-oxygenation-induced decreases in MTT reduction, release of LDH and activation of caspase-3, thus offering protection (figure 6.11, 6.12, 6.13 and 6.14). This protection was abolished when H9c2 cells were pre-treated for 30 min with the selective A₁R antagonist DPCPX (1 μM) prior to stimulation (figure 6.11). Moreover, pre-treatment with the G_{i/o}-protein inactivating pertussis toxin (100 ng/ml for 16 h) abolished A₁R-induced cell survival (figure 6.12), confirming the involvement of G_{i/o}-proteins. Finally, pre-treatment for 1 h with Z-DON (150 μM) or R283 (200 μM) prior to stimulation attenuated A₁R-induced cell survival (figure 6.13 and 6.14), confirming the involvement of TG2.

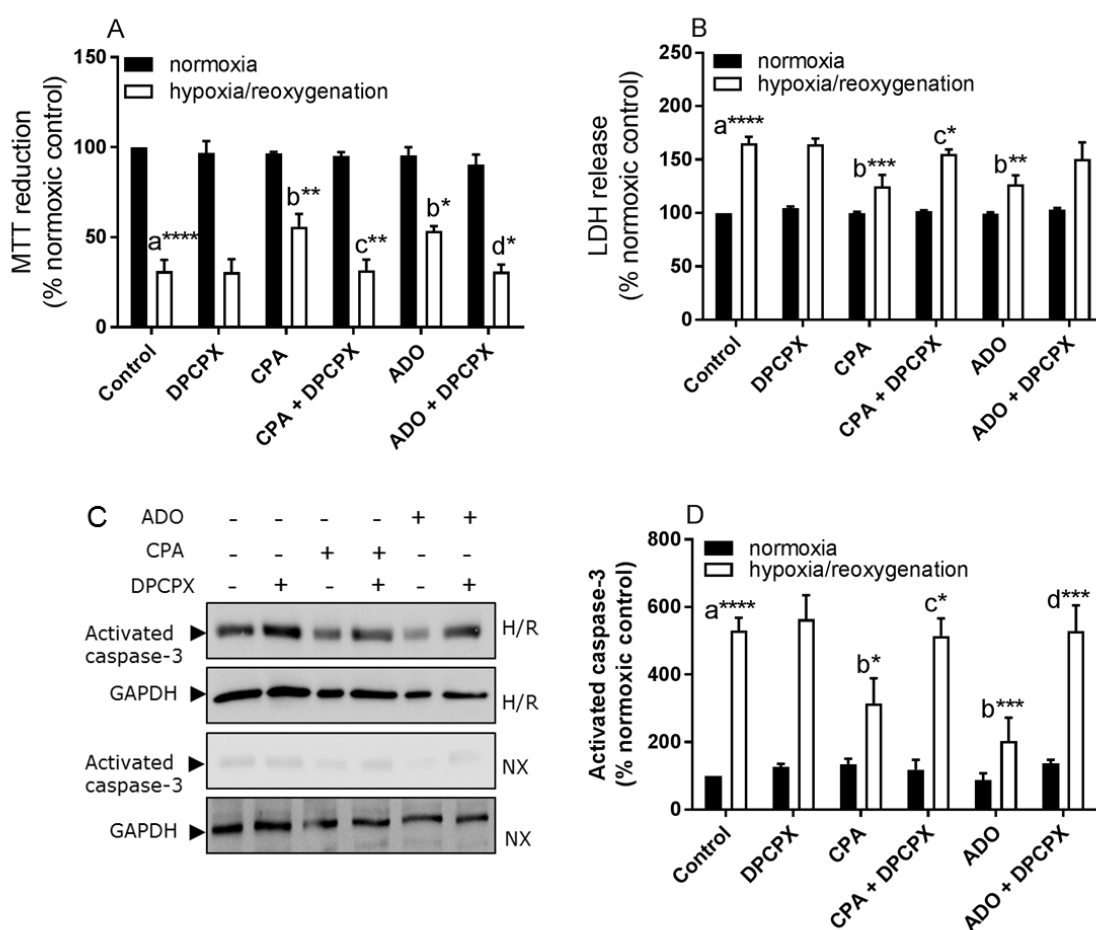


Fig 6.11: The effect of A₁R activation on hypoxia/re-oxygenation-induced cell death. Where indicated, H9c2 cells were pre-treated for 30 min with DPCPX (1 μM) before the addition of CPA (100 nM) or adenosine (ADO; 100 μM) for 10 min prior to 8 h hypoxia (1% O₂) followed by 18 h re-oxygenation (H/R) or normoxia (NX). Cell viability was

assessed by measuring the metabolic reduction of MTT by cellular dehydrogenases (A) and release of LDH into the culture medium (B). Caspase-3 activation was assessed via Western blotting using anti-activated caspase-3 antibody (C) and quantified caspase-3 data (D) are expressed as a percentage of normoxia control cell values (=100%). Data are expressed as a percentage of normoxia control cell values (=100%) and represent the mean \pm S.E.M. from four independent experiments. * P <0.05, ** P <0.01, *** P <0.001 and **** P <0.0001, (a) versus normoxia control, (b) versus H/R control, (c) versus 100 nM CPA in the presence of H/R, (d) versus 100 μ M ADO in the presence of H/R.

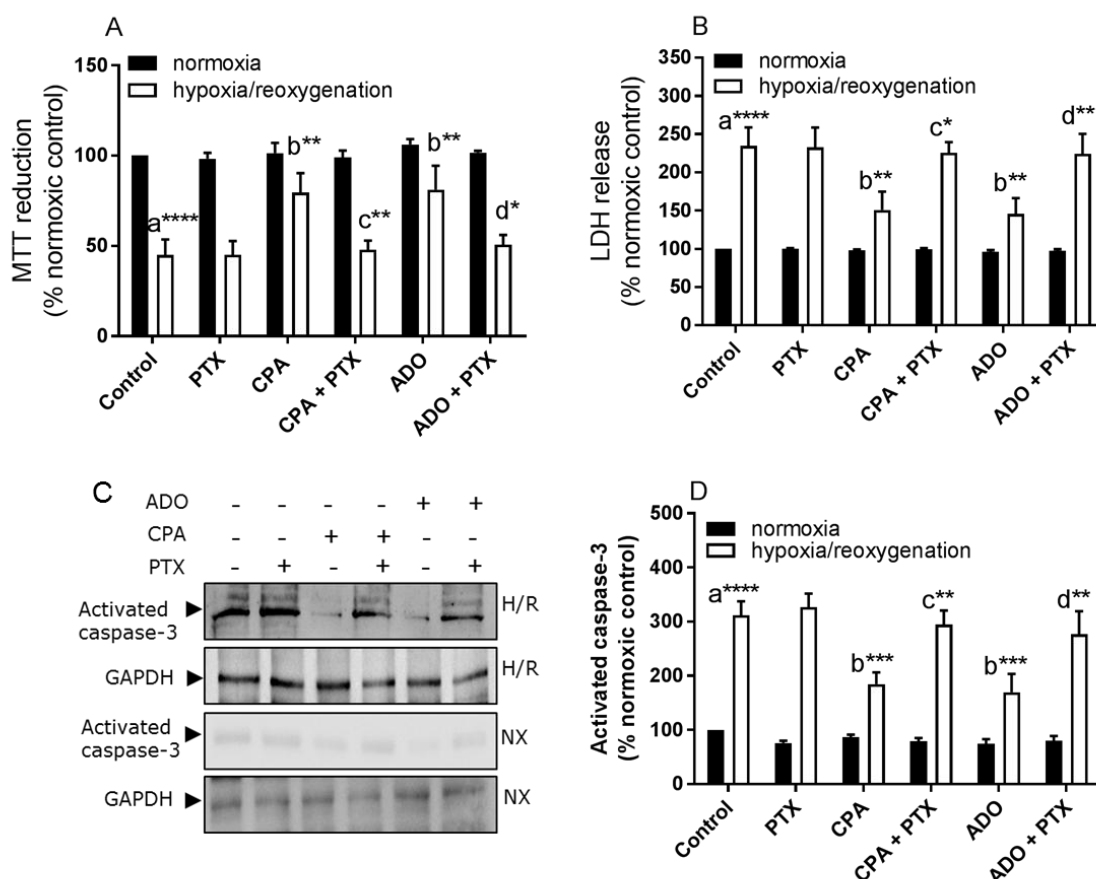


Fig 6.12: Role of $G_{i/o}$ -proteins in A_1R -induced pre-conditioning versus hypoxia/reoxygenation-induced cell death. Where indicated, H9c2 cells were pre-treated for 16 h with pertussis toxin (100 ng/ml) before the addition of CPA (100 nM) or adenosine (ADO; 100 μ M) for 10 min prior to 8 h hypoxia (1% O_2) followed by 18 h reoxygenation (H/R) or normoxia (NX). Cell viability was assessed by measuring the metabolic reduction of MTT by cellular dehydrogenases (A) and release of LDH into the culture medium (B). Caspase-3 activation was assessed via Western blotting using anti-activated caspase-3 antibody (C) and quantified caspase-3 data (D) are expressed as a percentage of normoxia control cell values (=100%). Data are expressed as a percentage of normoxia control cell values (=100%) and represent the mean \pm S.E.M. from four independent experiments. * P <0.05, ** P <0.01, *** P <0.001 and **** P <0.0001, (a) versus normoxia control, (b) versus H/R control, (c) versus 100 nM CPA in the presence of H/R, (d) versus 100 μ M ADO in the presence of H/R.

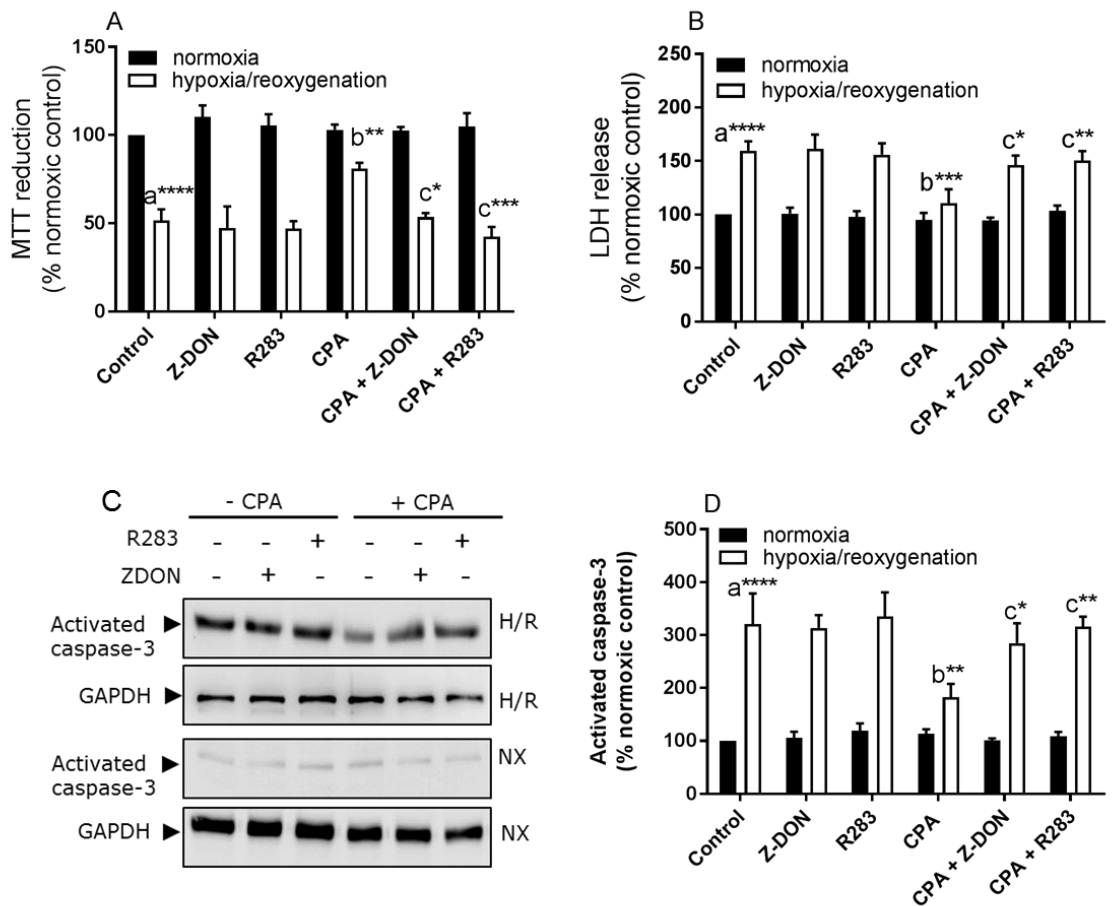


Fig 6.13: Role of TG2 in CPA-induced pre-conditioning versus hypoxia/reoxygenation-induced cell death. Where indicated, H9c2 cells were pre-treated for 1 h with Z-DON (150 μ M) or R283 (200 μ M) before the addition of CPA (100 nM) for 10 min prior to 8 h hypoxia (1% O₂) followed by 18 h re-oxygenation (H/R) or normoxia (NX). Cell viability was assessed by measuring the metabolic reduction of MTT by cellular dehydrogenases (A) and release of LDH into the culture medium (B). Caspase-3 activation was assessed via Western blotting using anti-activated caspase-3 antibody (C) and quantified caspase-3 data (D) are expressed as a percentage of normoxia control cell values (=100%). Data are expressed as a percentage of normoxia control cell values (=100%) and represent the mean \pm S.E.M. from four independent experiments. * P <0.05, ** P <0.01, *** P <0.001 and **** P <0.0001, (a) versus normoxia control, (b) versus H/R control, (c) versus 100 nM CPA in the presence of H/R.

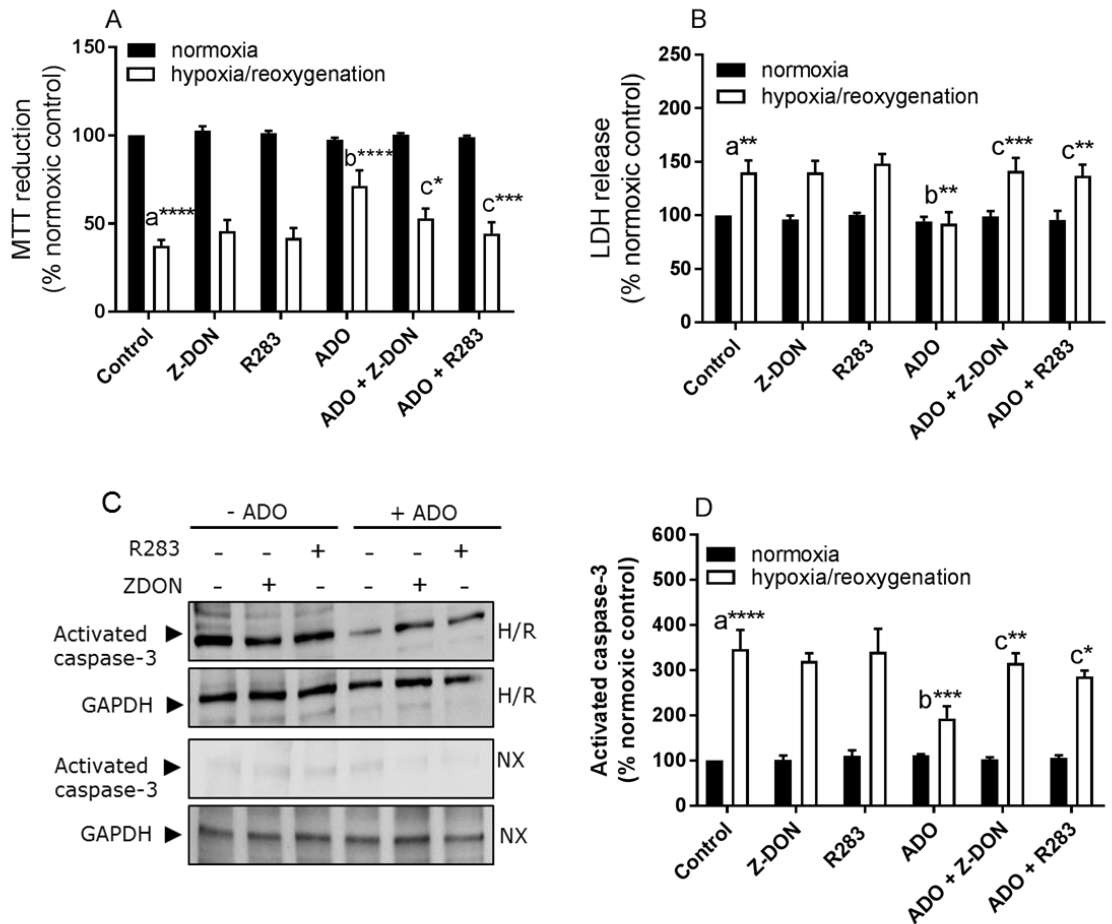


Fig 6.14: Role of TG2 in adenosine-induced pre-conditioning versus hypoxia/re-oxygenation-induced cell death. Where indicated, H9c2 cells were pre-treated for 1 h with Z-DON (150 μ M) or R283 (200 μ M) before the addition of adenosine (ADO; 100 μ M) for 10 min prior to 8 h hypoxia (1% O₂) followed by 18 h re-oxygenation (H/R) or normoxia (NX). Cell viability was assessed by measuring the metabolic reduction of MTT by cellular dehydrogenases (A) and release of LDH into the culture medium (B). Caspase-3 activation was assessed via Western blotting using anti-activated caspase-3 antibody (C) and quantified caspase-3 data (D) are expressed as a percentage of normoxia control cell values (=100%). Data are expressed as a percentage of normoxia control cell values (=100%) and represent the mean \pm S.E.M. from four independent experiments. * P <0.05, ** P <0.01, *** P <0.001 and **** P <0.0001, (a) versus normoxia control, (b) versus H/R control, (c) versus 100 μ M ADO in the presence of H/R.

A₁R-induced post-conditioning

For post-conditioning, H9c2 cells were treated with the pharmacological agents (or relevant media for appropriate control experiments) following 8 h hypoxic incubation but prior to 18 h of re-oxygenation. H9c2 cells were treated with CPA (100 nM) or adenosine (100 μ M) for 10 min following exposure to 8 h of hypoxia but prior to 18 h re-oxygenation. Both CPA and adenosine significantly attenuated hypoxia/re-oxygenation-induced decreases in MTT reduction, release of LDH and activation of caspase-3, consequently offering protection (figure 6.15, 6.16, 6.17 and 6.18). Pre-treatment for 30 min with the selective A₁R antagonist DPCPX (1 μ M) prior to stimulation abolished A₁R-induced cell survival (figure 6.15). Additionally, pre-treatment with the G_{i/o}-protein-inactivating pertussis toxin (100 ng/ml for 16 h)

abolished A₁R-induced-induced cell survival (figure 6.16), confirming the involvement of G_{i/o}-proteins. Finally, pre-treatment for 1 h with Z-DON (150 μM) or R283 (200 μM) prior to stimulation attenuated A₁R-induced cell survival (figure 6.17 and 6.18), confirming the involvement of TG2.

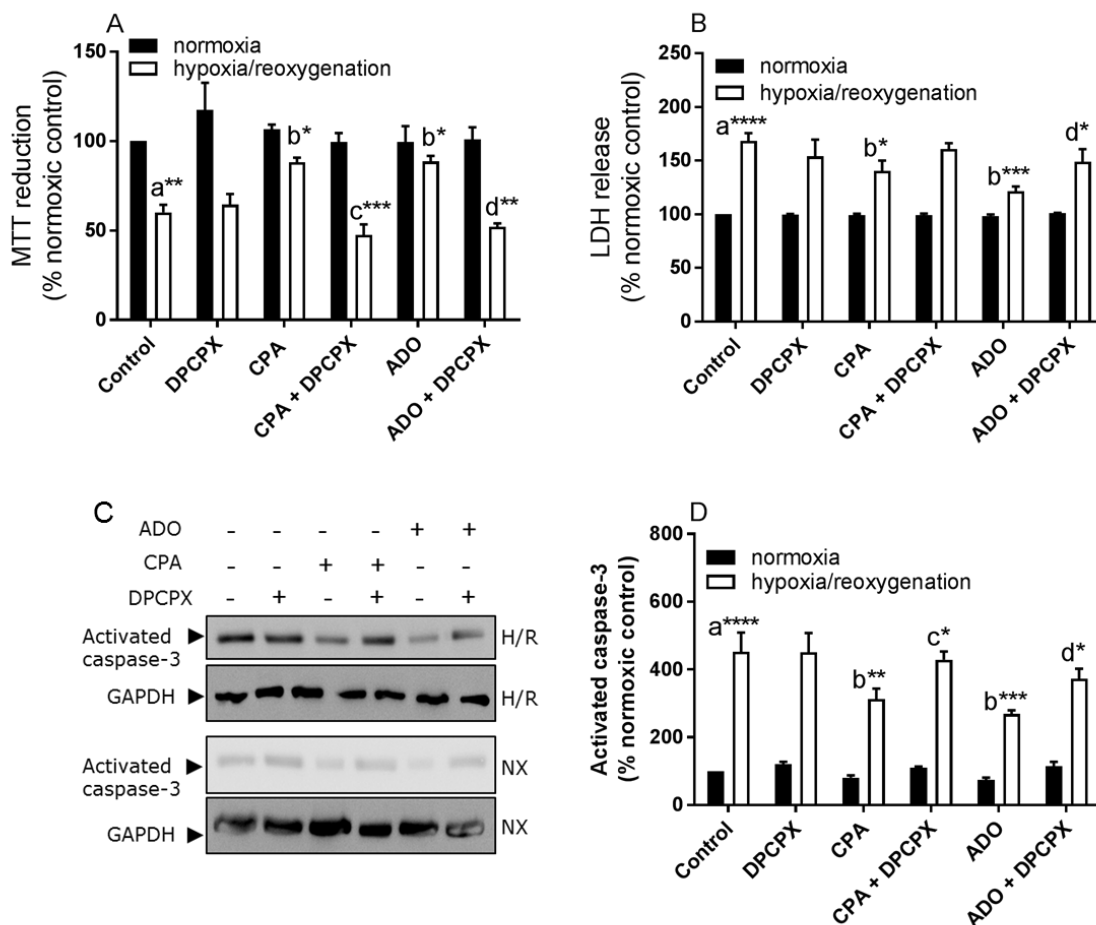


Fig 6.15: The effect of A₁R activation on hypoxia/re-oxygenation-induced cell death. Where indicated, H9c2 cells were exposed to 8 h hypoxia (1% O₂) followed by 18 h of re-oxygenation (H/R) or normoxia (NX). Cells were treated for the first 30 min of re-oxygenation with DPCPX (1 μM) before the addition of CPA (100 nM) or adenosine (ADO; 100 μM) for 10 min, which were then removed for the remainder of the re-oxygenation period. Cell viability was assessed by measuring the metabolic reduction of MTT by cellular dehydrogenases (A) and release of LDH into the culture medium (B). Caspase-3 activation was assessed via Western blotting using anti-activated caspase-3 antibody (C) and quantified caspase-3 data (D) are expressed as a percentage of normoxia control cell values (=100%). Data are expressed as a percentage of normoxia control cell values (=100%) and represent the mean ± S.E.M. from four independent experiments. **P*<0.05, ***P*<0.01, ****P*<0.001 and *****P*<0.0001, (a) versus normoxia control, (b) versus H/R control, (c) versus 100 nM CPA in the presence of H/R, (d) versus 100 μM ADO in the presence of H/R.

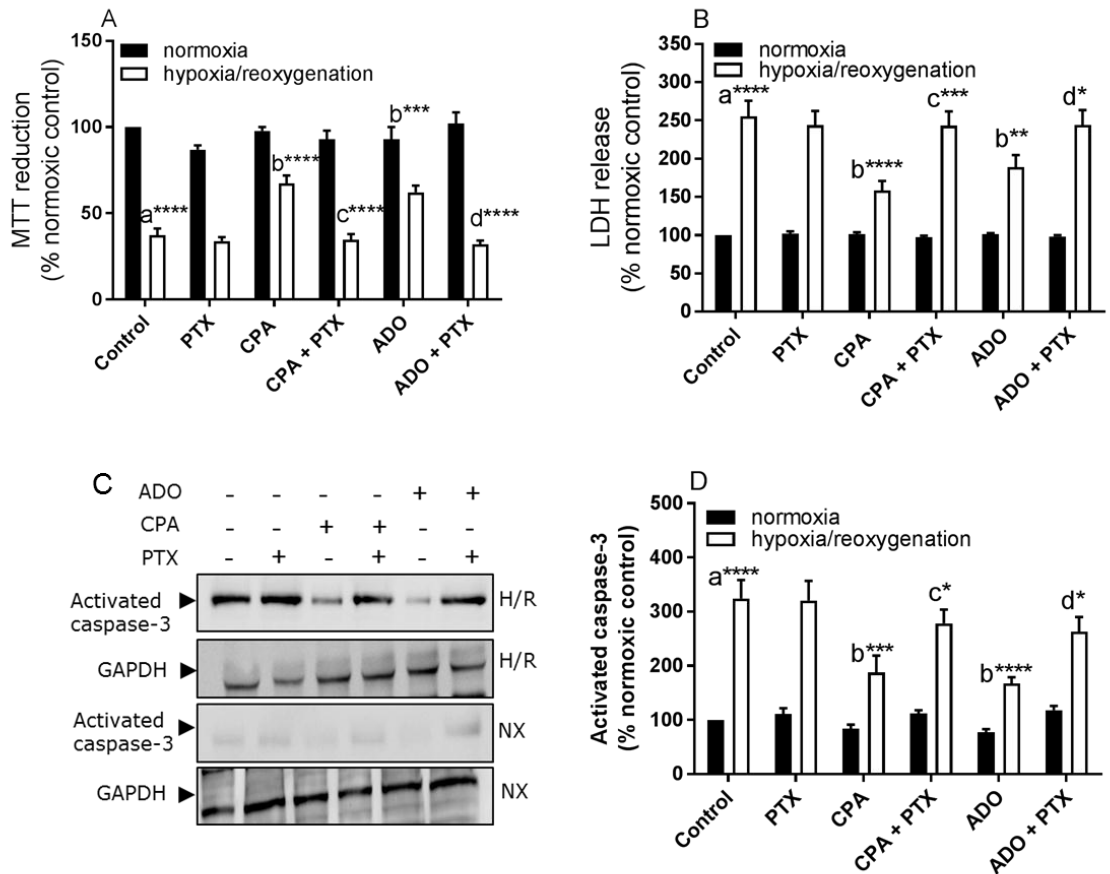


Fig 6.16: Role of $G_{i/o}$ -proteins in A_1R -induced post-conditioning versus hypoxia/re-oxygenation-induced cell death. Where indicated, H9c2 cells were exposed to 8 h hypoxia (1% O_2) followed by 18 h of re-oxygenation (H/R) or normoxia (NX). Cells were treated for the first 16 h of re-oxygenation with pertussis toxin (100 ng/ml) before the addition of CPA (100 nM) or adenosine (ADO; 100 μ M) for 10 min which were then removed for the remainder of re-oxygenation. Cell viability was assessed by measuring the metabolic reduction of MTT by cellular dehydrogenases (A) and release of LDH into the culture medium (B). Caspase-3 activation was assessed via Western blotting using anti-activated caspase-3 antibody (C) and quantified caspase-3 data (D) are expressed as a percentage of normoxia control cell values (=100%). Data are expressed as a percentage of normoxia control cell values (=100%) and represent the mean \pm S.E.M. from four independent experiments. * P <0.05, ** P <0.01, *** P <0.001 and **** P <0.0001, (a) versus normoxia control, (b) versus H/R control, (c) versus 100 nM CPA in the presence of H/R, (d) versus 100 μ M ADO in the presence of H/R.

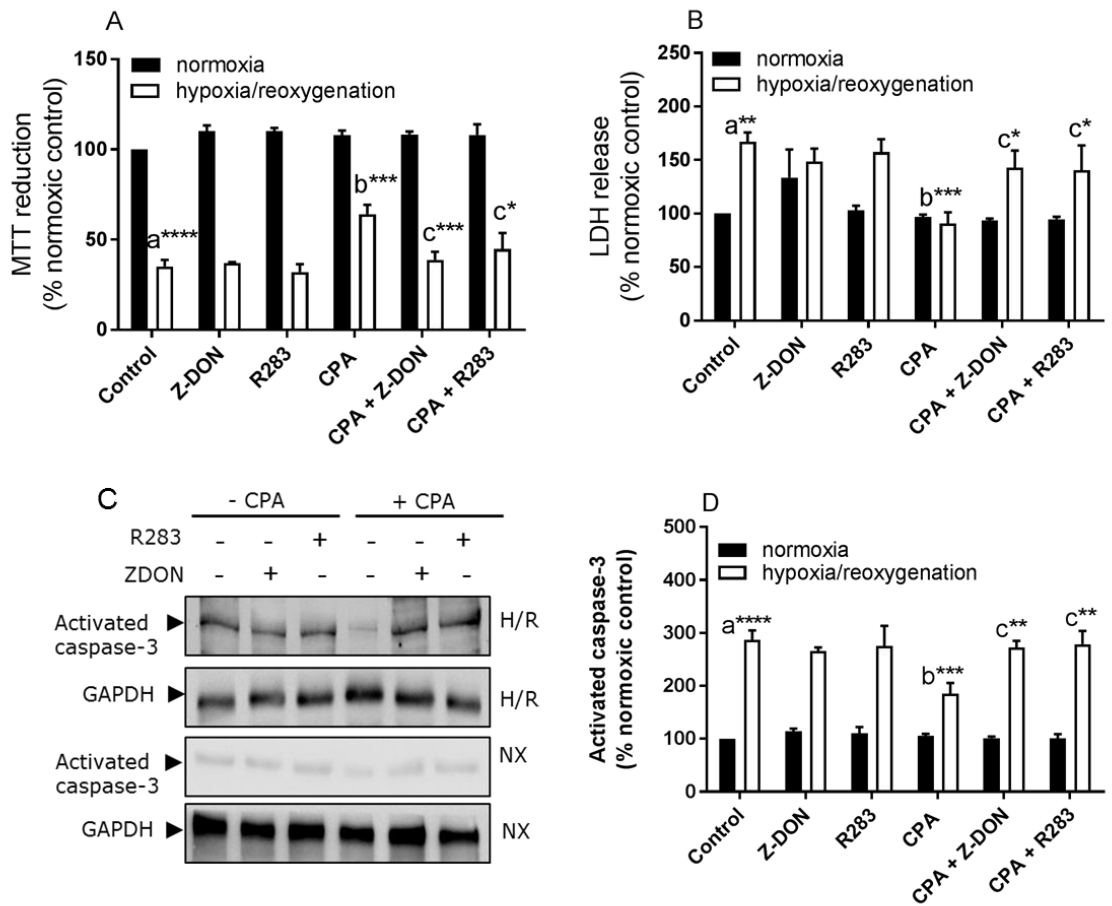


Fig 6.17: Role of TG2 in CPA-induced post-conditioning versus hypoxia/reoxygenation-induced cell death. Where indicated, H9c2 cells were exposed to 8 h hypoxia (1% O₂) followed by 18 h of re-oxygenation (H/R) or normoxia (NX). Cells were treated for the first 1 h of re-oxygenation with Z-DON (150 μM) or R283 (200 μM) before the addition of CPA (100 nM) for 10 min which was then removed for the remainder of the re-oxygenation period. Cell viability was assessed by measuring the metabolic reduction of MTT by cellular dehydrogenases (A) and release of LDH into the culture medium (B). Caspase-3 activation was assessed via Western blotting using anti-activated caspase-3 antibody (C) and quantified caspase-3 data (D) are expressed as a percentage of normoxia control cell values (=100%). Data are expressed as a percentage of normoxia control cell values (=100%) and represent the mean ± S.E.M. from four independent experiments. **P*<0.05, ***P*<0.01, ****P*<0.001 and *****P*<0.0001, (a) versus normoxia control, (b) versus H/R control, (c) versus 100 nM CPA in the presence of H/R.

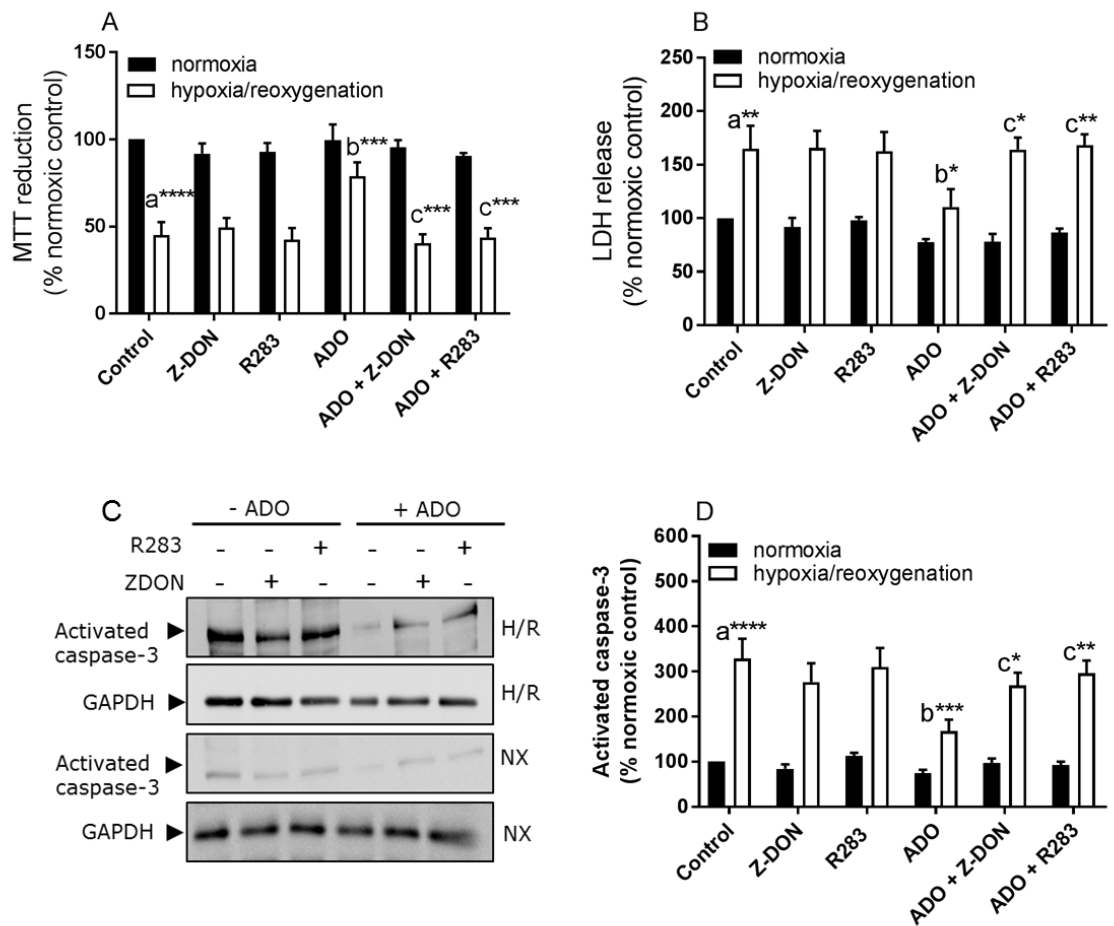


Fig 6.18: Role of TG2 in adenosine-induced post-conditioning versus hypoxia/reoxygenation-induced cell death. Where indicated, H9c2 cells were exposed to 8 h hypoxia (1% O₂) followed by 18 h of re-oxygenation (H/R) or normoxia (NX). Cells were treated for the first 1 h of re-oxygenation with Z-DON (150 μM) or R283 (200 μM) before the addition of adenosine (100 μM) for 10 min which was then removed for the remainder of the re-oxygenation period. Cell viability was assessed by measuring the metabolic reduction of MTT by cellular dehydrogenases (A) and release of LDH into the culture medium (B). Caspase-3 activation was assessed via Western blotting using anti-activated caspase-3 antibody (C) and quantified caspase-3 data (D) are expressed as a percentage of normoxia control cell values (=100%). Data are expressed as a percentage of normoxia control cell values (=100%) and represent the mean ± S.E.M. from four independent experiments. **P*<0.05, ***P*<0.01, ****P*<0.001 and *****P*<0.0001, (a) versus normoxia control, (b) versus H/R control, (c) versus 100 μM ADO in the presence of H/R.

6.5 Role of TG2 in β_2 -AR-induced cell survival against hypoxia/ re-oxygenation-induced cell death.

β_2 -AR-induced pre-conditioning

For pre-conditioning, H9c2 cells were treated with the pharmacological agents prior to the onset of hypoxia. Activation of the β_2 -AR with isoprenaline provided protection against hypoxia/re-oxygenation-induced cell death. H9c2 cells were treated with isoprenaline (10 μ M) for 20 min prior to exposure to 8 h of hypoxia followed by 18 h re-oxygenation. Isoprenaline significantly attenuated hypoxia/re-oxygenation-induced decrease in MTT reduction, release of LDH and activation of caspase-3, thus offering protection (figure 6.19, 6.20 and 6.21) and this protection was reversed when H9c2 cells were pre-treated for 30 min with the β_2 -AR selective (ICI 118551; 1 μ M) and non-selective (propranolol; 1 μ M) antagonists prior to stimulation (figure 6.19). Furthermore, pre-treatment with the $G_{i/o}$ -protein-inactivating pertussis toxin (100 ng/ml for 16 h) abolished isoprenaline-induced cell survival (figure 6.20), suggesting a prominent role of $G_{i/o}$ -proteins. Finally, pre-treatment for 1 h with Z-DON (150 μ M) or R283 (200 μ M) prior to stimulation attenuated isoprenaline-induced cell survival (figure 6.21), confirming the involvement of TG2.

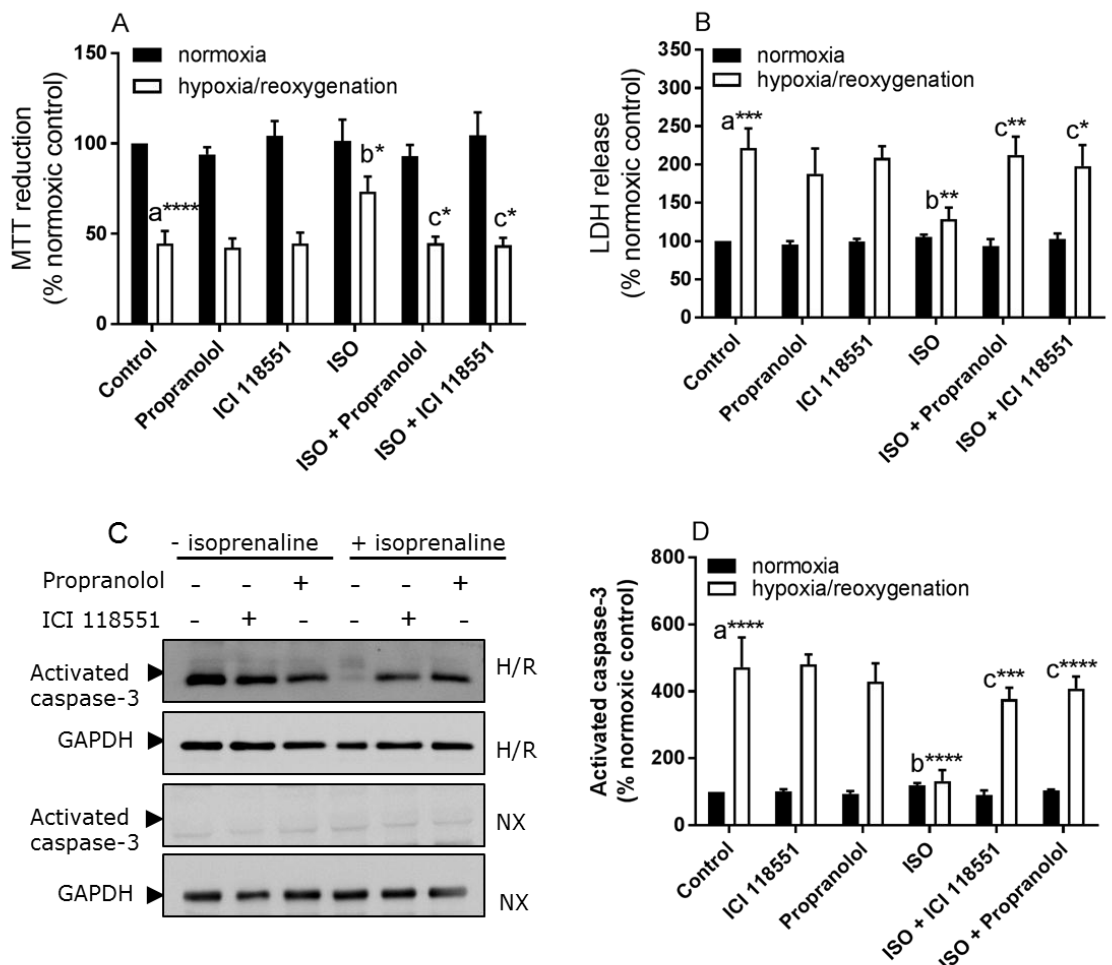


Fig 6.19: The effect of isoprenaline on hypoxia/re-oxygenation-induced cell death. Where indicated, H9c2 cells were pre-treated for 30 min with ICI 118551 (1 μ M) or propranolol (1 μ M) before the addition of isoprenaline (10 μ M) for 20 min, prior to 8 h hypoxia (1% O_2) followed by 18 h re-oxygenation (H/R) or normoxia (NX). Cell

viability was assessed by measuring the metabolic reduction of MTT by cellular dehydrogenases (A) and release of LDH into the culture medium (B). Caspase-3 activation was assessed via Western blotting using anti-activated caspase-3 antibody (C) and quantified caspase-3 data (D) are expressed as a percentage of normoxia control cell values (=100%). Data are expressed as a percentage of normoxia control cell values (=100%) and represent the mean \pm S.E.M. from four independent experiments. * P <0.05 and **** P <0.0001, (a) versus normoxia control, (b) versus H/R control, (c) versus 10 μ M isoprenaline in the presence of H/R.

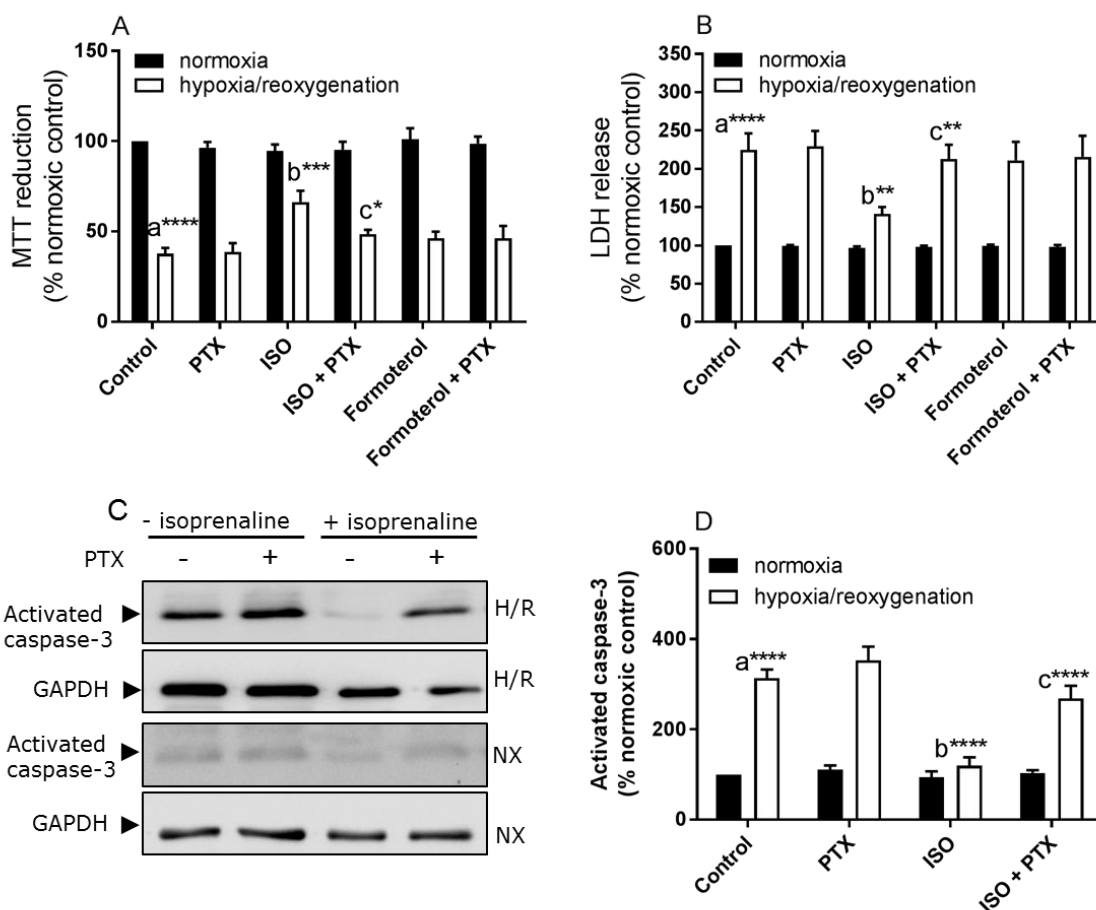


Fig 6.20: Role of $G_{i/o}$ -proteins in β_2 -AR-induced pre-conditioning versus hypoxia/re-oxygenation-induced cell death. Where indicated, H9c2 cells were pre-treated for 16 h with pertussis toxin (100 ng/ml) before the addition of isoprenaline (10 μ M) for 20 min prior to 8 h hypoxia (1% O_2) followed by 18 h re-oxygenation (H/R) or normoxia (NX). Cell viability was assessed by measuring the metabolic reduction of MTT by cellular dehydrogenases (A) and release of LDH into the culture medium (B). Caspase-3 activation was assessed via Western blotting using anti-activated caspase-3 antibody (C) and quantified caspase-3 data (D) are expressed as a percentage of normoxia control cell values (=100%). Data are expressed as a percentage of normoxia control cell values (=100%) and represent the mean \pm S.E.M. from four independent experiments. * P <0.05, ** P <0.01, *** P <0.001 and **** P <0.0001, (a) versus normoxia control, (b) versus H/R control, (c) versus 10 μ M isoprenaline in the presence of H/R.

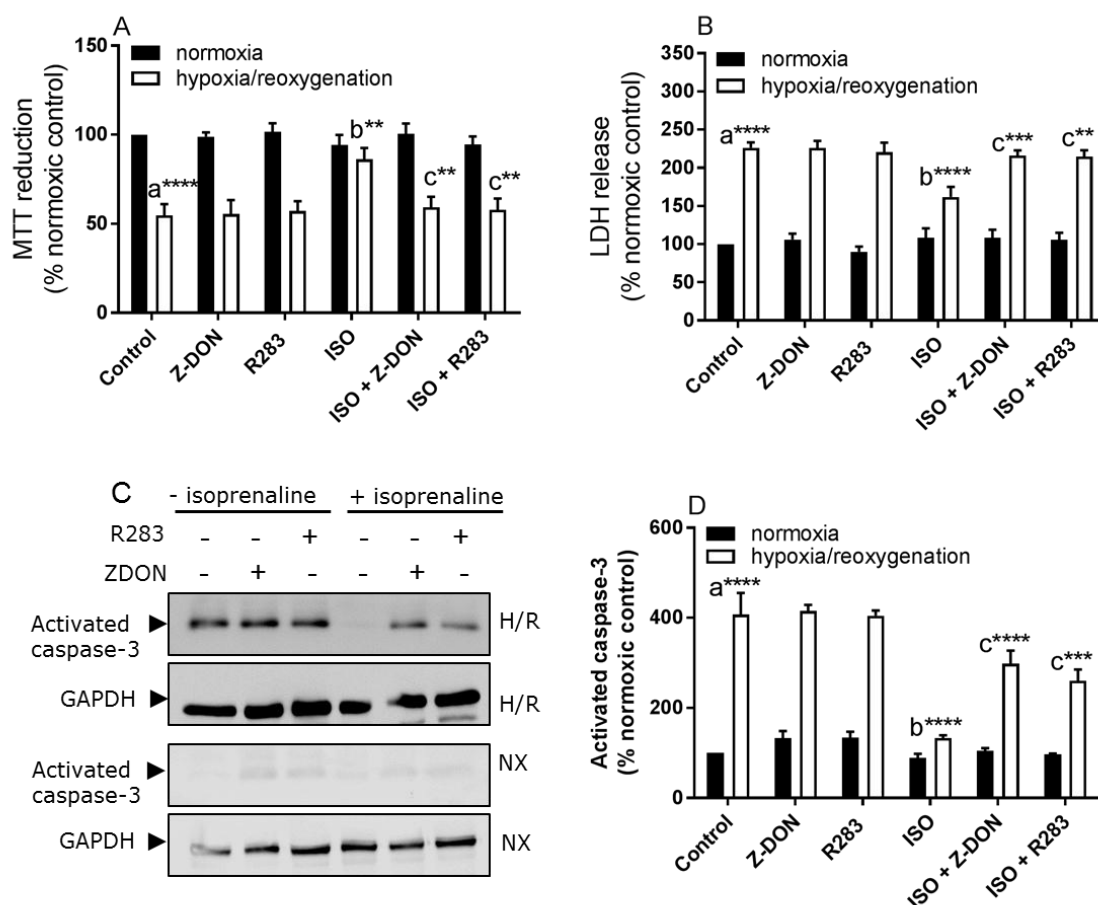


Fig 6.21: Role of TG2 in β_2 -AR-induced pre-conditioning versus hypoxia/re-oxygenation-induced cell death. Where indicated, H9c2 cells were pre-treated for 1 h with Z-DON (150 μ M) or R283 (200 μ M) before the addition of isoprenaline (10 μ M) for 20 min prior to 8 h hypoxia (1% O_2) followed by 18 h re-oxygenation (H/R) or normoxia (NX). Cell viability was assessed by measuring the metabolic reduction of MTT by cellular dehydrogenases (A) and release of LDH into the culture medium (B). Caspase-3 activation was assessed via Western blotting using anti-activated caspase-3 antibody (C) and quantified caspase-3 data (D) are expressed as a percentage of normoxia control cell values (=100%). Data are expressed as a percentage of normoxia control cell values (=100%) and represent the mean \pm S.E.M. from four independent experiments. * P <0.05, ** P <0.01, *** P <0.001 and **** P <0.0001, (a) versus normoxia control, (b) versus H/R control, (c) versus 10 μ M isoprenaline in the presence of H/R.

β_2 -AR-induced post-conditioning

For post-conditioning, H9c2 cells were treated with pharmacological agents (or relevant media for appropriate control experiments) following 8 h hypoxic incubation but prior to 18 h of re-oxygenation. H9c2 cells were treated with isoprenaline (10 μ M) for 20 min following exposure to 8 h of hypoxia but prior to 18 h re-oxygenation. Isoprenaline significantly attenuated the hypoxia/re-oxygenation-induced decrease in MTT reduction, release of LDH and activation of caspase-3, therefore offering protection (figure 6.22, 6.23 and 6.24). Pre-treatment for 30 min with the β_2 -AR selective (ICI 118551; 1 μ M) and non-selective (propranolol; 1 μ M) antagonists prior to stimulation abolished isoprenaline-induced cell survival (figure 6.22). Moreover,

pre-treatment with the $G_{i/o}$ -protein inactivating pertussis toxin (100 ng/ml for 16 h) abolished isoprenaline-induced cell survival (figure 6.23), confirming the involvement of $G_{i/o}$ -proteins. Finally, pre-treatment for 1 h with Z-DON (150 μ M) or R283 (200 μ M) prior to stimulation attenuated isoprenaline-induced cell survival (figure 6.24), confirming the involvement of TG2.

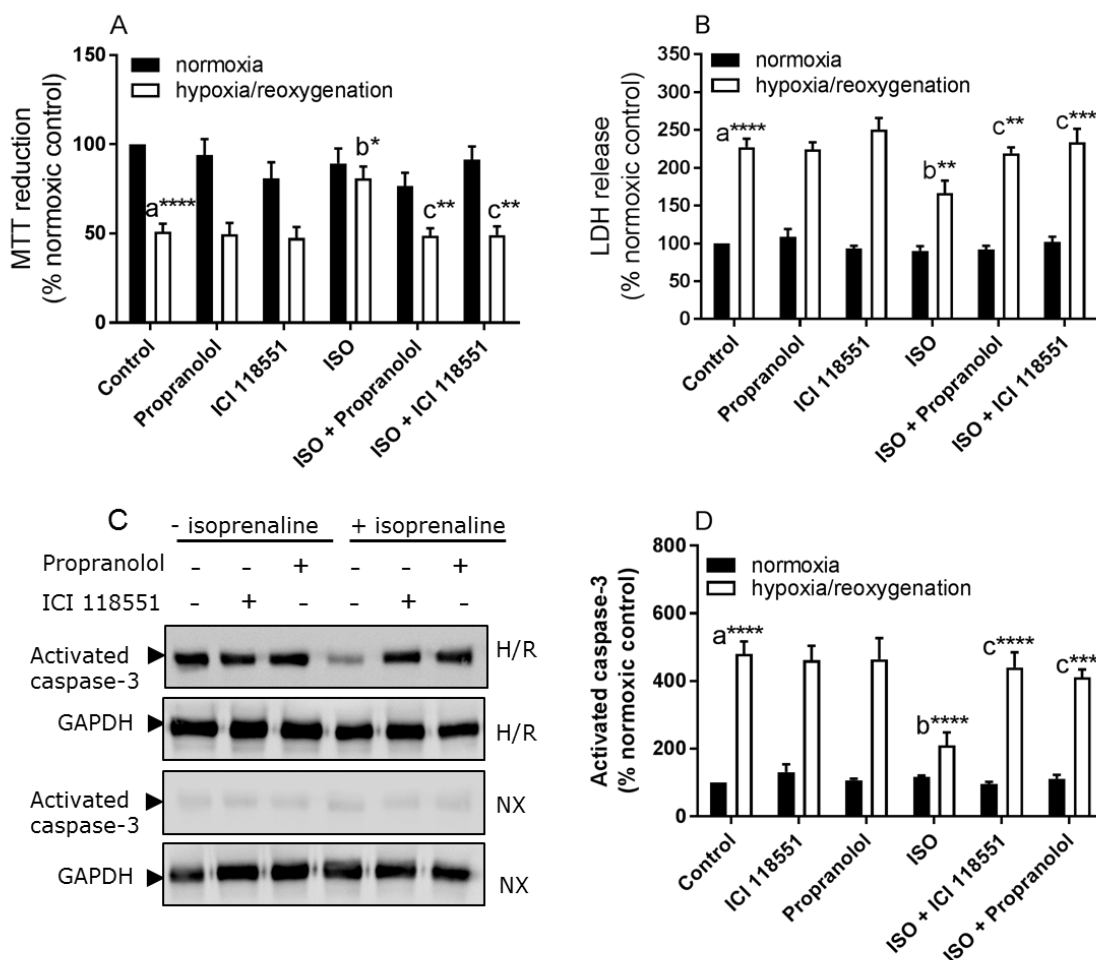


Fig 6.22: The effect of isoprenaline on hypoxia/re-oxygenation-induced cell death. Where indicated, H9c2 cells were exposed to 8 h hypoxia (1% O_2) followed by 18 h of re-oxygenation (H/R) or normoxia (NX). Cells were treated for the first 30 min of re-oxygenation with ICI 118551 (1 μ M) or propranolol (1 μ M) before the addition of isoprenaline (10 μ M) for 20 min which were then removed for the remainder of the re-oxygenation period. Cell viability was assessed by measuring the metabolic reduction of MTT by cellular dehydrogenases (A) and release of LDH into the culture medium (B). Caspase-3 activation was assessed via Western blotting using anti-activated caspase-3 antibody (C) and quantified caspase-3 data (D) are expressed as a percentage of normoxia control cell values (=100%). Data are expressed as a percentage of normoxia control cell values (=100%) and represent the mean \pm S.E.M. from four independent experiments. * P <0.05 and **** P <0.0001, (a) versus normoxia control, (b) versus H/R control, (c) versus 10 μ M isoprenaline in the presence of H/R.

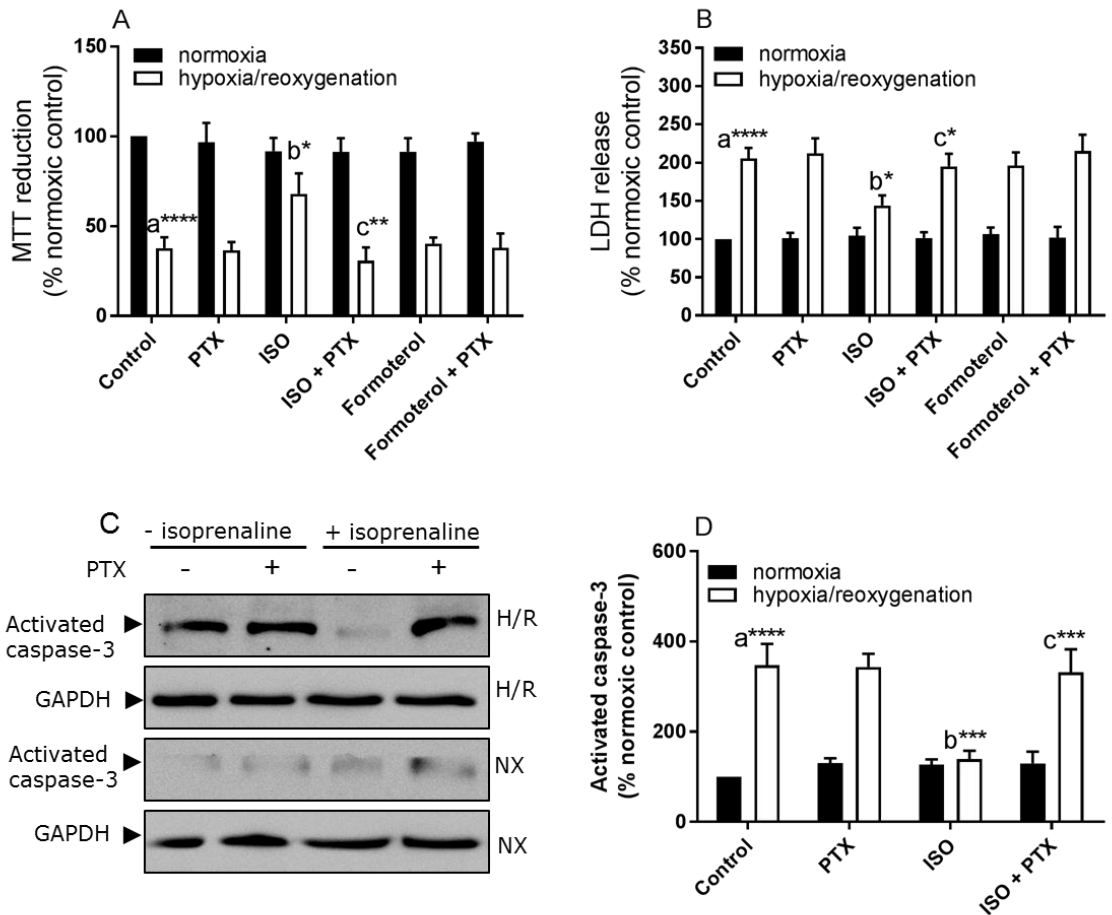


Fig 6.23: Role of $G_{i/o}$ -proteins in β_2 -AR-induced post-conditioning versus hypoxia/reoxygenation-induced cell death. Where indicated, H9c2 cells were exposed to 8 h hypoxia (1% O_2) followed by 18 h of re-oxygenation (H/R) or normoxia (NX). Cells were treated for the first 16 h of re-oxygenation with pertussis toxin (100 ng/ml) before the addition of isoprenaline (10 μ M) for 20 min which were then removed for the remainder of the re-oxygenation period. Cell viability was assessed by measuring the metabolic reduction of MTT by cellular dehydrogenases (A) and release of LDH into the culture medium (B). Caspase-3 activation was assessed via Western blotting using anti-activated caspase-3 antibody (C) and quantified caspase-3 data (D) are expressed as a percentage of normoxia control cell values (=100%). Data are expressed as a percentage of normoxia control cell values (=100%) and represent the mean \pm S.E.M. from four independent experiments. * P <0.05 and **** P <0.0001, (a) versus normoxia control, (b) versus H/R control, (c) versus 10 μ M isoprenaline in the presence of H/R.

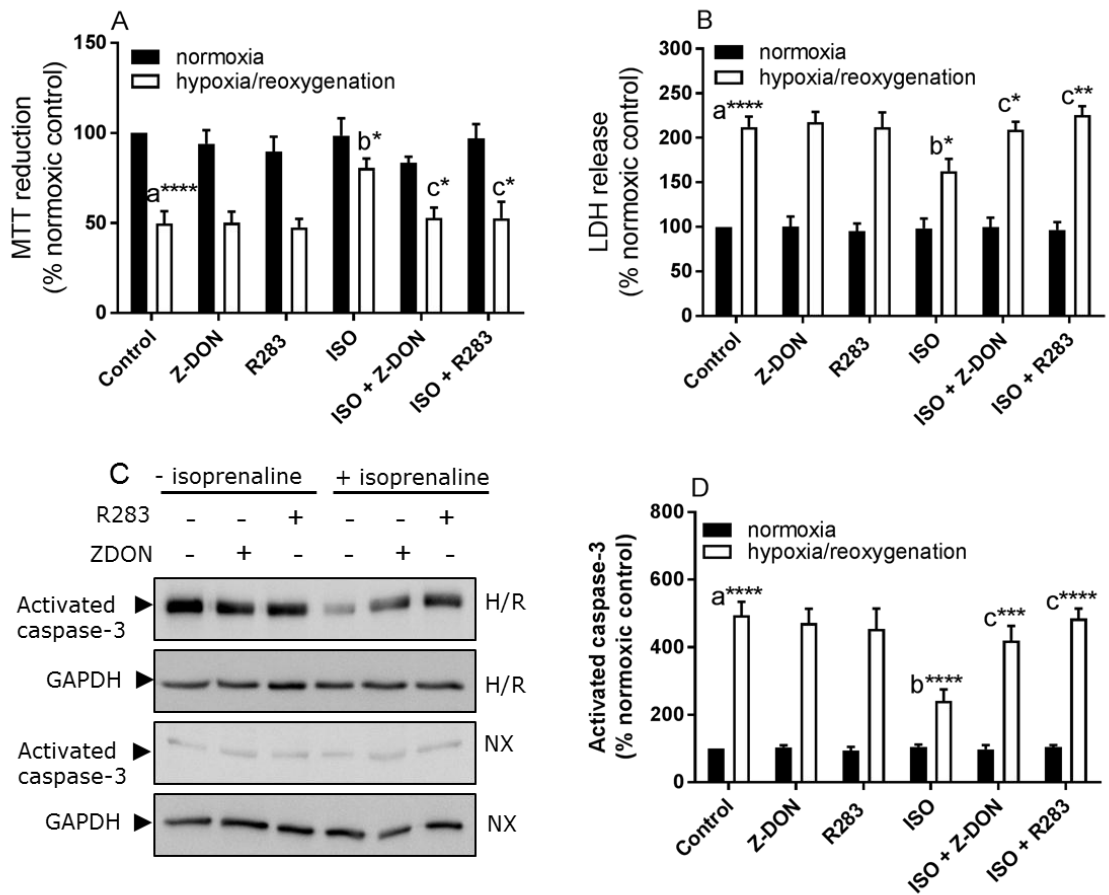


Fig 6.24: Role of TG2 in β_2 -AR-induced post-conditioning versus hypoxia/re-oxygenation-induced cell death. Where indicated, H9c2 cells were exposed to 8 h hypoxia (1% O_2) followed by 18 h of re-oxygenation (H/R) or normoxia (NX). Cells were treated for first 1 h of re-oxygenation with Z-DON (150 μ M) or R283 (200 μ M) before the addition of isoprenaline (10 μ M) for 20 min which were then removed for the remainder of the re-oxygenation period. Cell viability was assessed by measuring the metabolic reduction of MTT by cellular dehydrogenases (A) and release of LDH into the culture medium (B). Caspase-3 activation was assessed via Western blotting using anti-activated caspase-3 antibody (C) and quantified caspase-3 data (D) are expressed as a percentage of normoxia control cell values (=100%). Data are expressed as a percentage of normoxia control cell values (=100%) and represent the mean \pm S.E.M. from four independent experiments. * P <0.05 and **** P <0.0001, (a) versus normoxia control, (b) versus H/R control, (c) versus 10 μ M isoprenaline in the presence of H/R.

In conclusion, the data shown in this chapter provide sufficient evidence to support the notion that A_1 adenosine receptor- and β_2 adrenoceptor-induced TG2 activity is cardioprotective during simulated hypoxia and hypoxia/re-oxygenation injury.

6.6 Discussion.

The aim of this chapter was to evaluate the cardioprotective potential of A₁ adenosine receptor- and β₂ adrenoceptor-induced TG2 activity during simulated hypoxia and hypoxia/re-oxygenation injury.

Role of TG2 in A₁R-induced cell survival against hypoxia- and hypoxia/re-oxygenation-induced cell death:

H9c2 cells are derived from embryonic rat heart tissue and exhibit similar biochemical, morphological and electrophysiological properties to primary cardiac cells (Kimes and Brandt, 1976; Heschelet et al, 1991). These cells are increasingly being used as an *in vitro* model for studies relating to cardioprotection (see Han et al, 2005; Chen et al, 2010; Crawford et al, 2003; Sun et al, 2016) and H9c2 cells have been shown to be a good model for ischaemia/reperfusion injury (Fretwell and Dickenson, 2009; Urmaliya et al, 2009).

Activation of the G_{i/o}-coupled A₁ adenosine receptor has a well-documented role in cardioprotection in many models, including primary rat cardiomyocytes (Safran et al, 2001; Xiang et al, 2009) and H9c2 cells (Nagarkitti and Shaafi, 1998; Fretwell and Dickenson, 2011; Fretwell and Dickenson, 2009). A recent study showed that TG2 can be modulated by PKC and PKA and that it plays a role in cardioprotection in H9c2 cells (Almami et al, 2014). However, this study did not investigate the GPCR(s) involved in TG2-induced protection as non-specific activators of PKA (forskolin) and PKC (PMA) were used. It is known that the A₁R activates PKC and ERK1/2 and is implicated in cardioprotection (Germack and Dickenson, 2004; Li et al, 2006; Dana et al, 2000; Kudo et al, 2002). Since PKC and ERK1/2 pathways are also associated with modulation of TG activity (Mishra et al, 2007; Bollag et al, 2005), it is conceivable that the A₁ adenosine receptor could modulate TG2 activity via PKC and ERK1/2, and thereby play a role in cardioprotection in these cells.

Activation of the A₁R with the selective agonist CPA or the endogenous agonist adenosine significantly attenuated hypoxia- and hypoxia/re-oxygenation-induced decreases in MTT reduction, release of LDH and activation of caspase-3, thus offering protection. Loss of mitochondrial membrane integrity is measured by the metabolic reduction of MTT by cellular dehydrogenases and release of LDH into the culture medium indicates cell death. However, these approaches fail to distinguish between apoptosis and necrosis. Hence, activation of caspase-3 (which is specific to apoptosis) was also measured to distinguish between apoptosis and necrosis. It was found that caspase-3 was significantly activated revealing that the cells were undergoing apoptosis which was significantly decreased upon stimulation of A₁R. These findings suggest a role for the A₁R in cardioprotection, which was further confirmed by the use of the selective A₁R antagonist DPCPX and the G_{i/o}-protein inactivating pertussis toxin. DPCPX and pertussis toxin were able to significantly reverse the protection offered,

thus confirming the role of the A₁R and G_{i/o}-protein in cardioprotection. A role for the A₁R in both apoptosis and necrosis has also been documented in murine hearts over-expressing the cardiac A₁R (Regan *et al*, 2003). It was reported that, following ischaemia/reperfusion, less apoptosis and less necrosis occurred compared to wild-type controls (Regan *et al*, 2003).

The A₁R is cardioprotective under both pharmacological pre-conditioning and postconditioning in H9c2 cells. Not only was the protection offered by the A₁R reversed by antagonism and G_{i/o}-protein blockage but also inhibition of the enzyme TG2. At present, whilst the physiological function(s) of TG2 in cardiomyocytes is largely unknown, there is evidence for a role in modulating ischaemia/reperfusion injury by regulating ATP synthesis (Szondy *et al*, 2006). TG2 is also known to interact with or modulate a number of signalling pathways associated with cell survival against hypoxia and glucose deprivation-induced cell death, including hypoxia inducible factor 1 β , NF- κ B and PKB (Filiano *et al*, 2008; Wang *et al*, 2012). Hence it is of interest to identify TG2 protein substrates which are associated with cell survival/apoptosis in H9c2 cells. Therefore, chapter VII will be focussed on identification of protein substrates of TG2 in H9c2 cells.

Role of TG2 in β_2 -AR-induced cell survival against hypoxia and hypoxia/ re-oxygenation-induced cell death:

The role of β -AR in cardioprotection remains unclear and varies between different models and experimental procedures. In the current study, the selective β_2 -AR agonist, formoterol had no significant effect on hypoxia and hypoxia/re-oxygenation-induced decrease in MTT reduction or release of LDH. These observations are in contrast to previous studies reporting formoterol-induced cardioprotection in isolated rat hearts (Salie *et al*, 2011). The reason for the discrepancy between the present results and work by Salie *et al* (2011) is unclear but could be due to the use of different models (e.g. cell line versus isolated heart) and end points (cell viability assays versus infarct size) employed. Furthermore, simultaneous activation of PKA and EPAC in H9c2 cells induces cardioprotection against hypoxia/re-oxygenation injury via activation of PKC ϵ (Khaliulin *et al*, 2017). However, this study did not investigate PKA or EPAC activation via receptors but through direct activation of PKA using cell permeable cAMP analogues (Khaliulin *et al*, 2017). In marked contrast, the non-selective β -AR agonist, isoprenaline, significantly attenuated hypoxia and hypoxia/re-oxygenation-induced decrease in MTT reduction, release of LDH and caspase 3 activation. The functional studies carried out in chapter III imply that H9c2 cells express β -ARs with a rank order of β_2 -AR > β_1 -AR = β_3 -AR. The role of β_2 -AR in cardioprotection is well documented (Tong *et al*, 2005) and a study by Spear and colleagues reported the cardioprotective role of β_1 -AR (Spear *et al*, 2007). However, the protection offered by isoprenaline appears to occur through the β_2 -AR, based upon experiments performed with the

selective β_2 -AR antagonist ICI 118551. As reported in chapter V, isoprenaline predominantly signals via $G_{i/o}$ -proteins. This isoprenaline-induced protection is in good agreement with previous studies showing that isoprenaline-induced cell survival involved $G_{i/o}$ -protein coupling (Zhu et al, 2001; Salie et al, 2011). Furthermore, treatment with $G_{i/o}$ -protein inactivating pertussis toxin was able to significantly reverse the protection offered, thus confirming involvement of $G_{i/o}$ -protein in cardioprotection. Yano and colleagues have reported that in H9c2 cardiomyocytes, the β_2 -AR couples to $G_{i/o}$ proteins and activates pro-survival kinases such as PI-3K (Yano et al, 2007). PI-3K is a central component of the RISK pathway and it has also been demonstrated that β_2 -AR can activate the ERK1/2 pathway, which is another key player in the RISK pathway (Hausenloy et al, 2005; Galandrin and Bouvier, 2006; Tutor et al, 2007). From the results obtained in chapter V, it is clear that isoprenaline activates the ERK1/2 pathway in a $G_{i/o}$ -dependent manner while formoterol-induced ERK1/2 activation is independent of $G_{i/o}$ -protein. Isoprenaline-induced $G_{i/o}$ -dependent ERK1/2 activation could therefore be one of the pathways which offer protection.

Isoprenaline-induced cell survival is cardioprotective in both pharmacological preconditioning and postconditioning in H9c2 cells. Not only was the protection offered by the isoprenaline reversed by antagonism of the β_2 -AR and $G_{i/o}$ -protein blockage but also inhibition of the enzyme TG2. However, at present it is not clear why formoterol does not elicit increased cell survival, despite triggering TG2 and ERK1/2 activation. Possible explanations for this include: (i) only G_i -protein-mediated TG2 stimulation is cytoprotective, possibly via the selective activation of alternative enzymic functions of TG2 (e.g. protein kinase) not activated via G_s -dependent pathways; or (ii) opposing effects of robust formoterol-induced cAMP signalling on cell death which counteract TG2-induced cell survival. Overall these data highlight the need to carefully consider the signalling profiles (G_s versus G_i) when selecting β_2 -AR agonists for use in studies investigating cardioprotection.

In conclusion, the present study has revealed that A_1 adenosine receptor- and β_2 adrenoceptor-induced TG2 activity has a cardioprotective potential during simulated hypoxia and hypoxia/re-oxygenation injury in all the three experimental paradigms of preconditioning during hypoxia, preconditioning during hypoxia/re-oxygenation and postconditioning during hypoxia/re-oxygenation.

Chapter VII: Proteomic identification of agonist-mediated TG2 substrates and associated proteins

This chapter aims to identify novel TG2 substrates/interacting proteins in H9c2 cells following activation of the A₁ adenosine receptor and β₂-adrenoceptor using CaptAvidin™-agarose affinity chromatography, SWATH mass spectrometry, bioinformatics approaches and western blotting.

7.1 CaptAvidin™-agarose affinity chromatography.

In order to identify novel protein substrates associated with TG2, H9c2 cells were labelled with biotin-x-cadaverine and subsequently treated with CPA (100 nM), adenosine (100 μM), formoterol (1 μM) or isoprenaline (10 μM) in the presence or absence of TG2 inhibitors (150 μM Z-DON and 200 μM R283). Cell lysates were then subjected to CaptAvidin™-agarose affinity chromatography using CaptAvidin™-agarose sedimentation beads as described in section 2.9 (i) of chapter II and the gels stained, imaged and quantified as described in section 2.6 of chapter II.

Figure 7.1 shows that treatment with either 100 nM CPA or 100 μM adenosine for 10 min and figure 7.2 shows that treatment with either 1 μM formoterol or 10 μM isoprenaline for 20 min significantly increased the incorporation of biotin-X-cadaverine into several proteins of different molecular masses. However, it is notable that the intensity of several protein bands also decreased following these treatments, indicating reduced levels of transamidation and/or altered interactions with TG2 substrate binding partners. As expected, the incorporation of biotin-X-cadaverine into TG2 protein substrates was inhibited by pre-treatment with Z-DON and R283, thus signifying that these changes occur via interaction with TG2.

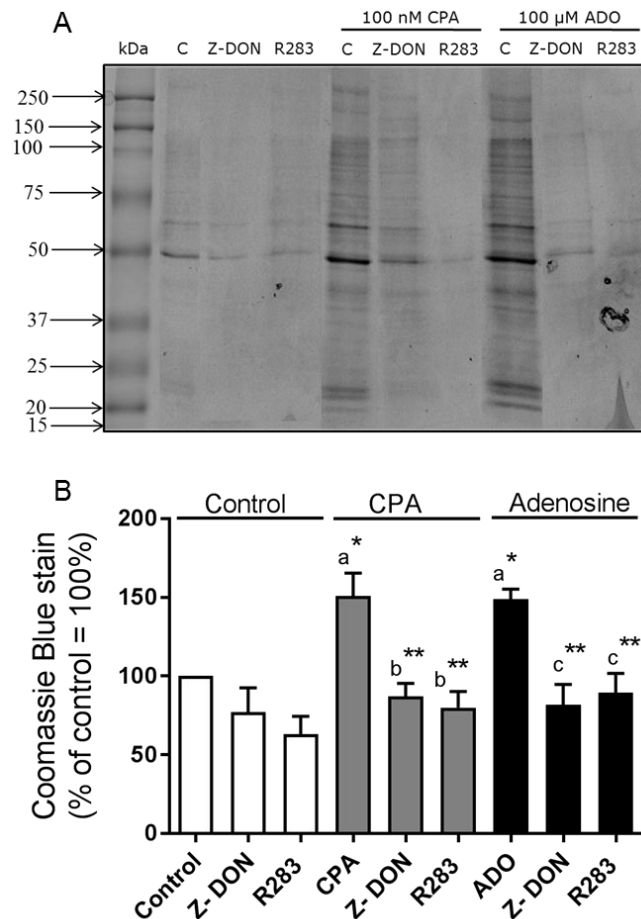


Fig. 7.1: Detection of *in situ* TG2 activity and protein substrates in CPA- and adenosine-treated H9c2 cells. Cells were incubated with 1 mM biotin-X-cadaverine for 6 h, after which they were treated for 1 h with the TG2 inhibitors Z-DON (150 μ M) or R283 (200 μ M) before stimulation with CPA (100 nM) or adenosine (100 μ M) for 10 min. Biotin-X-cadaverine-labelled proteins were enriched using CaptAvidin™ agarose sedimentation beads and eluted proteins were subjected to SDS-PAGE on 4-15% polyacrylamide gradient gels. (A) Coomassie blue staining of enriched biotin-X-cadaverine-labelled proteins following SDS-PAGE. (B) Quantification of protein substrates detected using Coomassie blue staining. Densitometry of each lane (total protein) was carried out using Advanced Image Data Analyser software (Fuji; version 3.52) and data are expressed as a percentage of basal TG2 protein substrate levels. Values are means \pm S.E.M. from three independent experiments. * P <0.05 and ** P <0.01, (a) versus control response, (b) versus CPA alone, (c) versus adenosine alone.

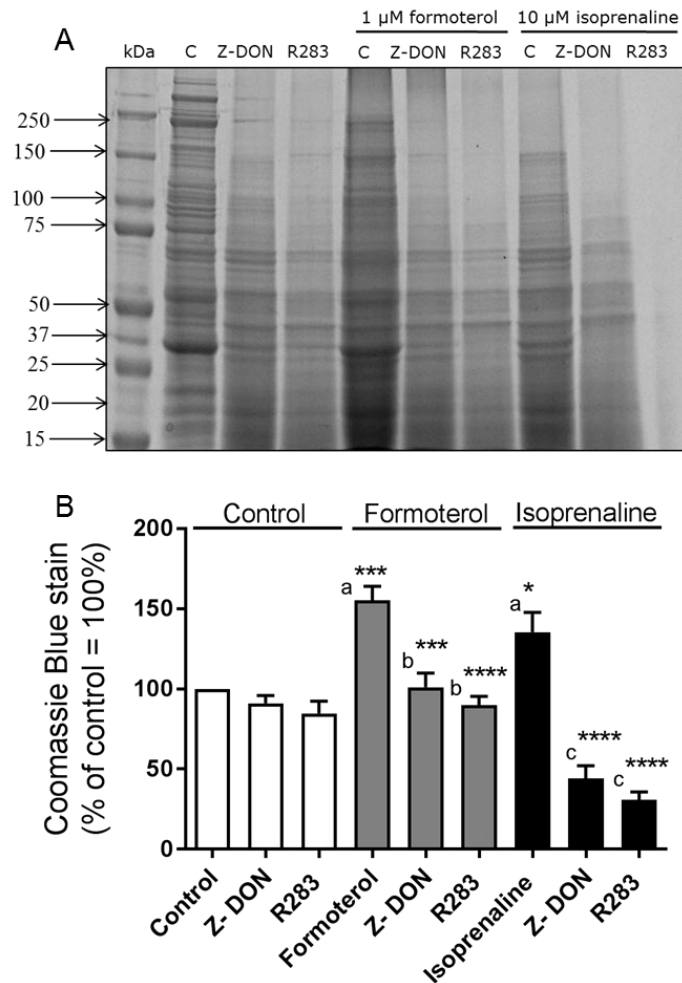


Fig. 7.2: Detection of *in situ* TG2 activity and protein substrates in formoterol- and isoprenaline-treated H9c2 cells. Cells were incubated with 1 mM biotin-X-cadaverine for 6 h, after which they were treated for 1 h with the TG2 inhibitors Z-DON (150 μ M) or R283 (200 μ M) before stimulation with formoterol (1 μ M) or isoprenaline (10 μ M) for 20 min. Biotin-X-cadaverine-labelled proteins were enriched using CaptAvidin™ agarose sedimentation beads and eluted proteins subjected to SDS-PAGE on 4-15% polyacrylamide gradient gels. (A) Coomassie blue staining of enriched biotin-X-cadaverine-labelled proteins following SDS-PAGE. (B) Quantification of protein substrates detected using Coomassie blue staining. Densitometry of each lane (total protein) was carried out using Advanced Image Data Analyser software (Fuji; version 3.52) and data are expressed as a percentage of basal TG2 protein substrate levels. Values are means \pm S.E.M. from three independent experiments. * P <0.05, *** P <0.001 and **** P <0.0001, (a) versus control response, (b) versus formoterol alone, (c) versus isoprenaline alone.

7.2 SWATH MS identification of proteins.

Lysates were digested with trypsin and prepared for SWATH MS (Sequential Windowed Acquisition of all Theoretical fragment ion Mass Spectra) analysis as described in section 2.9 (ii) of chapter II. SWATH MS is a recent technique which combines the advantages of traditional shotgun and selected reaction monitoring (SRM) techniques not only in the identification of proteins but also in their quantification following

treatments (Wang et al, 2015). The method is best described in two steps, namely: data dependent acquisition (DDA), to generate a spectral library; and data independent acquisition (DIA) to gather SWATH data. Firstly, all of the samples to be analysed (controls and treatments) are pooled together and run through the DDA mode (120 min LC run time fragmenting the top 30 proteins per MS cycle, 2.8s cycle time). Once the spectral library is constructed, the samples (individually) are then run in DIA mode (60 min LC run time, 100 variable window, 25 millisecond accumulation time per window, 3s cycle time). Once the DIA run is complete, the peptides are aligned in the PeakView 2.1 SWATH micro app (Sciex) with careful consideration of the +311.4429 mass shift (unimod.org modification accession number 800) due to tagging with biotin-X-cadaverine. The SWATH data is next extracted and quantified using OneOmics cloud processing software (<https://basespace.illumina.com/dashboard>; Lambert et al, 2013; for an overview refer to fig 7.3).

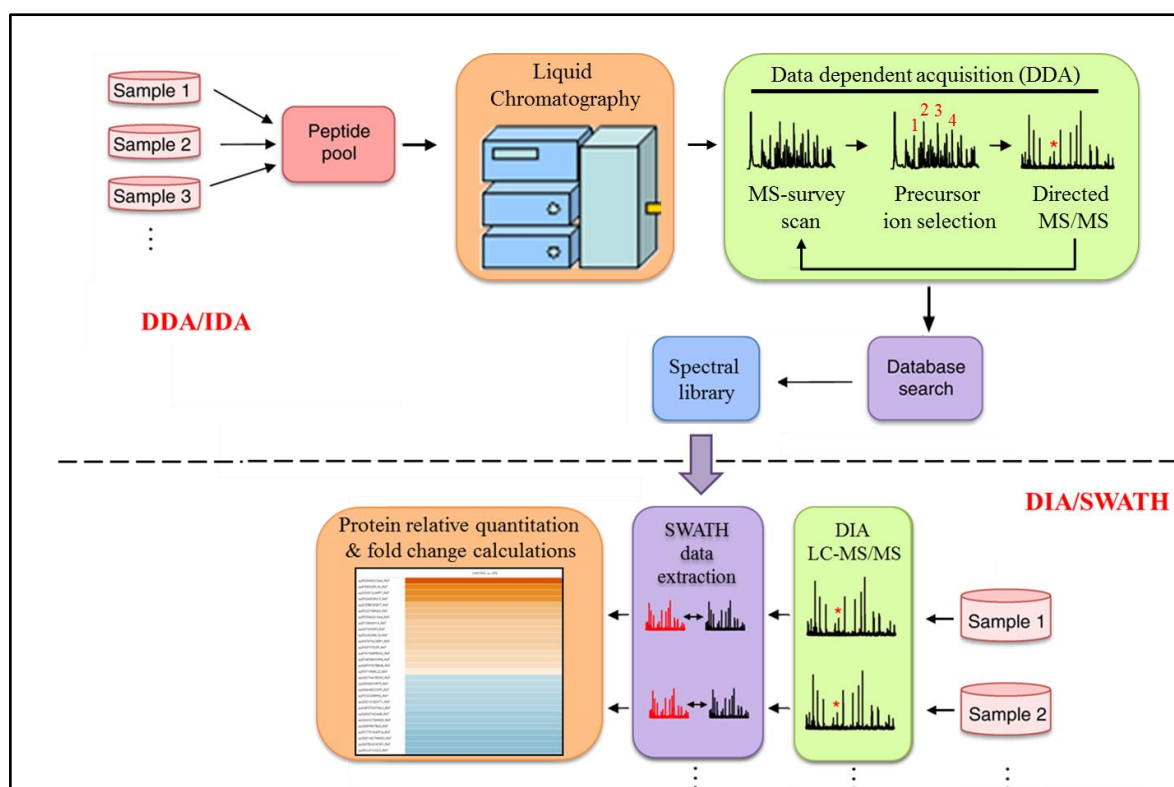


Fig. 7.3: SWATH MS protein profiling workflow. Firstly, all the samples were pooled and analysed by data-dependent acquisition, followed by SWATH MS/MS. To obtain a comprehensive protein coverage in the spectral library, all precursor ions were extracted and identified by UniProt database searching. Next, the samples were analysed individually by SWATH. The peptides were aligned to the spectral library and quantified using OneOmics cloud processing software (SCIEX). Figure adapted from Schmidt et al, (2011).

The results presented below are shown as agonist-induced fold-changes in proteins eluted from CaptAvidin™-agarose, compared to control unstimulated cells. Tables 1-4 illustrate proteins identified by SWATH-MS whose profile revealed an increase in CPA-, adenosine-, formoterol- or isoprenaline-treated cells when compared to untreated control cells. Tables 5-8 show proteins identified by SWATH-MS whose profile revealed a decrease in CPA-, adenosine-, formoterol- or isoprenaline-treated cells when compared to untreated control cells.

Table 1. Identification of proteins showing increased levels in eluates from CaptAvidin™-agarose columns following A₁R activation with 100 nM CPA.

Protein name	Uniprot accession	Uniprot name	Absolute fold change*
^a <i>Acidic leucine-rich nuclear phosphoprotein 32 family member A</i>	P49911	AN32A_RAT	5.38
^b <i>Hexokinase-1</i>	P05708	HXK1_RAT	5.16
^a <i>Nischarin</i>	Q4G017	NISCH_RAT	4.50
^c <i>Tropomyosin alpha-3 chain</i>	Q63610	TPM3_RAT	4.34
^d <i>Activated RNA polymerase II transcriptional coactivator p15</i>	Q63396	TCP4_RAT	3.34
^e <i>60S ribosomal protein L13</i>	P41123	RL13_RAT	3.10
^d <i>Histone H4</i>	P62804	H4_RAT	2.76
^e <i>Calcineurin B homologous protein 1</i>	P61023	CHP1_RAT	2.71
^f <i>Myeloid-associated differentiation marker</i>	Q6VBQ5	MYADM_RA T	2.66
^c <i>Nestin</i>	P21263	NEST_RAT	2.61
^e <i>60S ribosomal protein L30</i>	P62890	RL30_RAT	2.57
^f <i>Transmembrane protein 33</i>	Q9Z142	TMM33_RA T	2.49
^c <i>Tubulin alpha-3 chain</i>	Q68FR8	TBA3_RAT	2.14
^f <i>Homer protein homolog 3</i>	Q9Z2X5	HOME3_RA T	2.13
^g <i>Voltage-dependent anion-selective channel protein 1</i>	Q9Z2L0	VDAC1_RA T	2.11
^d <i>MIF4G domain-containing protein</i>	Q6AXU7	MI4GD_RA T	2.09
^f <i>Serine/threonine-protein phosphatase 2A 65 kDa regulatory subunit A beta isoform</i>	Q4QQT4	2AAB_RAT	2.08
^a <i>Phosphatidylinositol 4-kinase type 2-alpha</i>	Q99M64	P4K2A_RAT	2.02
^h <i>Extended synaptotagmin-1</i>	Q9Z1X1	ESYT1_RAT	1.89
ⁱ <i>Dolichyl-diphosphooligosaccharide--protein glycosyltransferase subunit 2</i>	P25235	RPN2_RAT	1.85
^d <i>Translation initiation factor eIF-2B subunit delta</i>	Q63186	EI2BD_RAT	1.78
^h <i>Coatomer subunit delta</i>	Q66H80	COPD_RAT	1.74
^d <i>Y-box-binding protein 3</i>	Q62764	YBOX3_RAT	1.66

H9c2 cells were pre-incubated with biotin-X-cadaverine prior to treatment with CPA (100 nM) and biotin-cadaverine-labelled proteins were captured and analysed by SWATH MS. *Absolute fold changes in CPA-treated samples versus control (n=4) were calculated using SCIEX OneOmics with parameters MLR weight > 0.15, confidence >60%, algorithms used described by Lambert *et al.*, (2013). Proposed novel TG2 targets not appearing in the TG2 substrate database (Csósz *et al.*, 2009) or identified by Yu *et al.* (2015) or Almami *et al.* (2014) are indicated in *italics*. Proteins are grouped according to their functions as follows: ^acell signalling; ^bmetabolism; ^ccytoskeletal; ^dtranscription/translation; ^evesicular trafficking/extracellular matrix constituent; ^fstructural/scaffolding protein; ^gapoptosis; ^hlipid/protein transport; ⁱprotein glycosylation; ^jprotein folding.

Table 2. Identification of proteins showing increased levels in eluates from CaptAvidin™-agarose columns following A₁R activation with 100 μM adenosine.

Protein name	Uniprot accession	Uniprot name	Absolute fold change*
^b <i>Citrate synthase, mitochondrial</i>	Q8VHF5	CISY_RAT	6.34
^c <i>Tropomyosin alpha-3 chain</i>	Q63610	TPM3_RAT	5.98
^c <i>Tropomyosin alpha-4 chain</i>	P09495	TPM4_RAT	5.86
^h Glutathione S-transferase P	P04906	GSTP1_RAT	5.63
^g <i>Annexin A5</i>	P14668	ANXA5_RAT	4.31
^d <i>RNA-binding protein 3</i>	Q925G0	RBM3_RAT	3.81
^c <i>Alpha-actinin-4</i>	Q9QXQ0	ACTN4_RAT	3.58
^d <i>60S ribosomal protein L18a</i>	P62718	RL18A_RAT	3.47
^c <i>Transgelin</i>	P31232	TAGL_RAT	3.13
^d <i>40S ribosomal protein S28</i>	P62859	RS28_RAT	2.88
^c <i>Tropomyosin alpha-1 chain</i>	P04692	TPM1_RAT	2.84
^b <i>Aspartate aminotransferase, mitochondrial</i>	P00507	AATM_RAT	2.75
^f <i>Myeloid-associated differentiation marker</i>	Q6VBQ5	MYADM_RAT	2.72
^e <i>Rab GDP dissociation inhibitor beta</i>	P50399	GDIB_RAT	2.57
^d Histone H4	P62804	H4_RAT	2.43
^j <i>Protein disulfide-isomerase</i>	P04785	PDIA1_RAT	2.21
^h <i>Lysosome-associated membrane glycoprotein 2</i>	P17046	LAMP2_RAT	2.06
^b L-lactate dehydrogenase A chain	P04642	LDHA_RAT	2.06
^g <i>Cytochrome c oxidase subunit 5B, mitochondrial</i>	P12075	COX5B_RAT	1.68
^d <i>Eukaryotic translation initiation factor 3 subunit J</i>	A0JPM9	EIF3J_RAT	1.38

H9c2 cells were pre-incubated with biotin-X-cadaverine prior to treatment with adenosine (100 μM) and biotin-cadaverine-labelled proteins were captured and analysed by SWATH MS. *Absolute fold changes in adenosine-treated samples versus control (n=4) were calculated using SCIEX OneOmics with parameters MLR weight > 0.15, confidence >60%, algorithms used described by Lambert *et al.*, (2013). Proposed novel TG2 targets not appearing in the TG2 substrate database (Csósz *et al.*, 2009) or identified by Yu *et al.* (2015) or Almami *et al.* (2014) are indicated in *italics*. Proteins are grouped according to their functions as follows: ^acell signalling; ^bmetabolism; ^ccytoskeletal; ^dtranscription/translation; ^evesicular trafficking/extracellular matrix constituent; ^fstructural/scaffolding protein; ^gapoptosis; ^hlipid/protein transport; ⁱprotein glycosylation; ^jprotein folding.

Table 3. Identification of proteins showing increased levels in eluates from CaptAvidin™-agarose columns following β_2 -AR activation with 1 μ M formoterol.

Protein name	Uniprot accession	Uniprot name	Absolute fold change*
^e Collagen alpha-1(I) chain	P02454	CO1A1_RAT	2.64
^a <i>Protein S100-A6</i>	P05964	S10A6_RAT	2.45
^e Collagen alpha-1(III) chain	P13941	CO3A1_RAT	2.40
^a <i>Protein SET</i>	Q63945	SET_RAT	2.26
^b L-lactate dehydrogenase A chain	P04642	LDHA_RAT	1.94
^g <i>Annexin A5</i>	P14668	ANXA5_RAT	1.91
^e Collagen alpha-2(I) chain	P02466	CO1A2_RAT	1.86
^b <i>Malate dehydrogenase, mitochondrial</i>	P04636	MDHM_RAT	1.84
^b D-3-phosphoglycerate dehydrogenase	O08651	SERA_RAT	1.65
^g <i>Galectin-1</i>	P11762	LEG1_RAT	1.62
^d <i>Ribonuclease inhibitor</i>	P29315	RINI_RAT	1.57
^d <i>Histone H1.5</i>	D3ZBN0	H15_RAT	1.46
^e <i>60S ribosomal protein L7</i>	P05426	RL7_RAT	1.32

H9c2 cells were pre-incubated with biotin-X-cadaverine prior to treatment with formoterol (1 μ M) and biotin-cadaverine-labelled proteins were captured and analysed by SWATH MS. *Absolute fold changes in formoterol-treated samples versus control (n=4) were calculated using SCIEX OneOmics with parameters MLR weight > 0.15, confidence >70%, algorithms used described by Lambert *et al.*, (2013). Proposed novel TG2 targets not appearing in the TG2 substrate database (Csósz *et al.*, 2009) or identified by Yu *et al.* (2015) or Almami *et al.* (2014) are indicated in *italics*. Proteins are grouped according to their functions as follows: ^acell signalling; ^bmetabolism; ^ccytoskeletal; ^dtranscription/translation; ^evesicular trafficking/extracellular matrix constituent; ^fstructural/scaffolding protein; ^gapoptosis; ^hlipid/protein transport; ⁱprotein glycosylation; ^jprotein folding.

Table 4. Identification of proteins showing increased levels in eluates from CaptAvidin™-agarose columns following β_2 -AR activation with 10 μ M isoprenaline.

Protein name	Uniprot accession	Uniprot name	Absolute fold change*
^b <i>Adenine phosphoribosyltransferase</i>	P36972	APT_RAT	2.61
^a <i>Protein S100-A6</i>	P05964	S10A6_RAT	2.46
^e Collagen alpha-1(III) chain	P13941	CO3A1_RAT	2.27
^g <i>Annexin A5</i>	P14668	ANXA5_RAT	2.15
^j <i>Protein disulfide-isomerase A5</i>	Q5I0H9	PDIA5_RAT	2.02
^a <i>Protein SET</i>	Q63945	SET_RAT	2.01
^b <i>Malate dehydrogenase, mitochondrial</i>	P04636	MDHM_RAT	1.96
^e Collagen alpha-1(I) chain	P02454	CO1A1_RAT	1.91
^b <i>Acetyl-CoA carboxylase 1</i>	P11497	ACACA_RAT	1.81
^b L-lactate dehydrogenase A chain	P04642	LDHA_RAT	1.75
^g <i>Caspase recruitment domain-containing protein 9</i>	Q9EPY0	CARD9_RAT	1.74
^b <i>Aldehyde dehydrogenase, mitochondrial</i>	P11884	ALDH2_RAT	1.73
^d <i>Ribonuclease inhibitor</i>	P29315	RINI_RAT	1.71

H9c2 cells were pre-incubated with biotin-X-cadaverine prior to treatment with isoprenaline (10 μ M) and biotin-cadaverine-labelled proteins were captured and analysed by SWATH MS. *Absolute fold changes in isoprenaline-treated samples versus control (n=4) were calculated using SCIEX OneOmics with parameters MLR weight > 0.15, confidence >70%, algorithms used described by Lambert et al., (2013). Proposed novel TG2 targets not appearing in the TG2 substrate database (Csósz et al., 2009) or identified by Yu et al. (2015) or Almami et al. (2014) are indicated in *italics*. Proteins are grouped according to their functions as follows: ^acell signalling; ^bmetabolism; ^ccytoskeletal; ^dtranscription/translation; ^evesicular trafficking/extracellular matrix constituent; ^fstructural/scaffolding protein; ^gapoptosis; ^hlipid/protein transport; ⁱprotein glycosylation; ^jprotein folding.

Table 5. Identification of proteins showing decreased levels in eluates from CaptAvidin™-agarose columns following A₁R activation with 100 nM CPA.

Protein name	Uniprot accession	Uniprot name	Absolute fold change*
^e 60S ribosomal protein L36	P39032	RL36_RAT	-7.71
^d 40S ribosomal protein S15	P62845	RS15_RAT	-6.32
^f PDZ and LIM domain protein 1	P52944	PDLI1_RAT	-5.17
^h Geranylgeranyl transferase type-2 subunit alpha	Q08602	PGTA_RAT	-4.93
^c Cofilin-1	P45592	COF1_RAT	-4.35
^c Calponin-1	Q08290	CNN1_RAT	-4.12
^d 40S ribosomal protein S24	P62850	RS24_RAT	-4.08
^c Nck-associated protein 1	P55161	NCKP1_RAT	-3.67
^d 40S ribosomal protein S29	P62275	RS29_RAT	-3.05
^h Copper-transporting ATPase 1	P70705	ATP7A_RAT	-2.96
^a Protein S100-A4	P05942	S10A4_RAT	-2.86
^e Granulins	P23785	GRN_RAT	-2.54
^d Histone H1.4	P15865	H14_RAT	-2.42
^d Eukaryotic translation initiation factor 5	Q07205	IF5_RAT	-2.34
^d 60S ribosomal protein L7a	P62425	RL7A_RAT	-2.31
^d Cysteine and glycine-rich protein 1	P47875	CSRP1_RAT	-2.27
^b Glyceraldehyde-3-phosphate dehydrogenase	P04797	G3P_RAT	-2.11
^h Protein-tyrosine sulfotransferase 2	Q5RJS8	TPST2_RAT	-2.10
^g Peroxiredoxin-2	P35704	PRDX2_RAT	-1.83
^j Heat shock protein HSP 90-beta	P34058	HS90B_RAT	-1.82
^e 60S ribosomal protein L14	Q63507	RL14_RAT	-1.77
^c Tubulin beta-5 chain	P69897	TBB5_RAT	-1.75
^d Eukaryotic translation initiation factor 2 subunit 1	P68101	IF2A_RAT	-1.74
^c Tubulin beta-4B chain	Q6P9T8	TBB4B_RAT	-1.73
^c Vacuolar protein sorting-associated protein 4A	Q793F9	VPS4A_RAT	-1.69
^b NADPH--cytochrome P450 reductase	P00388	NCPR_RAT	-1.63
^d 40S ribosomal protein S30	P62864	RS30_RAT	-1.46
^e 60S ribosomal protein L22	P47198	RL22_RAT	-1.34

H9c2 cells were pre-incubated with biotin-X-cadaverine prior to treatment with CPA (100 nM) and biotin-cadaverine-labelled proteins were captured and analysed by SWATH MS. *Absolute fold changes in CPA-treated samples versus control (n=4) were calculated using SCIEX OneOmics with parameters MLR weight > 0.15, confidence >60%, algorithms used described by Lambert *et al.*, (2013). Proposed novel TG2 targets not appearing in the TG2 substrate database (Csósz *et al.*, 2009) or identified by Yu *et al.* (2015) or Almami *et al.* (2014) are indicated in *italics*. Proteins are grouped according to their functions as follows: ^acell signalling; ^bmetabolism; ^ccytoskeletal; ^dtranscription/translation; ^evesicular trafficking/extracellular matrix constituent; ^fstructural/scaffolding protein; ^gapoptosis; ^hlipid/protein transport; ⁱprotein glycosylation; ^jprotein folding.

Table 6. Identification of proteins showing decreased levels in eluates from CaptAvidin™-agarose columns following A₁R activation with 100 μM adenosine.

Protein name	Uniprot accession	Uniprot name	Absolute fold change*
^d <i>Histone H2A type 2-A</i>	P0CC09	H2A2A_RAT	-100.00
^d <i>40S ribosomal protein S29</i>	P62275	RS29_RAT	-4.85
^d <i>Cysteine-rich protein 2</i>	P36201	CRIP2_RAT	-2.59
^c <i>Calponin-1</i>	Q08290	CNN1_RAT	-2.50
^d <i>Cysteine and glycine-rich protein 1</i>	P47875	CSRP1_RAT	-2.49
^f <i>PDZ and LIM domain protein 5</i>	Q62920	PDLI5_RAT	-2.42
^g <i>Cytochrome c oxidase subunit 6C-2</i>	P11951	CX6C2_RAT	-2.39
^c <i>Alpha-centractin</i>	P85515	ACTZ_RAT	-2.22
^e <i>Dynactin subunit 2</i>	Q6AYH5	DCTN2_RAT	-2.16
^d <i>40S ribosomal protein S2</i>	P27952	RS2_RAT	-2.09
^a <i>Integrin-linked protein kinase</i>	Q99J82	ILK_RAT	-2.07
^b <i>D-3-phosphoglycerate dehydrogenase</i>	O08651	SERA_RAT	-2.06
^c <i>Tubulin beta-4B chain</i>	Q6P9T8	TBB4B_RAT	-1.99
^b <i>Glyceraldehyde-3-phosphate dehydrogenase</i>	P04797	G3P_RAT	-1.91
^b <i>Pyrroline-5-carboxylate reductase 3</i>	Q5PQJ6	P5CR3_RAT	-1.89
^c <i>Tubulin beta-2A chain</i>	P85108	TBB2A_RAT	-1.88
^e <i>60S ribosomal protein L7a</i>	P62425	RL7A_RAT	-1.87
^d <i>40S ribosomal protein S25</i>	P62853	RS25_RAT	-1.81
^c <i>Tubulin beta-5 chain</i>	P69897	TBB5_RAT	-1.77
^f <i>26S protease regulatory subunit 4</i>	P62193	PRS4_RAT	-1.74
^d <i>Elongation factor 1-alpha 1</i>	P62630	EF1A1_RAT	-1.67
^e <i>60S ribosomal protein L10a</i>	P62907	RL10A_RAT	-1.62
^e <i>60S ribosomal protein L12</i>	P23358	RL12_RAT	-1.62
^e <i>60S ribosomal protein L23</i>	P62832	RL23_RAT	-1.60
^e <i>60S ribosomal protein L14</i>	Q63507	RL14_RAT	-1.58
^d <i>Heterogeneous nuclear ribonucleoprotein M</i>	Q62826	HNRPM_RAT	-1.56

H9c2 cells were pre-incubated with biotin-X-cadaverine prior to treatment with adenosine (100 μM) and biotin-cadaverine-labelled proteins were captured and analysed by SWATH MS. *Absolute fold changes in adenosine-treated samples versus control (n=4) were calculated using SCIEX OneOmics with parameters MLR weight > 0.15, confidence >60%, algorithms used described by Lambert *et al.*, (2013). Proposed novel TG2 targets not appearing in the TG2 substrate database (Csósz *et al.*, 2009) or identified by Yu *et al.* (2015) or Almami *et al.* (2014) are indicated in *italics*. Proteins are grouped according to their functions as follows: ^acell signalling; ^bmetabolism; ^ccytoskeletal; ^dtranscription/translation; ^evesicular trafficking/extracellular matrix constituent; ^fstructural/scaffolding protein; ^gapoptosis; ^hlipid/protein transport; ⁱprotein glycosylation; ^jprotein folding.

Table 7. Identification of proteins showing decreased levels in eluates from CaptAvidin™-agarose columns following β_2 -AR activation with 1 μ M formoterol.

Protein name	Uniprot accession	Uniprot name	Absolute fold change*
^e <i>Calumenin</i>	O35783	CALU_RAT	-3.27
^e <i>EH domain-containing protein 2</i>	Q4V8H8	EHD2_RAT	-2.76
^c <i>Myosin regulatory light polypeptide 9</i>	Q64122	MYL9_RAT	-2.65
^d <i>Cysteine and glycine-rich protein 1</i>	P47875	CSRP1_RAT	-2.46
^e Dynactin subunit 2	Q6AYH5	DCTN2_RAT	-2.40
^c <i>Actin, gamma-enteric smooth muscle</i>	P63269	ACTH_RAT	-2.36
^d <i>Transcription intermediary factor 1-beta</i>	O08629	TIF1B_RAT	-2.11
^g Lactadherin	P70490	MFGM_RAT	-2.07
^e Dynactin subunit 1	P28023	DCTN1_RAT	-2.03
^a <i>Four and a half LIM domains protein 1</i>	Q9WUH4	FHL1_RAT	-1.90
^c <i>Myosin light polypeptide 6</i>	Q64119	MYL6_RAT	-1.84
^c <i>Filamin-C</i>	D3ZHA0	FLNC_RAT	-1.80
^c Myosin-9	Q62812	MYH9_RAT	-1.73
^f <i>PDZ and LIM domain protein 7</i>	Q9Z1Z9	PDLI7_RAT	-1.72
^e <i>Alpha-centractin</i>	P85515	ACTZ_RAT	-1.72
^a Integrin beta-1	P49134	ITB1_RAT	-1.70
^c Tropomyosin alpha-1 chain	P04692	TPM1_RAT	-1.68
^a <i>Transforming growth factor beta-1-induced transcript 1 protein</i>	Q99PD6	TGFI1_RAT	-1.65
^a Rho-associated protein kinase 2	Q62868	ROCK2_RAT	-1.60
^e Ras-related protein Rab-7a	P09527	RAB7A_RAT	-1.53
^j Heat shock protein HSP 90-alpha	P82995	HS90A_RAT	-1.53
^c <i>LIM and SH3 domain protein 1</i>	Q99MZ8	LASP1_RAT	-1.43
^c <i>Myosin regulatory light chain RLC-A</i>	P13832	MRLCA_RAT	-1.43
^f <i>14-3-3 protein theta</i>	P68255	1433T_RAT	-1.41
^j Endoplasmic (Heat shock protein HSP 90-beta 1)	Q66HD0	ENPL_RAT	-1.38

H9c2 cells were pre-incubated with biotin-X-cadaverine prior to treatment with formoterol (1 μ M) and biotin-cadaverine-labelled proteins were captured and analysed by SWATH MS. *Absolute fold changes in formoterol-treated samples versus control (n=4) were calculated using SCIEX OneOmics with parameters MLR weight > 0.15, confidence >70%, algorithms used described by Lambert *et al.*, (2013). Proposed novel TG2 targets not appearing in the TG2 substrate database (Csósz *et al.*, 2009) or identified by Yu *et al.* (2015) or Almami *et al.* (2014) are indicated in *italics*. Proteins are grouped according to their functions as follows: ^acell signalling; ^bmetabolism; ^ccytoskeletal; ^dtranscription/translation; ^evesicular trafficking/extracellular matrix constituent; ^fstructural/scaffolding protein; ^gapoptosis; ^hlipid/protein transport; ⁱprotein glycosylation; ^jprotein folding.

Table 8. Identification of proteins showing decreased levels in eluates from CaptAvidin™-agarose columns following β_2 -AR activation with 10 μ M isoprenaline.

Protein name	Uniprot accession	Uniprot name	Absolute fold change*
^d <i>40S ribosomal protein S24</i>	P62850	RS24_RAT	-2.88
^d <i>Transcription intermediary factor 1-beta</i>	O08629	TIF1B_RAT	-2.87
^f <i>PDZ and LIM domain protein 5</i>	Q62920	PDLI5_RAT	-2.60
^d <i>Cysteine and glycine-rich protein 1</i>	P47875	CSRP1_RAT	-2.47
^g Lactadherin	P70490	MFGM_RAT	-2.24
^e Dynactin subunit 2	Q6AYH5	DCTN2_RAT	-1.90
^d <i>Elongation factor 1-delta</i>	Q68FR9	EF1D_RAT	-1.88
^a <i>Transforming growth factor beta-1-induced transcript 1 protein</i>	Q99PD6	TGFI1_RAT	-1.82
^e Dynactin subunit 1	P28023	DCTN1_RAT	-1.80
^a Integrin beta-1	P49134	ITB1_RAT	-1.79
^c Vimentin	P31000	VIME_RAT	-1.78
^d Eukaryotic translation initiation factor 5	Q07205	IF5_RAT	-1.68
^e <i>Cytoplasmic dynein 1 heavy chain 1</i>	P38650	DYHC1_RAT	-1.57
^j Heat shock protein HSP 90-alpha	P82995	HS90A_RAT	-1.56
^c <i>Tubulin beta-4B chain</i>	Q6P9T8	TBB4B_RAT	-1.52
^b Fatty acid synthase	P12785	FAS_RAT	-1.42
^f <i>14-3-3 protein theta</i>	P68255	1433T_RAT	-1.42
^f <i>14-3-3 protein zeta/delta</i>	P63102	1433Z_RAT	-1.38

H9c2 cells were pre-incubated with biotin-X-cadaverine prior to treatment with isoprenaline (10 μ M) and biotin-cadaverine-labelled proteins were captured and analysed by SWATH MS. *Absolute fold changes in isoprenaline-treated samples versus control (n=4) were calculated using SCIEX OneOmics with parameters MLR weight > 0.15, confidence >70%, algorithms used described by Lambert *et al.*, (2013). Proposed novel TG2 targets not appearing in the TG2 substrate database (Csósz *et al.*, 2009) or identified by Yu *et al.* (2015) or Almami *et al.* (2014) are indicated in *italics*. Proteins are grouped according to their functions as follows: ^acell signalling; ^bmetabolism; ^ccytoskeletal; ^dtranscription/translation; ^evesicular trafficking/extracellular matrix constituent; ^fstructural/scaffolding protein; ^gapoptosis; ^hlipid/protein transport; ⁱprotein glycosylation; ^jprotein folding.

In addition to the tables, figure 7.4 illustrates Venn diagrams representing the number of proteins which reveal agonist- and receptor-specific changes in levels of proteins eluted from CaptAvidin™-agarose compared to control unstimulated cells. Similar colours will be used hereafter to represent proteins showing increased- and/or decreased-levels in eluates from CaptAvidin™-agarose columns following receptor activation.

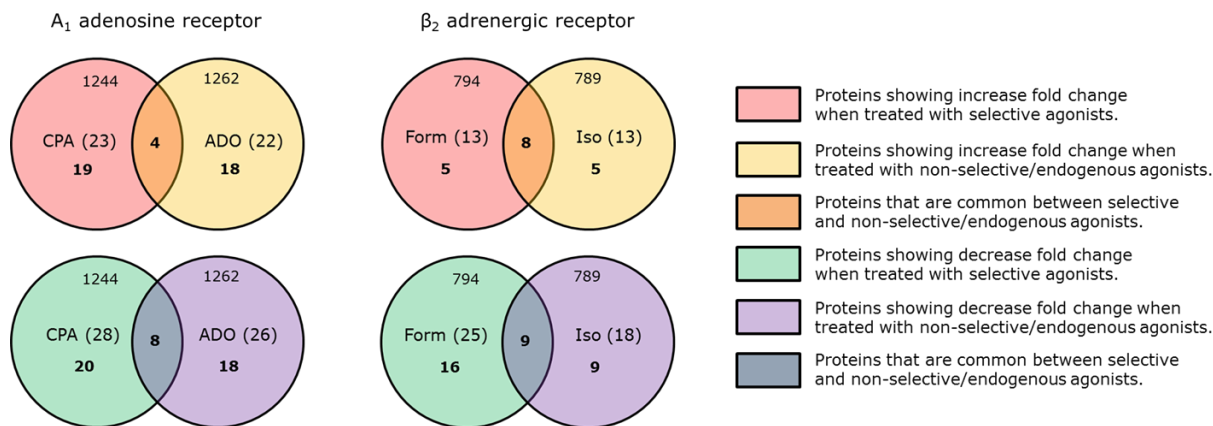


Fig. 7.4: Venn diagram illustrating number of proteins which reveal agonist- and receptor-specific changes in levels of proteins eluted from CaptAvidin™-agarose compared to control unstimulated cells. Numbers at the top of the circles represent total number of proteins identified, numbers in the brackets represent significant number of proteins in that data set as compared to control and the numbers in bold represent unique and/or similar proteins.

From the SWATH MS data analysis it can be seen that there are a significant number of novel increased and decreased proteins following A₁R or β₂-AR activation. There is a considerable overlap between proteins/substrates identified following treatment with selective versus non-selective/endogenous agonists, with changes in these protein levels occurring in the same direction. Furthermore, there are several proteins that are altered in the same direction in lysates subjected to ligands activating the A₁R and β₂-AR. This suggests that there are some common proteins/substrates of TG2 modulated by these receptors.

7.3 Pathway analysis.

Proteins identified from SWATH MS analysis showing increased/decreased levels in eluates from CaptAvidin™-agarose beads following stimulation of either A₁R and β₂-AR were further analysed using the Database for Annotation, Visualisation and Integrated Discovery (DAVID) v6.8 as described in section 2.9 (iii) of chapter II (<https://david.ncifcrf.gov/home.jsp>; Dennis et al, 2003). Data generated from selective/non-selective agonists for either A₁R and β₂-AR were pooled and processed to identify proteins significantly enriched in a pathway following these treatments. Figure 7.5 represents pathways identified by DAVID analysis as showing a significant enrichment of proteins following activation of the indicated receptor.

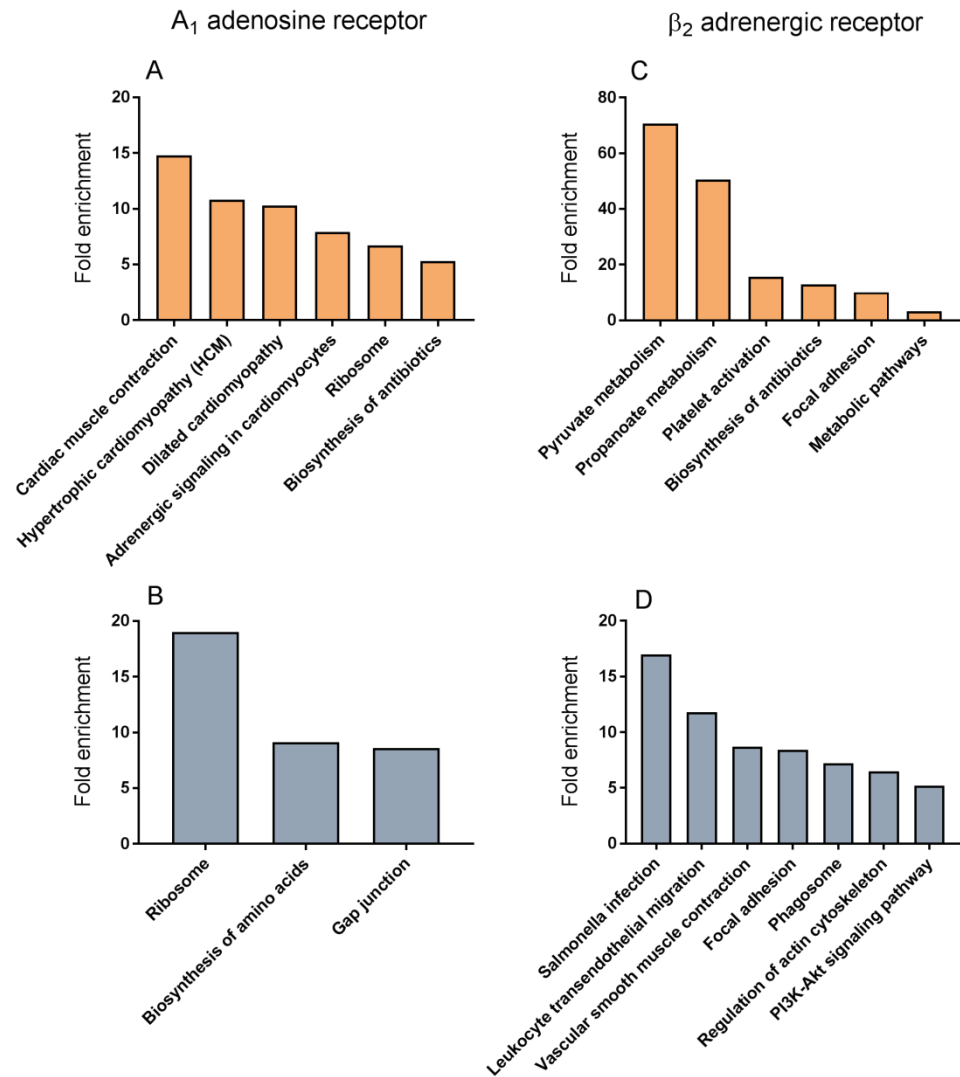


Fig. 7.5: Identification of pathways associated with the A₁R- and β₂-AR-induced TG2 protein substrates. (A, C) Pathways associated with the A₁R- and β₂-AR-induced TG2 protein substrates showing increased levels in eluates from CaptAvidin™-agarose columns. (B, D) Pathways associated with the A₁R- and β₂-AR-induced TG2 protein substrates showing decreased levels in eluates from CaptAvidin™-agarose columns.

Fold enrichment analysis carried out by the software can be defined as the ratio of two proportions. For instance, if 20/200 (i.e. 10%) of the input proteins are involved in "contraction of cardiac muscle" and the background information gathered from experimental evidence is 100/10000 proteins (i.e. 1%) associated with "contraction of cardiac muscle", then there is a 10% / 1% = 10 fold enrichment of the input proteins in the "contraction of cardiac muscle" pathway. Since fold enrichment is calculated in this manner, several proteins are associated with a number of pathways, as there is overlap between pathways. Tables 9-12 illustrate proteins identified by SWATH-MS whose profile is enriched in the pathways shown in figure 7.5.

Table 9. Identification of proteins significantly enriched in the stated pathways showing **increased** levels in eluates from CaptAvidin™-agarose columns following **A₁R** activation.

Pathway Name	Uniprot Accession	Protein Name
Cardiac muscle contraction	P12075	cytochrome c oxidase subunit 5B
	P04692	tropomyosin 1, alpha
	Q63610	tropomyosin 3
	P09495	tropomyosin 4
Hypertrophic cardiomyopathy (HCM)	P04692	tropomyosin 1, alpha
	Q63610	tropomyosin 3
	P09495	tropomyosin 4
Dilated cardiomyopathy	P04692	tropomyosin 1, alpha
	Q63610	tropomyosin 3
	P09495	tropomyosin 4
Adrenergic signaling in cardiomyocytes	Q4QQT4	protein phosphatase 2 scaffold subunit A beta
	P04692	tropomyosin 1, alpha
	Q63610	tropomyosin 3
	P09495	tropomyosin 4
Ribosome	P41123	ribosomal protein L13
	P62718	ribosomal protein L18A
	P62890	ribosomal protein L30-like
	P62859	ribosomal protein S28
Biosynthesis of antibiotics	Q8VHF5	citrate synthase
	P00507	glutamic-oxaloacetic transaminase 2
	P05708	hexokinase 1
	P04642	lactate dehydrogenase A

Proteins identified by SWATH MS analysis showing increased levels in eluates from CaptAvidin™-agarose columns following A₁R activation were further analysed by DAVID bioinformatics software with parameters count per protein > 2 and *P<0.05; algorithms used described by Huang et al, (2009). Proposed proteins/substrates of TG2 are involved in the corresponding significantly enriched pathway.

Table 10. Identification of proteins significantly enriched in the stated pathway showing **decreased** levels in eluates from CaptAvidin™-agarose columns following **A₁R** activation.

Pathway Name	Uniprot Accession	Protein Name
Ribosome	P23358	60S ribosomal protein L12-like
	P62864	FAU, ubiquitin like and ribosomal protein S30 fusion
	P62907	ribosomal protein L10A
	Q63507	ribosomal protein L14
	P47198	ribosomal protein L22
	P62832	ribosomal protein L23
	P39032	ribosomal protein L36
	P62425	ribosomal protein L7a
	P62845	ribosomal protein S15
	P27952	ribosomal protein S2
	P62850	ribosomal protein S24
	P62275	ribosomal protein S29
	P62853	ribosomal protein s25
Biosynthesis of amino acids	P04797	glyceraldehyde-3-phosphate dehydrogenase
	O08651	phosphoglycerate dehydrogenase
	Q5PQJ6	pyrroline-5-carboxylate reductase-like
Gap junction	P85108	tubulin, beta 2A class Iia
	Q6P9T8	tubulin, beta 4B class Ivb
	P69897	tubulin, beta 5 class I

Proteins identified by SWATH MS analysis showing decreased levels in eluates from CaptAvidin™-agarose columns following A₁R activation were further analysed by DAVID bioinformatics software with parameters count per protein > 2 and *P<0.05; algorithms used described by Huang et al, (2009). Proposed proteins/substrates of TG2 are involved in the corresponding significantly enriched pathway.

Table 11. Identification of proteins significantly enriched in the stated pathway showing **increased** levels in eluates from CaptAvidin™-agarose columns following β_2 -AR activation.

Pathway Name	Uniprot Accession	Protein Name
Pyruvate metabolism	P11497	acetyl-CoA carboxylase alpha
	P11884	aldehyde dehydrogenase 2 family (mitochondrial)
	P04642	lactate dehydrogenase A
	P04636	malate dehydrogenase 2
Propanoate metabolism	P11497	acetyl-CoA carboxylase alpha
	P04642	lactate dehydrogenase A
Platelet activation	P02454	collagen type I alpha 1 chain
	P02466	collagen type I alpha 2 chain
	P13941	collagen type III alpha 1 chain
Biosynthesis of antibiotics	P11884	aldehyde dehydrogenase 2 family (mitochondrial)
	P04642	lactate dehydrogenase A
	P04636	malate dehydrogenase 2
	O08651	phosphoglycerate dehydrogenase
Focal adhesion	P02454	collagen type I alpha 1 chain
	P02466	collagen type I alpha 2 chain
	P13941	collagen type III alpha 1 chain
Metabolic pathways	P11497	acetyl-CoA carboxylase alpha
	P36972	adenine phosphoribosyl transferase
	P11884	aldehyde dehydrogenase 2 family (mitochondrial)
	P04642	lactate dehydrogenase A
	P04636	malate dehydrogenase 2
	O08651	phosphoglycerate dehydrogenase

Proteins identified by SWATH MS analysis showing increased levels in eluates from CaptAvidin™-agarose columns following β_2 -AR activation were further analysed by DAVID bioinformatics software with parameters count per protein > 2 and * $P < 0.05$; algorithms used described by Huang et al, (2009). Proposed proteins/substrates of TG2 are involved in the corresponding significantly enriched pathway.

Table 12. Identification of proteins significantly enriched in the stated pathway showing **decreased** levels in eluates from CaptAvidin™-agarose columns following β_2 -AR activation.

Pathway Name	Uniprot Accession	Protein Name
Salmonella infection	P09527	RAB7A, member RAS oncogene family
	Q62868	Rho-associated coiled-coil containing protein kinase 2
	P38650	dynein cytoplasmic 1 heavy chain 1
	D3ZHA0	filamin C
Leukocyte transendothelial migration	Q62868	Rho-associated coiled-coil containing protein kinase 2
	P49134	integrin subunit beta 1
	P13832	myosin light chain 12A
	Q64122	myosin light chain 9
Vascular smooth muscle contraction	Q62868	Rho-associated coiled-coil containing protein kinase 2
	P63269	actin, gamma 2, smooth muscle, enteric
	Q64122	myosin light chain 9
Focal adhesion	Q62868	Rho-associated coiled-coil containing protein kinase 2
	D3ZHA0	filamin C
	P49134	integrin subunit beta 1
	P13832	myosin light chain 12A
Phagosome	Q64122	myosin light chain 9
	P09527	RAB7A, member RAS oncogene family
	P38650	dynein cytoplasmic 1 heavy chain 1
	P49134	integrin subunit beta 1
Regulation of actin cytoskeleton	Q6P9T8	tubulin, beta 4B class IVb
	Q62868	Rho-associated coiled-coil containing protein kinase 2
	P49134	integrin subunit beta 1
	P13832	myosin light chain 12A
PI3K-Akt signaling pathway	Q64122	myosin light chain 9
	Q66HD0	heat shock protein 90 beta family member 1
	P82995	heat shock protein HSP 90-alpha
	P49134	integrin subunit beta 1
	P68255	tyrosine 3-monooxygenase/tryptophan 5-monooxygenase activation protein, theta
P63102	tyrosine 3-monooxygenase/tryptophan 5-monooxygenase activation protein, zeta	

Proteins identified by SWATH MS analysis showing decreased levels in eluates from CaptAvidin™-agarose columns following β_2 -AR activation were further analysed by DAVID bioinformatics software with parameters count per protein > 2 and * $P < 0.05$; algorithms used described by Huang et al, (2009). Proposed proteins/substrates of TG2 are involved in the corresponding significantly enriched pathway.

From the pathway analysis, it can be clearly seen that there are a significant number of proteins enriched and allocated to a pathway upon activation of either A₁R or β₂-AR. This also implies a role for TG2 in these pathways, as the proteins analysed are TG2 substrates/interacting proteins.

7.4 Western blot confirmation of VDAC1 and HK1.

Confirmation of proteins identified by SWATH MS (one novel (HK1) and one known (VDAC1) substrate of TG2) was investigated using western blotting. Briefly, H9c2 cells were labelled with biotin-x-cadaverine and following labelling were treated with 100 nM CPA and 100 μM adenosine. Cell lysates were then subjected to CaptAvidin™-agarose affinity chromatography as described in section 2.9 (i) of chapter II. Following enrichment, immunoprecipitation of the lysate was carried out as described in section 2.7 of chapter II using VDAC1- and HK1- specific antibodies. Western blotting was carried out as described in section 2.6 of chapter II with minor modifications. Rather than using primary and secondary antibodies, blots were incubated overnight at 4°C with ExtrAvidin®-HRP (1:5000 dilution) to identify biotinylated proteins. Following incubation, the membranes were imaged and quantified.

Figures 7.6 and 7.7 illustrate that treatment with 100 nM CPA or 100 μM adenosine for 10 min significantly increased the incorporation of biotin-X-cadaverine into TG2 substrates, namely HK1 and VDAC1. Incorporation of biotin-X-cadaverine into both HK1 and VDAC1 was significantly inhibited by pre-treatment with Z-DON and R283, providing evidence that these changes occur via interaction with TG2.

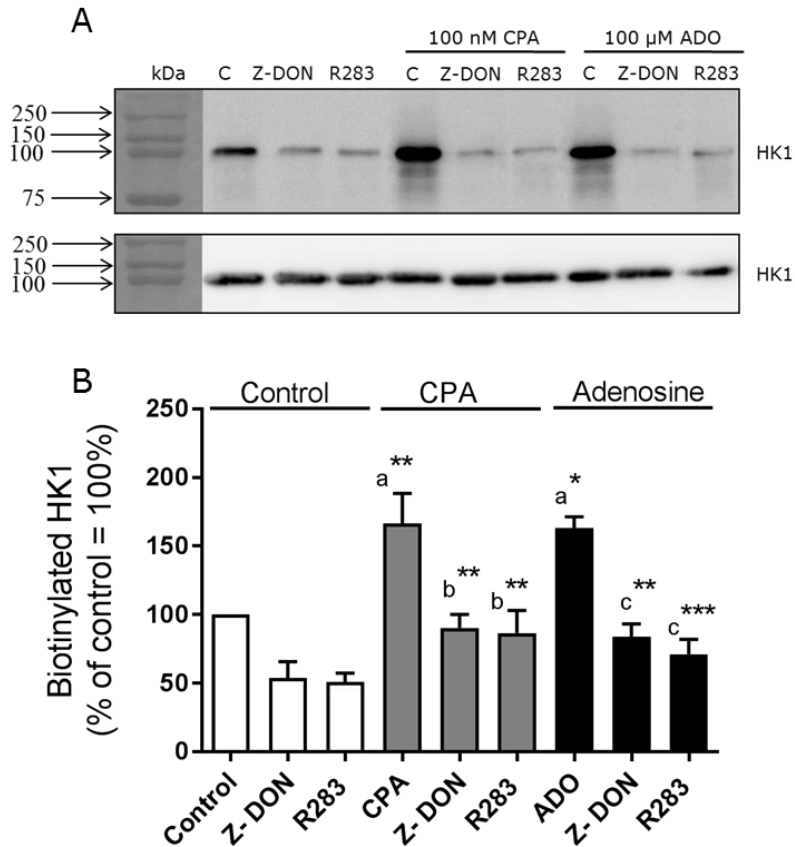


Fig. 7.6: Detection of hexokinase 1 as a TG2 protein substrate in CPA- and adenosine-treated H9c2 cells. Cells were incubated with 1 mM biotin-X-cadaverine for 6 h, after which they were treated for 1 h with the TG2 inhibitors Z-DON (150 μ M) or R283 (200 μ M) before stimulation with CPA (100 nM) or adenosine (100 μ M) for 10 min. Biotin-X-cadaverine-labelled proteins were enriched using CaptAvidin™ agarose sedimentation beads and eluted proteins were subjected to immunoprecipitation using a hexokinase 1 specific antibody. Samples were subsequently analysed by probing the blots with ExtrAvidin®-HRP. Quantified data for CPA- and adenosine-induced increases in HK1 are expressed as a percentage of that observed in control cells (100%). Values are means \pm S.E.M. from three independent experiments. * P <0.05, ** P <0.01 and *** P <0.001, (a) versus control response, (b) versus CPA alone, (c) versus adenosine alone.

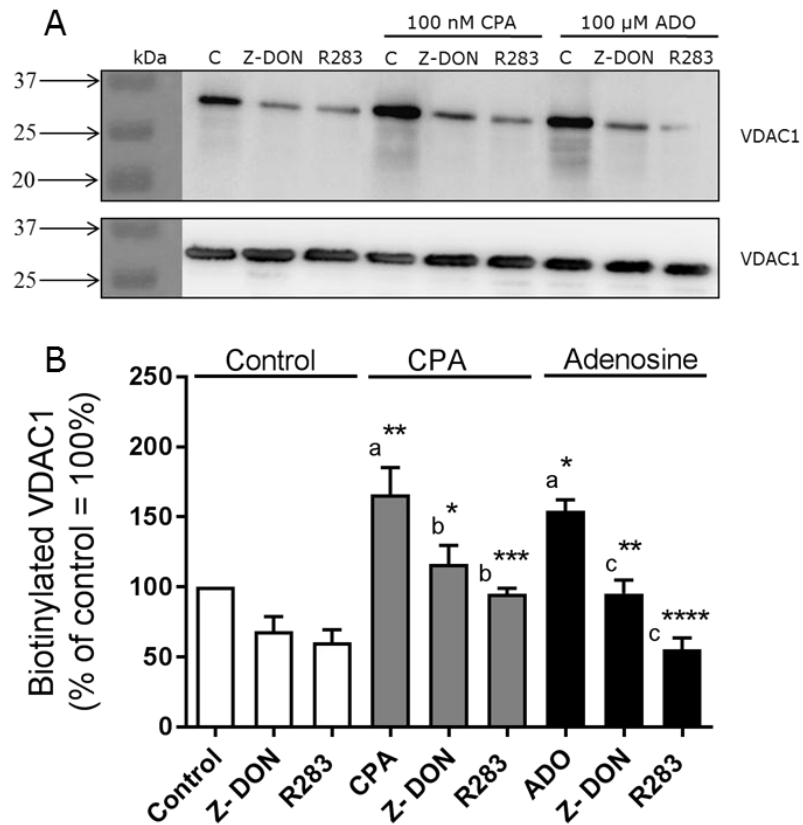


Fig. 7.7: Detection of Voltage-Dependent Anion Channel 1 (VDAC1) as a TG2 protein substrate in CPA- and adenosine-treated H9c2 cells. Cells were incubated with 1 mM biotin-X-cadaverine for 6 h, after which they were treated for 1 h with the TG2 inhibitors Z-DON (150 μM) or R283 (200 μM) before stimulation with CPA (100 nM) or adenosine (100 μM) for 10 min. Biotin-X-cadaverine-labelled proteins were enriched using CaptAvidin™ agarose sedimentation beads and eluted proteins were subjected to immunoprecipitation using a VDAC1 specific antibody. Samples were subsequently analysed by probing the blots with ExtrAvidin®-HRP. Quantified data for CPA- and adenosine-induced increases in VDAC1 are expressed as a percentage of that observed in control cells (100%). Values are means ± S.E.M. from three independent experiments. * $P < 0.05$, ** $P < 0.01$, *** $P < 0.001$ and **** $P < 0.0001$, (a) versus control response, (b) versus CPA alone, (c) versus adenosine alone.

From the data presented in this study, it can be concluded that this novel approach can be successfully used to identify and quantify TG2 substrates and to relate them to associated pathways.

7.5 Discussion.

This present study represents a novel proteomic approach to the identification of TG2 substrates. Furthermore, this study not only identifies novel substrates but also provides a quantitative analysis of their modification by TG2 in response to GPCR activation.

CaptAvidin™-agarose affinity chromatography

One recent study investigating TG2 substrates adopted a similar approach of enrichment using CaptAvidin™-agarose sedimentation beads followed by 2D-electrophoresis and MALDI-TOF analysis in H9c2 cells (Almami et al, 2014). However, this study used non-specific activators of PKA and PKC (forskolin and PMA) which do not target a specific GPCR and might have other effects on signalling/ TG2 and therefore the substrates of TG2. The proteomic findings of the present study targeted specific GPCRs to amplify responses generated by a single receptor and eliminate the possibility of direct activation of signalling pathways, which might have effects on TG2 and its substrates. However, one of the obvious shortcomings of this study is that even though activating one GPCR, signalling profiles can differ significantly between agonists at the same receptor (e.g. formoterol versus isoprenaline in chapter V) which could account for variability in the substrates identified. Biotin-X-cadaverine labelling of cells and its enrichment using CaptAvidin™-agarose sedimentation beads is widely used to identify enzyme substrates as well as to purify immunoglobulins (Morag, 1996; Bolivar, 2008). CaptAvidin™ has a selective nitrated tyrosine residue in its biotin-binding site, which reduces the affinity of biotinylated proteins above pH 10. Consequently, at acidic or neutral pH biotinylated proteins can be adsorbed (association constant $K_a = 10^9\text{M}^{-1}$) and released at pH 10 (Morag, 1996; Bolivar, 2008). This approach, followed by mass spectrometry has been applied previously to identify novel TG2 substrates (Ichikawa et al, 2008; Almami et al, 2014; Sileno et al, 2014).

SWATH MS identification of proteins

Despite providing several advantages over SRM and shotgun techniques, one of the obvious limitations of SWATH is that it requires preliminary selection of peptides to quantify from i.e. a spectral library generated from pooling samples and not directly searched against a database. It also allows monitoring of only a limited number of samples per run e.g. better elution of peptides is possible if the LC run is longer, however it's not feasible due to time and expense constraints. However, with this small limitation in mind the main advantage of SWATH is that it creates a permanent record of all theoretical fragment ion spectra in the sample that can be detected. This permanent record can be interrogated at a future date using an improved spectral library.

It is interesting to note that the confidence level used for the A₁R (60%) and β₂-AR (70%) analysis is different. This compromise in the confidence level can be explained by the differences in the injection methods applied, SWATH variable windows and the accumulation times used. Even though the instrument (SCIEC TripleTOF® 6600), column (YMC Triart C₁₈ 150mmX0.3mm 3 μl dam), constant gradient flow rate (5 μl/min) and LC run times (60 min) were similar, the injection methods were very different. The A₁R study used direct injection approach (samples directly injected onto the column) while during the β₂-AR study used an automated trapelute column prior to the sample reaching the column (an addition to the existing system). This trapelute column adds a desalting step which ensures that the sample is free of salts and detergents, which might interfere with the column binding and elution, as well as ionisation of the samples. Further differences in these studies were the SWATH variable windows and accumulation time. SWATH variable windows are a set of precursor acquisition windows, which are typically designed to cover the full mass range (400-1200 m/z), within the cycle time (usually 2-4 seconds). These windows can be variable, for instance, smaller windows (e.g. 5 Da) for dense m/z regions and wider windows (e.g. 25 Da) for lighter m/z regions and require optimisation for specific experiments. The A₁R study used 40 variable windows and a 50 millisecond accumulation time per window while the β₂-AR study used 100 variable windows and a 25 millisecond accumulation time per window. This difference makes the β₂-AR study much more sensitive as many more peptides were scanned with better precision. These more sensitive settings were not available during the A₁R study, due to the technique being quite novel at the time of these experiments being performed.

Once the protein lists were retrieved from the OneOmics, the proteins were searched against the TRANSDAB database (http://genomics.dote.hu/wiki/index.php/Main_Page; Csoz et al, 2009). TRANSDAB is a transglutaminase substrate database that contains an entry for each of the substrate proteins identified, source of organism used, information about the type of study (e.g. *in-vitro/in-vivo*) and its location (intracellular or extracellular) for the entire transglutaminase family. A significant limitation is that this database was last updated in February 2008. Hence, along with searching against the database, a manual literature search (using Pubmed) was performed to identify whether the given protein was a novel or known TG2 substrate.

Comparison of proteins either revealing an increase or decrease following treatment with selective/non-selective or endogenous agonists of the same receptor highlights some interesting similarities as well as differences. This could be explained as follows. Firstly, the non-selective/endogenous agonists could trigger TG2-mediated incorporation of biotin-X-cadaverine into several proteins via a different receptor belonging to the same family and as shown previously (chapter V), there could be a difference in the signalling pathway (i.e. G_s versus G_{1/o}) triggered even when activating

just a single receptor. Finally, it is important to bear in mind that only biotin-X-cadaverine-modified substrates have been considered for this study. TG2 can also incorporate other endogenous intracellular proteins (e.g. spermine, spermidine, putrescine) which have not been considered. When performing the analysis the mass shift (+311.4429) due to tagging with biotin-X-cadaverine was taken into account. However, since SWATH MS creates a permanent record of all theoretical fragment ion spectra in the sample, these modifications can be considered at a later date. This was not possible for this present study due to time and expense constraints. In relation to the current data, it is conceivable that the proteins that showed decreased levels in eluates from CaptAvidin™-agarose columns following A₁R and β₂-AR activation represent deamidation and/or altered transamidation and/or interactions with TG2 substrate binding partners. However, further work is necessary to determine the mechanism underlying the observed decreases.

Pathway analysis

To take an unbiased view of the substrates/interacting proteins identified and to select the most biologically relevant targets for further investigation, pathway analysis using DAVID bioinformatics software was implemented to examine the pathways where these proteins are most likely to function. Although it would have been ideal to investigate all of the proteins identified in the list, this was not technically possible due to time and expense constraints. For pathway analysis, proteins were pooled as the signalling profiles of selective/non-selective agonists are quite different and the purpose of this study was to identify substrates of TG2 upon activation of either A₁R or β₂-AR. It is quite clear that some of the substrates identified play significant roles in various pathways; for instance tropomyosin plays a role in contraction, hypertrophic and dilated cardiomyopathy and adrenergic signalling in cardiomyocytes. This illustrates the multifunctional role of a particular substrate in different pathways as well as crosstalk between pathways. Even though the software only considers the experimental data available for performing pathway analysis, one of the limitations is that it considers the organism as a whole and does not allow selection of a particular cell/tissue type. Hence, the pathways identified need to be scrutinized for relevance depending on the cell/tissue type. This does not mean that the protein is not present but simply that it does not perform this function in the given cell/tissue type. It might however play a function in the specific given cell type, which is different and is yet to be identified. For the purpose of this study only substrates that have been previously associated with cellular functions relevant to cardiac cells will be discussed.

i. Hexokinase 1:

Hexokinase 1 (HK1) is an enzyme involved in glycolysis and plays a key role in many metabolic pathways. Hexokinases carry out the first step of glycolysis by converting glucose to glucose-6-phosphate. Glucose-6-phosphate can then

continue to have either a catabolic or an anabolic fate. Thus, hexokinase acts as a gatekeeper for metabolic fates (Depre et al, 1999). Constant ATP generation and turnover via metabolism plays a key role in maintaining the heart's mechanical function and hence hexokinase acts as a regulator of metabolism (Depre et al, 1999; Calmettes et al, 2015). Apart from their metabolic function, hexokinases also have a role in regulating mPTP opening directly. HK1 is strongly anti-apoptotic when bound to the outer mitochondrial membrane, putatively to VDAC1 (Pastorino and Hoek, 2008; Shoshan-Barmatz et al, 2009). It has therefore been implicated in ischaemic preconditioning of the heart (Murry et al, 1986). During ischaemia, there is greater energy demand for cell survival. HK1 is hence recruited to mitochondria to maximise glucose-6-phosphate production to meet this demand. Also, when recruited to the mitochondrion, HK1 occupies binding sites which would otherwise be occupied by Bax and BAK to initiate apoptosis following this ischaemic insult (Southworth et al, 2007). Therefore, HK1 is an important substrate of TG2, which has been shown to be significantly increased upon the A₁R-induced TG2 activation (figure 7.6), and hence can be linked with A₁R-induced TG2-mediated cardioprotection seen in chapter VI.

ii. *Voltage-Dependent Anion Channel 1 (VDAC1):*

VDAC1, also known as outer mitochondrial membrane protein porin 1, is a voltage-dependent anion channel, which allows the flow of metabolites (e.g. pyruvate) and ions (e.g. Ca²⁺) across the outer mitochondrial membrane. It is known to interact with many proteins (e.g. BAX, dynein, mitochondrial heat-shock proteins 70 and 74, Hexokinases, etc; Schwarzer et al, 2002; Anflous-Pharayra et al, 2007; Martel et al, 2014) and is typically considered to be a pro-apoptotic protein (Shoshan-Barmatz et al, 2010; Prezma et al, 2013). However, recently an anti-apoptotic function of VDAC1 has been reported (Abu-Hamad et al, 2009; Shoshan-Barmatz et al, 2009; Arbel et al, 2012; Martel et al, 2014; Monaco et al, 2015). It is hypothesised that the protective effects of VDAC1 are due to its binding with HK1, which closes the mPTP and prevents Bax-induced translocation of cytochrome c and the activation of apoptosis (Arzoine et al, 2009; McCommis and Baines, 2012). Moreover, Rosa and colleagues recently recognised the neuro-protective effects of hexokinase and VDAC1 in several neurological disorders such as Alzheimer's disease (Rosa et al, 2016). TG2 has been extensively implicated in neurodegenerative pathologies and it could be speculated that VDAC1 and HK1 serving as its substrates mediate this protection. However, it is quite clear that in H9c2 cells VDAC1 serves as a substrate for TG2 (Figure 7.7; Almami et al, 2014). Since HK1 is a novel target identified in this present study, it suggests that the A₁R-induced TG2-mediated cardioprotection (Chapter VI) could be mediated via

HK1 and VDAC1 acting as TG2 substrates. However, further work is warranted to confirm this hypothesis.

iii. Protein S100-A6:

Protein S100-A6, also known as calyculin, is a Ca^{2+} -binding protein, which is known to interact with caldesmon, calponin, tropomyosin, actin and myosin (Donato et al, 2013). Its interaction with tropomyosin is well documented (Golitsina et al, 1996; Orre et al, 2007) and in fibroblasts it is known that depletion of S100-A6 results in disorganisation of tropomyosin-associated cytoskeletal filaments (Breen and Tang, 2003). Nedjadi and colleagues have also reported that in pancreatic cancer cell lines, depletion of S100-A6 results in loss of motility, which is partly caused by S100-A6 interaction with tropomyosin. Hence, it is conceivable that TG2-mediated modulation of Protein S100-A6 function plays a role in β_2 -AR-induced regulation of cardiomyocyte contractility. It is also suggested that S100-A6 inhibits apoptosis when its activation is induced by tumor necrosis factor- α via an NF- κ B-dependent manner (Tsoporis et al, 2008). When S100-A6 interacts with calyculin-binding protein/Siah-interacting protein (CacyBP/SIP), it exerts cardioprotective effects against ischaemia/reperfusion injury (Au et al, 2006; Schneider and Filipek, 2011). This suggests a possible role for S100A6 in β_2 -AR induced-cardioprotection.

iv. Tropomyosin:

Tropomyosin is a protein that is involved in contraction of muscle cells, whereas in non-muscle cells, it is responsible for maintaining cytoskeletal architecture. Along with the troponin complex, tropomyosin is associated with myosin and actin to regulate contractile functions (Wieczorek, 2016). It is therefore interesting to note that Myosin regulatory light polypeptide 9, Myosin light polypeptide 6, Myosin-9, Myosin regulatory light chain RLC-A, Actin, gamma-enteric smooth muscle, Alpha-actinin-4 are identified in this study. There are four isoforms of tropomyosin with further diversity resulting from alternative splicing, namely, tropomyosin 1 or α , tropomyosin 2 or β , tropomyosin 3 or γ and tropomyosin 4 or δ (Tropomyosin alpha-3 chain, Tropomyosin alpha-4 chain, Tropomyosin alpha-1 chain identified in this study), however, tropomyosin 3 or γ is not known to be expressed in cardiomyocytes (Bai et al, 2013). These isoforms play an important role during development of the heart as well as the rate of contraction and relaxation. For instance, in transgenic hearts and isolated cardiomyocytes, myofilaments containing tropomyosin 2 (β) demonstrate an increase in calcium sensitivity and a decrease in the rightward shift of Ca^{2+} -force relation induced by cAMP-dependent phosphorylation thereby increasing contraction rate (Palmiter et al,

1996). In order to fully understand the function of tropomyosin in the heart, a number of studies to define the expression and function of these isoforms have been undertaken (for reviews see Katz, 1969; Wieczorek et al, 2008; Bai et al, 2013; Wieczorek, 2016). The presence of tropomyosin in the present study demonstrates that H9c2 cells have a cardiomyocyte-like phenotype, as tropomyosin is a marker for cardiac muscle. It can also be conceived that TG2-mediated modulation of tropomyosin plays a role in cardiomyocyte contraction. Furthermore, the pathway analysis for increased levels in eluates from CaptAvidin™-agarose beads following stimulation of the A₁R illustrates cardiac muscle contraction, hypertrophic cardiomyopathy (HCM) and dilated cardiomyopathy pathways, which all contain the tropomyosin elements identified in this study. Convincing evidence exists that dysregulation of tropomyosin leads to various cardiomyopathies (Kamisago et al, 2000; Van Driest et al, 2002; Marques and De Oliveria, 2016) and hence it is likely that the detection of tropomyosin within this study and experimental data from previous studies allowed the software to identify these pathways.

v. *Acetyl-CoA carboxylase:*

Acetyl-CoA carboxylase and its derivatives are involved in regulation of cardiac energy metabolism by playing a key role in metabolic pathways as well as influencing the activity of other enzymes (such as carnitine palmitoyltransferase 1 and malonyl-CoA decarboxylase) either in an allosteric manner or by altering substrate availability (Kolwicz et al, 2013). The heart requires a massive rate of ATP production and turnover to maintain its continuous mechanical function, which is provided by the mitochondria. The cardiac mitochondria are not only responsible for generating ATP but are also accountable for maintaining Ca²⁺ homeostasis, Ca²⁺ signalling and apoptosis (Kolwicz et al, 2013). Although the metabolic network is responsible for generating ATP, metabolites generated during the process are known to regulate cell function. It is therefore interesting to note that Acetyl-CoA carboxylase 1, Adenine phosphoribosyl transferase, Aldehyde dehydrogenase 2 family (mitochondrial), Lactate dehydrogenase A, Malate dehydrogenase 2, Phosphoglycerate dehydrogenase are identified in this study. There have been a number of studies involved in identifying the role of metabolites in cardiac function as dysregulation of any one of them can cause impairment of cardiac function by attenuation of the metabolic pathway (for reviews see Bishop and Altschuld, 1969; Kolwicz et al, 2012; Maillet et al, 2013; Doenst et al, 2013; Alrob and Lopaschuk, 2014; Pietrocola et al, 2015; Munzel et al, 2015). Ca²⁺ overload during cardiac ischaemia/reperfusion injury is associated with the loss of mitochondrial function and opening of the permeability pore resulting in cell death. Studies have shown that TG2 knockout (TG2^{-/-}) ischaemia/reperfused

isolated hearts have increased infarct size and ventricular fibrillation as compared to ischaemia/reperfused wild type hearts (Szondy et al, 2006). Further interrogation of the molecular mechanisms underlying this phenomenon has led to the understanding that this sensitivity of TG2^{-/-} ischaemia/reperfused isolated hearts is not due to impaired adrenoceptor signalling but due to low baseline stores of high energy phosphates and defects in mitochondrial and ATPase function (Szondy et al, 2006). Piacentini and colleagues have shown that TG2 co-localizes with mitochondria and TG2 overexpression leads to mitochondrial hyperpolarization (Piacentini et al, 2002). Hence, these studies reveal a novel role for TG2 in the maintenance of mitochondrial respiratory function. Since most of the metabolic pathways identified in this study are associated with the mitochondria and are involved in its respiratory function to generate ATP, it is therefore likely that TG2 interacts with these metabolites and might play a role in the modulation of their activity.

From these findings, it is clear that the modulation of TG2 and its substrates by the A₁R and β₂-AR is very complex. Using proteomic approaches several novel TG2 substrates were identified and assigned to pathways to reveal their biological relevance. Two of the substrates were validated, demonstrating the accuracy of the new approach. Data presented here therefore supports the notion that TG2 substrates/interacting proteins show differential modulation upon activation of the A₁R and β₂-AR which can lead to various effects on cellular responses.

Chapter VIII: Conclusions and further work

8.1 General conclusions.

This present study has provided novel data contributing to the understanding of the modulation of tissue transglutaminase (TG2) activity via GPCRs (A_1 adenosine receptor and β_2 -adrenoceptor) in H9c2 cardiomyoblasts. This modulation was based upon a multi-protein kinase-dependent pathway. Investigation into the cytoprotection offered by the A_1 R and the β_2 -AR against hypoxia- and hypoxia/re-oxygenation induced cell death has revealed that TG2 has a pivotal role in pharmacological pre- and post-conditioning. Furthermore, identification of novel TG2 substrates/interacting proteins has illustrated differential modulation via the A_1 R and the β_2 -AR which may contribute to differences in their cellular/physiological responses.

8.2 Further work.

TG2 regulation by GPCRs

To extend this body of work, it would be interesting and novel to investigate potential GPCR modulation of other TG2 activities such as GTPase activity (Bailey et al, 2004), kinase activity (Thangaraju et al, 2016) and/or isopeptidase activity (Oertel et al, 2007). Assays are available e.g. isopeptidase-fluorogenic assay to evaluate isopeptidase activity of TG2 (Zedira, GmbH), which would enable these activities to be explored. Furthermore, since other TG isoforms (TG1 and TG3) are also expressed in H9c2 cells (chapter III- figure 3.12 and 3.13), it would be of interest to investigate if the activities of these enzymes can also be regulated by GPCRs. Also, it would be worthwhile to assess GPCR mediated activation of TG2 in cells derived from transgenic animals lacking TG2.

It would be important to implement another way of inhibiting TG2. The use of siRNA would allow silencing of TG2 without using pharmacological/chemical inhibitors which may not be 100% TG2 selective and hence would further confirm the findings of this study. Preliminary work has been already performed with regards to optimisation of TG2 siRNA (appendix 1). It was found that treatment with TG2 siRNA for 72 h could knock down ~50% of protein expression. However, further experiments could not be performed due to time constraints.

β_2 -AR signalling and biased agonism

An interesting avenue to explore would be to screen numerous β_2 -AR agonists and elucidate the signalling pathway activated by them in H9c2 cardiomyoblasts. The possible role of $G_{i/o}$ and G_s proteins could then be uncovered and perhaps this could be linked in with modulation of the enzyme TG2 as well as the cytoprotection offered by the β_2 -AR. It is known that noradrenaline (the endogenous full agonist) can fully activate β_2 -AR-mediated G_s signalling/cAMP signalling pathway (Heubach et al, 2003;

Wang et al, 2008) in murine heart and primary cardiomyocytes, whereas clenbuterol (full agonist) solely activates β_2 -AR-mediated G_i signalling/IP₃ signalling pathway (Siedlecka et al, 2008) in isolated rat ventricular myocytes. Similar properties of coupling to different G-proteins (G_s and G_i proteins) have been exhibited by isoprenaline and adrenaline (both full agonists; Heubach et al, 2003; Wang et al, 2008; Liu et al, 2009) in cardiomyocytes. This study investigated effects of formoterol (long-acting β_2 -AR agonist) and isoprenaline (non-selective β -AR agonist). It would be interesting to see if other long acting β_2 -AR agonists (salmeterol) and short acting β_2 -AR agonists such as (albuterol, metaproterenol, terbutaline) display similar phenomenon of coupling to $G_{i/o}$ and G_s proteins in H9c2 cardiomyoblasts.

TG2 phosphorylation

Another area of interest would be to determine the phosphorylation sites on TG2. Phosphoproteomic approaches would reveal which site(s) are being phosphorylated. For instance, ³²P tagging of ATP followed by strong cation-exchange chromatography and high accuracy multi-stage mass spectrometry could be one of the ways of identifying phosphoproteins. Previous studies have revealed that TG2 is phosphorylated by PKA at Ser²¹⁵ and Ser²¹⁶ (Mishra and Murphy, 2006) and at an unknown site(s) by PTEN-induced putative kinase 1 (PINK1; Min et al., 2015). It is also known that phosphorylation of TG2 by PKA at Ser²¹⁶ inhibits its transamidase activity and enhances its kinase activity (Mishra et al, 2007; Wang et al, 2012). Phosphoproteomic studies have also identified numerous phosphorylation sites in human TG2 (Ser⁵⁶, Ser⁶⁰, Tyr²¹⁹, Thr³⁶⁸, Tyr³⁶⁹, Ser⁴¹⁹, Ser⁴²⁷, Ser⁵³⁸, Ser⁵⁴¹ and Ser⁶⁰⁸; Rikova et al, 2007; Imami et al, 2008; Kettenbach et al, 2011; Bian et al, 2014; Palacios-Moreno et al, 2015) and rat TG2 (Tyr⁴⁴, Thr⁵⁸, Ser⁶⁸ and Ser⁴⁴⁹; Hoffert et al, 2006; Lundby et al, 2012). This study has shown that TG2 is phosphorylated upon activation of the A₁R and the β_2 -AR. Inhibition of an individual protein kinase that phosphorylates TG2 (e.g. ERK1/2, PKC etc.) and then performing phosphoproteomic analysis would reveal exactly which site on TG2 is phosphorylated by which protein kinase which is activated upon stimulation of the A₁R and the β_2 -AR. At present the relationship between the A₁R and the β_2 -AR-induced TG2 activity and phosphorylation is not known. Since the A₁R and the β_2 -AR induce TG2 activity in a time-dependent manner, it would be interesting to examine if this time course matches TG2 phosphorylation induced by these receptors.

TG2 substrates

The present study has identified several novel TG2 substrates/interacting proteins which illustrate differential modulation upon activation of the A₁R and the β_2 -AR, thus leading to various effects on cellular responses. This has uncovered several proteins which could make good targets for future work. It would be necessary to validate more of the identified substrates/interacting proteins and examine if they are

associated with cytoprotection. Moreover, also determine how TG2 modulation could potentially alter its biological function, cellular localisation and turnover. This would be achieved by using subcellular fractionation (to isolate various compartments) followed by functional assays (ELISA).

TG2 cardioprotection and signalling pathways

It is known that the A₁R activates the RISK pathway (ERK1/2 and PKB) during ischaemic and ischaemia/reperfusion conditions (Cohen and Downey, 2015). However, it has not been investigated if the β₂-AR activates the RISK pathway under these conditions and hence would form an area of interest. It is known that the β₂-AR activates both ERK1/2 and PKB under normal conditions (Yang et al, 2010; Zhang et al, 2011). Therefore, it is conceivable that the β₂-AR activates both ERK1/2 and PKB under hypoxic conditions. As the A₁R activates TG2 and RISK pathways, it is possible that there could be a link between the protection offered by TG2 and these pathways under hypoxia and hypoxia/reoxygenation conditions. Also, it would be interesting to check if the switching between G_{i/o} and G_s proteins by different β₂-AR agonists plays a role in activation of the RISK pathway. Furthermore, it is known that TG2 binds to hypoxia inducible factor 1β (HIF1β) and suppresses HIF activity in neurons under ischaemic conditions (Filiano et al, 2008). It was later found that nuclear localisation of TG2 is necessary for suppression of HIF activity which is not dependent on TG2's interaction with HIF1β (Gundemir et al, 2013). Hence, it would be of interest to assess TG2's interaction with HIF1β and HIF signalling in H9c2 cardiomyocytes.

Alternative models

Extending this study to the use of isolated rat cardiomyocytes and ventricle strips would be the initial next steps to undertake, closely followed by the use of Langendorff-perfused rat heart and *in-vivo* studies. These approaches represent more physiological relevant models for the study of cardiovascular diseases and would validate the novel data obtained using H9c2 cardiomyoblasts. It would also be interesting to extend this study to neuronal cells as they reflect yet another area that is commonly subjected to ischaemic and ischaemic/reperfusion insult during stroke and would further add to the current understanding of the cytoprotective mechanism of TG2.

8.3 Concluding remarks.

In conclusion, this study has shown for the first time that activation of the A₁ adenosine receptor and the β₂-adrenoceptor modulates TG2 activity and phosphorylation via a multi protein kinase and extracellular Ca²⁺-dependent pathway in H9c2 cells. In addition, cytoprotection offered by the A₁R and β₂-AR against hypoxia and hypoxia/re-oxygenation injury is dependent on TG2. This study has also identified novel TG2 substrates/interacting proteins which could be potential therapeutic targets.

It is anticipated that this study will lead to further investigation into the modulation of TG2 by GPCRs, its role in pathophysiological circumstances such as ischaemia/reperfusion injury and potentially lead to novel drug discovery by either targeting TG2 or one of its substrates identified. Figure 8.1 summarises the findings of this study.

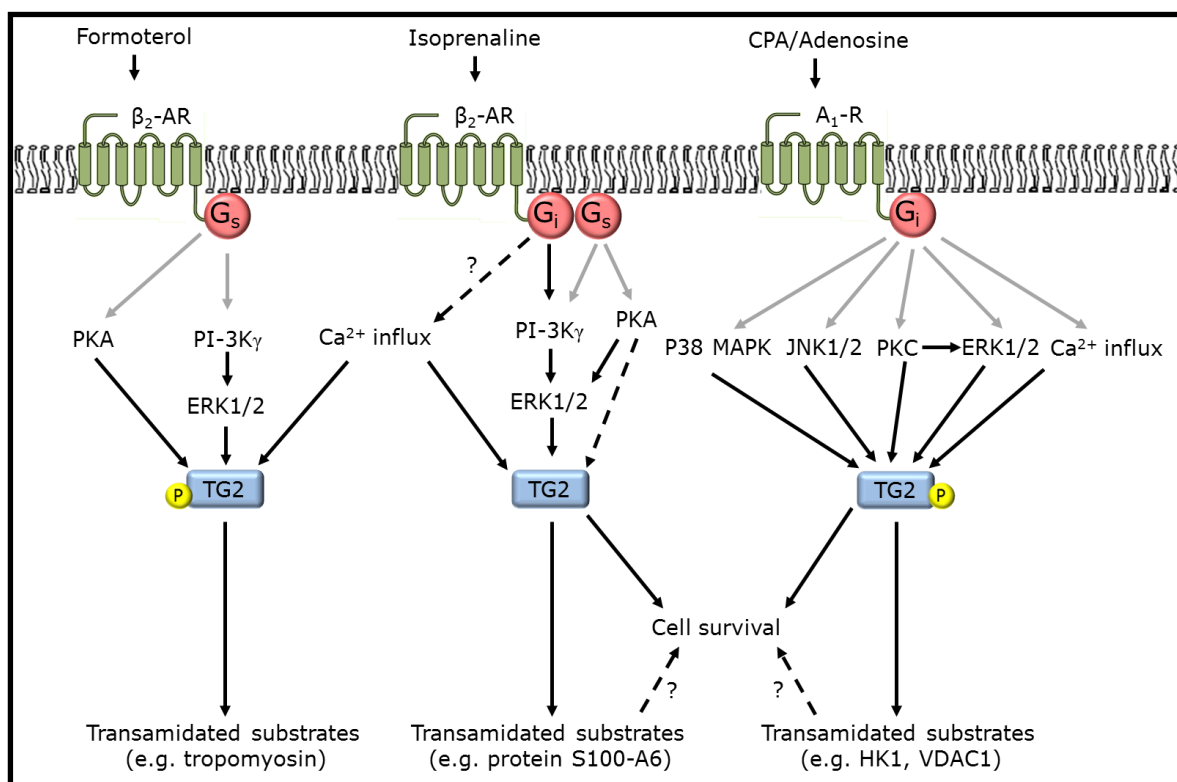


Fig 8.1: Summary of the findings in this study. Briefly, stimulation of the A₁ adenosine receptor (A₁R) by selective and endogenous agonists (CPA and adenosine, respectively) triggers activation of protein kinases (PKC, ERK1/2, JNK1/2 and p38 MAPK) along with influx of extracellular Ca²⁺ leading to increases in TG2 activity and TG2 phosphorylation. Similarly, stimulation of the β₂-adrenoceptor (β₂-AR) by selective and non-selective agonists (formoterol and isoprenaline, respectively) triggers activation of protein kinases via G_s- and G_{i/o}- proteins (PKA, PI-3K_γ and ERK1/2) along with influx of extracellular Ca²⁺ leading to increases in TG2 activity and TG2 phosphorylation. Cytoprotection against hypoxia and hypoxia/re-oxygenation was offered by the A₁R- and isoprenaline-mediated pre- and post-conditioning and was dependent on TG2. Substrate identification by SWATH-MS revealed several novel TG2 proteins/substrates which might be involved in cell survival. Solid black arrows represent findings of this study, dashed arrows represent findings of this study which need further work or were inconclusive and grey arrows represent published findings (not from the present study).

Bibliography

Abbracchio MP, Ceruti S, Barbieri D, Franceschi C, Malorni W, Biondo L, Burnstock G, Cattabeni F. (1995) A novel action for adenosine: apoptosis of astroglial cells in rat brain primary cultures. *Biochem Biophys Res Commun.* **213**(3):908-15.

Abo Alrob O, Lopaschuk GD. (2014) Role of CoA and acetyl-CoA in regulating cardiac fatty acid and glucose oxidation. *Biochem Soc Trans.* **42**(4):1043-51.

Abu-Hamad S, Arbel N, Calo D, Arzoine L, Israelson A, Keinan N, Ben-Romano R, Friedman O, Shoshan-Barmatz V. (2009) The VDAC1 N-terminus is essential both for apoptosis and the protective effect of anti-apoptotic proteins. *J Cell Sci.* **122**(Pt 11):1906-16.

Abu-Hamad S, Zaid H, Israelson A, Nahon E, Shoshan-Barmatz V. (2008) Hexokinase-I protection against apoptotic cell death is mediated via interaction with the voltage-dependent anion channel-1: mapping the site of binding. *J Biol Chem.* **283**(19):13482-90.

Adameova A, Goncalvesova E, Szobi A, Dhalla NS. (2016) Necroptotic cell death in failing heart: relevance and proposed mechanisms. *Heart Fail Rev.* **21**(2):213-21.

Agle KA, Vongsa RA, Dwinell MB. (2010) Calcium mobilization triggered by the chemokine CXCL12 regulates migration in wounded intestinal epithelial monolayers. *J Biol Chem.* **285**(21):16066-75.

Agnihotri N, Kumar S, Mehta K. (2013) Tissue transglutaminase as a central mediator in inflammation-induced progression of breast cancer. *Breast Cancer Res.* **15**(1):202.

Aikawa R, Komuro I, Yamazaki T, Zou Y, Kudoh S, Tanaka M, Shiojima I, Hiroi Y, Yazaki Y. (1997) Oxidative stress activates extracellular signal-regulated kinases through Src and Ras in cultured cardiac myocytes of neonatal rats. *J Clin Invest.* **100**(7):1813-21.

Akimov SS, Belkin AM. (2001) Cell surface tissue transglutaminase is involved in adhesion and migration of monocytic cells on fibronectin. *Blood.* **98**(5):1567-76.

Akimov SS, Krylov D, Fleischman LF, Belkin AM. (2000) Tissue transglutaminase is an integrin-binding adhesion coreceptor for fibronectin. *J Cell Biol.* **148**(4):825-38.

Alexander SP, Davenport AP, Kelly E, Marrion N, Peters JA, Benson HE, Faccenda E, Pawson AJ, Sharman JL, Southan C, Davies JA; CGTP Collaborators. (2015) The

- Concise Guide to PHARMACOLOGY 2015/16: G protein-coupled receptors. *Br J Pharmacol.* **172**(24):5744-869.
- Almami I, Dickenson JM, Hargreaves AJ, Bonner PL. (2014) Modulation of transglutaminase 2 activity in H9c2 cells by PKC and PKA signalling: a role for transglutaminase 2 in cytoprotection. *Br J Pharmacol.* **171**(16):3946-60.
- Altamirano F, Wang ZV, Hill JA. (2015) Cardioprotection in ischaemia-reperfusion injury: novel mechanisms and clinical translation. *J Physiol.* **593**(17):3773-88.
- Altuntas S, D'Eletto M, Rossin F, Hidalgo LD, Farrace MG, Falasca L, Piredda L, Cocco S, Mastroberardino PG, Piacentini M, Campanella M. (2014) Type 2 Transglutaminase, mitochondria and Huntington's disease: menage a trois. *Mitochondrion.* **19**(Pt A):97-104.
- Anderson ME, Brown JH, Bers DM. (2011) CaMKII in myocardial hypertrophy and heart failure. *J Mol Cell Cardiol.* **51**(4):468-73.
- Andringa G, Lam KY, Chegary M, Wang X, Chase TN, Bennett MC. (2004) Tissue transglutaminase catalyzes the formation of alpha-synuclein crosslinks in Parkinson's disease. *FASEB J.* **18**(7):932-4.
- Anflous-Pharayra K, Cai ZJ, Craigen WJ. (2007) VDAC1 serves as a mitochondrial binding site for hexokinase in oxidative muscles. *Biochim Biophys Acta.* **1767**(2):136-42.
- Antonyak MA, Li B, Regan AD, Feng Q, Dusaban SS, Cerione RA. (2009) Tissue transglutaminase is an essential participant in the epidermal growth factor-stimulated signaling pathway leading to cancer cell migration and invasion. *J Biol Chem.* **284**(27):17914-25.
- Antonyak MA, McNeill CJ, Wakshlag JJ, Boehm JE, Cerione RA. (2003) Activation of the Ras-ERK pathway inhibits retinoic acid-induced stimulation of tissue transglutaminase expression in NIH3T3 cells. *J Biol Chem.* **278**(18):15859-66.
- Arbel N, Ben-Hail D, Shoshan-Barmatz V. (2012) Mediation of the antiapoptotic activity of Bcl-xL protein upon interaction with VDAC1 protein. *J Biol Chem.* **287**(27):23152-61.
- Arzoine L, Zilberberg N, Ben-Romano R, Shoshan-Barmatz V. (2009) Voltage-dependent anion channel 1-based peptides interact with hexokinase to prevent its anti-apoptotic activity. *J Biol Chem.* **284**(6):3946-55.

- Au KW, Kou CY, Woo AY, Chim SS, Fung KP, Cheng CH, Waye MM, Tsui SK. (2006) Calcyclin binding protein promotes DNA synthesis and differentiation in rat neonatal cardiomyocytes. *J Cell Biochem.* **98**(3):555-66.
- Auchampach JA, Bolli R. (1999) Adenosine receptor subtypes in the heart: therapeutic opportunities and challenges. *Am J Physiol.* **276**(3 Pt 2):H1113-6.
- Bae J, Lee YS, Jeoung D. (2006) Down-regulation of transglutaminase II leads to impaired motility of cancer cells by inactivation of the protein kinase, Akt, and decrease of reactive oxygen species. *Biotechnol Lett.* **28**(15):1151-8.
- Baek KJ, Das T, Gray C, Antar S, Murugesan G, Im MJ. (1993) Evidence that the Gh protein is a signal mediator from alpha 1-adrenoceptor to a phospholipase C. I. Identification of alpha 1-adrenoceptor-coupled Gh family and purification of Gh7 from bovine heart. *J Biol Chem.* **268**(36):27390-7.
- Baek KJ, Das T, Gray CD, Desai S, Hwang KC, Gacchui R, Ludwig M, Im MJ. (1996) A 50 KDa protein modulates guanine nucleotide binding of transglutaminase II. *Biochemistry.* **35**(8):2651-7.
- Baek KJ, Kang S, Damron D, Im M. (2001) Phospholipase Cdelta1 is a guanine nucleotide exchanging factor for transglutaminase II (Galpha h) and promotes alpha 1B-adrenoreceptor-mediated GTP binding and intracellular calcium release. *J Biol Chem.* **276**(8):5591-7.
- Bai F, Wang L, Kawai M. (2013) A study of tropomyosin's role in cardiac function and disease using thin-filament reconstituted myocardium. *J Muscle Res Cell Motil.* **34**(3-4):295-310.
- Bailey CD, Graham RM, Nanda N, Davies PJ, Johnson GV. (2004) Validity of mouse models for the study of tissue transglutaminase in neurodegenerative diseases. *Mol Cell Neurosci.* **25**(3):493-503.
- Bailey CD, Johnson GV. (2005) Tissue transglutaminase contributes to disease progression in the R6/2 Huntington's disease mouse model via aggregate-independent mechanisms. *J Neurochem.* **92**(1):83-92.
- Baker JG. (2005) Evidence for a secondary state of the human beta3-adrenoceptor. *Mol Pharmacol.* **68**(6):1645-55.
- Baker JG. (2005) The selectivity of beta-adrenoceptor antagonists at the human beta1, beta2 and beta3 adrenoceptors. *Br J Pharmacol.* **144**(3):317-22.

- Baker JG. (2010) The selectivity of beta-adrenoceptor agonists at human beta1-, beta2- and beta3-adrenoceptors. *Br J Pharmacol.* **160**(5):1048-61.
- Baldwin AS Jr. (2001) Series introduction: the transcription factor NF-kappaB and human disease. *J Clin Invest.* **107**(1):3-6.
- Ballard-Croft C, Kristo G, Yoshimura Y, Reid E, Keith BJ, Mentzer RM Jr, Lasley RD. (2005) Acute adenosine preconditioning is mediated by p38 MAPK activation in discrete subcellular compartments. *Am J Physiol Heart Circ Physiol.* **288**(3):H1359-66.
- Ballarín M, Fredholm BB, Ambrosio S, Mahy N. (1991) Extracellular levels of adenosine and its metabolites in the striatum of awake rats: inhibition of uptake and metabolism. *Acta Physiol Scand.* **142**(1):97-103.
- Barve V, Ahmed F, Adsule S, Banerjee S, Kulkarni S, Katiyar P, Anson CE, Powell AK, Padhye S, Sarkar FH. (2006) Synthesis, molecular characterization, and biological activity of novel synthetic derivatives of chromen-4-one in human cancer cells. *J Med Chem.* **49**(13):3800-8.
- Basheer R, Arrigoni E, Thatte HS, Greene RW, Ambudkar IS, McCarley RW. (2002) Adenosine induces inositol 1,4,5-trisphosphate receptor-mediated mobilization of intracellular calcium stores in basal forebrain cholinergic neurons. *J Neurosci.* **22**(17):7680-6.
- Bayascas JR, Alessi DR. (2005) Regulation of Akt/PKB Ser473 phosphorylation. *Mol Cell.* **18**(2):143-5.
- Beattie WS, Wijeyesundera DN, Karkouti K, McCluskey S, Tait G, Mitsakakis N, Hare GM. (2010) Acute surgical anemia influences the cardioprotective effects of beta-blockade: a single-center, propensity-matched cohort study. *Anesthesiology.* **112**(1):25-33.
- Beavo JA, Rogers NL, Crofford OB, Hardman JG, Sutherland EW, Newman EV. (1970) Effects of xanthine derivatives on lipolysis and on adenosine 3',5'-monophosphate phosphodiesterase activity. *Mol Pharmacol.* **6**(6):597-603.
- Becker LB. (2004) New concepts in reactive oxygen species and cardiovascular reperfusion physiology. *Cardiovasc Res.* **61**(3):461-70.
- Begg GE, Carrington L, Stokes PH, Matthews JM, Wouters MA, Husain A, Lorand L, Iismaa SE, Graham RM. (2006a) Mechanism of allosteric regulation of transglutaminase 2 by GTP. *Proc Natl Acad Sci U S A.* **103**(52):19683-8.

- Begg GE, Holman SR, Stokes PH, Matthews JM, Graham RM, Iismaa SE. (2006) Mutation of a critical arginine in the GTP-binding site of transglutaminase 2 disinhibits intracellular cross-linking activity. *J Biol Chem.* **281**(18):12603-9.
- Belardinelli L, Isenberg G. (1983) Actions of adenosine and isoproterenol on isolated mammalian ventricular myocytes. *Circ Res.* **53**(3):287-97.
- Bergamini CM. (1988) GTP modulates calcium binding and cation-induced conformational changes in erythrocyte transglutaminase. *FEBS Lett.* **239**(2):255-8.
- Berlot CH, Bourne HR. (1992) Identification of effector-activating residues of Gs alpha. *Cell.* **68**(5):911-22.
- Bernassola F, Federici M, Corazzari M, Terrinoni A, Hribal ML, De Laurenzi V, Ranalli M, Massa O, Sesti G, McLean WH, Citro G, Barbetti F, Melino G. (2002) Role of transglutaminase 2 in glucose tolerance: knockout mice studies and a putative mutation in a MODY patient. *FASEB J.* **16**(11):1371-8.
- Bernstein D, Fajardo G, Zhao M, Urashima T, Powers J, Berry G, Kobilka BK. (2005) Differential cardioprotective/cardiotoxic effects mediated by beta-adrenergic receptor subtypes. *Am J Physiol Heart Circ Physiol.* **289**(6):H2441-9.
- Bernstein D, Fajardo G, Zhao M. (2011) The role of β -adrenergic receptors in heart failure: differential regulation of cardiotoxicity and cardioprotection. *Prog Pediatr Cardiol.* **31**(1):35-38.
- Berrutti L, Silverman JS. (1996) Cardiac myxoma is rich in factor XIIIa positive dendrophages: immunohistochemical study of four cases. *Histopathology.* **28**(6):529-35.
- Bian Y, Song C, Cheng K, Dong M, Wang F, Huang J, Sun D, Wang L, Ye M, Zou H. (2014) An enzyme assisted RP-RPLC approach for in-depth analysis of human liver phosphoproteome. *J Proteomics.* **96**:253-62.
- Bice JS, Jones BR, Chamberlain GR, Baxter GF. (2016) Nitric oxide treatments as adjuncts to reperfusion in acute myocardial infarction: a systematic review of experimental and clinical studies. *Basic Res Cardiol.* **111**(2):23.
- Bishop SP, Altschuld RA. (1970) Increased glycolytic metabolism in cardiac hypertrophy and congestive failure. *Am J Physiol.* **218**(1):153-9.
- Boehm JE, Singh U, Combs C, Antonyak MA, Cerione RA. (2002) Tissue transglutaminase protects against apoptosis by modifying the tumor suppressor protein p110 Rb. *J Biol Chem.* **277**(23):20127-30.

- Bollag WB, Zhong X, Dodd ME, Hardy DM, Zheng X, Allred WT. (2005) Phospholipase d signaling and extracellular signal-regulated kinase-1 and -2 phosphorylation (activation) are required for maximal phorbol ester-induced transglutaminase activity, a marker of keratinocyte differentiation. *J Pharmacol Exp Ther.* **312**(3):1223-31.
- Bolli R. (2007) Preconditioning: a paradigm shift in the biology of myocardial ischemia. *Am J Physiol Heart Circ Physiol.* **292**(1):H19-27.
- Bondar A, Lazar J. (2017) G protein Gi1 exhibits basal coupling but not preassembly with G protein-coupled receptors. *J Biol Chem.* pii: jbc.M116.768127. doi: 10.1074/jbc.M116.768127. [Epub ahead of print].
- Bonney S, Hughes K, Eckle T. (2014) Anesthetic cardioprotection: the role of adenosine. *Curr Pharm Des.* **20**(36):5690-5.
- Boucher M, Pesant S, Falcao S, de Montigny C, Schampaert E, Cardinal R, Rousseau G. (2004) Post-ischemic cardioprotection by A2A adenosine receptors: dependent of phosphatidylinositol 3-kinase pathway. *J Cardiovasc Pharmacol.* **43**(3):416-22.
- Brady AR, Gibbs JS, Greenhalgh RM, Powell JT, Sydes MR; (2005) POBBLE trial investigators. Perioperative beta-blockade (POBBLE) for patients undergoing infrarenal vascular surgery: results of a randomized double-blind controlled trial. *J Vasc Surg.* **41**(4):602-9.
- Bragança B, Oliveira-Monteiro N, Ferreirinha F, Lima PA, Faria M, Fontes-Sousa AP, Correia-de-Sá P. (2016) Ion Fluxes through KCa2 (SK) and Cav1 (L-type) Channels Contribute to Chronoselectivity of Adenosine A1 Receptor-Mediated Actions in Spontaneously Beating Rat Atria. *Front Pharmacol.* **7**:45.
- Brahmadevara N, Shaw AM, MacDonald A. (2004) ALpha1-adrenoceptor antagonist properties of CGP 12177A and other beta-adrenoceptor ligands: evidence against beta(3)- or atypical beta-adrenoceptors in rat aorta. *Br J Pharmacol.* **142**(4):781-7.
- Brahmadevara N, Shaw AM, MacDonald A. (2003) Evidence against beta 3-adrenoceptors or low affinity state of beta 1-adrenoceptors mediating relaxation in rat isolated aorta. *Br J Pharmacol.* **138**(1):99-106.
- Brawley L, Shaw AM, MacDonald A. (2000a) Beta 1-, beta 2- and atypical beta-adrenoceptor-mediated relaxation in rat isolated aorta. *Br J Pharmacol.* **129**(4):637-44.

- Brawley L, Shaw AM, MacDonald A. (2000b) Role of endothelium/nitric oxide in atypical beta-adrenoceptor-mediated relaxation in rat isolated aorta. *Eur J Pharmacol.* **398**(2):285-96.
- Breen EC, Tang K. (2003) Calcyclin (S100A6) regulates pulmonary fibroblast proliferation, morphology, and cytoskeletal organization in vitro. *J Cell Biochem.* **88**(4):848-54.
- Briones AM, Daly CJ, Jimenez-Altayo F, Martinez-Revelles S, Gonzalez JM, McGrath JC, Vila E. (2005) Direct demonstration of beta1- and evidence against beta2- and beta3-adrenoceptors, in smooth muscle cells of rat small mesenteric arteries. *Br J Pharmacol.* **146**(5):679-91.
- Bristow MR, Ginsburg R, Umans V, Fowler M, Minobe W, Rasmussen R, Zera P, Menlove R, Shah P, Jamieson S, et al. (1986) Beta 1- and beta 2-adrenergic-receptor subpopulations in nonfailing and failing human ventricular myocardium: coupling of both receptor subtypes to muscle contraction and selective beta 1-receptor down-regulation in heart failure. *Circ Res.* **59**(3):297-309.
- Brodde OE, Bruck H, Leineweber K. (2006) Cardiac adrenoceptors: physiological and pathophysiological relevance. *J Pharmacol Sci.* **100**(5):323-37.
- Brodde OE. (1988) The functional importance of beta 1 and beta 2 adrenoceptors in the human heart. *Am J Cardiol.* **62**(5):24C-29C.
- Bruns RF. (1990) Adenosine receptors. Roles and pharmacology. *Ann N Y Acad Sci.* **603**:211-25; discussion 225-6.
- Brust TB, Cayabyab FS, MacVicar BA. (2007) C-Jun N-terminal kinase regulates adenosine A1 receptor-mediated synaptic depression in the rat hippocampus. *Neuropharmacology.* **53**(8):906-17.
- Brust TF, Hayes MP, Roman DL, Burris KD, Watts VJ. (2015) Bias analyses of preclinical and clinical D2 dopamine ligands: studies with immediate and complex signaling pathways. *J Pharmacol Exp Ther.* **352**(3):480-93.
- Buja LM. (2005) Myocardial ischemia and reperfusion injury. *Cardiovasc Pathol.* **14**(4):170-5.
- Bungay PJ, Owen RA, Coutts IC, Griffin M. (1986) A role for transglutaminase in glucose-stimulated insulin release from the pancreatic beta-cell. *Biochem J.* **235**(1):269-78.

- Bylund, D.B., Bond, R.A., Clarke, D.E., Eikenburg, D.C., Hieble, J.P., Langer, S.Z., et al. (1998) Adrenoceptors. The IUPHAR compendium of receptor characterization and classification. London: IUPHAR Media. 58–74.
- Cabrera-Vera TM, Vanhauwe J, Thomas TO, Medkova M, Preininger A, Mazzoni MR, Hamm HE. (2003) Insights into G protein structure, function, and regulation. *Endocr Rev.* **24**(6):765-81.
- Calmettes G, Ribalet B, John S, Korge P, Ping P, Weiss JN. (2015) Hexokinases and cardioprotection. *J Mol Cell Cardiol.* **78**:107-15.
- Candi E, Melino G, Lahm A, Ceci R, Rossi A, Kim IG, Ciani B, Steinert PM. (1998) Transglutaminase 1 mutations in lamellar ichthyosis. Loss of activity due to failure of activation by proteolytic processing. *J Biol Chem.* **273**(22):13693-702.
- Candi E, Oddi S, Paradisi A, Terrinoni A, Ranalli M, Teofoli P, Citro G, Scarpato S, Puddu P, Melino G. (2002) Expression of transglutaminase 5 in normal and pathologic human epidermis. *J Invest Dermatol.* **119**(3):670-7.
- Cannavo A, Koch WJ. (2017) Targeting β 3-Adrenergic Receptors in the Heart: Selective Agonism and β -Blockade. *J Cardiovasc Pharmacol.* **69**(2):71-78.
- Caputo I, D'Amato A, Troncone R, Auricchio S, Esposito C. (2004) Transglutaminase 2 in celiac disease: minireview article. *Amino Acids.* **26**(4):381-6.
- Carracedo A, Pandolfi PP. (2008) The PTEN-PI3K pathway: of feedbacks and cross-talks. *Oncogene.* **27**(41):5527-41.
- Carré DA, Mitchell CH, Peterson-Yantorno K, Coca-Prados M, Civan MM. (2000) Similarity of A(3)-adenosine and swelling-activated Cl(-) channels in nonpigmented ciliary epithelial cells. *Am J Physiol Cell Physiol.* **279**(2):C440-51.
- Carroll R, Yellon DM. (2000) Delayed cardioprotection in a human cardiomyocyte-derived cell line: the role of adenosine, p38MAP kinase and mitochondrial KATP. *Basic Res Cardiol.* **95**(3):243-9.
- Carvajal K, Moreno-Sánchez R. (2003) Heart metabolic disturbances in cardiovascular diseases. *Arch Med Res.* **34**(2):89-99.
- Champion HC, Kass DA. (2004) Calcium handler mishandles heart. *Nat Med.* **10**(3):239-40.

- Chen SL, Yang CT, Yang ZL, Guo RX, Meng JL, Cui Y, Lan AP, Chen PX, Feng JQ. (2010) Hydrogen sulphide protects H9c2 cells against chemical hypoxia-induced injury. *Clin Exp Pharmacol Physiol.* **37**(3):316-21.
- Chen Z, Xiong C, Pancyr C, Stockwell J, Walz W, Cayabyab FS. (2014) Prolonged adenosine A1 receptor activation in hypoxia and pial vessel disruption focal cortical ischemia facilitates clathrin-mediated AMPA receptor endocytosis and long-lasting synaptic inhibition in rat hippocampal CA3-CA1 synapses: differential regulation of GluA2 and GluA1 subunits by p38 MAPK and JNK. *J Neurosci.* **34**(29):9621-43.
- Chen-Izu Y, Xiao RP, Izu LT, Cheng H, Kuschel M, Spurgeon H, Lakatta EG. (2000) G(i)-dependent localization of beta(2)-adrenergic receptor signaling to L-type Ca(2+) channels. *Biophys J.* **79**(5):2547-56.
- Chesley A, Lundberg MS, Asai T, Xiao RP, Ohtani S, Lakatta EG, Crow MT. (2000) The beta(2)-adrenergic receptor delivers an antiapoptotic signal to cardiac myocytes through G(i)-dependent coupling to phosphatidylinositol 3'-kinase. *Circ Res.* **87**(12):1172-9.
- Chruscinski AJ, Rohrer DK, Schauble E, Desai KH, Bernstein D, Kobilka BK. (1999) Targeted disruption of the beta2 adrenergic receptor gene. *J Biol Chem.* **274**(24):16694-700.
- Chuderland D, Seger R. (2008) Calcium regulates ERK signaling by modulating its protein-protein interactions. *Commun Integr Biol.* **1**(1):4-5.
- Ciruela F, Albergaria C, Soriano A, Cuffí L, Carbonell L, Sánchez S, Gandía J, Fernández-Dueñas V. (2010) Adenosine receptors interacting proteins (ARIPs): Behind the biology of adenosine signaling. *Biochim Biophys Acta.* **1798**(1):9-20.
- Civantos Calzada B, Aleixandre de Artiñano A. (2001) Alpha-adrenoceptor subtypes. *Pharmacol Res.* **44**(3):195-208.
- Clarke, D.D., Mycek, M.J., Neidle, A., Waelsch, H. (1957) The incorporation of amines into proteins. *Arch. Biochem. Biophys.* **79**, 338-354.
- Cohen MV, Downey JM. (2008) Adenosine: trigger and mediator of cardioprotection. *Basic Res Cardiol.* **103**(3):203-15.
- Cohen MV, Downey JM. (2015) Signalling pathways and mechanisms of protection in pre- and postconditioning: historical perspective and lessons for the future. *Br J Pharmacol.* **172**(8):1913-32.

Colak G, Johnson GV. (2012) Complete transglutaminase 2 ablation results in reduced stroke volumes and astrocytes that exhibit increased survival in response to ischemia. *Neurobiol Dis.* **45**(3):1042-50.

Communal C, Colucci WS, Singh K. (2000) p38 mitogen-activated protein kinase pathway protects adult rat ventricular myocytes against beta -adrenergic receptor-stimulated apoptosis. Evidence for Gi-dependent activation. *J Biol Chem.* **275**(25):19395-400.

Communal C, Singh K, Sawyer DB, Colucci WS. (1999) Opposing effects of beta(1)- and beta(2)-adrenergic receptors on cardiac myocyte apoptosis : role of a pertussis toxin-sensitive G protein. *Circulation.* **100**(22):2210-2.

Contractor, Hussain, Rasmus Haarup Lie, Colin Cunningham, Jing Li, Nicolaj B. Støttrup, Cedric Manlihot, Hans Erik Bøtker, Michael R. Schmidt, J. Colin Forfar, Houman Ashrafian, Andrew Redington, and Rajesh K. Kharbanda. (2016) "Adenosine Receptor Activation in the "Trigger" Limb of Remote Pre-Conditioning Mediates Human Endothelial Conditioning and Release of Circulating Cardioprotective Factor(s)." *JACC: Basic to Translational Science* **1.6**: 461-71.

Cooke RM, Brown AJ, Marshall FH, Mason JS. (2015) Structures of G protein-coupled receptors reveal new opportunities for drug discovery. *Drug Discov Today.* **20**(11):1355-64.

Cordella-Miele E, Miele L, Beninati S, Mukherjee AB. (1993) Transglutaminase-catalyzed incorporation of polyamines into phospholipase A2. *J Biochem.* **113**(2):164-73.

Corvol JC, Studler JM, Schonn JS, Girault JA, Hervé D. (2001) Galpha(olf) is necessary for coupling D1 and A2a receptors to adenylyl cyclase in the striatum. *J Neurochem.* **76**(5):1585-8.

Cotecchia S. (2010) The α 1-adrenergic receptors: diversity of signaling networks and regulation. *J Recept Signal Transduct Res.* **30**(6):410-9.

Crawford RM, Jovanović S, Budas GR, Davies AM, Lad H, Wenger RH, Robertson KA, Roy DJ, Ranki HJ, Jovanović A. (2003) Chronic mild hypoxia protects heart-derived H9c2 cells against acute hypoxia/reoxygenation by regulating expression of the SUR2A subunit of the ATP-sensitive K⁺ channel. *J Biol Chem.* **278**(33):31444-55.

Csosz E, Meskó B, Fésüs L. (2009) Transdab wiki: the interactive transglutaminase substrate database on web 2.0 surface. *Amino Acids.* **36**(4):615-7.

Daaka Y, Luttrell LM, Lefkowitz RJ. (1997) Switching of the coupling of the beta2-adrenergic receptor to different G proteins by protein kinase A. *Nature*. **390**(6655):88-91.

Dai Y, Dudek NL, Patel TB, Muma NA. (2008) Transglutaminase-catalyzed transamidation: a novel mechanism for Rac1 activation by 5-hydroxytryptamine_{2A} receptor stimulation. *J Pharmacol Exp Ther*. **326**(1):153-62.

Dana A, Skarli M, Papakrivopoulou J, Yellon DM. (2000) Adenosine A(1) receptor induced delayed preconditioning in rabbits: induction of p38 mitogen-activated protein kinase activation and Hsp27 phosphorylation via a tyrosine kinase- and protein kinase C-dependent mechanism. *Circ Res*. **86**(9):989-97.

Dangel V, Giray J, Ratge D, Wisser H. (1996) Regulation of beta-adrenoceptor density and mRNA levels in the rat heart cell-line H9c2. *Biochem J*. **317** (Pt3):925-31.

Dardik R, Inbal A. (2006) Complex formation between tissue transglutaminase II (tTG) and vascular endothelial growth factor receptor 2 (VEGFR-2): proposed mechanism for modulation of endothelial cell response to VEGF. *Exp Cell Res*. **312**(16):2973-82.

D'Argenio G, Amoroso DC, Mazzone G, Vitaglione P, Romano A, Ribecco MT, D'Armiento MR, Mezza E, Morisco F, Fogliano V, Caporaso N. (2010) Garlic extract prevents CCl₄-induced liver fibrosis in rats: The role of tissue transglutaminase. *Dig Liver Dis*. **42**(8):571-7.

Das T, Baek KJ, Gray C, Im MJ. (1993) Evidence that the Gh protein is a signal mediator from alpha 1-adrenoceptor to a phospholipase C. II. Purification and characterization of a Gh-coupled 69-kDa phospholipase C and reconstitution of alpha 1-adrenoceptor, Gh family, and phospholipase C. *J Biol Chem*. **268**(36):27398-405.

Datta S, Antonyak MA, Cerione RA. (2007) GTP-binding-defective forms of tissue transglutaminase trigger cell death. *Biochemistry*. **46**(51):14819-29.

Daubney J, Bonner PL, Hargreaves AJ, Dickenson JM. (2015) Cardioprotective and cardiotoxic effects of quercetin and two of its in vivo metabolites on differentiated h9c2 cardiomyocytes. *Basic Clin Pharmacol Toxicol*. **116**(2):96-109.

Davel AP, Brum PC, Rossoni LV. (2014) Isoproterenol induces vascular oxidative stress and endothelial dysfunction via a Gi α -coupled β ₂-adrenoceptor signaling pathway. *PLoS One*. **9**(3):e91877.

De Bernardi MA, Rabins SJ, Colangelo AM, Brooker G, Mocchetti I. (1996) TrkA mediates the nerve growth factor-induced intracellular calcium accumulation. *J Biol Chem.* **271**(11):6092-8.

de Moissac D, Gurevich RM, Zheng H, Singal PK, Kirshenbaum LA. (2000) Caspase activation and mitochondrial cytochrome C release during hypoxia-mediated apoptosis of adult ventricular myocytes. *J Mol Cell Cardiol.* **32**(1):53-63.

de Wit RJ, Hekstra D, Jastorff B, Stec WJ, Baraniak J, Van Driel R, Van Haastert PJ. (1984) Inhibitory action of certain cyclophosphate derivatives of cAMP on cAMP-dependent protein kinases. *Eur J Biochem.* **142**(2):255-60.

Deasey S, Shanmugasundaram S, Nurminskaya M. (2013) Tissue-specific responses to loss of transglutaminase 2. *Amino Acids.* **44**(1):179-87.

Dennis G Jr, Sherman BT, Hosack DA, Yang J, Gao W, Lane HC, Lempicki RA. (2003) DAVID: Database for Annotation, Visualization, and Integrated Discovery. *Genome Biol.* **4**(5):P3.

Depre C, Taegtmeyer H. (2000) Metabolic aspects of programmed cell survival and cell death in the heart. *Cardiovasc Res.* **45**(3):538-48.

Depre C, Vanoverschelde JL, Taegtmeyer H. (1999) Glucose for the heart. *Circulation.* **99**(4):578-88.

Dessy C, Balligand JL. (2010) Beta3-adrenergic receptors in cardiac and vascular tissues emerging concepts and therapeutic perspectives. *Adv Pharmacol.* **59**:135-63.

Devereaux PJ, Yang H, Yusuf S, Guyatt G, Leslie K, Villar JC, Xavier D, Chrolavicius S, Greenspan L, Pogue J, Pais P, Liu L, Xu S, Málaga G, Avezum A, Chan M, Montori VM, Jacka M, Choi P. (2008) Effects of extended-release metoprolol succinate in patients undergoing non-cardiac surgery (POISE trial): a randomised controlled trial. *Lancet.* **371**(9627):1839-47.

Devic E, Xiang Y, Gould D, Kobilka B. (2001) Beta-adrenergic receptor subtype-specific signaling in cardiac myocytes from beta(1) and beta(2) adrenoceptor knockout mice. *Mol Pharmacol.* **60**(3):577-83.

Devic E, Xiang Y, Gould D, Kobilka B. (2001) Beta-adrenergic receptor subtype-specific signaling in cardiac myocytes from beta(1) and beta(2) adrenoceptor knockout mice. *Mol Pharmacol.* **60**(3):577-83.

- Di Lisa F, Menabò R, Canton M, Petronilli V. (1998) The role of mitochondria in the salvage and the injury of the ischemic myocardium. *Biochim Biophys Acta*. **1366**(1-2):69-78.
- Dickenson JM, Blank JL, Hill SJ. (1998) Human adenosine A1 receptor and P2Y2-purinoreceptor-mediated activation of the mitogen-activated protein kinase cascade in transfected CHO cells. *Br J Pharmacol*. **124**(7):1491-9.
- Dickenson JM, Camps M, Gierschik P, Hill SJ. (1995) Activation of phospholipase C by G-protein beta gamma subunits in DDT1MF-2 cells. *Eur J Pharmacol*. **288**(3):393-8.
- Dickenson JM, Hill SJ. (1993) Adenosine A1-receptor stimulated increases in intracellular calcium in the smooth muscle cell line, DDT1MF-2. *Br J Pharmacol*. **108**(1):85-92.
- Dixon AK, Gubitzi AK, Sirinathsinghji DJ, Richardson PJ, Freeman TC. (1996) Tissue distribution of adenosine receptor mRNAs in the rat. *Br J Pharmacol*. **118**(6):1461-8.
- Dobson JG Jr, Fenton RA. (1997) Adenosine A2 receptor function in rat ventricular myocytes. *Cardiovasc Res*. **34**(2):337-47.
- Doenst T, Nguyen TD, Abel ED. (2013) Cardiac metabolism in heart failure: implications beyond ATP production. *Circ Res*. **113**(6):709-24.
- Donato R, Cannon BR, Sorci G, Riuzzi F, Hsu K, Weber DJ, Geczy CL. (2013) Functions of S100 proteins. *Curr Mol Med*. **13**(1):24-57.
- Downward J. (1999) How BAD phosphorylation is good for survival. *Nat Cell Biol*. **1**(2):E33-5.
- Dudek SM, Johnson GV. (1994) Transglutaminase facilitates the formation of polymers of the betaamyloid peptide. *Brain Res* **651**:129-133
- Dumaz N, Milne DM, Jardine LJ, Meek DW. (2001) Critical roles for the serine 20, but not the serine 15, phosphorylation site and for the polyproline domain in regulating p53 turnover. *Biochem J*. **359**(Pt 2):459-64.
- Eckert RL, Kaartinen MT, Nurminskaya M, Belkin AM, Colak G, Johnson GV, Mehta K. (2014) Transglutaminase regulation of cell function. *Physiol Rev*. **94**(2):383-417.
- Eckert RL, Sturniolo MT, Broome AM, Ruse M, Rorke EA. (2005) Transglutaminase function in epidermis. *J Invest Dermatol*. **124**(3):481-92.

- Edinger AL, Thompson CB. (2004) Death by design: apoptosis, necrosis and autophagy. *Curr Opin Cell Biol.* **16**(6):663-9.
- Ekhterae D, Lin Z, Lundberg MS, Crow MT, Brosius FC 3rd, Núñez G. (1999) ARC inhibits cytochrome c release from mitochondria and protects against hypoxia-induced apoptosis in heart-derived H9c2 cells. *Circ Res.* **85**(12):e70-7.
- Ethier MF, Madison JM. (2006) Adenosine A1 receptors mediate mobilization of calcium in human bronchial smooth muscle cells. *Am J Respir Cell Mol Biol.* **35**(4):496-502.
- Facchiano A, Facchiano F. (2009) Transglutaminases and their substrates in biology and human diseases: 50 years of growing. *Amino Acids.* **36**(4):599-614.
- Facchiano F, Facchiano A, Facchiano AM. (2006) The role of transglutaminase-2 and its substrates in human diseases. *Front Biosci.* **11**:1758-73.
- Fajardo G, Zhao M, Berry G, Wong LJ, Mochly-Rosen D, Bernstein D. (2011) β 2-adrenergic receptors mediate cardioprotection through crosstalk with mitochondrial cell death pathways. *J Mol Cell Cardiol.* **51**(5):781-9.
- Fajardo G, Zhao M, Powers J, Bernstein D. (2006) Differential cardiotoxic/cardioprotective effects of beta-adrenergic receptor subtypes in myocytes and fibroblasts in doxorubicin cardiomyopathy. *J Mol Cell Cardiol.* **40**(3):375-83.
- Fassina G, de Biasi M, Ragazzi E, Caparrotta L. (1991) Adenosine: a natural modulator of L-type calcium channels in atrial myocardium? *Pharmacol Res.* **23**(4):319-26.
- Faye C, Chautard E, Olsen BR, Ricard-Blum S. (2009) The first draft of the endostatin interaction network. *J Biol Chem.* **284**(33):22041-7.
- Faye C, Inforzato A, Bignon M, Hartmann DJ, Muller L, Ballut L, Olsen BR, Day AJ, Ricard-Blum S. (2010) Transglutaminase-2: a new endostatin partner in the extracellular matrix of endothelial cells. *Biochem J.* **427**(3):467-75.
- Feng JF, Rhee SG, Im MJ. (1996) Evidence that phospholipase delta1 is the effector in the Gh (transglutaminase II)-mediated signaling. *J Biol Chem.* **271**(28):16451-4.
- Fenton RA, Shea LG, Doddi C, Dobson JG Jr. (2010) Myocardial adenosine A(1)-receptor-mediated adenoprotection involves phospholipase C, PKC-epsilon, and p38 MAPK, but not HSP27. *Am J Physiol Heart Circ Physiol.* **298**(6):H1671-8.

- Feoktistov I, Biaggioni I. (1997) Adenosine A2B receptors. *Pharmacol Rev.* **49**(4):381-402.
- Ferdinandy P, Schulz R, Baxter GF. (2007) Interaction of cardiovascular risk factors with myocardial ischemia/reperfusion injury, preconditioning, and postconditioning. *Pharmacol Rev.* **59**(4):418-58.
- Ferrero P, Said M, Sánchez G, Vittone L, Valverde C, Donoso P, Mattiazzi A, Mundiña-Weilenmann C. (2007) Ca²⁺/calmodulin kinase II increases ryanodine binding and Ca²⁺-induced sarcoplasmic reticulum Ca²⁺ release kinetics during beta-adrenergic stimulation. *J Mol Cell Cardiol.* **43**(3):281-91.
- Fésüs L, Szondy Z. (2005) Transglutaminase 2 in the balance of cell death and survival. *FEBS Lett.* **579**(15):3297-302.
- Filiano A, Tucholski J, Dolan P, Colak G, Johnson G. (2010) Transglutaminase 2 protects against ischemic stroke. *Neurobiology of disease.* **39**(3):334-343.
- Filiano AJ, Bailey CD, Tucholski J, Gundemir S, Johnson GV. (2008) Transglutaminase 2 protects against ischemic insult, interacts with HIF1beta, and attenuates HIF1 signaling. *FASEB J.* **22**(8):2662-75.
- Fliss H, Gattinger D. (1996) Apoptosis in ischemic and reperfused rat myocardium. *Circ Res.* **79**(5):949-56.
- Fok JY, Ekmekcioglu S, Mehta K. (2006) Implications of tissue transglutaminase expression in malignant melanoma. *Mol Cancer Ther.* **5**(6):1493-503.
- Folk JE. (1983) Mechanism and basis for specificity of transglutaminase-catalyzed epsilon-(gamma-glutamyl) lysine bond formation. *Adv Enzymol Relat Areas Mol Biol.* **54**:1-56.
- Frank KF, Bölck B, Brixius K, Kranias EG, Schwinger RH. (2002) Modulation of SERCA: implications for the failing human heart. *Basic Res Cardiol.* **97** Suppl 1:I72-8.
- Fredholm BB, IJzerman AP, Jacobson KA, Klotz KN, Linden J. (2001) International Union of Pharmacology. XXV. Nomenclature and classification of adenosine receptors. *Pharmacol Rev.* **53**(4):527-52.
- Fredholm BB, IJzerman AP, Jacobson KA, Linden J, Müller CE. (2011) International Union of Basic and Clinical Pharmacology. LXXXI. Nomenclature and classification of adenosine receptors--an update. *Pharmacol Rev.* **63**(1):1-34.

- Fredholm BB. (2014) Adenosine--a physiological or pathophysiological agent? *J Mol Med(Berl)*. **92**(3):201-6.
- Freissmuth M, Waldhoer M, Bofill-Cardona E, Nanoff C. (1999) G protein antagonists. *Trends Pharmacol Sci*. **20**(6):237-45.
- Fretwell L, Dickenson JM. (2009) Role of large-conductance Ca(2+) -activated potassium channels in adenosine A(1) receptor-mediated pharmacological preconditioning in H9c2 cells. *Eur J Pharmacol*. **618**(1-3):37-44.
- Fretwell L, Dickenson JM. (2011) Role of large-conductance Ca²⁺-activated K⁺ channels in adenosine A₁ receptor-mediated pharmacological postconditioning in H9c2 cells. *Can J Physiol Pharmacol*. **89**(1):24-30.
- Freund KF, Doshi KP, Gaul SL, Claremon DA, Remy DC, Baldwin JJ, Pitzenberger SM, Stern AM. (1994) Transglutaminase inhibition by 2-[(2-oxopropyl)thio]imidazolium derivatives: mechanism of factor XIIIa inactivation. *Biochemistry*. **33**(33):10109-19.
- Freund S, Ungerer M, Lohse MJ. (1994) A1 adenosine receptors expressed in CHO-cells couple to adenylyl cyclase and to phospholipase C. *Naunyn Schmiedebergs Arch Pharmacol*. **350**(1):49-56.
- Fryer RM, Auchampach JA, Gross GJ. (2002) Therapeutic receptor targets of ischemic preconditioning. *Cardiovasc Res*. **55**(3):520-5.
- Fryer RM, Pratt PF, Hsu AK, Gross GJ. (2001) Differential activation of extracellular signal regulated kinase isoforms in preconditioning and opioid-induced cardioprotection. *J Pharmacol Exp Ther*. **296**(2):642-9.
- Fu Q, Chen X, Xiang YK. (2013) Compartmentalization of β-adrenergic signals in cardiomyocytes. *Trends Cardiovasc Med*. **23**(7):250-6.
- Fu Q, Xu B, Liu Y, Parikh D, Li J, Li Y, Zhang Y, Riehle C, Zhu Y, Rawlings T, Shi Q, Clark RB, Chen X, Abel ED, Xiang YK. (2014) Insulin inhibits cardiac contractility by inducing a Gi-biased β2-adrenergic signaling in hearts. *Diabetes*. **63**(8):2676-89.
- Galandrin S, Bouvier M. (2006) Distinct signaling profiles of beta1 and beta2 adrenergic receptor ligands toward adenylyl cyclase and mitogen-activated protein kinase reveals the pluridimensionality of efficacy. *Mol Pharmacol*. **70**(5):1575-84.
- Galaz-Montoya M, Wright SJ, Rodriguez GJ, Lichtarge O, Wensel TG. (2017) Beta-2 Adrenergic Receptor Activation Mobilizes Intracellular Calcium via a Non-Canonical

cAMP-Independent Signaling Pathway. *J Biol Chem*. pii:jbc.M117.787119. doi: 10.1074/jbc.M117.787119. [Epub ahead of print].

Gao Z, Ni Y, Szabo G, Linden J. (1999) Palmitoylation of the recombinant human A1 adenosine receptor: enhanced proteolysis of palmitoylation-deficient mutant receptors. *Biochem J*. **342** (Pt 2):387-95.

Gaudry CA, Verderio E, Jones RA, Smith C, Griffin M. (1999) Tissue transglutaminase is an important player at the surface of human endothelial cells: evidence for its externalization and its colocalization with the beta(1) integrin. *Exp Cell Res*. **252**(1):104-13.

Gay EA, Urban JD, Nichols DE, Oxford GS, Mailman RB. (2004) Functional selectivity of D2 receptor ligands in a Chinese hamster ovary hD2L cell line: evidence for induction of ligand-specific receptor states. *Mol Pharmacol*. **66**(1):97-105.

Gaziano TA, Bitton A, Anand S, Abrahams-Gessel S, Murphy A. (2010) Growing epidemic of coronary heart disease in low- and middle-income countries. *Curr Probl Cardiol*. **35**(2):72-115.

Gentile V, Porta R, Chiosi E, Spina A, Valente F, Pezone R, Davies PJ, Aladik A, Illiano G. (1997) tTGase/G alpha h protein expression inhibits adenylate cyclase activity in Balb-C 3T3 fibroblasts membranes. *Biochim Biophys Acta*. **1357**(1):115-22.

Germack R, Dickenson JM. (2000) Activation of protein kinase B by the A(1)-adenosine receptor in DDT(1)MF-2 cells. *Br J Pharmacol*. **130**(4):867-74.

Germack R, Dickenson JM. (2005) Adenosine triggers preconditioning through MEK/ERK1/2 signalling pathway during hypoxia/reoxygenation in neonatal rat cardiomyocytes. *J Mol Cell Cardiol*. **39**(3):429-42.

Germack R, Dickenson JM. (2004) Characterization of ERK1/2 signalling pathways induced by adenosine receptor subtypes in newborn rat cardiomyocytes. *Br J Pharmacol*. **141**(2):329-39.

Germack R, Griffin M, Dickenson JM. (2004) Activation of protein kinase B by adenosine A1 and A3 receptors in newborn rat cardiomyocytes. *J Mol Cell Cardiol*. **37**(5):989-99.

Gerwins P, Fredholm BB. (1995) Activation of adenosine A1 and bradykinin receptors increases protein kinase C and phospholipase D activity in smooth muscle cells. *Naunyn Schmiedebergs Arch Pharmacol*. **351**(2):186-93.

- Gesek FA. (1996) Alpha 2-adrenergic receptors activate phospholipase C in renal epithelial cells. *Mol Pharmacol.* **50**(2):407-14.
- Glynn Dennis Jr., Brad T. Sherman, Douglas A. Hosack, Jun Yang, Michael W. Baseler, H. Clifford Lane, Richard A. Lempicki. DAVID: Database for Annotation, Visualization, and Integrated Discovery. *Genome Biology* 2003 **4**(5): P3.
- Goddard AD, Watts A. (2012) Regulation of G protein-coupled receptors by palmitoylation and cholesterol. *BMC Biol.* **10**:27.
- Goldsmith ZG, Dhanasekaran DN. (2007) G protein regulation of MAPK networks. *Oncogene.* **26**(22):3122-42.
- Golitsina NL, Kordowska J, Wang CL, Lehrer SS. (1996) Ca²⁺-dependent binding of calyculin to muscle tropomyosin. *Biochem Biophys Res Commun.* **220**(2):360-5.
- Gomis R, Sener A, Malaisse-Lagae F, Malaisse WJ. (1983) Transglutaminase activity in pancreatic islets. *Biochim Biophys Acta.* **760**(3):384-8.
- Gottlieb RA, Burlison KO, Kloner RA, Babior BM, Engler RL. (1994) Reperfusion injury induces apoptosis in rabbit cardiomyocytes. *J Clin Invest.* **94**(4):1621-8.
- Gottlob K, Majewski N, Kennedy S, Kandel E, Robey RB, Hay N. (2001) Inhibition of early apoptotic events by Akt/PKB is dependent on the first committed step of glycolysis and mitochondrial hexokinase. *Genes Dev.* **15**(11):1406-18.
- Granneman JG. (2001) The putative beta4-adrenergic receptor is a novel state of the beta1-adrenergic receptor. *Am J Physiol Endocrinol Metab.* **280**(2):E199-202.
- Gregg CJ, Steppan J, Gonzalez DR, Champion HC, Phan AC, Nyhan D, Shoukas AA, Hare JM, Barouch LA, Berkowitz DE. (2010) β 2-adrenergic receptor-coupled phosphoinositide 3-kinase constrains cAMP-dependent increases in cardiac inotropy through phosphodiesterase 4 activation. *Anesth Analg.* **111**(4):870-7.
- Grenard P, Bates MK, Aeschlimann D. (2001) Evolution of transglutaminase genes: identification of a transglutaminase gene cluster on human chromosome 15q15. Structure of the gene encoding transglutaminase X and a novel gene family member, transglutaminase Z. *J Biol Chem.* **276**(35):33066-78.
- Griffin M, Casadio R, Bergamini CM. (2002) Transglutaminases: nature's biological glues. *Biochem J.* **368**(Pt 2):377-96.

- Gross SR, Balklava Z, Griffin M. (2003) Importance of tissue transglutaminase in repair of extracellular matrices and cell death of dermal fibroblasts after exposure to a solarium ultraviolet A source. *J Invest Dermatol.* **121**(2):412-23.
- Grosso H, Mouradian MM. (2012) Transglutaminase 2: biology, relevance to neurodegenerative diseases and therapeutic implications. *Pharmacol Ther.* **133**(3):392-410.
- Guan WJ, Xia KD, Ma YT, Liu YT, Shi YT, Jiang H, Shen L, Xia K, Li JD, Tang BS, Wang JL. (2013) Transglutaminase 6 interacts with polyQ proteins and promotes the formation of polyQ aggregates. *Biochem Biophys Res Commun.* **437**(1):94-100.
- Guimarães S, Moura D. (2001) Vascular adrenoceptors: an update. *Pharmacol Rev.* **53**(2):319-56.
- Gundemir S, Colak G, Feola J, Blouin R, Johnson GV. (2013) Transglutaminase 2 facilitates or ameliorates HIF signaling and ischemic cell death depending on its conformation and localization. *Biochim Biophys Acta.* **1833**(1):1-10.
- Gundemir S, Colak G, Tucholski J, Johnson GV. (2012) Transglutaminase 2: a molecular Swiss army knife. *Biochim Biophys Acta.* **1823**(2):406-19.
- Gundlfinger A, Bischofberger J, Jochenning FW, Torvinen M, Schmitz D, Breustedt J. (2007) Adenosine modulates transmission at the hippocampal mossy fibre synapse via direct inhibition of presynaptic calcium channels. *J Physiol.* **582**(Pt1):263-77.
- Guo A, Villén J, Kornhauser J, Lee KA, Stokes MP, Rikova K, Possemato A, Nardone J, Innocenti G, Wetzel R, Wang Y, MacNeill J, Mitchell J, Gygi SP, Rush J, Polakiewicz RD, Comb MJ. (2008) Signaling networks assembled by oncogenic EGFR and c-Met. *Proc Natl Acad Sci U S A.* **105**(2):692-7.
- Halestrap AP, Richardson AP. (2015) The mitochondrial permeability transition: a current perspective on its identity and role in ischaemia/reperfusion injury. *J Mol Cell Cardiol.* **78**:129-41.
- Han JA, Park SC. (2000) Transglutaminase-dependent modulation of transcription factor Sp1 activity. *Mol Cells.* **10**(6):612-8.
- Han XJ, Chae JK, Lee MJ, You KR, Lee BH, Kim DG. (2005) Involvement of GADD153 and cardiac ankyrin repeat protein in hypoxia-induced apoptosis of H9c2 cells. *J Biol Chem.* **280**(24):23122-9.

- Hansen PR. (1995) Role of neutrophils in myocardial ischemia and reperfusion. *Circulation*. **91**(6):1872-85.
- Hansson T, Ulfgren AK, Lindroos E, DannAEus A, Dahlbom I, Klareskog L. (2002) Transforming growth factor-beta (TGF-beta) and tissue transglutaminase expression in the small intestine in children with coeliac disease. *Scand J Immunol*. **56**(5):530-7.
- Haroon ZA, Hettasch JM, Lai TS, Dewhirst MW, Greenberg CS. (1999) Tissue transglutaminase is expressed, active, and directly involved in rat dermal wound healing and angiogenesis. *FASEB J*. **13**(13):1787-95.
- Hartley DM, Zhao C, Speier AC, Woodard GA, Li S, Li Z, Walz T. (2008) Transglutaminase induces protofibril-like amyloid beta-protein assemblies that are protease-resistant and inhibit long-term potentiation. *J Biol Chem*. **283**(24):16790-800.
- Hartzell HC, Fischmeister R. (1992) Direct regulation of cardiac Ca²⁺ channels by G proteins: neither proven nor necessary? *Trends Pharmacol Sci*. **13**(10):380-5.
- Hartzell HC, Méry PF, Fischmeister R, Szabo G. (1991) Sympathetic regulation of cardiac calcium current is due exclusively to cAMP-dependent phosphorylation. *Nature*. **351**(6327):573-6.
- Hasegawa G, Suwa M, Ichikawa Y, Ohtsuka T, Kumagai S, Kikuchi M, Sato Y, Saito Y. (2003) A novel function of tissue-type transglutaminase: protein disulphide isomerase. *Biochem J*. **373**(Pt 3):793-803.
- Haskó G, Pacher P. (2012) Regulation of macrophage function by adenosine. *Arterioscler Thromb Vasc Biol*. **32**(4):865-9.
- Hausenloy DJ, Tsang A, Mocanu MM, Yellon DM. (2005) Ischemic preconditioning protects by activating prosurvival kinases at reperfusion. *Am J Physiol Heart Circ Physiol*. **288**(2):H971-6.
- Hausenloy DJ, Tsang A, Yellon DM. (2005) The reperfusion injury salvage kinase pathway: a common target for both ischemic preconditioning and postconditioning. *Trends Cardiovasc Med*. **15**(2):69-75.
- Hausenloy DJ, Yellon DM. (2006) Survival kinases in ischemic preconditioning and postconditioning. *Cardiovasc Res*. **70**(2):240-53.
- Head BP, Patel HH, Roth DM, Lai NC, Niesman IR, Farquhar MG, Insel PA. (2005) G-protein-coupled receptor signaling components localize in both sarcolemmal and

intracellular caveolin-3-associated microdomains in adult cardiac myocytes. *J Biol Chem.* **280**(35):31036-44.

Head BP, Patel HH, Roth DM, Murray F, Swaney JS, Niesman IR, Farquhar MG, Insel PA. (2006) Microtubules and actin microfilaments regulate lipid raft/caveolae localization of adenylyl cyclase signaling components. *J Biol Chem.* **281**(36):26391-9.

Headrick JP, Ashton KJ, Rose'meyer RB, Peart JN. (2013) Cardiovascular adenosine receptors: expression, actions and interactions. *Pharmacol Ther.* **140**(1):92-111.

Headrick JP, Peart JN, Reichelt ME, Haseler LJ. (2011) Adenosine and its receptors in the heart: regulation, retaliation and adaptation. *Biochim Biophys Acta.* **1808**(5):1413-28.

Headrick JP. (1996) Ischemic preconditioning: bioenergetic and metabolic changes and the role of endogenous adenosine. *J Mol Cell Cardiol.* **28**(6):1227-40.

Hegde A, Strachan RT, Walker JK. (2015) Quantification of beta adrenergic receptor subtypes in beta-arrestin knockout mouse airways. *PLoS One.* **10**(2):e0116458.

Heifetz A, James T, Morao I, Bodkin MJ, Biggin PC. (2016) Guiding lead optimization with GPCR structure modeling and molecular dynamics. *Curr Opin Pharmacol.* **30**:14-21.

Hein TW, Wang W, Zoghi B, Muthuchamy M, Kuo L. (2001) Functional and molecular characterization of receptor subtypes mediating coronary microvascular dilation to adenosine. *J Mol Cell Cardiol.* **33**(2):271-82.

Hemmings BA, Restuccia DF. (2012) PI3K-PKB/Akt pathway. *Cold Spring Harb Perspect Biol.* **4**(9):a011189.

Herrera R, Sebolt-Leopold JS. (2002) Unraveling the complexities of the Raf/MAP kinase pathway for pharmacological intervention. *Trends Mol Med.* **8**(4Suppl):S27-31.

Hescheler J, Meyer R, Plant S, Krautwurst D, Rosenthal W, Schultz G. (1991) Morphological, biochemical, and electrophysiological characterization of a clonal cell (H9c2) line from rat heart. *Circ Res.* **69**(6):1476-86.

Heubach JF, Blaschke M, Harding SE, Ravens U, Kaumann AJ. (2003) Cardiostimulant and cardiodepressant effects through overexpressed human

beta2-adrenoceptors in murine heart: regional differences and functional role of beta1-adrenoceptors. *Naunyn Schmiedebergs Arch Pharmacol.* **367**(4):380-90.

Hillenbrand M, Schori C, Schöppe J, Plückthun A. (2015) Comprehensive analysis of heterotrimeric G-protein complex diversity and their interactions with GPCRs in solution. *Proc Natl Acad Sci U S A.* **112**(11):E1181-90.

Hochhauser E, Leshem D, Kaminski O, Cheporko Y, Vidne BA, Shainberg A. (2007) The protective effect of prior ischemia reperfusion adenosine A1 or A3 receptor activation in the normal and hypertrophied heart. *Interact Cardiovasc Thorac Surg.* **6**(3):363-8.

Hoffert JD, Pisitkun T, Wang G, Shen RF, Knepper MA. (2006) Quantitative phosphoproteomics of vasopressin-sensitive renal cells: regulation of aquaporin-2 phosphorylation at two sites. *Proc Natl Acad Sci U S A.* **103**(18):7159-64.

Hoffner G, Djian P. (2005) Transglutaminase and diseases of the central nervous system. *Front Biosci.* **10**:3078-92.

Holloway AC, Qian H, Pipolo L, Ziogas J, Miura S, Karnik S, Southwell BR, Lew MJ, Thomas WG. (2002) Side-chain substitutions within angiotensin II reveal different requirements for signaling, internalization, and phosphorylation of type 1A angiotensin receptors. *Mol Pharmacol.* **61**(4):768-77.

Hothi SS, Gurung IS, Heathcote JC, Zhang Y, Booth SW, Skepper JN, Grace AA, Huang CL. (2008) Epac activation, altered calcium homeostasis and ventricular arrhythmogenesis in the murine heart. *Pflugers Arch.* **457**(2):253-70.

Hsu TC, Huang CY, Chiang SY, Lai WX, Tsai CH, Tzang BS. (2008) Transglutaminase inhibitor cystamine alleviates the abnormality in liver from NZB/W F1 mice. *Eur J Pharmacol.* **579**(1-3):382-9.

Hu L, Wang J, Zhu H, Wu X, Zhou L, Song Y, Zhu S, Hao M, Liu C, Fan Y, Wang Y, Li Q. (2016) Ischemic postconditioning protects the heart against ischemia-reperfusion injury via neuronal nitric oxide synthase in the sarcoplasmic reticulum and mitochondria. *Cell Death Dis.* **7**:e2222.

Huang da W, Sherman BT, Lempicki RA. (2009) Bioinformatics enrichment tools: paths toward the comprehensive functional analysis of large gene lists. *Nucleic Acids Res.* **37**(1):1-13.

Huang da W, Sherman BT, Lempicki RA. (2009) Systematic and integrative analysis of large gene lists using DAVID bioinformatics resources. *Nat Protoc.* **4**(1):44-57.

- Huang Q, Yang L, Luo J, Guo L, Wang Z, Yang X, Jin W, Fang Y, Ye J, Shan B, Zhang Y. (2015) SWATH enables precise label-free quantification on proteome scale. *Proteomics*. **15**(7):1215-23.
- Huang YC, Wei KC, Chang CN, Chen PY, Hsu PW, Chen CP, Lu CS, Wang HL, Gutmann DH, Yeh TH. (2014) Transglutaminase 2 expression is increased as a function of malignancy grade and negatively regulates cell growth in meningioma. *PLoS One*. **9**(9):e108228.
- Huang, L., Xu, A.-M., & Liu, W. (2015). Transglutaminase 2 in cancer. *American Journal of Cancer Research*. **5**(9), 2756–2776.
- Hulme JT, Westenbroek RE, Scheuer T, Catterall WA. (2006) Phosphorylation of serine 1928 in the distal C-terminal domain of cardiac CaV1.2 channels during beta1-adrenergic regulation. *Proc Natl Acad Sci U S A*. **103**(44):16574-9.
- Hunter T. (1995) When is a lipid kinase not a lipid kinase? When it is a protein kinase. *Cell*. **83**(1):1-4.
- Hwang JY, Mangala LS, Fok JY, Lin YG, Merritt WM, Spannuth WA, Nick AM, Fiterman DJ, Vivas-Mejia PE, Deavers MT, Coleman RL, Lopez-Berestein G, Mehta K, Sood AK. (2008) Clinical and biological significance of tissue transglutaminase in ovarian carcinoma. *Cancer Res*. **68**(14):5849-58.
- Hwang KC, Gray CD, Sivasubramanian N, Im MJ. (1995) Interaction site of GTP binding Gh (transglutaminase II) with phospholipase C. *J Biol Chem*. **270**(45):27058-62.
- Ichikawa A, Ishizaki J, Morita M, Tanaka K, Ikura K. (2008) Identification of new amine acceptor protein substrate candidates of transglutaminase in rat liver extract: use of 5-(biotinamido) pentylamine as a probe. *Biosci Biotechnol Biochem*. **72**(4):1056-62.
- Iismaa SE, Aplin M, Holman S, Yiu TW, Jackson K, Burchfield JG, Mitchell CJ, O'Reilly L, Davenport A, Cantley J, Schmitz-Peiffer C, Biden TJ, Cooney GJ, Graham RM. (2013) Glucose homeostasis in mice is transglutaminase 2 independent. *PLoS One*. **8**(5):e63346.
- Iismaa SE, Graham RM. (2003) Dissecting cardiac hypertrophy and signaling pathways: evidence for an interaction between multifunctional g proteins and prostanoids. *Circ Res*. **92**(10):1059-61.

Iismaa SE, Mearns BM, Lorand L, Graham RM. (2009) Transglutaminases and disease: lessons from genetically engineered mouse models and inherited disorders. *Physiol Rev.* **89**(3):991-1023.

Im MJ, Graham RM. (1990) A novel guanine nucleotide-binding protein coupled to the alpha 1-adrenergic receptor. I. Identification by photolabeling or membrane and ternary complex preparation. *J Biol Chem.* **265**(31):18944-51.

Im MJ, Riek RP, Graham RM. (1990) A novel guanine nucleotide-binding protein coupled to the alpha 1-adrenergic receptor. II. Purification, characterization, and reconstitution. *J Biol Chem.* **265**(31):18952-60.

Imami K, Sugiyama N, Kyono Y, Tomita M, Ishihama Y. (2008) Automated phosphoproteome analysis for cultured cancer cells by two-dimensional nanoLC-MS using a calcined titania/C18 biphasic column. *Anal Sci.* **24**(1):161-6.

Imhof A, Wolffe AP. (1999) Purification and properties of the Xenopus Hat1 acetyltransferase: association with the 14-3-3 proteins in the oocyte nucleus. *Biochemistry.* **38**(40):13085-93.

Inagaki K, Chen L, Ikeno F, Lee FH, Imahashi K, Bouley DM, Rezaee M, Yock PG, Murphy E, Mochly-Rosen D. (2003) Inhibition of delta-protein kinase C protects against reperfusion injury of the ischemic heart in vivo. *Circulation.* **108**(19):2304-7.

Insel PA, Snead A, Murray F, Zhang L, Yokouchi H, Katakia T, Kwon O, Dimucci D, Wilderman A. (2012) GPCR expression in tissues and cells: are the optimal receptors being used as drug targets? *Br J Pharmacol.* **165**(6):1613-6.

Ito K, Nakazato T, Yamato K, Miyakawa Y, Yamada T, Hozumi N, Segawa K, Ikeda, Y, Kizaki M. (2004) Induction of apoptosis in leukemic cells by homovanillic acid derivative, capsaicin, through oxidative stress: implication of phosphorylation of p53 at Ser-15 residue by reactive oxygen species. *Cancer Res.* **64**(3):1071-8.

Itoh G, Tamura J, Suzuki M, Suzuki Y, Ikeda H, Koike M, Nomura M, Jie T, Ito K. (1995) DNA fragmentation of human infarcted myocardial cells demonstrated by the nick end labeling method and DNA agarose gel electrophoresis. *Am J Pathol.* **146**(6):1325-31.

Itoh H, Gilman AG. (1991) Expression and analysis of Gs alpha mutants with decreased ability to activate adenylyl cyclase. *J Biol Chem.* **266**(24):16226-31.

Jeitner TM, Pinto JT, Krasnikov BF, Horswill M, Cooper AJ. (2009) Transglutaminases and neurodegeneration. *J Neurochem.* **109** Suppl 1:160-6.

- Jensen BC, O'Connell TD, Simpson PC. (2011) Alpha-1-adrenergic receptors: targets for agonist drugs to treat heart failure. *J Mol Cell Cardiol.* **51**(4):518-28.
- Jiang WG, Ye L, Sanders AJ, Ruge F, Kynaston HG, Ablin RJ, Mason MD. (2013) Prostate transglutaminase (TGase-4, TGaseP) enhances the adhesion of prostate cancer cells to extracellular matrix, the potential role of TGase-core domain. *J Transl Med.* **11**:269.
- Jockers R, Linder ME, Hohenegger M, Nanoff C, Bertin B, Strosberg AD, Marullo S, Freissmuth M. (1994) Species difference in the G protein selectivity of the human and bovine A1-adenosine receptor. *J Biol Chem.* **269**(51):32077-84.
- Johnson K, Hashimoto S, Lotz M, Pritzker K, Terkeltaub R. (2001) Interleukin-1 induces pro-mineralizing activity of cartilage tissue transglutaminase and factor XIIIa. *Am J Pathol.* **159**(1):149-63.
- Johnson TS, Knight CR, el-Alaoui S, Mian S, Rees RC, Gentile V, Davies PJ, Griffin M. (1994) Transfection of tissue transglutaminase into a highly malignant hamster fibrosarcoma leads to a reduced incidence of primary tumour growth. *Oncogene.* **9**(10):2935-42.
- Jones RA, Kotsakis P, Johnson TS, Chau DY, Ali S, Melino G, Griffin M. (2006) Matrix changes induced by transglutaminase 2 lead to inhibition of angiogenesis and tumor growth. *Cell Death Differ.* **13**(9):1442-53.
- Jones RA, Nicholas B, Mian S, Davies PJ, Griffin M. (1997) Reduced expression of tissue transglutaminase in a human endothelial cell line leads to changes in cell spreading, cell adhesion and reduced polymerisation of fibronectin. *J Cell Sci.* **110** (Pt 19):2461-72.
- Jordan JE, Zhao ZQ, Vinten-Johansen J. (1999) The role of neutrophils in myocardial ischemia-reperfusion injury. *Cardiovasc Res.* **43**(4):860-78.
- Jost P, Fasshauer M, Kahn CR, Benito M, Meyer M, Ott V, Lowell BB, Klein HH, Klein J. (2002) Atypical beta-adrenergic effects on insulin signaling and action in beta(3)-adrenoceptor-deficient brown adipocytes. *Am J Physiol Endocrinol Metab.* **283**(1):E146-53.
- Jung SM, Jandu S, Steppan J, Belkin A, An SS, Pak A, Choi EY, Nyhan D, Butlin M, Viegas K, Avolio A, Berkowitz DE, Santhanam L. (2013) Increased tissue transglutaminase activity contributes to central vascular stiffness in eNOS knockout mice. *Am J Physiol Heart Circ Physiol.* **305**(6):H803-10.

Kalfa TA, Connor JA, Begtrup AH. EPB42-Related Hereditary Spherocytosis. 2014 Mar 13 [updated 2016 Nov 10]. In: Pagon RA, Adam MP, Ardinger HH, Wallace SE, Amemiya A, Bean LJH, Bird TD, Ledbetter N, Mefford HC, Smith RJH, Stephens K, editors. GeneReviews® [Internet]. Seattle (WA): University of Washington, Seattle; 1993-2017. Available from <http://www.ncbi.nlm.nih.gov/books/NBK190102/>

Kamisago M, Sharma SD, DePalma SR, Solomon S, Sharma P, McDonough B, Smoot L, Mullen MP, Woolf PK, Wigle ED, Seidman JG, Seidman CE. (2000) Mutations in sarcomere protein genes as a cause of dilated cardiomyopathy. *N Engl J Med.* **343**(23):1688-96.

Kamp TJ, Hell JW. (2000) Regulation of cardiac L-type calcium channels by protein kinase A and protein kinase C. *Circ Res.* **87**(12):1095-102.

Kanchan K, Fuxreiter M, Fésüs L. (2015) Physiological, pathological, and structural implications of non-enzymatic protein-protein interactions of the multifunctional human transglutaminase 2. *Cell Mol Life Sci.* **72**(16):3009-35.

Kang SK, Kim DK, Damron DS, Baek KJ, Im MJ. (2002) Modulation of intracellular Ca(2+) via alpha(1B)-adrenoceptor signaling molecules, G alpha(h) (transglutaminase II) and phospholipase C-delta 1. *Biochem Biophys Res Commun.* **293**(1):383-90.

Kang SK, Yi KS, Kwon NS, Park KH, Kim UH, Baek KJ, Im MJ. (2004) Alpha1B-adrenoceptor signaling and cell motility: GTPase function of Gh/transglutaminase 2 inhibits cell migration through interaction with cytoplasmic tail of integrin alpha subunits. *J Biol Chem.* **279**(35):36593-600.

Karpuj MV, Becher MW, Springer JE, Chabas D, Youssef S, Pedotti R, Mitchell D, Steinman L. (2002) Prolonged survival and decreased abnormal movements in transgenic model of Huntington disease, with administration of the transglutaminase inhibitor cystamine. *Nat Med.* **8**(2):143-9.

Karpuj MV, Garren H, Slunt H, Price DL, Gusella J, Becher MW, Steinman L. (1999) Transglutaminase aggregates huntingtin into nonamyloidogenic polymers, and its enzymatic activity increases in Huntington's disease brain nuclei. *Proc Natl Acad Sci U S A.* **96**(13):7388-93.

Kase H, Iwahashi K, Nakanishi S, Matsuda Y, Yamada K, Takahashi M, Murakata C, Sato A, Kaneko M. (1987) K-252 compounds, novel and potent inhibitors of protein kinase C and cyclic nucleotide-dependent protein kinases. *Biochem Biophys Res Commun.* **142**(2):436-40.

- Katritch V, Cherezov V, Stevens RC. (2013) Structure-function of the G protein-coupled receptor superfamily. *Annu Rev Pharmacol Toxicol.* **53**:531-56.
- Katz AM. (1970) Contractile proteins of the heart. *Physiol Rev.* **50**(1):63-158.
- Kaumann A, Bartel S, Molenaar P, Sanders L, Burrell K, Vetter D, Hempel P, Karczewski P, Krause EG. (1999) Activation of beta2-adrenergic receptors hastens relaxation and mediates phosphorylation of phospholamban, troponin I, and C-protein in ventricular myocardium from patients with terminal heart failure. *Circulation.* **99**(1):65-72.
- Kaumann AJ, Molenaar P. (1997) Modulation of human cardiac function through 4 beta-adrenoceptor populations. *Naunyn Schmiedebergs Arch Pharmacol.* **355**(6):667-81.
- Kaumann AJ, Sanders L. (1993) Both beta 1- and beta 2-adrenoceptors mediate catecholamine-evoked arrhythmias in isolated human right atrium. *Naunyn Schmiedebergs Arch Pharmacol.* **348**(5):536-40.
- Kelsen SG, Anakwe OO, Aksoy MO, Reddy PJ, Dhanesekaran N, Penn R, Benovic JL. (1997) Chronic effects of catecholamines on the beta 2-adrenoceptor system in cultured human airway epithelial cells. *Am J Physiol.* **272**(5 Pt 1):L916-24.
- Kenakin T, Christopoulos A. (2013) Signalling bias in new drug discovery: detection, quantification and therapeutic impact. *Nat Rev Drug Discov.* **12**(3):205-16.
- Kenakin T, Watson C, Muniz-Medina V, Christopoulos A, Novick S. (2012) A simple method for quantifying functional selectivity and agonist bias. *ACS Chem Neurosci.* **3**(3):193-203.
- Kenakin T. (2009) Biased agonism. *F1000 Biol Rep.* **1**:87.
- Kenakin T. (2007) Functional selectivity through protean and biased agonism: who steers the ship? *Mol Pharmacol.* **72**(6):1393-401.
- Kersten JR, Orth KG, Pagel PS, Mei DA, Gross GJ, Warltier DC. (1997) Role of adenosine in isoflurane-induced cardioprotection. *Anesthesiology.* **86**(5):1128-39.
- Kettenbach AN, Schweppe DK, Faherty BK, Pechenick D, Pletnev AA, Gerber SA. (2011) Quantitative phosphoproteomics identifies substrates and functional modules of Aurora and Polo-like kinase activities in mitotic cells. *Sci Signal.* **4**(179):rs5.

- Khaliulin I, Bond M, James AF, Dyar Z, Amini R, Johnson JL, Suleiman MS. (2017) Functional and cardioprotective effects of simultaneous and individual activation of protein kinase A and Epac. *Br J Pharmacol.* **174**(6):438-453.
- Kim SJ, Peppas A, Hong SK, Yang G, Huang Y, Diaz G, Sadoshima J, Vatner DE, Vatner SF. (2003) Persistent stunning induces myocardial hibernation and protection: flow/function and metabolic mechanisms. *Circ Res.* **92**(11):1233-9.
- Kim SY, Grant P, Lee JH, Pant HC, Steinert PM. (1999) Differential expression of multiple transglutaminases in human brain. Increased expression and cross-linking by transglutaminases 1 and 2 in Alzheimer's disease. *J Biol Chem.* **274**(43):30715-21.
- Kimes BW, Brandt BL. (1976) Properties of a clonal muscle cell line from rat heart. *Exp Cell Res.* **98**(2):367-81.
- Kingwell K. (2016) Receptor pharmacology: The many faces of G protein-coupled receptors. *Nat Rev Drug Discov.* **15**(9):602-3.
- Király R, Demény M, Fésüs L. (2011) Protein transamidation by transglutaminase 2 in cells: a disputed Ca²⁺-dependent action of a multifunctional protein. *FEBS J.* **278**(24):4717-39.
- Kojima S, Kuo TF, Tatsukawa H, Hirose S. (2010) Induction of cross-linking and silencing of Sp1 by transglutaminase during liver injury in ASH and NASH via different ER stress pathways. *Dig Dis.* **28**(6):715-21.
- Kolwicz SC Jr, Olson DP, Marney LC, Garcia-Menendez L, Synovec RE, Tian R. (2012) Cardiac-specific deletion of acetyl CoA carboxylase 2 prevents metabolic remodeling during pressure-overload hypertrophy. *Circ Res.* **111**(6):728-38.
- Kolwicz SC Jr, Purohit S, Tian R. (2013) Cardiac metabolism and its interactions with contraction, growth, and survival of cardiomyocytes. *Circ Res.* **113**(5):603-16.
- Kong L, Korthuis RJ. (1997) Melanoma cell adhesion to injured arterioles: mechanisms of stabilized tethering. *Clin Exp Metastasis.* **15**(4):426-31.
- Konkar AA, Zhai Y, Granneman JG. (2000) beta1-adrenergic receptors mediate beta3-adrenergic-independent effects of CGP 12177 in brown adipose tissue. *Mol Pharmacol.* **57**(2):252-8.
- Korge P, Ping P, Weiss JN. (2008) Reactive oxygen species production in energized cardiac mitochondria during hypoxia/reoxygenation: modulation by nitric oxide. *Circ Res.* **103**(8):873-80.

Kozłowska H, Szymaska U, Schlicker E, Malinowska B. (2003) Atypical beta-adrenoceptors, different from beta 3-adrenoceptors and probably from the low-affinity state of beta 1-adrenoceptors, relax the rat isolated mesenteric artery. *Br J Pharmacol.* **140**(1):3-12.

Kranias EG, Hajjar RJ. (2012) Modulation of cardiac contractility by the phospholamban/SERCA2a regulatome. *Circ Res.* **110**(12):1646-60.

Krasnikov BF, Kim SY, McConoughey SJ, Ryu H, Xu H, Stavrovskaya I, Iismaa SE, Mearns BM, Ratan RR, Blass JP, Gibson GE, Cooper AJ. (2005) Transglutaminase activity is present in highly purified nonsynaptosomal mouse brain and liver mitochondria. *Biochemistry.* **44**(21):7830-43.

Kudo M, Wang Y, Xu M, Ayub A, Ashraf M. (2002) Adenosine A(1) receptor mediates late preconditioning via activation of PKC-delta signaling pathway. *Am J Physiol Heart Circ Physiol.* **283**(1):H296-301.

Kull B, Svenningsson P, Fredholm BB. (2000) Adenosine A(2A) receptors are colocalized with and activate g(olf) in rat striatum. *Mol Pharmacol.* **58**(4):771-7.

Kuncio GS, Tsyganskaya M, Zhu J, Liu SL, Nagy L, Thomazy V, Davies PJ, Zern MA. (1998) TNF-alpha modulates expression of the tissue transglutaminase gene in liver cells. *Am J Physiol.* **274**(2 Pt 1):G240-5.

Kuno A, Critz SD, Cui L, Solodushko V, Yang XM, Krahn T, Albrecht B, Philipp S, Cohen MV, Downey JM. (2007) Protein kinase C protects preconditioned rabbit hearts by increasing sensitivity of adenosine A2b-dependent signaling during early reperfusion. *J Mol Cell Cardiol.* **43**(3):262-71.

Kuo TF, Tatsukawa H, Matsuura T, Nagatsuma K, Hirose S, Kojima S. (2012) Free fatty acids induce transglutaminase 2-dependent apoptosis in hepatocytes via ER stress-stimulated PERK pathways. *J Cell Physiol.* **227**(3):1130-7.

Kuschel M, Zhou YY, Cheng H, Zhang SJ, Chen Y, Lakatta EG, Xiao RP. (1999) G(i) protein-mediated functional compartmentalization of cardiac beta(2)-adrenergic signaling. *J Biol Chem.* **274**(31):22048-52.

Kuschel M, Zhou YY, Spurgeon HA, Bartel S, Karczewski P, Zhang SJ, Krause EG, Lakatta EG, Xiao RP. (1999) beta2-adrenergic cAMP signaling is uncoupled from phosphorylation of cytoplasmic proteins in canine heart. *Circulation.* **99**(18):2458-65.

Kuznetsov V, Pak E, Robinson RB, Steinberg SF. (1995) Beta 2-adrenergic receptor actions in neonatal and adult rat ventricular myocytes. *Circ Res.* **76**(1):40-52.

Kuznetsov AV, Javadov S, Sickinger S, Frotschnig S, Grimm M. (2015) H9c2 and HL-1 cells demonstrate distinct features of energy metabolism, mitochondrial function and sensitivity to hypoxia-reoxygenation. *Biochim Biophys Acta*. **1853**(2):276-84.

Lader AS, Xiao YF, Ishikawa Y, Cui Y, Vatner DE, Vatner SF, Homcy CJ, Cantiello HF. (1998) Cardiac G α overexpression enhances L-type calcium channels through an adenylyl cyclase independent pathway. *Proc Natl Acad Sci U S A*. **95**(16):9669-74.

Laemmli UK, Mölbert E, Showe M, Kellenberger E. (1970) Form-determining function of the genes required for the assembly of the head of bacteriophage T4. *J Mol Biol*. **49**(1):99-113.

Lai TS, Bielawska A, Peoples KA, Hannun YA, Greenberg CS. (1997) Sphingosylphosphocholine reduces the calcium ion requirement for activating tissue transglutaminase. *J Biol Chem*. **272**(26):16295-300.

Lai TS, Greenberg CS. (2013) TGM2 and implications for human disease: role of alternative splicing. *Front Biosci (Landmark Ed)*. **18**:504-19.

Lambert JP, Ivosev G, Couzens AL, Larsen B, Taipale M, Lin ZY, Zhong Q, Lindquist S, Vidal M, Aebersold R, Pawson T, Bonner R, Tate S, Gingras AC. (2013) Mapping differential interactomes by affinity purification coupled with data-independent mass spectrometry acquisition. *Nat Methods*. **10**(12):1239-45.

Lange M, Smul TM, Blomeyer CA, Redel A, Klotz KN, Roewer N, Kehl F. (2006) Role of the beta1-adrenergic pathway in anesthetic and ischemic preconditioning against myocardial infarction in the rabbit heart in vivo. *Anesthesiology*. **105**(3):503-10.

Leblais V, Jo SH, Chakir K, Maltsev V, Zheng M, Crow MT, Wang W, Lakatta EG, Xiao RP. (2004) Phosphatidylinositol 3-kinase offsets cAMP-mediated positive inotropic effect via inhibiting Ca²⁺ influx in cardiomyocytes. *Circ Res*. **95**(12):1183-90.

Lee KH, Lee N, Lim S, Jung H, Ko YG, Park HY, Jang Y, Lee H, Hwang KC. (2003) Calreticulin inhibits the MEK1,2-ERK1,2 pathway in alpha 1-adrenergic receptor/Gh-stimulated hypertrophy of neonatal rat cardiomyocytes. *J Steroid Biochem Mol Biol*. **84**(1):101-7.

Lee KN, Arnold SA, Birckbichler PJ, Patterson MK Jr, Fraij BM, Takeuchi Y, Carter HA. (1993) Site-directed mutagenesis of human tissue transglutaminase: Cys-277

- is essential for transglutaminase activity but not for GTPase activity. *Biochim Biophys Acta*. **1202**(1):1-6.
- Lee MY, Chung S, Bang HW, Baek KJ, Uhm D. (1997) Modulation of large conductance Ca²⁺-activated K⁺ channel by Galphah (transglutaminase II) in the vascular smooth muscle cell. *Pflugers Arch*. **433**(5):671-3.
- Lerner A, Neidhöfer S, Matthias T (2015) Transglutaminase 2 and Anti Transglutaminase 2 Autoantibodies in Celiac Disease and Beyond: Anti-Transglutaminase 2 Autoantibodies: Friends or Enemies. *Immunome Res* **11**: 100.
- Lewis CJ, Gong H, Brown MJ, Harding SE. (2004) Overexpression of beta 1-adrenoceptors in adult rat ventricular myocytes enhances CGP 12177A cardiostimulation: implications for 'putative' beta 4-adrenoceptor pharmacology. *Br J Pharmacol*. **141**(5):813-24.
- Lewis TE, Milam TD, Klingler DW, Rao PS, Jaggi M, Smith DJ, Hemstreet GP, Balaji KC. (2005) Tissue transglutaminase interacts with protein kinase A anchor protein 13 in prostate cancer. *Urol Oncol*. **23**(6):407-12.
- Li J, Bai C, Guo J, Liang W, Long J. (2017) NDUFA4L2 protects against ischaemia/reperfusion-induced cardiomyocyte apoptosis and mitochondrial dysfunction by inhibiting complex I. *Clin Exp Pharmacol Physiol*. **44**(7):779-786.
- Li DY, Tao L, Liu H, Christopher TA, Lopez BL, Ma XL. (2006) Role of ERK1/2 in the anti-apoptotic and cardioprotective effects of nitric oxide after myocardial ischemia and reperfusion. *Apoptosis*. **11**(6):923-30.
- Li F, Zhang J, Cao X, Wang L, Li D, Song S, Ye B, Fan C. (2009) Adenosine detection by using gold nanoparticles and designed aptamer sequences. *Analyst*. **134**(7):1355-60.
- Li X, Wei XL, Meng LL, Chi MG, Yan JQ, Ma XY, Jia YS, Liang L, Yan HT, Zheng JQ. (2009) Involvement of tissue transglutaminase in endothelin 1-induced hypertrophy in cultured neonatal rat cardiomyocytes. *Hypertension*. **54**(4):839-44.
- Liao P, Wang SQ, Wang S, Zheng M, Zheng M, Zhang SJ, Cheng H, Wang Y, Xiao RP. (2002) p38 Mitogen-activated protein kinase mediates a negative inotropic effect in cardiac myocytes. *Circ Res*. **90**(2):190-6.
- Lilley GR, Skill J, Griffin M, Bonner PL. (1998) Detection of Ca²⁺-dependent transglutaminase activity in root and leaf tissue of monocotyledonous and dicotyledonous plants. *Plant Physiol*. **117**(3):1115-23.

Linden J, Thai T, Figler H, Jin X, Robeva AS. (1999) Characterization of human A(2B) adenosine receptors: radioligand binding, western blotting, and coupling to G(q) in human embryonic kidney 293 cells and HMC-1 mast cells. *Mol Pharmacol.* **56**(4):705-13.

Linden J. (1994) Cloned adenosine A3 receptors: pharmacological properties, species differences and receptor functions. *Trends Pharmacol Sci.* **15**(8):298-306.

Linden J. (2001) Molecular approach to adenosine receptors: receptor-mediated mechanisms of tissue protection. *Annu Rev Pharmacol Toxicol.* **41**:775-87.

Lindsay MA, Bungay PJ, Griffin M. (1990) Transglutaminase involvement in the secretion of insulin from electroporated rat islets of Langerhans. *Biosci Rep.* **10**(6):557-61.

Liu GS, Cohen MV, Mochly-Rosen D, Downey JM. (1999) Protein kinase C-epsilon is responsible for the protection of preconditioning in rabbit cardiomyocytes. *J Mol Cell Cardiol.* **31**(10):1937-48.

Liu GS, Thornton J, Van Winkle DM, Stanley AW, Olsson RA, Downey JM. (1991) Protection against infarction afforded by preconditioning is mediated by A1 adenosine receptors in rabbit heart. *Circulation.* **84**(1):350-6.

Liu JJ, Horst R, Katritch V, Stevens RC, Wüthrich K. (2012) Biased signalling pathways in β 2-adrenergic receptor characterized by 19F-NMR. *Science.* **335**(6072):1106-10.

Liu Q, Hofmann PA. (2003) Modulation of protein phosphatase 2a by adenosine A1 receptors in cardiomyocytes: role for p38 MAPK. *Am J Physiol Heart Circ Physiol.* **285**(1):H97-103.

Liu R, Ramani B, Soto D, De Arcangelis V, Xiang Y. (2009) Agonist dose-dependent phosphorylation by protein kinase A and G protein-coupled receptor kinase regulates beta2 adrenoceptor coupling to G(i) proteins in cardiomyocytes. *J Biol Chem.* **284**(47):32279-87.

Liu J, Sui H, Zhao J, Wang Y. (2017) Osmotin Protects H9c2 Cells from Simulated Ischemia-Reperfusion Injury through AdipoR1/PI3K/AKT Signaling Pathway. *Front Physiol.* **8**:611.

Lochner A, Genade S, Tromp E, Podzuweit T, Moolman JA. (1999) Ischemic preconditioning and the beta-adrenergic signal transduction pathway. *Circulation.* **100**(9):958-66.

- Long X, Boluyt MO, Hipolito ML, Lundberg MS, Zheng JS, O'Neill L, Cirielli C, Lakatta EG, Crow MT. (1997) p53 and the hypoxia-induced apoptosis of cultured neonatal rat cardiac myocytes. *J Clin Invest.* **99**(11):2635-43.
- López-Neblina F, Toledo-Pereyra LH. (2006) Phosphoregulation of signal transduction pathways in ischemia and reperfusion. *J Surg Res.* **134**(2):292-9.
- Lorand L, Conrad SM. (1984) Transglutaminases. *Mol Cell Biochem.* **58**(1-2):9-35.
- Lorand L, Graham RM. (2003) Transglutaminases: crosslinking enzymes with pleiotropic functions. *Nat Rev Mol Cell Biol.* **4**(2):140-56.
- Lundby A, Secher A, Lage K, Nordsborg NB, Dmytriyev A, Lundby C, Olsen JV. (2012) Quantitative maps of protein phosphorylation sites across 14 different rat organs and tissues. *Nat Commun.* **3**:876.
- Macdonald A, Campbell DG, Toth R, McLauchlan H, Hastie CJ, Arthur JS. (2006) Pim kinases phosphorylate multiple sites on Bad and promote 14-3-3 binding and dissociation from Bcl-XL. *BMC Cell Biol.* **7**:1.
- MacDonald, M. E., Ambrose, C. M., Dujao, M. P. and et al. (1993). A novel gene containing a trinucleotide repeat that is expanded and unstable on Huntington's disease chromosomes. *Cell* **72**:971-983.
- Macdougall DA, Agarwal SR, Stopford EA, Chu H, Collins JA, Longster AL, Colyer J, Harvey RD, Calaghan S. (2012) Caveolae compartmentalise β 2-adrenoceptor signals by curtailing cAMP production and maintaining phosphatase activity in the sarcoplasmic reticulum of the adult ventricular myocyte. *J Mol Cell Cardiol.* **52**(2):388-400.
- Mackintosh C. (2004) Dynamic interactions between 14-3-3 proteins and phosphoproteins regulate diverse cellular processes. *Biochem J.* **381**(Pt 2):329-42.
- Maillet M, van Berlo JH, Molkenin JD. (2013) Molecular basis of physiological heart growth: fundamental concepts and new players. *Nat Rev Mol Cell Biol.* **14**(1):38-48.
- Majno G, Joris I. (1995) Apoptosis, oncosis, and necrosis. An overview of cell death. *Am J Pathol.* **146**(1):3-15.
- Makaula S, Lochner A, Genade S, Sack MN, Awan MM, Opie LH. (2005) H-89, a non-specific inhibitor of protein kinase A, promotes post-ischemic cardiac contractile recovery and reduces infarct size. *J Cardiovasc Pharmacol.* **45**(4):341-7.

- Mäkitie LT, Kanerva K, Andersson LC. (2009) Ornithine decarboxylase regulates the activity and localization of rhoA via polyamination. *Exp Cell Res.* **315**(6):1008-14.
- Malhotra R, Lin Z, Vincenz C, Brosius FC 3rd. (2001) Hypoxia induces apoptosis via two independent pathways in Jurkat cells: differential regulation by glucose. *Am J Physiol Cell Physiol.* **281**(5):C1596-603.
- Malorni W, Farrace MG, Matarrese P, Tinari A, Ciarlo L, Mousavi-Shafaei P, D'Eletto M, Di Giacomo G, Melino G, Palmieri L, Rodolfo C, Piacentini M. (2009) The adenine nucleotide translocator 1 acts as a type 2 transglutaminase substrate: implications for mitochondrial-dependent apoptosis. *Cell Death Differ.* **16**(11):1480-92.
- Mangala LS, Fok JY, Zorrilla-Calancha IR, Verma A, Mehta K. (2007) Tissue transglutaminase expression promotes cell attachment, invasion and survival in breast cancer cells. *Oncogene.* **26**(17):2459-70.
- Mangano DT, Goldman L. (1995) Preoperative assessment of patients with known or suspected coronary disease. *N Engl J Med.* **333**(26):1750-6.
- Mangoni ME, Barrère-Lemaire S. (2004) Adenosine receptors, heart rate, and cardioprotection. *Cardiovasc Res.* **62**(3):447-9.
- Manni S, Mauban JH, Ward CW, Bond M. (2008) Phosphorylation of the cAMP-dependent protein kinase (PKA) regulatory subunit modulates PKA-AKAP interaction, substrate phosphorylation, and calcium signaling in cardiac cells. *J Biol Chem.* **283**(35):24145-54.
- Marais E, Genade S, Strijdom H, Moolman JA, Lochner A. (2001) p38 MAPK activation triggers pharmacologically-induced beta-adrenergic preconditioning, but not ischaemic preconditioning. *J Mol Cell Cardiol.* **33**(12):2157-77.
- Marques MA, de Oliveira GA. (2016) Cardiac Troponin and Tropomyosin: Structural and Cellular Perspectives to Unveil the Hypertrophic Cardiomyopathy Phenotype. *Front Physiol.* **7**:429.
- Martel C, Wang Z, Brenner C. (2014) VDAC phosphorylation, a lipid sensor influencing the cell fate. *Mitochondrion.* **19**(Pt A):69-77.
- Martens D, Lohse MJ, Rauch B, Schwabe U. (1987) Pharmacological characterization of A1 adenosine receptors in isolated rat ventricular myocytes. *Naunyn Schmiedebergs Arch Pharmacol.* **336**(3):342-8.

Martin A, De Vivo G, Gentile V. (2011) Possible role of the transglutaminases in the pathogenesis of Alzheimer's disease and other neurodegenerative diseases. *Int J Alzheimers Dis.* **1**:865432.

Martin NP, Whalen EJ, Zamah MA, Pierce KL, Lefkowitz RJ. (2004) PKA-mediated phosphorylation of the beta1-adrenergic receptor promotes Gs/Gi switching. *Cell Signal.* **16**(12):1397-403.

Mastroberardino PG, Farrace MG, Viti I, Pavone F, Fimia GM, Melino G, Rodolfo C, Piacentini M. (2006) "Tissue" transglutaminase contributes to the formation of disulphide bridges in proteins of mitochondrial respiratory complexes. *Biochim Biophys Acta.* **1757**(9-10):1357-65.

Mastroberardino PG, Iannicola C, Nardacci R, Bernassola F, De Laurenzi V, Melino G, Moreno S, Pavone F, Oliverio S, Fesus L, Piacentini M. (2002) 'Tissue' transglutaminase ablation reduces neuronal death and prolongs survival in a mouse model of Huntington's disease. *Cell Death Differ.* **9**(9):873-80.

Mastroberardino PG, Piacentini M. (2010) Type 2 transglutaminase in Huntington's disease: a double-edged sword with clinical potential. *J Intern Med.* **268**(5):419-31.

Matlung HL, Neele AE, Groen HC, van Gaalen K, Tuna BG, van Weert A, de Vos J, Wentzel JJ, Hoogenboezem M, van Buul JD, VanBavel E, Bakker EN. (2012) Transglutaminase activity regulates atherosclerotic plaque composition at locations exposed to oscillatory shear stress. *Atherosclerosis.* **224**(2):355-62.

McCommis KS, Baines CP. (2012) The role of VDAC in cell death: friend or foe? *Biochim Biophys Acta.* **1818**(6):1444-50.

McGrath JC. (2015) Localization of α -adrenoceptors: JR Vane Medal Lecture. *Br J Pharmacol.* **172**(5):1179-94.

Medina DL, Toro MJ, Santisteban P. (2000) Somatostatin interferes with thyrotropin-induced G1-S transition mediated by cAMP-dependent protein kinase and phosphatidylinositol 3-kinase. Involvement of RhoA and cyclin E x cyclin-dependent kinase 2 complexes. *J Biol Chem.* **275**(20):15549-56.

Mehta K, Fok J, Miller FR, Koul D, Sahin AA. (2004) Prognostic significance of tissue transglutaminase in drug resistant and metastatic breast cancer. *Clin Cancer Res.* **10**(23):8068-76.

Mehta K, Fok JY, Mangala LS. (2006) Tissue transglutaminase: from biological glue to cell survival cues. *Front Biosci.* **11**:173-85.

- Mehta K, Kumar A, Kim HI. (2010) Transglutaminase 2: a multi-tasking protein in the complex circuitry of inflammation and cancer. *Biochem Pharmacol.* **80**(12):1921-9.
- Messerli FH, Bangalore S, Yao SS, Steinberg JS. (2009) Cardioprotection with beta-blockers: myths, facts and Pascal's wager. *J Intern Med.* **266**(3):232-41.
- Métrich M, Lucas A, Gastineau M, Samuel JL, Heymes C, Morel E, Lezoualc'h F. (2008) Epac mediates beta-adrenergic receptor-induced cardiomyocyte hypertrophy. *Circ Res.* **102**(8):959-65.
- Mhaouty-Kodja S. (2004) Galpha/tissue transglutaminase 2: an emerging G protein in signal transduction. *Biol Cell.* **96**(5):363-7.
- Milakovic T, Tucholski J, McCoy E, Johnson GV. (2004) Intracellular localization and activity state of tissue transglutaminase differentially impacts cell death. *J Biol Chem.* **279**(10):8715-22.
- Miller-Fleming L, Olin-Sandoval V, Campbell K, Ralser M. (2015) Remaining Mysteries of Molecular Biology: The Role of Polyamines in the Cell. *J Mol Biol.* **427**(21):3389-406.
- Milligan G, Kostenis E. (2006) Heterotrimeric G-proteins: a short history. *Br J Pharmacol.* **147** Suppl 1:S46-55.
- Min B, Kwon YC, Choe KM, Chung KC. (2015) PINK1 phosphorylates transglutaminase 2 and blocks its proteasomal degradation. *J Neurosci Res.* **93**(5):722-35.
- Minneman KP. (1988) Alpha 1-adrenergic receptor subtypes, inositol phosphates, and sources of cell Ca²⁺. *Pharmacol Rev.* **40**(2):87-119.
- Mishra S, Melino G, Murphy LJ. (2007) Transglutaminase 2 kinase activity facilitates protein kinase A-induced phosphorylation of retinoblastoma protein. *J Biol Chem* **282**(25):18108-15.
- Mishra S, Murphy LJ. (2006) Phosphorylation of transglutaminase 2 by PKA at Ser216 creates 14-3-3 binding sites. *Biochem Biophys Res Commun.* **347**(4):1166-70.
- Mishra S, Murphy LJ. (2006) The p53 oncoprotein is a substrate for tissue transglutaminase kinase activity. *Biochem Biophys Res Commun.* **339**(2):726-30.

- Mishra S, Murphy LJ. (2004) Tissue transglutaminase has intrinsic kinase activity: identification of transglutaminase 2 as an insulin-like growth factor-binding protein-3 kinase. *J Biol Chem.* **279**(23):23863-8.
- Mishra S, Saleh A, Espino PS, Davie JR, Murphy LJ. (2006) Phosphorylation of histones by tissue transglutaminase. *J Biol Chem.* **281**(9):5532-8.
- Mitchell CH, Peterson-Yantorno K, Carré DA, McGlenn AM, Coca-Prados M, Stone RA, Civan MM. (1999) A3 adenosine receptors regulate Cl⁻ channels of nonpigmented ciliary epithelial cells. *Am J Physiol.* **276**(3 Pt 1):C659-66.
- Mocanu MM, Baxter GF, Yue Y, Critz SD, Yellon DM. (2000) The p38 MAPK inhibitor, SB203580, abrogates ischaemic preconditioning in rat heart but timing of administration is critical. *Basic Res Cardiol.* **95**(6):472-8.
- Moens AL, Claeys MJ, Timmermans JP, Vrints CJ. (2005) Myocardial ischemia/reperfusion-injury, a clinical view on a complex pathophysiological process. *Int J Cardiol.* **100**(2):179-90.
- Monaco G, Decrock E, Arbel N, van Vliet AR, La Rovere RM, De Smedt H, Parys JB, Agostinis P, Leybaert L, Shoshan-Barmatz V, Bultynck G. (2015) The BH4 domain of anti-apoptotic Bcl-XL, but not that of the related Bcl-2, limits the voltage-dependent anion channel 1 (VDAC1)-mediated transfer of pro-apoptotic Ca²⁺ signals to mitochondria. *J Biol Chem.* **290**(14):9150-61.
- Moolman JA, Hartley S, Van Wyk J, Marais E, Lochner A. (2006a) Inhibition of myocardial apoptosis by ischaemic and beta-adrenergic preconditioning is dependent on p38 MAPK. *Cardiovasc Drugs Ther.* **20**(1):13-25.
- Moolman, JA, Salie, R, Lochner, A (2006c) The mechanism of 0-adrenergic preconditioning (fJPC) depends on activation of adenosine A(3) receptors by endogenous adenosine and involves the PI3-K/PKB signal transduction pathway. *Journal of Molecular and Cellular Cardiology* **41**(4): 741-742.
- Morisco C, Zebrowski DC, Vatner DE, Vatner SF, Sadoshima J. (2001) Beta-adrenergic cardiac hypertrophy is mediated primarily by the beta(1)-subtype in the rat heart. *J Mol Cell Cardiol.* **33**(3):561-73.
- Morgan AJ, Murray KJ, Challiss RA. (1993) Comparison of the effect of isobutylmethylxanthine and phosphodiesterase-selective inhibitors on cAMP levels in SH-SY5Y neuroblastoma cells. *Biochem Pharmacol.* **45**(12):2373-80.

- Motomura S, Reinhard-Zerkowski H, Daul A, Brodde OE. (1990) On the physiologic role of beta-2 adrenoceptors in the human heart: in vitro and in vivo studies. *Am Heart J.* **119**(3 Pt 1):608-19.
- Munshi R, Pang IH, Sternweis PC, Linden J. (1991) A1 adenosine receptors of bovine brain couple to guanine nucleotide-binding proteins Gi1, Gi2, and Go. *J Biol Chem.* **266**(33):22285-9.
- Münzel T, Gori T, Keaney JF Jr, Maack C, Daiber A. (2015) Pathophysiological role of oxidative stress in systolic and diastolic heart failure and its therapeutic implications. *Eur Heart J.* **36**(38):2555-64.
- Murry CE, Jennings RB, Reimer KA. (1986) Preconditioning with ischemia: a delay of lethal cell injury in ischemic myocardium. *Circulation.* **74**(5):1124-36.
- Murthy KS, Makhlof GM. (1995) Adenosine A1 receptor-mediated activation of phospholipase C-beta 3 in intestinal muscle: dual requirement for alpha and beta gamma subunits of Gi3. *Mol Pharmacol.* **47**(6):1172-9.
- Murthy, S.N., Iismaa, S., Begg, G., Freymann, D.M., Graham, R.M., and Lorand, L. (2002). Conserved tryptophan in the core domain of transglutaminase is essential for catalytic activity. *Proc Natl Acad Sci U S A* **99**: 2738-2742.
- MYCEK MJ, CLARKE DD, NEIDLE A, WAELSCH H. (1959) Amine incorporation into insulin as catalyzed by transglutaminase. *Arch Biochem Biophys.* **84**:528-40.
- Myneni VD, Hitomi K, Kaartinen MT. (2014) Factor XIII-A transglutaminase acts as a switch between preadipocyte proliferation and differentiation. *Blood.* **124**(8):1344-53.
- Myrsky E, Kaukinen K, Syrjänen M, Korponay-Szabó IR, Mäki M, Lindfors K. (2008) Coeliac disease-specific autoantibodies targeted against transglutaminase 2 disturb angiogenesis. *Clin Exp Immunol.* **152**(1):111-9.
- Naga Prasad SV, Jayatilleke A, Madamanchi A, Rockman HA. (2005) Protein kinase activity of phosphoinositide 3-kinase regulates beta-adrenergic receptor endocytosis. *Nat Cell Biol.* **7**(8):785-96.
- Nagarkatti DS, Sha'afi RI. (1998) Role of p38 MAP kinase in myocardial stress. *J Mol Cell Cardiol.* **30**(8):1651-64.
- Nakaoka H, Perez DM, Baek KJ, Das T, Husain A, Misono K, Im MJ, Graham RM. (1994) Gh: a GTP-binding protein with transglutaminase activity and receptor signalling function. *Science.* **264**(5165):1593-6.

- Nardacci R, Lo Iacono O, Ciccocanti F, Falasca L, Adesso M, Amendola A, Antonucci G, Craxì A, Fimia GM, Iadevaia V, Melino G, Ruco L, Tocci G, Ippolito G, Piacentini M. (2003) Transglutaminase type II plays a protective role in hepatic injury. *Am J Pathol.* **162**(4):1293-303.
- Nasa Y, Yabe K, Takeo S. (1997) Beta-adrenoceptor stimulation-mediated preconditioning-like cardioprotection in perfused rat hearts. *J Cardiovasc Pharmacol.* **29**(4):436-43.
- Nedjadi T, Kitteringham N, Campbell F, Jenkins RE, Park BK, Navarro P, Ashcroft F, Tepikin A, Neoptolemos JP, Costello E. (2009) S100A6 binds to annexin 2 in pancreatic cancer cells and promotes pancreatic cancer cell motility. *Br J Cancer.* **101**(7):1145-54.
- Nelson TE, Gruol DL. (2004) The chemokine CXCL10 modulates excitatory activity and intracellular calcium signaling in cultured hippocampal neurons. *J Neuroimmunol.* **156**(1-2):74-87.
- Neves SR, Ram PT, Iyengar R. (2002) G protein pathways. *Science.* **296**(5573):1636-9.
- Nichols M, Townsend N, Scarborough P, Rayner M. (2014) Cardiovascular disease in Europe 2014: epidemiological update. *Eur Heart J.* **35**(42):2950-9.
- Nikolaev VO, Bünemann M, Schmitteckert E, Lohse MJ, Engelhardt S. (2006) Cyclic AMP imaging in adult cardiac myocytes reveals far-reaching beta1-adrenergic but locally confined beta2-adrenergic receptor-mediated signaling. *Circ Res.* **99**(10):1084-91.
- Nikolaev VO, Bünemann M, Schmitteckert E, Lohse MJ, Engelhardt S. (2006) Cyclic AMP imaging in adult cardiac myocytes reveals far-reaching beta1-adrenergic but locally confined beta2-adrenergic receptor-mediated signaling. *Circ Res.* **99**(10):1084-91.
- Nikolaev VO, Moshkov A, Lyon AR, Miragoli M, Novak P, Paur H, Lohse MJ, Korchev YE, Harding SE, Gorelik J. (2010) Beta2-adrenergic receptor redistribution in heart failure changes cAMP compartmentation. *Science.* **327**(5973):1653-7.
- Niu X, Watts VL, Cingolani OH, Sivakumaran V, Leyton-Mange JS, Ellis CL, Miller KL, Vandegaer K, Bedja D, Gabrielson KL, Paolucci N, Kass DA, Bouch LA. (2012) Cardioprotective effect of beta-3 adrenergic receptor agonism: role of neuronal nitric oxide synthase. *J Am Coll Cardiol.* **59**(22):1979-87.

Nurminskaya M, Magee C, Faverman L, Linsenmayer TF. (2003) Chondrocyte-derived transglutaminase promotes maturation of preosteoblasts in periosteal bone. *Dev Biol.* **263**(1):139-52.

Nurminskaya MV, Belkin AM. (2012) Cellular functions of tissue transglutaminase. *Int Rev Cell Mol Biol.* **294**:1-97.

Odi BO, Coussons P. (2014) Biological functionalities of transglutaminase 2 and the possibility of its compensation by other members of the transglutaminase family. *Scientific World Journal.* **1**:714561.

Oertel K, Hunfeld A, Specker E, Reiff C, Seitz R, Pasternack R, Dodt J. (2007) A highly sensitive fluorometric assay for determination of human coagulation factor XIII in plasma. *Anal Biochem.* **367**(2):152-8.

Oestreich EA, Malik S, Goonasekera SA, Blaxall BC, Kelley GG, Dirksen RT, Smrcka AV. (2009) Epac and phospholipase Cepsilon regulate Ca²⁺ release in the heart by activation of protein kinase Cepsilon and calcium-calmodulin kinase II. *J Biol Chem.* **284**(3):1514-22.

Offermanns S, Simon MI. (1995) G alpha 15 and G alpha 16 couple a wide variety of receptors to phospholipase C. *J Biol Chem.* **270**(25):15175-80.

Okamoto T, Murayama Y, Hayashi Y, Inagaki M, Ogata E, Nishimoto I. (1991) Identification of a Gs activator region of the beta 2-adrenergic receptor that is autoregulated via protein kinase A-dependent phosphorylation. *Cell.* **67**(4):723-30.

Olah ME, Stiles GL. (1995) Adenosine receptor subtypes: characterization and therapeutic regulation. *Annu Rev Pharmacol Toxicol.* **35**:581-606.

Oliverio S, Amendola A, Di Sano F, Farrace MG, Fesus L, Nemes Z, Piredda L, Spinedi A, Piacentini M. (1997) Tissue transglutaminase-dependent posttranslational modification of the retinoblastoma gene product in promonocytic cells undergoing apoptosis. *Mol Cell Biol.* **17**(10):6040-8.

Onaran HO, Ambrosio C, Uğur Ö, Madaras Koncz E, Grò MC, Vezzi V, Rajagopal S, Costa T. (2017) Systematic errors in detecting biased agonism: Analysis of current methods and development of a new model-free approach. *Sci Rep.* **7**:44247.

Orre LM, Pernemalm M, Lengqvist J, Lewensohn R, Lehtiö J. (2007) Up-regulation, modification, and translocation of S100A6 induced by exposure to ionizing radiation revealed by proteomics profiling. *Mol Cell Proteomics.* **6**(12):2122-31.

- Osaki M, Oshimura M, Ito H. (2004) PI3K-Akt pathway: its functions and alterations in human cancer. *Apoptosis*. **9**(6):667-76.
- Ostrom RS, Gregorian C, Drenan RM, Xiang Y, Regan JW, Insel PA. (2001) Receptor number and caveolar co-localization determine receptor coupling efficiency to adenylyl cyclase. *J Biol Chem*. **276**(45):42063-9.
- Otani H, Matsuhisa S, Akita Y, Kyoi S, Enoki C, Tatsumi K, Fujiwara H, Hattori R, Imamura H, Iwasaka T. (2006) Role of mechanical stress in the form of cardiomyocyte death during the early phase of reperfusion. *Circ J*. **70**(10):1344-55.
- Ou H, Haendeler J, Aebly MR, Kelly LA, Cholewa BC, Koike G, Kwitek-Black A, Jacob HJ, Berk BC, Miano JM. (2000) Retinoic acid-induced tissue transglutaminase and apoptosis in vascular smooth muscle cells. *Circ Res*. **87**(10):881-7.
- Pac-Soo CK, Mathew H, Ma D. (2015) Ischaemic conditioning strategies reduce ischaemia/reperfusion-induced organ injury. *Br J Anaesth*. **114**(2):204-16.
- Palacios-Moreno J, Foltz L, Guo A, Stokes MP, Kuehn ED, George L, Comb M, Grimes ML. (2015) Neuroblastoma tyrosine kinase signaling networks involve FYN and LYN in endosomes and lipid rafts. *PLoS Comput Biol*. **11**(4):e1004130.
- Palczewski K. (2006) G protein-coupled receptor rhodopsin. *Annu Rev Biochem*. **75**:743-67.
- Palmer TM, Gettys TW, Stiles GL. (1995) Differential interaction with and regulation of multiple G-proteins by the rat A3 adenosine receptor. *J Biol Chem*. **270**(28):16895-902.
- Palmiter KA, Kitada Y, Muthuchamy M, Wieczorek DF, Solaro RJ. (1996) Exchange of beta- for alpha-tropomyosin in hearts of transgenic mice induces changes in thin filament response to Ca²⁺, strong cross-bridge binding, and protein phosphorylation. *J Biol Chem*. **271**(20):11611-4.
- Park ES, Won JH, Han KJ, Suh PG, Ryu SH, Lee HS, Yun HY, Kwon NS, Baek KJ. (1998) Phospholipase C-delta1 and oxytocin receptor signalling: evidence of its role as an effector. *Biochem J*. **331** (Pt 1):283-9.
- Park KS, Kim HK, Lee JH, Choi YB, Park SY, Yang SH, Kim SY, Hong KM. (2010) Transglutaminase 2 as a cisplatin resistance marker in non-small cell lung cancer. *J Cancer Res Clin Oncol*. **136**(4):493-502.

- Parsons M, Young L, Lee JE, Jacobson KA, Liang BT. (2000) Distinct cardioprotective effects of adenosine mediated by differential coupling of receptor subtypes to phospholipases C and D. *FASEB J.* **14**(10):1423-31.
- Pastorino JG, Hoek JB. (2008) Regulation of hexokinase binding to VDAC. *J Bioenerg Biomembr.* **40**(3):171-82.
- Patel HH, Murray F, Insel PA. (2008) Caveolae as organizers of pharmacologically relevant signal transduction molecules. *Annu Rev Pharmacol Toxicol.* **48**:359-91.
- Peart JN, Headrick JP. (2007) Adenosinergic cardioprotection: multiple receptors, multiple pathways. *Pharmacol Ther.* **114**(2):208-21.
- Penumatsa K, Abualkhair S, Wei L, Warburton R, Preston I, Hill NS, Watts SW, Fanburg BL, Toksoz D. (2014) Tissue transglutaminase promotes serotonin-induced AKT signaling and mitogenesis in pulmonary vascular smooth muscle cells. *Cell Signal.* **26**(12):2818-25.
- Pereira L, Cheng H, Lao DH, Na L, van Oort RJ, Brown JH, Wehrens XH, Chen J, Bers DM. (2013) Epac2 mediates cardiac β 1-adrenergic-dependent sarcoplasmic reticulum Ca²⁺ leak and arrhythmia. *Circulation.* **127**(8):913-22.
- Perry MJ, Mahoney SA, Haynes LW. (1995) Transglutaminase C in cerebellar granule neurons: regulation and localization of substrate cross-linking. *Neuroscience.* **65**(4):1063-76.
- Peter AK, Bjerke MA, Leinwand LA. (2016) Biology of the cardiac myocyte in heart disease. *Molecular Biology of the Cell* **27**(14):2149-2160.
- Philipp S, Yang XM, Cui L, Davis AM, Downey JM, Cohen MV. (2006) Postconditioning protects rabbit hearts through a protein kinase C-adenosine A2b receptor cascade. *Cardiovasc Res.* **70**(2):308-14.
- Phillips AB, Ko W. (2007) Effects of ischemic preconditioning and adenosine pretreatment on myocardial function and energetics in a clinically relevant model. *Life Sci.* **81**(17-18):1355-61.
- Piacentini M, Farrace MG, Piredda L, Matarrese P, Ciccocanti F, Falasca L, Rodolfo C, Giammarioli AM, Verderio E, Griffin M, Malorni W. (2002) Transglutaminase overexpression sensitizes neuronal cell lines to apoptosis by increasing mitochondrial membrane potential and cellular oxidative stress. *J Neurochem.* **81**(5):1061-72.

- Pierce KD, Furlong TJ, Selbie LA, Shine J. (1992) Molecular cloning and expression of an adenosine A2b receptor from human brain. *Biochem Biophys Res Commun.* **187**(1):86-93.
- Pietrocola F, Galluzzi L, Bravo-San Pedro JM, Madeo F, Kroemer G. (2015) Acetyl coenzyme A: a central metabolite and second messenger. *Cell Metab.* **21**(6):805-21.
- Piper HM, Kasseckert S, Abdallah Y. (2006) The sarcoplasmic reticulum as the primary target of reperfusion protection. *Cardiovasc Res.* **70**(2):170-3.
- Poldermans D, Boersma E, Bax JJ, Thomson IR, van de Ven LL, Blankensteijn JD, Baars HF, Yo TI, Trocino G, Vigna C, Roelandt JR, van Urk H. (1999) The effect of bisoprolol on perioperative mortality and myocardial infarction in high-risk patients undergoing vascular surgery. Dutch Echocardiographic Cardiac Risk Evaluation Applying Stress Echocardiography Study Group. *N Engl J Med.* **341**(24):1789-94.
- Porter GW, Khuri FR, Fu H. (2006) Dynamic 14-3-3/client protein interactions integrate survival and apoptotic pathways. *Semin Cancer Biol.* **16**(3):193-202.
- Porzio O, Massa O, Cunsolo V, Colombo C, Malaponti M, Bertuzzi F, Hansen T, Johansen A, Pedersen O, Meschi F, Terrinoni A, Melino G, Federici M, Decarlo N, Menicagli M, Campani D, Marchetti P, Ferdaoussi M, Froguel P, Federici G, Vaxillaire M, Barbetti F. (2007) Missense mutations in the TGM2 gene encoding transglutaminase 2 are found in patients with early-onset type 2 diabetes. Mutation in brief no. 982. Online. *Hum Mutat.* **28**(11):1150.
- Prezma T, Shteinfer A, Admoni L, Raviv Z, Sela I, Levi I, Shoshan-Barmatz V. (2013) VDAC1-based peptides: novel pro-apoptotic agents and potential therapeutics for B-cell chronic lymphocytic leukemia. *Cell Death Dis.* **4**:e809.
- Przedborski S, Vila M, Jackson-Lewis V. (2003) Neurodegeneration: what is it and where are we? *J Clin Invest.* **111**(1):3-10.
- Qin Q, Downey JM, Cohen MV. (2003) Acetylcholine but not adenosine triggers preconditioning through PI3-kinase and a tyrosine kinase. *Am J Physiol Heart Circ Physiol.* **284**(2):H727-34.
- Quan G, Choi JY, Lee DS, Lee SC. (2005) TGF-beta1 up-regulates transglutaminase two and fibronectin in dermal fibroblasts: a possible mechanism for the stabilization of tissue inflammation. *Arch Dermatol Res.* **297**(2):84-90.

Rajagopal S, Ahn S, Rominger DH, Gowen-MacDonald W, Lam CM, Dewire SM, Violin JD, Lefkowitz RJ. (2011) Quantifying ligand bias at seven-transmembrane receptors. *Mol Pharmacol.* **80**(3):367-77.

Rajagopal S. (2013) Quantifying biased agonism: understanding the links between affinity and efficacy. *Nat Rev Drug Discov.* **12**(6):483.

Ralevic V, Burnstock G. (1998) Receptors for purines and pyrimidines. *Pharmacol Rev.* **50**(3):413-92.

Randhawa PK, Jaggi AS. (2016) Unraveling the role of adenosine in remote ischemic preconditioning-induced cardioprotection. *Life Sci.* **155**:140-6.

Rankovic Z, Brust TF, Bohn LM. (2016) Biased agonism: An emerging paradigm in GPCR drug discovery. *Bioorg Med Chem Lett.* **26**(2):241-50.

Rauhavirta T, Hietikko M, Salmi T, Lindfors K. (2016) Transglutaminase 2 and Transglutaminase 2 Autoantibodies in Celiac Disease: a Review. *Clin Rev Allergy Immunol.* [Epub ahead of print].

Rebecchi MJ, Pentylala SN. (2000) Structure, function, and control of phosphoinositide-specific phospholipase C. *Physiol Rev.* **80**(4):1291-335.

Regan SE, Broad M, Byford AM, Lankford AR, Cerniway RJ, Mayo MW, Matherne GP. (2003) A1 adenosine receptor overexpression attenuates ischemia-reperfusion-induced apoptosis and caspase 3 activity. *Am J Physiol Heart Circ Physiol.* **284**(3):H859-66.

Reiter E, Ahn S, Shukla AK, Lefkowitz RJ. (2012) Molecular mechanism of β -arrestin-biased agonism at seven-transmembrane receptors. *Annu Rev Pharmacol Toxicol.* **52**:179-97.

Reiter MJ. (2004) Cardiovascular drug class specificity: beta-blockers. *Prog Cardiovasc Dis.* **47**(1):11-33.

Rikova K, Guo A, Zeng Q, Possemato A, Yu J, Haack H, Nardone J, Lee K, Reeves C, Li Y, Hu Y, Tan Z, Stokes M, Sullivan L, Mitchell J, Wetzel R, Macneill J, Ren JM, Yuan J, Bakalarski CE, Villen J, Kornhauser JM, Smith B, Li D, Zhou X, Gygi SP, Gu TL, Polakiewicz RD, Rush J, Comb MJ. (2007) Global survey of phosphotyrosine signaling identifies oncogenic kinases in lung cancer. *Cell.* **131**(6):1190-203.

Risso G, Blaustein M, Pozzi B, Mammi P, Srebrow A. (2015) Akt/PKB: one kinase, many modifications. *Biochem J.* **468**(2):203-14.

- Roberts SJ, Molenaar P, Summers RJ. (1993) Characterization of propranolol-resistant (-)-[125I]-cyanopindolol binding sites in rat soleus muscle. *Br J Pharmacol.* **109**(2):344-52.
- Roberts SJ, Russell FD, Molenaar P, Summers RJ. (1995) Characterization and localization of atypical beta-adrenoceptors in rat ileum. *Br J Pharmacol.* **116**(6):2549-56.
- Robinet A, Hoizey G, Millart H. (2005) PI 3-kinase, protein kinase C, and protein kinase A are involved in the trigger phase of beta1-adrenergic preconditioning. *Cardiovasc Res.* **66**(3):530-42.
- Robinson AJ, Dickenson JM. (2001) Regulation of p42/p44 MAPK and p38 MAPK by the adenosine A(1) receptor in DDT(1)MF-2 cells. *Eur J Pharmacol.* **413**(2-3):151-61.
- Rocha-Singh KJ, Honbo NY, Karliner JS. (1991) Hypoxia and glucose independently regulate the beta-adrenergic receptor-adenylate cyclase system in cardiac myocytes. *J Clin Invest.* **88**(1):204-13.
- Rodolfo C, Mormone E, Matarrese P, Ciccocanti F, Farrace MG, Garofano E, Piredda L, Fimia GM, Malorni W, Piacentini M. (2004) Tissue transglutaminase is a multifunctional BH3-only protein. *J Biol Chem.* **279**(52):54783-92.
- Rohrer DK, Desai KH, Jasper JR, Stevens ME, Regula DP Jr, Barsh GS, Bernstein D, Kobilka BK. (1996) Targeted disruption of the mouse beta1-adrenergic receptor gene: developmental and cardiovascular effects. *Proc Natl Acad Sci U S A.* **93**(14):7375-80.
- Rosa JC, César MC. (2016) Role of Hexokinase and VDAC in Neurological Disorders. *Curr Mol Pharmacol.* **9**(4):320-331.
- Rosenbaum DM, Rasmussen SG, Kobilka BK. (2009) The structure and function of G-protein-coupled receptors. *Nature.* **459**(7245):356-63.
- Rozec B, Gauthier C. (2006) beta3-adrenoceptors in the cardiovascular system: putative roles in human pathologies. *Pharmacol Ther.* **111**(3):652-73.
- Ruan Q, Quintanilla RA, Johnson GV. (2007) Type 2 transglutaminase differentially modulates striatal cell death in the presence of wild type or mutant huntingtin. *J Neurochem.* **102**(1):25-36.

- Ruan Q, Tucholski J, Gundemir S, Johnson Voll GV. (2008) The Differential Effects of R580A Mutation on Transamidation and GTP Binding Activity of Rat and Human Type 2 Transglutaminase. *Int J Clin Exp Med.* **1**(3):248-59.
- Sabourin J, Antigny F, Robin E, Frieden M, Raddatz E. (2012) Activation of transient receptor potential canonical 3 (TRPC3)-mediated Ca²⁺ entry by A1 adenosine receptor in cardiomyocytes disturbs atrioventricular conduction. *J Biol Chem.* **287**(32):26688-701.
- Safran N, Shneyvays V, Balas N, Jacobson KA, Nawrath H, Shainberg A. (2001) Cardioprotective effects of adenosine A1 and A3 receptor activation during hypoxia in isolated rat cardiac myocytes. *Mol Cell Biochem.* **217**(1-2):143-52.
- Sailer A, Houlden H. (2012) Recent advances in the genetics of cerebellar ataxias. *Curr Neurol Neurosci Rep.* **12**(3):227-36.
- Salie R, Moolman JA, Lochner A. (2012) The mechanism of beta-adrenergic preconditioning: roles for adenosine and ROS during triggering and mediation. *Basic Res Cardiol.* **107**(5):281.
- Salie R, Moolman JA, Lochner A. (2011) The role of β -adrenergic receptors in the cardioprotective effects of beta-preconditioning (β PC). *Cardiovasc Drugs Ther.* **25**(1):31-46.
- Salvatore CA, Tilley SL, Latour AM, Fletcher DS, Koller BH, Jacobson MA. (2000) Disruption of the A(3) adenosine receptor gene in mice and its effect on stimulated inflammatory cells. *J Biol Chem.* **275**(6):4429-34.
- Sanada S, Kitakaze M. (2004) Ischemic preconditioning: emerging evidence, controversy, and translational trials. *Int J Cardiol.* **97**(2):263-76.
- Sane DC, Kontos JL, Greenberg CS. (2007) Roles of transglutaminases in cardiac and vascular diseases. *Front Biosci.* **12**:2530-45.
- Santhanam L, Tuday EC, Webb AK, Dowzicky P, Kim JH, Oh YJ, Sikka G, Kuo M, Halushka MK, Macgregor AM, Dunn J, Gutbrod S, Yin D, Shoukas A, Nyhan D, Flavahan NA, Belkin AM, Berkowitz DE. (2010) Decreased S-nitrosylation of tissue transglutaminase contributes to age-related increases in vascular stiffness. *Circ Res.* **107**(1):117-25.
- Sarang Z, Molnár P, Németh T, Gomba S, Kardon T, Melino G, Cotecchia S, Fésüs L, Szondy Z. (2005) Tissue transglutaminase (TG2) acting as G protein protects hepatocytes against Fas-mediated cell death in mice. *Hepatology.* **42**(3):578-87.

- Sarang Z, Tóth B, Balajthy Z, Köröskényi K, Garabuczi E, Fésüs L, Szondy Z. (2009) Some lessons from the tissue transglutaminase knockout mouse. *Amino Acids*. **36**(4):625-31.
- Saraste A, Pulkki K, Kallajoki M, Henriksen K, Parvinen M, Voipio-Pulkki LM. (1997) Apoptosis in human acute myocardial infarction. *Circulation*. **95**(2):320-3.
- Sarbassov DD, Guertin DA, Ali SM, Sabatini DM. (2005) Phosphorylation and regulation of Akt/PKB by the rictor-mTOR complex. *Science*. **307**(5712):1098-101.
- Sarsero D, Molenaar P, Kaumann AJ, Freestone NS. (1999) Putative beta 4-adrenoceptors in rat ventricle mediate increases in contractile force and cell Ca²⁺: comparison with atrial receptors and relationship to (-)-[3H]-CGP 12177 binding. *Br J Pharmacol*. **128**(7):1445-60.
- Satpathy M, Cao L, Pincheira R, Emerson R, Bigsby R, Nakshatri H, Matei D. (2007) Enhanced peritoneal ovarian tumor dissemination by tissue transglutaminase. *Cancer Res*. **67**(15):7194-202.
- Schaertl S, Prime M, Wityak J, Dominguez C, Munoz-Sanjuan I, Pacifici RE, Courtney S, Scheel A, Macdonald D. (2010) A profiling platform for the characterization of transglutaminase 2 (TG2) inhibitors. *J Biomol Screen*. **15**(5):478-87.
- Schäfer M, Pönicke K, Heinroth-Hoffmann I, Brodde OE, Piper HM, Schlüter KD. (2001) Beta-adrenoceptor stimulation attenuates the hypertrophic effect of alpha-adrenoceptor stimulation in adult rat ventricular cardiomyocytes. *J Am Coll Cardiol*. **37**(1):300-7.
- Schaper J, Kostin S. (2005) Cell death and adenosine triphosphate: the paradox. *Circulation*. **112**(1):6-8.
- Schmidt A, Beck M, Malmström J, Lam H, Claassen M, Campbell D, Aebersold R. (2011) Absolute quantification of microbial proteomes at different states by directed mass spectrometry. *Mol Syst Biol*. **7**:510.
- Schmitt JM, Stork PJ. (2000) beta 2-adrenergic receptor activates extracellular signal-regulated kinases (ERKs) via the small G protein rap1 and the serine/threonine kinase B-Raf. *J Biol Chem*. **275**(33):25342-50.
- Schneider G, Filipek A. (2011) S100A6 binding protein and Siah-1 interacting protein (CacyBP/SIP): spotlight on properties and cellular function. *Amino Acids*. **41**(4):773-80.

- Scholz KP, Miller RJ. (1991) GABAB receptor-mediated inhibition of Ca²⁺ currents and synaptic transmission in cultured rat hippocampal neurones. *J Physiol.* **444**:669-86.
- Schömig A. (1990) Catecholamines in myocardial ischemia. Systemic and cardiac release. *Circulation.* **82**(3 Suppl):II13-22.
- Schreiber KL, Paquet L, Allen BG, Rindt H. (2001) Protein kinase C isoform expression and activity in the mouse heart. *Am J Physiol Heart Circ Physiol.* **281**(5):H2062-71.
- Schulte G, Fredholm BB. (2003) Signalling from adenosine receptors to mitogen-activated protein kinases. *Cell Signal.* **15**(9):813-27.
- Schuppan D, Hahn EG. (2002) Biomedicine. Gluten and the gut-lessons for immune regulation. *Science.* **297**(5590):2218-20.
- Schwartz DD. (1997) Activation of alpha-2 adrenergic receptors inhibits norepinephrine release by a pertussis toxin-insensitive pathway independent of changes in cytosolic calcium in cultured rat sympathetic neurons. *J Pharmacol Exp Ther.* **282**(1):248-55.
- Schwartz LM, Lagranha CJ. (2006) Ischemic postconditioning during reperfusion activates Akt and ERK without protecting against lethal myocardial ischemia-reperfusion injury in pigs. *Am J Physiol Heart Circ Physiol.* **290**(3):H1011-8.
- Schwarzer C, Barnikol-Watanabe S, Thinner FP, Hilschmann N. (2002) Voltage-dependent anion-selective channel (VDAC) interacts with the dynein light chain Tctex1 and the heat-shock protein PBP74. *Int J Biochem Cell Biol.* **34**(9):1059-70.
- Sener A, Dunlop ME, Gomis R, Mathias PC, Malaisse-Lagae F, Malaisse WJ. (1985) Role of transglutaminase in insulin release. Study with glycine and sarcosine methylesters. *Endocrinology.* **117**(1):237-42.
- Seurin D, Lombet A, Babajko S, Godeau F, Ricort JM. (2013) Insulin-like growth factor binding proteins increase intracellular calcium levels in two different cell lines. *PLoS One.* **8**(3):e59323.
- Shafiei M, Mahmoudian M. (1999) Atypical beta-adrenoceptors of rat thoracic aorta. *Gen Pharmacol.* **32**(5):557-62.
- Shcherbakova OG, Hurt CM, Xiang Y, Dell'Acqua ML, Zhang Q, Tsien RW, Kobilka BK. (2007) Organization of beta-adrenoceptor signaling compartments by sympathetic innervation of cardiac myocytes. *J Cell Biol.* **176**(4):521-33.

Shenoy SK, Drake MT, Nelson CD, Houtz DA, Xiao K, Madabushi S, Reiter E, Premont RT, Lichtarge O, Lefkowitz RJ. (2006) beta-arrestin-dependent, G protein-independent ERK1/2 activation by the beta2 adrenergic receptor. *J Biol Chem.* **281**(2):1261-73.

Sheth S, Brito R, Mukherjea D, Rybak LP, Ramkumar V. (2014) Adenosine receptors: expression, function and regulation. *Int J Mol Sci.* **15**(2):2024-52.

Shin DM, Kang J, Ha J, Kang HS, Park SC, Kim IG, Kim SJ. (2008) Cystamine prevents ischemia-reperfusion injury by inhibiting polyamination of RhoA. *Biochem Biophys Res Commun.* **365**(3):509-14.

Shizukuda Y, Buttrick PM. (2002) Subtype specific roles of beta-adrenergic receptors in apoptosis of adult rat ventricular myocytes. *J Mol Cell Cardiol.* **34**(7):823-31.

Shoshan-Barmatz V, Keinan N, Abu-Hamad S, Tyomkin D, Aram L. (2010) Apoptosis is regulated by the VDAC1 N-terminal region and by VDAC oligomerization: release of cytochrome c, AIF and Smac/Diablo. *Biochim Biophys Acta.* **1797**(6-7):1281-91.

Shoshan-Barmatz V, Zakar M, Rosenthal K, Abu-Hamad S. (2009) Key regions of VDAC1 functioning in apoptosis induction and regulation by hexokinase. *Biochim Biophys Acta.* **1787**(5):421-30.

Shrestha R, Tatsukawa H, Shrestha R, Ishibashi N, Matsuura T, Kagechika H, Kose S, Hitomi K, Imamoto N, Kojima S. (2015) Molecular mechanism by which acyclic retinoid induces nuclear localization of transglutaminase 2 in human hepatocellular carcinoma cells. *Cell Death Dis.* **6**:e2002.

Shryock JC, Belardinelli L. (1997) Adenosine and adenosine receptors in the cardiovascular system: biochemistry, physiology, and pharmacology. *Am J Cardiol.* **79**(12A):2-10.

Shweke N, Boulos N, Jouanneau C, Vandermeersch S, Melino G, Dussaule JC, Chatziantoniou C, Ronco P, Boffa JJ. (2008) Tissue transglutaminase contributes to interstitial renal fibrosis by favoring accumulation of fibrillar collagen through TGF-beta activation and cell infiltration. *Am J Pathol.* **173**(3):631-42.

Siedlecka U, Arora M, Kolettis T, Soppa GK, Lee J, Stagg MA, Harding SE, Yacoub MH, Terracciano CM. (2008) Effects of clenbuterol on contractility and Ca²⁺ homeostasis of isolated rat ventricular myocytes. *Am J Physiol Heart Circ Physiol.* **295**(5):H1917-26.

- Siegel M, Khosla C. (2007) Transglutaminase 2 inhibitors and their therapeutic role in disease states. *Pharmacol Ther.* **115**(2):232-45.
- Sileno S, D'Oria V, Stucchi R, Alessio M, Petrini S, Bonetto V, Maechler P, Bertuzzi F, Grasso V, Paolella K, Barbetti F, Massa O. (2014) A possible role of transglutaminase 2 in the nucleus of INS-1E and of cells of human pancreatic islets. *J Proteomics.* **96**:314-27.
- Simonis G, Briem SK, Schoen SP, Bock M, Marquetant R, Strasser RH. (2007) Protein kinase C in the human heart: differential regulation of the isoforms in aortic stenosis or dilated cardiomyopathy. *Mol Cell Biochem.* **305**(1-2):103-11.
- Simpson P. (1983) Norepinephrine-stimulated hypertrophy of cultured rat myocardial cells is an alpha 1 adrenergic response. *J Clin Invest.* **72**(2):732-8.
- Singh RN, McQueen T, Mehta K. (1995) Detection of the amine acceptor protein substrates of transglutaminase with 5-(biotinamido) pentylamine. *Anal Biochem.* **231**(1):261-3.
- Singh US, Kunar MT, Kao YL, Baker KM. (2001) Role of transglutaminase II in retinoic acid-induced activation of RhoA-associated kinase-2. *EMBO J.* **20**(10):2413-23.
- Singh US, Pan J, Kao YL, Joshi S, Young KL, Baker KM. (2003) Tissue transglutaminase mediates activation of RhoA and MAP kinase pathways during retinoic acid-induced neuronal differentiation of SH-SY5Y cells. *J Biol Chem.* **278**(1):391-9.
- Sivaramakrishnan M, Shooter GK, Upton Z, Croll TI. (2013) Transglutaminases and receptor tyrosine kinases. *Amino Acids.* **44**(1):19-24.
- Sivaraman V, Hausenloy DJ, Kolvekar S, Hayward M, Yap J, Lawrence D, Di Salvo C, Yellon DM. (2009) The divergent roles of protein kinase C epsilon and delta in simulated ischaemia-reperfusion injury in human myocardium. *J Mol Cell Cardiol.* **46**(5):758-64.
- Skeberdis VA, Jurevicius J, Fischmeister aR. (1997) Beta-2 adrenergic activation of L-type Ca⁺⁺ current in cardiac myocytes. *J Pharmacol Exp Ther.* **283**(2):452-61.
- Skeberdis VA, Jurevicius J, Fischmeister R. (1997) Pharmacological characterization of the receptors involved in the beta-adrenoceptor-mediated stimulation of the L-type Ca²⁺ current in frog ventricular myocytes. *Br J Pharmacol.* **121**(7):1277-86.

Slaughter TF, Achyuthan KE, Lai TS, Greenberg CS. (1992) A microtiter plate transglutaminase assay utilizing 5-(biotinamido)pentylamine as substrate. *Anal Biochem.* **205**(1):166-71.

Small K, Feng JF, Lorenz J, Donnelly ET, Yu A, Im MJ, Dorn GW 2nd, Liggett SB. (1999) Cardiac specific overexpression of transglutaminase II (G(h)) results in a unique hypertrophy phenotype independent of phospholipase C activation. *J Biol Chem.* **274**(30):21291-6.

Smith PK, Krohn RI, Hermanson GT, Mallia AK, Gartner FH, Provenzano MD, Fujimoto EK, Goeke NM, Olson BJ, Klenk DC. (1985) Measurement of protein using bicinchoninic acid. *Anal Biochem.* **150**(1):76-85. Erratum in: *Anal Biochem* 1985 May 15;163(1):279.

Smrcka AV, Sternweis PC. (1993) Regulation of purified subtypes of phosphatidylinositol-specific phospholipase C beta by G protein alpha and beta gamma subunits. *J Biol Chem.* **268**(13):9667-74.

Sneddon WB, Magyar CE, Willick GE, Syme CA, Galbiati F, Bisello A, Friedman PA. (2004) Ligand-selective dissociation of activation and internalization of the parathyroid hormone (PTH) receptor: conditional efficacy of PTH peptide fragments. *Endocrinology.* **145**(6):2815-23.

Solaini G, Harris DA. (2005) Biochemical dysfunction in heart mitochondria exposed to ischaemia and reperfusion. *Biochem J.* **390**(Pt 2):377-94.

Solenkova NV, Solodushko V, Cohen MV, Downey JM. (2006) Endogenous adenosine protects preconditioned heart during early minutes of reperfusion by activating Akt. *Am J Physiol Heart Circ Physiol.* **290**(1):H441-9.

Sollid LM, Scott H. (1998) New tool to predict celiac disease on its way to the clinics. *Gastroenterology.* **115**(6):1584-6.

Soltis AR, Saucerman JJ. (2010) Synergy between CaMKII substrates and β -adrenergic signaling in regulation of cardiac myocyte Ca(2+) handling. *Biophys J.* **99**(7):2038-47.

Somvanshi RK, Qiu X, Kumar U. (2013) Isoproterenol induced hypertrophy and associated signaling pathways are modulated by somatostatin in H9c2 cells. *Int J Cardiol.* **167**(3):1012-22.

Somvanshi RK, War SA, Chaudhari N, Qiu X, Kumar U. (2011) Receptor specific crosstalk and modulation of signaling upon heterodimerization between β 1-adrenergic receptor and somatostatin receptor-5. *Cell Signal.* **23**(5):794-811.

Soto D, De Arcangelis V, Zhang J, Xiang Y. (2009) Dynamic protein kinase activities induced by beta-adrenoceptors dictate signaling propagation for substrate phosphorylation and myocyte contraction. *Circ Res.* **104**(6):770-9.

Southworth R, Davey KA, Warley A, Garlick PB. (2007) A reevaluation of the roles of hexokinase I and II in the heart. *Am J Physiol Heart Circ Physiol.* **292**(1):H378-86.

Spear JF, Prabu SK, Galati D, Raza H, Anandatheerthavarada HK, Avadhani NG. (2007) beta1-Adrenoreceptor activation contributes to ischemia-reperfusion damage as well as playing a role in ischemic preconditioning. *Am J Physiol Heart Circ Physiol.* **292**(5):H2459-66.

Stahl EL, Zhou L, Ehlert FJ, Bohn LM. (2015) A novel method for analyzing extremely biased agonism at G protein-coupled receptors. *Mol Pharmacol.* **87**(5):866-77.

Stamnaes J, Fleckenstein B, Sollid LM. (2008) The propensity for deamidation and transamidation of peptides by transglutaminase 2 is dependent on substrate affinity and reaction conditions. *Biochim Biophys Acta.* **1784**(11):1804-11.

Stamnaes J, Pinkas DM, Fleckenstein B, Khosla C, Sollid LM. (2010) Redox regulation of transglutaminase 2 activity. *J Biol Chem.* **285**(33):25402-9.

Staus DP, Wingler LM, Strachan RT, Rasmussen SG, Pardon E, Ahn S, Steyaert J, Kobilka BK, Lefkowitz RJ. (2014) Regulation of β 2-adrenergic receptor function by conformationally selective single-domain intrabodies. *Mol Pharmacol.* **85**(3):472-81.

Steinberg SF. (1999) The molecular basis for distinct beta-adrenergic receptor subtype actions in cardiomyocytes. *Circ Res.* **85**(11):1101-11.

Steinberg SF. (2012) Cardiac actions of protein kinase C isoforms. *Physiology (Bethesda).* **27**(3):130-9.

Stephens P, Grenard P, Aeschlimann P, Langley M, Blain E, Errington R, Kipling D, Thomas D, Aeschlimann D. (2004) Crosslinking and G-protein functions of transglutaminase 2 contribute differentially to fibroblast wound healing responses. *J Cell Sci.* **117**(Pt 15):3389-403.

Steppan J, Bergman Y, Viegas K, Armstrong D, Tan S, Wang H, Melucci S, Hori D, Park SY, Barreto SF, Isak A, Jandu S, Flavahan N, Butlin M, An SS, Avolio A, Berkowitz DE, Halushka MK, Santhanam L. (2017) Tissue Transglutaminase

Modulates Vascular Stiffness and Function Through Crosslinking-Dependent and Crosslinking-Independent Functions. *J Am Heart Assoc.* **6**(2).

Steppan J, Sikka G, Jandu S, Barodka V, Halushka MK, Flavahan NA, Belkin AM, Nyhan D, Butlin M, Avolio A, Berkowitz DE, Santhanam L. (2014) Exercise, vascular stiffness, and tissue transglutaminase. *J Am Heart Assoc.* **3**(2):e000599.

Sterin-Borda L, Gómez RM, Borda E. (2002) Role of nitric oxide/cyclic GMP in myocardial adenosine A1 receptor-inotropic response. *Br J Pharmacol.* **135**(2):444-50.

Stockwell J, Jakova E, Cayabyab FS. (2017) Adenosine A1 and A2A Receptors in the Brain: Current Research and Their Role in Neurodegeneration. *Molecules.* **22**(4). pii: E676.

Straiker AJ, Borden CR, Sullivan JM. (2002) G-protein alpha subunit isoforms couple differentially to receptors that mediate presynaptic inhibition at rat hippocampal synapses. *J Neurosci.* **22**(7):2460-8.

Strasser, RH, Krimmer, J, Braun-Duallaeus, R, Marquetant, R, Kubler, W (1990) Dual sensitization of the adrenergic system in early myocardial ischemia: Independent regulation of the P-adrenergic receptors and the adenylyl cyclase. *Journal of Molecular and Cellular Cardiology* **22**(12): 1405-1423.

Sun L, Fan H, Yang L, Shi L, Liu Y. (2015) Tyrosol prevents ischemia/reperfusion-induced cardiac injury in H9c2 cells: involvement of ROS, Hsp70, JNK and ERK, and apoptosis. *Molecules.* **20**(3):3758-75.

Sun L, Zhao M, Yang Y, Xue RQ, Yu XJ, Liu JK, Zang WJ. (2016) Acetylcholine Attenuates Hypoxia/Reoxygenation Injury by Inducing Mitophagy Through PINK1/Parkin Signal Pathway in H9c2 Cells. *J Cell Physiol.* **231**(5):1171-81.

Sunahara RK, Insel PA. (2016) The Molecular Pharmacology of G Protein Signaling Then and Now: A Tribute to Alfred G. Gilman. *Mol Pharmacol.* **89**(5):585-92.

Suto N, Ikura K, Sasaki R. (1993) Expression induced by interleukin-6 of tissue-type transglutaminase in human hepatoblastoma HepG2 cells. *J Biol Chem.* **268**(10):7469-73.

Swaminathan PD, Purohit A, Hund TJ, Anderson ME. (2012) Calmodulin-dependent protein kinase II: linking heart failure and arrhythmias. *Circ Res.* **110**(12):1661-77.

Syrovatkina V, Alegre KO, Dey R, Huang XY. (2016) Regulation, Signaling, and Physiological Functions of G-Proteins. *J Mol Biol.* **428**(19):3850-68.

- Szondy Z, Mastroberardino PG, Váradi J, Farrace MG, Nagy N, Bak I, Viti I, Wieckowski MR, Melino G, Rizzuto R, Tószaki A, Fesus L, Piacentini M. (2006) Tissue transglutaminase (TG2) protects cardiomyocytes against ischemia/reperfusion injury by regulating ATP synthesis. *Cell Death Differ.* **13**(10):1827-9.
- Tanaka M, Ito H, Adachi S, Akimoto H, Nishikawa T, Kasajima T, Marumo F, Hiroe M. (1994) Hypoxia induces apoptosis with enhanced expression of Fas antigen messenger RNA in cultured neonatal rat cardiomyocytes. *Circ Res.* **75**(3):426-33.
- Tatsukawa H, Furutani Y, Hitomi K, Kojima S. (2016) Transglutaminase 2 has opposing roles in the regulation of cellular functions as well as cell growth and death. *Cell Death Dis.* **7**(6):e2244.
- Tatsukawa H, Kojima S. (2010) Recent advances in understanding the roles of transglutaminase 2 in alcoholic steatohepatitis. *Cell Biol Int.* **34**(3):325-34.
- Tatsukawa H, Sano T, Fukaya Y, Ishibashi N, Watanabe M, Okuno M, Moriwaki H, Kojima S. (2011) Dual induction of caspase 3- and transglutaminase-dependent apoptosis by acyclic retinoid in hepatocellular carcinoma cells. *Mol Cancer.* **10**:4.
- Tatsumi T, Shiraishi J, Keira N, Akashi K, Mano A, Yamanaka S, Matoba S, Fushiki S, Fliss H, Nakagawa M. (2003) Intracellular ATP is required for mitochondrial apoptotic pathways in isolated hypoxic rat cardiac myocytes. *Cardiovasc Res.* **59**(2):428-40.
- Tchivileva IE, Tan KS, Gambarian M, Nackley AG, Medvedev AV, Romanov S, Flood PM, Maixner W, Makarov SS, Diatchenko L. (2009) Signaling pathways mediating beta3-adrenergic receptor-induced production of interleukin-6 in adipocytes. *Mol Immunol.* **46**(11-12):2256-66.
- Tee AE, Marshall GM, Liu PY, Xu N, Haber M, Norris MD, Iismaa SE, Liu T. (2010) Opposing effects of two tissue transglutaminase protein isoforms in neuroblastoma cell differentiation. *J Biol Chem.* **285**(6):3561-7.
- Telci D, Wang Z, Li X, Verderio EA, Humphries MJ, Baccarini M, Basaga H, Griffin M. (2008) Fibronectin-tissue transglutaminase matrix rescues RGD-impaired cell adhesion through syndecan-4 and beta1 integrin co-signaling. *J Biol Chem.* **283**(30):20937-47.
- Terzic A, Pucéat M, Vassort G, Vogel SM. (1993) Cardiac alpha 1-adrenoceptors: an overview. *Pharmacol Rev.* **45**(2):147-75.

- Thangaraju K, Biri B, Schlosser G, Kiss B, Nyitray L, Fésüs L, Király R. (2016) Real-time kinetic method to monitor isopeptidase activity of transglutaminase 2 on protein substrate. *Anal Biochem.* **505**:36-42.
- Thomas H, Beck K, Adamczyk M, Aeschlimann P, Langley M, Oita RC, Thiebach L, Hils M, Aeschlimann D. (2013) Transglutaminase 6: a protein associated with central nervous system development and motor function. *Amino Acids.* **44**(1):161-77.
- Thornton JD, Liu GS, Olsson RA, Downey JM. (1992) Intravenous pretreatment with A1-selective adenosine analogues protects the heart against infarction. *Circulation.* **85**(2):659-65.
- Toker A, Marmiroli S. (2014) Signaling specificity in the Akt pathway in biology and disease. *Adv Biol Regul.* **55**:28-38.
- Tolentino PJ, Waghray A, Wang KK, Hayes RL. (2004) Increased expression of tissue-type transglutaminase following middle cerebral artery occlusion in rats. *J Neurochem.* **89**(5):1301-7.
- Tomura H, Itoh H, Sho K, Sato K, Nagao M, Ui M, Kondo Y, Okajima F. (1997) Betagamma subunits of pertussis toxin-sensitive G proteins mediate A1 adenosine receptor agonist-induced activation of phospholipase C in collaboration with thyrotropin. A novel stimulatory mechanism through the cross-talk of two types of receptors. *J Biol Chem.* **272**(37):23130-7.
- Tong H, Bernstein D, Murphy E, Steenbergen C. (2005) The role of beta-adrenergic receptor signaling in cardioprotection. *FASEB J.* **19**(8):983-5.
- Toone, E. (2011). *Advances in Enzymology and Related Areas of Molecular Biology*. 1st ed. Hoboken: *John Wiley & Sons, Incorporated.* **78**:PMID22220470
- Tota B, Angelone T, Cerra MC. (2014) The surging role of Chromogranin A in cardiovascular homeostasis. *Front Chem.* **2**:64.
- Tota B, Gentile S, Pasqua T, Bassino E, Koshimizu H, Cawley NX, Cerra MC, Loh YP, Angelone T. (2012) The novel chromogranin A-derived serpinin and pyroglutaminated serpinin peptides are positive cardiac β -adrenergic-like inotropes. *FASEB J.* **26**(7):2888-98.
- Tóth B, Garabuczi E, Sarang Z, Vereb G, Vámosi G, Aeschlimann D, Blaskó B, Bécsi B, Erdődi F, Lacy-Hulbert A, Zhang A, Falasca L, Birge RB, Balajthy Z, Melino G, Fésüs L, Szondy Z. (2009) Transglutaminase 2 is needed for the formation of an

efficient phagocyte portal in macrophages engulfing apoptotic cells. *J Immunol.* **182**(4):2084-92.

Towbin H, Staehelin T, Gordon J. (1979) Electrophoretic transfer of proteins from polyacrylamide gels to nitrocellulose sheets: procedure and some applications. *Proc Natl Acad Sci U S A.* **76**(9):4350-4.

Tracey, W. (1998) "Selective activation of adenosine A3 receptors with N6-(3-chlorobenzyl)-5'-N-methylcarboxamidoadenosine (CB-MECA) provides cardioprotection via KATP channel activation." *Cardiovascular Research* **40**(1): 138-45.

Trigwell SM, Lynch PT, Griffin M, Hargreaves AJ, Bonner PL. (2004) An improved colorimetric assay for the measurement of transglutaminase (type II)-(gamma-glutamyl) lysine cross-linking activity. *Anal Biochem.* **330**(1):164-6.

Trump BF, Berezsky IK. (1996) The role of altered $[Ca^{2+}]_i$ regulation in apoptosis, oncosis, and necrosis. *Biochim Biophys Acta.* **1313**(3):173-8.

Tsoporis JN, Izhar S, Parker TG. (2008) Expression of S100A6 in cardiac myocytes limits apoptosis induced by tumor necrosis factor-alpha. *J Biol Chem.* **283**(44):30174-83.

Tucholski J, Johnson GV. (2003) Tissue transglutaminase directly regulates adenylyl cyclase resulting in enhanced cAMP-response element-binding protein (CREB) activation. *J Biol Chem.* **278**(29):26838-43.

Tutor AS, Penela P, Mayor F Jr. (2007) Anti-beta1-adrenergic receptor autoantibodies are potent stimulators of the ERK1/2 pathway in cardiac cells. *Cardiovasc Res.* **76**(1):51-60.

Urban JD, Clarke WP, von Zastrow M, Nichols DE, Kobilka B, Weinstein H, Javitch JA, Roth BL, Christopoulos A, Sexton PM, Miller KJ, Spedding M, Mailman RB. (2007) Functional selectivity and classical concepts of quantitative pharmacology. *J Pharmacol Exp Ther.* **320**(1):1-13.

Urmaliya VB, Church JE, Coupar IM, Rose-Meyer RB, Pouton CW, White PJ. (2009) Cardioprotection induced by adenosine A1 receptor agonists in a cardiac cell ischemia model involves cooperative activation of adenosine A2A and A2B receptors by endogenous adenosine. *J Cardiovasc Pharmacol.* **53**(5):424-33.

Van Driest SL, Ackerman MJ, Ommen SR, Shakur R, Will ML, Nishimura RA, Tajik AJ, Gersh BJ. (2002) Prevalence and severity of "benign" mutations in the beta-

- myosin heavy chain, cardiac troponin T, and alpha-tropomyosin genes in hypertrophic cardiomyopathy. *Circulation*. **106**(24):3085-90.
- Vanhaesebroeck B, Alessi DR. (2000) The PI3K-PDK1 connection: more than just a road to PKB. *Biochem J*. **346** Pt 3:561-76.
- Velasco CE, Turner M, Cobb MA, Virmani R, Forman MB. (1991) Myocardial reperfusion injury in the canine model after 40 minutes of ischemia: effect of intracoronary adenosine. *Am Heart J*. **122**(6):1561-70.
- Verderio EA, Johnson T, Griffin M. (2004) Tissue transglutaminase in normal and abnormal wound healing: review article. *Amino Acids*. **26**(4):387-404.
- Verma A, Guha S, Diagaradjane P, Kunnumakkara AB, Sanguino AM, Lopez-Berestein G, Sood AK, Aggarwal BB, Krishnan S, Gelovani JG, Mehta K. (2008) Therapeutic significance of elevated tissue transglutaminase expression in pancreatic cancer. *Clin Cancer Res*. **14**(8):2476-83.
- Verma A, Guha S, Wang H, Fok JY, Koul D, Abbruzzese J, Mehta K. (2008) Tissue transglutaminase regulates focal adhesion kinase/AKT activation by modulating PTEN expression in pancreatic cancer cells. *Clin Cancer Res*. **14**(7):1997-2005.
- Verma A, Mehta K. (2007) Tissue transglutaminase-mediated chemoresistance in cancer cells. *Drug Resist Updat*. **10**(4-5):144-51.
- Verma A, Wang H, Manavathi B, Fok JY, Mann AP, Kumar R, Mehta K. (2006) Increased expression of tissue transglutaminase in pancreatic ductal adenocarcinoma and its implications in drug resistance and metastasis. *Cancer Res*. **66**(21):10525-33.
- Veza R, Habib A, FitzGerald GA. (1999) Differential signaling by the thromboxane receptor isoforms via the novel GTP-binding protein, Gh. *J Biol Chem*. **274**(18):12774-9.
- Wallace AW, Au S, Cason BA. (2011) Perioperative β -blockade: atenolol is associated with reduced mortality when compared to metoprolol. *Anesthesiology*. **114**(4):824-36.
- Wallukat G. (2002) The beta-adrenergic receptors. *Herz*. **27**(7):683-90.
- Walther DJ, Peter JU, Winter S, Hölting M, Paulmann N, Grohmann M, Vowinkel J, Alamo-Bethencourt V, Wilhelm CS, Ahnert-Hilger G, Bader M. (2003) Serotonylation of small GTPases is a signal transduction pathway that triggers platelet alpha-granule release. *Cell*. **115**(7):851-62.

- Wang JL, Yang X, Xia K, Hu ZM, Weng L, Jin X, Jiang H, Zhang P, Shen L, Guo JF, Li N, Li YR, Lei LF, Zhou J, Du J, Zhou YF, Pan Q, Wang J, Wang J, Li RQ, Tang BS. (2010) TGM6 identified as a novel causative gene of spinocerebellar ataxias using exome sequencing. *Brain*. **133**(Pt 12):3510-8.
- Wang Y, Ande SR, Mishra S. (2012) Phosphorylation of transglutaminase 2 (TG2) at serine-216 has a role in TG2 mediated activation of nuclear factor-kappa B and in the downregulation of PTEN. *BMC Cancer*. **12**:277.
- Wang Y, De Arcangelis V, Gao X, Ramani B, Jung YS, Xiang Y. (2008) Norepinephrine- and epinephrine-induced distinct beta2-adrenoceptor signaling is dictated by GRK2 phosphorylation in cardiomyocytes. *J Biol Chem*. **283**(4):1799-807.
- Wang Z, Telci D, Griffin M. (2011) Importance of syndecan-4 and syndecan -2 in osteoblast cell adhesion and survival mediated by a tissue transglutaminase-fibronectin complex. *Exp Cell Res*. **317**(3):367-81.
- Wang, Jing, Quanhu Sheng, and Yu Shyr. (2015) "SWATH-MS in proteomics: current status." *International Journal of Computational Biology and Drug Design* **8**(3):192.
- Wang M, Sun GB, Du YY, Tian Y, Liao P, Liu XS, Ye JX, Sun XB. (2017) Myricitrin Protects Cardiomyocytes from Hypoxia/Reoxygenation Injury: Involvement of Heat Shock Protein 90. *Front Pharmacol*. **8**:353.
- Watkins SJ, Borthwick GM, Arthur HM. (2011) The H9C2 cell line and primary neonatal cardiomyocyte cells show similar hypertrophic responses in vitro. *In Vitro Cell Dev Biol Anim*. **47**(2):125-31.
- Webster KA, Discher DJ, Kaiser S, Hernandez O, Sato B, Bishopric NH. (1999) Hypoxia-activated apoptosis of cardiac myocytes requires reoxygenation or a Ph shift and is independent of p53. *J Clin Invest*. **104**(3):239-52.
- Wettschureck N, Offermanns S. (2005) Mammalian G proteins and their cell type specific functions. *Physiol Rev*. **85**(4):1159-204.
- White TE, Dickenson JM, Alexander SP, Hill SJ. (1992) Adenosine A1-receptor stimulation of inositol phospholipid hydrolysis and calcium mobilisation in DDT1 MF-2 cells. *Br J Pharmacol*. **106**(1):215-21.
- Wieczorek DF, Jagatheesan G, Rajan S. (2008) The role of tropomyosin in heart disease. *Adv Exp Med Biol*. **644**:132-42.

- Wieczorek, DF. (2016) Tropomyosin: an effector of cardiac remodeling. *International Journal of Medical and Biological Frontiers*. **22**(1), 1-17.
- Williams H, Pease RJ, Newell LM, Cordell PA, Graham RM, Kearney MT, Jackson CL, Grant PJ. (2010) Effect of transglutaminase 2 (TG2) deficiency on atherosclerotic plaque stability in the apolipoprotein E deficient mouse. *Atherosclerosis*. **210**(1):94-9.
- Woo AY, Xiao RP. (2012) β -Adrenergic receptor subtype signaling in heart: from bench to bedside. *Acta Pharmacol Sin*. **33**(3):335-41.
- Wu D, Jiang H, Simon MI. (1995) Different alpha 1-adrenergic receptor sequences required for activating different G alpha subunits of Gq class of G proteins. *J Biol Chem*. **270**(17):9828-32.
- Wu Y, Temple J, Zhang R, Dzhura I, Zhang W, Trimble R, Roden DM, Passier R, Olson EN, Colbran RJ, Anderson ME. (2002) Calmodulin kinase II and arrhythmias in a mouse model of cardiac hypertrophy. *Circulation*. **106**(10):1288-93.
- Wu ZK, Iivainen T, Pehkonen E, Laurikka J, Tarkka MR. (2002) Ischemic preconditioning suppresses ventricular tachyarrhythmias after myocardial revascularization. *Circulation*. **106**(24):3091-6.
- Xi L, Das A, Zhao ZQ, Merino VF, Bader M, Kukreja RC. (2008) Loss of myocardial ischemic postconditioning in adenosine A1 and bradykinin B2 receptors gene knockout mice. *Circulation*. **118**(14 Suppl):S32-7.
- Xia Z, Li H, Irwin MG. (2016) Myocardial ischaemia reperfusion injury: the challenge of translating ischaemic and anaesthetic protection from animal models to humans. *Br J Anaesth*. **117** Suppl 2:ii44-ii62.
- Xia ZP, Sun L, Chen X, Pineda G, Jiang X, Adhikari A, Zeng W, Chen ZJ. (2009) Direct activation of protein kinases by unanchored polyubiquitin chains. *Nature*. **461**(7260):114-9.
- Xiang F, Huang YS, Zhang DX, Chu ZG, Zhang JP, Zhang Q. (2010) Adenosine A1 receptor activation reduces opening of mitochondrial permeability transition pores in hypoxic cardiomyocytes. *Clin Exp Pharmacol Physiol*. **37**(3):343-9.
- Xiang Y, Kobilka B. (2003) The PDZ-binding motif of the beta2-adrenoceptor is essential for physiologic signaling and trafficking in cardiac myocytes. *Proc Natl Acad Sci U S A*. **100**(19):10776-81.

- Xiang Y, Kobilka BK. (2003) Myocyte adrenoceptor signaling pathways. *Science*. **300**(5625):1530-2.
- Xiang Y, Rybin VO, Steinberg SF, Kobilka B. (2002) Caveolar localization dictates physiologic signaling of beta 2-adrenoceptors in neonatal cardiac myocytes. *J Biol Chem*. **277**(37):34280-6.
- Xiang YK. (2011) Compartmentalization of beta-adrenergic signals in cardiomyocytes. *Circ Res*. **109**(2):231-44.
- Xiao RP, Hohl C, Altschuld R, Jones L, Livingston B, Ziman B, Tantini B, Lakatta EG. (1994) Beta 2-adrenergic receptor-stimulated increase in cAMP in rat heart cells is not coupled to changes in Ca²⁺ dynamics, contractility, or phospholamban phosphorylation. *J Biol Chem*. **269**(29):19151-6.
- Xiao RP, Ji X, Lakatta EG. (1995) Functional coupling of the beta 2-adrenoceptor to a pertussis toxin-sensitive G protein in cardiac myocytes. *Mol Pharmacol*. **47**(2):322-9.
- Xiao RP, Zhang SJ, Chakir K, Avdonin P, Zhu W, Bond RA, Balke CW, Lakatta EG, Cheng H. (2003) Enhanced G(i) signaling selectively negates beta2-adrenergic receptor(AR)--but not beta1-AR-mediated positive inotropic effect in myocytes from failing rat hearts. *Circulation*. **108**(13):1633-9.
- Xiao RP. (2001) Beta-adrenergic signaling in the heart: dual coupling of the beta2-adrenergic receptor to G(s) and G(i) proteins. *Sci STKE*. **104**:re15.
- Xiao, R. P., and E. G. Lakatta. (1993) "Beta 1-adrenoceptor stimulation and beta 2-adrenoceptor stimulation differ in their effects on contraction, cytosolic Ca²⁺, and Ca²⁺ current in single rat ventricular cells." *Circulation Research* **73**(2): 286-300.
- Xin W, Tran TM, Richter W, Clark RB, Rich TC. (2008) Roles of GRK and PDE4 activities in the regulation of beta2 adrenergic signaling. *J Gen Physiol*. **131**(4):349-64.
- Xu Z, Downey JM, Cohen MV. (2001) Amp 579 reduces contracture and limits infarction in rabbit heart by activating adenosine A2 receptors. *J Cardiovasc Pharmacol*. **38**(3):474-81.
- Xu Y, Gu Q, Tang J, Qian Y, Tan X, Yu Z, Qu C. (2017) Substance P Attenuates Hypoxia/Reoxygenation-Induced Apoptosis Via the Akt Signalling Pathway and the NK1-Receptor in H9C2Cells. *Heart Lung Circ* **17**(pii):31420-8.

- Yabe K, Ishishita H, Tanonaka K, Takeo S. (1998) Pharmacologic preconditioning induced by beta-adrenergic stimulation is mediated by activation of protein kinase C. *J Cardiovasc Pharmacol.* **32**(6):962-8.
- Yanagawa Y, Hiraide S, Matsumoto M, Shimamura K, Togashi H. (2014) Enhanced transglutaminase 2 expression in response to stress-related catecholamines in macrophages. *Immunobiology.* **219**(9):680-6.
- Yang H, Raymer K, Butler R, Parlow J, Roberts R. (2006) The effects of perioperative beta-blockade: results of the Metoprolol after Vascular Surgery (MaVS) study, a randomized controlled trial. *Am Heart J.* **152**(5):983-90.
- Yang X, Zheng J, Xiong Y, Shen H, Sun L, Huang Y, Sun C, Li Y, He J. (2010) Beta-2 adrenergic receptor mediated ERK activation is regulated by interaction with MAGI-3. *FEBS Lett.* **584**(11):2207-12.
- Yang Z, Sun W, Hu K. (2009) Adenosine A(1) receptors selectively target protein kinase C isoforms to the caveolin-rich plasma membrane in cardiac myocytes. *Biochim Biophys Acta.* **1793**(12):1868-75.
- Yano N, Ianus V, Zhao TC, Tseng A, Padbury JF, Tseng YT. (2007) A novel signalling pathway for beta-adrenergic receptor-mediated activation of phosphoinositide 3-kinase in H9c2 cardiomyocytes. *Am J Physiol Heart Circ Physiol.* **293**(1):H385-93.
- Yates, L, Mardon, HL, Broadley, KJ (2003) Preconditioning against myocardial stunning by betaadrenoceptor stimulation with isoprenaline. 11th Meeting on Adrenergic Mechanisms, Porto, Portugal. *Autonomic and Autacoid Pharmacology* **23**: P7.
- Yellon DM, Hausenloy DJ. (2005) Realizing the clinical potential of ischemic preconditioning and postconditioning. *Nat Clin Pract Cardiovasc Med.* **2**(11):568-75.
- Yeung PK, Kolathuru SS (2015) Therapeutic Potential of Adenosine Transport Modulators for Cardiovascular Protection. *Cardiol Pharmacol* **4**:e127.
- Yu CH, Chou CC, Lee YJ, Khoo KH, Chang GD. (2015) Uncovering protein polyamination by the spermine-specific antiserum and mass spectrometric analysis. *Amino Acids.* **47**(3):469-81.
- Yuan L, Siegel M, Choi K, Khosla C, Miller CR, Jackson EN, Piwnicka-Worms D, Rich KM. (2007) Transglutaminase 2 inhibitor, KCC009, disrupts fibronectin assembly in the extracellular matrix and sensitizes orthotopic glioblastomas to chemotherapy. *Oncogene.* **26**(18):2563-73.

- Zainelli GM, Ross CA, Troncoso JC, Fitzgerald JK, Muma NA. (2004) Calmodulin regulates transglutaminase 2 cross-linking of huntingtin. *J Neurosci.* **24**(8):1954-61.
- Zatta AJ, Kin H, Lee G, Wang N, Jiang R, Lust R, Reeves JG, Mykytenko J, Guyton RA, Zhao ZQ, Vinten-Johansen J. (2006) Infarct-sparing effect of myocardial postconditioning is dependent on protein kinase C signalling. *Cardiovasc Res.* **70**(2):315-24.
- Zaugg M, Schaub MC. (2008) Beta3-adrenergic receptor subtype signaling in senescent heart: nitric oxide intoxication or "endogenous" beta blockade for protection? *Anesthesiology.* **109**(6):956-9.
- Zaugg M, Schaub MC. (2004) Cellular mechanisms in sympatho-modulation of the heart. *Br J Anaesth.* **93**(1):34-52.
- Zaugg M, Schaub MC. (2005) Genetic modulation of adrenergic activity in the heart and vasculature: implications for perioperative medicine. *Anesthesiology.* **102**(2):429-46.
- Zhang J, Antonyak MA, Singh G, Cerione RA. (2013) A mechanism for the upregulation of EGF receptor levels in glioblastomas. *Cell Rep.* **3**(6):2008-20.
- Zhang J, Lesort M, Guttman RP, Johnson GV. (1998) Modulation of the in situ activity of tissue transglutaminase by calcium and GTP. *J Biol Chem.* **273**(4):2288-95.
- Zhang J, Zhi HY, Ding F, Luo AP, Liu ZH. (2005) Transglutaminase 3 expression in C57BL/6J mouse embryo epidermis and the correlation with its differentiation. *Cell Res.* **15**(2):105-10.
- Zhang R, Khoo MS, Wu Y, Yang Y, Grueter CE, Ni G, Price EE Jr, Thiel W, Guatimosim S, Song LS, Madu EC, Shah AN, Vishnivetskaya TA, Atkinson JB, Gurevich VV, Salama G, Lederer WJ, Colbran RJ, Anderson ME. (2005) Calmodulin kinase II inhibition protects against structural heart disease. *Nat Med.* **11**(4):409-17.
- Zhang W, Yano N, Deng M, Mao Q, Shaw SK, Tseng YT. (2011) β -Adrenergic receptor-PI3K signaling crosstalk in mouse heart: elucidation of immediate downstream signalling cascades. *PLoS One.* **6**(10):e26581.
- Zhao ZQ, Corvera JS, Halkos ME, Kerendi F, Wang NP, Guyton RA, Vinten-Johansen J. (2003) Inhibition of myocardial injury by ischemic postconditioning

during reperfusion: comparison with ischemic preconditioning. *Am J Physiol Heart Circ Physiol.* **285**(2):H579-88.

Zhou P, Zhao YT, Guo YB, Xu SM, Bai SH, Lakatta EG, Cheng H, Hao XM, Wang SQ. (2009) Beta-adrenergic signaling accelerates and synchronizes cardiac ryanodine receptor response to a single L-type Ca²⁺ channel. *Proc Natl Acad Sci U S A.* **106**(42):18028-33.

Zhou, T., Zhou, Z., Zhou, S., & Huang, F. (2016) Real-time monitoring of contractile properties of H9C2 cardiomyoblasts by using a quartz crystal microbalance. *Analytical Methods* **8**(3), 488-495

Zhou YY, Cheng H, Bogdanov KY, Hohl C, Altschuld R, Lakatta EG, Xiao RP. (1997) Localized cAMP-dependent signaling mediates beta 2-adrenergic modulation of cardiac excitation-contraction coupling. *Am J Physiol.* **273**(3 Pt2):H1611-8.

Zhu WZ, Wang SQ, Chakir K, Yang D, Zhang T, Brown JH, Devic E, Kobilka BK, Cheng H, Xiao RP. (2003) Linkage of beta1-adrenergic stimulation to apoptotic heart cell death through protein kinase A-independent activation of Ca²⁺/calmodulin kinase II. *J Clin Invest.* **111**(5):617-25.

Zhu HL, Wei X, Qu SL, Zhang C, Zuo XX, Feng YS, Luo Q, Chen GW, Liu MD, Jiang L, Xiao XZ, Wang KK. (2011) Ischemic postconditioning protects cardiomyocytes against ischemia/reperfusion injury by inducing MIP2. *Exp Mol Med.* **43**(8):437-45.

Zhu WZ, Zheng M, Koch WJ, Lefkowitz RJ, Kobilka BK, Xiao RP. (2001) Dual modulation of cell survival and cell death by beta(2)-adrenergic signaling in adult mouse cardiac myocytes. *Proc Natl Acad Sci U S A.* **98**(4):1607-12.

Zordoky BN, El-Kadi AO. (2007) H9c2 cell line is a valuable in vitro model to study the drug metabolizing enzymes in the heart. *J Pharmacol Toxicol Methods.* **56**(3):317-22.

Appendix

Transfection with siRNAs:

H9c2 cells were seeded in 6-well flat-bottomed plates (45,000 cells/well) and cultured for 24 h in fully supplemented DMEM. Cells were transfected using the Accell siRNA delivery system (Dharmacon, Lafayette, CO). Briefly, the medium was removed and replaced with Accell delivery medium containing either TG2-specific siRNA targeting ORF of rat TG2 mRNA, positive control (GAPDH-targeting siRNA) or negative control (non-targeting control siRNA; Dharmacon, Lafayette, CO). Cells were incubated for 24, 48 and 72 h in the same media and following incubation, cells were lysed and subjected to western blotting as described in chapter II section 2.6 to detect TG2 and GAPDH. β -actin was used as loading control in these experiments.

Western blot analysis revealed that at 72 h, 39.25 ± 4.29 knockdown of TG2 protein expression was achieved (figure A.1) and therefore this time point would be suitable for future experiments. GAPDH siRNA was used as a positive control to check if the siRNA delivery mechanism was working. At 72 h, 36.57 ± 3.76 knockdown of GAPDH protein expression was achieved (figure A.1). It should also be noted that there was no significant difference between growth media and delivery media for either TG2 (84% of control) or GAPDH (92% of control) protein expression and the β -actin expression was unaltered in all conditions.

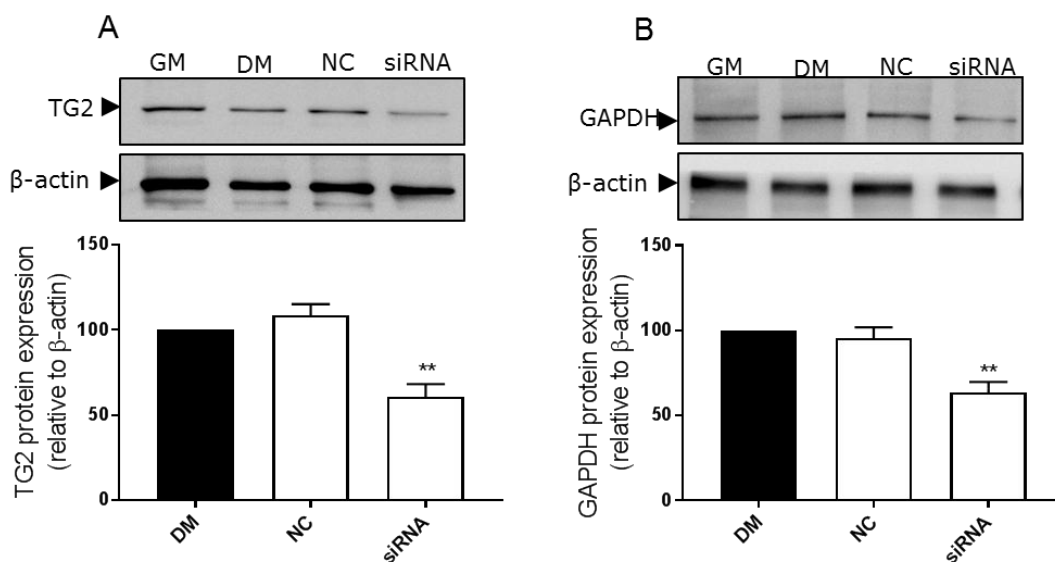


Fig A.1: Protein expression of TG2 and GAPDH in H9c2 cells. Cell lysates (15 μ g) from mitotic H9c2 cells treated with growth media (GM), delivery media (DM), negative control siRNA (NC), TG2 specific (A) and GAPDH specific (B) siRNAs for 72 h were analysed for TG2 and GAPDH protein expression by western blotting. Quantified data are expressed as percentage of control for TG2 and GAPDH protein expression relative to β -actin and represent the mean \pm S.E.M. from three independent experiments.